ATMOSPHERIC OZONE 1985

ASSESSMENT OF OUR UNDERSTANDING OF THE PROCESSES CONTROLLING ITS PRESENT DISTRIBUTION AND CHANGE

VOLUME II

NATIONAL AERONAUTICS AND SPACE ADMINISTRATION
FEDERAL AVIATION ADMINISTRATION • NATIONAL OCEANIC AND ATMOSPHERIC ADMINISTRATION
UNITED NATIONS ENVIRONMENT PROGRAM • WORLD METEOROLOGICAL ORGANIZATION
COMMISSION OF THE EUROPEAN COMMUNITIES • BUNDESMINISTERIUM FÜR FORSCHUNG UND TECHNOLOGIE

VOLUME II

TABLE OF CONTENTS

SPECIAL INTRODUCTION FOR CHAPTERS 8, 9, 10, and 11

HYDROGEN CYCLE

NITROGEN CYCLE

CHLORINE CYCLE

R.T. Watson

OXYGEN, HYDROGEN, NITROGEN, AND HALOGENATED SPECIES: OBSERVATIONS AND INTERPRETATION

Understanding the chemical composition and future behavior of the stratosphere cannot be achieved through laboratory simulation experiments because of the scale and complexity of atmospheric phenomena. The atmosphere is a complex chemical system with photochemical lifetimes of species ranging from nanoseconds to years, strongly influenced by dynamical and radiative processes. Consequently, at present and for the foreseeable future, heavy reliance must be placed on theoretical models. However, these models must be checked against atmospheric observations at every opportunity. A wide variety of in-situ and remote sensing techniques are now being used to determine the atmospheric concentrations of a large number of chemical species at a limited number of geographical locations from ground, aircraft, balloon, and rocket platforms. This type of data predominantly tests the radiative and chemical aspects of the models. A major advance in the last few years has been the demonstration of a capability to make global measurements of temperature and the concentrations of several species from satellites. Such new measurements are required to test the coupling of dynamics, chemistry, and radiation in the multidimensional models. In the longer term, future field and satellite programs will be needed to overcome our greatest limitation, which is a shortage of data. At present, the available measurements are inadequate for a complete test of the theoretical models.

The chemical processes controlling atmospheric ozone have already been described in detail in Chapter 2. Consequently, it is sufficient here to simply restate the key conclusion that atmospheric ozone is chemically controlled through a series of catalytic cycles involving members of the oxygen, hydrogen, nitrogen, chlorine, and to a lesser extent the bromine families. The chemical coupling that exists within and between the species of the HO_x, NO_x, and ClO_x families can be simply illustrated as shown in Figures SI-1, SI-2, and SI-3. The classical catalytic cycle that destroys odd oxygen can be written:

$$X + O_3 \rightarrow XO + O_2 \qquad (1)$$
$$\underline{O + XO \rightarrow X + O_2} \qquad (2)$$
$$\text{net:} \quad O + O_3 \rightarrow 2O_2 \qquad (3)$$
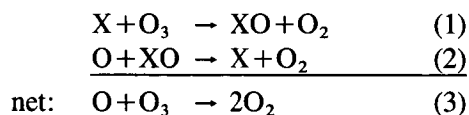
where $X = H$, OH, NO, Cl, or Br.

In order to model quantitatively the roles of hydrogen-, nitrogen-, and chlorine-containing species in controlling the distribution of atmospheric ozone, it is vital to measure and understand their total budgets. In addition, it is essential to understand the photochemical partitioning between the active and inactive species within each family. Therefore, the key chemical constituents of importance in understanding the spatial and temporal distribution of atmospheric ozone include the source gases (H_2O, CH_4, N_2O, and the halogenated alkanes) and the active and inactive inorganic species from the oxygen ($O(^3P)$, $O(^1D)$, and O_3), hydrogen (H, OH, HO_2, and H_2O_2), nitrogen (N, NO, NO_2, NO_3, N_2O_5, $ClONO_2$, HO_2NO_2, and HNO_3), and chlorine (Cl, ClO, HOCl, HCl, and $ClONO_2$) families. Active species are defined as being those species which directly participate in the catalytic cycles which destroy odd oxygen, i.e. OH and HO_2 (HO_x), NO and NO_2 (NO_x), and Cl and ClO (ClO_x). It should be noted that NO_x plays the major role in controlling ozone throughout most of the stratosphere in today's atmosphere (see Figure 8-1). However, even if the emissions of CFC's do not increase but remain constant at the present level, ClO_x will play an increasingly important, even dominant, role in controlling ozone in the middle and upper stratosphere as the concentration of ClO_x approaches its steady state value.

Since the previous WMO assessment report in 1982 there has been a continued expansion of the atmospheric chemical composition data base, including the temporary reservoir species $ClONO_2$, N_2O_5, and HO_2NO_2. Therefore, we now have at least some measurements of most key species. While many of these observations have been isolated measurements of single species, they have provided a valuable

Figure SI-1. Schematic of the Hydrogen Cycle.
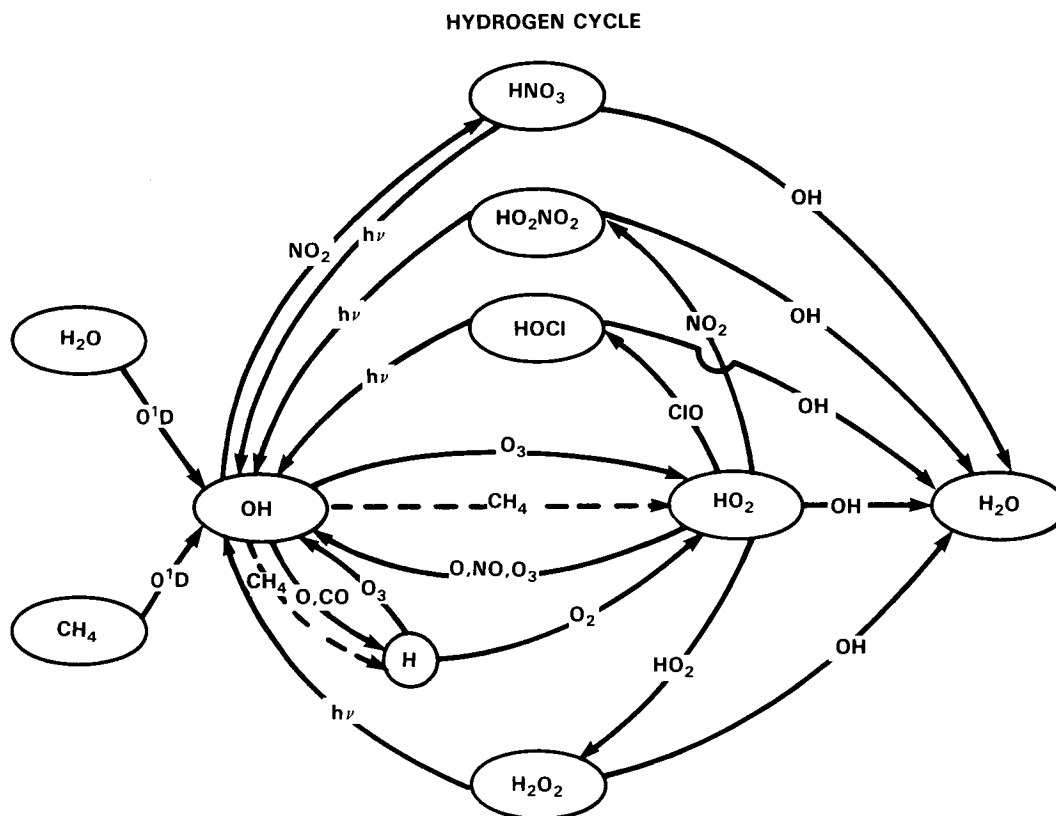
yet limited test of our knowledge of atmospheric photochemistry. However, it is now well recognized that the simultaneous measurement of several photochemically coupled species in the same air mass is necessary for the required critical test of photochemical theory; such tests are not possible from isolated measurements of single species. While there have been only a limited number of such simultaneous measurements to date, there is currently a growing emphasis to implement such a measurement strategy.

A major limitation in our ability to critically compare atmospheric observations with theoretical predictions at the time of writing the previous WMO assessment report (1982) was our lack of knowledge of the accuracy and precision of the atmospheric chemical composition measurements. Differences between measurements of the same species made at different times and places could be ascribed either to atmospheric variability or to measurement inaccuracies. Consequently, a major effort has been expended during the last four years to determine the accuracy and precision of atmospheric chemical composition measurements by conducting a series of international intercomparison balloon campaigns where chemical constituents were measured using a variety of observational techniques simultaneously in time and space. The inter-comparison campaigns performed to date include:

(a) a series of three campaigns, employing both *in-situ* and remote sensing balloon and rocket-borne instruments, to measure ozone.

(b) two campaigns utilizing remote sensing balloon-borne instruments (13 on the first, and 18 on the second), using eight different techniques including grating spectrometers, radiometers, and Fourier transform

interferometers, to measure several key atmospheric constituents including HNO_3, NO_2, NO, HCl, HF, O_3, H_2O, CH_4, and OH. These sensors covered the visible, infrared, far-infrared, and microwave region of the electromagnetic spectrum in both absorption and emission.

(c) three campaigns employing *in-situ* and remote sensing balloon-borne instruments to measure water vapor.

(d) *in-situ* cryogenic grab sampling techniques to measure source gases such as CH_4, N_2O, and chlorofluorocarbons (including $CFCl_3$ and CF_2Cl_2).

The data from these intercomparison campaigns which is described more fully in Appendix C is currently in the final stages of analysis. The results have shown that some of our current measurements, such as those for O_3, are accurate to better than ten percent. Others are accurate to no better than a factor of two, e.g. those for NO_2.

Within the last four years, several newly developed *in-situ* and remote sensing techniques have been demonstrated for species for which there had been inadequate measurements, e.g. OH. In addition, some existing techniques have been improved which will result in greater sensitivity for a number of species, e.g. ClO and O_3 by balloon-borne microwave emission. This newly developed and improved instrumentation will augment existing instrumentation in order to measure nearly all key atmospheric species over a significant altitude range with the accuracy and precision required to critically test our understanding of atmospheric photochemistry. Techniques that have been demonstrated within the last four years include:
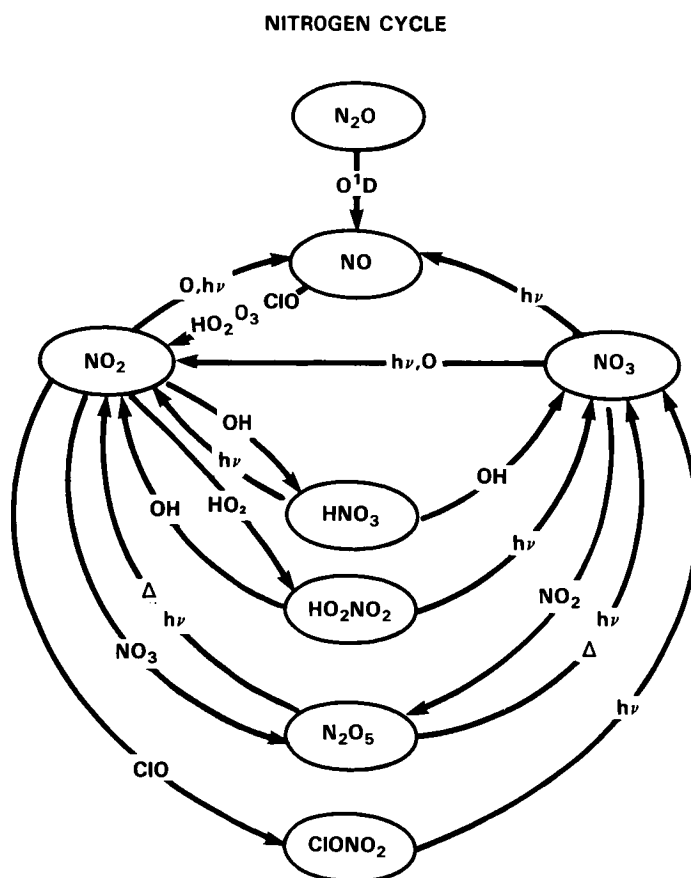
NITROGEN CYCLE

Figure SI-2. Schematic of the Nitrogen Cycle.

395
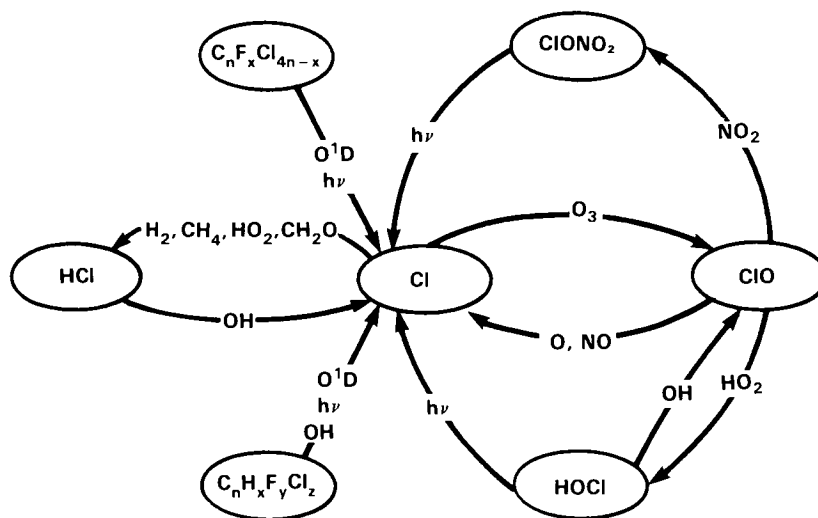
Figure SI-3. Schematic of the Chlorine Cycle.

(a) Two balloon-borne far-infrared emission interferometers for remote sensing detection of OH;

(b) Balloon-borne laser induced fluorescence systems for *in-situ* and range resolved detection of OH;

(c) A balloon-borne laser diode absorption system for *in-situ* detection of NO and NO_2;

(d) A shuttle-borne high resolution infrared absorption interferometer (ATMOS) for detection of a wide range of chemical constituents including several of the temporary reservoir species, e.g. $ClONO_2$, N_2O_5, and HO_2NO_2;

(e) A ground-based microwave emission system for remote detection of species including ClO, HO_2, and O_3;

(f) A balloon-borne cryogenic matrix isolation technique for *in-situ* detection of HO_2 and NO_2;

(g) Ground-based lidar systems for remote detection of O_3 and temperature.

As stated earlier, the single greatest advance during the last four years has been the analysis, validation and release of data obtained by instruments flown on the Nimbus 7, Applications Explorer II (AEM-2), and Solar Mesospheric Explorer satellites. These data includes seven months of Limb Infrared Monitor of the Stratosphere (LIMS) (HNO_3, NO_2, O_3, H_2O, temperature); four years of Stratospheric and Mesospheric Sounder (SAMS) (CH_4, N_2O, temperature), four years of Solar Backscatter Ultraviolet/Total Ozone Monitoring System (SBUV/TOMS) (O_3 (column and vertical distribution) and solar flux); three years of Stratospheric Aerosol and Gas Experiment (SAGE) (O_3, NO_2, aerosols); and Solar Mesospheric Explorer (SME) (O_3, NO_2, aerosols, solar flux). In addition, five years of polar stratospheric aerosol data are available from the SAMS II experiment. These data have now been processed and archived at the National Space Science Data Center in Greenbelt, Maryland, USA.

A brief description of each of these satellite instruments will now be presented:

(1) The Limb Infrared Monitor of the Stratosphere (LIMS):

The LIMS instrument is a six channel limb scanning infrared radiometer that was launched on the Nimbus 7 spacecraft in a circular Sun synchronous polar orbit on October 24, 1978. LIMS scanned across the Earth's limb, and measured the radiation emitted by the atmosphere as a function of height above the surface. The radiances measured in two channels at 15 μm were used to derive vertical temperature distributions as a function of pressure. These were then used with radiances measured by channels centered at 9.6, 6.7, 11.3, and 6.2 μm to retrieve the vertical distributions of O_3, H_2O, HNO_3, and NO_2, respectively. The instrument's detectors were cooled to 63K by subliming solid methane cryogen in order to achieve high radiometric signal-to-noise with a narrow field of view. The cryogen system was designed for a seven month lifetime, so LIMS data spanned the period October 1978 - May 1979. Each retrieval provides a profile with a vertical resolution of about 2 km for temperature, O_3, and HNO_3, and 4 km for NO_2 and H_2O. The profiles extend from 10 to 65 km for temperature and O_3, and 10 to 50 km for NO_2, HNO_3, and H_2O. Retrievals were performed every 4 degrees of latitude from 64 °S to 84 °N, resulting in about 7000 profiles per day. The local times of overpass were close to 1 PM and 11 PM over a wide range of latitudes, but changed rapidly at high latitudes near the terminator.

(2) The Stratospheric and Mesospheric Sounder (SAMS):

The SAMS instrument is a multichannel infrared limb-scanning radiometer using both conventional and pressure modulation techniques, in the emission mode, to measure atmospheric temperature (using the 15 μm CO_2 band) and the abundances of a number of minor atmospheric constituents including CH_4, N_2O and H_2O. CH_4 and N_2O were measured using a common optical chain and detector at 7.8 μm. Consequently, these gases could not be measured simultaneously and were observed on alternative 24 hour periods. H_2O was measured at 6.3 μm but no data has yet been archived due to retrieval difficulties. The instrument flew aboard the Nimbus 7 satellite and operated successfully for more than four years providing profiles from 20 mbar (~ 28 km) to 0.3 mbar (~ 58 km) with a vertical resolution of approximately 8 km every 10 degrees from about 50° S to 70° N. As with the LIMS instrument, the local times of overpass were close to 1 PM and 11 PM at all but high latitudes.

(3) The Solar Backscatter Ultraviolet/Total Ozone Monitoring System (SBUV/TOMS):

The SBUV and TOMS instruments were launched on the Nimbus 7 satellite and are still operating. Consequently, they have so far provided a continuous 7 year data set starting in October 1978 for the vertical distribution and total column content of O_3 from 80° N to 80° S. The SBUV instrument is a nadir-viewing double monochromator, with a field of view of 200 by 200 km, which measures the radiances backscattered from the atmosphere at 12 discrete wavelengths from 255 to 340 nm with a 1 nm bandpass, and continuously scans wavelength ranging between 160 and 400 nm. Radiances between 255 and 306 nm are used in the O_3 profile inversion, while radiances between 312 and 340 nm are used to calculate total O_3. In order to calculate backscattered albedo, the ratio of backscattered radiance to extraterrestrial solar irradiance must be measured daily by employing a diffuser plate. The retrieved O_3 profiles extend from about 25 to 55 km with an altitude resolution of approximately 8 km.

The TOMS instrument is similar in concept to the SBUV instrument but has two distinct differences i.e., it has only 6 discrete wavelength channels, and incorporates a side scan feature with approximately 50 by 50 km field of view. These differences result in the TOMS instrument being limited to total O_3

measurements only, but with true global daily coverage and a significantly enhanced capability to observe small spatial scale features. As the SBUV and TOMS measurements are restricted to the sunlit portion of the Earth this means that continuous spatial coverage thoughout the year is from 60°N–60°S, with coverage to the poles by TOMS only in the summer season.

4) The Stratospheric Aerosol and Gas Experiment (SAGE):

The SAGE instrument is a four channel Sun photometer that measures atmospheric attenuation during each solar occultation (sunrise or sunset). SAGE was launched on the AEM-2 satellite during February 1979 with an orbital inclination of 55 degrees. It operated for 34 months but due to a battery problem SAGE sunrise measurements were terminated in August 1979 and only sunset measurements were continued. The four spectral channels were centered at 1000, 600, 450, and 385 nm. The four wavelength transmission profiles are inverted to produce vertical profiles of aerosol extinction, O_3, and NO_2. The vertical resolution is 1 km for O_3 and aerosol extinction measured at 1000 nm, and the vertical resolution is 3 km for NO_2 and aerosol extinction measured at 450 nm. The vertical ranges of O_3, NO_2, and aerosol extinction measurements were 10-50, 20-40, and 2-35 km, respectively (the lower limit for O_3 and aerosol profiles was normally limited by the cloud top height) with a latitude coverage of about 80° S to 80° N over a two week period.

An improved version of the SAGE instrument, SAGE 2, was recently launched on the Earth Radiation Budget Experiment satellite (ERBE). SAGE 2 has 7 channels and will measure H_2O in addition to O_3, NO_2, and aerosol extinction.

(5) The Solar Mesospheric Explorer (SME):

The SME satellite was launched in October 1981 in a Sun synchronous polar orbit. It has four limb scanning instruments that are used to measure O_3, the O_3 photodissociation rate, temperature, H_2O, thermal emission, and NO_2. In addition it has two instruments to measure the solar ultraviolet radiation and to detect solar proton events. The satellite spins at a rate of 5 rpm enabling the limb scanning instruments to obtain vertical profiles every 12 seconds along its orbit track. The local equator crossing time is approximately 3 PM. The duty cycle of the instruments is about 30% which results in complete latitudinal coverage, but incomplete longitudinal coverage, with most of the data being taken over the North American Continent.

O_3 density is measured between 50 and 70 km altitude with an ultraviolet spectrometer which detects solar radiation scattered by the atmosphere at 265 and 297 nm. Differential absorption by O_3 at these two wavelengths produces an absolute measurement of the O_3 density along the line of sight of the limb viewing instrument. An onion peeling inversion algorithm converts the observed Raleigh scattered sunlight including O_3 absorption into O_3 density as a function of altitude with a vertical resolution of approximately 3.5 km.

O_3 density is also determined with a near infrared spectrometer which measures the airglow at 1270 nm. This emission is the result of the photodissociation of O_3 which produces O_2 in excited states. Vertical profiles of O_3 densities can be deduced from 50 to 90 km from these data.

NO_2 densities can be measured between 20 and 40 km altitude with a visible spectrometer detecting solar radiation scattered by the atmosphere in the spectral region of the spectrum near 440 nm. Differential absorption by NO_2 in this spectral region produces an absolute measurement of NO_2 in a manner similar to O_3. The El Chichon eruption of April 1982 injected a large number of scattering particles into the

atmosphere, interrupting NO_2 observations for almost two years. Algorithms are currently being developed to retrieve NO_2 in the two year period following the El Chichon eruption.

H_2O and temperature measurements were to be made using an infrared spectrometer operated in the emission mode at 6.3 and 15 μm respectively. Unfortunately no data has yet been archived because of difficulties in retrieving atmospheric temperatures due to low signal-to-noise ratios caused by the high operating temperature of the instrument.

The next four chapters review, and compare to both one-dimensional and two-dimensional model descriptions of the present day stratosphere, the stratospheric measurements of oxygen, hydrogen, nitrogen, and halogen containing species obtained from ground, aircraft, balloon, rocket, shuttle, and satellite-based instruments.

OXYGEN SPECIES
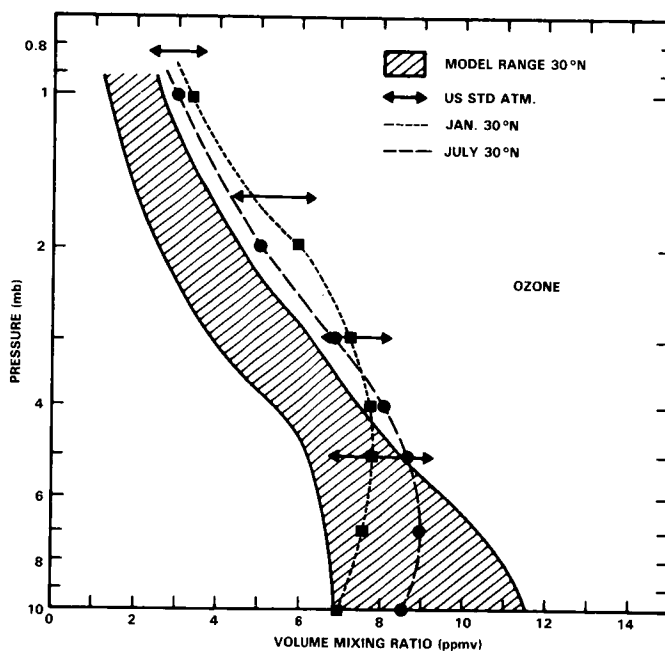
Panel Members

G. Brasseur and A.J. Miller, Co-Chairmen

P.K. Bhartia   P. McCormick
A. Fleig   G. Megie
L. Froidevaux   R. Nagatani
D. Heath   J.M. Russell, III
E. Hilsenrath   R.J. Thomas
J.A. Logan

CHAPTER 8

OXYGEN SPECIES: OBSERVATIONS AND INTERPRETATION

TABLE OF CONTENTS

8.0 INTRODUCTION

The problems related to odd oxygen (O_3, O and O(^{1}D)) in the atmosphere and especially to ozone (O_3) have been extensively discussed in the last 10-20 years. Ozone is indeed the only atmospheric constituent which effectively absorbs ultraviolet solar radiation from about 250 to 310 nm, protecting plant and animal life from exposure to harmful radiation (UV-B). Moreover, since the absorbed solar energy is converted into thermal energy, the absorption of UV light by ozone constitutes the principal source of heat in the middle atmosphere and is therefore responsible for the existence of the stratosphere, a layer with a positive temperature gradient and a considerable static stability.

The possible long-term decrease in the ozone amount is therefore expected not only to increase the UV-B irradiance at the earth's surface, but also to modify the thermal structure or the atmosphere with potential consequences on the general circulation and on the global and local climate of the Earth.

As indicated previously in Chapter 2, stratospheric and mesospheric ozone is produced by photodissociation of molecular oxygen

$$O_2 + h\nu \rightarrow O + O \tag{1}$$

followed by a three-body recombination reaction

$$O + O_2 + M \rightarrow O_3 + M \tag{2}$$

Its destruction can occur by recombination with atomic oxygen

$$O + O_3 \rightarrow 2O_2 \tag{3}$$

This reaction, however, can be catalyzed by a number of atmospheric species such as the pairs of radicals OH and HO_2, NO and NO_2, or Cl and ClO. A representative picture of the height-dependent percent contribution of these cycles to the odd oxygen loss at mid-latitudes is shown in Figure 8-1. The direct recombination (Chapman, 1930) plays its major role near the stratopause while the effect of nitrogen (Crutzen, 1970), which is the globally dominant ozone loss occurs essentially in the middle and lower stratosphere. Destruction by hydrogen compounds dominates in the mesosphere, at low altitude in the troposphere and near the tropopause. Chlorine plays a significant role (and will play an even larger role in the future) in the upper stratosphere.

The ozone balance is thus controlled on the one hand by the solar irradiance and its penetration into the denser layers of the atmosphere and on the other hand by the atmospheric abundance or species involved in the O_x, HO_x, NO_x and ClO_x systems. These chemical families will be considered in detail in the next three chapters.

The purpose of this chapter is to determine how the spatial distribution of ozone, as predicted by numerical models, compares with observations. Since numerical predictions of the future ozone trend are based on models which make use of this complex chemistry, it is important to state how well we understand that chemistry and what are the possible sources of discrepancies between models and observations. Toward this, we will develop a set of reference ozone profiles against which to compare current numerical calculations.
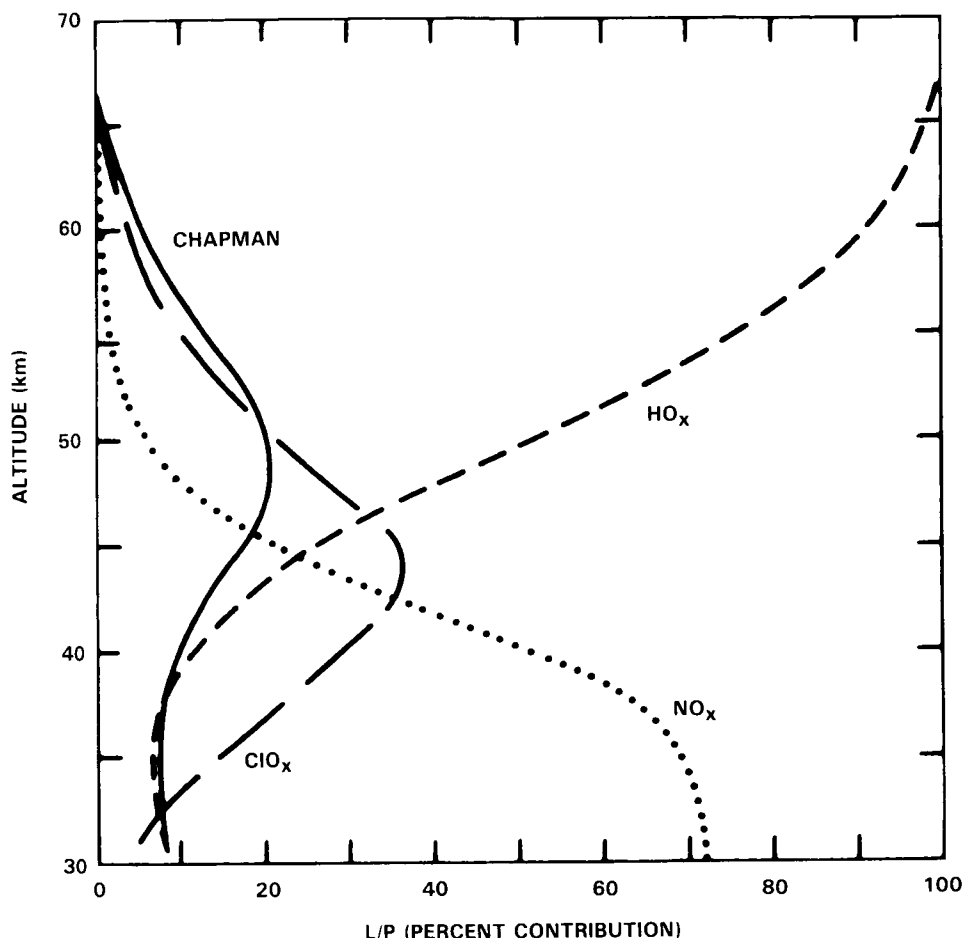
Figure 8-1. Ratio (in percent) of the odd oxygen loss rate due to the Chapman, HO_x, NO_x, ClO_x mechanisms to the odd oxygen production rate (based on mid-latitude diurnal average calculation with the Caltech 1-D model; JPL 1985 recommended photochemical data). L and P are the O_x loss and production rates respectively.

The comparison between measured and calculated ozone distributions is not always straightforward. Indeed, below about 25 km, the photochemical lifetime of odd oxygen is long compared to the characteristic time for meridional and vertical transport. In the lower stratosphere, the ozone distribution is thus heavily influenced by dynamics and the large ozone variability which is observed reflects effects due to advection, large scale planetary waves, turbulence, etc. In the upper stratosphere and in the mesosphere, ozone can more easily be used to test our present knowledge of the chemistry since the chemical lifetime of odd oxygen is short and the direct influence of transport processes is weak. Figure 8-2, taken from the 2-D model of Garcia and Solomon (1985), shows the O_x photochemical lifetime as a function of altitude and the resulting regions of dynamical and chemical control. Most of the analyses reported in the present chapter will focus on ozone between 30 and 70 km altitude. Even in this region, however, transport processes can influence the ozone distribution, in particular at high latitudes during the winter and spring seasons, when large scale planetary waves and stratospheric warmings occur. In an attempt to isolate the photochemical effects, one should therefore also try to avoid the above regions, unless one can track a certain air parcel and analyze the ozone changes within it, as they relate to temperature or other observable chemical changes.

LOG$_{10}$ O$_X$ PHOTOCHEMICAL LIFETIME (sec)
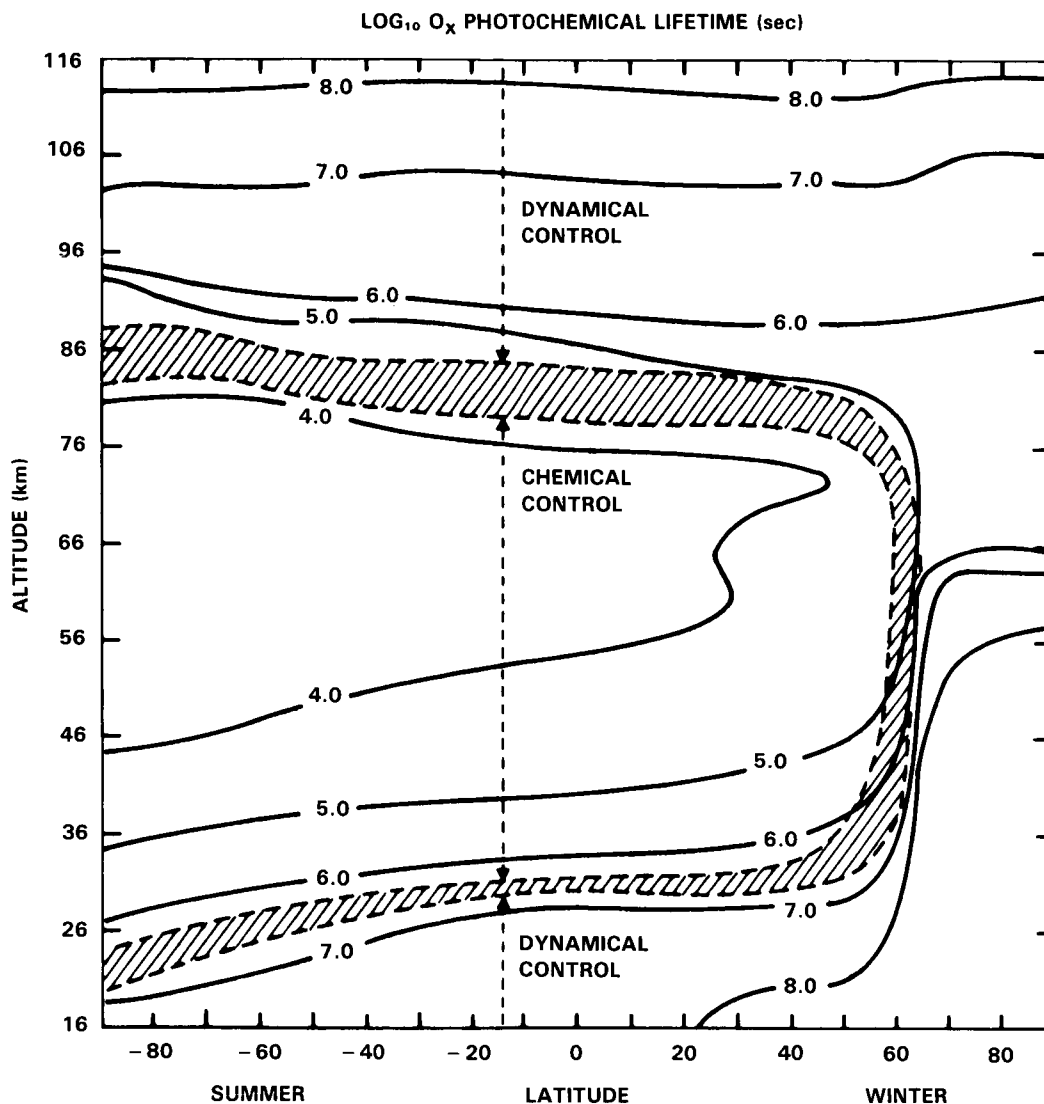
Figure 8-2. Photochemical lifetime of the O$_X$ family and the region of transition from photochemical to dynamical control (shaded) (From Garcia and Solomon, 1985).

8.1 OZONE REFERENCE PROFILES

Our approach within this section is to utilize recent satellite observations as well as ground-based data to provide the necessary global coverage. Because the Solar Backscatter Ultraviolet (SBUV) instrument, launched in 1978, provides the longest data record of the satellite systems, we focus on these data as the basic system. A major feature of this section, however, is a discussion of the comparison of SBUV versus LIMS, SAGE and SME satellite systems as well as the ground-based observations to provide evidence of the absolute accuracy of the profiles. This, combined with the estimates of sampling errors and year-to-year variations provides the basic confidence estimates of the observations for the model comparisons.

8.1.1 Instruments

8.1.1.1 Satellite Systems

General descriptions of the satellite systems are described above such that within this section we will focus on the error analyses pertinent to our understanding of the random and absolute error characteristics.

The operating characteristics of the SBUV system are presented in Tables 8-1 and 8-2 (Bhartia, personal communication) where Table 8-1 pertains to time invariant errors and Table 8-2 the random error component. We see that at 1 mbar the combined time-invariant error is about 7% and decreases to about 3% for total ozone. For the random error component the combined error is about 5% except at the upper end of the profile data where it increases to 10%.

Table 8-1. Nimbus-7 SBUV Systematic Error Summary (Bhartia and Fleig, Personal Communication).

Error Source	Ozone Mixing Ratio Error (%)					Total Ozone
	.4 mb	1 mb	3 mb	10 mb	30 mb	
1. Ozone absorption cross-section	3	3	3	3	3	3
2. Wavelength calibration	0.5	0.5	0.6	0.7	0.7	0.7
3. Radiometric calibration	7	5	3	2	2	1
4. Retrieval error	10	3	2	4	5	1
RSS of (1) thru (4)	13	7	5	5	6	3

Notes: a) Values are maximum possible error (1 σ confidence) from each error source in mid latitudes
  b) Error 1 applies only for SBUV comparisons with non-UV instruments. Within Ultraviolet errors should be less than 1%.
  c) Errors 1 and 4 should be ignored in comparing similar SBUV instruments on different satellites.

Total ozone measurements made by the SBUV have been compared with those from over 60 Dobson stations (Bhartia *et al.*, 1984a). The result is that SBUV is lower, on average, by about 8% and the standard deviation of the differences is consistent with the estimates of about 2% precision on each instrument type.

With respect to comparisons of SBUV profiles, Bhartia *et al.* (1984b) have compared the results with Umkehr and balloon ozonesonde information. The biases are generally less than 10%, but are functions of layer height and latitude. The precision of the SBUV measurements is found to be better than 8% from pressures between 1 and 64 mbar and better than 15% from 64 to 253 mbar.

The biases between SBUV and the ground-based observations, discussed above, are believed to be largely due to inconsistencies in the ozone absorption cross sections used for the various measurement systems. This is currently being reexamined utilizing new absorption coefficients derived by Bass and

Table 8-2. Nimbus-7 SBUV Random Error Summary (Bhartia and Fleig, Personal Communication).

Error Source	Ozone Mixing Ratio Error (%)					Total Ozone
	.4 mb	**1 mb**	**3 mb**	**10 mb**	**30 mb**	
1. Instrument noise	2	1	1	2	2	0.5
2. Atmospheric temp	1	0.5	1	1	1	1
3. Retrieval error	10	3	2	4	5	2
RSS of (1) thru (3)	10	3	2.5	5	5	2

Notes: a) Errors listed are R.M.S. values for typical mid latitude measurements. During winter months or under disturbed atmospheric conditions. Errors 2 and 3 may be larger by a factor of 2.

b) Vertical resolution of SBUV derived profiles is ~8 km. Resolution related limitations are not included.

Paur (personal communication) and recently recommended by the International Ozone Commission for use in the satellite retrievals.

For the LIMS experiment, details of the preflight calibration are presented by Gille and Russell (1984). Within Table 8-3 are presented the LIMS systematic errors (Remsberg et al., 1984a) and we see that the errors are about 20% save at the lower and upper end of the profiles where they increase to 40%. The authors note that the random ozone radiometric errors are about equal to the systematic radiometric errors from 30 to 0.3 mbar.

An extensive program of correlative balloon underflights was carried out to aid in validation of LIMS data. The results of the correlative measurement comparisons, accuracy calculations, and precision estimates are presented by Remsberg et al., 1984a. Comparisons with sets of correlative ozone profiles show mean differences of less than 10% from 7 to 50 mbar for mid-latitude balloon borne sensors and 16% from 0.3 to 50 mbar for rocket data. Such results are well within the uncertainties for the correlative sensors themselves. Agreement with balloon measurements degrades somewhat at tropical latitudes in the lower stratosphere. LIMS detects significant vertical structure in the ozone profile even below the ozone mixing ratio peak. Preliminary comparisons with Umkehr data at four stations show generally good agreement from 1 to 30 mbar.

Results of comparison between SAGE and ground-based data have been summarized by McCormick et al. (1984) for 5 sets during 1979-1980. The intercomparisons included data taken with electrochemical ozone (ECC) balloonsondes and chemiluminescent and optical rocketsondes. The average mean difference for 17 separate comparisons between the SAGE and ECC balloonsonde observations over the altitudes 18-28 km was 9.3% with a standard deviation of 2.8%. Excluding comparisons separated by greater than 500 km reduces the average mean difference to 8.9% and the standard deviation to 2.1%. The average mean difference between SAGE and three optical rocketsonde observations over the altitudes 25-50 km was 11% and between SAGE and two chemiluminescent rocketsondes over the altitudes 20-60 km was 13.5%. Considering the differences in vertical resolution, experimental errors, and ozone time and space

gradients, the agreement between SAGE-derived ozone profiles and these correlative measurements is considered very good. In addition, isopleths of ozone mixing ratio versus latitude and altitude are in good agreement with previously published results.

Within Tables 8-4 and 8-5 are presented the systematic and random error components, respectively. We see that the systematic component is about 2.5% and the random component is of the order of 10% except at the highest level where it is 40%. This value, however, is a worst case scenario for 1 km resolution.

Rusch et al. (1984) have examined the error characteristics of the SME experiment and in Table 8-6 and 8-7 we reproduce their results for the systematic and random components, respectively. We see that the systematic errors are about 16% over the entire range, while the random errors are about 6% at 48 km increasing to about 14% at 68 km.

Table 8-3. LIMS O_3 Channel Systematic Error Sensitivity Results.

Error Parameter	O_3 Mixing Ratio Error, %						
	100 mb	30 mb	10 mb	3 mb	1 mb	0.3 mb	0.1 mb
1. Systematic radiometric errors*	5	2	1	1	2	5	20
2. Temperature profile bias (± 2 K)	34	32	20	12	10	12	12
3. O_3 spectral parameters	15	12	10	8	8	8	8
4. IFOV side lobes	14	2	2	3	6	20	31
5. Deconvolution error	5	5	5	5	5	5	5
6. rss of rows 1-5	40	35	23	16	15	26	40

* Random O_3 radiometric errors are about equal to the systematic radiometric errors from 30 to 0.3 mbar.

Table 8-4. SAGE Ozone Systematic Error Summary (McCormick and Chu, Personal Communication).

Error Source	1 mb	7 mb	50 mb	100 mb	Total Ozone
1. Ozone absorption cross-section	1.5%	1.5%	1.5%	1.5%	1.5%
2. Wavelength calibration	2.0%	2.0%	2.0%	2.0%	2.0%
3. Rayleigh correction	0.5%	0.5%	0.5%	0.5%	0.5%
	2.5%	2.5%	2.5%	2.5%	2.5%

Table 8-5. SAGE Ozone Random Error Summary (McCormick and Chu, Personal Communication).

Error Source	1 mb	7 mb	50 mb	100 mb	Total Ozone
1. Measurement noise	40%	5%	10%	10%	1.0%
2. Atmospheric temperature	0.3%	0.2%	0.2%	0.5%	0.2%
3. Aerosol correction	0	0	1.0%	2%	0.5%
4. Tropospheric ozone	0	0	0	0	1%
	40%	5%	10.1%	10.2%	1.5%

Notes: a) Error 1 applies only when SAGE data are used at 1 km altitude resolution. Error magnitude can be reduced by vertical averaging giving an improvement factor of $\sqrt{N}$, where N is the number of km altitude being averaged; i.e., the 10% error at 50 mb can be reduced to approximately 3.3% when 10 km vertical averaging is done.

b) SAGE ozone profiles begin at cloud top altitude. Total ozone is determined using climatology mean for the tropospheric ozone component.

8.1.1.2 Ground-Based Systems

As the ground-based data systems (except for the recent LIDAR results) have been extensively discussed in the recent reports of Hudson and Reed (1979) and WMO (1982), we will present here only a brief overview and update as required.

8.1.1.3 Total Ozone

The most widely used tool for monitoring total ozone continues to be the Dobson ozone spectrophotometer. This instrument is a quartz-prism double-monochromator, which measures the differential attenuation of sunlight in adjacent spectral bands in the UV Huggins bands of ozone. By use of a double wavelength pair method with direct sunlight, measurements precise to ±2% are possible. Empirical relationships between measurements on direct sunlight and zenith skylight have been derived. This allows a less accurate estimation of total ozone on partly cloudy and cloudy days.

In the U.S.S.R., a filter photometer system, the M-83, is used for total ozone measurements. In a direct comparison with the Dobson spectrophotometer, Bojkov (1969) found differences as large as 40 percent. These differences, which depend on the solar zenith angle and the season, apparently arise from the use of broadband filters and the assumption of constant ozone absorption coefficients. The U.S.S.R. has about 35 M-83 instrument reporting stations. Error estimates of the Dobson system are presented by Hudson and Reed (1979). We note, however, that this table does not take into consideration the recently derived ozone absorption coefficients of Bass and Paur.

It should be noted here that Dobson spectrophotometers are no longer being produced. A. W. Brewer has developed a grating ozone spectrophotometer which is now available commercially. Preliminary evaluation indicates that the Brewer instrument provides direct sun total ozone observations of precision comparable to the Dobson (Kerr et al., 1976) and, in addition, provides information on the total SO_2 content.

Table 8-6. SME UV ozone systematic error summary (Rusch *et al.*, 1984).

Altitude, km	Day 11	Day 101	Day 191	Day 280	rms Average
% Error Due to Uncertainty in Sensitivity					
48	15.0	15.9	16.8	15.1	15.7
50	17.0	17.7	17.4	17.3	17.3
52	17.7	18.2	17.5	17.4	17.7
54	17.4	18.1	17.4	16.9	17.5
56	16.9	17.5	17.2	16.6	17.0
58	17.6	17.6	16.6	17.2	17.3
60	17.8	18.3	17.0	16.6	17.4
62	17.2	18.5	17.8	15.0	17.2
64	15.9	16.9	17.7	14.2	16.2
66	14.5	15.9	15.6	12.4	14.7
68	13.4	14.9	14.2	10.6	13.4
% Error Due to Polarization Errors					
48	1.6	1.5	1.5	2.1	1.7
50	1.6	1.6	1.4	1.8	1.6
52	1.8	1.8	1.4	1.9	1.8
54	2.0	2.1	1.5	2.8	2.2
56	2.1	2.3	1.6	3.2	2.4
58	2.1	2.3	1.8	2.7	2.2
60	2.1	2.3	1.9	3.2	2.5
62	2.2	2.2	2.0	3.6	2.6
64	2.2	2.1	2.1	4.0	2.7
66	3.1	4.5	2.3	5.9	4.2
68	4.0	4.6	2.7	6.8	4.7
% Error Due to Uncertainties in Dead Time Constants					
48	1.4	1.2	1.0	3.0	1.8
50	1.6	1.4	1.3	1.9	1.6
52	1.7	1.5	1.5	2.4	1.8
54	1.7	1.5	1.5	3.5	2.2
56	1.7	1.4	1.3	3.5	2.1
58	1.5	1.1	1.2	2.5	1.7
60	1.3	0.9	0.9	3.3	1.9
62	1.2	0.8	0.7	4.4	2.3
64	1.5	0.7	0.7	5.5	2.9
66	1.3	1.1	0.7	2.8	1.7
68	1.7	1.1	1.0	3.5	2.1
% Error Due to Uncertainties in Ozone Absorption Cross Sections					
48	5.8	5.1	4.9	6.2	5.5
50	5.4	4.9	4.9	5.7	5.2
52	5.1	4.9	5.0	5.6	5.2
54	5.1	5.1	5.1	5.9	5.3
56	5.2	5.4	5.2	6.3	5.5
58	5.4	5.6	5.2	6.2	5.6
60	5.6	5.6	5.2	6.4	5.7
62	6.1	5.4	5.1	6.8	5.9
64	6.6	5.0	4.9	7.3	6.0
66	4.6	4.2	4.5	5.1	4.6
68	4.1	3.5	4.2	5.1	4.3
% Error (Year Total)					
48	16.9				
50	18.3				
52	18.7				
54	18.6				
56	18.3				
58	18.4				
60	18.7				
62	18.5				
64	17.8				
66	16.1				
68	15.0				

Vertical Distribution of Ozone

8.1.1.4 Umkehr Method

Estimates of the vertical ozone distribution have been made with the Dobson instrument using the "Umkehr" effect (Gotz *et al.*, 1934).

Table 8-7. SME UV ozone random error summary (Rusch *et al.*, 1984).

Altitude, km	Day 11	Day 101	Day 191	Day 280	rms Average
% Error Due to Noise and Data Compression					
48	2.5	3.4	2.9	4.3	3.4
50	1.9	2.5	2.2	4.1	2.8
52	2.3	2.0	2.8	4.5	3.0
54	3.3	2.4	3.8	5.4	3.9
56	3.5	3.1	4.7	5.3	4.2
58	3.1	3.6	4.9	5.2	4.3
60	4.6	4.0	4.4	7.2	5.2
62	6.3	4.9	4.9	7.3	5.9
64	6.2	6.5	7.8	8.7	7.3
66	9.5	6.6	9.6	9.4	8.8
68	11.0	7.3	11.6	10.5	10.2
% Error Due to Temperature and Pressure Errors and Altitude Assignment of the Data					
48	3.7	4.4	4.6	5.2	4.5
50	5.4	6.8	6.7	6.9	6.5
52	6.7	8.5	8.0	8.8	8.0
54	7.5	9.4	8.6	10.5	9.1
56	7.8	9.7	8.6	10.7	9.3
58	7.4	9.4	8.3	10.0	8.8
60	6.9	8.9	7.8	10.6	8.7
62	7.2	8.4	7.5	11.0	8.6
64	7.5	8.4	7.9	12.3	9.2
66	6.1	8.6	8.9	9.4	8.4
68	7.4	10.0	11.4	11.0	10.1
% Error (Year Total)					
48	5.6				
50	7.1				
52	8.5				
54	9.9				
56	10.3				
58	9.9				
60	10.1				
62	10.6				
64	11.9				
66	12.2				
68	14.4				

Recently, a new method for obtaining ozone profiles, known as the "short Umkehr," has been tested and accepted. The short Umkehr method requires zenith sky measurements on the A, C, and D wavelength pairs of the Dobson ozone spectrophotometer while the solar zenith angle is between 80 and 89 degrees. It has been shown by DeLuisi (1970) in a theoretical-numerical study that such measurements should contain at least as much information about the ozone profile as do the conventional Umkehr observations taken on the C wavelength pair while the solar zenith angle is between 60 and 90 degrees. The short Umkehr requires about one-third of the observing time needed for the conventional Umkehr.

This reduced observing time gives the short Umkehr at least three distinct advantages over the conventional Umkehr. First, there is less chance that significant changes in the ozone profile will occur during the course of the observation; second, there is a better chance that the zenith sky will remain clear; and third; it costs less per Umkehr observation in terms of observer time.

Hudson and Reed (1979) present the error estimates of the Umkehr method. As for the Dobson total ozone, this does not consider the impact of the Bass and Paur ozone absorption coefficients. We note that one recent development in the Umkehr measurement program has been the distribution of automated Dobson instruments at 7 sites. Instruments are currently operative at Boulder, Colorado; Mauna Loa, Hawaii; Haute Provence, France; Poker Flat, Alaska and Perth, Australia. Initiation of operations at Huancayo, Peru is planned for this year and a seventh site is under consideration.

8.1.1.5 Balloonsondes

For determinations of the vertical ozone distribution with good vertical resolution, direct soundings are required. Optical balloonsondes, using differential absorption techniques analogous to the Dobson method, were designed by Kulcke and Paetzold (1957), Vassy (1958), and Kobayashi et al. (1966). Above the ozone maximum, these methods have limited vertical resolution, but potentially good absolute accuracy.

Electrochemicalsondes, using the reaction of ozone with an aqueous solution of potassium iodide, were later developed by Brewer and Milford (1966), Komhyr (1965), and Kobayashi and Toyama (1966). These can be flown day or night and have better vertical resolution than the opticalsondes below 25 km. In practice, data from the electrochemicalsondes must be adjusted by coincident independent total ozone observations, and all such sondes require air pump efficiency corrections. Intercomparison between balloonsondes shows agreement within about 6 percent after corrections are applied.

The sensors in both the ECC and Brewer-Mast sondes are based on the reaction of ozone with the iodide ion to form molecular iodine, but the sondes differ in the design of the electrochemical cell. The reaction is not specific for ozone. Sulfur dioxide causes a negative interference of one mole of O_3 per mole of SO_2, while NO_2 gives a slight positive interference (Katz, 1977; Schenkel and Broder, 1982). Contamination by NO_2 should be unimportant at rural sites, where concentrations of NO_x are 0.2-10 ppbv (Logan, 1983). Surface concentrations of SO_2 at rural sites in the eastern U.S. are between 5 ppbv and 15 ppbv in winter, but below 5 ppbv during other seasons (Mueller and Hidy, 1983). Similar values are reported for southern Germany (Reiter and Kanter, 1982). Concentrations above the boundary layer are generally below 1 ppbv (Blumenthal et al., 1981; Georgii and Meixner, 1980). Sonde data from the boundary layer in polluted areas may therefore be contaminated by SO_2.

Comparison of the integrated ozone profile recorded by the BM sonde with concurrent measurement of the ozone column recorded by a Dobson spectrophotometer indicates that the sonde results are too low by 10%-30% (e.g. Dütsch, 1966). Results from ECC sondes agree more closely with Dobson measurements

(Kohmyr, 1969; Torres and Bandy, 1978). In practice, individual soundings are multiplied by a correction factor, to ensure that the integrated ozone column is equal to the Dobson measurement of the ozone column. This procedure requires an estimate of the amount of ozone above the altitude reached by the sonde, about 30 km (Dütsch *et al.*, 1970). There is no real justification for this scaling procedure, since it has not been demonstrated that the response of the sondes is linear with respect to ozone over the entire altitude range. The scaling procedure introduces errors due to uncertainty in the ozone amount above 30 km and errors associated with the Dobson technique.

Intercomparison flights have shown that the ECC sonde gives higher concentrations of tropospheric ozone than the BM sonde by 12-20%, after correction to the Dobson column. Systematic differences were not apparent in the stratosphere (Attmannspacher and Dütsch, 1970; 1981). Laboratory tests in a flight simulator suggest that the ECC sonde overestimates the concentration of tropospheric ozone by 10%-15% (Barnes *et al.*, 1985). No such test results have been published for the BM sonde. De Muer (1976) reported that descent data for the BM sonde tend to be about 25% higher than ascent data in the troposphere, implying that published data (based on ascent values) may underestimate tropospheric ozone. These last results appear inconsistent with the combined conclusions of Barnes *et al.* (1985) and Attmannspacher and Dütsch (1981). Uncertainties in the response of these sondes to ozone at concentrations characteristic of the troposphere should be resolved by careful laboratory and field studies.

Although the United States funded balloon ozonesonde networks from 1964 through 1966, these measurements have been discontinued. The only station flying sondes routinely in the United States as described above is Wallops Island, Virginia, on about a weekly basis. Other than this station, our information on the vertical ozone distribution in the lower stratosphere comes from approximately 10 stations in Canada, Japan, Europe, and Australia. Error estimates of the current operational balloonsonde systems are presented by Hudson and Reed (1979).

Recently, it has been indicated that a modified electrochemical balloonsonde would be capable of reliable ozone measurements up to about 40 km. This instrument is currently being deployed at three sites; Hilo, Hawaii; Boulder, Colorado and Edmonton, Canada with once-per-week launches scheduled.

During 1983-84, a balloon ozone intercomparison campaign was conducted under NASA sponsorship whose purpose was to assess the accuracy and precision of various ozone measurement systems under development as well as those flown operationally. The results have been reported by Hilsenrath *et al.* (1984) and the following are some initial results:

The difference among 5 *in situ* UV photometers flown together was about ±3% during ascent to about 41 km. During float at 42 km the difference nearly doubled. During descent, the difference decreased to about ±2% which is much closer to the expected accuracy of these instruments. A complement of electrochemical sondes flown with the UV photometers agreed with them in the range of 0-20% depending on the sonde and altitude. Some electrochemical sondes gave systematically lower ozone values at pressures lower than 10 mbar (31 km). One comparison between an *in situ* UV and a solar absorption photometer indicated 10% difference in the stratosphere where the *in situ* measurement was lower. Balloonsondes also showed systematically lower values than concurrent Umkehr and SBUV satellite observations in this altitude range. Intercomparisons among all the instruments in the troposphere showed 20-30% differences. A comparison of pressure measurements performed by several experimenters resulted in differences as high as ±15% from the average measurement.

411

8.1.1.6 Rocketsondes

For altitudes above 30 km, optical and chemiluminescence techniques have been adapted for the sounding rocket. These methods can operate at altitudes up to approximately 70 km. The earliest successful rocket data were acquired by Johnson *et al.* (1952) using a spectrograph launched at sunrise. This technique has been more recently employed by Krueger (1969), Nagata *et al.* (1971), and Weeks and Smith (1968), using UV filter radiometers. Carver *et al.* (1966) have used the moon for nighttime measurements. Hilsenrath *et al.* (1969) have used the chemiluminescent method for day and night soundings. By use of preflight multipoint calibrations and inflight flow-rate measurements, they find agreement within 10 percent of optical results. Randhawa (1967) has used a similar method on small rockets; however, his measured ozone concentrations above 35 km are generally two to five times greater than those of the other investigators.

In September 1979, International Rocket Ozonesonde Intercomparisons were held under FAA, NASA and WMO sponsorship at Wallops Island, Virginia. Results of this intercomparison should be available in the near future.

The United States is currently operating one rocket ozone station at Wallops Island, Virginia, using a modified Krueger optical technique (Holland, personal communication). This effort is, basically, in support of satellite observations and is limited to only a few observations per year.

8.1.1.7 Lidar

The recent development of powerful tunable lasers has opened a new experimental field for spectroscopic studies of atmospheric trace constituents. As part of it, the differential absorption laser technique (DIAL) has already been used for ground-based measurements of minor constituents in the boundary layer (Cahen *et al.*, 1981, Frederiksson *et al.*, 1979; Murray *et al.*, 1977).

Vertical concentration profiles of atmospheric ozone have also been recorded by using UV and IR lidar systems; however, these measurements have been restricted either to the boundary layer (e.g., Asai *et al.*, 1979; Bufton *et al.*, 1979: Browell *et al*, 1981) or to the stratosphere (Megie *et al.*, 1977; Uchino *et al.*, 1980). Pelon and Megie (1982a) describe the evaluation and realization of a ground-based UV lidar system for continuous monitoring of the ozone number density profile from the ground up to the 25-30 km range.

The emission performances of the laser system and the receiver characteristics have been summarized by Pelon and Megie (1982a). The full sequence of a DIAL measurement is computer controlled and a real time analysis of the data can be performed. The reliability of the various subsystems and experimental procedures have been tested during several field experiments in 1980-1981. The main characteristics of the measurements can be summarized as follows:

— Vertical profiles of the ozone number density are obtained for clear sky conditions from the ground up to 25 km. This altitude range has been recently extended up to 40 km (Pelon and Megie, 1982b).

Three ozone profiles corresponding to the altitude ranges 0-8 km, 7-17 km, 15-28 km are successively obtained within a 15 min acquisition time. This sequential experimental procedure results from the optimization criteria of the DIAL method.

The relative accuracy corresponding to a 1σ standard deviation on the ozone number density for each individual profile is:

(1) Better than 5% at tropospheric altitude levels for a vertical resolution of 450 m.

(2) Minimum in the 23-28 km altitude range where it decreases down to 20% at the uppermost level for a vertical resolution of 1.2 km and a 15 min. acquisition time.

8.1.2. Satellite Data Comparisons

As described above, a critical element of this chapter is a discussion of the comparison of SBUV versus other types of data to provide evidence of the absolute accuracy of the profile. Within the previous section we have discussed the comparisons with ground-based information; in this section we will focus on the satellite intercomparisons. Specifically, in April 1979 the SBUV, LIMS and SAGE instruments were all operative and as they utilize three entirely different measurement techniques their comparisons provide an excellent opportunity to assess our capability to measure ozone in an absolute sense.

Inasmuch as actual overpass coincidences of the satellite data are very few, our approach is to compare the zonal average for the month, recognizing that the SAGE coverage is inherently more limited than the others at a specific latitude. For these comparisons the SBUV Ozone Processing Team has recalculated the zonal averages utilizing the algorithm with the updated absorption coefficients (Bhartia and Fleig, personal communication) such that the latest estimates of each data set are provided.

The results for 45 °N (actually 44 °N for LIMS and SBUV) and the Equator are presented in Figure 8-3. At 45 °N we see that there is, overall, very good agreement in the shape of the 3 profiles with the largest disparity in the lower stratosphere between about 30 to 10 mbar. Standard deviations of the three data sets are included both in ppmv and percentage of the mean at 30-, 10-, 5-, 2-, 1 and 0.5 mbar. We see that in the middle stratosphere the agreement is excellent and the standard deviation is only about 3%. Above this level the standard deviation increases to about 7% and in the lower levels increases to about 15%.

At the Equator we see that SAGE and SBUV are in agreement at the lower levels with LIMS larger than either, but that SAGE then crosses over to indicate the largest maximum of the three data sets. Above the maximum SBUV and LIMS show very good agreement with SAGE considerably greater than the others. The relative maximum in the SAGE data at about 1.5 mbar results in an increase of the standard deviation at 2 mbar to about 10% versus its value of about 3% at 45 °N.

On the basis of the above, one can see that it is very difficult with such a limited sample to ascribe specific limits of uncertainty in the absolute value of the measured ozone. Therefore, for discussion purposes later in this section we suggest the following (1 standard deviation) limits as representing our capability to determine ozone in an absolute sense from satellite data:

- 15% 30 to 10 mbar

- 6% 10 to 0.5 mbar

Note that the above estimates are well within the RMS of the instrument systematic error summaries above of about 30% and 16%, respectively.
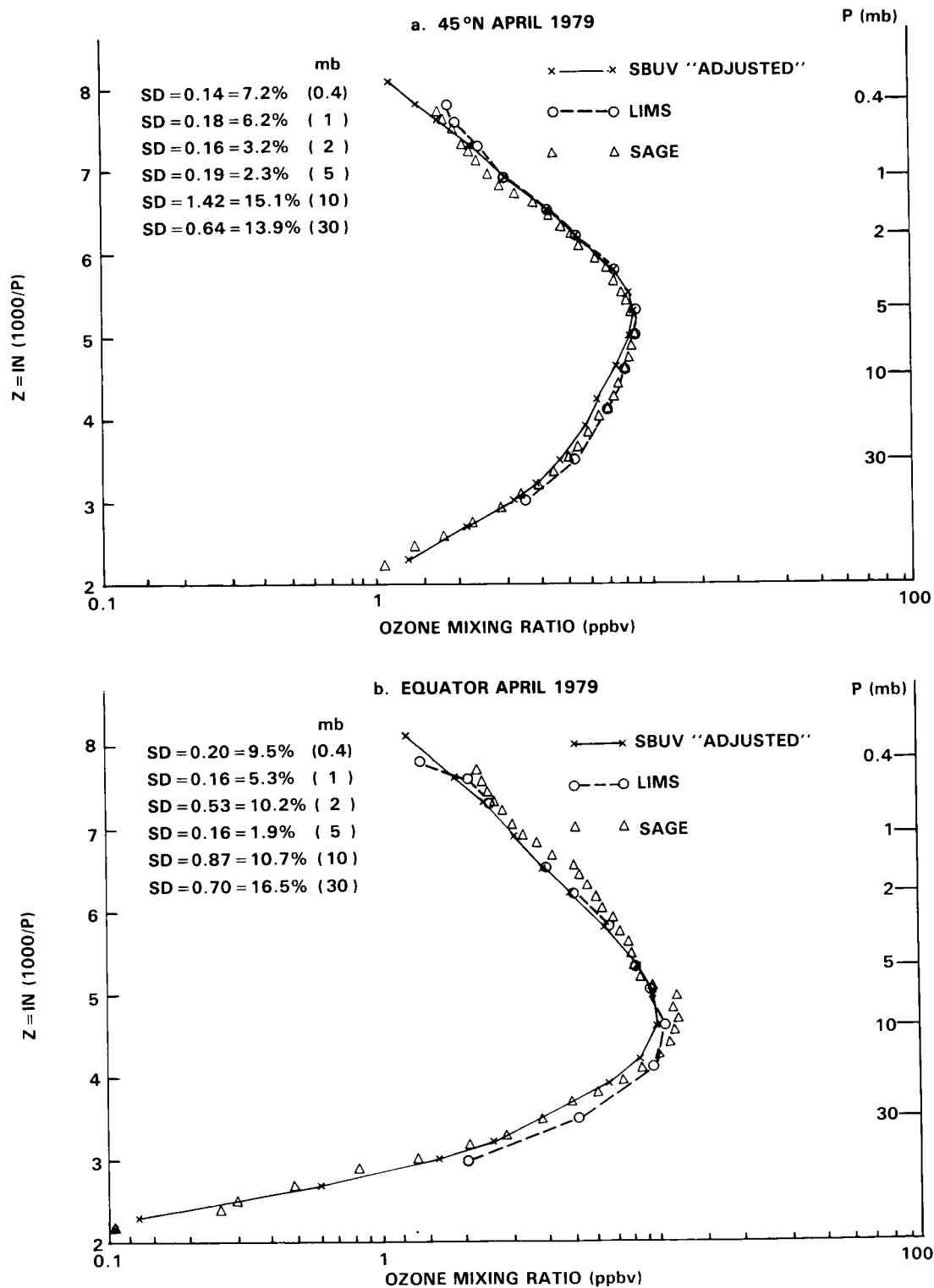
a. 45°N APRIL 1979

	mb	
SD = 0.14 = 7.2%	(0.4)	
SD = 0.18 = 6.2%	(1)	
SD = 0.16 = 3.2%	(2)	
SD = 0.19 = 2.3%	(5)	
SD = 1.42 = 15.1%	(10)	
SD = 0.64 = 13.9%	(30)	

x———x SBUV "ADJUSTED"
o———o LIMS
△ △ SAGE

Z = IN (1000/P)

OZONE MIXING RATIO (ppbv)

P (mb)

b. EQUATOR APRIL 1979

	mb	
SD = 0.20 = 9.5%	(0.4)	
SD = 0.16 = 5.3%	(1)	
SD = 0.53 = 10.2%	(2)	
SD = 0.16 = 1.9%	(5)	
SD = 0.87 = 10.7%	(10)	
SD = 0.70 = 16.5%	(30)	

x———x SBUV "ADJUSTED"
o———o LIMS
△ △ SAGE

Z = IN (1000/P)

OZONE MIXING RATIO (ppbv)

P (mb)

Figure 8-3. Monthly average ozone profile (ppmv) for April 1979 SBUV, LIMS and SAGE instruments at 45°N (a) and Equator (b).

414

8.1.3 Confidence Estimation of Mean Monthly Zonal Averages

When we compute a mean monthly zonal average ozone profile, there are several sources of error as well as natural variability that must be considered. Specified in terms of standard deviation, these are:

S_1 — the random measurement errors of the SBUV instrument;

S_2 — the random error of the daily true zonal average due to incomplete sampling (i.e., 14 points per day) extended to the domain of a monthly average;

S_3 — natural variability within a month, i.e., representativeness of the monthly average;

S_4 — natural year-to-year variability, representativeness of the multiyear average;

S_5 — absolute value of the measurement system.

The first two components have been extensively covered in the National Plan for Stratospheric Ozone Monitoring (FCM, 1982) and will be briefly summarized here.

For the SBUV instrument, the random error term, S_1, is estimated to be about 2.5% for total ozone and about 10% for the vertical distribution. When we determine the zonal average over a 5° latitude band, this encompasses about 28 data points. The contribution to the total uncertainty variance is:

$$a) \quad \frac{S_1^2}{28 \times 30} = \frac{(25)^2}{840} = 0.007\% \text{ total}$$

$$b) \quad \frac{S_1^2}{28 \times 30} = \frac{(10)^2}{840} = 0.12\% \text{ vertical profile}$$

When we determine the 5° daily zonal average from the 28 data points, however, an additional sampling error occurs due to incomplete sampling of the traveling wave patterns. This is about 1% for the SBUV (Wilcox, personal communication). We will assume this to be independent of pressure, although this is most likely very conservative for the profiles. Also, we will assume that the sampling errors are correlated in time such that there are only 10 independent observations per month. The contribution of this term to the uncertainty variance is:

$$\frac{S_2^2}{10} = \frac{(1)^2}{10} = 0.10\%$$

In the case of the S_3 component, which is the representativeness of the monthly average value or the error in utilizing the daily measured values to determine the monthly average, we have made the assumption that there are only 10 independent data points during the month. The results are indicated in Table 8-8 for the 4 months of depiction at low-, mid- and high-latitudes for 30- and 1- mbar. We see that the within month standard error is generally within 2%, but that it can be as large as 7% during certain periods such as high-latitude winter.

415

Table 8-8. SBUV Within Month Standard Error (%) 1978-1979.

	30 mbar	1 mbar
January		
70	7	7
40	4	3
0	2	2
−40	2	2
−80	2	1
April		
80	3	3
40	2	1
0	1	1
−40	2	2
−80	4	1
July		
80	1	2
40	1	2
0	2	1
−40	2	6
−70	1	4
October		
80	4	1
40	2	2
0	2	1
−40	2	3
−70	7	3

For the profile comparisons, then, we should utilize the following values of S_3^2

$S_3^2 = 4$ low-latitude and summer

$S_3^2 = 16$ mid- and high-latitude spring/fall

$S_3^2 = 49$ mid- and high-latitude winter

A subtle point is raised in this regard in that with the virtually complete sample of SBUV (at least in daytime) the variation within month does not represent an error or uncertainty in the monthly average. As the current models seek to emulate only the monthly average and not a daily value, inclusion of this term in the overall uncertainty is not warranted at this time. At such time when three-dimensional models are available this term should be included within the comparisons.

For the S_4 term that encompasses the natural variability we have little or no indication from theory as to what to expect save possibly that due to solar variations. We, however, consider that to be a "regular" feature that we should be able to detect and not part of the year-to-year variability. With no theoretical framework to guide us, we have utilized the 4 year SBUV record and calculated at 10° latitude increments the standard deviation between years for the 4 year average. The results at 60°N, equator and 60°S are presented in Figure 8-4 as a function of pressure and month. The standard error is the standard deviation divided by 2.

We see that the standard deviation calculated in this manner, which includes certain elements of S_3, is relatively small being generally on the order of 4% or less. The exception is the winter of each hemisphere where it becomes about 6% at 1 mbar of the Northern Hemisphere and 8% for the Southern Hemisphere. On this basis we will utilize values of S_4^2 (standard error) as follows:

$S_4^2 = 4$ low-latitude, summer and spring

$S_4^2 = 16$ mid-and high-latitude winter

Adding the measurement variances plus the year-to-year variance, while excluding the within month variance as described above, we see that the uncertainty of the monthly average is dominated by the year-to-year variation. For purposes of estimating the uncertainties of the SBUV profiles, then, we will utilize the following values:

$\sigma\,(\%) = 2\%$ Low-latitude, summer, spring, fall

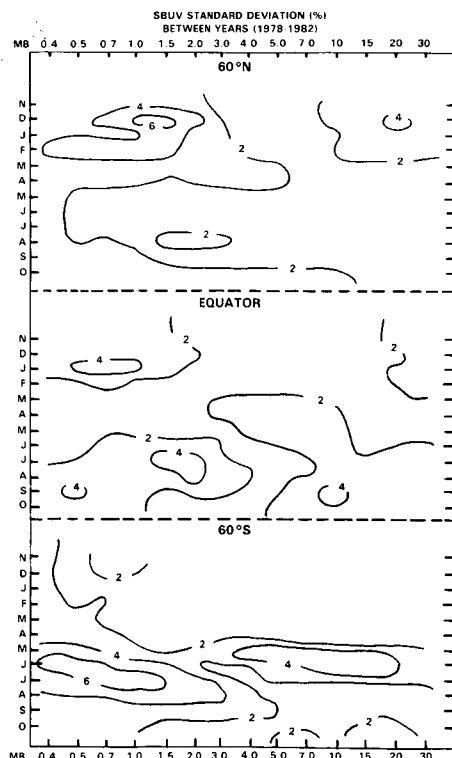$\sigma\,(\%) = 4\%$ Mid-and high latitudes winter

Figure 8-4. SBUV standard deviation (percent) between years (1978–1981) at 60°N (top), Equator (middle) and 60°S (bottom).

OXYGEN SPECIES

8.1.4 Average Vertical Profiles/Total Ozone

In the last section we combine the various elements described above to present our "best" estimate of the vertical ozone profiles/total ozone values along with the uncertainty estimates as determined from the previous elements. Presented in Figures 8-5 and 8-6 are the vertical ozone profiles (in units of volume mixing ratio ppmv) as a function of height with the following scales:

- The vertical scale is linear with scale height, defined as
  $Z = \ln(1000/P)$

- Included also are the decadal units of pressure in mbar along with the geometric altitude (km) as determined by multiplying Z by the approximate scale height of 7 km (Standard Atmosphere, 1966). Note that over an annual cycle the geometric altitude may change by several kilometers so that these values should be regarded as approximate only.

In order to provide information over the annual cycle and latitude domain we have selected for presentation the following data:

- Months: January, July

- Latitude: Equator, 30°N, 30°S, 45°N, 45°S, 60°N, 60°S

For each data source the curves are based on:

- Balloonsondes — The data are averaged for the period 1979-1983 in Umkehr layers within the latitude bands, 52.5-90°N(60°N), 37.5-52.5°N(45°N), 15°S-15°N(Equator), 37.5-52.5°S(45°S) and 52.5-90°S(60°S) (Hilsenrath, private communication).

- SBUV — The data are averaged for the period Nov. 1978 — Oct. 1981 at the specific latitudes as interpolated from the monthly average synoptic charts. This includes the total ozone value.

- Adjusted SBUV — These are the SBUV profiles multiplied by an average adjustment factor provided by the SBUV Ozone Processing Team (private communication) mainly to account for the recently adopted ozone absorption coefficients. Such adjustments are presented to indicate the sign and magnitude of their effect as is anticipated for the final processed data.

- SME (UV and IR) — The data are averaged for the period 1982-1984. Note that as described above the longitudinal coverage is not complete.

As a simple consistency check we have calculated the total ozone from the SBUV profiles from 0.4 to 30 mbar and the balloonsondes from 30 to 1000 mbar and compared the results against the SBUV total ozone measurements. The results are presented in Table 8-9. From above we would anticipate that the SBUV total ozone should be on the order of 8% lower than the combined SBUV-balloonsonde calculations. This is because the balloonsondes are normalized to the Dobson measurements and the SBUV is about 8% lower than the Dobsons. If the combined total ozone is very different from the 8% value then this raises the question of representativeness of the balloon profile possibly due to the number of stations in the region and/or to the number of points at the stations.

Table 8-9. Comparison of Total Ozone Calculated from Ozone Profile Versus Total Ozone Determined from SBUV.

60°N	Jan.	April	July	Oct.
SBUV (.4-30 mb)	117.1	133.9	129.5	121.5
Balloonsondes (30-1000 mb)	283.9	329.4	236.0	212.4
Total	401.0	463.3	365.5	333.9
SBUV	362.0	399.7	319.3	291.8
SBUV — Total (%)	−9.7%	−14.2%	−12.6%	−12.6%

45°N	Jan.	April	July	Oct.
SBUV (.4-30 mb)	134.0	148.5	150.3	140.3
Balloonsondes (30-1000 mb)	220.6	258.9	193.5	165.2
Total	354.6	407.4	343.8	305.5
SBUV	340.7	360.4	307.1	277.5
SBUV — Total (%)	−3.9%	−11.5%	−10.7%	−9.2%

30°N	Jan.	April	July	Oct.
SBUV (.4-30 mb)	145.2	161.9	165.1	158.8
Balloonsondes (30-1000 mb)	182.4	211.2	—	117.8
Total	327.6	373.1	—	276.6
SBUV	269.9	300.5	279.7	258.2
SBUV — Total (%)	−17.6%	−19.5%	—	−6.7%

Equator	Jan.	April	July	Oct.
SBUV (.4-30 mb)	174.3	176.3	176.1	178.1
Balloonsondes (30-1000 mb)	82.6	84.3	97.0	129.0
Total	256.9	260.6	273.1	307.1
SBUV	230.9	239.3	245.7	245.2
SBUV — Total (%)	−10.1%	−8.2%	−10.0%	−20.2%

45°S	Jan.	April	July	Oct.
SBUV (.4-30 mb)	150.2	139.1	129.4	148.0
Balloonsondes (30-1000 mb)	124.6	152.2	206.6	190.7
Total	274.8	291.3	336.0	338.7
SBUV	292.6	273.5	308.9	338.0
SBUV — Total (%)	+6.5%	−6.1%	−8.1%	−0.2%

OXYGEN SPECIES

From Table 8-9 we see that the latitudes with the best consistency are 45 °N, where the largest number of stations exist, and the equator, where the fewer observations seem to have lesser impact. The significant exception to this is in October at the Equator where the balloonsondes indicate very large values that do not appear reasonable. At the other latitudes the results appear to be more sensitive to the available data and the comparisons in the region should be made with appropriate care.

For the upper level profiles, looking first at January — Equator, Figure 8-5 (d) we see overall excellent agreement of the SME-IR data with the SBUV data in the overlap region. The SME-UV data indicate a positive bias against the others although the two SME curves tend to merge at about 1 mbar. SBUV adjusted values tend to be lower than unadjusted values with the major impact in the lower layers.

As we move away from the Equator into the Northern Hemisphere we see increasing disparity of SME, both with SBUV and with itself. The former is undoubtedly due in part to the limited sampling in the winter hemisphere while the latter must be due to the instrument/algorithm differences. In the Southern, summer Hemisphere the overall agreement is much better, but SME maintains a positive bias. Note also that toward higher latitudes the sense of the SBUV adjustment changes at the lower levels with the adjusted SBUV larger than unadjusted.

For the Southern Hemisphere winter, July, Figure 8-6, we see that a similar pattern emerges with the SME greater than SBUV with the tendency of the two to merge at about the 1 mbar level. The summer SME values are quite consistent as was the case for Southern Hemisphere January profiles, but we note that the winter values seem more consistent than their Northern Hemisphere counterparts.

Finally, in the previous sections we have attempted to resolve the question as to the uncertainties in the average profiles and have divided the uncertainities into absolute and random components. In this section we combine the two components to achieve what we feel is our best estimate of the overall uncertainties and in Figures 8-5 and 8-6 we plot the two standard deviation uncertainty bars at 1 and 10 mbar. The values are based on the following combined elements:

- Low latitude/summer/spring/fall

  | 30-10 mbar | $1\sigma = 15.1\%$ | $2\sigma = 30.2\%$ |

  | 10-0.4 mbar | $1\sigma = 6.3\%$ | $2\sigma = 12.6\%$ |

- Mid- and high-latitude winter

  | 30-10 mbar | $1\sigma = 15.5\%$ | $2\sigma = 31.0\%$ |

  | 10-0.4 mbar | $1\sigma = 7.2\%$ | $2\sigma = 14.4\%$ |

8.2 COMPARISON OF CALCULATED AND OBSERVED OZONE PROFILES

Total ozone has been observed for many years at various stations located in different parts of the world. A climatology of these data has been presented for example by London (1980b), indicating that the average ozone column reaches a maximum between 70 and 75 °N at the end of March and that the maximum observed in the Southern hemisphere is smaller and located at somewhat lower latitudes and earlier in the season, than that of the Northern Hemisphere. Two-dimensional time-dependent models with a classical Eulerian or a diabatic circulation can produce satisfactory fits to the above observations. Moreover, as shown by Figure 8-7a and b, the meridional distribution of ozone provided by 2-D models below 35 km
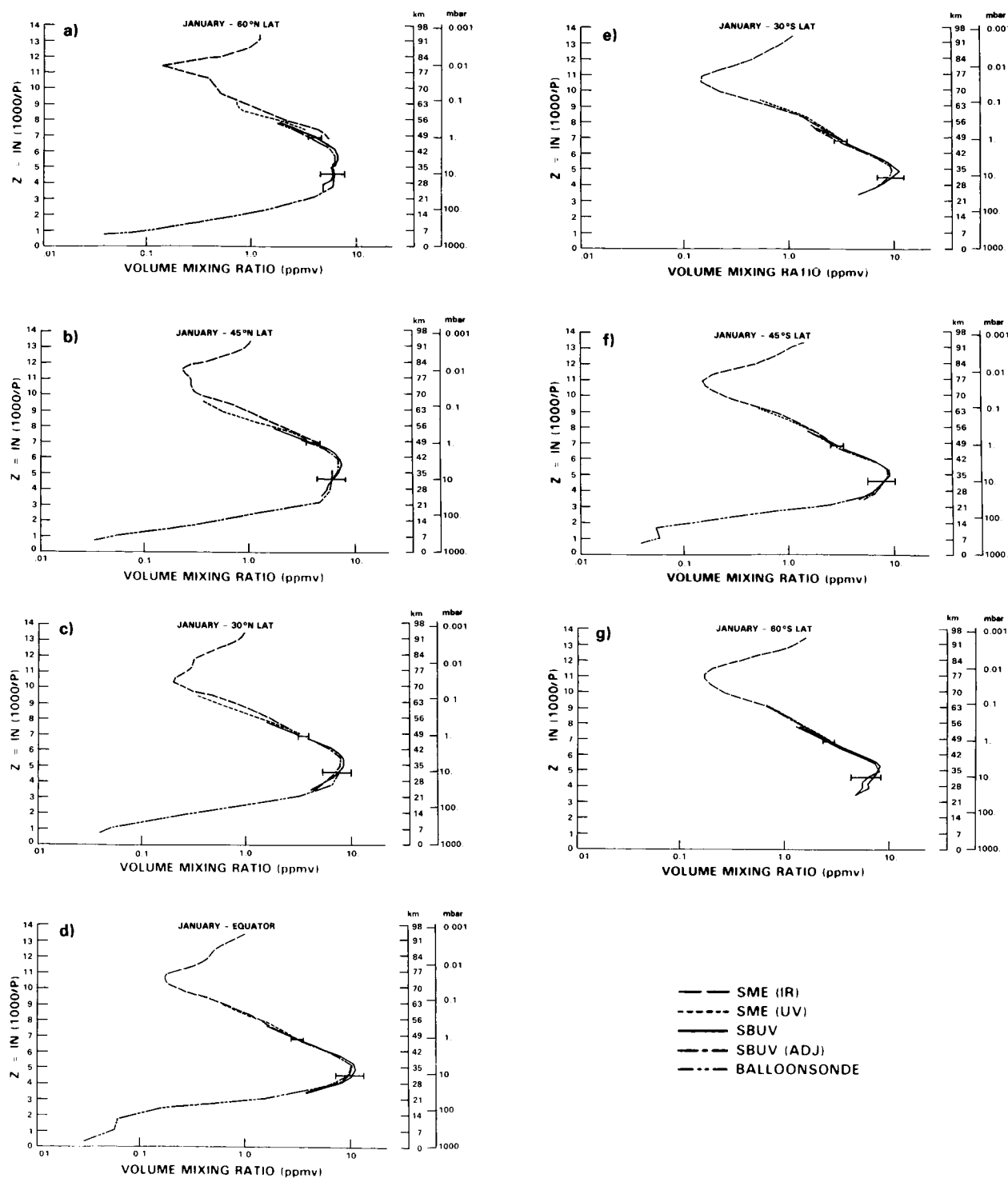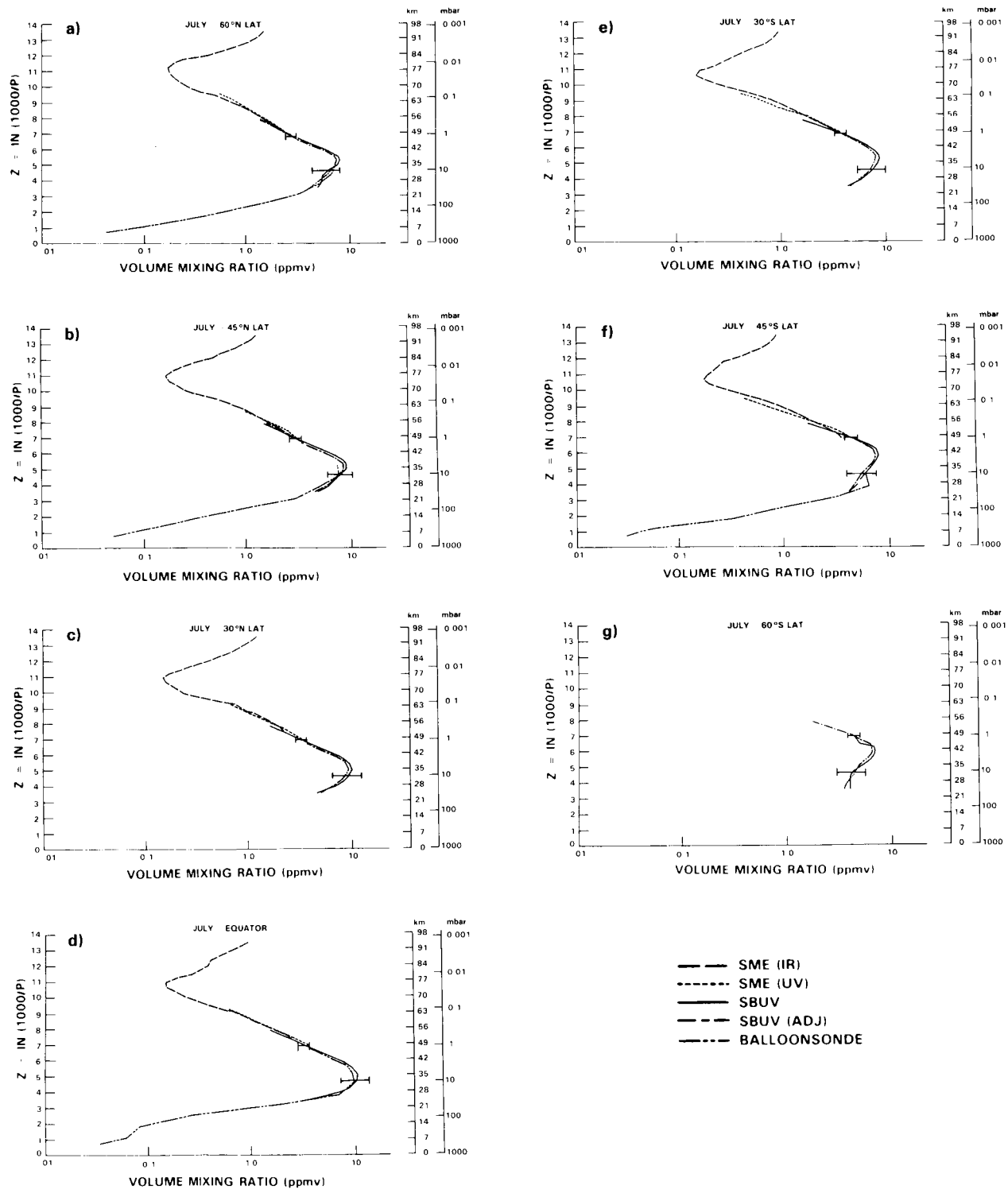
OXYGEN SPECIES

Figure 8-5. Average ozone vertical profiles (ppmv) for January at 60°N (a), 45°N (b), 30°N (c), Equator (d), 30°S (e), 45°S (f) and 60°S (g) for SME (UV and IR), SBUV (adjusted for Bass and Paur coefficients and unadjusted) and balloonsondes. Also plotted are 95% uncertainty bars (see text) on SBUV data at 1- and 10-mbar.
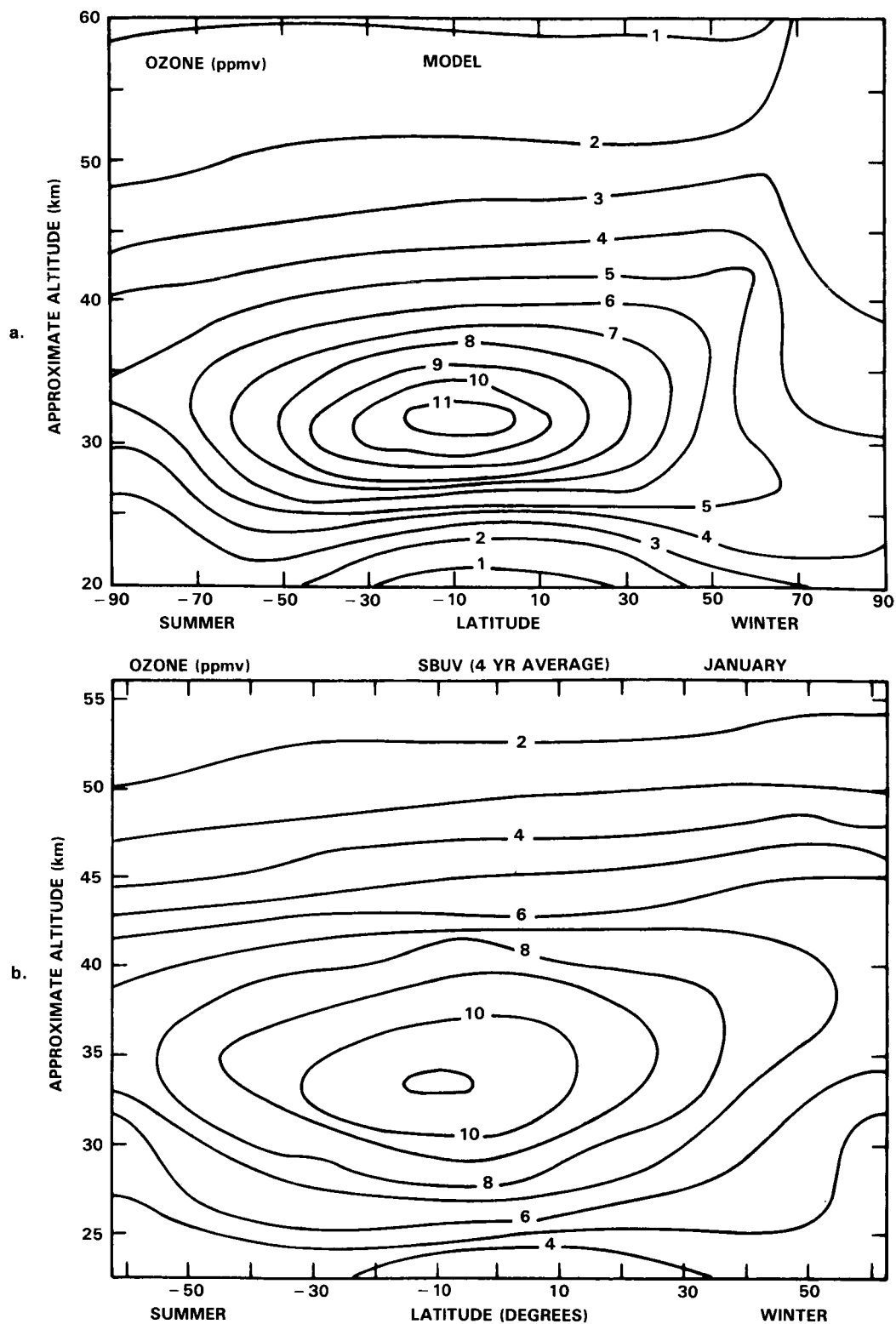
Figure 8-6. Average ozone vertical profiles (ppmv) for July at 60°N (a), 45°N (b), 30°N (c), Equator (d), 30°S (e), 45°S (f) and 60°S (g) for SME (UV and IR), SBUV (adjusted for Bass and Paur coefficients and unadjusted) and baloonsondes. Also plotted are 95% uncertainty bars (see text) on SBUV data at 1- and 10-mbar.

Figure 8-7. Two dimensional distribution of the ozone mixing ratio (ppmv).
(a) : Model calculation by Solomon et al. (1985b).
(b) : Four year average of SBUV data.

423

are in good agreement with the climatology of O_3 resulting from satellite observations. These results, however, depend more on the transport parameterization than on the chemical scheme adopted in the model. A validation of the chemistry should preferably deal with comparisons of ozone distributions in the upper stratosphere and in the mesosphere.

In addition to numerous rocket and balloon observations, space borne experiments (SBUV, LIMS, SAGE, SME and ATMOS) have provided a large data base of ozone concentrations in the region where photochemical equilibrium conditions should apply to O_3. The standard deviation arising from comparisons between a subset of these observations (see previous sections) using completely different techniques, is about 6 percent above 6 mbar whereas there are significantly larger systematic uncertainties in each experiment, so that the reported vertical profiles can essentially be considered to represent absolute values.

Several model calculations in the stratosphere (Ko and Sze, 1983; Froidevaux et al., 1985a; as well as those reported in Chapter 12) and in the mesosphere (Prather, 1981; Solomon et al., 1983; Allen et al., 1984; Aikin et al., 1984; Rusch and Eckman, 1985) have been used for an interpretation of ozone data. The more recent studies generally include a reduced O_2 absorption cross section in the Herzberg continuum, as suggested by the stratospheric solar flux measurements of Frederick and Mentall (1982), Hermann and Mentall (1982), Anderson and Hall (1983), as well as the laboratory work of Cheung et al. (1984) and Johnston et al. (1984). Note however that the cross sections derived by Pirre et al. (1985) from flux measuremenis in the stratosphere are higher than the data deduced from the other recent experiments. As indicated by Froidevaux and Yung (1982), Brasseur et al. (1983b), Ko and Sze (1983) and Jackman and Guthrie (1985), the use of these lower O_2 cross sections (see Chapter 7) has reduced the calculated concentrations of several gases, in particular ozone, in the middle and upper stratosphere.

Figure 8-8 shows the range of ozone mixing ratios calculated at 30 °N for winter and summer conditions by the two-dimensional models under consideration in this report. The profile from the Rutherford Appleton Laboratory, however, has not been included in the figure since this model uses a very low chlorine abundance. The model range is typically $\pm 20\%$ about the average profile, which probably reflects the combined effects of slightly different dynamical and photochemical representations, in addition to the seasonal effects. These theoretical profiles are compared with a representative distribution of the ozone mixing ratio for January and July, respectively, based on SME (UV and IR), SBUV and balloon ozonesondes (see Figure 8-5). Also shown at selected levels for historical comparison are the ozone values (and their standard deviation) of the U.S. Standard Atmosphere, 1976. Other measurements at northern mid-latitudes, such as the OGO 4 BUV satellite data (London et al., 1977), the SAGE data (Reiter and McCormick, 1982) and the LIMS data (Remsberg et al., 1984a), generally fall within the bounds of this Standard Atmosphere.

In the upper stratosphere, the 2-D model results appearing in Figure 8-8, as well as recent 1-D model calculations (e.g. Ko and Sze, 1983; Froidevaux, 1983; Froidevaux et al., 1985a; Brasseur et al., 1985) predict concentrations which are 30 to 50 percent lower than the values representative of mid-latitude observations. Similar discrepancies in the mesosphere have been found from SME data (Solomon et al., 1983a; Rusch and Eckman, 1985). Since the temperature in the middle atmosphere is directly controlled by the ozone amount, the absolute temperature value derived by radiative models should be somewhat underestimated, especially near the stratopause, if the low O_3 concentration currently predicted by photochemical models is used.
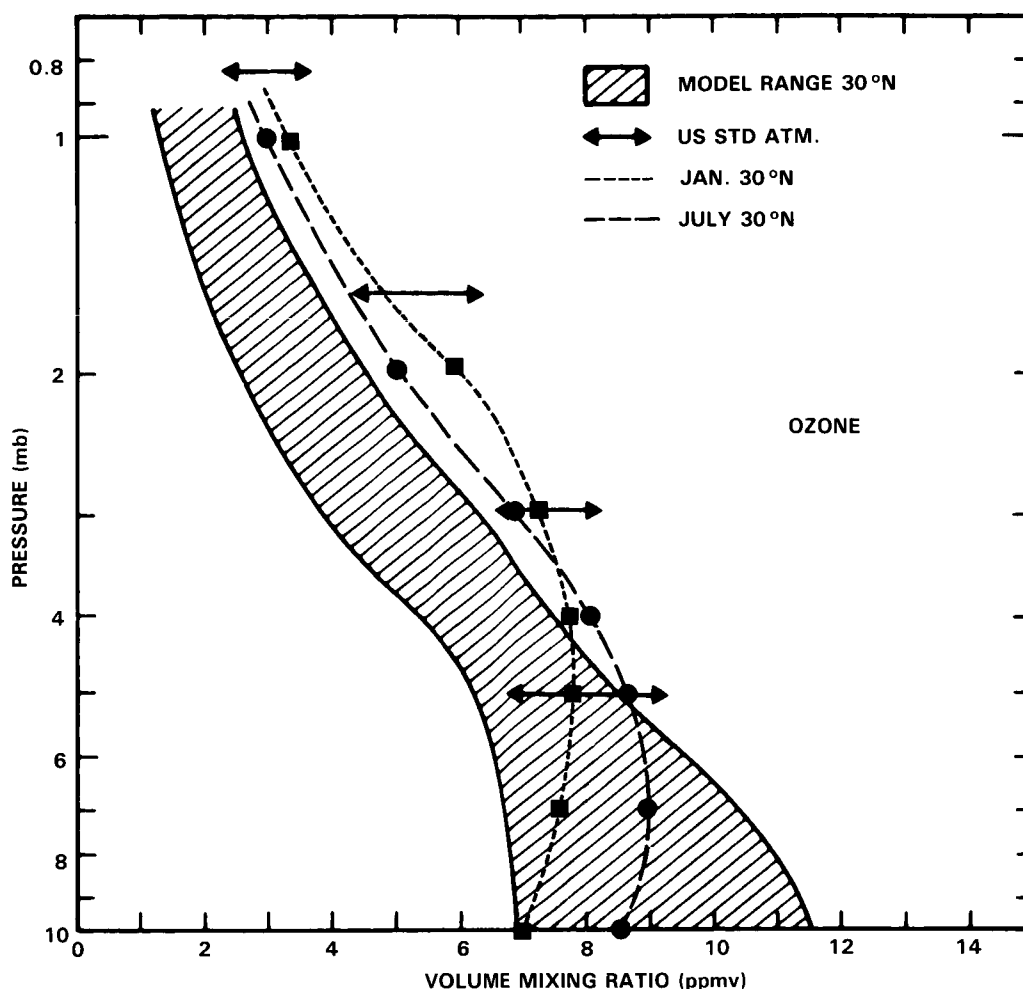
Figure 8-8. Vertical distribution of the ozone mixing ratio in the upper stratosphere. The shaded area includes 2-D model results obtained for winter and summer conditions at 30°N (see Chapter 12). The O_3 mixing ratio given by the US Standard Atmosphere as well as representative observations at 30°N for January and July are also indicated. (See Figures 8-5 and 8-6.)

In order to attempt to understand the source of these discrepancies, the uncertainties in the production and loss processes due to all catalyzing mechanisms and involving O_x, HO_x, NO_x, and ClO_x should first be investigated. In the altitude range where photochemical equilibrium conditions are satisfied, the ozone balance can be written

$$P(O_x) = L_{O_x} + L_{HO_x} + L_{NO_x} + L_{ClO_x} = L(O_x) \tag{4}$$

or, to a good approximation, (Johnston and Podolske, 1978; Froidevaux et al., 1985a)

$$J_{O_2} (O_2) = k_1 (O) (O_3) + k_2 (O) (HO_2)$$

$$+ k_3 (O_3) (HO_2) + k_4 (O_3) (H) + k_5 (O) (NO_2)$$

$$+ k_6 (O) (ClO) \tag{5}$$

425

where the ith k value represents the rate constant for the reactions between the species in the ith term on the right-hand side of the above equation.

These source and sink terms in the stratosphere have been evaluated by Schmailzl and Crutzen (1985), using N_2O and CH_4 distributions from SAMS (Jones and Pyle, 1984), ozone from LIMS (Gille and Russell, 1984) or SBUV (Frederick et al., 1983b), water vapor and temperature from LIMS. The distributions of other species, including ClO_x, were calculated with a 2-D model. A significant imbalance in the odd oxygen budget is found with an overproduction in the lower stratosphere and an extra loss above 30 km.

Schmailzl and Crutzen (1985) indicate that, in order to balance the ozone budget, one requires either a smaller NO production rate compared to the one derived from the SAMS N_2O data or modifications in the chemical scheme which is used for stratospheric studies.

Jackman et al. (1985a,b) have done a similar study using the LIMS data for O_3, H_2O, HNO_3, NO_2 and temperature in a zonally averaged form. Adopting a ClO_x mixing ratio of 3 ppbv at the stratopause and fixing CH_4 according to the SAMS data, they have calculated the $L(O_x)/ P(O_x)$ ratio for different months during which LIMS was operating. An example is given by Figure 8-9. Again, the ozone budget is unbalanced, as values of $L(O_x)/P(O_x)$ of 1.3 to 1.5 are found in the photochemical region. These results are in good agreement with those of Schmailzl and Crutzen (1985). While the imbalance is quite large, Jackman et al. (1986) point out that the total model uncertainty associated with the value of $L(O_x)/P(O_x)$ is close to 1.7, so that the imbalance may still be due to inaccuracies in the included chemistry and species concentrations.

Frederick et al. (1984) also find that the expected ozone abundances are 20-27% below the SBUV data for pressures less than 7.8 mbar, and that the observed seasonal behavior (phase) is also in some disagreement with calculations. Analyses of LIMS data also show the existence of a model ozone deficit in the upper stratosphere and lower mesosphere (Froidevaux et al., 1985b).

While it is true that the error bars associated with both model and observational ozone results overlap, it is not very satisfying to interpret this as an indication that there is really no problem in modelling ozone in the upper stratosphere and lower mesosphere. Froidevaux et al. (1985a) have performed a sensitivity analysis (with a 1-D model) which shows that no reasonable change in any one or two parameters can resolve the systematic model ozone deficit. They argue that the (O) to (O_3) ratio is an important quantity, since the atomic oxygen concentration enters in most of the odd oxygen loss terms (Equation (5). In view of the fact that there exists only one simultaneous measurement of O and O_3 (Anderson, 1980), and that this particular determination seems to have been affected by systematic errors in the O_3 observation (see Froidevaux et al., 1985a), new in situ determinations of the (O) to (O_3) ratio are needed in order to test the "pure O_x" chemical system in isolation.

Indeed, according to the current ozone theory, the O to O_3 concentration ratio is given by the simple expression

$$\frac{[O]}{[O_3]} = \frac{J_{O_3}}{k(T)\ [M]\ [O_2]} = \frac{J_{O_3}}{0.21\ k(T)\ [M]^2} \tag{6}$$

where J_{O_3} is the photodissociation frequency of ozone, [M] is the total concentration and k(T) the temperature dependent rate constant of reaction $O + O_2 + M$. The pure odd oxygen chemistry can thus
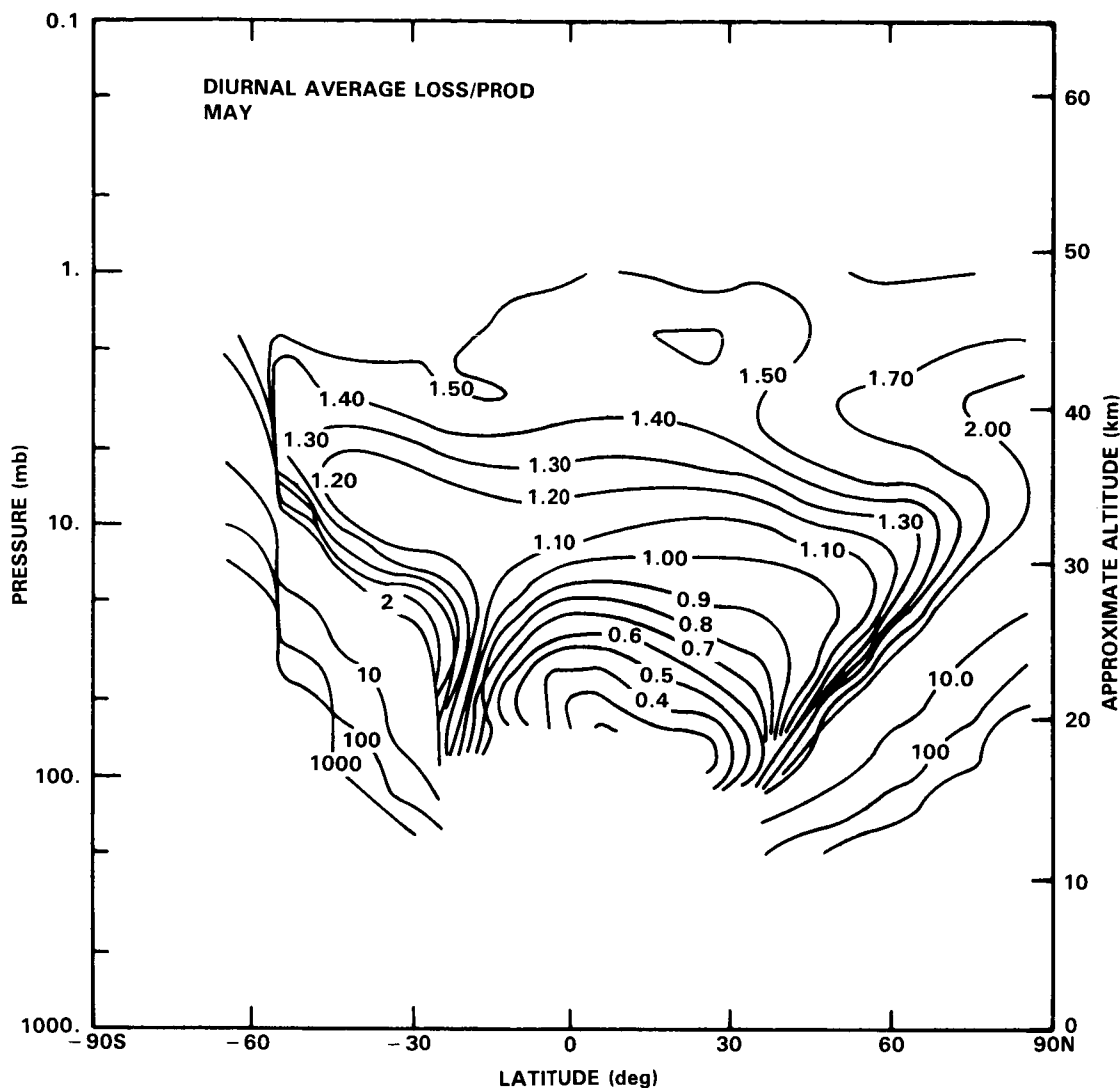
Figure 8-9. Calculated ratio of the odd oxygen loss rate to the production rate making use of temperature and trace species concentration reported by LIMS and SAMS in May 1979 (from Jackman *et al.,* 1986).

easily be tested by measuring simultaneously, at a given pressure level, the O and O_3 concentrations together with the temperature and the O_3 column density above this level. The photodissociation coefficient of O_3 can be estimated without significant error for a given solar zenith angle, assuming that the spectral distribution of the solar irradiance and of the O_3 (and O_2) absorption cross section are accurately known.

This conceptually simple chemical test has never been made so far, despite the fact that the destruction rate of odd oxygen or concentration ratios such as [NO]/[NO_2] or [Cl]/[ClO] in the upper stratosphere are usually derived by assuming that expression (6) is verified.

Finally it should be stated, as mentioned by Pallister and Tuck (1983) that a detailed observation of the 24 hour waveform of the ozone concentration in the upper stratosphere also provides a means of testing current photochemical mechanisms. For this purpose, measurements require good relative rather than good absolute accuracy. Such useful measurements have begun to be exploited by Aimedieu *et al.* (1981).

OXYGEN SPECIES

Given the ozone imbalance in the upper stratosphere and mesosphere, and the fact that dynamical effects on the mean ozone value are generally expected to be small throughout most of that region (note that 2-D and 1-D models both yield similarly low O_3 values), one is left with three main options in order to reduce or eliminate this imbalance:

1) In the currently accepted photochemical scheme, find a way to decrease the odd oxygen loss rate (whereby increasing the ozone abundance).

2) In the currently accepted photochemical scheme, find a way to increase the odd oxygen production rate.

3) Change the currently accepted photochemical scheme, so as to eliminate the ozone discrepancy.

In all the above cases, the resulting changes in species concentrations other than $[O_3]$ should not be so large as to produce significant problems of another kind. Currently, it does not appear that the mean observed concentration of HO_x, NO_x and ClO_x are systematically and significantly overestimated by the models, although there is still enough uncertainty in the observed distribution of these species not to preclude changes in their model concentrations that could reduce the ozone imbalance.

In the mesosphere, where the odd hydrogen photochemistry dominates, HO_x related sensitivity analyses need to be performed in order to try to understand differences between models and observations (see Allen *et al.*, 1984). The model ozone deficit in comparison with SME data (see Figure 8-10) could indeed be explained by errors in the hydrogen chemistry. The mesospheric water vapor abundance and
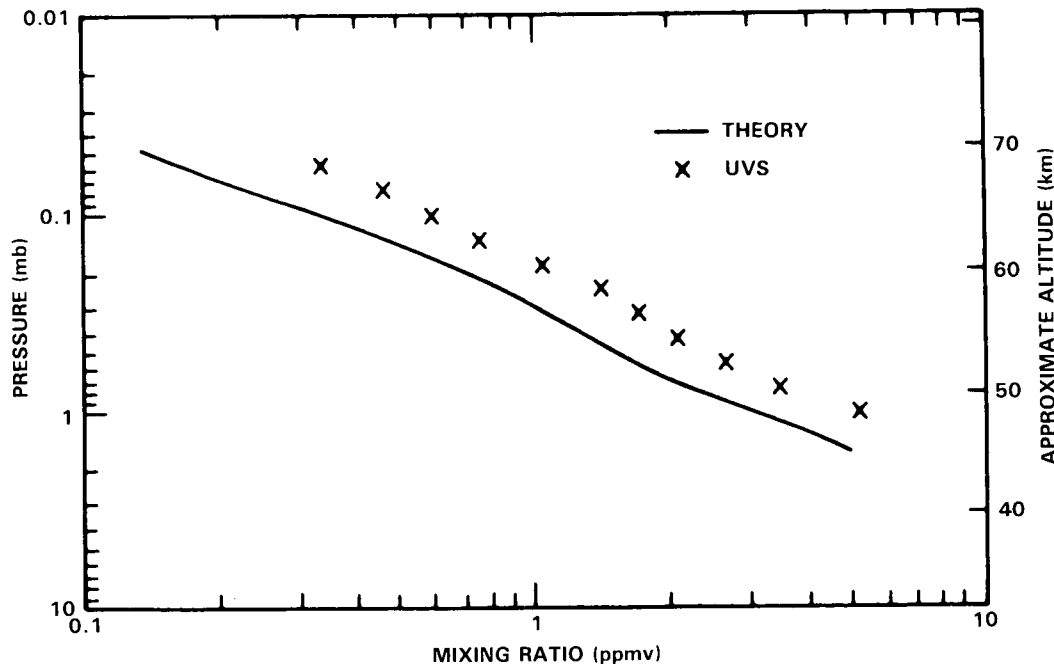

Figure 8-10. Comparison of measured weekly averaged ozone mixing ratio (crosses) to model calculations (solid line) for day 360 of 1983 (latitude 40°, solar zenith angle 76.4°). Data are from the Solar Mesosphere Explorer (from Rusch and Eckman, 1985).

some HO_x-related photochemical parameters are not very well known, nor are the rates of O_2 and H_2O photolysis in the Schumann-Runge bands (Solomon et al., 1983a; Rusch and Eckman, 1985). The latter authors find that good agreement with the measurements can be obtained if the efficiency of the odd hydrogen catalytic cycle is decreased by 30-50%. One notes that even if such a change is not unreasonable (and within the total uncertainty associated with model parameters and concentrations), this type of reduction in the HO_x catalytic efficiency will have very little impact on ozone in the 35-45 km region, where a significant discrepancy also exists.

In terms of the odd oxygen production rate, there are clearly some remaining uncertainties in the photodissociation rate of O_2 in the Schumann-Runge bands and Herzberg continuum, despite recent analyses of the cross section values in those wavelength regions. A large increase in J_{O_2} (by about a factor of two) would be required in order to eliminate the ozone discrepancy above 35 km. It does not appear that such a change is within the range of uncertainty in J_{O_2} given current laboratory work. In fact, recent reductions in the measured Herzberg continuum cross sections have led to a decrease in J_{O_2} and (O_3) in the upper stratosphere. In the Schumann-Runge bands, a decrease in the underlying continuum absorption could lead to some increase in the upper stratospheric flux at those wavelengths, although the effect on JO is diluted by the Herzberg region. Nevertheless, further high-resolution laboratory studies in the Schumann-Runge bands could be worthwhile.

Possibly important additional sources of odd oxygen have been considered (this case now refers to option 3, i.e. missing chemistry). For example, Cicerone and McCrumb (1980) have indicated that the photodissociation of heavy molecular oxygen ($^{18}O\ ^{16}O$) might provide a source of odd oxygen in the atmosphere. A recent line by line calculation of the related photodissociation coefficient by Blake et al. (1984) shows however that this process can only contribute a maximum of 3 percent of the O_2 photodissociation. More recently, Frederick and Cicerone (1985) have indicated that, if the dissociation cross section of the excited $O_2(a^1\Delta g)$ molecule has a maximum value of order 10^{-19} cm^2, the process O_2 $(a^1\Delta g)$ +hν $\rightarrow$ O_2 $(c^3\Sigma_u)$ $\rightarrow$ $O(^3P)$ + $O(^3P)$ has the potential to provide a substantial source of odd oxygen (comparable to the J_{O_2}source) in the upper stratosphere and mesosphere. This potential source appears to be ruled out, however, by recent laboratory measurements of absorption by O_2 ($^1\Delta g$) (Simonaitis and Leu, 1985); these data yield an upper limit for the cross section of 8×10^{-22} cm^2.

8.3 OZONE AND TEMPERATURE CORRELATIONS

In this section, developments concerning the two observational and theoretical relations between the ozone and temperature fields are reviewed. The analysis of such relations can broaden our view of the photochemistry and dynamics of the stratosphere and could prove useful in an attempt to understand the model ozone deficit (above 35 km) discussed in the previous section.

The dependence of chemical reaction rate constants upon temperature is the primary cause of the ozone sensitivity to temperature. When dynamics and chemistry are both important, one expects differing relationships between ozone and temperature perturbations as a function of height, whether these perturbations are spatial (e.g. longitudinal wave-like phenomena about zonal mean quantities) or temporal. The mechanistic model of Hartmann and Garcia (1979) showed that the eddy fields of velocity, temperature, and ozone mixing ratio associated with planetary wave disturbances exhibit characteristic phase relationships. In the lower stratosphere, where ozone can be regarded as an inert tracer, temperature and ozone perturbations are expected to be very nearly in phase, whereas a 180° phase shift is found in the upper stratosphere, where photochemistry should dominate over dynamics. A transition region exists in the middle stratosphere, where significant ozone transport can still be produced (see also Kawahira, 1982).

OXYGEN SPECIES

Such general relationships between local temperature and ozone fields have been deduced from various upper stratospheric satellite data for some time (Barnett *et al.*, 1975; Ghazi *et al.*, 1976; Ghazi and Barnett, 1980b; Krueger *et al.*, 1980; Gille *et al.*, 1980b; Wang *et al.*, 1983; Barth *et al.*, 1983; Miller *et al.*, 1984). Chandra (1985) has recently discussed the existence of an interesting global oscillation in ozone and temperature at 2 mbar (with period of 3-5 weeks) based on 2 years (1970-1982) of data from the Selective Chopper Radiometer (SCR) and Backscattered Ultraviolet (BUV) experiments on Nimbus 4. The Limb Infrared Monitor of the Stratosphere (LIMS) experiment also obtained strong evidence for the spatial and temporal anti-correlation between simultaneously measured ozone and temperature fields (Keating *et al.*, 1985; Froidevaux *et al.*, 1985b). Figures 8-11(a) through 8-11(c) were selected from the references mentioned above in order to display a variety of upper stratospheric situations where the out-of-phase relation between ozone and temperature has been observed. As shown in some of the above references, an in-phase relation at lower altitudes has also been observed.
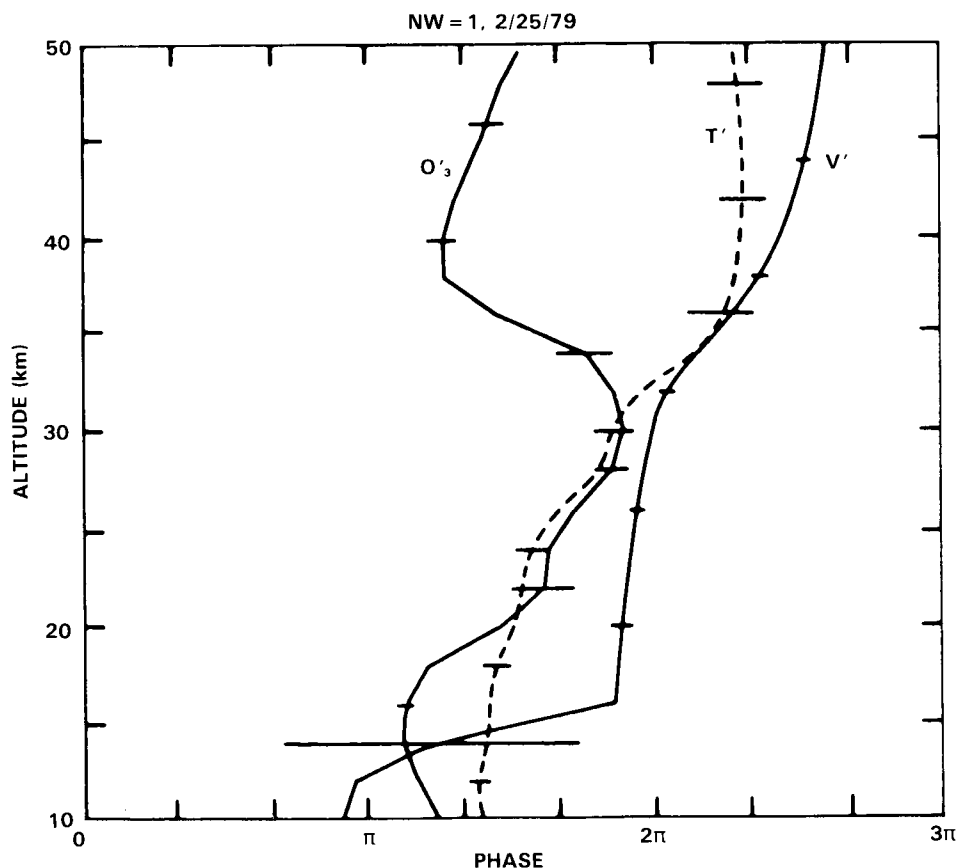

Figure 8-11.a Phase relationship between ozone (solid line), temperature (dashed line) and eddy meriodional velocity (solid and dashed line) waves (wave-number 1) during the late February 1979 warming. This figure is taken from an analysis of SAGE ozone data and meteorological information by Wang *et al.* (1983). The difference between an out-of-phase relationship between ozone and temperature in the upper stratosphere and in-phase relationship in the lower stratosphere is clearly seen.
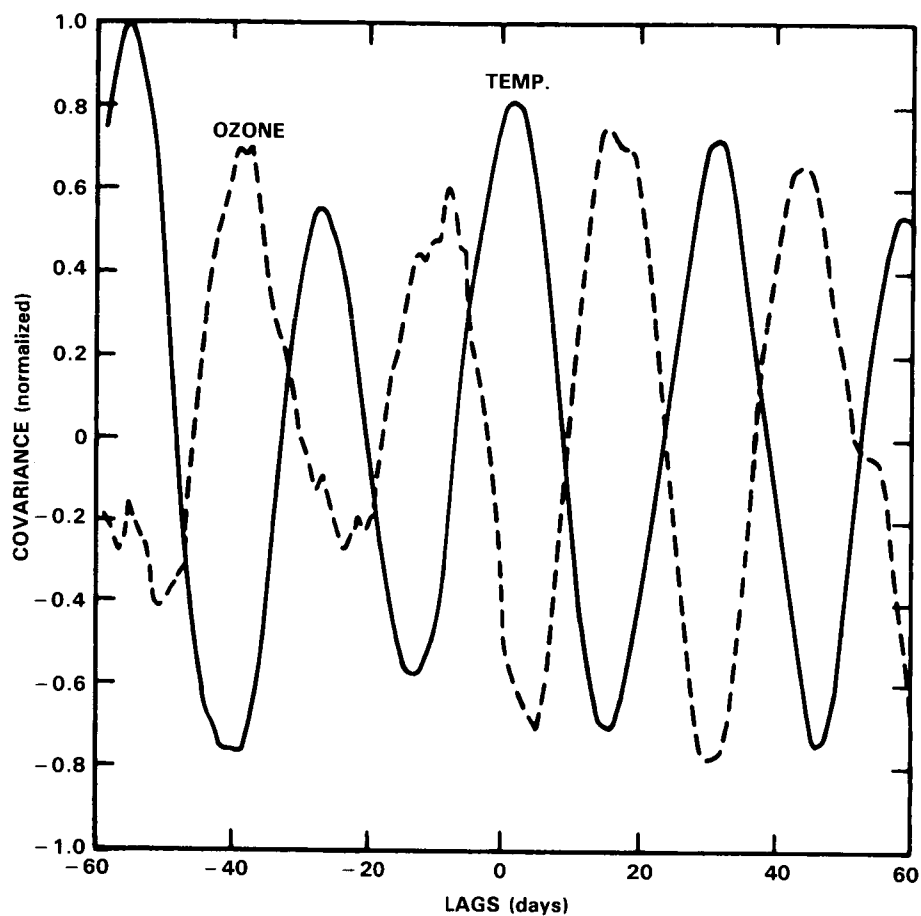
Figure 8-11.b Covariance of $F_{10.7}$ solar index and temperature and $F_{10.7}$ and ozone mixing ratio of 2 mbar in the tropics. This analysis (Chandra, 1985, see text for data sources) displays the anticorrelation between ozone and temperature fields as a function of time.
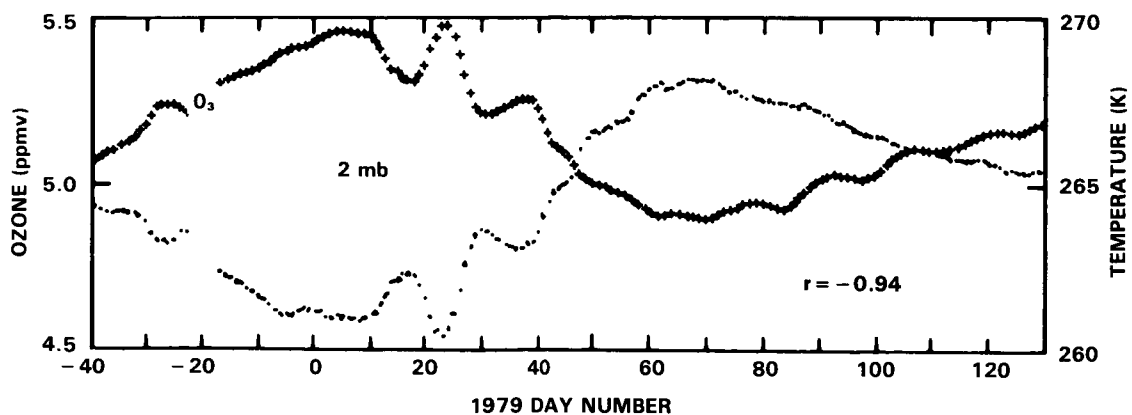

Figure 8-11.c Comparison between 5 day running means of O_3 (ppmv) and temperature (K) at 2 mbar as measured by Nimbus 7 LIMS. Data are zonal means averaged between $0°\pm20°$ latitude (from Keating *et al.*, 1985).

431

While the broad scheme depicted above (an upper stratospheric photochemical control of ozone with an associated out-of-phase relation between O_3 and T, and a lower stratospheric dynamical control with O_3 and T approximately in phase) might well hold for part of the globe during most seasons, one should be cautious not to blindly interpret observed phase relations in terms of "pure" photochemistry or "pure" dynamics. Indeed, Rood and Douglass (1985), Douglass *et al.* (1985), and Stolarski and Douglass (1985) have discussed this point by analyzing the individual terms (photochemical and dynamical) in the continuity equation for the perturbed fields of O_3 and T. This was done for both model and observational analyses, the latter case referring to winter satellite data from Nimbus 7 (SBUV ozone), NOAA 5 and Tiros-N (temperature). One conclusion from the above studies is that a strong anti-correlation between the O_3 and T eddy fields, coupled with a good agreement between the observed ozone perturbation and that deduced from photochemical equilibrium, does not necessarily imply that the individual dynamical terms are not important, compared to the photochemical terms (although the net dynamical contribution is small). In fact, the dynamically-induced phase differences between ozone and temperature waves can mimic the relationship expected from photochemical equilibrium. Moreover, dynamic forcing in the transition region can lead to a wide range of correlations between ozone and temperature perturbations.

The LIMS observations of ozone and temperature provide the best data available (simultaneous measurements with same instrument, good height resolution and observational precision) to quantitatively analyze ozone-temperature correlations. One way to do this is by evaluating the parameter $\theta = \partial \ln([O_3]/[M],/\partial(1/T)$ which relates to the ozone sensitivity to temperature changes. Expected values of θ can be algebraically estimated for individual cycles (O_x, HO_x, NO_x, or ClO_x), and approximate expressions for the combined chemistry can be obtained as well (Barnett *et al.*, 1975a; Haigh and Pyle, 1982). An illustration of the expected relative importance of the individual cycles as a function of height, as well as the combined result for all cycles together, is given in Figure 8-12, taken from the recent analysis of LIMS observations (mid-latitudes, May 1979) by Froidevaux *et al.* (1985b). These results come from an iterative algebraic solution to the odd oxygen photochemical balance equation, and include opacity feedback effects. The above study also reveals that there are regions of disagreement between the observed and theoretical values of θ particularly in the 3-5 mbar range, where model results are typically much higher (a factor of two) than the values inferred from LIMS data, even for statistically significant correlation coefficients between ozone and temperature. Uncertainties in the current chemistry or in the relative importance of the various cycles cannot account for these large differences, but dynamical contributions – as mentioned above – could play a role in this problem. The above authors also argue that short-term (less than a day) temperature fluctuations cannot be "tracked" by ozone in the middle and lower stratosphere, where its photochemical lifetime increases rapidly, and that such a phenomenon might be responsible for the disagreement in θ values (i.e., the lack of photochemical equilibrium). Frederick (1981) has discussed a similar effect in relation to the longitudinal phase differences between ozone and temperature fields. The value of θ itself, in addition to the correlation coefficient for O_3 and T, might serve as a useful diagnostic of the absence of photochemical equilibrium; its evaluation is more direct than the calculation of individual dynamical terms in the continuity equation. Agreement between the observed and predicted θ values, however, does not necessarily imply that dynamical terms are negligible and that photochemical control is strictly established. This could limit the usefulness of θ as a test of the model photochemistry.

Despite the interesting emerging analyses of ozone-temperature correlations, it does not appear that such analyses can readily lead to possible solutions to the significant model ozone deficit question raised in the previous section.
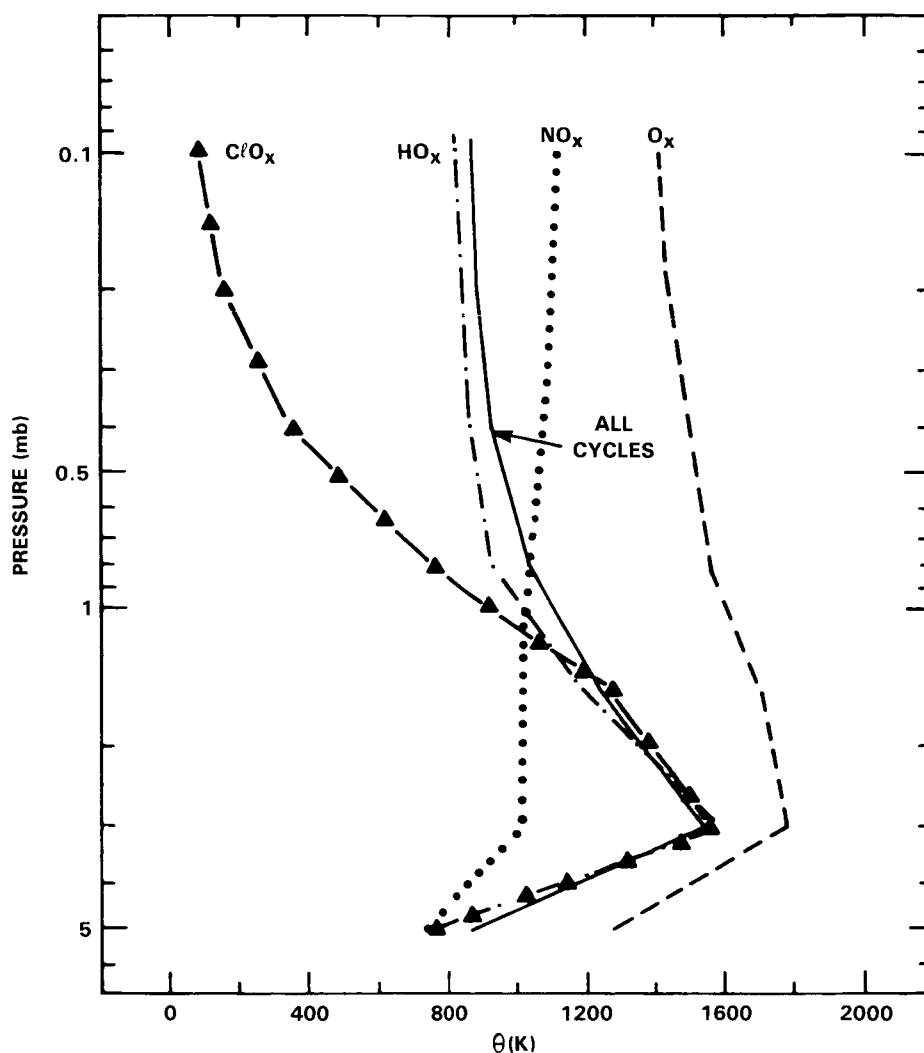
Figure 8-12. Theoretical estimate of sensitivity parameter θ (see text) in the upper stratosphere/lower mesosphere for individual chemical cycles (O_x, HO_x, NO_x and ClO_x) and all cycles combined. Model is for May 30°N and uses O_3, NO_2, H_2O and T data from LIMS (Froidevaux *et al.*, 1985b).

8.4 OZONE AND SOLAR VARIABILITY

Since the formation of ozone results from the photodissociation of molecular oxygen in the Herzberg continuum (stratosphere) and in the Schumann-Runge bands (mesosphere), one should expect slight changes in the O_3 mixing ratio with solar activity. As indicated in Chapter 6, the irradiance received at the earth is known to vary over a 27 day rotation of the Sun with typical values of 5 to 7 percent in the 175-210 nm region, 3 percent between 210 and 250 nm and 1 percent or less beyond 260 nm.

Analyses of the ozone response to short term solar variability have been reported recently by Hood (1984), Gille *et al.* (1984c), Chandra (1985) and Keating *et al.* (1985). These are based on different methods and on data from various sources. It might be interesting to briefly review these studies in order to see if their conclusions are in accord with the model predictions.

OXYGEN SPECIES

Hood (1984) has used the Nimbus 4 BUV ozone measurements (Fleig *et al.*, 1981) to estimate the response of upper stratospheric O_3 to UV changes. Since, at these heights, the temperature is negatively correlated with ozone (see Section 8.4), this endogenic component of the O_3 variation has been removed approximately by using a photochemical model in which the temperature was modified as a function of time according to the measurements by the Nimbus 4 Selective Chopper Radiometer. The residual ozone mixing ratio at low latitude was found to contain short term variations positively correlated with variations in the radiometric 10.7 cm flux and in the 180-190 nm UV flux as determined by the model of Lean *et al.* (1982) based on ground-based Ca II K line measurements.

Chandra (1985), however, using the same data as Hood (1984) showed that the oscillations in tropical ozone and temperature are apparently related to higher latitude waves and that the observed variability in ozone near the equator should probably be attributed to planetary waves rather than solar UV oscillations.

Using a statistical spectral method to treat ozone distributions reported by the LIMS instrument and solar irradiances measured by the SBUV experiment, both on board Nimbus 7, Gille *et al.* (1984c) have found that the ratio of the percentage O_3 response in the tropics to the percentage UV change at 205 nm increases with altitude from 0.17 at 30 km to 0.38 at 54 km reaching probably 0.60 at 60 km (see Figure 8-13). Keating *et al.* (1985), adopting data from the same source, have corrected for temperature
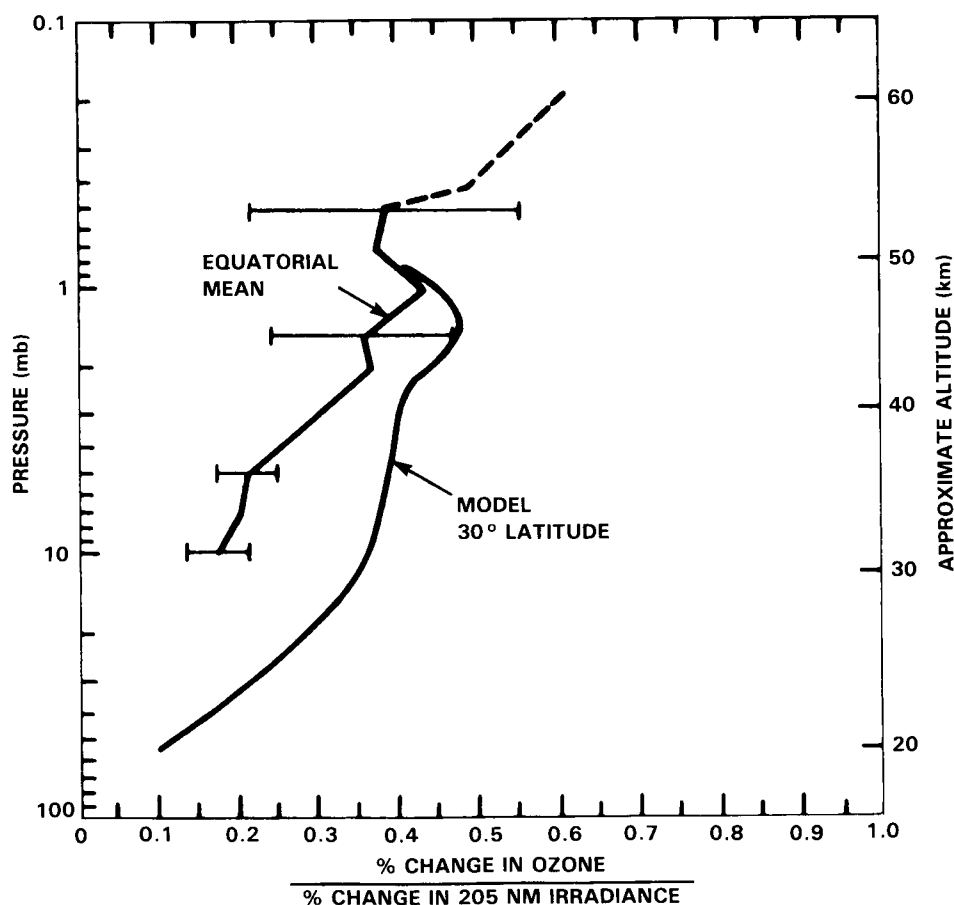

Figure 8-13. Sensitivity of the ozone concentration to a 1% change in the UV irradiance at 205 nm. Values derived from the LIMS and SBUV data compared with a model simulation (Gille et al.,1984c).

434

variations by making use of the temperature data measured simultaneously by LIMS to derive at each level a relation between temperature and ozone variations. This method allows to extract endogenic effects due to dynamics and in particular to planetary waves. The small residual variations can be attributed to exogenic solar influence since they correlate strongly with the variability in the measured solar irradiance at 205 nm (Figure 8-14). The percentage change in ozone relative to the percentage change in the UV flux at 205 nm is estimated to be of the order of 0.3 between 5 and 0.5 mbar, and to increase significantly above the stratopause. These results as well as those of Gille *et al.* (1984c), are in reasonable agreement with theoretical model predictions below about 40-50 km. Above this level, the predicted sensitivity of ozone to UV is considerably lower than the sensitivity inferred from the data. This discrepancy is consistent with the ozone imbalance discussed previously since it could be resolved by reducing the effect of odd hydrogen on the odd oxygen loss or by increasing the contribution of short wave radiation to the O_3 production.

Solar induced modifications of the ozone layer in relation with the 11 year solar cycle have been recently studied by Natarajan *et al.* (1980/81), Brasseur and Simon (1981) and Garcia *et al.* (1984). Some of this work as well as previous studies have been reviewed by Keating *et al.* (1981). Moreover, an analysis of 7 years of Nimbus 4 BUV data by Chandra (1984) has shown that the globally-averaged ozone in the upper stratosphere, when corrected for instrument drift, decreased by 3 to 4 percent from 1970 (solar maximum) to 1976 (solar minimum).
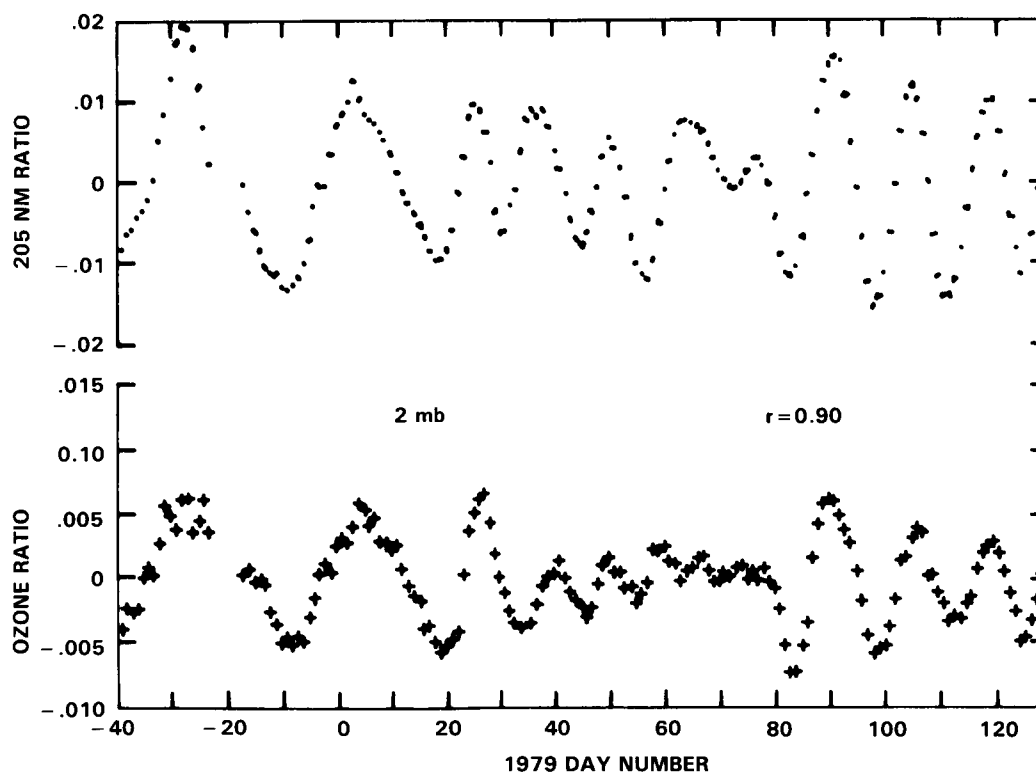

Figure 8-14. Relation between relative variation in the ozone mixing ratio (lower curve) and in the solar UV irradiance at 205 nm (upper curve) at 2 mbar after correcting for temperature effect. The ozone values refer to a zonal mean averaged over ± 40° latitude (from Keating *et al.*, 1985).

OXYGEN SPECIES

The recent model of Garcia *et al.* (1984), based on the model by Lean *et al.* (1982) for solar variability at wavelengths shorter than 200 nm, shows, from solar minimum to solar maximum, an increase in the ozone concentration of less than 5 percent in the stratosphere but considerably higher in the upper mesosphere and lower thermosphere (Figure 8-15). The reduction predicted in the lower mesosphere is attributed mostly to the increase in the dissociation of water vapor and the resulting increase in the HO_x-catalyzed ozone destruction. The negative change computed at high latitude near the stratopause reflects the increase in odd nitrogen as a result of higher production of NO_x in the thermosphere and its downward transport near the polar region. These predicted changes should be considered as upper limits since the model by Lean *et al.*, predicts higher solar variability than inferred directly from the SME data (see Chapter 7).
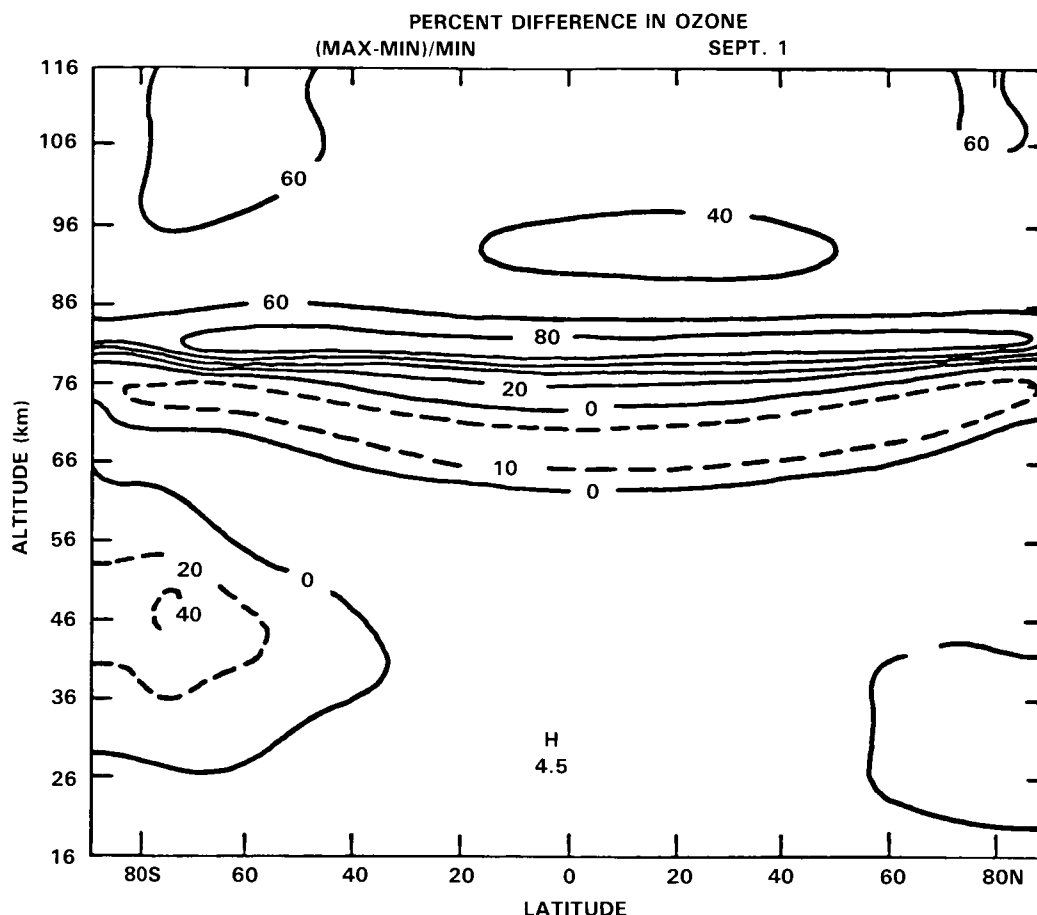

Figure 8-15. Ozone density variation over the course of the 11 year cycle of solar activity as calculated by Garcia *et al.* (1984).

From these studies, one may conclude that most of the short-term ozone variations observed on a global scale even in the tropics, are related to planetary wave activity but that a refined treatment of the data can reveal small oscillations induced by variations in the solar output. It is estimated that a 5-6 percent change in the solar irradiance at 205 nm over a solar rotation period (27 days) leads to a fluctuation in mid and upper stratospheric ozone on the order of 2-3 percent. No detectable change in the ozone column should be expected.

436

Ozone also responds to long-term variations in the solar output related to the 11-year cycle. The corresponding change in mid-stratospheric ozone is expected to be less than 5 percent and the variation of the ozone column should be of the order of 1 to 3 percent.

8.5 OZONE AND SOLAR PROTON EVENTS

Particle precipitation events (generally high latitude solar proton events or SPEs) have been studied intensively mostly during the last few years. Very few such studies had been published much prior to the 1981 WMO Report. The interest in these events stems from the opportunity that they provide for analyses of the perturbed middle atmosphere in a kind of "natural laboratory" experiment. Our understanding of the complex interactions affecting ozone can be tested and furthered by studying simultaneous observations of particle precipitation events and related changes in the ozone abundance.

Since the initial evidence of ozone changes resulting from an SPE reported by Weeks *et al.* (1972), based on rocket measurements between 50 and 70 km, analyses of ozone satellite data from the Nimbus 4 BUV experiment (Heath *et al.*, 1977; Fabian *et al.*, 1979; Reagan *et al.*, 1981; McPeters *et al.*, 1981; Solomon and Crutzen, 1981; Rusch *et al.*, 1981), the Nimbus 7 SBUV experiment (McPeters and Jackman, 1985; Jackman and McPeters, 1985), and the Solar Mesosphere Explorer (Thomas *et al.*, 1983b; Solomon *et al.*, 1983b) have all produced qualitatively similar correlations between SPEs and ozone. Nine such events have now led to identifiable ozone depletions.

The theoretical interpretation relies on HO_x or NO_x related catalytic destruction of ozone. The added HO_x or NO_x radicals (in the models) are products that follow the degradation of primary particles, dissociative and ionizing effects of secondary electrons on N_2, O_2, and other species, and subsequent neutral and ion chemistry in the middle atmosphere (Swider and Keneshea, 1973; Crutzen *et al.*, 1975; Frederick, 1976; Swider *et al.*, 1978; Crutzen and Solomon, 1980; Rusch *et al.*, 1981; Solomon *et al.*, 1981). Both short-term (1 day or less) and long-term (1 week or more) ozone responses have been observed, these responses being understood as a product of HO_x (short-lived) and NO_x (long-lived) related chemistry, respectively. It is expected that the HO_x radicals will be mostly responsible for ozone changes above the stratopause, while NO_x production effects become important mostly below that level. Model and observational results for ozone depletions at heights between 60 and 85 km agree reasonably well. Below 45 km, the observed ozone decrease associated with the large SPE that occurred on August 4, 1972, follows approximately the predicted response. Also, one expects a relative increase in the ozone depletion as the solar zenith angle increases, due to the increased importance of the SPE HO_x source (independent of solar zenith angle), relative to the (angle-dependent) natural source from H_2O. Such an effect has been analyzed in a few cases (Solomon *et al.*, 1983b see Figure 8-16; Jackman and McPeters, 1985), and the observed relative ozone decrease with solar zenith angle appears to be fairly well represented by the above explanation.

Despite these encouraging results, McPeters *et al.* (1981) and Jackman and McPeters (1985) have pointed out that some ozone depletions observed between 50 and 60 km are significantly larger than the predicted values. Results from a totally self-consistent calculation are in much worse disagreement with observations than calculations using observed ozone depletions to determine relevant values of the radiation field as a function of height. In either case, it is difficult to account for the observed ozone depletions, even if model parameters are allowed to vary within reasonable bounds. Whether this problem is due to an incomplete understanding of the HO_x-related chemistry, to uncertainties in the absorption cross sections for O_2 or O_3, or to some other reason remains to be seen.
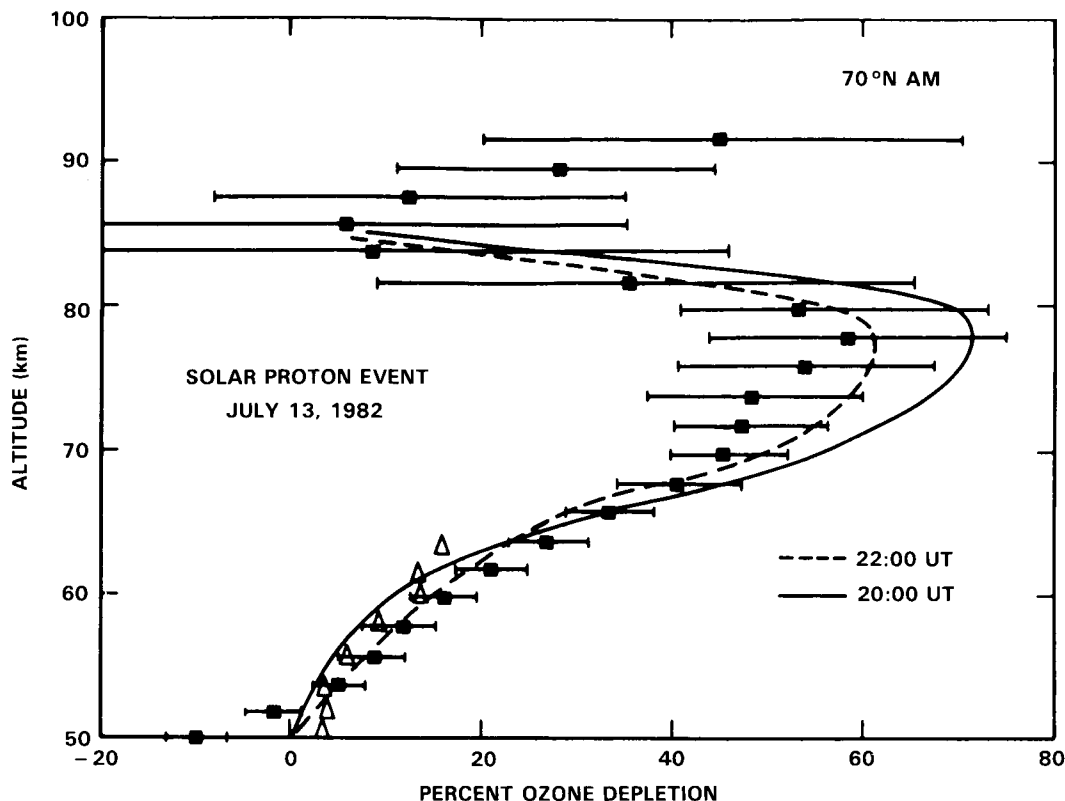
437

Figure 8-16. Observed and calculated ozone depletion during the solar proton event of July 13, 1982 (from Solomon *et al.*, 1983b).

The solution to this problem could be related to the ozone balance problem above 35 km. This should provide additional motivation for closely studying relationships between particle precipitation events and the ozone abundance near the stratopause.

8.6 OZONE VARIATIONS ASSOCIATED WITH EL CHICHON/EL NINO

Within Chapter 14 discussion is presented on the extended total ozone minimum observed during the winter of 1982-1983 and referred to as the "ozone hole," Figure 14-2. The timing of this phenomenon has been related to either or both of two separate events; the volcanic eruption of El Chichon in March-April of 1982 and the large atmospheric circulation anomalies associated with the El Nino of this time period.

With respect to the El Chichon, the arguments suggestive of a volcanic association have been presented by Dütsch (1985) and Vupputuri (1985). An ozone decrease on the order of 10 percent is observed between 100 and 30 mbar from ozone balloonsonde data that is connected through its timing and attributes to the El Chichon event. Two possible mechanisms were proposed; aerosol heterogeneous chemistry and direct chlorine injection.

Quiroz (1983 a,b) and Angell *et al.* (1985), on the other hand, point out that the '82-83' period was, coincidentally, that of a major El Nino event which has been associated with extraordinary climatic anomalies in the troposphere. Quiroz (1983a) has specifically demonstrated the difficulty of separating the stratospheric temperature signal from the two events and it is clear that considerable work must be done for the ozone data.

8.7 SUMMARY AND SUGGESTIONS FOR FUTURE RESEARCH

In this chapter, questions related to odd oxygen have dealt primarily with the photochemically dominated altitude region, i.e. the upper stratosphere and lower mesosphere. The absolute abundance of ozone and relationships between ozone and imposed variations in atmospheric temperature, solar UV flux and solar proton precipitation are being studied with the help of an increasingly accurate and large data base (from spaceborne experiments in particular), and increasingly accurate models of the middle atmosphere. From the analyses carried out in the last few years, several possibly related problems appear to exist in our understanding of the region above about 35 km.

Comparisons of SBUV, LIMS and SAGE profiles for April 1979 indicate a standard deviation of about 15% from 25-30 km which decreases to about 6% from 30-55 km. As these three instruments use such different techniques, these values represent our ability to measure the ozone profile in an absolute sense. These values are within the root mean square systematic error summaries. In the lower levels where the satellite data overlap with the ozone balloonsondes there is more ambiguity, but it appears that the balloonsondes are systematically lower than SBUV above about 32 km. The cause of this pattern is not currently recognized.

Utilizing SBUV as the basic data source for four year zonal average profiles, the random uncertainties appear to be about 4% in mid- and high-latitude winter and about 2% elsewhere.

The observed ozone abundance above 35 km is significantly underestimated by model calculations. This model deficit is typically 30-50%, and in some cases is as large as a factor of two. This ozone imbalance can only marginally be accepted as being due to the combined errors in the models and observations. It is not clear which of the possible solutions (underestimate of the model O_x production rate, overestimate of the model O_x loss rate, or missing chemistry) is most likely at present. Suggestions for future research include: a) Laboratory work to reduce the model uncertainties in key photochemical parameters, in particular HO_x radical chemistry and absorption cross sections for O_2 (Schumann-Runge bands and Herzberg continuum) and O_3 ($O(^1D)$ channel); b) Stratospheric measurements relating to the above cross section determinations (i.e., high resolution solar flux data within as large an altitude range as possible, from 180 to 250 nm); c) better understanding of the local ozone photochemical balance in the upper stratosphere (i.e., simultaneous measurements of the key radical species involved). However a quantitatively accurate observational determination of the O_3 balance is not possible, due to the importance of the local dynamics and since the required accuracy in the measurements of the individual parameters cannot yet be achieved; d) Precise measurements of the [O]/[O_3] ratio; e) A search for possible additional production mechanisms; f) Measurement and detailed consideration of the diurnal waveform of O_3 as a means of testing photochemistry in the upper stratosphere; g) Continued use of models to test the expected ozone sensitivity to newly arising recommendations of photochemical parameters; h) More detailed analyses of radiative and dynamical effects on ozone with the use of observations as well as multidimensional models.

In addition, comparisons of theoretical and observed relationships between ozone and temperature, ozone and solar UV, and ozone and solar proton events reveal a number of discrepancies which require further analyses.

The problems discussed in the present chapter, in particular the significant ozone imbalance in the photochemically-controlled region of the middle atmosphere, limit the confidence that can be attached to model predictions of future ozone changes in response to long-term increases in the emission or source gases.
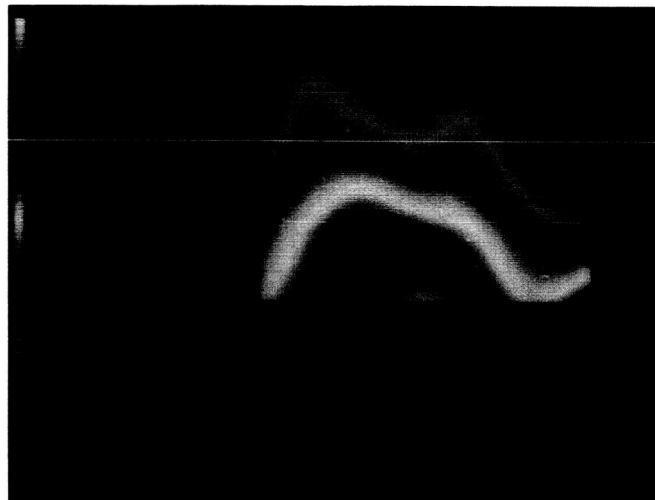
OXYGEN SPECIES

With respect to requirements for future effort, we also recommend the following:

1. Resolve the causes of the ozone measurement biases between SBUV, LIMS, SAGE as well as balloonsondes and, thereby, reduce the absolute error estimates.

2. Determine the impact of implementation of the Bass and Paur ozone absorption coefficients in the ground based measurements and compare the results with satellite observations.

3. Continue development of the ground based profile measurement program with particular emphasis on the following:

   a. Determination of the El Chichon aerosol impact on Umkehr measurements.
   b. Development of the high altitude (about 40 km) balloon sampling system with specific attention to the adjustment procedure to match the Dobson total ozone measurement.
   c. Development of a Lidar system capable of routine ozone and temperature measurements in the troposphere and stratosphere, especially above about 40 km.

CHAPTER ⑨

HYDROGEN SPECIES

Panel Members

H.I. Schiff, Chairman

C. Burnett — R. Jones
B. Carli — D. Kley
W.B. DeMore — M. Prather
R. deZafra — J.M. Russell, III
W.F.J. Evans — U. Schmidt
P.D. Guthrie — W.A. Traub
R.F. Hampson — R.T. Watson
W. Heaps

CHAPTER 9

HYDROGEN SPECIES: OBSERVATIONS AND INTERPRETATION

TABLE OF CONTENTS

9.0 INTRODUCTION

This chapter discusses measurements of the members of the HO_x family - OH, HO_2 and H_2O_2 - and their major source gases, H_2O, and CH_4. Emphasis will be placed on measurements which have been made since the 1982 WMO report.

The effects of HO_x on ozone destruction are both direct and indirect. Direct control is believed to dominate in the mesosphere and upper stratosphere. At lower altitudes, NO_x and ClO_x are more important in determining ozone loss but HO_x is closely coupled to the other two families and strongly influences their catalytic efficiencies.

The OH radical is mainly responsible for this coupling. In the case of NO_x interactions OH deactivates the chain carrier NO_2 by converting it to the inactive reservoir molecule HNO_3. The deactivation is, however, only temporary, since photolysis and reaction of OH with HNO_3 regenerates the chain carriers. In contrast, the primary interaction of OH with the ClO_x family is to convert the inactive HCl molecule to the chain carrier, Cl. The ClO_x cycle also interacts with the hydrogen cycle through CH_4 which provides the main chain termination step by reaction with Cl to form HCl. This mechanism may lead to substantial latitudinal and perhaps seasonal variations in the efficiency of the chlorine catalysis of ozone (Gidel *et al.*, 1983; Solomon and Garcia, 1984b). For these reasons OH is considered to be the most important member of the HO_x family and a key species in atmospheric chemistry.

The other chain carrier in the catalytic cycle of ozone destruction, HO_2, is coupled to the NO_x family largely by its reaction with NO which affects the partitioning of the chain carriers in both families. The HO_x and NO_x families are also coupled through the $HO_2 + NO_2 + M$ reaction forming the temporary reservoir species, HO_2NO_2. Although H_2O_2 does not directly affect ozone loss it is a major sink molecule for HO_x in the lower stratosphere where it can be transported down through the tropopause and removed. Its measurement therefore provides important information to our understanding of the overall HO_x budget.

Water vapor provides the primary source of stratospheric hydroxyl radicals through reaction with $O(^1D)$. Intermediate steps in the overall oxidation of CH_4 to CO_2 and H_2O generate HO_2 radicals. Molecular hydrogen represents a small source of HO_x in the stratosphere. Concentration measurements of H_2O and CH_4 provide tests for stratospheric transport and chemistry in multidimensional models. Their concentrations are coupled since the hydrogen content of stratospheric air, primarily $(H_2O + 2 \times CH_4)$ should remain constant as CH_4 is converted into H_2O.

Significant advances have been made in the measurement of all these HO_x species since the 1982 WMO assessment and the data base for these measurements has been extended appreciably.

The remainder of the chapter describes the measurement techniques, the available data, an assessment of the data reliability, and a comparison of the data with theoretical distributions of stratospheric HO_x species predicted from one and two dimensional photochemical models.

9.1 HYDROXYL (OH) MEASUREMENTS

9.1.1 Balloon-borne Measurements of OH

The only new measurements reported for the OH vertical profile since the 1982 WMO assessment were obtained using a balloon-borne laser radar system (LIDAR [Heaps and McGee, 1985]). A crude measurement using this technique was made in 1980 and an improved instrument was flown in October 1983.

HYDROGEN SPECIES

Radiation at 282 nm is transmitted into the atmosphere and is absorbed by the OH radical. Collisions with other atmospheric molecules redistribute the energy into a number of vibrational and rotational levels leading to two bands of fluorescence in the 306 nm - 315 nm region. The strength of the fluorescence is related to the OH concentration [Heaps et al., 1982].

The results from the October, 1983 flight of the lidar system are shown in Figure 9-1a. The closed circles represent all the OH profile measurements made using the in situ resonance fluorescence technique up to 1983 and the curves are results from current 2-D models (see Chapter 12). Open circles are from the 1980 LIDAR flight. The crosses are the new lidar data. The vertical bars represent the altitude range through which the gondola ascended while the measurements were being made. The horizontal bars represent one standard deviation of uncertainty arising from counting statistics which ranged from about ±5% at 38 km to ±100% at 28 km. The accuracy of all the measurements is ±50% resulting from the accumulated uncertainty of the calibration. Each measurement corresponds to 1,000 laser shots requiring approximately 4 minutes. The maximum raw signal observed was ~0.6 photons/shot. The measurements were obtained at a range of 75-150 meters from the gondola. Although this is close enough to the balloon for outgassing contamination to be a consideration, these measurements are thought to be of good quality because the ascent rate was too rapid for balloon borne contaminants to diffuse into the measurement volume. Later measurements at float (not shown in the figure) show effects that are probably attributable to contamination arising on a time scale of 10-30 minutes. Measurements made at ranges out to 0.5 km agree to within the stated precision with this profile although they have a poorer signal-to-noise ratio.

As can be seen in the figure this profile is generally lower than most previous measurements made by Anderson [1976] using the in situ resonance fluorescence technique and is slightly lower than the range predicted by models. The measurements are, however, within the combined uncertainty of the models and the measurements. It is evident that the measurements are insufficient to provide a critical test of HO_x photochemistry.

It has long been recognized that simultaneous measurements of multiple species are required for meaningful comparisons between theory and measurements. A minimum set for OH would be O_3 and H_2O. The lidar system makes an O_3 measurement simultaneously with OH measurements by using differential absorption. No satisfactory H_2O lidar technique has been developed to date. Simultaneous measurements of H_2O by in situ techniques cannot be obtained on the same gondola due to differences in sampling strategy, i.e., the lidar's flight profile involves long duration at float. Consequently a second balloon would be needed for the H_2O measurements.

Three other balloon-borne instruments have been developed for OH profile measurements. Although all have been flown, results are not yet available for inclusion in this report at this time. Two of these instruments involve remote-sensing far infrared emission in the 60 - 250 cm⁻¹ region measured by Fourier-transform spectrometers (FTS) in a limb-sounding mode.

The Carli (Instituto di Ricerca Onde Elettromagnetiche) group uses an FTS with a wire grid beamsplitter optimized for longer wavelength, He⁴ as well as He³ cooled bolometers, and an apodized resolution of 0.007 cm⁻¹ [Carli, et al., 1983, 1984, 1985a]. The Traub group (Smithsonian Astronomical Observatory) uses an FTS with a Mylar beamsplitter optimized for shorter wavelengths, He⁴ cooled Ge:Ga photoconductors, and an apodized resolution of 0.064 cm⁻¹ (Traub et al., 1982).

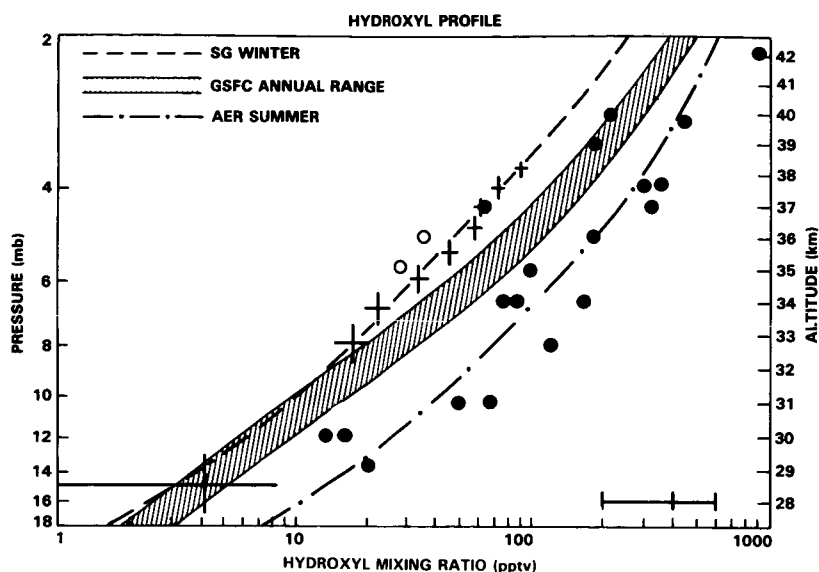HYDROXYL PROFILE

Figure 9-1a. OH concentration versus altitude. The circles represent all stratospheric OH measurements prior to 1983: filled circles were obtained by Anderson (1976) using lamps to excite fluorescence and have typical uncertainties of ±30%; open circles are from Heaps and McGee, 1983. The crosses are results from the October 1983 flight of Heaps and McGee (1985) taken from Palestine, Texas, 10:30 local time. The height of the crosses represents the altitude range of the measurements; the width of the crosses present the precision (1σ). The bar at the bottom of the figure represents the accuracy esti-mates for all the points. Also shown are representative results from several current 2-D models (— — —, Solomon and Garcia Winter; —·—, AER Summer). The seasonal range shown for the GSFC model is typical for models of this type. Additional details of the models are presented in Chapter 12.
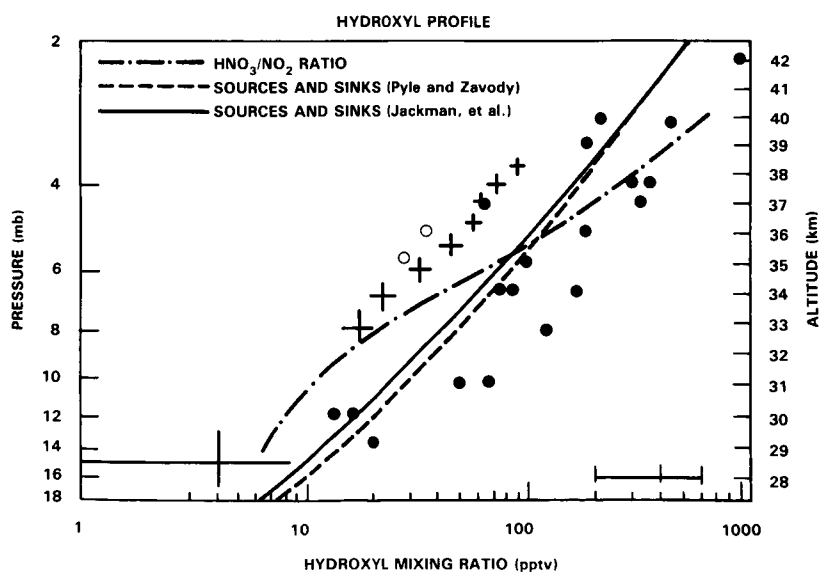
HYDROXYL PROFILE

Figure 9-1b. Data as in Figure 9.1a. The —·—; — — —; ———; lines represent the OH profiles inferred by Pyle and Zavody from the HNO_3/NO_2 ratio; by Pyle and Zavody from the sources and sinks; and by Jackman *et al.* from the sources and sinks.

Since OH has a strongly increasing mixing ratio with height, the measured signal is generally dominated by emissions from higher altitudes and consequently remote sensing techniques are most sensitive at altitudes below the instrument but above about 30 km. The recovered OH abundances are progressively less accurate below this altitude.

Both the Carli and Traub instruments have OH data from two flights each, which have not yet been fully analyzed. However the following qualitative results are available:

During the BIC-2 campaign on 20 June 1983, both instruments were launched at Palestine, Texas at the same time but on different gondolas. The measurement of OH near 118 cm^{-1} provides a common point of comparison. On the basis of repeated observations along upward-looking lines of sight, from early afternoon to about midnight, a monotonically decreasing signal is seen, in accord with theoretical expectations. The nighttime signal levels out at a fraction of the daytime signal, indicating that there is still a measurable amount of OH above the balloon. This is also in accord with theoretical models, which, although predicting a strong decrease in stratospheric OH after sunset, also predict a modest increase in mesospheric OH near 80 km, which can account for the detected signal.

Preliminary profile calculations indicate that meaningful concentration measurements can be obtained down to about 25 km from a float altitude of about 38 km.

A final instrument uses an *in situ* fluorescence method similar to that used to make the first OH measurements [Anderson, 1976] except that the resonance lamp is replaced by a laser system. Radiation from a frequency-doubled dye laser, pumped by a Cu vapor laser, is tuned to a number of specific OH absorption features near 282 nm and illuminates a multipath cell through which the atmospheric sample flows. The OH concentration is measured by its induced fluorescence as the balloon descends. The instrument is calibrated in the laboratory by simulating a flow under stratospheric conditions and injecting known quantities of OH into the measurement volume. This instrument can, in principle, provide OH measurements from balloon float altitudes down to the upper troposphere. Although it has been flown once, no results from this instrument are available at the time of writing this report.

9.1.2 Inferred OH Profiles

Pyle *et al.* [1983] derived an OH profile based on the ratio of HNO_3 to NO_2 using LIMS observations. The photochemical equilibrium between these species breaks down in the lower stratosphere, however, and the LIMS HNO_3 measurements do not appear to be consistent with other measurements above about 35 km [Gille *et al.*, 1984b, Jackman *et al.*, 1985a].

An alternative approach is to assume equilibrium between total sources and sinks of OH. If the source and sink terms can then be constrained by observations, the equilibrium OH profile can be derived. This approach has been used by Pyle and Zavody [1985a] and by Jackman *et al.* [1985a], using 2-D models with full chemistry, constrained by LIMS and SAMS observations of O_3, H_2O, HNO_3, NO_2, CH_4 and temperature. The resulting profiles for 32 °N in winter from these studies and from the HNO_3/NO_2 ratio are shown in Figure 9-1b.

9.1.3 Ground Based OH Measurements

Column amounts of OH have been obtained, by Burnett and Burnett (1983a), with a Pepsios spectrometer measuring solar absorption of the P1(1) (0.0) line at 308.2 nm. The high resolution and luminosity

of this instrument enables it to clearly distinguish the sharp terrestrial OH absorption feature from the relatively broad solar Fraunhofer lines. Uncertainty, due to statistical noise for a single 3-minute line scan at a solar zenith angle of 30° is about 10%.

The total vertical column abundance, Nv(OH) (cm^{-2}) is derived from the slant path absorption measurements using an independently determined oscillator strength, the appropriate rotational population distribution for middle atmospheric temperatures, and the geometric correction to the vertical column [Burnett and Burnett, 1981]. Uncertainty in these factors should not total more than a few per cent. Since absorption measurements are inherently relative, the method provides absolute values for the column amounts.

Figure 9-2 shows the hydroxyl radical profile from 16-90 km from the model of Solomon and Garcia for the daytime average at 37°N in summer. It can be seen that the total column density of OH in the stratosphere (16-48 km) and mesosphere (48-90 km) are approximately equal. The column density of OH in the troposphere is assumed to be approximately 9% of the total.

The OH column abundances observed at Fritz Peak Observatory in Colorado in 1981-82 are shown in Figure 9-3 as a function of the solar zenith angle, χ. About 1000 sets of data were taken, representing approximately one third of the days of each season. The bars represent the standard error of the mean and the curve represents the best empirical fit to the data.
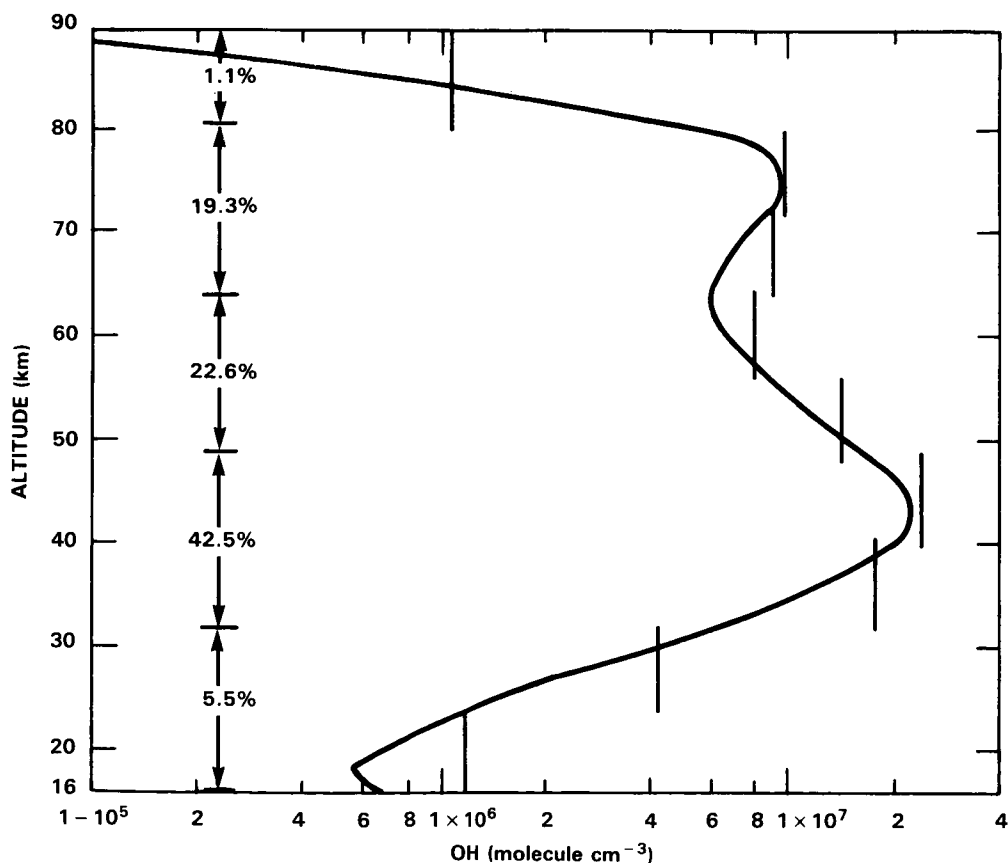

Figure 9-2. Hydroxyl profile from 16-90 km from the model of Solomon and Garcia. OH number density (molecule cm^{-3}) for the daytime average at 37°N in summer. The tropospheric column of OH is assumed to be approximately 9%.
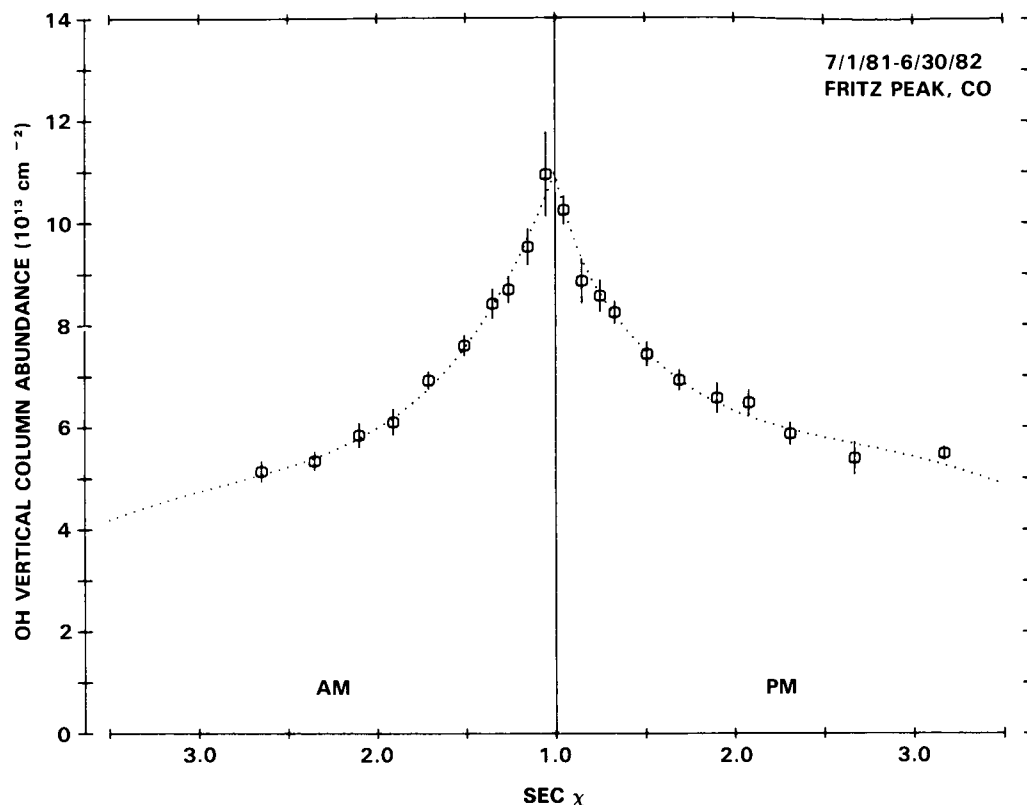
Figure 9-3. OH vertical column abundances, July 1, 1981, to June 30, 1982. A full year of OH data taken between July 1981 and June 1982 is shown plotted as a function of sec χ, where χ is the solar zenith angle. The averages were determined with each month's average for a given sec χ weighted equally in order to compensate for varying number of data sets per month. (Burnett and Burnett, 1984).

The dependence of the column abundance on solar zenith angle is in accord with photochemical theory. The total measured column abundances are also in general agreement with theory. For example, the column abundances for a solar zenith angle of 30° ranged from 6.6 × 10^{13} cm^{-2} in 1977–79 to 9.4 × 10^{13}cm^{-2} in 1981–1982.

The long-term variability can best be seen from the "normalized abundances" obtained by dividing the observed abundances by the values on the empirical sec χ distribution curve, a procedure which, to a first approximation, eliminates the χ-dependence, Figure 9-4a shows the normalized abundances at Fritz Peak during 1977–1984. The levels appear to have increased in the 1977–1980 period, coinciding with the approach to maximum solar activity in the solar cycle [Burnett and Burnett, 1982]. The dashed line in the figure represents one empirical fit to the data, showing a 30% increase. Photochemical models do not predict this trend.

Figure 9-4b shows a seasonal variation of 28%, with winter maxima and summer minima obtained when the long term variation is subtracted from the normalized abundances [Burnett and Burnett, 1984]. The seasonal variation appears to be independent of the long term change. Seasonal temperature changes in the OH rotational population distribution, and seasonal variations in incident solar radiation can account for part of this variation, but a seasonal OH abundance variation of about 21% remains, which must be due to other seasonal changes in atmospheric behavior. Recently observed (LIMS and SAMS data) seasonal cycles in stratospheric O$_3$, H$_2$O, NO$_2$ and CH$_4$ may lead to substantial variation in OH.
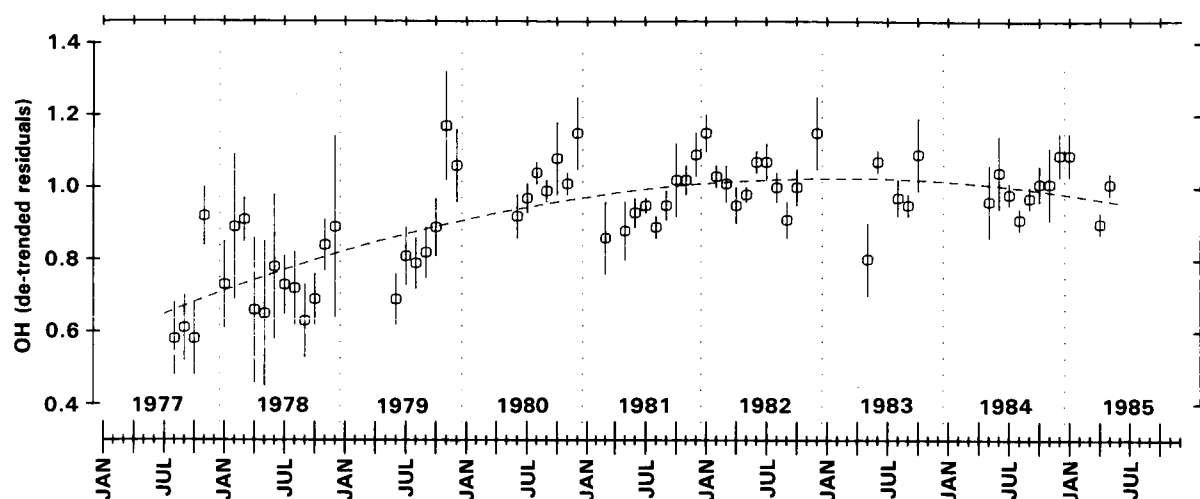
Figure 9-4a. Normalized monthly OH abundances, 1977-1985 at Fritz Peak Observatory, Colorado (40°N, 105°W). OH abundances have been normalized with respect to the best fit curve representing the 1981-82 AM data. Bars represent the standard error of the mean $\sigma/\overline{N}$. The dashed line is one empirical fit to the long term trend.
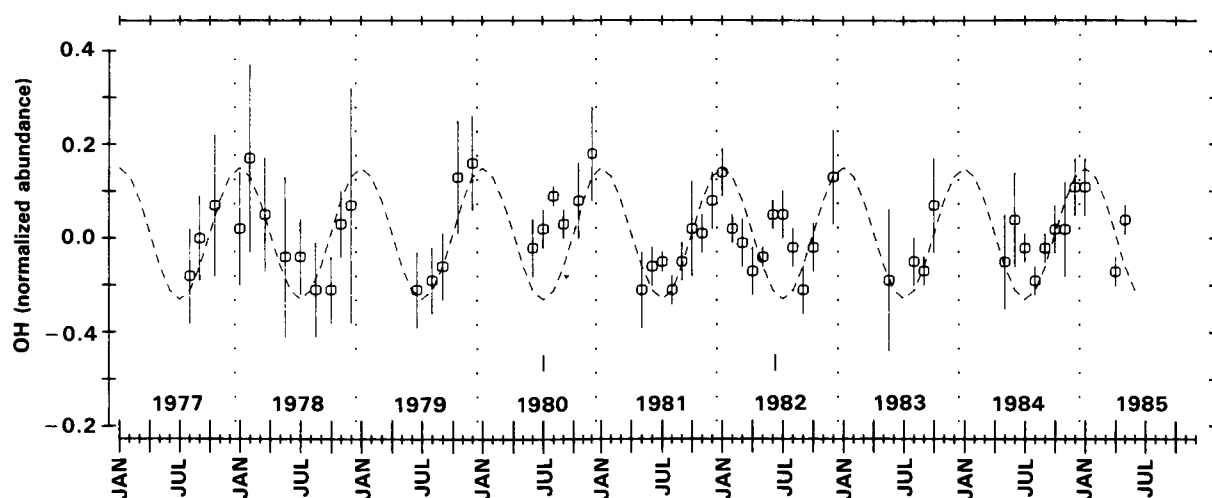

Figure 9-4b. OH residual abundances: seasonal variation, 1977–1985. The empirical long term trend has been removed from the normalized OH abundances from Figure 9-4a. While most departures from the seasonal curve may be attributed to experimental uncertainty, the deviations which appear in summer 1980 and 1982 may be related to the volcanic eruptions of Mount St. Helens and El Chichon, respectively.

447

Column abundances measured at Fritz Peak show a morning (AM) and afternoon (PM) dependence. The AM-PM asymmetry has a large persistent seasonal variation [Burnett and Burnett, 1984]. AM abundances exceed PM abundances in the Spring; PM abundances exceed AM abundances in the fall. Figure 9-5 shows the asymmetry to vary seasonally with an amplitude of 27% around a 7% offset favoring PM abundances. The phase of this behavior is shown in the figure to be identical to that for the seasonal variation in total ozone at this latitude. However, the asymmetry behavior appears to depend on location since the Florida data seems to lack the seasonal behavior. Since such temporal variations can only occur where the lifetimes for the HO_x family are longer than 2 hours, these observations indicate a large contribution of mesospheric OH to the measured column abundances.

The column abundances show other geographical differences. The abundances measured during the winter and spring of 1980 at Boca Raton, FL (26°N, 80°W) were 40% greater than those measured at
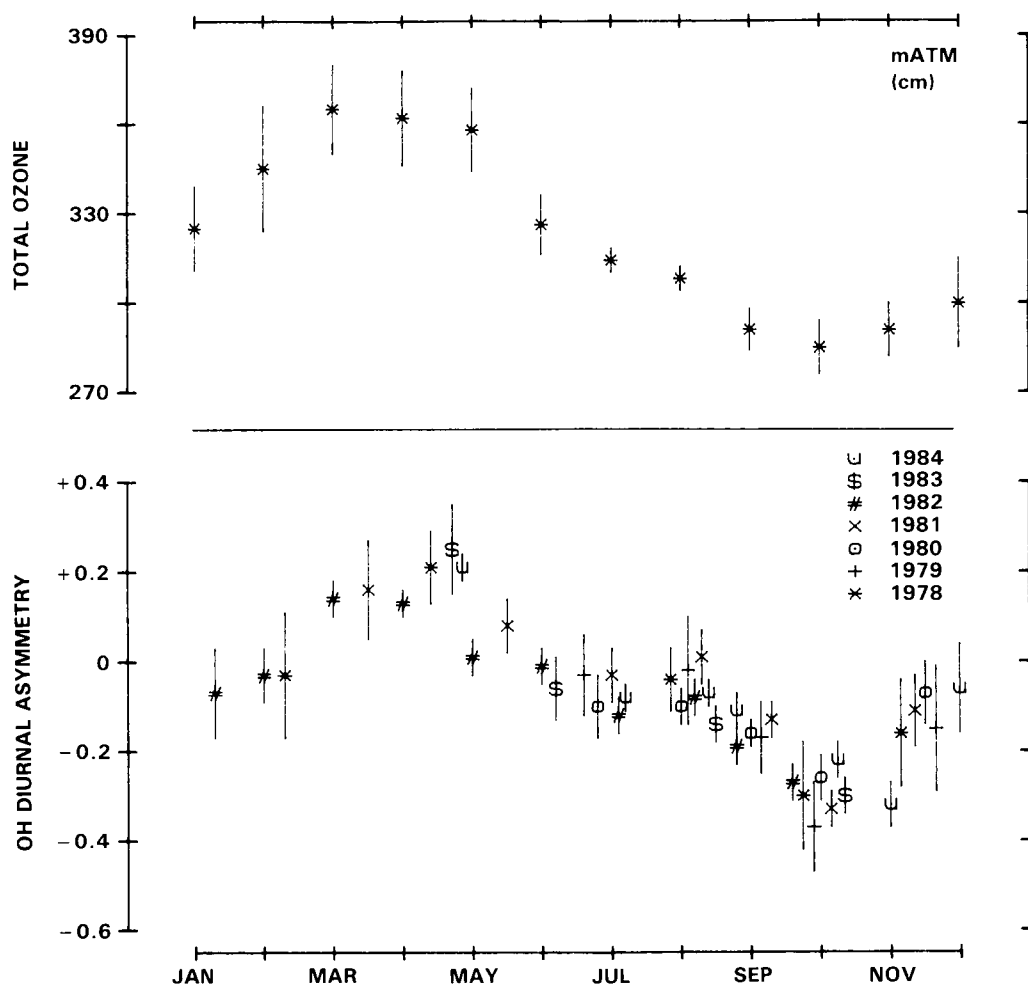

Figure 9-5. Average diurnal asymmetry: 1978–1984. The differences between the average morning residual abundances, R_{AM} and the PM residual abundance R_{PM} are plotted by month. A difference of −0.20 would be interpreted as a month in which afternoon abundances were 20% higher than the corresponding morning values. Data for local noon ± 1 hour have been omitted. The 1978–1982 Boulder ozone measurements by R. Grass, NOAA, Geophysical Monitoring for Climatic Change (personal communication, 1983), are shown for comparison.

Fritz Peak, CO during the same period although the measurements made during the same period in 1983 were essentially identical at both locations. Measurements made at Poker Flat, AK (65 °N, 148 °W) during the summer of 1983 were some 30% higher than those observed at Colorado and Florida for the same zenith angles.

Interesting observations were made during the volcanic eruptions in May, 1980 and April, 1982. Burnett and Burnett [1984] observed a positive OH column perturbation of 30% in the edge of the El Chichon cloud in 1982.

The observations made during the partial solar eclipse of May, 1984 were quite unexpected. The measurements made during the eclipse, compared with the average of those made during the preceding 3 days are shown in Figure 9-6. There is an initial decrease in the total column of about 50% followed by recovery and an overshoot of nearly the same magnitude before the end of the eclipse. The continuing transient following the eclipse is increasingly damped, approaching baseline values 2-hour after eclipse [Burnett and Burnett, 1985]. These surprisingly large changes in transient column OH abundances provide a challenging time-dependent test for theoretical models.
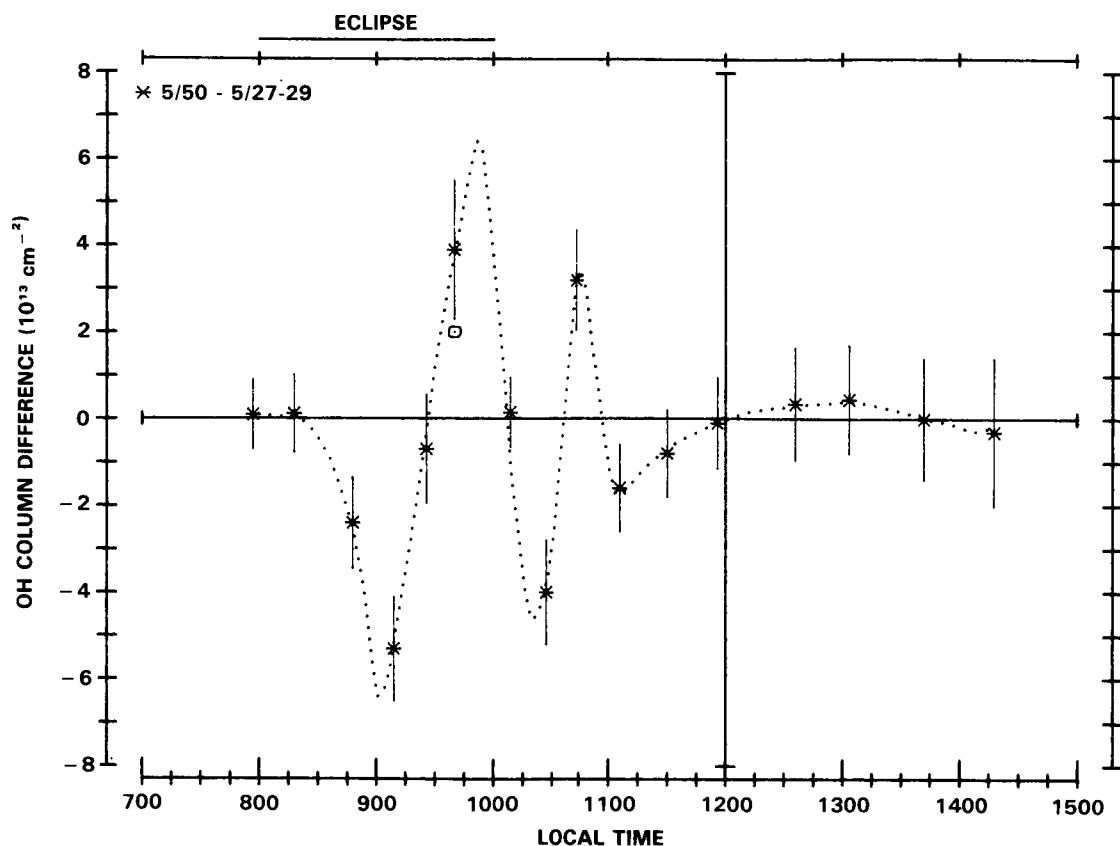

Figure 9-6. OH vertical column abundance departures from baseline values for the partial eclipse event of May 30, 1984. Nv = Nv(5/30)−Nv(5/27−29), where Nv(5/30) are the OH abundance data for 5/30 and Nv(5/27−29) is the corresponding average baseline for the 5/27, 28 and 29 data. An alternative point, $\square$, is shown for the possible interpretation of a smoother baseline at 0945 LT. The abundance drop of $5 \times 10^{13}/cm^2$ and subsequent overshoot during the eclipse period are evident. These excursions and the transient oscillation after the termination of the eclipse are several times the observational uncertainties. The dashed curve is thought to be a good representation of this oscillatory behavior (Burnett and Burnett, 1985).

449

9.2 HYDROPEROXYL (HO₂) MEASUREMENTS

9.2.1 *In situ* Vertical Profile Measurements of HO₂

The balloon-borne, *in situ*, cryogenic sampling technique for HO_2 measurements described by Mihelcic, *et al.* [1978] has been improved and used in a series of flights by Helten, *et al.* [1984a; personal communication, 1985] to obtain vertical profile data over the range 16 to 34 km. Observations have been conducted during September and October of 1980 and 1983 over Aire sur l'Adour in southern France (44 °N).

The cryogenic sampling technique traps all free radicals on a liquid nitrogen cooled, gold plated, copper finger in a matrix of H_2O or D_2O. Up to 10 samples may be collected in sequence during a controlled balloon descent and a vertical resolution of about 3 km is typically obtained. The matrix is isolated and free radical samples are returned to a laboratory for identification and determination of concentration via electron spin resonance spectroscopy.

The signals assigned to HO_2 also include other peroxy radicals, RO_2. However, the most abundant of these radicals in the stratosphere is CH_3O_2 and model calculations predict that the concentrations of these radicals are less than 10% as large as the HO_2 concentrations and can therefore be neglected within the uncertainties of the measurements.

Only three data points from the two flights in 1980 have been published to date (Helten *et al.*, 1984a). The overall uncertainty in the measured concentrations is estimated by the authors to be ±40% for this published data.

Due to technical modifications associated with the other flights, remaining recent data may be subject to small changes in calibration. The results of these flights are reported here, with the caveat that the uncertainties and the accuracy are subject to change once the calibration factors have been finally determined. The authors expect to reduce the overall uncertainty to a value of less than 25% for this data.

The preliminary data from Helten *et al.* (personal communication, 1985) is shown in Figure 9-7. In general the flights reached a maximum altitude of about 34 km and the controlled descent was initiated after dawn at a rate of about 1 m/s. The measurements which were made at high solar zenith angle are shown as open symbols. Since theoretical models predict negligible quantities of HO_2 near 30 km before dawn, rising rapidly over ~3 hours to values within ~25% of the midday maximum, interpretation of the Helten *et al.* data requires input from diurnal modeling to adjust the data to a vertical HO_2 profile at the same time of day. The primary effect will be to shift the data above 25 km to higher values. It should be noted that the 1-D model profile in Figure 9-7 represents the midday maximum mixing ratio, while the 2-D model profiles represent the seasonal range (winter-summer) of the daytime average mixing ratio.

9.2.2 Ground Based HO₂ Measurements

A ground based mm wave rotational emission line measurement reported by de Zafra, *et al.* (1984) provides a measure of HO_2 column amounts above 35 km. A triplet of transitions, spaced about 40 MHz apart near 265.7 GHz, was observed, using a cryogenically cooled mm-wave heterodyne receiver located at Mauna Kea, Hawaii (19.5 °N). The measurement was made over several days in late September and early October, 1982.
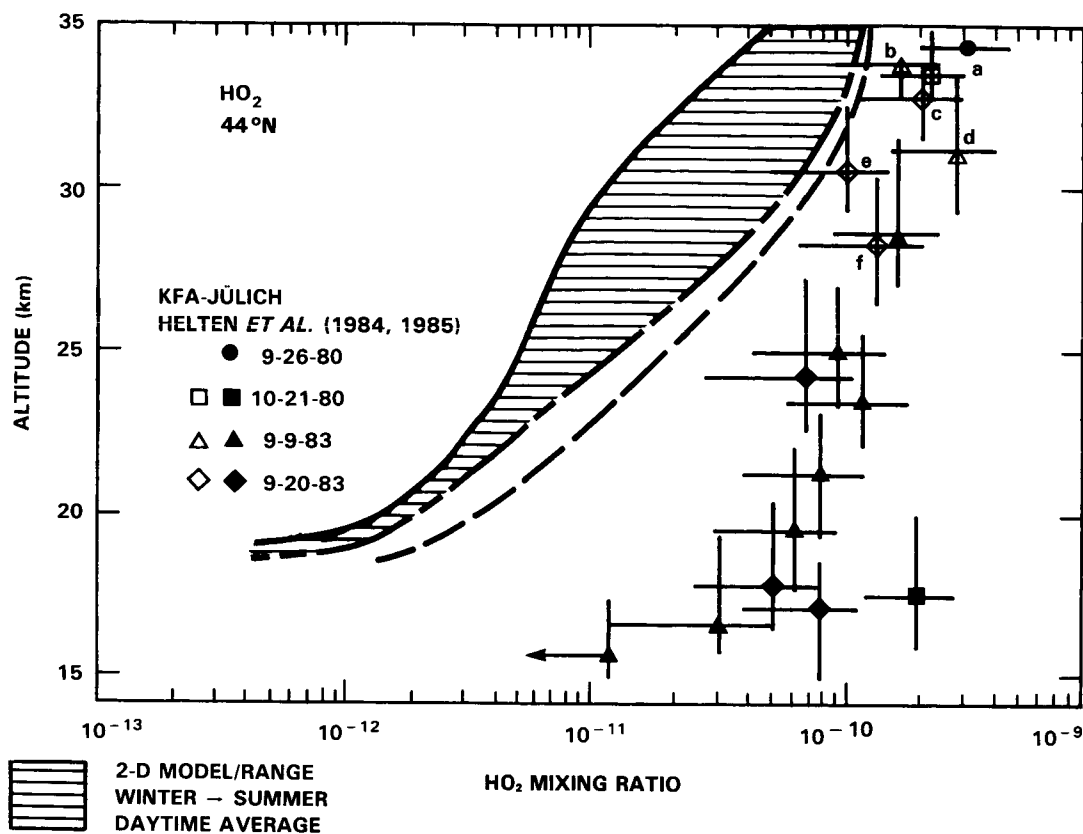
Figure 9-7. *In situ* observations of HO₂, employing the matrix isolation technique of Helten *et al.* (1984a). The samples were collected during several balloon flights at local time between sunrise and approximately noontime. Data for observations made within 3 hours after sunrise are plotted with open symbols, because they should be adjusted (upward in mixing ratio) due to the rather strong diurnal variation of HO₂ within this time period. The zenith angle for these samples are as follows: a: 88.1-78.1; b: 62.3-53.3; c: 95.8-83.9; d: 55.0-46.6; e: 86.8-77.2; f: 80.7-70.5. The dashed line represents a typical altitude profile for HO₂ at midday calculated by Prather using a one-dimensional photochemical model.

In the mm wave emission technique the absolute intensity and the pressure broadened line shape of molecular rotational emission lines are measured. The frequency resolution available allows precise measurements of pressure broadened line shapes. The integrated line intensity is proportional to the molecular column density. Vertical profile information is obtained by best fitting the observed line shape to assumed profiles. In the altitude range below approximately 70 km, where pressure broadening dominates Doppler broadening, each small altitude increment contributes a Lorentzian line shape whose intensity is determined by molecular concentration and whose width is determined by the mean pressure over the altitude increment. The authors estimate that their method is insensitive below 35 km due to the low concentrations of HO₂ in this region of the atmosphere. Below this altitude, the signal attributed to the total lineshape is too weak and broad to be clearly distinguished from baseline curvature of instrumental origin which may be present in the output. This ground based data therefore shares only a small region of overlap with *in situ* balloon-borne measurements [Mihelcic *et al.*, 1978; Anderson, *et al.*, 1981; Helten *et al.*, 1984a; personal communication, 1985].

To minimize the effect of diurnal variation on the measurement value, observing was started about four hours after sunrise each day and continued no later than one hour before sunset. On the basis of

full diurnal models by Ko and Sze (1983) and Froidevaux (1983), the authors estimate that a 10-15% correction should be applied to their integrated results when comparing to a theoretical midday peak.

The accuracy of these ground-based results depends on calibration of the mm wave receiver sensitivity and the accuracy with which tropospheric attenuation by water vapor can be determined. The authors estimate the overall, one-sigma, uncertainty for these effects, combined in quadrature, to be 15%. A further uncertainty affecting conversion of the observed line shape and emission intensity to a correctly scaled vertical profile arises from lack of an accurate measure of the pressure broadening coefficient for HO_2 in air. Measured coefficients for other molecules lead to an error estimate of $\pm 10\%$ from this source. Combination of this uncertainty with that above, again in quadrature, results in an overall estimate of 18% for the total one-sigma error involved in determining column densities above 35 km from the measured data.

The error within which the mixing ratio may be determined at any given altitude depends on that altitude, being worst at the extremes covered here. The strongest of the three measured transitions is compared with the vertical profiles a, b, and c of Figure 9-8 in Figure 9-9. The signal-to-noise ratio of the data seems clearly sufficient to distinguish between vertical profiles a, b, and c in the region above 35 km. It clearly agrees best with profile a. The first of these is typical of profiles obtained using the faster $O + HO_2$ rates currently used and first recommended in JPL 82-57, while the second is typical of the older values recommended in WMO (1982). Profile c is an arbitrary profile designed to accommodate the much higher
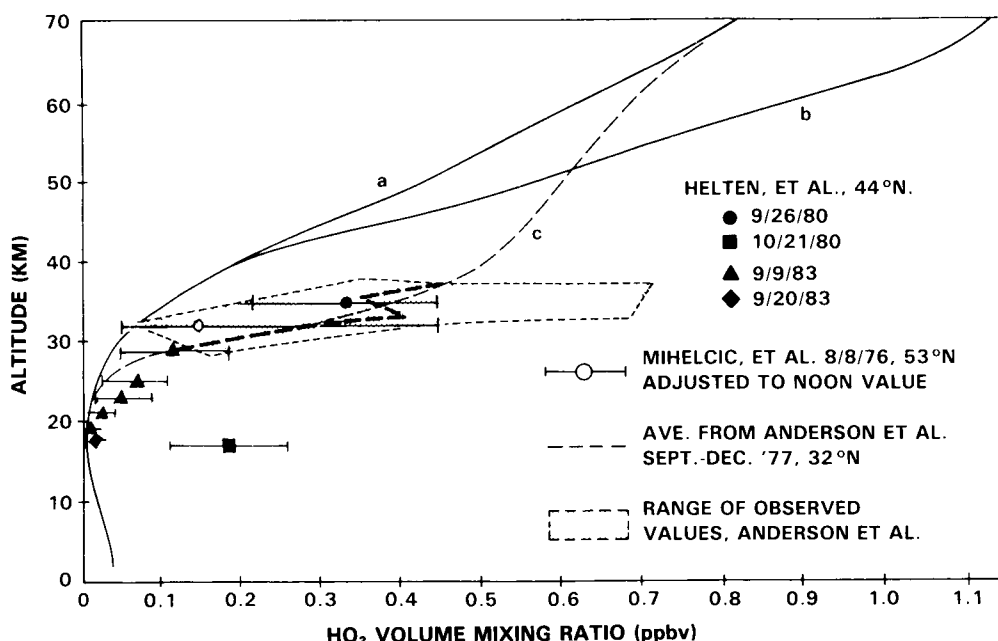

Figure 9-8. Theoretical midday mixing ratios for 30°N as a function of altitude, compared with data. Curves a, b, and c define synthesized lineshapes and amplitudes compared against ground based mm data in Figure 9-9 Curve (a) is typical of recent 1 and 2-D models using JPL 82-57 chemistry and curve (b) is typical of the same models using WMO (1982) or similar chemistry embodying a slower reaction rate for $O + HO_2$. Curve (c) is an arbitrary profile chosen to blend typical lower altitude data with mesospheric theory predictions. Experimental values of Helten *et al.* (1984a; personal communication, 1985) are limited to those with a mean solar zenith angle of ~55°N and would be subject to relatively small diurnal corrections to midday values. Data of Anderson *et al.* (1981) were taken near local noon. (Adapted from de Zafra, *et al.*, 1984).
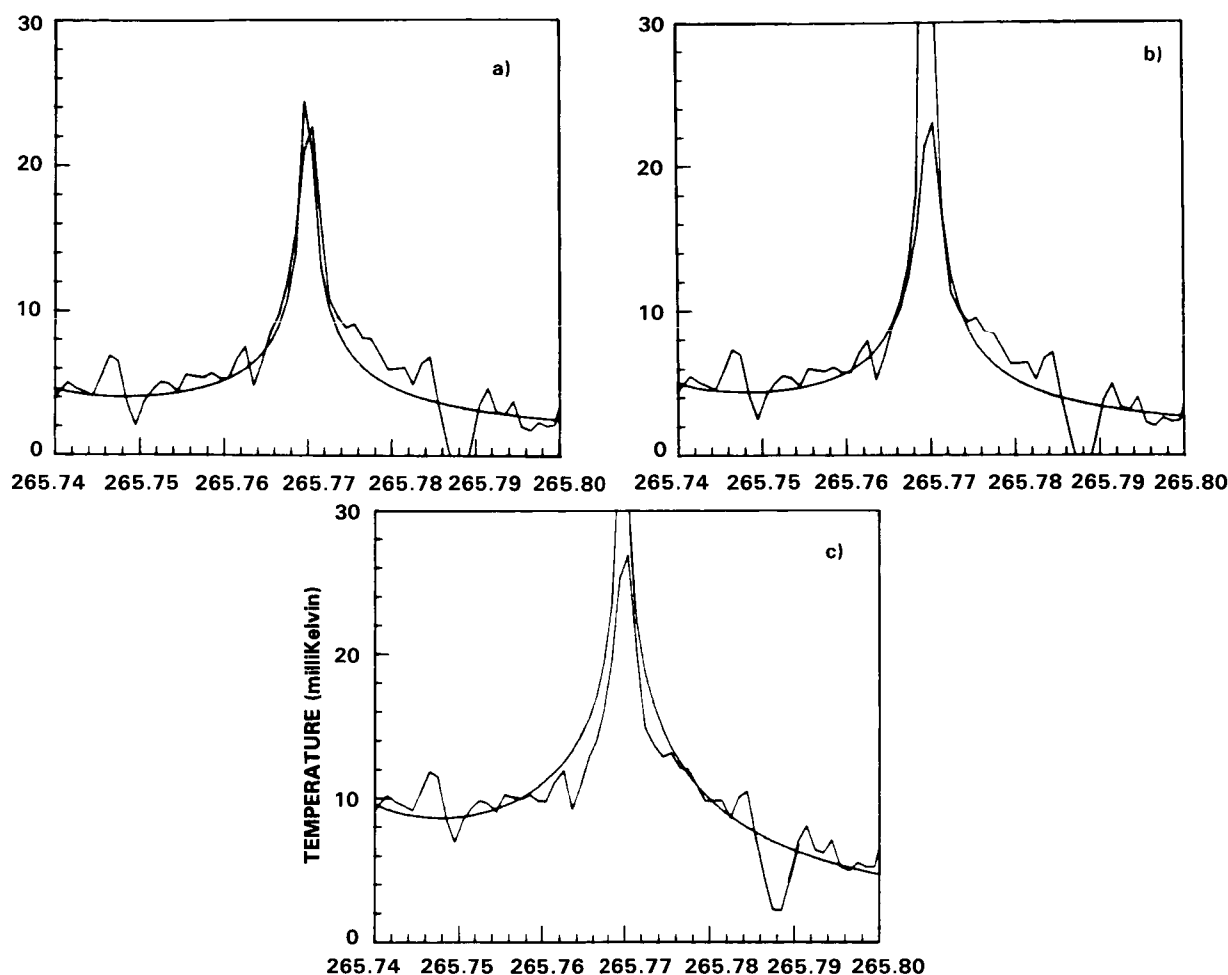
Figure 9-9. Observed HO_2 lineshape of the strongest component from the line triplet at 265 GHz after removal of contributing background from all species except HO_2. The smooth line profiles in a, b, and c have been synthesized from the corresponding vertical profiles of Figure 9-8. The ordinates are in milliKelvin equivalent blackbody radiation and the abscissa in GHz. The required diurnal correction of +(10–15)% to midday values (see text) has not been made to the experimental data. This compensates for a positive correction of approximately equal magnitude, also not applied, to convert theoretical mixing ratios for 30°N (from Figure 9-8) to 20°N for comparison with this data. (From de Zafra, *et al.* 1984). Baselines appear to vary from (a) to (c) due to the influence of line wings from the two other members of the triplet lying to the left as the assumed vertical distribution changes.

in situ values of HO_2 mixing ratio reported at lower altitudes by Anderson, *et al.* (1981) and the more recent results from Helten, (personal communication, 1985) merging with the theoretical values at 60-70 km. There is clearly an inconsistency between the ground-based and *in situ* measurements of HO_2.

9.2.3 Comparisons of Theory and Observations for HO_2

The *in situ* measurements in the 20-35 km range are difficult to reconcile with current theory, being higher than modelled concentrations by factors ranging from more than 2 at 35 km to about 10 below 25 km. Such high concentrations of HO_2, along with current reaction rate coefficients, would lead to predictions of H_2O_2 and HNO_4 concentrations well above the observed upper limits.

Significant problems are encountered in reconciling the high measurements of HO_2 with the low measurements of OH reported in Section 9.2.1. The ratio of HO_2 to OH is thought to be well understood and to depend mainly on the reactions of HO_2 with NO and O_3 and the reaction of OH with O_3. If the HO_2/OH ratio is anywhere near as large as that obtained by combining the HO_2 data of Helten et al. and the OH data of Heaps and McGee, substantial changes in currently accepted chemistry will be required. In fact, converting all the OH to HO_2 does not yield sufficient HO_2 to agree with the measurements. Since the main destruction process for the termination of the HO_x chain above 30 km is the recombination of OH and HO_2, a reduction in the rate coefficient for this recombination reaction in order to increase the predicted HO_2 concentration would also increase the predicted OH concentration, further increasing the discrepancy with the measurements of Heaps and McGee. If substantial changes are required in our description of HO_x chemistry then our understanding of the ozone budget would be significantly impacted since HO_x reactions currently account for as much as half of the ozone loss below 25 km, and OH and HO_2 strongly influence the atmospheric chemistry of nitrogen and chlorine species.

9.3 HYDROGEN PEROXIDE (H_2O_2) MEASUREMENTS

Hydrogen peroxide is theoretically expected in the stratosphere at concentrations within the detection range of several current techniques. However, attempts by three separate groups have failed to make conclusive detection of this molecule. Current 2D theoretical models predict that, at mid-latitudes, H_2O_2 should have a mixing ratio peak in the 30 to 35 km range, and should vary seasonally from a summer high of about 0.35 ppbv to a winter low of about 0.15 ppbv. The diurnal variation in this altitude range is predicted to be about 10 percent at most, with a maximum at night.

A tentative detection of H_2O_2 was reported by Waters et al. (1981) using a balloon-borne, microwave limb sounding spectrometer, looking at the thermal emission from a rotational line at 205 GHz (1.5 mm wavelength). The reported value was 1.1 ± 0.5 ppbv in a layer between about 27 and 35 km (in February at 32 °N) which is nearly an order of magnitude larger than current theoretical values for this altitude range and season. This tentative detection has not been confirmed in subsequent attempts.

Chance and Traub (1984) reported an altitude-dependent upper limit for H_2O_2, using a limb sounding, balloon-borne, far-infrared Fourier transform spectrometer looking at the 112.2 cm^{-1} rotational Q branch in thermal emission. The observations were made in January at a latitude of 34 °N. The altitudes of the six layers examined ranged from about 22 to 38 km. The most sensitive region of comparison with theoretical models was in the 26 to 34 km range where the measured upper limits of H_2O_2 ranged from 0.05 to 0.14 ppbv. These limits were set by background noise in the spectra and represent twice its standard deviation; in no instance was a clearly identifiable spectral feature observed which exceeded this noise level. These upper limits are shown in Figure 9-10 , along with four theoretical curves for the appropriate season and latitude. Each of these models uses the NASA-JPL (1985) kinetic and photochemical rate coefficients (see Appendix A). With future improvements, this technique should be adequate to detect the higher concentrations expected in summer at the same latitude.

An upper limit for H_2O_2 was reported by de Zafra et al. (1985b) using a ground-based millimeter wave spectrometer looking for a 270 GHz (1.1. mm wavelength) rotational line in thermal emission. The measurements were made in May and June from Mauna Kea, Hawaii (20 °N). After 55 hours integration, no signal was detected above the background noise. The authors have interpreted this null result in terms of the signal intensity to be expected from a particular model profile, compared against the noise level reached during data integration. They conclude that no more than twice the H_2O_2 mixing ratio predicted over the 30-50 km range for a model output for 19 °N by Sze and Ko (using JPL 82 chemistry) would
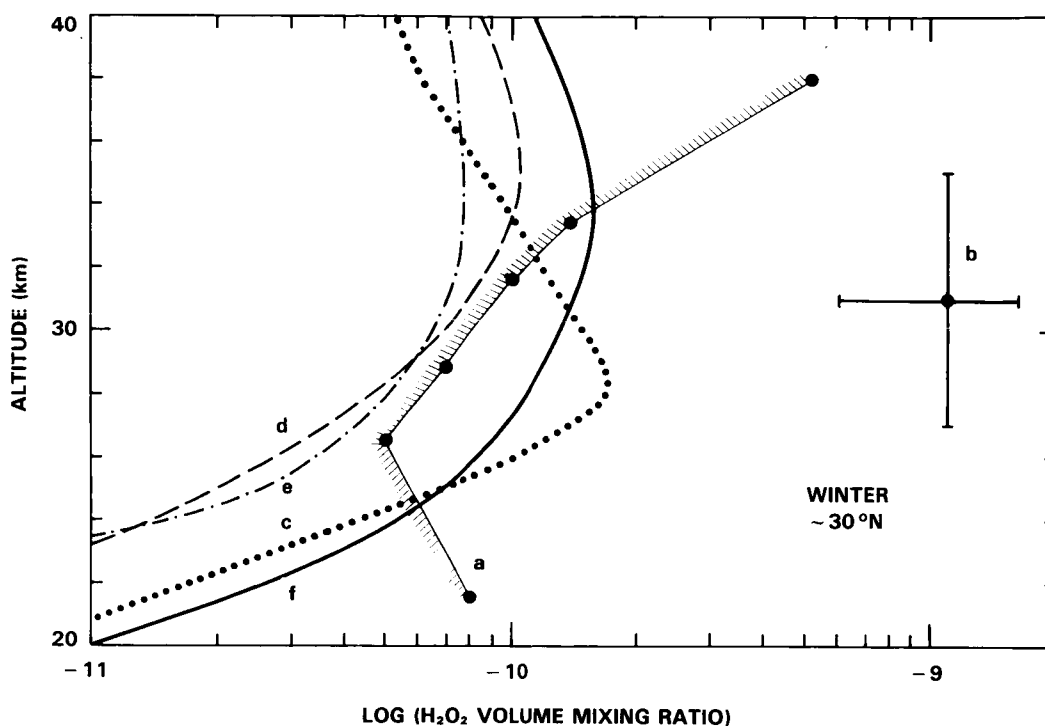
LOG (H₂O₂ VOLUME MIXING RATIO)

Figure 9-10. (a) H_2O_2 measured upper limits by Chance and Traub (1984) for January at 34°N from balloon-borne far IR spectroscopy.

(b) H_2O_2 tentative detection by Waters *et al.* (1981), for February at 32°N from balloon-borne microwave limb sounding spectroscopy.

For comparison, four H_2O_2 theoretical profiles are shown, each using 2-D calculations and JPL-1985 reaction rate data, for winter at 30°N:

(c) A. Owens, private communication.

(d) S. Solomon and R. Garcia, private communication.

(e) P. Guthrie, private communication.

(f) M. Ko, private communication.

The relatively large dispersion in theoretical values may be largely attributable to relatively small differences in assumed abundances of O_3, NO_2 and H_2O, as discussed by Connell *et al.* (1985).

have been detectable with a signal-to-noise ratio of one. At 32 km, where the theoretical H_2O_2 mixing ratio profile has the peak theoretical value, this implies a one-standard-deviation upper limit of about 0.5 ppbv.

The abundance and vertical distribution of H_2O_2 is very sensitive to variations in the long-lived trace species O_3, NO_y, and H_2O. The range of theoretical variation in H_2O_2 mixing ratios allowed by known or probable variabilities in these species has been addressed by Connell, *et al.* (1985) using a diurnally average 1-D model. Their results, which extend over the range 15-35 km, are shown as the shaded region in Figure 9-11. They conclude that temporal variations as large as a factor of 4 to 5 may be expected within the altitude range considered. Since these calculations assumed NASA-JPL (1981) kinetic parameters they should not be compared too rigorously with the other profiles shown in the figures but should be taken to indicate the range of variability expected. The inclusion of error limits in these quantities would extend the region of variability or uncertainty shown in Figure 9-10.
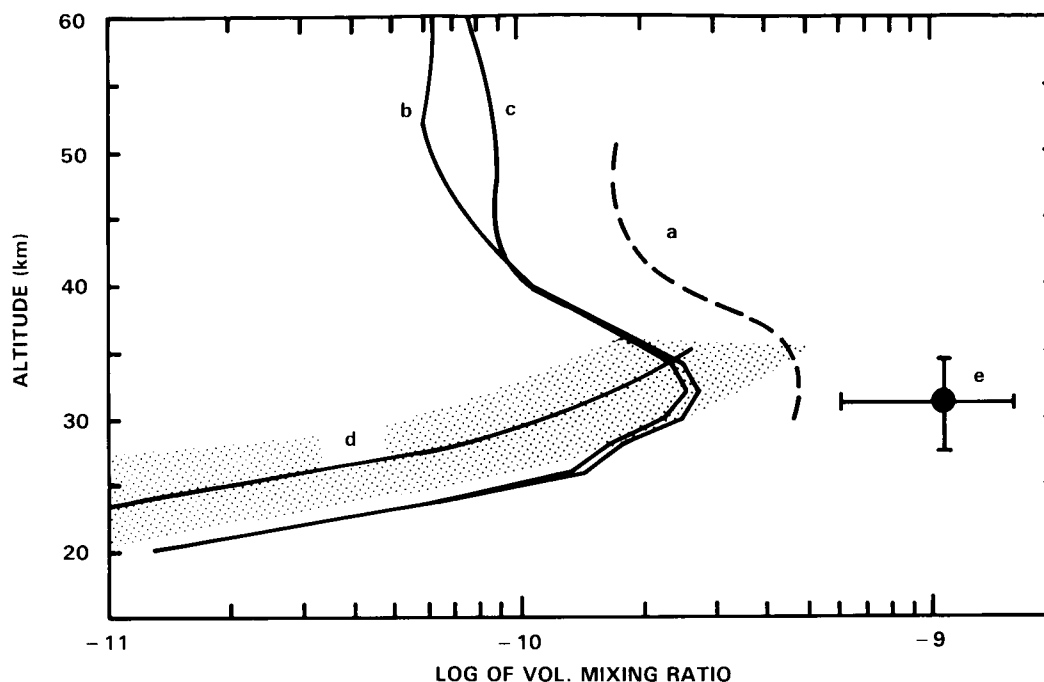
Figure 9-11. (a) H_2O_2 measured upper limit by de Zafra *et al.* (1985b), for May–June at 20 °N from ground-based mm wave emission spectroscopy. (b) Day and (c) Night H_2O_2 theoretical profiles, using 2-D calculations and JPL 82-57 reaction rate data, for the same season and latitude (D. Sze and M. Ko, private communication, (1983). (d) Diurnally-averaged 1-D theoretical H_2O_2 profile using JPL 81-3 reaction rate data (Connell *et al.,* 1985); the shaded region shows the possible range of values of H_2O_2 from variations in O_3, NO_2 and H_2O. (e) H_2O_2 tentative detection by Waters *et al.* (1981), for February at 32 °N from balloon-borne microwave limb sounding spectroscopy.

In summary, there has not yet been any clear detection of stratospheric H_2O_2 despite initial attempts by three groups using different techniques, spectral features and seasons. Judged both by modelling predictions and by the upper limits set by two of these detection efforts, the tentative detection reported by Waters *et al.* appears to be either an anomalous event or an erroneous identification. With improvements in detection techniques measurements of this species are anticipated in the near future.

9.4 WATER (H_2O) MEASUREMENTS

9.4.1 *In Situ* Vertical Profile Measurements of H_2O

There are two important results that have emerged from *in situ* observations since WMO (1982). The first of these deals with the question of the existence and location of a hygropause or minimum in the mixing ratio of H_2O. The hygropause was first seen in *in situ* data and has now been confirmed by LIMS satellite results which show that the region of minimum H_2O in the lower stratosphere extends from ~30 °N to 30 °S and up to ~40 mbar (22 km). The second result concerns the degree of water vapor stratification with altitude in the stratosphere. Both of these points will be discussed in more detail later.

There are two *in situ* measurements techniques which have been used. The first of these, the Ly-α hygrometer (Kley and Stone, 1978) is based on the dissociation of H_2O by Ly (α) (121.6 nm) radiation to produce electronically excited OH* radicals.

$$H_2O + h\nu \rightarrow OH^* + H$$
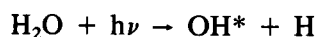
The intensity of the $OH^* \rightarrow OH + h\nu'$ fluorescence is a measure of the H_2O mixing ratio. The accuracy of the method depends on the accuracy with which the cross section (σ) of water at 121.6 nm is known. Kley (1984) has measured σ and estimated the accuracy, $\Delta\sigma/\sigma$ to be 6% at the 95% confidence level. The accuracy is also a function of pressure and, therefore, of altitude. This is because the quenching process:

$$OH^* + M \rightarrow products$$
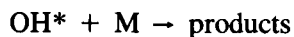
is pressure dependent. The rate coefficient for quenching is estimated to be known with an accuracy of $\pm 20\%$. This error source does not influence the total accuracy of the instrument in the lower stratosphere but becomes the major source of uncertainty at altitudes above 38 km. Other sources of error are considered to be small. These include contamination effects, i.e., possible contributions to the signal from water carried aloft with the instrument or balloon. During the main measurement period the instrument is deployed on a rapidly descending parachute where any balloon wake is absent.

Table 9-1 gives the total estimated accuracy (63% confidence) as a function of height. (X = mixing ratio, σ = estimated fractional percentage total error, including precision).

Table 9-1. Accuracy of the Ly (α) Hygrometer for Various Altitudes (%)

z (km)	10	15	20	25	28	30	38	40
$\sigma X/X$	7.0	7.0	7.0	7.0	7.3	7.5	10.0	12.7

The precision of the Ly-α hygrometer is 2% (one sigma standard deviation at typical stratospheric mixing ratios for integration times of 1 second). If small scale variability is observed, it is considered to be real if the amplitude exceeds 0.2 ppmv at a mean value of $\sim$5 ppmv.

The second method is the frost-point hygrometer (Mastenbrook, 1968). This technique operates on the principle that an equilibrium exists between the water vapor pressure in the atmosphere and an ice surface at the frost-point temperature. The instrument has been used extensively in past soundings and recently (1977) was redesigned to incorporate solid state circuitry and to develop an instrument for routine measurements by a monitoring network. NOAA has made monthly soundings from Boulder, Colorado, with the new instrument since 1981 (Mastenbrook and Oltmans, 1983). A conservative estimate of the H_2O mixing ratio accuracy is $\pm 17\%$ ($\pm 1\,°C$ frost point temperature).

Eight profiles of water vapor across the tropical tropopause have been reported by Kley et al. (1982, 1983). These were obtained during the NASA sponsored Stratospheric-Tropospheric Exchange-Experiment in 1980. Figure 9-12 shows the mean profiles for water vapor and temperature measured on the eight flights. The mean water vapor mixing ratio of the hygropause was 3.4 ppmv with a standard deviation of 0.24 ppmv. Table 9-2 gives a list of tropical soundings of the mixing ratio of water vapor at the hygropause by *in situ* instruments.

457

Table 9-2. Mixing Ratio of Water Vapor at the Hygropause

Hygropause Mixing Ratio	Location	Time of Measurement	Reference
3.4	Trinidad W.I.	monthly, 1964 and 1965	Mastenbrook, (1968)
2.7	Brazil	27 Sept 1978	Kley *et al.* (1979)
3.4	Panama	8 values Aug/Sept 1980	Kley *et al.* (1982, 1983)
3.1	Wyoming*	Feb. 1 1979	Danielsen and Kley (1985)

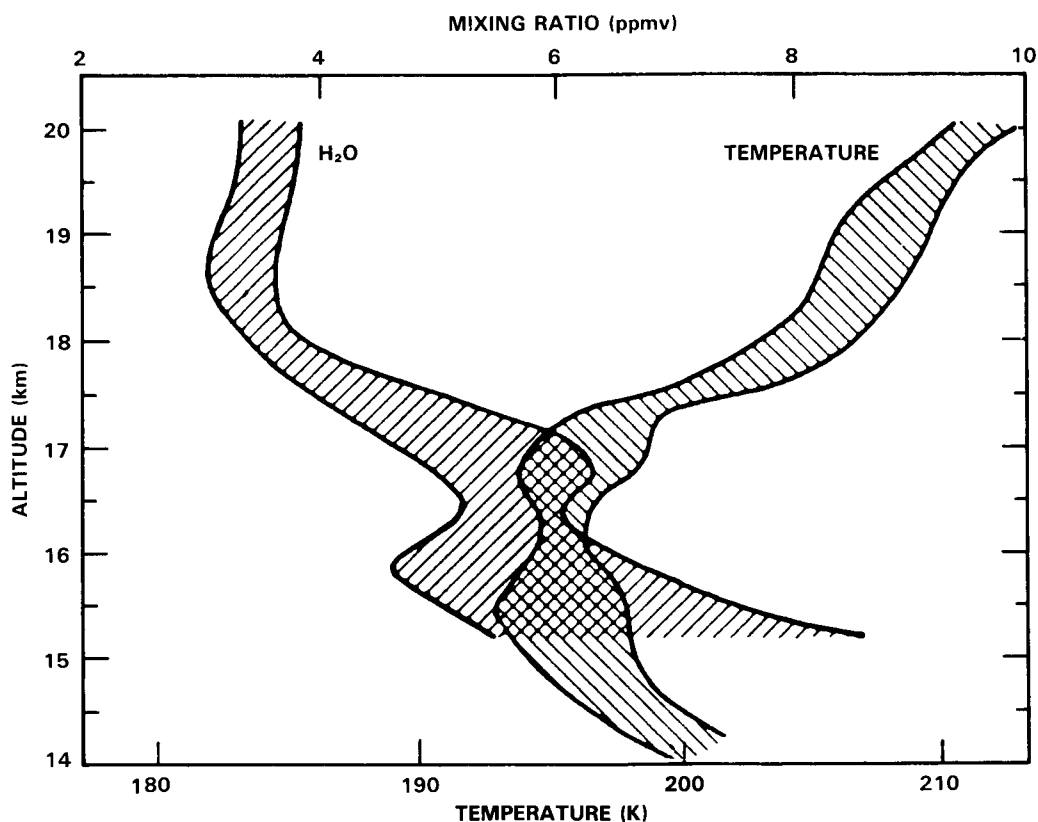*As discussed by Danielsen and Kley (1985), the air traveled to Wyoming from the tropics in about 5 days.

Figure 9-12. Standard deviations from the mean (± 1σ) of eight profiles of H_2O and temperature measured by instruments on the NASA U-2 aircraft over Panama, 1980. Areas between the lines defining − 1σ and + 1σ are hatched. The H_2O data has been multiplied by a factor of 0.88 due to changes in the calibration factor.
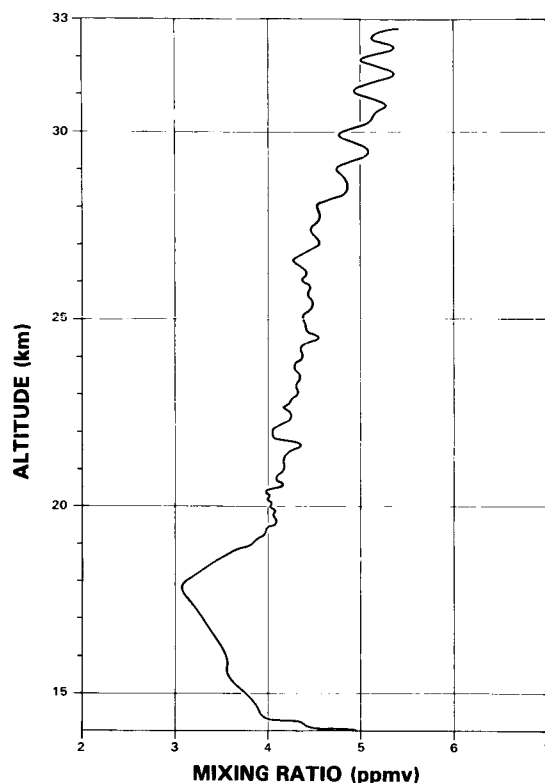
Figure 9-13. Microstructure of water vapor observed over Palestine, Texas, May 7, 1981 (Kley *et al.*, 1985, unpublished).

These *in situ* data provide evidence for a mixing ratio of slightly less than 3.4 ppmv at the tropical hygropause. Compared to this, the LIMS data discussed later are slightly lower (≈ 2.7 ppmv). However, a secular trend has been observed in water vapor mixing ratio in the lower stratosphere at extratropical latitudes (cf Foot, 1984, and references therein) which may or may not be present in the tropics. Furthermore, Mastenbrook and Oltmans (1983) find a weak quasi-bienniel oscillation (QBO) in the water mixing ratio over Washington, D.C. and Boulder, Colorado. A similar QBO discussed by Hyson (1978) is present over Australia. Because of a lack of data nothing can be said about a QBO in the tropical stratosphere. A direct comparison of hygropause mixing ratios from LIMS and balloon *in situ* measurements is therefore not possible. The Wyoming flight (Danielsen and Kley, 1985) was made during the time that LIMS operated and the observed minimum of the mixing ratio of 3.1 ppmv was traced back to the lower tropical stratosphere. Although the travel time was short (≈ 5 days) some "filling up" of the minimum could have occurred during the transit, so that 3.1 ppmv would represent an upper limit of the hygropause mixing ratio consistent with the LIMS value. Further studies are required to resolve the discrepancy between the satellite and the *in situ* results.

Kley *et al.* (1980) reported a very strong vertical stratification of stratospheric water vapor. Since the time of the early measurement, similar features have been found on subsequent flights. Figure 9-13 gives a more recent example. Kley *et al.* suggest that this oscillatory behavior of middle and upper stratospheric water vapor is most probably of photochemical origin via CH_4 oxidation. This conclusion is derived from the argument that the amplitude of the oscillation tends to grow larger with increasing

altitude which indicates that any variability which might be generated by the dynamics of the troposphere/ stratosphere exchange process cannot be responsible. Changes in water vapor mixing ratio, due to photochemistry, happen on a long time scale (> 1 year) in the stratosphere. The observed local variability must, it seems, be caused by quasi-horizontal, highly stratified and stable advection from regions of the stratosphere where, due to the slow photochemistry, large scale anticorrelative regions of H_2O and CH_4 exist. The most plausible explanation of the oscillation over a fixed location is long-range transport from those regions. Wind speeds must be highly oscillatory in altitude but stable over several days in order to achieve the observed variability.

A number of other water vapor profiles have been measured since WMO (1982), using mass spectrometric, cryogenic sampling and remote sensing techniques. Descriptions of these techniques are not included here. Many of them have been used in the *in situ* H_2O vapor and BIC intercomparison campaigns and are discussed in Appendix C. Rippel (1984a) recently conducted occultation measurements of H_2O at Aire Sur L'Adour (44° N) from a balloon over the altitude range 26 to 38 km and obtained an essentially constant mixing ratio of ~3.5 to 4.0 ppmv. In general all the data since WMO (1982) (i.e. satellite, BIC, and *in situ*) are consistent with the picture of increasing mixing ratio with altitude in the tropics and low values of ~3 ppmv at the hygropause location. The *in situ* measurements shown in Figures 9-14 and 9-15 and the remote sensing measurements shown in Figures 9-16 and 9-17 made during the *in situ* and BIC campaigns, respectively, are typical.
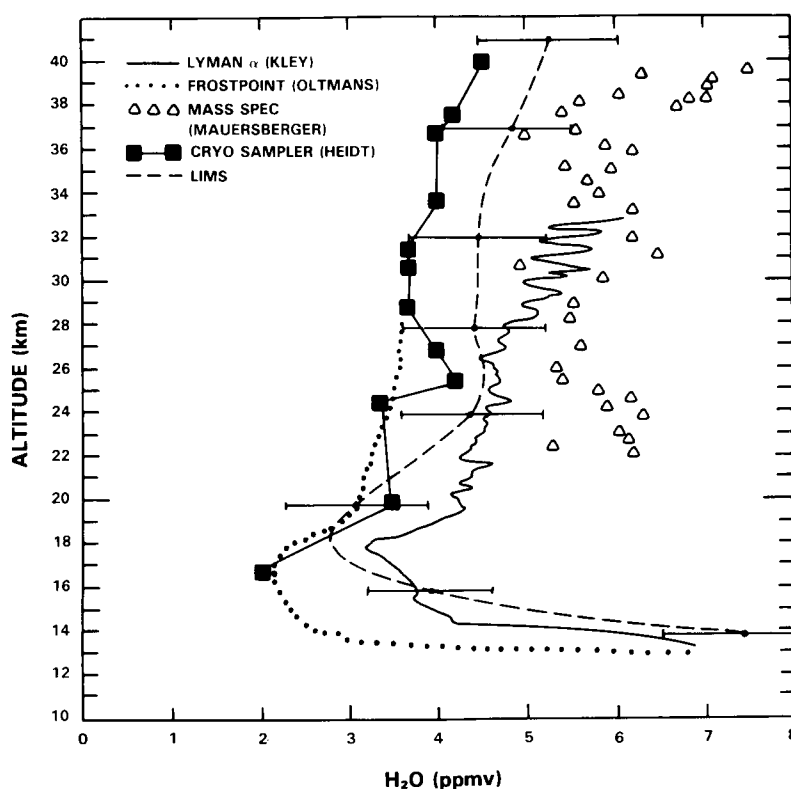

Figure 9-14. Final results from the *in situ* samplers of stratospheric water vapor of the first International Water Vapor Intercomparison, held over Palestine, Texas, May 7, 1981. (see Appendix C). LIMS zonal mean profile for 32°N and May 6–10, 1979 is given by dashed line.
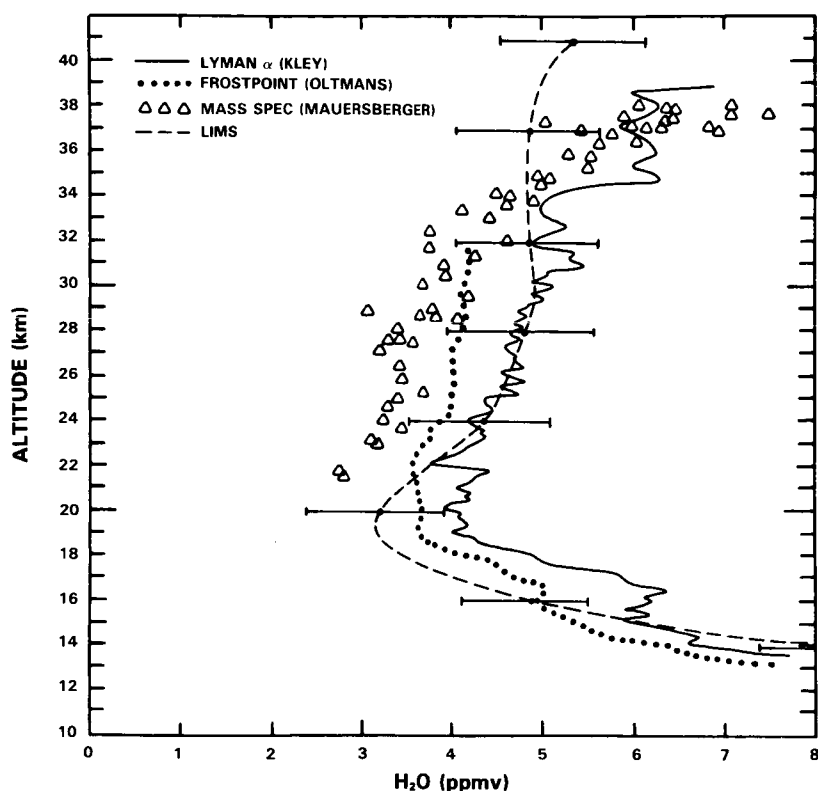
Figure 9-15. Preliminary results from the in situ samplers of stratospheric water vapor of the second International Water Vapor Intercomparison, held over Palestine, Texas, October 11, 1983. (see Appendix C). LIMS Zonal Mean Profile for 32 °N and October 27-31, 1978 is given by dashed line.

9.4.2 LIMS Water Vapor Measurements

The LIMS instrument is a limb scanning radiometer with six channels centered at wavelengths between 6.2 μm and 15 μm. It flew aboard the Nimbus 7 spacecraft operating from the time of launch on October 24, 1978, until the end of the planned lifetime of the solid cryogen cooler on May 28, 1979. The standard IR limb sounding approach was used; vertical profiles of radiance emitted by the 15 μm CO_2 band were inverted to obtain temperature profiles and this information was then used with the 6.3 μm band water vapor radiances (covering the 1370 cm^{-1} to 1560 cm^{-1} range) to obtain vertical water vapor mixing ratio profiles. The vertical resolution of the measurements was 4 km. These data have been reduced and archived in the National Space Sciences Data Center (NSSDC). The archived results cover the altitude range from about 100 mb (16 km) to 1 mb (50 km) and extend from 64 °S to 84 °N in 4 ° latitude increments. The measurements were made night and day almost continuously during the mission (11 days on, 1 day off duty cycle).

An extensive discussion of efforts to validate the LIMS water vapor results has been presented by Russell *et al.* (1984c). The validation approach included detailed ground simulations taking various experimental error sources into account in order to assess accuracy and precision, verification of calculated precision values by studying consecutive orbital data, and comparisons with data collected in 13 balloon underflights to obtain further confidence in orbital results. Five LIMS profiles, covering ± 2 ° of latitude were averaged and compared to balloon data. The mean difference with balloon results was ~ 7 to $\sim 20\%$ (~ 0.1 to 0.3 ppmv) over the 5 to 100 mb (~ 40 km to ~ 16 km) range. The primary systematic error sources in order of importance are temperature profile errors, molecular oxygen absorption coefficient
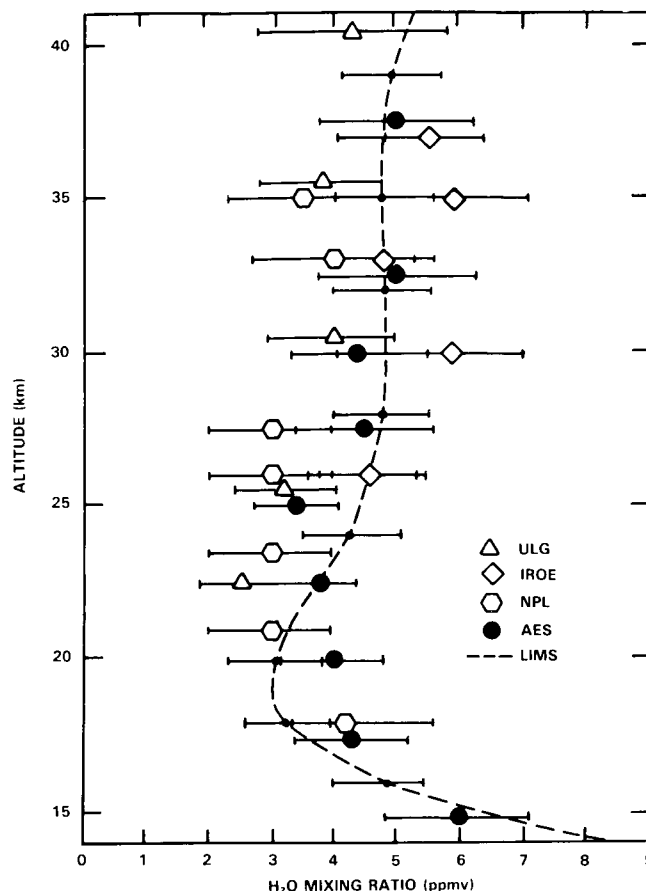
461

Figure 9-16. H₂O profiles obtained during BIC I using remote sensing techniques. The AES data were obtained on September 22, NPL and IROE data on October 5, 1982. The error bars of each measurement are one standard deviation and include both random and estimated systematic errors. The LIMS 5 day zonal mean profile for October 27–31, 1978, is also shown in the figure. Such a comparison presumes that interannual variability is small and that the BIC air mass is representative of the zonal mean.

errors (for altitudes < 20 km), spectral parameter errors, instrument vertical field of view errors, and other instrumental effects. Temperature error effects are dominant at all levels above about 18 km. The estimated single profile accuracy is 20% from 20 km to 45 km and 30 to 35% at 50 km. The LIMS data showed apparent profile-to- profile variations in mixing ratios which approach 40% near 50 km. Such variations are only of the order of 10% below 30 km. These variations occurred somewhat randomly along an orbit track and are believed to be due to a combination of spacecraft motion effects and possibly small variations in radiance bias error. For these and other reasons, the LIMS team has placed more confidence in zonal mean profiles rather than single profiles. The comparisons with balloon data showing overlap of the LIMS and balloon data error bars, and the high precision estimated from orbital data give high confidence in the LIMS results.

Of special interest are the error estimates for zonal mean profiles at tropical latitudes in the 50 mb (20 km) to 70 mb (18 km) range where the hygropause (Kley *et al.*, 1982) is located. The major error sources in this pressure range are temperature and molecular oxygen effects. Spatial sampling biases due to loss of data from cloud contamination in the tropics is also a consideration at 70 mb (18km) and below. As discussed in Remsberg *et al.* (1984b), simulations were done using realistic LIMS temperature bias errors of $+1$K at 50 mb (20 km) and $+4$K at 70 mb (18km) (Gille *et al.*, 1984b) combined with a
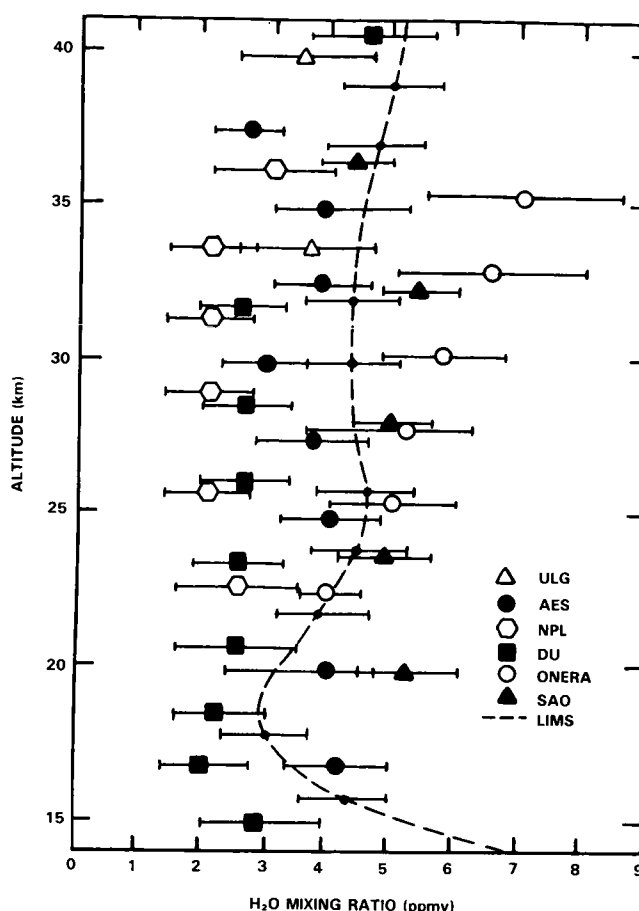
462

Figure 9-17. H$_2$O profiles obtained during BIC II using remote sensing techniques. The AES, SAO, NPL, and ONERA data were obtained on June 20. The DU and ULG data were obtained on June 17, 1983. The error bars of each measurement are one standard deviation and include both random and estimated systematic errors. The LIMS 5-day zonal mean profile for May 23–27, 1979, is also shown in the figure.

20% uncertainty in O$_2$ emission. Temperature bias error effects near the tropopause are not too severe due to compensating differences in vertical resolution of the temperature and H$_2$O channels (Russell *et al.*, 1984c). Based on these calculations, it was estimated that between ±15° latitude the archived results are too low by 0.3 ppmv at 50 mb and 0.6 ppmv at 70 mb with much smaller biases at ±25° latitude. Even after allowing for such biases a distinct hygropause is still evident. Remsberg *et al.* (1984c) also point out that the altitude position of the minimum water vapor mixing ratio in the lower stratosphere for tropical latitudes is likely to be 1 to 2 km too high.

Russell *et al.* (1984c) have noted that there is an apparent diurnal variation in water vapor (day values higher than night values) of about 1 ppmv to 2 ppmv at 1 mb (50 km) decreasing to negligible values at about 10 mb (30 km). This is most likely due to day/night temperature effects from LIMS temperature profiles used for retrieval or non-local thermodynamic equilibrium effects (not included in LIMS H$_2$O retrievals). An unaccounted-for physical phenomenon giving a radiance change equal only to the radiance noise can cause this effect. As a result, the nighttime results are probably more reliable, especially for quantitative studies of vertical mixing ratio changes.

Table 9-3. LIMS Estimated Accuracy and Precision for H_2O Measurements

Parameter	Altitude			
	16 km	18 – 20 km	20 – 40 km	50 km
Accuracy (ppmv)				
tropics (1)	±0.7	±0.3 to ±0.6	±0.8	±1.5
mid and high latitudes	±0.4	±0.4	±0.8	±1.5
Precision ppmv (2)	±0.1	±0.3	±0.3	±0.5

(1) These apply to single profiles. Some systematic effects will be reduced when zonal mean profiles are calculated. Thus the estimates are somewhat conservative.

(2) These values apply to single profiles as determined by calculating standard deviations of a series of 6 sequential scans about the 6 scan mean as a function of latitude.

Ground simulation and orbital results were both in accord, giving single profile precision values which varied from 0.1 ppmv to 0.3 ppmv in the altitude range from 16 km to 40 km. Again, the precision of the zonal mean product is improved over the single profile results (e.g. by a factor of 2 for daily zonal means). The largest variation occurs near the stratopause where the standard deviation of the daily zonal mean about the monthly zonal mean is typically 0.4 ppmv to 0.8 ppmv. At least part of this variation is due to true atmospheric changes, but some portion is due to the spacecraft motion or radiance bias effects discussed above. A summary of estimated LIMS water vapor accuracy and precision is included in Table 9-3.

Typical water vapor zonal mean nighttime profiles for November 1978 from LIMS are shown in Figure 9-18. The profiles show a clear, well developed minimum in mixing ratio (hygropause) that occurs above the tropopause. This feature is evident at low to mid latitudes between 100 mb (16km) to 30 mb (24km). There is a slight trace of the hygropause present even at 56 °S. Other features that should be noted are an increase in mixing ratio with height in tropical latitudes that appears to be consistent with the methane oxidation theory (see section 2.4.8) and a constant mixing ratio profile or even a slight decrease with altitude at mid to high latitudes. There are some variations in the profile during the seven months of LIMS data, but this general description suffices to describe the distribution.

The zonal mean pressure versus latitude cross sections of monthly averaged nighttime water vapor are shown in Figures 9-19 and 9-20. A number of important characteristics emerge upon examination of these plots. The results show a broad minimum in mixing ratio that persists during all 7 months and occurs mainly in the tropics in the pressure range from 100 mb (16 km) to 30 mb (24km). Based on LIMS latitude versus longitude plots and time series analyses, we can conclude that variability in the latitude-altitude hygropause area is small over the life of LIMS and is quite uniform with longitude.
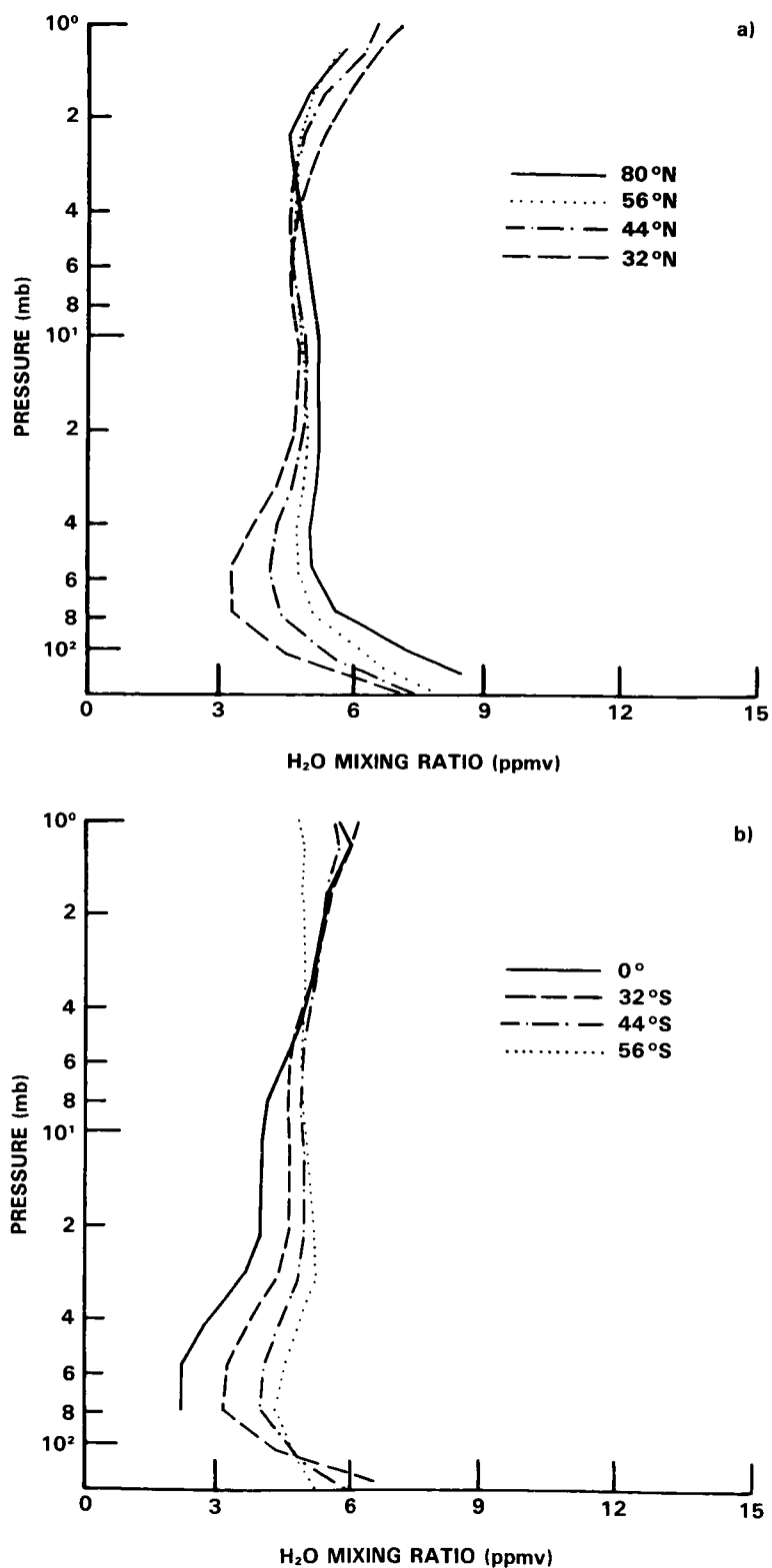
Figure 9-18. (a) LIMS Monthly Mean H_2O Mixing Ratio for November 1978 in the Northern Hemisphere. (b) LIMS Monthly Mean H_2O Mixing Ratio for November, 1978 in the Southern Hemisphere.

465
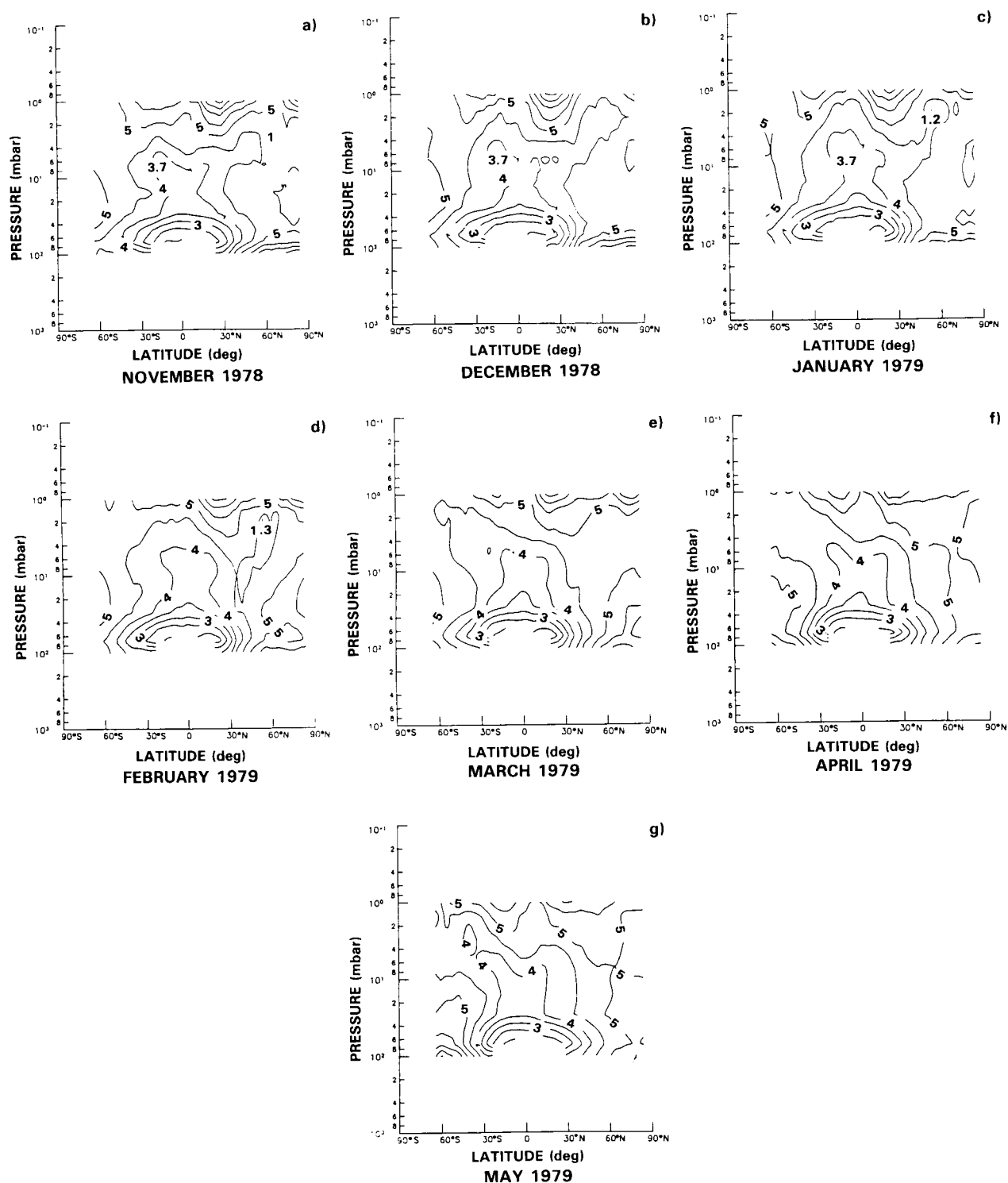
Figure 9-19. LIMS monthly zonal mean water vapor pressure versus latitude cross sections for (a) November, and (b) December, 1978, and (c) January, (d) February, (e) March, (f) April, and (g) May, 1979 (0.5 ppmv contour intervals)

466

a)

b)

c)

d)

e)

f)

g)
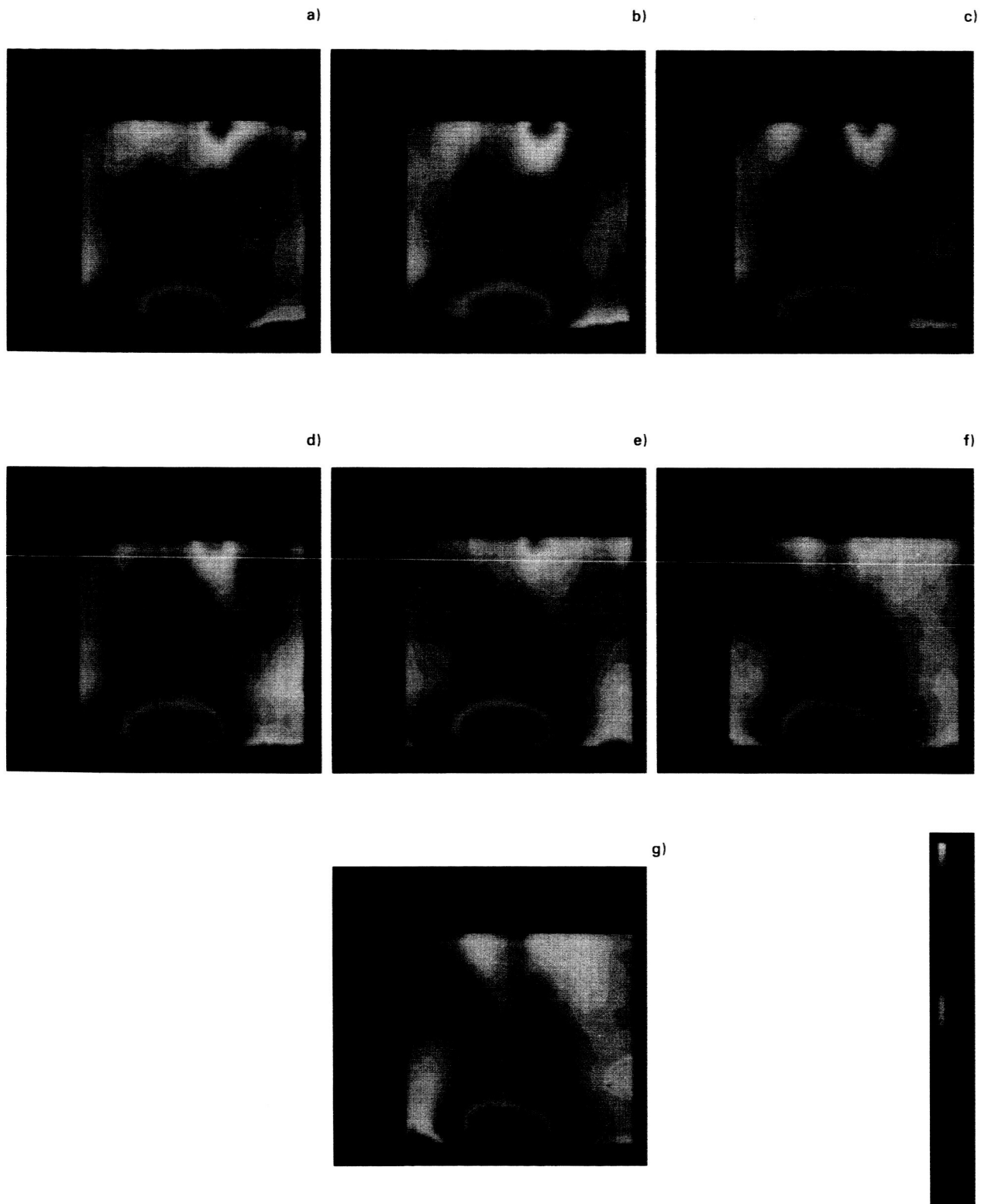
Figure 9-20 . LIMS monthly zonal mean water pressure versus latitude vapor cross section for (a) November, and (b) December, 1978, and (c) January, (d) February, (e) March, (f) April, and (g) May, 1979.

In the tropics near the 10 mb (~ 30 km) level, the presence of a double minimum in mixing ratio exists which correlates closely with a double maximum in SAMS CH_4 and N_2O measurements. This suggests an upward motion carrying water vapor from the dry region below and then branching northward and southward. In November, the "dry" contours (e.g. 4 to 4.5 ppmv) extend toward the 1 mb (≈ 50 km) level at high northern latitudes. At the same time, in high altitudes and latitudes of the Southern Hemisphere, a broad region of higher mixing ratio (5 ppmv) exists. This picture gradually changes until in March the "dry" contours have reversed to extend southward and upward. In May, the Southern Hemisphere low water vapor air extends further toward high altitudes and southern latitudes. This is further emphasized in Figure 9-21, which compares LIMS H_2O and SAMS CH_4 monthly zonal mean results. Note that where LIMS H_2O is low, SAMS CH_4 is high. The tropical methane source region is obvious in this figure. There are regions of maximum H_2O mixing ratio near the 1 mb (≈ 50 km) level in the tropics that occur on each side of the equator and tend to persist in all 7 months. The maximum values are consistent with the oxidation of methane as a water vapor source.

There is an increasing gradient of mixing ratio poleward both north and south at all levels from 100 mb to about 4 mb. Here, the direction of the gradient gradually reverses with increasing altitude. In the lower
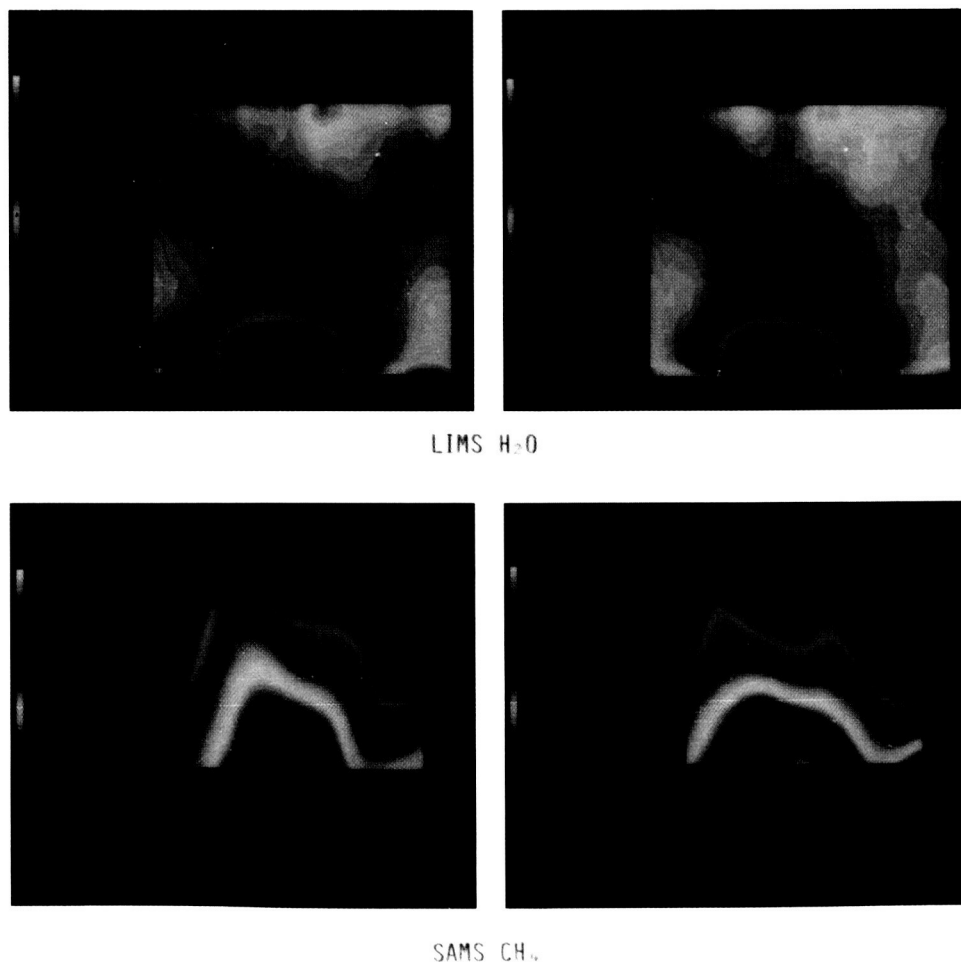

LIMS H_2O

SAMS CH_4

Figure 9-21. LIMS H_2O and SAMS CH_4 monthly zonal mean pressure versus latitude cross sections for March and April 1979.

stratosphere, the data imply the presence of a low altitude net circulation with the strongest circulation toward the summer pole. Such an implied mechanistic circulation is counter to the calculated circulations reported in Chapter 6 which show stronger net transport by waves towards the winter pole in the lower stratosphere. Note the elongated contours of minimum mixing ratio extending horizontally from the hygropause region in the 100 mb (16 km) to 30 mb (24 km) range to about 60° S during November through March but then going through a rather quick reversal so that in May, the low mixing ratio contours extend to 60° N. This behavior is accompanied by a significant change in mixing ratio in the low stratosphere at high latitudes. In the Northern Hemisphere, at 60° N and 100 mb (16 km) in November, the mixing ratio is 6.5 ppmv. During the mission, it gradually decays to 6 ppmv in March and 5 ppmv in May. At the same time, at 60° S the opposite trend occurs, i.e. in November the mixing ratio is 4.5 ppmv, 5 ppmv in March, and 6.5 ppmv in May. Examination of the changes in each hemisphere near 60° latitude and at levels up to about 40 mb (22km) show a general increase in water vapor during winter. The data seem to suggest a mechanistic model where water vapor is being mixed into the stratosphere from the troposphere during these times, possibly because of northern advection of water vapor through the tropopause break region near 30°N.

It is apparent that the LIMS water vapor cross sections contain much information not only on the water vapor budget in the stratosphere but also on the net circulation patterns as suggested in this brief description. Since CH_4 oxidation, the primary source of H_2O, is generally much slower than transport effects over most of the stratosphere, the water data should be useful in transport studies. Nevertheless, both processes must be considered in attempting to understand the observed distribution. A combination of SAMS and LIMS data should prove to be most helpful in any such studies.

The variability in zonal mean water vapor observed by LIMS in the 16 km to 50 km range is generally small with the greatest changes occurring in the high latitudes of the winter hemisphere. Figures 9-22a,b show pressure versus latitude cross sections of the standard deviation of daily zonal mean profiles about the monthly zonal mean for November and May. Throughout most of the stratosphere, this variation is very small (< 0.2 ppmv). Evidence of increased changes at high winter or fall latitudes in the middle stratosphere is indicated by the closed contour at ≈60°N in November and 45°S in May. The changes at the extreme upper altitude near 1 mb are in part real, but it is difficult to say how much of this variation is driven by the spacecraft motion and the variable bias problem discussed previously.

One of the important questions that prevailed prior to LIMS dealt with the issue of spatial and temporal variability of H_2O. Much of this question has been answered by LIMS results. Figure 9-23a,b shows 5-day zonal mean latitude versus time cross sections at 50 mb (≈20 km) and 10 mb (≈30 km). These pressure levels were chosen to show changes in the hygropause region and in the mid stratosphere. The lowest water values at 50 mb occur in the ≈±15° latitude range and have a value of ≈2.7 ppmv (2.4 + 0.3 ppmv for the temperature bias effect). The variation in these minimum values (cf Figure 9-23) is only ~0.3 ppmv over the life of LIMS. Note the rather sharp latitudinal gradients. The region of greatest "short term" variability lies above ≈50°N in winter and is on the order of 0.5 ppmv. The greatest long term changes occur in the high latitudes of both hemispheres as already discussed. The same kind of plot at 10 mb (30 km) shows a rather different picture. The latitudinal gradients are greatly reduced at 10 mb and the variation is < 0.25 ppmv at all latitudes up to about 50N and on the order of 0.3 ppmv at higher latitudes. Variations at all altitudes for the equator and 60°S are shown in Figures 9-24a,b. The vertical mixing ratio gradient at 60°S is much smaller than at the equator throughout the mission. The mixing ratio is nearly constant with altitude until fall and early winter approaches. At that time, there is a mixing ratio rise in the lower stratosphere and a slight decline near 50 km. There appears to be more variability at the equator than at 60°S most of the time although absolute variation differences are still small.

HYDROGEN SPECIES

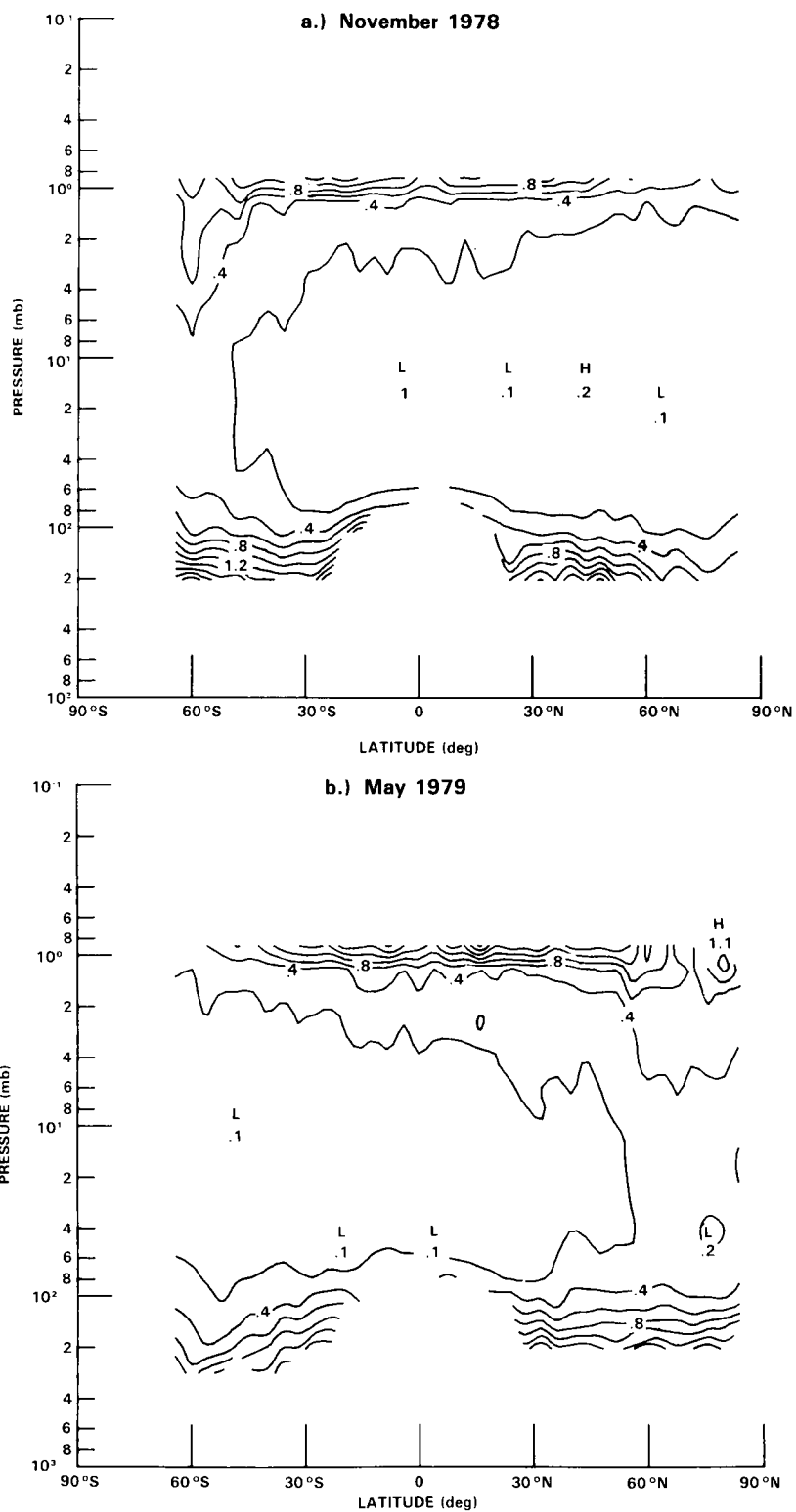**Figure 9-22.** LIMS H_2O standard deviation of daily zonal mean profiles about zonal mean for (a) November, 1978 and (b) May 1979
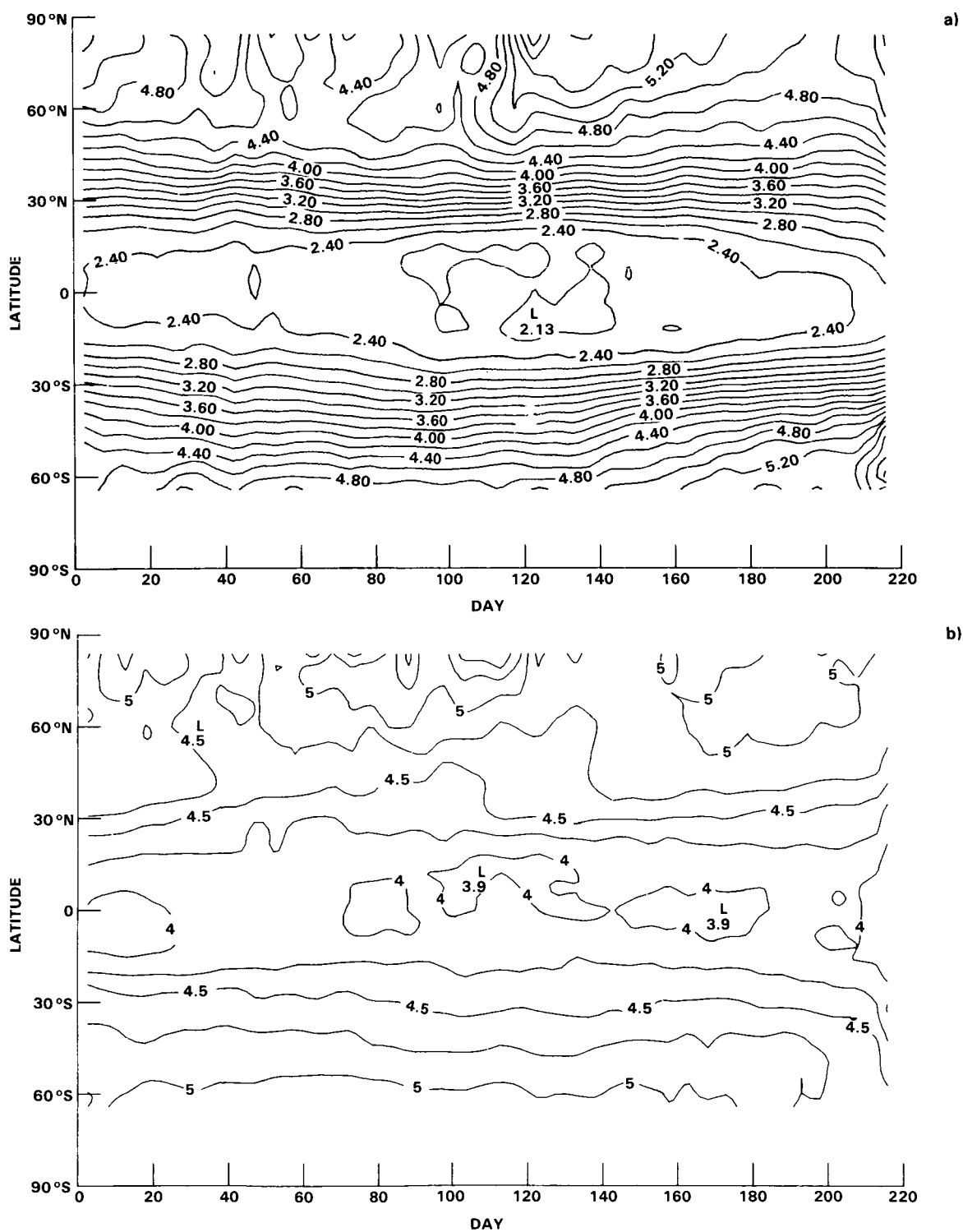
470

Figure 9-23. LIMS H_2O latitude versus time cross section at (a) 50 mb and (b) 10 mb (0.25 ppmv intervals, 5 day means).
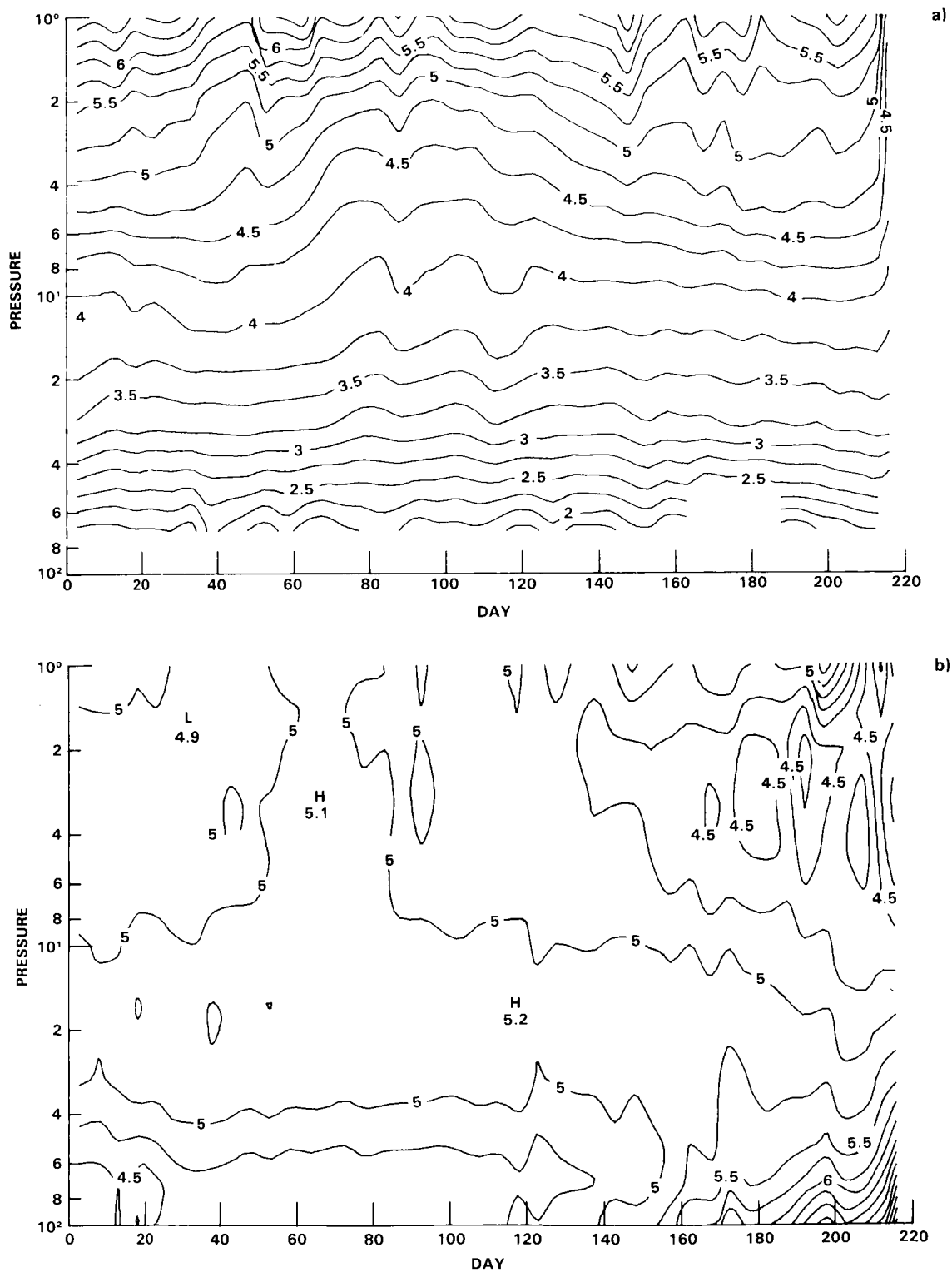
471

Figure 9-24. LIMS H₂O pressure versus time cross section at (a) the Equator and 60 °S (0.25 ppmv intervals, 5 day means).

472

Figure 9-25 is a polar stereographic plot of water vapor at 50 mb (≈ 20 km) for February 2, 1979, Northern Hemisphere. This plot was made from the LIMS mapped results. Mapping was done using the sequential estimator Kalman filter method of Rodgers (1976b). Up to 13 Fourier coefficients were obtained defining a zonal mean and six longitudinal wave numbers at each of 38 LIMS latitude points $\sim 4°$ increments. Because fewer profiles are available (due to cloud contamination) for the low altitude 50 mb analysis, (Figure 9-25) only the largest wave numbers, up to wave number 4 have been calculated. The strong meridional gradient showing the extension of the hygropause to mid latitudes is evident, with some interesting variations at high latitude that seem to reflect the advection of low water vapor to higher latitudes. The high latitude variations are typical of dynamically disturbed periods. Longitudinal variations are also present at low latitudes, but the amplitude is only of the order of 0.2 ppmv.

In summary, the LIMS H_2O data show a zonal mean vertical profile which increases with increasing altitude in the tropics to a maximum value of ≈ 5.5 to 6 ppmv at the [1mb] 50 km level. The profile in mid to high latitudes shows either a constant value or a slight decrease with altitude. The zonal mean altitude versus latitude cross section shows a broad region of low mixing ratio (≈ 2-3 ppmv) [the hygropause] from 35 °N/S to 45 °N/S and extending to ~ 40 mb. The data show evidence of dry air being carried upward and branching north and south in accord with the Brewer-Dobson theory. The strongest implied net circulation is toward the winter pole at high altitudes. The high latitude ($> 50°$), winter, lower stratosphere ($p > \approx 60$ mb) appears to be a region where water enters the stratosphere from below. It is not clear, however, how important this is in terms of the total water vapor budget or what the exact mechanism could be. A latitudinal gradient in mixing ratio exists at all times during the LIMS mission with a poleward increase at low to middle stratosphere altitudes and a poleward decrease higher up. Variability in the zonal mean mixing ratio is small most of the time and is greatest in winter high latitudes. Longitudinal variability in the tropics is < 0.5 ppmv and on the order of 1 to 1.5 ppmv at mid and high latitudes.

Comparisons were made between LIMS and balloon H_2O measurements as part of the *in situ* and BIC intercomparison campaigns. It should be noted though that LIMS data were taken about 4 years earlier. Therefore, care must be exercised in making such comparisons. The comparison is valid to the extent that interannual variability is small. Examples of these comparisons are shown in Figures 9-14 to 9-17 and are discussed in Appendix C. In general, the vertical profile structures are similar and the uncertainties in the measurements overlap. A major discrepancy exists between satellite results and the mean of three February profiles measured by Evans (1983) during 1977, 1978 and 1979 at 58 °N. Evans (1983) shows low mixing ratio (≈ 2.5 ppmv) in the lower stratosphere as contrasted with values of 4.5 to 5 ppmv from LIMS. The reason for these differences are not known at present.

9.4.3 Measurements of H_2O in the Upper Stratosphere and Mesosphere

The water vapor content in the upper stratosphere and in the mesosphere and its temporal variation have been the subject of a recent series of studies using ground-based microwave spectroscopy to measure the $6_{1,6}$ - $5_{2,3}$ rotational emission line of water vapor at 22.2 GHz (Thacker *et al.*, 1981, Bevilacqua, *et al.*, 1983, Schwartz *et al.*, 1983, Bevilacqua *et al.*, 1985). The weak transition yields an unsaturated line even when looking through tropospheric water vapor from a sea-level location, and with a moderately high resolution, filter-bank spectrometer ($<$ a few tens of KHz per channel) the narrow collision-broadened mesospheric component of the water vapor emission may be singled out for study. The techniques used for recovering a vertical profile from the observed pressured-broadened line shape, as well as the capabilities of the equipment being used, have been steadily improved during the course of these measurements. With the exception of the last cited reference, all of this work was carried out at the Haystack Observatory in Massachusetts (72 °W, 42 °N) at various times of year. Recently, a second instrument has been built and operated by Jet Propulsion Laboratory at Pasadena, CA (117 °W, 34 °N).

Earlier conclusions regarding vertical profiles and mixing ratios (Thacker *et al.*, 1981, Gibbins *et al.*, 1982) have been somewhat modified by improved data reduction and deconvolution procedures [Bevilacqua *et al.*, 1983] but four general conclusions remain.
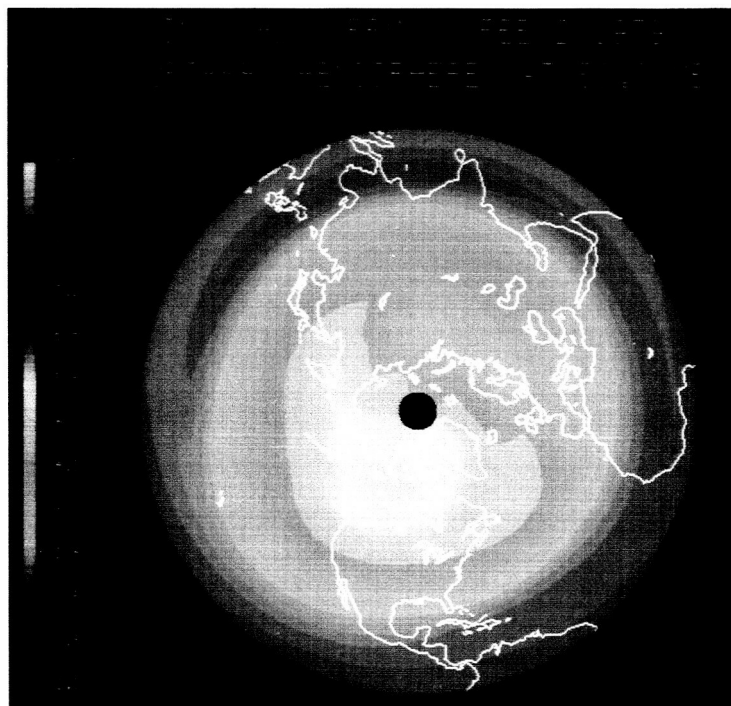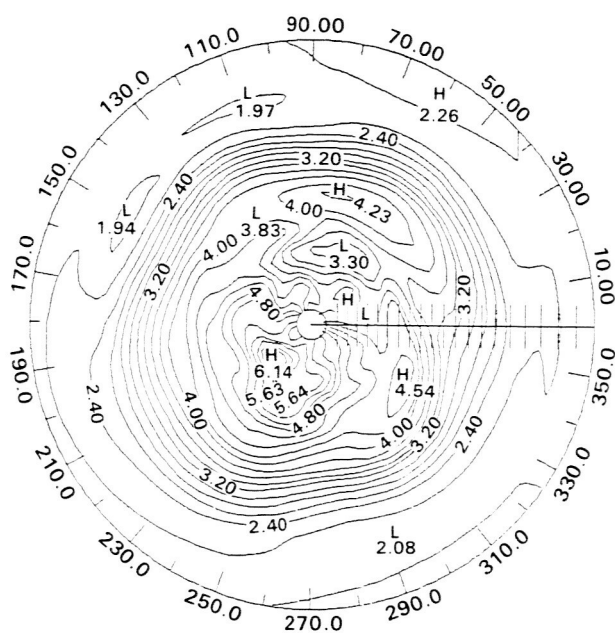
Figure 9-25a and b. Polar stereographic map of LIMS H_2O at 50 mb for Northern Hemisphere for February 2, 1979 (0.20 ppmv intervals).

(1) A significant variability is observed in the mesospheric water vapor profile and column density on a time scale of < 1 day.

(2) Above approximately 65 km, the mixing ratio decreases more rapidly than predicted on the basis of "standard" values for the vertical component of the upper mesospheric eddy diffusion coefficient (see Figures 9-26 and 9-27). Evidence of this decrease is also seen in unpublished LIMS data and the Spacelab I Grille Spectrometer results and (Lippens et al., 1984).

(3) Water vapor increases throughout the stratosphere and lower mesosphere to a peak in mixing ratio in the range of 55 to 65 km altitude.

(4) There is some evidence for seasonal variation in mesospheric water vapor (see Figures 9-26, 9-27).
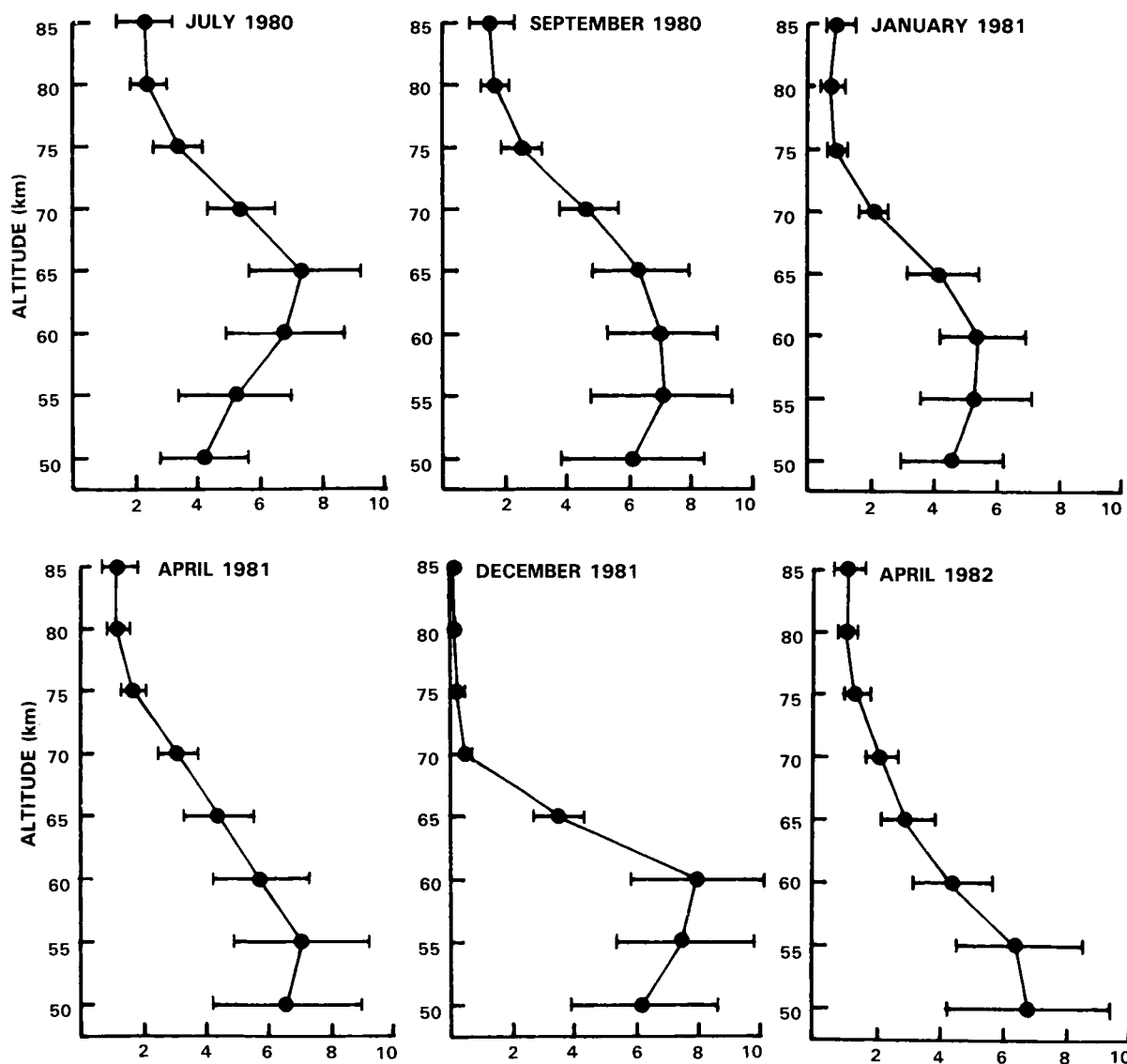
Figure 9-26. Averaged water vapor mixing ratio profiles retrieved by deconvolution of pressure-broadened line shapes. The horizontal bars represent 1σ error levels in the profile retrievals. Data from Haystack Observatory, Massachusetts (42°N). From Bevilacqua, et al. 1983.

475
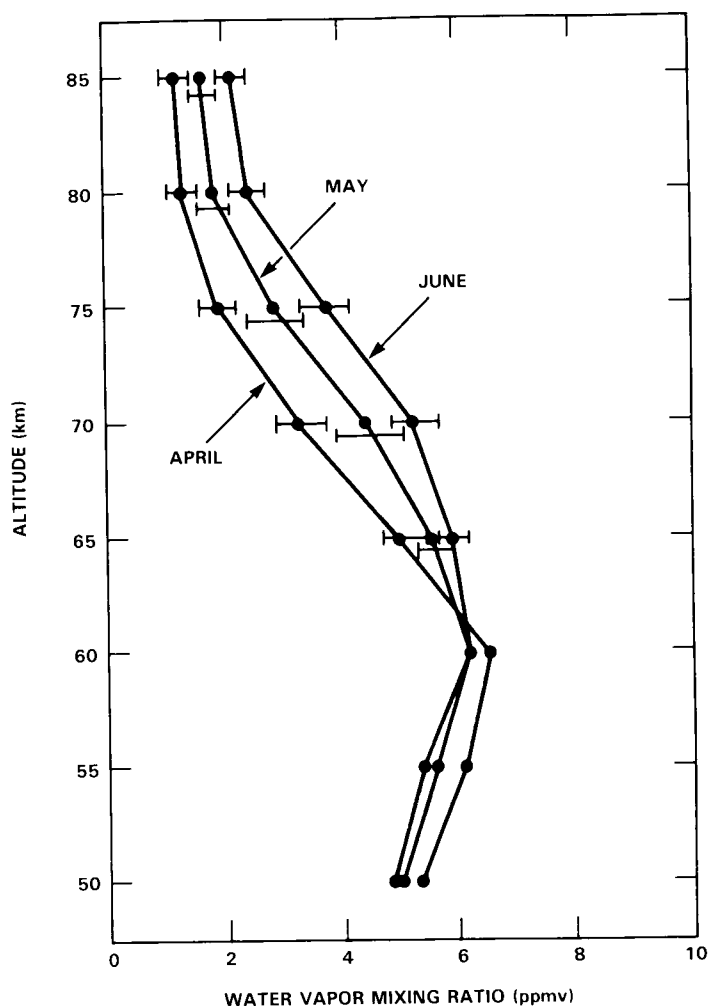
Figure 9-27. Monthly-mean water vapor profiles measured at Pasadena, California (34 °N) over the period March 27, 1984 to April 11, 1984 and May 4, 1984 to July 1, 1984 showing evidence for a seasonal trend towards larger mixing ratios above 65 km.

9.5 METHANE (CH₄) MEASUREMENTS

9.5.1 Vertical Profiles of CH₄ by *In Situ* Measurements

Most of the measurements of low and mid stratospheric CH_4 have been made using the cryogenic sampling technique. Two groups are responsible for the bulk of these measurements, one at the Kernforschungsanlage, Julich (KFA), and the other at the Max-Planck Institut fur Aeronomie, Lindau (MPI).

Improvements have been made in the technique by both groups. The new balloon-borne cryosamplers allow collection of up to 15 distinct samples per flight, each having a volume of at least 20 1 STP. The samples are collected beneath the balloon during slow descent to avoid contamination of the samples by the balloon or the gondola structure, During the 20 to 30 minutes required to collect a sample, the balloon descends over a range of about 1-2 km in the middle stratosphere and a range of less than 0.5 km in the lower stratosphere. This determines the vertical resolution of the observations.

Analyses of the samples are made in the laboratory using gas chromatographic techniques, which give high sensitivity and precision. The precision of the analyses is about 3%. In instances where two samples were collected simultaneously the measured CH_4 mixing ratios were found to differ by less than 4%, indicating that the error in the sampling process is comparable with the precision of the analysis. The accuracy of the calibration is of the order of 5%.

The vertical profile data was extended into the upper stratosphere and mesosphere by a set of new measurements made by a group at the University of Pittsburgh (Zipf et al. unpublished 1985). A rocket borne cryogenic whole air sampler is used that condenses large air samples (~4 1 STP) on gold plated cold fingers cooled to 15 K. Typical height intervals for distinct samples that are collected during a rocket flight are about 3 km at altitudes below 50 km and increase to about 5 km above 70 km altitude. After recovery the samples are transferred into stainless steel containers and their CH_4 content measured by gas chromatography. The samples are calibrated against commercial calibration gases to an accuracy of better than 5%. The precision of the analyses is estimated by the authors to be about 1%.

The vertical profiles obtained from these in situ measurements are shown in Figures 9-28a and 9-28b. The composite data display the same principal features as those discussed in the last assessment document (WMO, 1982) for mid-latitudes. However, more structure is revealed as a result of the improved vertical resolution.

The variance of CH_4 mixing ratios increases with altitude. Up to altitudes of about 24 km it is less than 10% (compared with an experimental accuracy of ~3-5%), but at higher altitudes relatively large deviations from the "average" vertical distribution are observed. The spread of observed mixing ratios is as large as 0.3 ppmv around 30 km. For the data presented in Figure 9-28a, this is most clearly apparent in the two observations made in October 1982 and late September 1980. Both flights show mixing ratios above 26 km that are considerably lower than the other data observed in this altitude range (Schmidt et al., 1984). All the other profiles display mixing ratio values in excess of 0.7 ppmv around 30 km altitude, and rather weak gradients in the middle stratosphere compared to the sharp decreases observed lower down (< 24 km).

Some individual profiles display a stepwise structure (Fabian et al., 1981b, Schmidt et al., 1984) reminiscent of the structure seen in the H_2O profiles (Figure 9-28b). Since the large number of samples collected per sampling flight allows better height resolution, the existence of layers with rather weak mixing ratio gradients is clearly visible. In the case of the profile observed on 9/10/83 the nearly uniform layer extends over almost 10 km. Because of the long (years) photochemical time constants for CH_4 destruction at these altitudes, structure of this kind is thought to be due to the effects of horizontal transport processes (Ehhalt and Tonnissen, 1980). In support of this explanation, recent in situ observations at 44 °N have shown similar structure in the profiles of other long-lived trace gases, such as N_2O, CF_2Cl_2, and $CFCl_3$ (Schmidt et al. 1984). The relative variance of the mixing ratio of long-lived gases that is caused by such structures is quite different for different species. Ehhalt et al. (1983a) have shown that these differences are reduced when the local mean standard deviation of a given species is normalized to its vertical gradient. They defined the ratio:

$$\Delta = \delta(z)/\frac{dH}{dz}$$

as the 'equivalent displacement height'. This quantity shows very similar vertical profiles for various long-lived species, and even for ozone in the lower stratosphere which shows that the scatter in the observation is due to common causes other than experimental uncertainties.
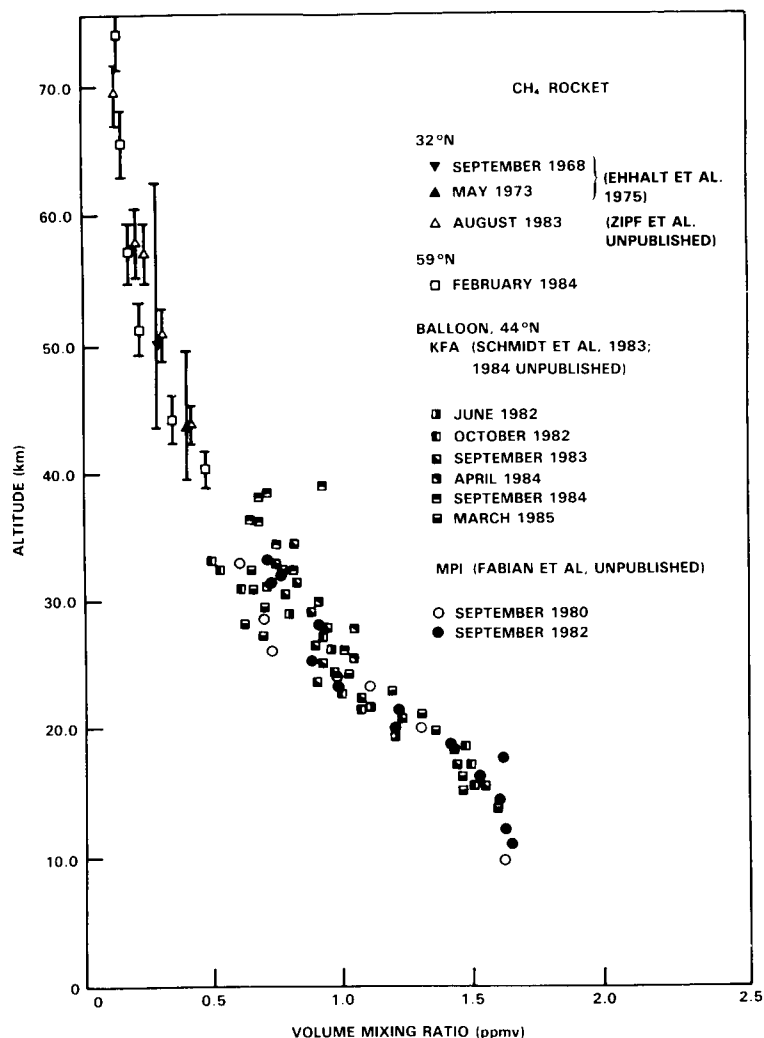
Figure 9-28a. *In situ* measurements of the CH₄ mixing ratio by balloon-borne and rocket-borne cryogenic sampling techniques in the stratosphere and lower mesosphere.

This behavior is in general agreement with the features seen in the SAMS data for northern mid-latitudes in autumn (see Figure 9-29). At levels above 10 mb (31 km) the SAMS data show enhanced latitudinal gradients for this time period. For active dynamical conditions one might therefore expect air masses for higher latitudes with low CH₄ mixing ratios to be transported towards the equator. During the summer months the SAMS data show a more uniform distribution of the CH₄ mixing ratio (Figure 9-29). Again this is confirmed by the moderate variance in the *in situ* data obtained during the other flights.

The upper stratosphere and mesosphere data obtained with the rocket borne cryosampler (Zipf *et al.*, unpublished, 1985) are also shown in Figure 9-28a. They constitute an important addition and extension of the earlier *in situ* observations made by Ehhalt *et al.* (1975). The new data show CH₄ mixing ratios decreasing from 0.48 ppmv at about 40 km to values of 0.14 ppmv at about 75 km. They agree well with the average CH₄ distribution as derived from the SAMS observations at these latitudes. The lower mesosphere observations are still too limited to allow for any assessment of the range of variation of the CH₄ mixing ratio in that region.

478
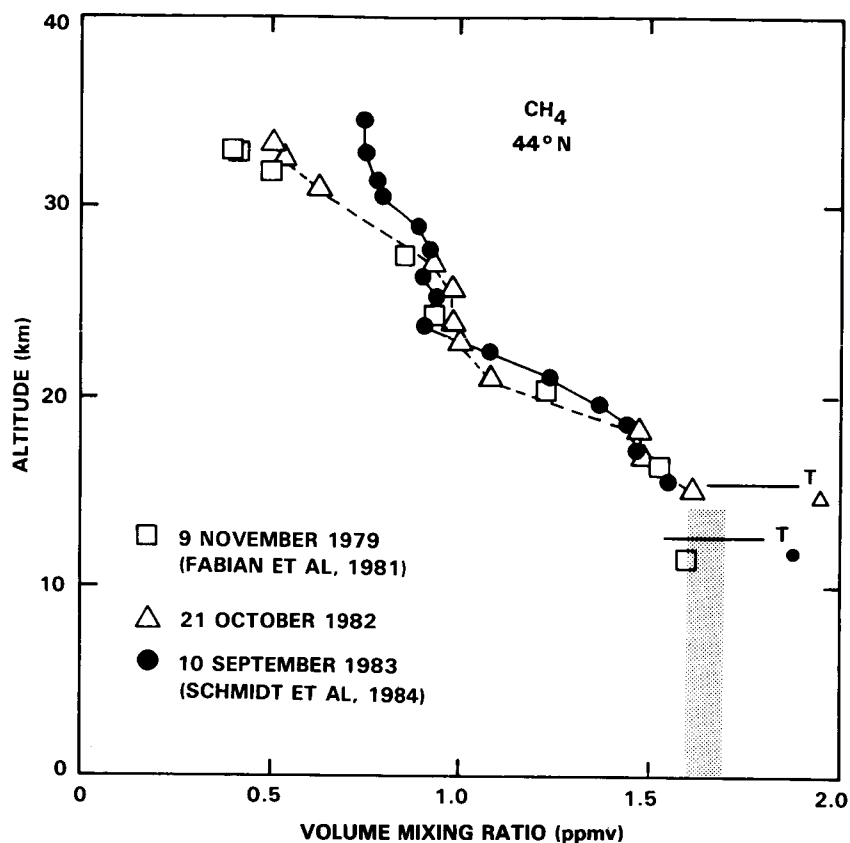
Figure 9-28b. In situ measurements of the CH₄ mixing ratio in the stratosphere (from Fabian *et al.,* 1981 and Schmidt *et al.,* 1984). These data form a subset of the data in Figure 9-28a.

9.5.2 Vertical Profiles of CH₄ by Remote Sensing

A number of CH_4 profile measurements were made during the two balloon intercomparison campaigns (BIC) in Sept/Oct 1982 and May 1983 (Figure 9-30). Details of results of these campaigns as well as a discussion of the accuracies and precisions of the various instruments may be found in Appendix C.

A grille spectrometer was flown on the Spacelab One mission (December 3, 1983 launch) to measure the abundances of a number of minor atmospheric constituents. The instrument (Laurent *et al.,* 1983) uses solar absorption spectroscopy to observe spectral features of CH_4 at around 3000 cm⁻¹. Scans of spectral features taken at different tangent heights were used to derive mixing ratio profiles in the upper stratosphere and mesosphere at two locations at 27°N, 161°E and 176°W. The experimenters (Muller *et al.,*1985) report high accuracy and precision, with 1σ errors of ~15% at all levels. A breakdown of this figure into individual error sources and with altitude is given by Ackerman *et al.* (1985).

Two profiles obtained by the grille spectrometer, taken 1.5 hours apart, are shown in Figure 9-31. Different spectral features around 3000 cm⁻¹ were used for the two retrievals. The data extend from ~27 km to above 70 km and show high mixing ratios (1 - 1.5 ppmv) in the low stratosphere, falling to ~0.5 ppmv at 50 km. Above 50 km the profiles show different characteristics, that taken at 161°E showing a continued gradual fall-off and that at 176°W showing a more uniformly mixed region centered at 65 km with some indication of an increase above. The data therefore show that little or no longitudinal

479

HYDROGEN SPECIES
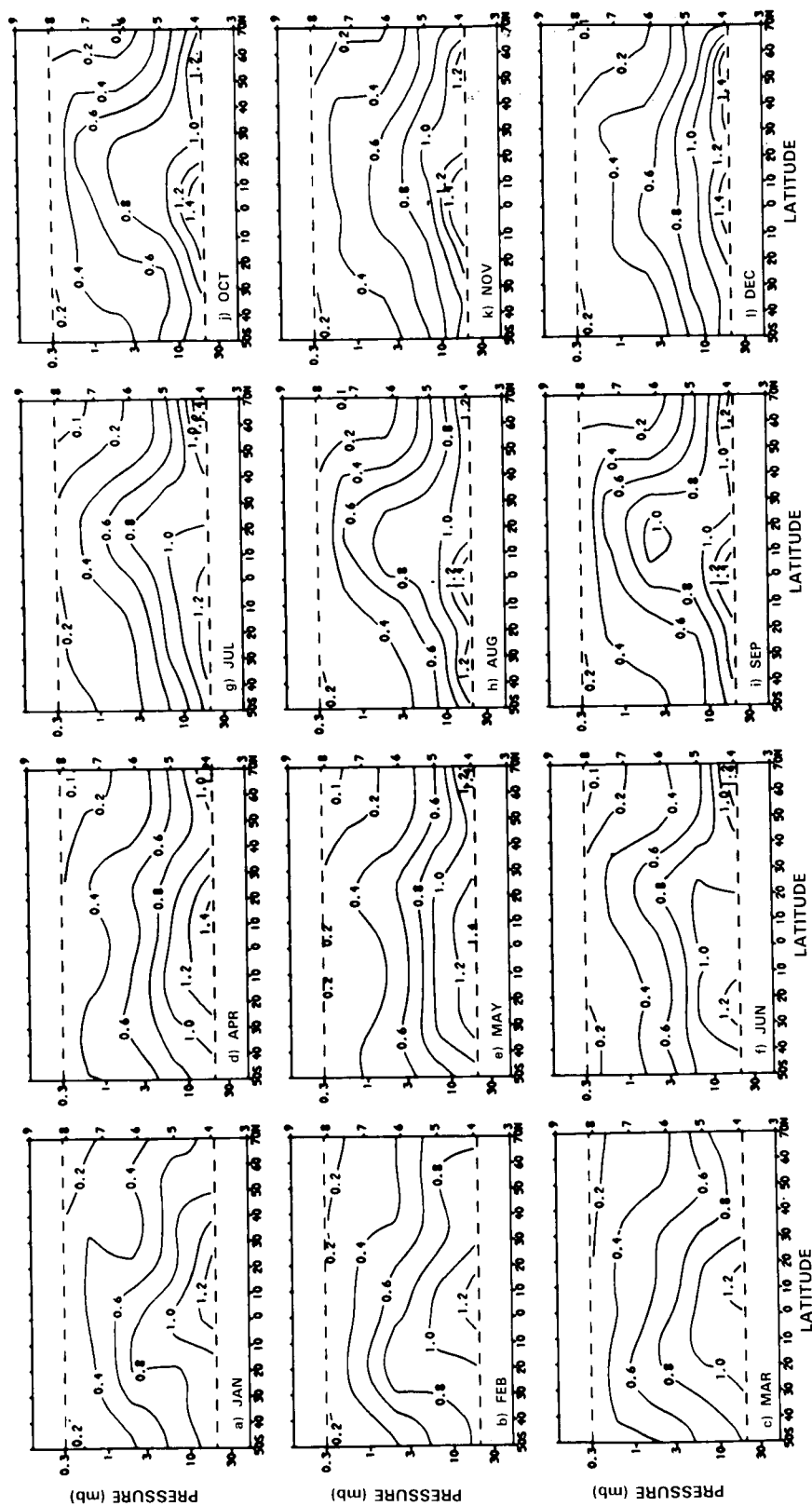
Figure 9-29. Monthly mean zonal mean cross-sections of methane (ppmv) for 1979 measured by the Stratospheric and Mesospheric Sounder (SAMS) instrument on Nimbus 7 (taken from Jones and Pyle, 1984. Note that the coverage is asymmetric about the equator, extending from 50°S – 70°N.

C-2
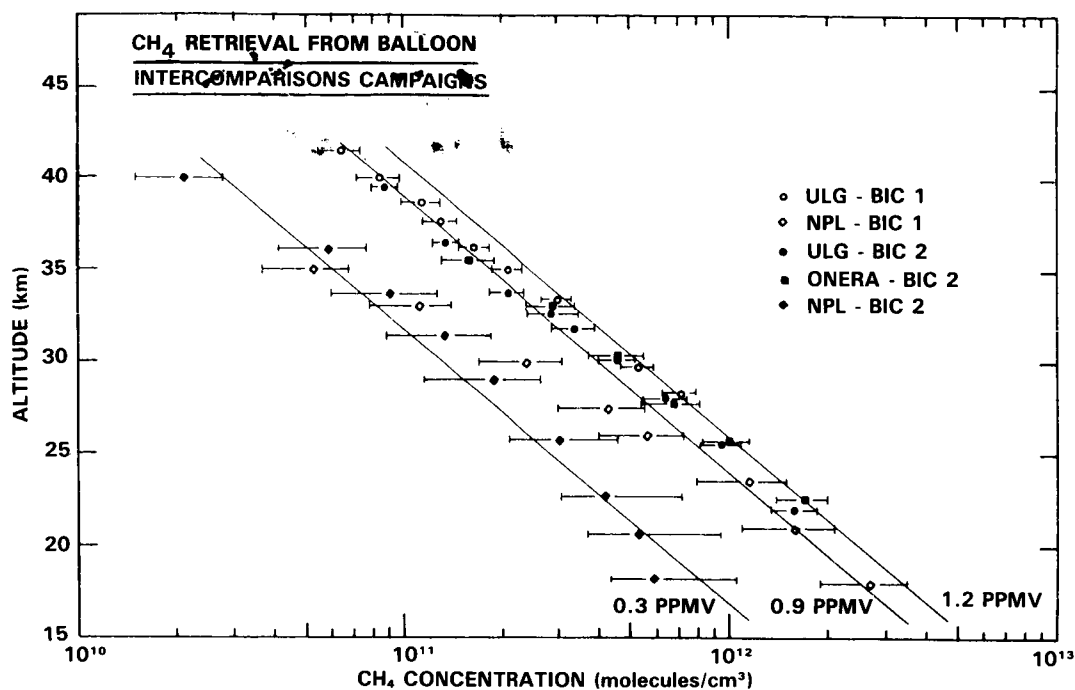
Figure 9-30. Methane concentration profiles retrieved during BIC I (open signs) and BIC II (filled signs). The error bars associated to the retrieved points do not include uncertainties on spectroscopic parameters used in the retrievals.

structure existed in the stratosphere at that time and location, with apparently more variability in the mesosphere (Ackerman *et al.* 1985).

9.5.3 Satellite Measurements of CH₄

The SAMS instrument launched on the Nimbus 7 satellite in October 1978 was a multichannel, limb scanning, infrared radiometer measuring atmospheric temperature, line-of-sight pressure and the abundances of a number of minor atmospheric constituents. Measurements of thermal emission from the ν_4 band of CH_4 between 1200 and 1340 cm^{-1} were used to derive CH_4 mixing ratios between 20 mb (~ 28 km) and 0.3 mb (~ 58 km) with a vertical resolution of ~ 8 km. The orbit configuration and viewing geometry of SAMS provided coverage from 50°S to 70°N each day.

Details of the instrument design may be found in Drummond *et al.* (1980). The use of a common optical chain and detector for both the CH_4 and the N_2O channels meant that these gases could not be observed simultaneously and were measured on alternate 24 hour periods. With the SAMS duty cycle of three operational days in four, CH_4 measurements were thus made on about 12 days per month.

The details of the CH_4 channel on SAMS were, in many respects, similar to those of the N_2O channel, which has been described in the NO_x chapter. A statistical inversion method was used to retrieve mixing ratios from the radiance data. Details of this and the instrument calibration procedures may be found in Rodgers *et al.* (1984) and Wale and Peskett (1984) respectively.

A detailed investigation of the sources of errors in the SAMS CH_4 observations has been described by Jones and Pyle (1984). They found that systematic errors in the retrieved CH_4 fields fell into four main
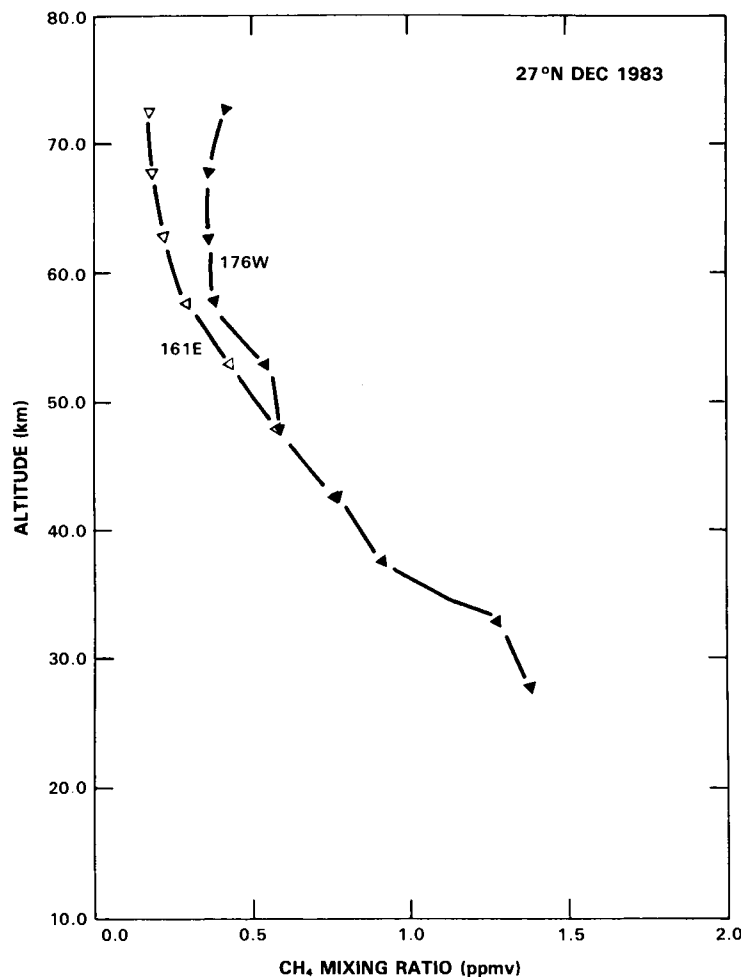
Figure 9-31. Profiles of CH₄ (ppmv) measured by the grille spectrometer on Spacelab One (Ackerman *et al.*, 1985). Errors on the data are estimated to be ± 15%. The two profiles were obtained 1.5 hours apart.

categories: (1) uncertainties in the spectroscopy of CH_4 and of any other overlapping gases (mainly N_2O); (2) instrumental and calibration uncertainties; (3) limitations and simplifications in the retrieval method and algorithm, and (4) inaccurate knowledge of the atmospheric state (mainly the temperature structure).

To estimate the impacts of these various systematic error sources, a synthetic radiance profile was computed using typical mixing ratio and temperature profiles with all the uncertain parameters set to their nominal values. The simulated data set was then retrieved with the uncertain parameters offset, in turn, to their uncertainty limits, and the profiles thus obtained compared each time with the original.

There was a significant random component to the error budget even when zonal means were considered. The effects of this on the retrieved profiles was quantified during the retrieval process by means of an error covariance matrix. In practice, only the diagonal elements of this matrix were used. This simplification, which ignores correlations between measurement errors at different levels of the atmosphere, tends to overestimate the random error at all levels.

A summary of the error budget of the SAMS CH_4 observations is shown for various pressure levels in Table 9-4.

Table 9-4. SAMS Estimated Accuracy and Precision for CH_4 Measurements

Pressure Level (mbar)	20		7		2		0.6		0.2	
1. Spectroscopy	±	7%	±	7%	±	5%	±	5%	±	5%
2. Field of View	±	2%	±	1%	±	3%	±	6%	±	3%
3. Mean PMC Pressure	±	3%	±	2%	±	6%	±	6%	±	3%
4. Uncompensated Doppler shifts	±	1.5%	±	1%	±	1.5%	±	6%	±	7%
5. Zonal Averaging	±	8%	±	8%	±	8%	±	8%	±	8%
6. Interference of N_2O	±	5%	±	2%	±	0.5%	—			
7. Temperature (2K)	±	50%	±	15%	±	10%	±	10%	±	10%
8. Line-of-sight attitude (+ 0.006)	±	4%	±	2%	±	6%	±	10%	±	6%
9. RMS of latitude and time dependent errors	±	51%	±	15%	±	12%	±	17%	±	14%
10. RMS of bias errors	±	9%	±	6%	±	8%	±	10%	±	7%
11. Net RMS accuracy	±52%		±	18%	±17%		±	21%	±	17%
12. Precision of monthly mean cross section	±5–15%		±3–10%		±3–13%		±4–13%		±20–40%	

Overall, the most important error sources are thought to be uncertainties in spectroscopy, the direct evaluation from zonal mean radiance and temperature profiles of a zonal mean mixing ratio profile, and uncertainties in the line of sight attitude and atmospheric temperature. The effects of uncompensated Doppler shifts contribute somewhat at upper levels (above 0.6 mb). The net RMS accuracy is ~20% above 7 mb, increasing, due to uncertainties in atmospheric temperature below, to ~50% at 20 mb. By comparison, random errors on a monthly mean zonal mean cross section vary between 3 and 15% below 0.6 mb, depending on the temperature and mixing ratio fields, increasing somewhat above this level.

The data from the three year period, 1978-81 have been studied in detail. Figures 9-29 (a)-(l) and 9-32 show monthly mean cross sections of CH_4 measured by SAMS for January to December 1979. The data are not symmetric about the equator, extending from 50°S to 70°N. Useful coverage is obtained between ~20 and 0.2 mb, covering the middle and upper stratosphere and the low mesosphere. Each monthly mean comprises approximately 12 days data per month.

The gross structure shown by these data is of a low stratosphere, low latitude mixing ratio maximum of ~1.2 ppmv at 20 mb (27 km), falling to 0.3 - 0.1 ppmv at the stratopause. Closer inspection reveals pronounced seasonal differences.

In January 1979 (Figures 9-29a and 9-32a) there was a marked asymmetry in the CH_4 field, with a region of elevated mixing ratio extending from the equator at 20 mb, tilting into the Southern (summer) Hemisphere, reaching ~20°S by the stratopause level. This feature persisted through February (Figures 9-29b and 32b), giving rise to sharp latitudinal gradients at high southern latitudes, with somewhat weaker gradients in the Northern Hemisphere. By March (Figures 9-29c and 32c) a second maximum began to emerge in the Northern Hemisphere as the first began to subside giving, by March and April (Figures 9-29c and d and 32c and d), an almost symmetrical appearance with, on a fixed pressure surface, two low latitude mixing ratio maxima separated by an equatorial minimum. This changeover continued

Figure 9-32. Monthly mean zonal cross-sections of methane (ppmv) measured by the Stratospheric
(a-f) and Mesospheric Sounder (SAMS) instrument on Nimbus 7 for (a) January 1979, (b)
February 1979, (c) March 1979, (d) April 1979, (e) May 1979 and (f) June 1979. These
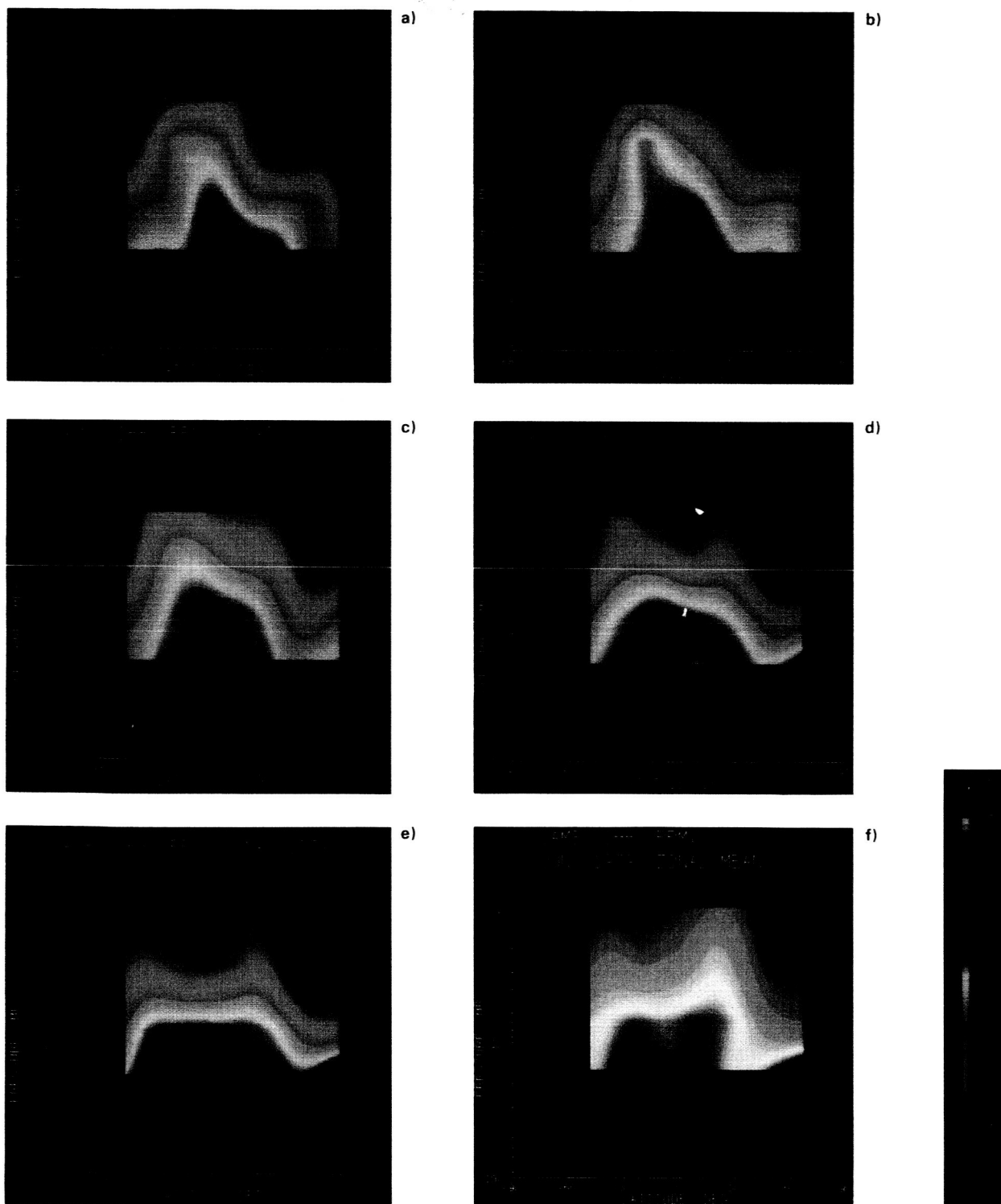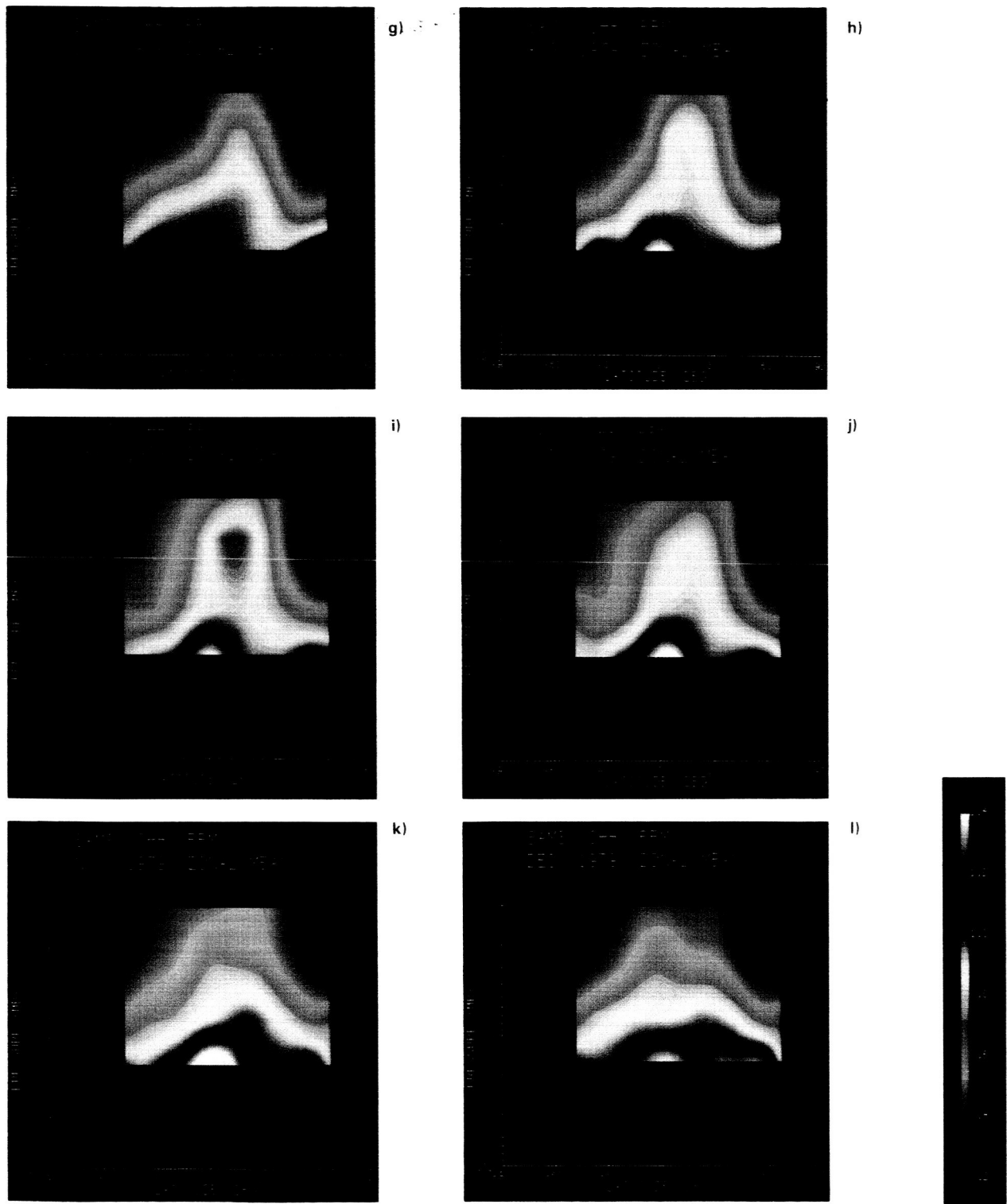data form a subset of the data shown in Figure 9-29.

Figure 9-32. Monthly mean zonal cross-sections of methane (pppmv) measured by the Stratospheric and
(g-l) Mesospheric Sounder (SAMS) instrument on Nimbus 7 for each month in 1979 beginning
with (g) July through (l) December 1979. These data form a subset of the data shown
in Figure 9-29.

through June (Figures 9-29f and 32f) giving, by July (Figures 9-29g and 32g), a single maximum extending into the Northern Hemisphere. The distribution observed during July was essentially a reversal of that seen during January, with sharp latitudinal gradients at high northern latitudes and weaker gradients everywhere in the Southern Hemisphere.

The behavior during the second half of 1979 differed in many respects from that of the first. During August and September (Figures 9-29h and i, and 32h and i), the Northern Hemisphere maximum intensified considerably, giving rise to an almost uniformly mixed region at high northern latitudes in the upper stratosphere until October (Figures 9-29j and 32j). Interestingly, the pronounced "double peak" structure evident during May that year was not repeated. In the final three months of 1979 the maximum subsided to give an almost symmetrical distribution by December (Figures 9-29l and 32l).

Three years of CH_4 data have now been examined. It appears (Jones, 1984) that, while minor differences do occur from year to year, the seasonal behavior remained essentially unchanged from that of 1979. For example, Figure 9-33 shows monthly mean cross-sections for January, April, July and October for the years 1979, 1980 and 1981. These months are chosen to emphasize the contrast between the methane distributions observed at different times of the year. All three years show regions of elevated mixing ratio extending into the summer hemisphere in January and July, with the "double peak" apparent in all three years, although less markedly in April 1981, being most pronounced during May of that year.

While the similarities between the structure seen during the three years are obvious, some differences warrant comment. Figure 9-34 shows time marches of CH_4 mixing ratios at 3 levels (10, 3, and 1 mb) at 65 °N for the three years of data. While the three summers (April to September) are remarkably consistent from year to year, the winter periods differ markedly. For example, while the vertical gradient was maintained throughout the winter of 1979/80, there were periods in both 1978/79 and 1980/81 when there was no decrease of CH_4 with height at this latitude. The arrows on the upper margin of the figure identify the active periods during each winter. For the purposes of the study these were identified with maxima in the 10 mb temperature at the north pole as indicated by Labitzke (1979) and Labitzke et al. (1980, 1981). The large arrows denote major (~20 K) increases, the smaller arrows more minor ones. The major events in the CH_4 time marches are correlated with the active periods during the warmings which differ from year to year.

The CH_4 data from SAMS have shown many new and hitherto unseen features. Foremost among these is the branching of air into the summer hemisphere giving, at certain times of the year, a "double peak" in mixing ratio with a local minimum at the equator. Similar features have been observed for N_2O (Jones and Pyle, 1984) and H_2O (Russell et al., 1984c), both measured from the Nimbus 7 satellite.

There are substantial semiannual variations in the data. For example, no "double peak" is seen in the latter half of the years studied to date. Seasonal changes show a high degree of consistency from year to year, with some differences in the winter hemispheres. It would appear that the three years of SAMS CH_4 data represent a useful climatology of that gas.

The global data sets on CH_4 (and N_2O) from SAMS and on H_2O from LIMS offer an important opportunity for understanding the transport of tracers in the stratosphere. One of the most interesting features of the observed fields is the presence, at certain times of the year, of 'double peaks' in equatorial latitudes. This structure was not anticipated by theory.

Recent modelling work appears to have explained the 'double peaks' and helped in the general understanding of transport processes. In a two dimensional model study, Gray and Pyle (1985) were able to
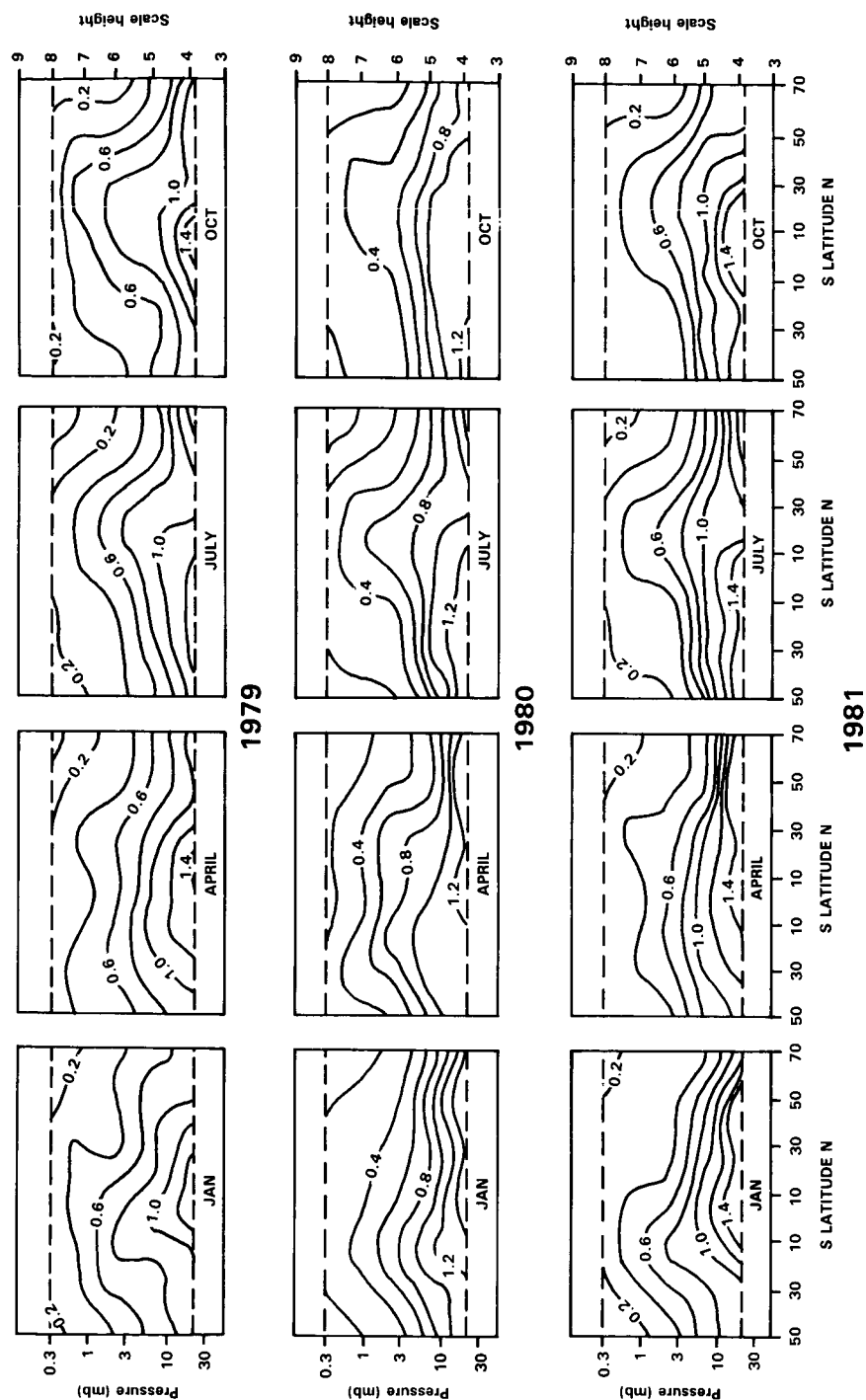
Figure 9-33. Monthly mean zonal mean cross-sections of methane (ppmv) for January, April, July and October for the years 1979, 1980 and 1981. Note the asymmetric coverage about the equator. The cross sections illustrate the small interannual variability compared with the marked seasonal changes. Note that the "double peak" is seen in all three years of data (from Jones, 1984).

487

reproduce the main features of the equatorial behavior only when they included the forcing of the semi-annual oscillation. They successfully modelled the double peak improving the seasonal behavior in low latitudes compared with model studies excluding the semiannual oscillation (see Chapter 12.6). This particular model interpretation of the satellite data has pointed to an important role for equatorial dynamics in determining the observed distributions of tracers. Solomon *et al.* (1986) have also reproduced the double peak in CH_4 in a model study in which the transport is effected by the diabatic circulation, diagnosed from LIMS ozone and temperature data. They find excellent agreement with the observed CH_4 fields in low latitudes (see Chapter 12.6 for a more complete discussion).

Another interesting feature of CH_4 data from SAMS is the presence of regions of weak and strong horizontal gradients. These can throw some light on the importance of eddy transport. Weak gradients generally lie along observed isotropic surfaces indicating strong mixing. The relationship of the mixing to the 'surf zone' ideas of McIntyre and Palmer (1984) is still to be explained in detail.
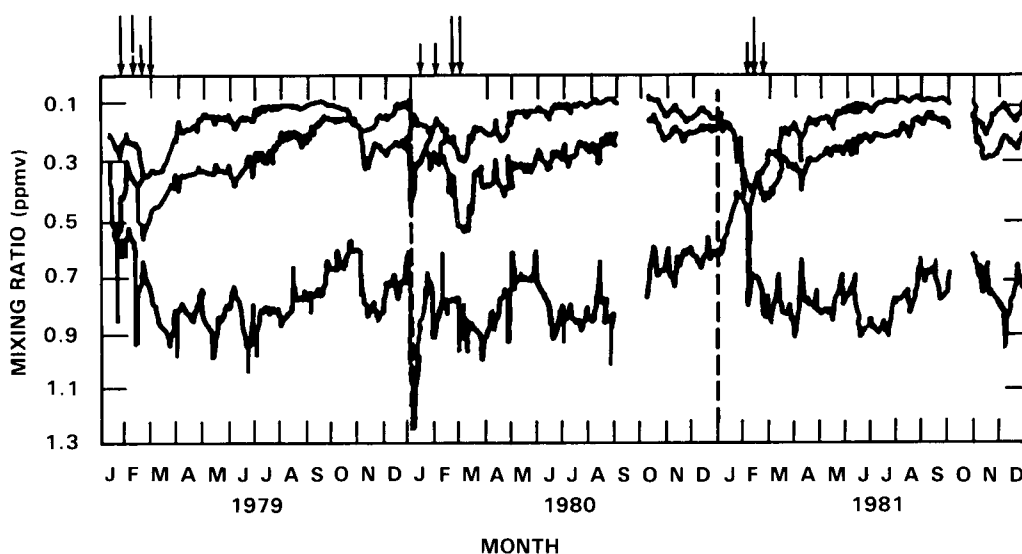
Figure 9-34. Mixing ratios of CH_4 at 10, 3 and 1 mb for the latitude band centered at 65°N for the period 1979–81 measured by SAMS. While relatively little variability is seen, particularly at upper levels during the summer, marked fluctuations correlating with warming events (arrows) are seen during winter months (from Jones, 1984).

9.5.4 Intercomparison of CH_4 Data

The different measurement times, locations, and techniques prevent a direct intercomparison of all the CH_4 data presented above. For example, no upper stratospheric *in situ* measurements were made during the lifetime of the SAMS instrument. While comparisons such as those during BIC and MAP-GLOBUS are described elsewhere, this section aims at giving an overall picture of the consistency of the CH_4 data now available. Since the only new data in the Southern Hemisphere has come from the SAMS instrument, such a comparison is only meaningful for the Northern Hemisphere.

Only the SAMS instrument provided high quality zonal mean data. Comparison of this data with *in situ* and other local measurements is limited by the substantial variability exhibited by the *in situ* data and the absence of any clearly defined seasonal behavior (see e.g. Figure 9-34). The approach taken here follows

that adopted by Jones and Pyle (1984). Annual mean profiles from SAMS have been plotted with all the available *in situ* data within specific latitude bands. Figures 9-35 to 9-38 show such comparisons at equatorial latitudes, 20–40°N, 40–60°N and 60–70°N respectively.

At equatorial latitudes (Figure 9-35) there has been no new, *in situ* data since WMO 1982. The SAMS data extends to much higher level at this latitude (55 km compared with 35 km), and is in good agreement at low levels (~30 km).

A variety of new observations have been made between 20°N–40°N (Figure 9-36) since WMO 1982. Despite the different techniques used, there is a broad consistency in the CH_4 profiles in this latitude range, with CH_4 mixing ratios falling almost linearly from 1.6 ppmv at the tropopause to around 0.5 ppmv at 50 km. Above this level both the rocket borne, *in situ* and the grille spectrometer profiles show the gradient lessening. The profiles obtained during the balloon intercomparison campaigns deviate somewhat from this picture, as described in Appendix C.

There is also good consistency in the range 40–60° N (Figure 9-37) between the SAMS data and the *in situ* measurements (both balloon and rocket) above ~30 km, with some suggestion that the SAMS data has a positive bias at lower altitudes as discussed by Jones and Pyle (1984). The 1975 AES profile
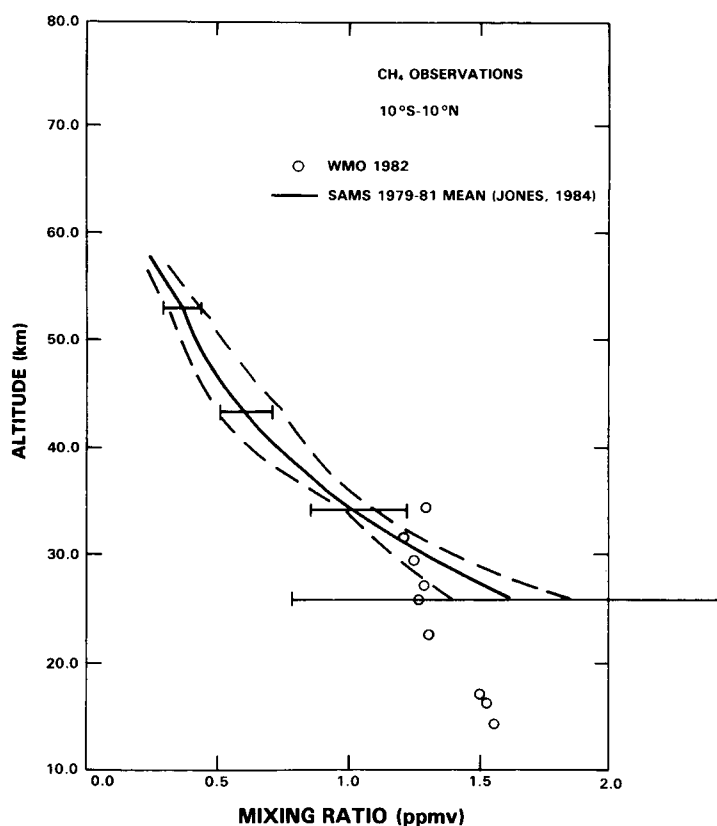
Figure 9-35. Comparison of the SAMS 1979–81 mean vertical profile for CH_4 between 10°S and 10°N (Jones, 1984) with *in situ* data taken within the same latitude band. The dashed lines represent the standard deviation of the monthly mean SAMS profiles over this period and the horizontal bars the estimated measurement accuracy.

appears to be rather low below 25 km. Evans (1985) suggests that this is an indication of a trend in atmospheric CH_4. The data at this latitude show a clear picture of mixing ratios falling almost linearly up to ~40 km from around 1.5 ppmv to ~0.4 ppmv, with much weaker gradients above.

There are no new *in situ* observations at latitudes higher than 60°N. Between 60 - 70°N the SAMS annual mean profile shows good agreement with the earlier *in situ* data (Figure 9-38). The data show a sharp fall off in mixing ratio to around 0.25 ppmv at 40 km with a more uniformly mixed region above, similar to the behavior observed between 40-60°N.

9.5.5 Total Hydrogen Content of the Stratosphere

Current understanding of stratospheric chemistry predicts that CH_4 is oxidized into CO_2 and H_2O. If there is no heterogeneous removal of water from the stratosphere, hydrogen should be conserved in
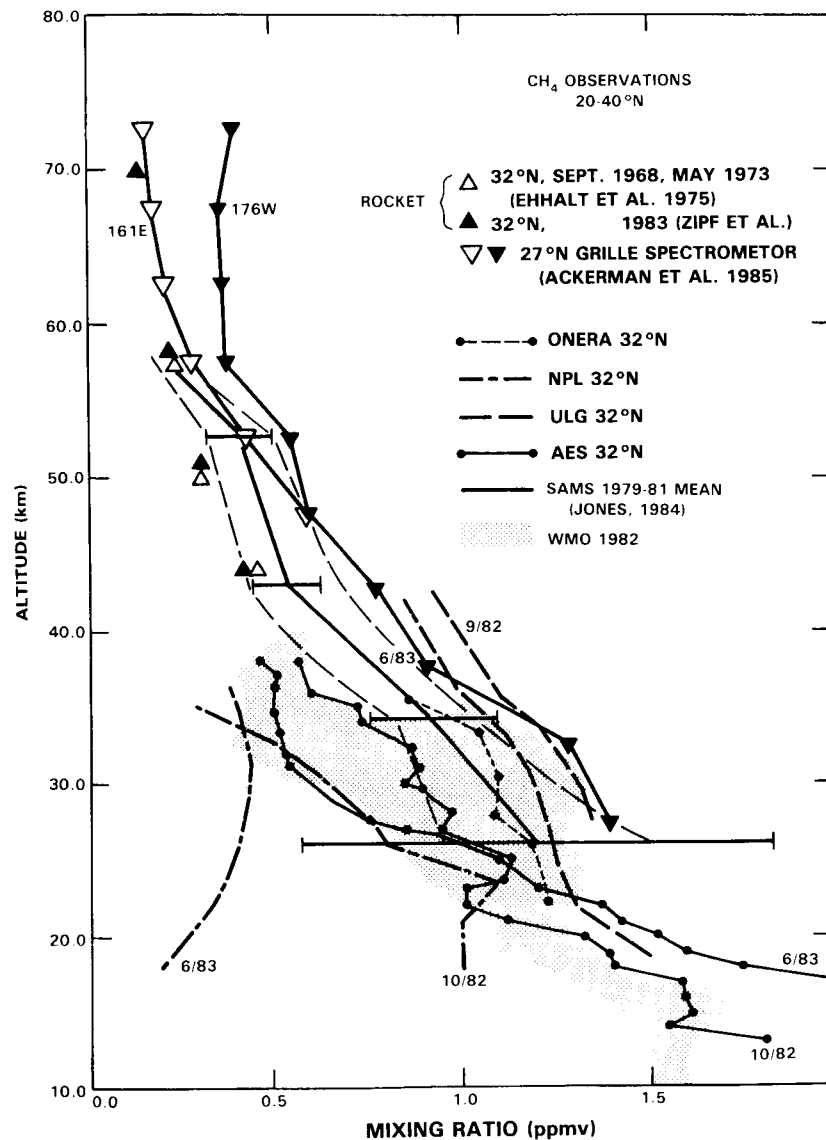
Figure 9-36. As for Figure 9-35 except for latitudes 20-40°N.

490

this process. The total hydrogen should be closely approximated by the sum $2 \times CH_4 + H_2O$. Strictly speaking, molecular hydrogen (H_2) should also be included, but since its contribution is less than either of the other species and it is essentially uniformly distributed with height (see for example Ehhalt *et al.* (1975a); Volz *et al.* (1981)) its omission does not have serious consequences and may in most cases be treated as an offset of approximately 0.5 ppmv (H_2).

The total hydrogen content of stratospheric air using local measurements has been investigated by Pollock *et al.* (1980) and Rinsland *et al.* (1984b). The former study was based on 6 flights of a balloon-borne cryogenic sampler between 1975 and 1978 and included molecular hydrogen in the sum. The study of Rinsland (1984) used CH_4 and H_2O profiles derived from solar occultation spectra taken during a single flight of a balloon-borne Fourier transform interferometer. The two studies show a good degree of consistency, giving approximately 6 ppmv of total hydrogen.

Jones *et al.* (1985) have combined simultaneous satellite data for CH_4 and H_2O. They showed that, for the 30 to 40 km region from 60°S to 80°N, the sum of $H_2O + 2 \times CH_4$ is, on average, about 6 ppmv,
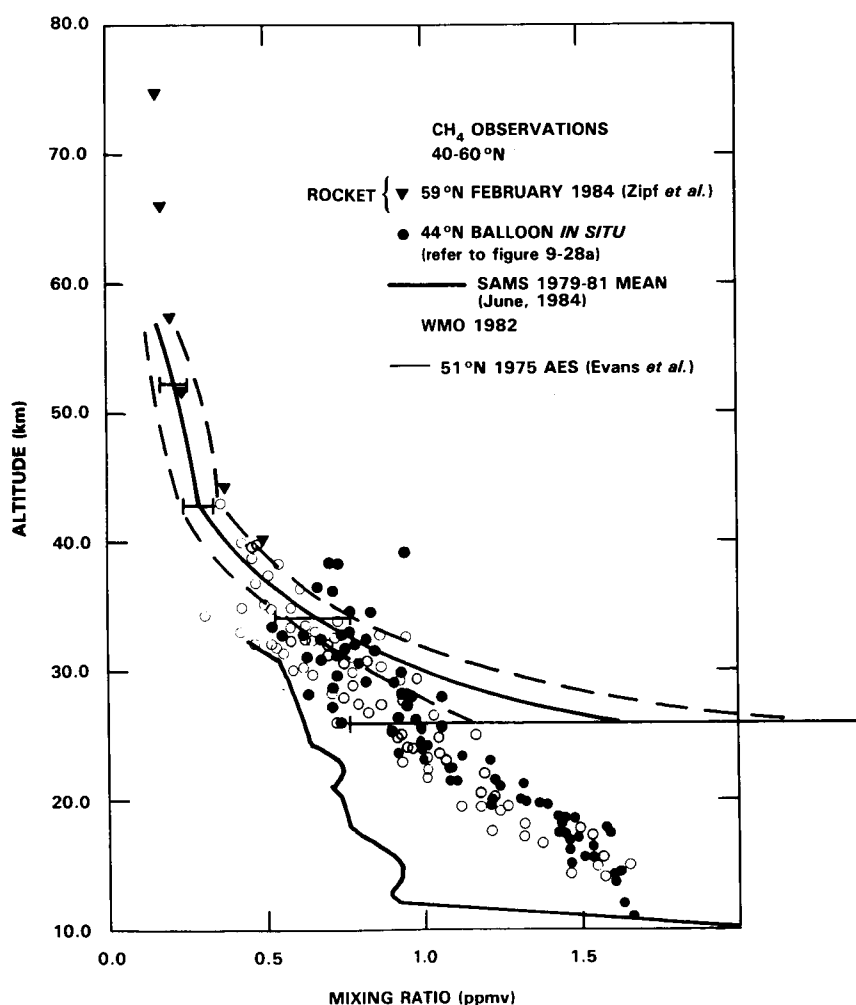
Figure 9-37. As for Figure 9-35 except for latitudes 40-60°N.

491
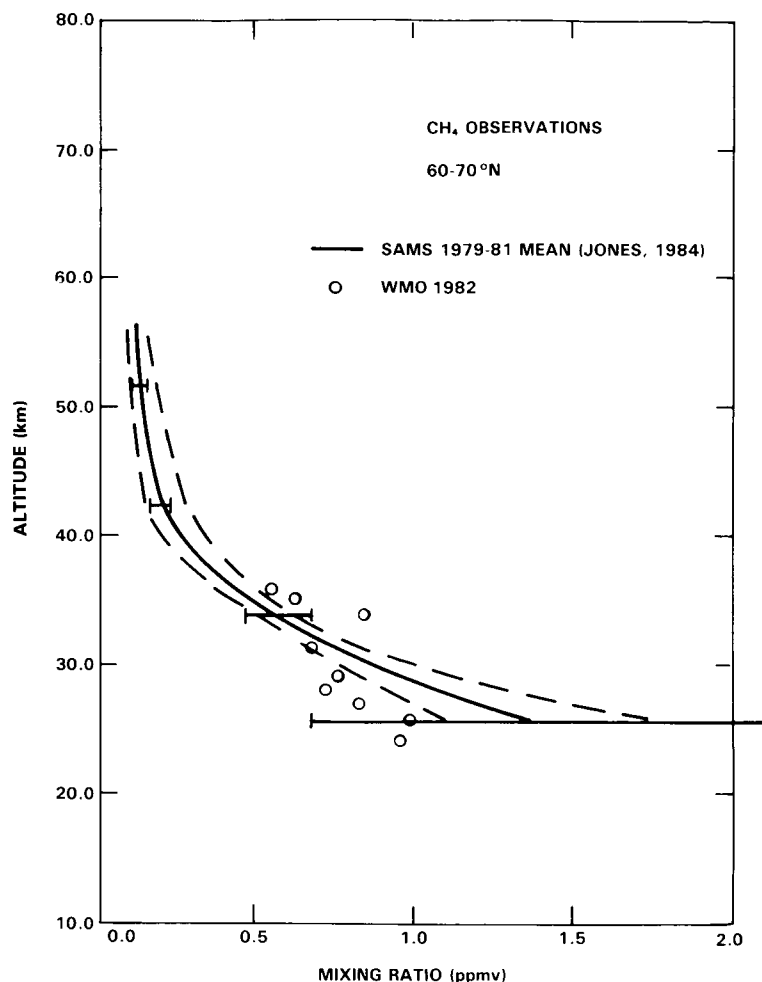
Figure 9-38. As for Figure 9-35 except for latitudes between 60–70°N.

to an accuracy of ±0.5 ppmv. Figure 9-39 and 9-40 show cross-sections of this sum based on monthly mean observations from January and May 1979 respectively, from the LIMS and SAMS instruments. Structure in this sum above 3 mb is not significant when compared with the estimated error in the sum (~0.5 ppmv). Other months examined reveal the same featureless fields. The fact that the sum is so invariant in time and space points to CH_4 and H_2O forming a chemical family in which CH_4 is the dominant stratospheric source of water vapor, i.e., the CH_4 oxidation hypothesis is correct. The decrease in CH_4 with increasing altitudes and latitudes must therefore be accompanied by a corresponding increase in H_2O. The variations of the sum at the 10% accuracy level may reflect the precision of the satellite data rather than a true atmospheric variation.

The demonstration of the CH_4 oxidation process in the stratosphere raises the interesting question of whether this uniformity in total hydrogen conservation holds to the 10% level on a local, *in situ* basis throughout the middle stratosphere. If this were the case, the circulation of water in the stratosphere would be highly constrained so that all air entering the stratosphere must have been processed through the same, hygroscopic cold trap. Variations in total hydrogen in the order of 10% in individual air parcels might
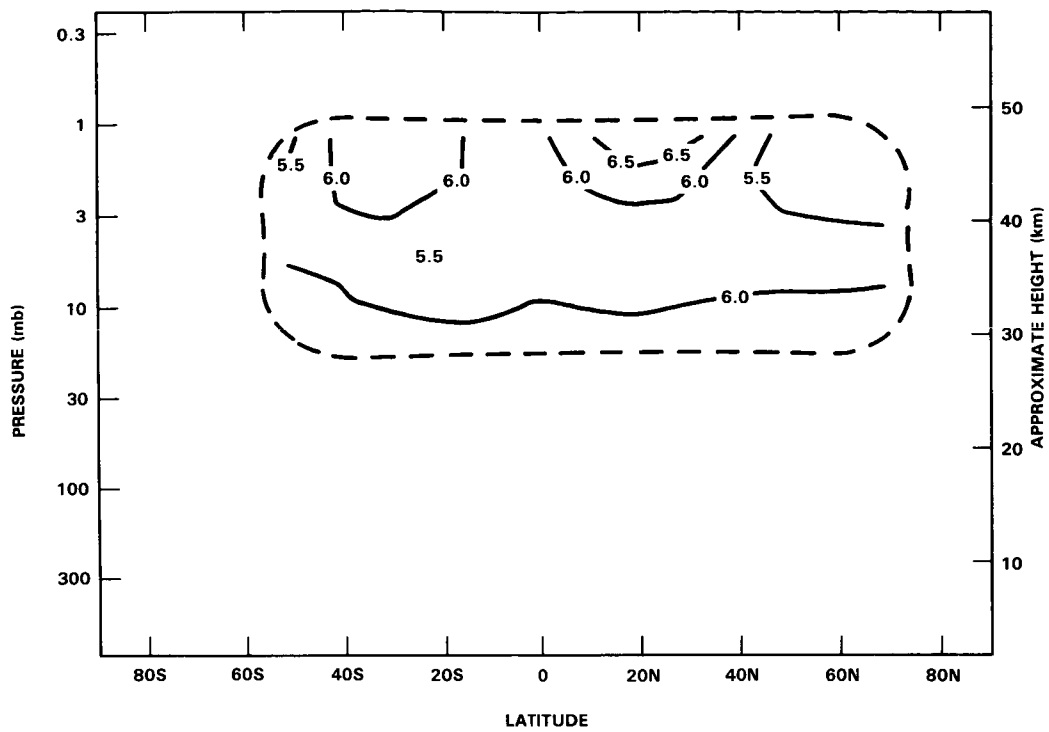
Figure 9-39. Cross section of $2 \times CH_4 + H_2O$ from SAMS and LIMS data. The data were derived from January, 1979 monthly mean data. (Jones *et al.*, 1985).
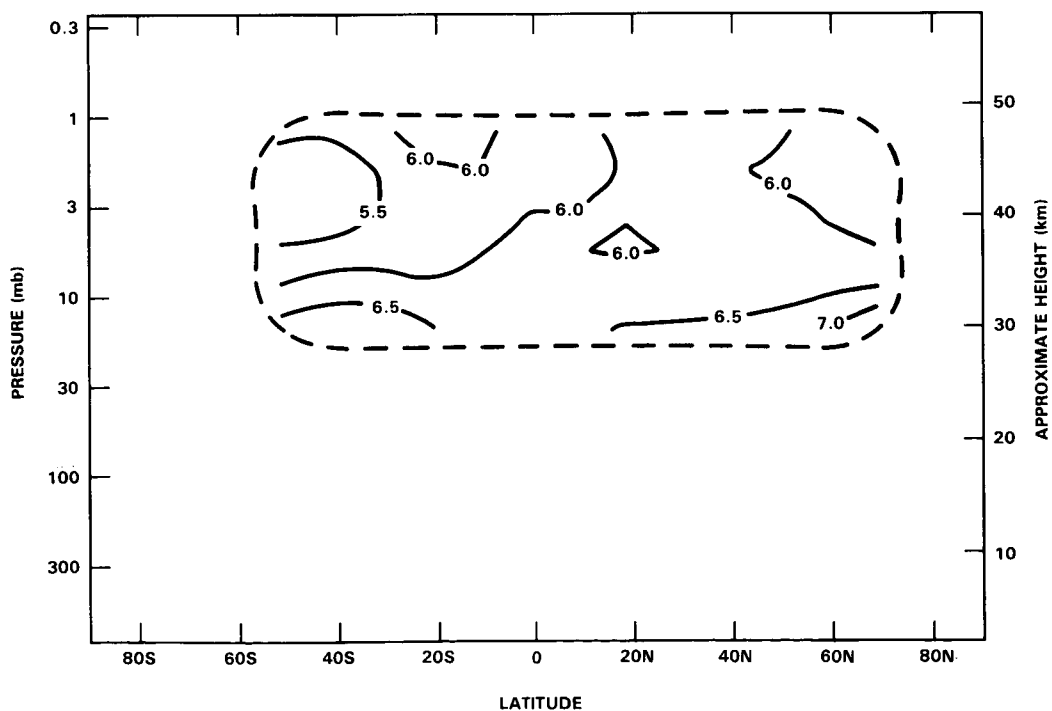
Figure 9-40. Cross section of $2 \times CH_4 + H_2O$ for May, 1979 from SAMS and LIMS data.

493

be expected if air entering the stratosphere passed through a cold trap at the tropical tropopause with seasonally or spatially varying temperatures or if more than one mechanism is responsible for drying the stratosphere.

The recent measurements by Kley *et al.* show structure in water vapor concentrations, with vertical features as small as 100 m in the lower stratosphere. This variability may be associated either with differing photochemical evolution among air parcels (i.e., conversion of CH_4 into H_2O) or with inherent variations in the hygroscopic mechanisms which dry out stratospheric air. In either case the existence of thin, distinct layers with differing composition must be evaluated in terms of their role in large-scale transport of trace species in the stratosphere, especially since no current models are capable of resolving these features.

9.6 CONCLUSIONS

The data base for OH, HO_2 and H_2O_2 vertical profiles has not expanded in a major way since the last assessment.

Only one new OH profile measurement has been obtained. It extended over an altitude range of 28–38 km. The new profile is lower than most of the earlier profiles and current model predictions. However, given the precision of the data and the wide range of values predicted by the models the discrepancy cannot be considered to be serious. It is clear that the data is insufficient to provide a critical test of the HO_x partitioning and budget. The profile data for OH has been complemented by 7 years of quasi-continuous, ground-based, solar absorption column measurements which show a long term trend, seasonal, diurnal and geographical variability and response to volcanic eruptions and solar eclipse. This column data for OH is a valuable record awaiting theoretical interpretation.

For HO_2, two independent data sets, obtained from balloon-borne *in situ* cryogenic sampling and ground-based mm-wave techniques cover the range 16–34 km and 35–60 km, respectively. The HO_2 concentrations measured in the 16–34 km range are substantially higher than those predicted from theoretical models, and are not consistent with the ground-based mm wave observations. This discrepancy suggests a problem either in the *in situ* measurements or in our current understanding of HO_x chemistry. The HO_2 measurements in the 35–60 km range are consistent with current theoretical predictions.

Although there have been only a limited number of observations of OH and HO_2 profiles over the past four years there have been major advances in observing systems for these species. Four new, balloon-borne instruments have demonstrated their capabilities for observing the diurnal variability of OH, and the potential for HO_2 measurements looks promising. A substantial expansion of the data bases for both these species is anticipated.

Major improvements have occurred in our knowledge of the spatial and temporal distributions of stratospheric and mesospheric H_2O and CH_4. While most of these improvements have come from satellite observations, significant new information has also been obtained from balloon *in situ* and ground-based measurements, particularly for H_2O. Clear evidence has been obtained for the existence of a hygropause, a region of minimum H_2O mixing ratios, just above the tropopause. Structure in the vertical profiles for both species, but especially for H_2O has been observed as a result of the improved vertical resolution (~ 0.5 km) of the *in situ* measurements. Also measurements both by *in situ*-sampler and remote methods have extended the data for H_2O and CH_4 throughout the mesosphere.

Observations by the LIMS instrument on Nimbus 7 over the period October, 1978 to May 1979 have revealed the global distributions (64 °S to 84 °N) of H_2O from 100 to 1 mb (16 to 50 km) for the first

time. The key observations are: (a) the zonal means show a region of low mixing ratio (~ 3 ppmv) at ~ 60 mb (~ 22 km) extending over low latitudes (the hygropause region); (b) the mixing ratio generally increased poleward and upwards in tropical regions reaching a maximum value of ~ 6 ppmv; (c) the variability in mean zonal mixing ratios is small except in high latitude winter; (d) the longitudinal variability in mixing ratio is 0.5 ppmv in the tropics, and ranges from 1 to 1.5 ppmv at mid-to-high latitudes.

The SAMS instrument on Nimbus 7 has provided near global observations ($50\,°S$ to $70\,°N$) of CH_4 from October, 1978 to June, 1983 from 20 to 0.3 mb (27 to 55 km). The data show: (a) a low latitude, low statospheric maximum, with mixing ratios generally decreasing polewards and upwards; (b) gradients in the vertical distributions exhibit a wide range depending on latitude and season; (c) significant seasonal changes with a marked asymmetry between the equinoxes each year; (d) little interannual variability.

The satellite data set of H_2O and CH_4 have clearly demonstrated that air is transported upward and poleward from the tropics. The transport of dry air in this fashion is consistent with the Brewer-Dobson hypothesis. The combination of these data sets has demonstrated that the total hydrogen budget of the stratosphere, viz H_2O + 2 CH_4, is relatively constant at values ranging from 6 to 7 ppmv. The satellite data also shows enhanced H_2O levels in the lower stratosphere at high latitudes (> 50) in the winter indicating that not all the H_2O in the stratosphere can be explained by exchange in the tropics and CH_4 oxidation. Simulation of the observed variability in the spatial and temporal distribution of CH_4 and H_2O utilizing multidimensional models present a major challenge to the modelling community.

9.7 FUTURE RESEARCH NEEDS

Despite the fundamental role of the HO_x family (HO, HO_2, H_2O_2) in stratospheric chemistry, the data base for that group remains one of the poorest of all species in the atmosphere. Very few definitive measurements are available for the needed quantities, which are the concentrations of the species, the partitioning between the family members, and the latitudinal, diurnal, and seasonal variations.

Ultimately, measurements must be made simultaneously of as many family members as possible, and it will also be especially important to make concurrent measurements of those species such as O, O_3, NO, etc., which control the partitioning between family members.

A substantial complement of instrumentation exists for the *in situ* and remote sensing of the HO_x species. The principal need at the present time is for the verification and application of these capabilities. The achievement of this goal has been greatly hindered by unreliability and failure of the balloon platforms, which are required for virtually all of these instruments. There is thus an urgent need for the resolution of the balloon reliability problem, and it is doubtful that a substantial data base on HO_x can be acquired until this has been accomplished (this is obviously also true for measurements of NO_x and ClO_x species).

Ground-based instruments, which are free of the limitations of balloon platforms, may have a useful role in future programs, provided that adequate accuracy, sensitivity, and altitude resolution can be achieved. The existing data base of Burnett for column OH should be fully exploited. However, total column measurements of OH suffer from the disadvantage of domination by the mesospheric component, and in any case total OH measurements alone do not provide an adequate test of model validity.

The mesospheric region requires further observational and theoretical investigation, because ozone concentrations in that part of the atmosphere are photochemically controlled and the photochemistry is dominated by the HO_x family. The mesosphere thus provides a good test of HO_x chemistry.

495

HYDROGEN SPECIES

Beyond the capabilities of the existing instrumentation, and without regard for the choice of platform, there is a general need for development of new sensors with increased accuracy, reliability, and sensitivity. However, such development must not in any way impede the expeditious implementation of existing instruments.

One of the principal requirements for understanding the chemistry of HO_x is the development of a method for global monitoring of H_2O, with good signal-to-noise ratio, which can be accurately calibrated and supported by ground truth (*in situ* or actual ground-based) measurements. In this connection ATMOS data may be useful for correlative measurements of H_2O vapor. Further development of microwave ground-based measurements is also warranted. All of these measurements must be made on a long term basis, both to verify the methods and to observe trends.

The mechanism of H_2O exchange with the troposphere, which is the subject of another chapter, must be fully understood in order to predict future effects of possible atmospheric changes on the rate of H_2O influx into the stratosphere. Observations such as enhanced H_2O vapor concentrations in the high latitude, lower stratosphere regions must be understood.

A clearer picture is needed of the overall hydrogen balance, particularly the contribution of CH_4 oxidation to H_2O and the relative importance of H_2. These objectives will require continuous global measurements of the CH_4 concentrations and altitude profiles, along with those of H_2O.

Further laboratory research is needed in support of instrument development, calibration, and sensitivity improvement. Accurate measurements of pressure broadening coefficients are especially important. As discussed in the chapter on chemistry, some laboratory simulations of HO_x/O_3 photochemistry may prove to be useful for testing the accuracy and completeness of the photochemical models.

CHAPTER **10**
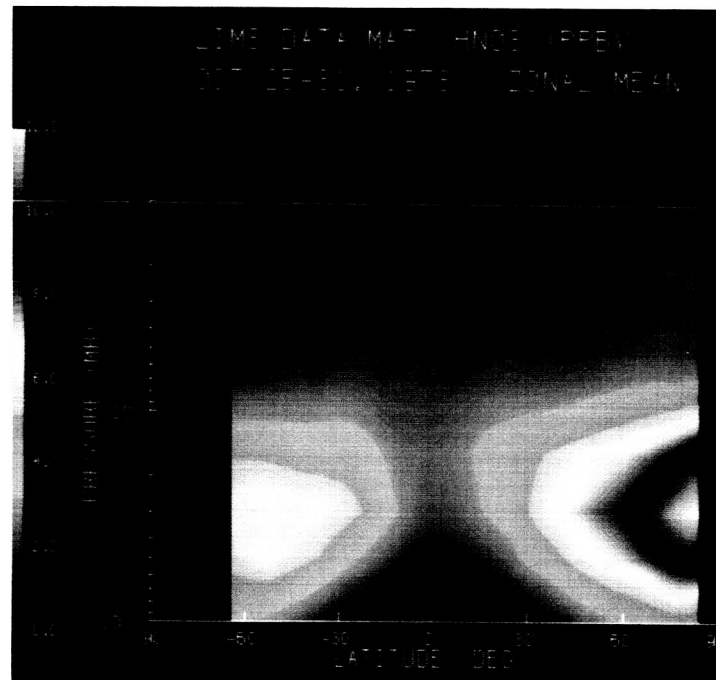
NITROGEN SPECIES

Panel Members

J.E. Harries, Chairman

G. Brasseur	A.J. Owens
M.T. Coffey	J. Pyle
H. Fischer	B.A. Ridley
J. Gille	H. Roscoe
R. Jones	A.L. Schmeltekopf
N. Louisnard	S. Solomon
M.P. McCormick	N.D. Sze
J. Noxon	

CHAPTER 10
NITROGEN SPECIES: OBSERVATIONS AND INTERPRETATION

TABLE OF CONTENTS

10.0 INTRODUCTION

Total odd nitrogen (NO_y) may be defined as the sum of all active nitrogen species that interchange photochemically with one another on a time scale of the order of weeks or less, i.e. $NO + NO_2 + NO_3 + 2N_2O_5 + ClONO_2 + HNO_4 + HNO_3$. The interchange of the NO and NO_2 free radicals occurs on a time scale of minutes in the sunlit atmosphere, and can result in a catalytic loss process for stratospheric ozone. As noted in the Introduction to this and the other species chapters in this report, $NO + NO_2$ reactions dominate the processes controlling the ozone balance in the contemporary stratosphere; further increased chlorine abundances may change this situation, but presently this dominance is evident. As a result, accurate direct measurements of the NO_2/NO ratio in the stratosphere must be considered central to any verification of ozone chemistry. Significant progress regarding this question is now available from balloon observations, as discussed in Section 10.1 and 10.3. It is also important to understand spatial and temporal variations in NO and NO_2, both on scales ranging from a few hundred meters or a few seconds, to global and seasonal levels, in order to evaluate the role played by variations in NO_y insofar as the diverse behaviour of stratospheric ozone is concerned. Both *in situ* and satellite techniques have revealed important insights into these questions, as will be shown below.

Study of the odd nitrogen family must also include the longer-lived reservoir species, such as N_2O_5, $ClONO_2$, HNO_3, and HNO_4. N_2O_5 plays a particularly important role in the diurnal and seasonal variability of NO and NO_2, because of its unique chemical properties. N_2O_5 is produced during the night via the reactions:

$$NO_2 + O_3 \rightarrow NO_3 + O_2$$

$$NO_3 + NO_2 + M \rightarrow N_2O_5 + M \tag{2}$$
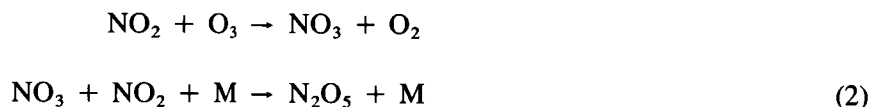
This process occurs almost exclusively at night because NO_3 is destroyed rapidly by photolysis in the sunlit atmosphere, and is therefore present in quantity only at night. The N_2O_5 produced at night then photolyzes in the sunlit atmosphere on a time scale of hours to days, depending on altitude and temperature:

$$N_2O_5 + h\upsilon \rightarrow NO_2 + NO_3$$

$$\rightarrow 2NO_2 + O \tag{3}$$
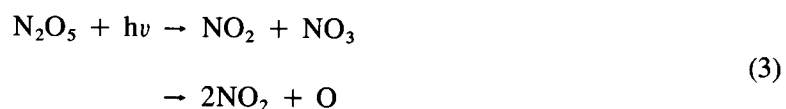
In a twelve hour night at midlatitude in summer, perhaps 50% of the NO_2 present at sunset is converted to N_2O_5 near 10 mbar, and subsequently slowly released in the following day. Therefore, this species plays a critical role in the diurnal variations of NO and NO_2. Similar, but substantially less important roles are played by $ClONO_2$, and HNO_4 in the contemporary atmosphere. HNO_3 is produced via

$$OH + NO_2 + M \rightarrow HNO_3 + M \tag{4}$$

and destroyed by photolysis and reaction with OH:

$$HNO_3 + h\upsilon \rightarrow NO_2 + OH \tag{5}$$

$$HNO_3 + OH \rightarrow H_2O + NO_3 \tag{6}$$

497

Because the time scale for loss of HNO_3 is generally longer than a few days to weeks at the altitudes where it is present in large quantities, HNO_3 is of importance to our understanding of NO_y on somewhat larger temporal and spatial scales.

We have briefly reviewed how the principal members of the NO_y family are related chemically to one another, but we must also consider the production and loss of the family as a whole, as well as its relationship to atmospheric transport processes. The various sources of NO_y will be discussed in detail in Section 10.3, but here we briefly mention that the primary source of stratospheric NO_y is provided by N_2O via the reaction:

$$N_2O + O(^1D) \rightarrow 2NO. \tag{7}$$

N_2O, in turn, is strongly controlled by atmospheric transport. Balloon observations before 1981 revealed large latitudinal gradients in N_2O vertical distributions; further balloon and particularly satellite observations of this constituent have not only quantified our knowledge of NO_y sources, but have also led to a greatly improved understanding of atmospheric transport.

Another manifestation of the importance of transport in NO_y distributions is provided by the Noxon "cliff" phenomenon, first observed in ground based studies in 1977 (Noxon 1979). A cliff is an abrupt decrease in NO_2 column abundance as a function of latitude, in winter by as much as a factor of 4 in only 5-10° of latitude. Other ground based and aircraft studies, however, obtained much less dramatic changes in NO_2. Noxon (1979) showed that particular meteorological conditions characterize the NO_2 "cliff" phenomenon; i.e. large scale wave activity seemed to be a prerequisite for cliff formation. Recent theoretical work has shown that this phenomenon is likely to be related to N_2O_5 chemistry and transport. The broad spatial and temporal coverage of satellite NO_2 observations, under varied meteorological conditions, has led to a much more complete understanding of the cliff than previously possible. Balloon data have also revealed the precise altitudes where the NO_2 variations occur during cliff conditions, with very high vertical resolution: yet another example of the role of transport processes in variations in NO_y column abundance, both from aircraft and satellite data.

These and other aspects of stratospheric nitrogen species are discussed in this chapter, with the aim of reviewing the status of observational data and theory. Particular emphasis is placed on advances in our interpretation of observations with regard to developments since the last major NASA/WMO assessment report. This chapter is organised as follows:

Section 10.1   reviews observational data from non-satellite platforms;
Section 10.2   considers the somewhat explosive growth in available satellite data in the past four years;
Section 10.3   then presents a discussion of some of the most important scientific issues which have been addressed, taking into account new results from atmospheric models (mainly 2-D), and the comparison of these model results with observational data.
Section 10.4   presents a summary and conclusions; and
Section 10.5   recommends future research needs.

The chapter shows that remarkable progress in our knowledge of odd nitrogen chemical and physical balances has occurred in recent years, but that many processes are still far from perfectly understood.

10.1 NON-SATELLITE DATA

Balloon, ground-based and aircraft measurements have always played a central role in our understanding of stratospheric chemistry and in confirming photochemical theory. Recently, the emphasis of balloon-borne measurements has shifted to a more detailed testing of photochemistry and dynamics. Diurnal cycle measurements within a moving air parcel can be conveniently made by balloons. *In situ* measurements made from balloons and rockets retrieve data at vertical scales far beyond the capabilities of remote sensing methods, leading to improved understanding of small scale variability. Ground based observations can provide continuous time series data at particular points, revealing important temporal information.

In this section, *in situ* and remote data on odd nitrogen species will be presented and intercompared. Results from several measurement techniques will be compared, and photochemical variations associated with their interpretation (i.e. as a function of local time) will be considered. As described in the Introduction (10.0), it is also of interest to examine the total NO_y abundance obtained from the sum of available observations of the constituent family members. This provides a test of our understanding of the chemical and transport budget of the family as a whole (see Section 10.3). To this end, best estimate profiles for NO, NO_2 and HNO_3 are evaluated from their composite database.

10.1.1 Nitric Oxide (NO)

In contrast to the large amount of data available for nitrogen dioxide and nitric acid from satellite retrievals (LIMS, SAGE, SME), no such direct temporal and spatial information exists for nitric oxide. Instead, most of our knowledge of the distribution of nitric oxide in the stratosphere results from discrete measurements made from the ground, from high-altitude balloons, aircraft, rockets, and, more recently, the Space Shuttle platforms. Additional information can be inferred from measurements of nitrogen dioxide; daytime to nighttime differences from satellite observations can provide at a minimum a lower limit to the nitric oxide abundance. Nitric oxide can also be estimated from satellite measurements of nitrogen dioxide, temperature and ozone if the photodissociation rate of nitrogen dioxide is known, since the two free radicals, NO and NO_2, are in photochemical equilibrium in the sunlit atmosphere.

Since the last detailed assessments of 1981 and 1982, further measurements have been made using new techniques and by different groups. These include *in situ* optical and chemiluminescence measurements, daytime observations using the pressure modulator radiometer (PMR) and sunset occultation measurements. Simultaneous *in situ* and long-path measurements of nitric oxide and nitrogen dioxide have been obtained (Louisnard *et al.*, 1983, and McFarland *et al.*, 1985). Most importantly, some instrument intercomparison studies were undertaken during the MAP-GLOBUS and BIC-2 balloon campaigns. Seasonal changes in the altitude distribution of NO have been observed at high latitudes in North America.

Table 10-1 summarizes most of the *in situ* balloon and aircraft experiments that have been undertaken. Excluded from consideration are the experiments listed in the footnote. Further, only those experiments for the summer and fall seasons at latitudes from 32 to 44 °N are considered explicitly; this restriction allows the inclusion of most of the studies, by the largest number of techniques, and eliminates possible biases due to seasonal or latitudinal variation. Observations at other latitudes are consistent with the lack of marked variations in the total column measurements in summer and fall discussed in Section 10.1.11.

The observations of nitric oxide can be conveniently separated into measurements made below and above about 32 km. There are two reasons for this separation: (1) many of the techniques were designed

to operate optimally in one of these two altitude regions; (2) the variance of the observations by different techniques are quite different for the two regions. The data sets obtained within a few hours of local noon are considered first.

Table 10-1a. *In situ* Observations of Stratospheric Nitric Oxide.

	Group	Location	Date	Alt (km)	$\pm$ Error (%)
A	Webster and Menzies	32 °N	Oct 16/83	36	30
*B	Kondo *et al.*	44 °N	Sept 20/83	7-32	5-10
*BB	Fabian *et al.*	44 °N	Sept 20/83		
C	McFarland *et al.*	32 °N	Nov 04/81	22-32	20
D		32 °N	Jul 08/82	21-30	20
E		51 °N	Aug 10/82	22-32	20
F	Horvath *et al.*	38 °N	Aug 29/78	32-51	20-30
G		38 °N	Oct 01/79	31-47	20-25
H		38 °N	Oct 10/80	29-46	20
J		38 °N	Jul 23/81+	29-54	10-20
K	Weiler *et al.*	44 °N	Jun 26/77	31-33	20
L		44 °N	Jun 6/78	14-31	7-20
M	Drummond *et al.*	43 °N	Jun 27/76	12-45	25
N	Maier *et al.*	32 °N	Apr 26/77	27-38	25-34
O	Patel *et al.*	32 °N	Oct 19/73	28	8
P	Patel *et al.*	33 °N	May 22/74	25,28	30
Q	Loewenstein *et al.*	32-44 °N	Summer/75/Fall/76	18.3,21.3	25
R	Loewenstein *et al.*	50 °N	Summer/75/Fall/76	18.3,21.3	25
S	Roy *et al.*	34 °S	Dec 11/77	12-33	30
T		34 °S	Dec 13/77	15-33	30
U	Galbally *et al.*	34 °S	May 15/79	18-33	30
V		34 °S	Oct 10/79	14-33	30
W	Ridley and Schiff	32 °N	Oct 25/77	15-33	—
X		32 °N	Oct 30/78	14-40	—
Y		32 °N	Nov 08/78	14-40	—
Z	Ridley and Hastie	51 °N	Aug 28/76	17-34	—
ZZ		51 °N	Aug 12/78	14-33	—

*MAP-GLOBUS Intercomparison
+Two flights.

Other observations have been reported but are not included in this review. Most of the early measurements by the York University group were rejected because sampling problems likely existed (Ridley and Schiff, 1981). The results of McGhan *et al.* (1979) were not considered because the instrument was damaged during the launch process and it did not operate completely according to design. (Data reported from this flight above 27 km are in good agreement with the majority of the balloon measurements for 32 °N.) The June 26/78 flight results reported by Weiler *et al.* (1980) were also not considered because of a mechanical malfunction that increased the error estimate to $\pm$ 50%. The results from the resonance fluorescence technique of Anderson and co-workers (1979) were not considered. As well, the early rocket flights of Mason and Horvath (1976) are not included in the analysis. Instead, only the data obtained during parachute descent from the rocket apogee are discussed (Horvath *et al.*, 1983).

Table 10-1b. Oxford University Pressure Modulated Radiometer Measurements of NO

June/75	44 °N	Drummond and Jarnot, 1978
Sept/78	32 °N	Roscoe et al., 1981
Oct/80	32 °N	Roscoe et al., 1985
Oct/82	32 °N	Roscoe et al., 1985
*June/83	32 °N	Roscoe et al., 1985

Table 10-1c. Sunset Solar Occultation Measurements of NO

May/73	44 °N	Ackerman et al., 1975
May/74	44 °N	Ackerman et al., 1975
Sept/80	44 °N	Louisnard et al., 1983
*June/83	32 °N	Louisnard et al., 1985
Oct/79	33 °N	Rinsland et al., 1984c

*BIC 2 Intercomparison

10.1.1.1 Balloon and Aircraft Observations below 32 km

Figure 10-1 gives the data obtained below about 32 km for the 32-44 °N latitude band from the balloon and aircraft measurements of Table 10-1. For clarity, and where appropriate, only hand-drawn curves through the reported data are given. Data reported since the 1981 WMO assessment are emphasized by heavier printing. Two of these profiles (B and BB of Table 10-1) were obtained simultaneously; these two observations are in substantial disagreement below 24 km but above this altitude the agreement is very good and consistent with the majority of other measurements.

Considering the $\pm$ 20-30% error of individual experiments, several profiles appear disproportionately low. The first is the data below 34 km of Maier et al. (1978). This flight was made near local noon on April 26, 1977 but the shape resembles several winter profiles obtained near 50 °N that are discussed in a subsequent section. Upper atmospheric meteorological charts have not been examined to determine if unusual dynamics could explain the low values. Since there are no other winter/spring measurements for this latitude band to corroborate this unusual profile, the values reported below 34 km are not included in the ensuing analysis. Second, although the instrument flown by Weiler et al. (1980) employed an on-board calibration system, these observations also appear anomalously low below about 30 km. A third flight also gave mixing ratios of only 0.2 to 0.3 ppbv between 15 and 26 km. Fabian (private communication) has indicated that the earlier flights of Weiler et al. (1980) suffered from uncertainties in the determination of the zero level signal of the instrument. Consequently these flights are not considered further. The profile of Drummond et al. (1977) is also about a factor of two smaller than the bulk of the data shown in Figure 10-1. There is a reasonable explanation of this result. The payload was launched shortly after visible sunrise on the ground. Morning solar zenith angles at 10, 20, 30 and 40 km were approximately 84, 79, 73, and 67 degrees. Burkhardt et al. (1975), Ridley et al. (1977) and McFarland et al. (1985) have measured the growth of nitric oxide and/or nitrogen dioxide during the morning at constant altitudes. These studies observed a growth of almost a factor of two during the morning which is attributed to the slow photolysis of N_2O_5 that was formed overnight. Consequently, the profile of Drummond et al. (1977) is expected to be significantly lower than the bulk of the other measurements that were made near local noon or in the afternoon.
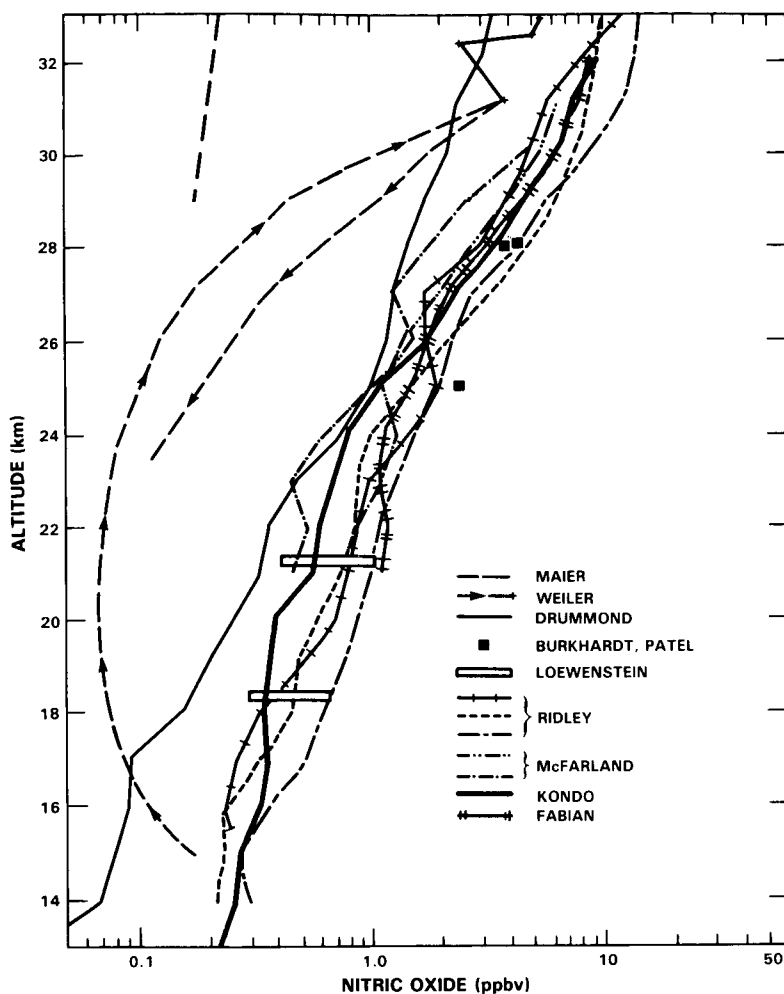
Figure 10-1. Balloon and aircraft observations of NO below 32 km in the latitude range 32–44°N.

The remaining profiles form a reasonably consistent data set and allow a best estimate of the altitude distribution for the 30-40 °N latitude region, the summer through fall season, daytime conditions and below 32 km by calculating a simple weighted average.

From the hand-drawn altitude profile curves, mixing ratios were noted at 1 km intervals. The mean and standard deviation of the mean were calculated. All of the measurements made since 1980 with instrumentation designed to operate optimally below about 32 km were assigned a weighting factor of two simply because of technological improvements and the experience gained with calibration standards and sampling methods. The aircraft measurements near 18 and 21 km were assigned a weighting factor of four simply due to the volume of data obtained by that group. The result is given in Figure 10-2. This mean profile does not include flights K, L, M, N of Table 10-1.
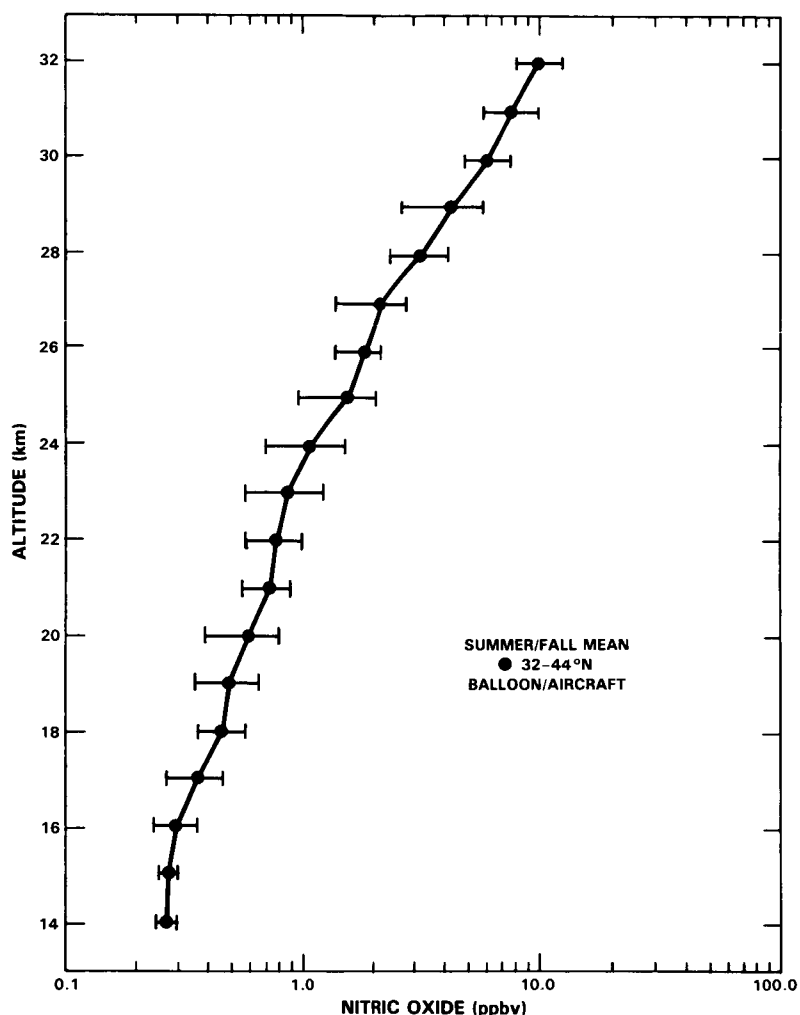
Figure 10-2. Best estimate of NO profile 32–44°N latitude, up to 32 km.

10.1.1.2 Observations at Higher Altitudes

There are also a large number of observations for the summer/fall season at 32-44 °N both from instruments designed to operate only above about 30 km and from some of the previously discussed balloon experiments. There are also a number of recent observations from the Oxford PMR instrument. Although this is not an *in situ* technique, it does allow measurements during high sun conditions. All of these data were obtained in the afternoon and are included in the analysis of the observations for this altitude regime.

Above about 35 km, nitric oxide begins to dominate total odd-nitrogen. Near 40 km, nitric oxide is almost equivalent to total odd-nitrogen in current atmospheric models. Unfortunately, NO profiles measured by different techniques differ by as much as a factor of 4 to 6 in the 30-45 km region.

Figure 10-3 contains all of the non-occultation data from Table 10-1 for 32-44 °N above 29 km and for the summer/fall seasons. Flights K and L and N below 34 km are not included for the reasons given previously. Clearly, the range is large; at 36 km the mixing ratio ranges from a low of 2.8 ppbv from the PMR flight to a high of 17 ppbv from the diode laser instrument of Webster and Menzies (1984).
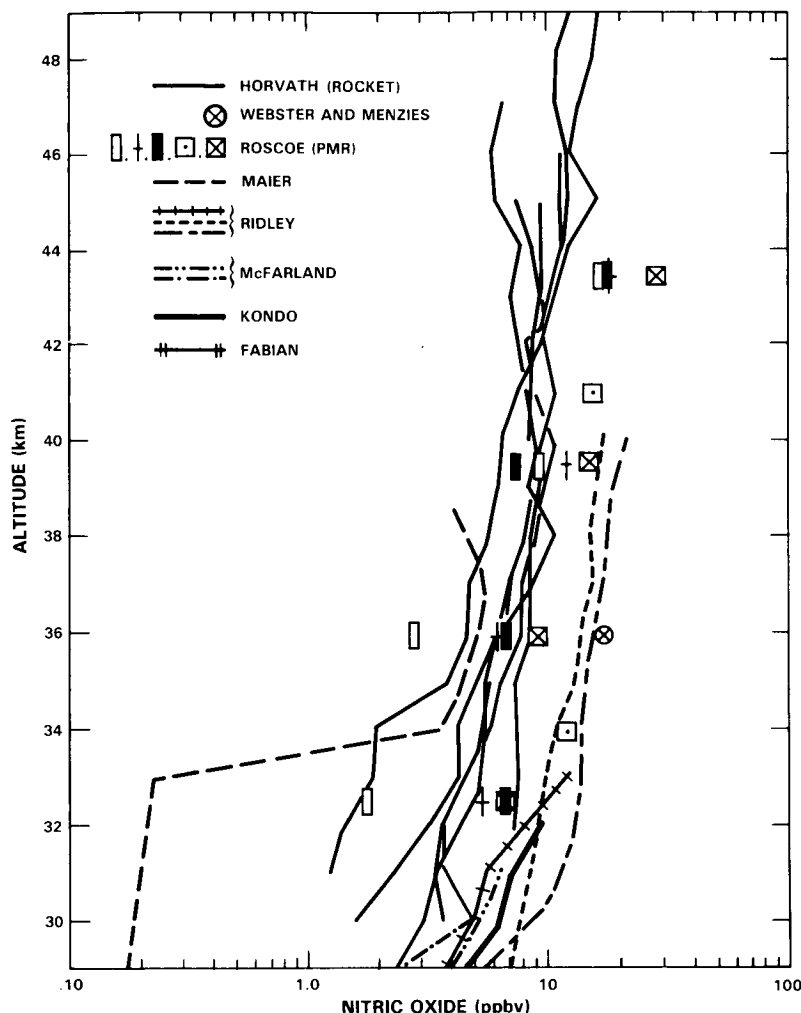
Figure 10-3. Non-occultation measurements of NO above 29 km for latitudes between 32 and 44°N.

The bulk of the higher altitude measurements have been obtained by Horvath *et al.* (1983), using a rocket-borne chemiluminescence instrument. A close examination of the rocket profiles of Figure 10-3 reveals that the variance between profiles increases markedly at altitudes below about 35 km; at 32 km there is over a factor of 5 difference in the mixing ratio. This is in contrast to the majority of the *in situ* balloon results in the 30-32 km of Figure 10-1. The average of the rocket data at 32 km is a factor of 2.8 lower than the mean derived from the balloon measurements shown in Figure 10-2; a discrepancy noted in the WMO assessment of 1981 and one that still needs to be resolved. Part of the difference and the increased variance of lower altitudes may be due to a loss in cryopump efficiency in the rocket instrument below 32-33 km (Horvath, private communication). None of the rocket measurements shown in Figure 10-3 employed an in-flight calibration procedure. More recently, in-flight calibration was employed on a flight in winter (January 1983). The results at 30 km agreed very well with a value near 2.8 ppbv, and the in-flight calibration confirmed the preflight laboratory calibration. Since substantial seasonal differences have been observed at more northern latitudes, these observations do not necessarily substantiate the summer/fall values near 30 km.

However, the variance in the measurements from the other instruments in Figure 10-3 is also large. Consequently, in an attempt to estimate the high altitude distribution of NO, the rocket data below 34 km is not considered. Even so, a broad range remains in the data.

Figure 10-4 shows the best estimate of the NO profile from the data in Figures 10-1 and 10-3. The profile above 30 km was determined by averaging the data by technique (rocket, balloon chemiluminescence, PMR and diode laser) rather than by averaging individual profiles. Flight M was included since diurnal trends are not expected to substantially perturb the data. This average profile above 32 km must be considered to have substantially larger uncertainty than that at altitudes below 32 km. Certainly, the confidence in the profile at altitudes where nitric oxide is expected to dominate the abundance of NO_y is not high.

10.1.1.3 Other Information

Further information about stratospheric nitric oxide can be derived from satellite measurements of nitrogen dioxide. These observations are discussed in detail in Sections 10.2 and 10.3. There are also

Figure 10-4. Best estimate of NO profile from all techniques, 14 to 50 km, 32–44 °N latitude.

505

a few recent long-path solar occultation retrievals of nitric oxide. Together, these data bases can be examined to determine whether the range of mixing ratios at high altitudes can be further refined.

Zonal mean profiles for nitrogen dioxide at 32 °N in the summer/fall season during the afternoon (about 1300 local time) and at night (about 2300 local time) are available from the LIMS retrievals 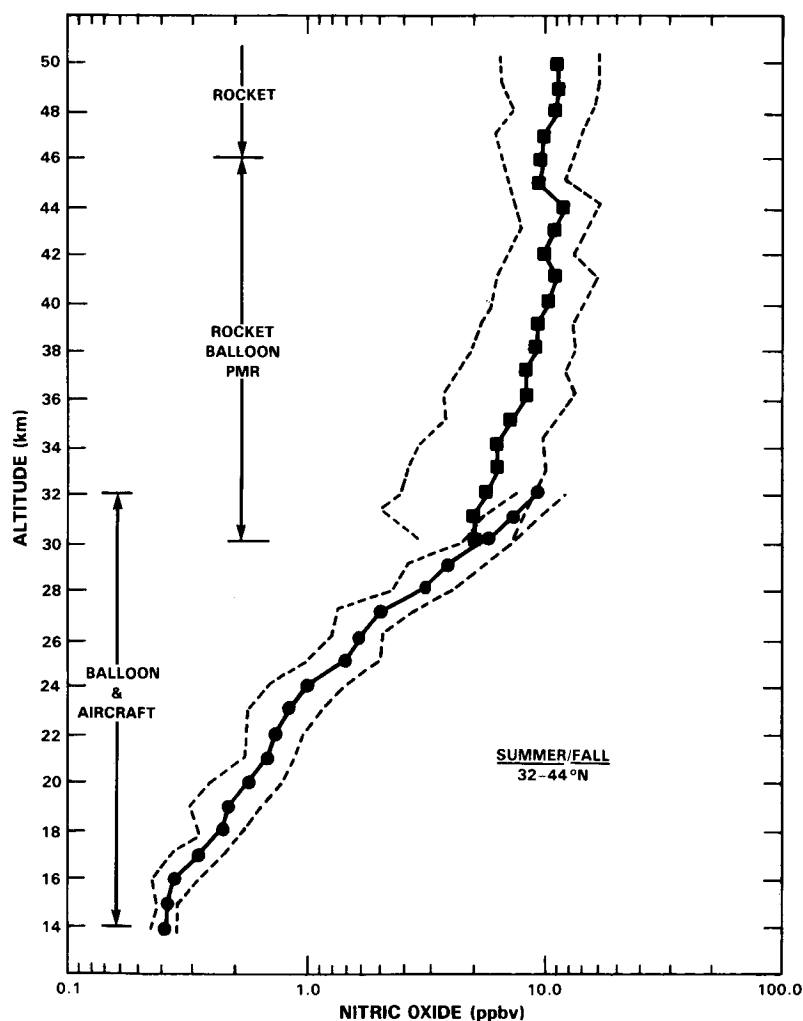(see Section 10.2.1). Near 40 km, the daytime abundance is 2-3 ppbv while the nighttime abundance is 15-16 ppbv. The difference of 12-14 ppbv provides at least a lower limit to the afternoon abundance of nitric oxide. The difference should be larger and depends on the amount of nitrogen dioxide converted to NO_3 and N_2O_5 between sunset and 2330 (see Section 10.3). In any event, the lower limit difference is only about 25% larger than the mean at 40 km in Figure 10-4. At 34 km a similar analysis yields a lower limit of 10-11 ppbv, about 50% larger than the mean in Figure 10-4. Of course these differences depend upon the uncertainties in the satellite retrievals.

10.1.1.4 Solar Occultation Retrievals

Solar occultation measurements of nitric oxide during sunset have been reported since as early as 1973 (Ackerman et al., 1973, 1975). The method has the advantage that absorption features of many different stratospheric species are recorded simultaneously. Mixing ratio profiles from this technique have not been discussed so far because they are not directly comparable to the daytime in situ and PMR data of Figures 10-1 and 10-3. Although the measurement technique is straightforward, the deconvolution of the infrared absorption as a function of zenith angle to obtain an altitude profile is particularly complicated for nitric oxide, for two reasons. First, as the solar zenith angle increases beyond 90° during sunset, nitric oxide is converted to nitrogen dioxide as both the photodissociation rate of nitrogen dioxide and, at appropriate altitudes, the atomic oxygen concentration decrease. Second, deconvolution techniques usually employ an "onion peeling" procedure in which NO is assumed constant in layers of about 2 km. Altitude gradients of nitric oxide within the layer further complicate the analysis. To obtain the best estimate of the profile of nitric oxide equivalent to sunset (a zenith angle of 90°) a diurnal model should be applied (Boughner et al., 1980). Rinsland et al. (1984a) have developed this reduction technique to show that a sunset profile of NO with a model input yields a mixing ratio near 18 km about a factor of 1.7 larger than a retrieval with no model input. The difference was a strong function of altitude; above about 20 km the difference decreases from about 10% to zero near 33 km.

Once a 90° sunset profile is derived, a comparison with high sun in situ or PMR data requires a knowledge of the afternoon to sunset variation of nitric oxide. This variation should depend upon altitude for three reasons. First the vertical distribution of N_2O_5 and its photodissociation coefficient depend strongly on altitude. Photolysis of N_2O_5 during the morning and afternoon would tend to increase nitric oxide. Second, due to multiple scattering and the decreasing contribution of surface albedo, the photodissociation coefficient of NO_2 is expected to decrease in the afternoon towards sunset. Partitioning of the sum of NO and NO_2 should shift to lower NO. Third, the decrease in the atomic oxygen concentration with increasing afternoon zenith angle would tend to decrease nitric oxide. The detailed diurnal variation varies from model to model. However, the decay of nitric oxide near sunset has been observed in detail by Ridley and Schiff (1981), Knight et al. (1982) and Kondo et al. (1985). At 32 km, Kondo et al. (1985) have observed a slow decay of about 25% as the zenith angle increased from 80-90° and a rapid decay to zero nitric oxide by 94°. Near 40 km, the decay was not observed until near 90° (Ridley and Schiff, 1981). Consequently, it is reasonable to assume that the solar occultation measurements for 90° and at altitudes above 34 km are about 15% below afternoon in situ measurements. At lower altitudes, 90° occultation profiles are expected to be even lower than daytime in situ and PMR profiles.

Figure 10-5 shows the results of three recent interpretations of sunset spectra. The first, by Rinsland *et al.* (1984a), is obtained by a model modified deconvolution to 90° of spectra obtained by Blatherwick *et al.* (1980) from a balloon flight on October 10, 1979. The other two profiles (Louisnard *et al.,* 1983) do not include this type of correction. The errors estimated for these profiles are near ± 20% above about 30 km. Included in this figure is the result from the PMR instrument which was obtained simultaneously with the Louisnard *et al.* occultation profile of June 1983 (BIC 2). The PMR data were the result of signal integration over a three hour period ending one-half hour before a 90° zenith angle. There is good agreement between the BIC 2 instruments below 38 km, with the PMR results being larger on average as would be expected.

At high altitudes (above 30 km) the occultation data tend to nitric oxide values that fall between the extremes of the data of Figures 10-1 and 10-3. Consequently, these data do not help to decrease the range of the uncertainty in the high altitude measurements.
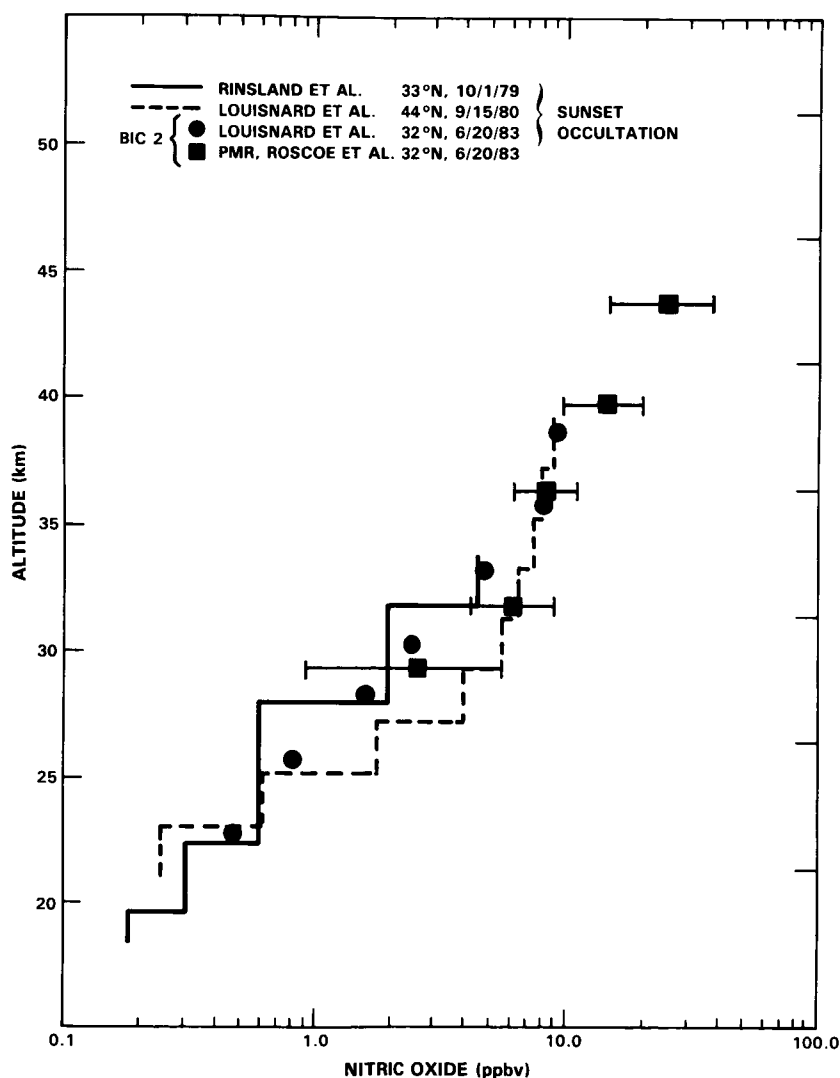

Figure 10-5. Sunset observations of stratospheric NO.

507

10.1.1.5 Seasonal Variations

The variation of nitric oxide with season observed near 18 and 21 km by Loewenstein *et al.* (1978a, b) was summarized in the 1981 WMO report. Total stratospheric column densities have also been measured as a function of latitude in the summer and winter seasons. These observations are discussed in detail in Section 10.1.11. Although these data provide valuable information, they do not reveal the changes in the altitude distribution in the stratosphere.

Altitude distributions of nitric oxide and other trace species have been measured at latitudes between 50 and 54 °N over western North America in winter (Ridley *et al.*, 1984; Knight *et al.*, 1982; Evans *et al.*, 1982a; McFarland *et al.*, 1985). Several rocket flights at 38 °N and one at 50 °N have been reported for the winter season by Horvath *et al.* (1983). The winter balloon experiments were inspired by the unique observations by Noxon (1979) concerning the variation with latitude and season of the column abundance of nitrogen dioxide.

Figure 10-6 shows observations of NO by McFarland *et al.* (1985) for December 15, 1982 near 50 °N. NO_2 was also observed to be greatly reduced below 28 km relative to summer observations. The seasonal change is in agreement with observations made earlier by Ridley *et al.* (1984). Both Knight *et al.* (1982) and Solomon and Garcia (1983a, b) suggested that the reduction of nitric oxide and nitrogen dioxide was likely to be due to the formation of N_2O_5 at northern latitudes in winter under certain meteorological conditions. Evans *et al.* (1982a) suggested that heterogeneous conversion to nitric acid might also contribute to the reduction. It is unfortunate that no winter profiles below 30 km have been obtained at more southerly latitudes. Such observations could provide further information on the role of N_2O_5 in winter.

Solomon and Garcia (1983a, b) and further work by Noxon and co-workers (1983) have demonstrated in detail the sensitivity of the winter distribution of nitric oxide and nitrogen dioxide to the variances in winter dynamics at high latitudes over North America.

10.1.2 Nitrogen dioxide (NO_2)

A variety of airborne and ground-based measurement programs have established some aspects of the latitudinal, seasonal and diurnal variability of stratospheric NO_2. The column abundance of NO_2 increases with increasing latitude, and summertime high latitude column amounts are a factor of three more than equatorial column amounts. The latitude distribution also depends on season with high latitude winter column amounts a factor of 2 to 3 less than summer abundances. Diurnal variations have also been observed; sunrise column amounts and altitude profiles are about a factor of two to three lower than sunset abundances. The situation during the transition from night to day (sunset or sunrise) is not well defined. There is also evidence that large scale air motions can alter the NO_2 abundance by a factor of two in a few days.

To establish a complete picture of stratospheric NO_2, measurements are required at many latitudes, for many times during a year, throughout the day. All these measurements, of course, have not been made. Observations tend to cluster at the locations of balloon launch facilities. For legitimate comparison we must group measurements with regard to location and time.

Table 10-2 lists most of the balloon-borne observations of NO_2. Most of the methods employ long-path optical techniques, either infrared (IR) emission or visible or IR absorption. Most of the absorption methods use the rising or setting sun as the light source (solar occultation). Since the 1981 WMO assessment, several *in situ* methods have been used to obtain daytime observations.
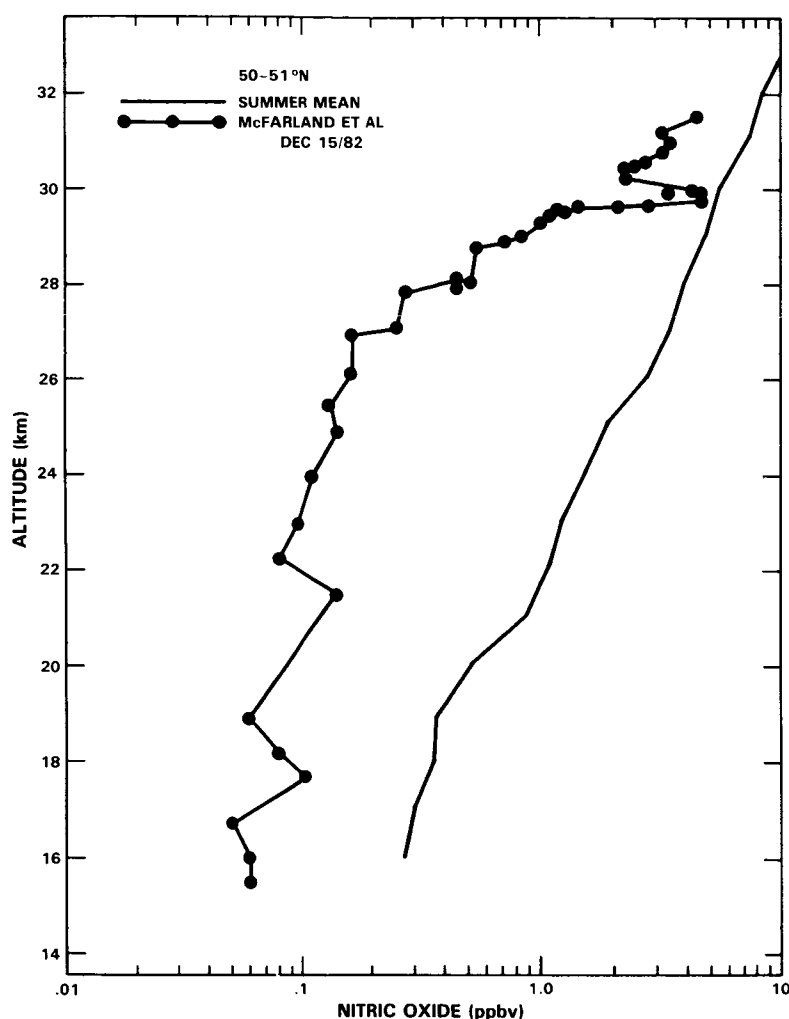
Figure 10-6. Summer and winter NO profiles by the same technique showing seasonal variability.

Figure 10-7 contains sunset vertical profiles from a number of techniques in the latitude range of 30-35 °N. Equator wards of about 40 °N there is little seasonal variation so measurements from all seasons may be compared. Since the 1981 assessment there was an extensive international measurement program, the Balloon Intercomparison Campaign (BIC 1 in September and October 1982 and BIC 2 in June 1983) which provided a number of remote observations of NO_2. A new technique using a gas correlation radiometer in a solar occultation mode (Fischer *et al.*, 1985a) has produced two sunset profiles which are included in Figure 10-7. The solid curve is a hand drawn mean from the values presented in WMO 1981 from visible and infrared absorption techniques at sunset. In general, the uncertainties are ± 20% for values between 28 and 38 km.

BIC results are not yet published and some obvious systematic instrumental differences have not been resolved. One suggestion of the BIC results is a decrease in the NO_2 during BIC 1 as compared to the BIC 2 time period, which may have been due to abnormal stratospheric conditions caused by the eruption

Table 10-2. Measurements of Profiles of NO_2 from Balloons

| O=solar occultation | SR=sunrise | BIC 1=Sep/Oct 82, 32°N, SS | N=night |
| E=thermal emission | SS=sunset | BIC 2=Jun 83, 32°N, SS | |

Group	Instrument	Flights	Reference
IASB	grille	May 74, 44°N, SS	Ackerman et al. 1978/79
ONERA	spectrometer,	May 78, 44°N, SS	Borghi et al. 1983
ONERA	1600cm⁻¹,O	Apr 79, 32°N, SS	Borghi et al. 1983
ONERA	1600cm⁻¹,O	Sep 80, 44°N, SS	Louisnard et al. 1983
ONERA	1600cm⁻¹,O	May 82, 44°N, SR	Louisnard et al. 1985
ONERA	1600cm⁻¹,O	BIC 2	—
Denver U	spectrometer,	Dec 67, 34°N, SS	Murcray et al. 1973
Denver U	1600cm⁻¹,O	Oct 79, 33°N, SS	Blatherwick et al. 1980
NPL	cooled spectr,	May 81, 32°N, pm	—
NPL	1600cm⁻¹,	BIC 1, pm	—
NPL	wideband, E	BIC 2, pm	—
Oxford U	PMR, 1600cm⁻¹,E	Jun 75, 44°N, am+N	Drummond & Jarnot 1978
Oxford U	PMR, 1600cm⁻¹,E	Sep 78, 32°N, pm	Roscoe et al. 1981
Oxford U	PMR, 1600cm⁻¹,E	Oct 80, 32°N, pm+N	Roscoe et al. 1985a
Oxford U	PMR, 1600cm⁻¹,E	May 81, 32°N, pm+N	Roscoe et al. 1985a
Oxford U	PMR, 1600cm⁻¹,E	BIC 1, pm+N	Roscoe et al. 1985a
Oxford U	PMR, 1600cm⁻¹,E	BIC 2, pm+N	Roscoe et al. 1985a
Met Inst,	gas correlation,	Jul 78, 48°N, SR	Fischer et al. 1985b
Munich	1600cm⁻¹,O	Feb 79, 32°N, SS	Fischer et al. 1985b
	1600cm⁻¹,O	May 79, 32°N, SS	Fischer et al. 1985b
York U	laser, in situ	Jul 83, 51°N, pm	Hastie et al. 1985
NOAA,	chemilumines,	Nov 81, 32°N, pm	McFarland et al. 1985
Boulder	in situ	Jul 82, 32°N, pm	McFarland et al. 1985
Boulder	chemilumines	Aug 82, 51°N, pm	McFarland et al. 1985
Julich	matrix isol,	Sep 83, 44°N, am	Helten et al. 1984a, b
Julich	ESR, in situ	Sep 83, 44°N, N+am	Helten et al. 1984a, b
Denver U	scanning	Feb 77, 33°N, SS,	Goldman et al. 1978
Tokyo U	spectrometer,	May 78, 40°N, SS,	Ogawa et al. 1981
Tokyo U	440nm, O	Nov 82, 67°S, SS+SR	—
Tokyo U	440nm, O	BIC 2	—
CNRS	440nm, O	Sep 79, 44°N, day	Pommereau 1982
CNRS	440nm, O	BIC 2	—
U PM. Curie	440nm, star O	Sep 79, 44°N, N	Naudet et al. 1984
U PM. Curie	440nm, star O	Sep 81, 44°N, N	Naudet et al. 1984
AES	fixed	Jul 74, 58°N, SS	Kerr & McElroy 1976
AES	spectr,	Aug 75, 5°N, SS+SR	Kerr & McElroy 1976
AES	440nm, O	Aug 75, 5°N, SS+SR)	Kerr et al. 1982
AES	440nm, O	Aug 76, 5°N, SS+SR	Kerr et al. 1982
AES	440nm, O	Aug 76, 5°N, SS+SR	Kerr et al. 1982
AES	440nm, O	Aug 77, 5°N, SR	—
AES	440nm, O	Dec 77, 32°N, SS	—
AES	440nm, O	Nov 78, 32°N, SS	—
AES	440nm, O	Oct 80, 32°N, SS	—
AES	440nm, O	Oct 79, 34°S, SR	—
AES	440nm, O	Oct 79, 34°S, SS	—
AES	440nm, O	BIC 1	
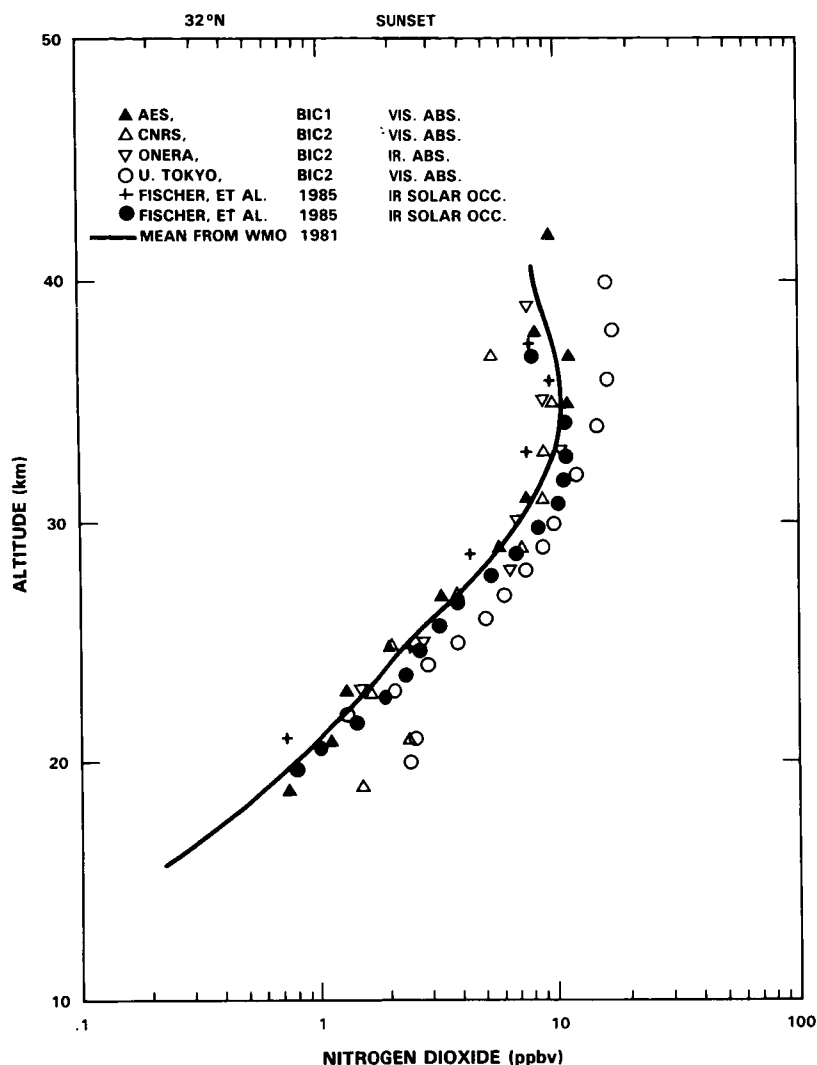
Figure 10-7. Sunset NO₂ profiles from a number of techniques in the latitude range 30–35°N.

of the volcano El Chichon in April 1982. The difference (a factor of 1.5 to 2) is supported by ground based and aircraft measurements of the NO_2 column. The possibility of such sporadic and apparently temporary effects adds another dimension to the variability in stratospheric NO_2.

In situ and emission measurements made during the day should represent a lower NO_2 amount at every altitude as compared with a sunset determination (up to a factor of two less at 30 km). Figure 10-8 contains daytime NO_2 profiles from a number of sources. The daytime profiles are significantly less than sunset profiles, as expected. Variation in the profiles is nearly encompassed by the measurement uncertainties. To strictly compare daytime measurements consideration must be given to the exact time of day of the measurements.

It is clear from observations, especially those of the AES group (Kerr *et al.*, 1982), that sunrise NO_2 ($\chi = 90°$, am) is about a factor of two lower than sunset NO_2 ($\chi = 90°$ pm). Observations during a
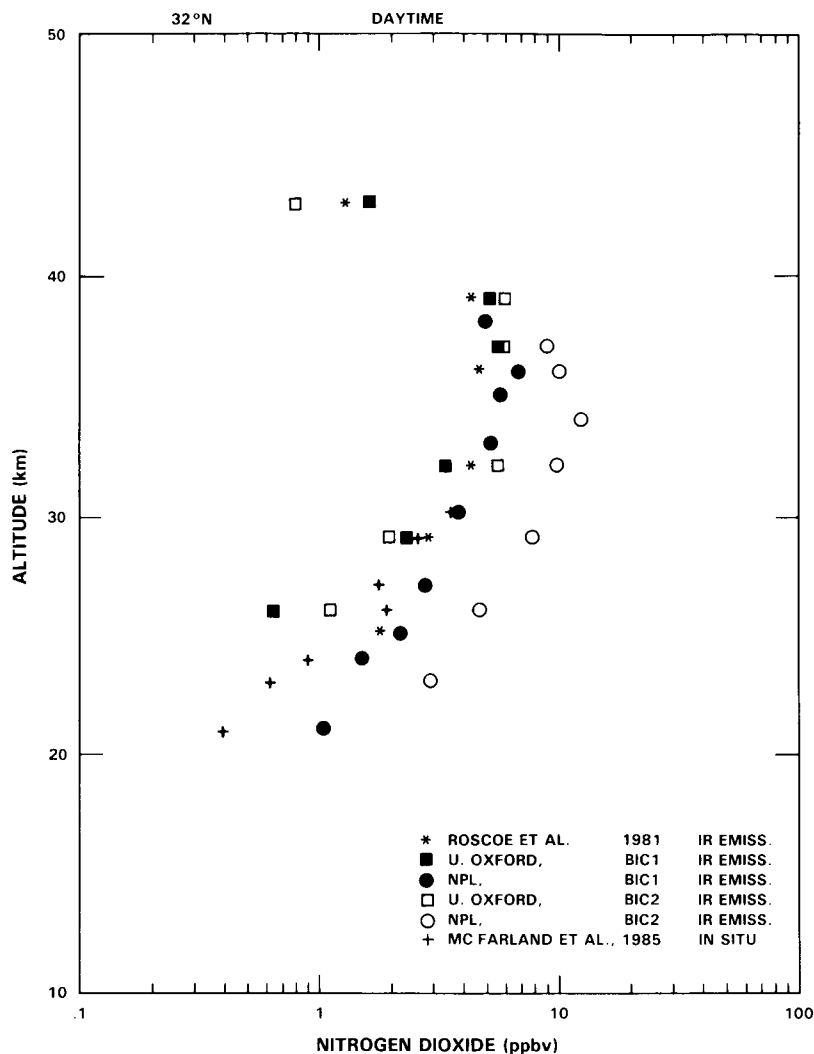
Figure 10-8. Daytime NO₂ profiles near 32°N.

day with the same instrument have shown slow diurnal changes in NO_2 amounts (Roscoe *et al.*, 1981; Pommereau, 1982; Flaud *et al.*, 1983). As discussed in the previous Section (10.1.1) several factors may contribute to this daytime variation. First, release of NO and NO_2 from nighttime reservoirs, especially N_2O_5, would cause a daytime increase of NO and NO_2. Little is known about the stratospheric abundance of N_2O_5 and the photolysis rate of N_2O_5 is a strong function of altitude. Second, due to multiple scattering and the change in the contribution of surface or cloud albedo with zenith angle, the photodissociation coefficient of NO_2 (J_{NO_2}) exhibits a diurnal dependence. From noon to sunset, J_{NO_2} is expected to decrease especially as $\chi \rightarrow 90°$. Third, the atomic oxygen concentration at higher altitudes also exhibits a strong zenith angle dependence. Consequently, NO_2 is expected to increase in the afternoon towards sunset at the expense of NO. Considerable debate remains as to the magnitude of the change in NO_2 at a given altitude as sunset is approached; models are not consistent in their treatment of multiple scattering and albedo for curved earth geometry. Nevertheless, observations made near local noon are not expected to agree with sunset solar occulation measurements that are equivalent to a solar angle of 90° (cf. Rinsland

et al., 1984c). Thus careful attention must be given to the time (solar angle) of the measurements if observations from different techniques are to be intercompared. The same attention must be given to comparisons of observations with predictions from photochemical/transport computer models.

Figure 10-9 shows daytime and sunset NO_2 measurements which have been reported since WMO 1981 in the latitude range of 40 to 50°N. The open symbols (Louisnard *et al.*, 1983) are from infrared solar occultation measurements at sunset using a grille spectrometer, the solid line is a hand drawn mean of the measurements reported in WMO 1981 by the same spectrometer in earlier years. A recent development is an *in situ* measurement of daytime NO_2 using a matrix isolation ESR spectroscopy technique (Helten *et al.*, 1984a, b). The agreement between the *in situ* and remote occultation measurements is encouraging. *In situ* measurements are not susceptible to the uncertainties in NO_2 photochemistry which affect the retrieval of remote occultation measurements. Future, more numerous comparisons of *in situ* and remote observations would make a valuable contribution to our understanding of the NO_2 data base.
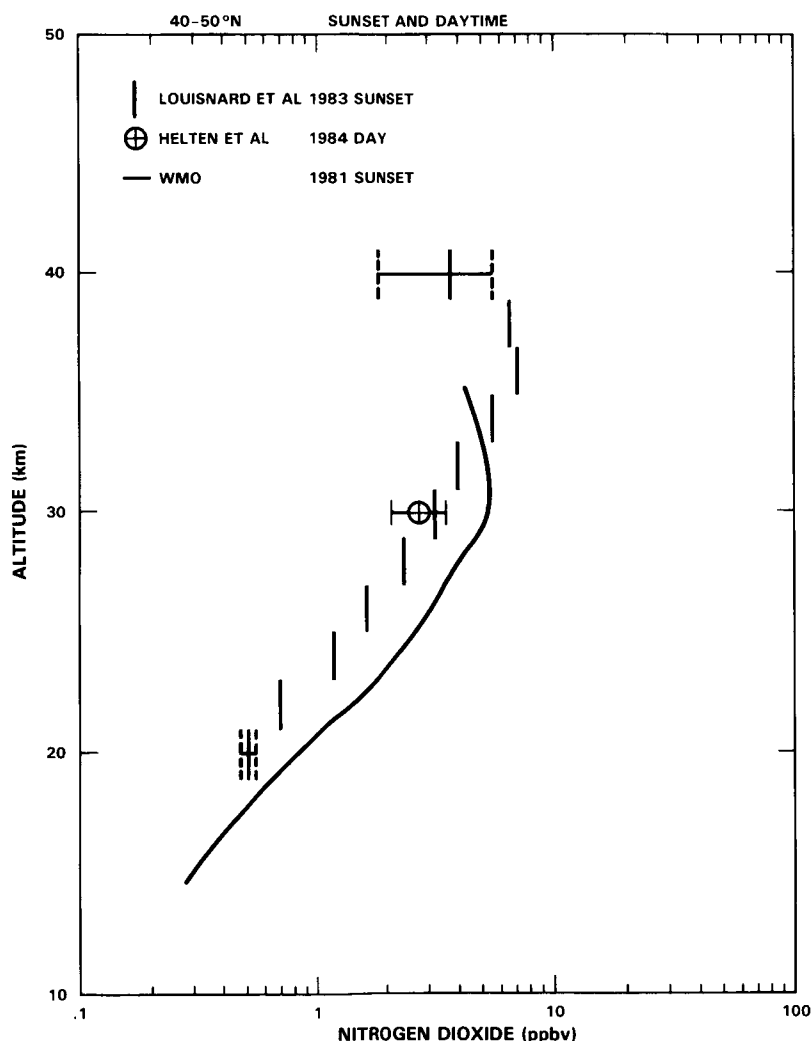
Figure 10-9. Daytime and sunset observations of NO_2 from 40 to 50°N latitude.

NITROGEN SPECIES

New measurements reported from 50 to 60 °N are from an *in situ* technique based on infrared tunable diode laser absorption spectroscopy (Hastie and Miller, 1985) and an *in situ* profile determined using a chemiluminescence technique (McFarland *et al.*, 1985). Figure 10-10 shows the daytime *in situ* measurements and a remote sunset profile published in 1982 (Kerr *et al.*, 1982) which are essentially the same data presented in WMO 1981. At these higher latitudes one must distinguish measurements made in different seasons. The observations in Figure 10-9 were all in summer and no profile measurements have been made at high latitudes in winter to test the seasonal variability calculated by models. As was the case at lower latitudes the noontime profile is uniformly less than the sunset profile.

As described above, measurements of sunrise NO_2 should not be the same as nighttime measurements. Figure 10-11 contains the relatively few observations of nighttime and sunrise NO_2 profiles. The two sunrise observations agree well and are rather less than most of the nighttime observations as our understanding of nighttime photochemistry would predict. Profiles produced for sunrise and sunset by visible absorption spectrometry (Kerr *et al.*, 1982) indicate a factor of two increase from sunrise to sunset at all altitudes; the magnitude of the increase is in agreement with column measurements from aircraft (Coffey *et al.*, 1981a).
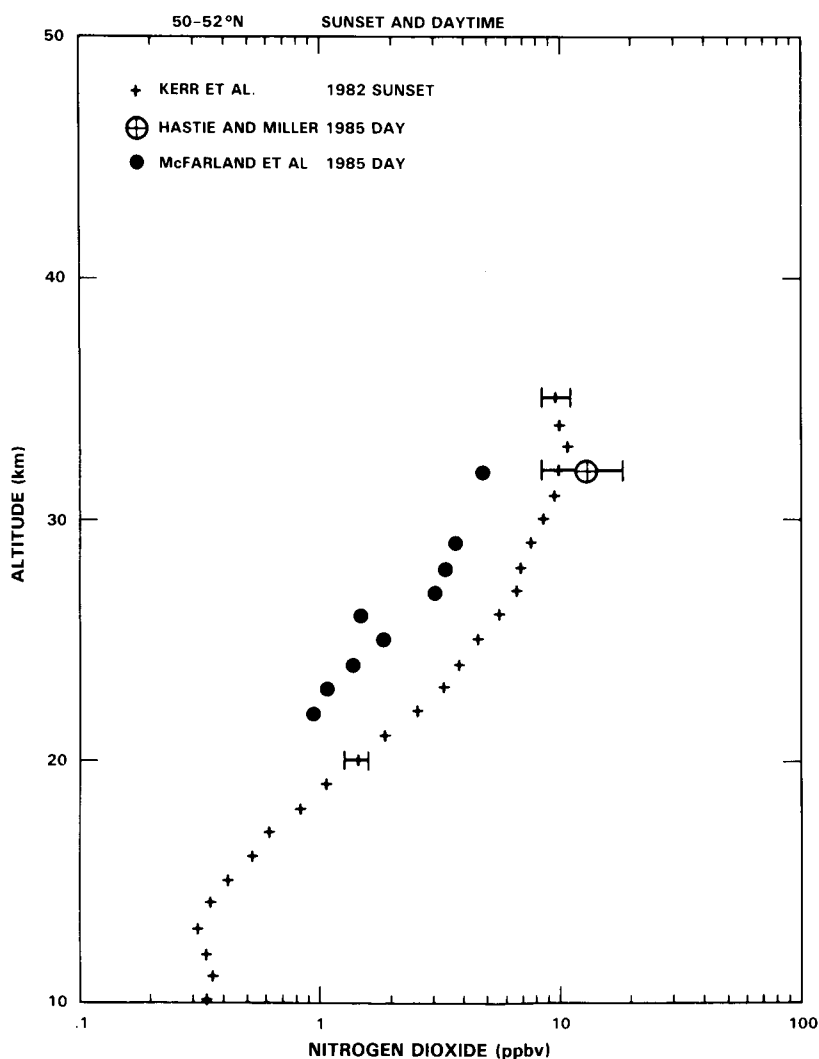
Figure 10-10. Daytime and sunset observations of NO_2 from 50 to 52 °N latitude.

514

Having examined each of the latitudinal groups of measurements one may attempt to discern a latitudinal trend in the NO_2 vertical profile. Figure 10-12 contains a representative sunset profile from each of the latitude ranges. Some liberty has been taken in selecting a profile in the 30 to 35 °N range since there may have been unusual effects in the BIC 1 results due to perturbations resulting from the El Chichon eruption. Also plotted in the figure are summertime profiles for various latitudes from the LIMS and SAGE satellite-borne instruments. The LIMS measurements are appropriate to a local time of 13:00 hours, the SAGE profiles are for sunset so our simple model implies that the LIMS profile should show less NO_2 than SAGE. Figure 10-12 shows that the NO_2 vertical profile does not change substantially in shape or magnitude from 30 to 45 °N but the profile at 60 °N is considerably different. Reasonable agreement is shown between the balloon and satellite observations over much of the range of overlap, though the substantial differences at 50-60 °N need to be explained.
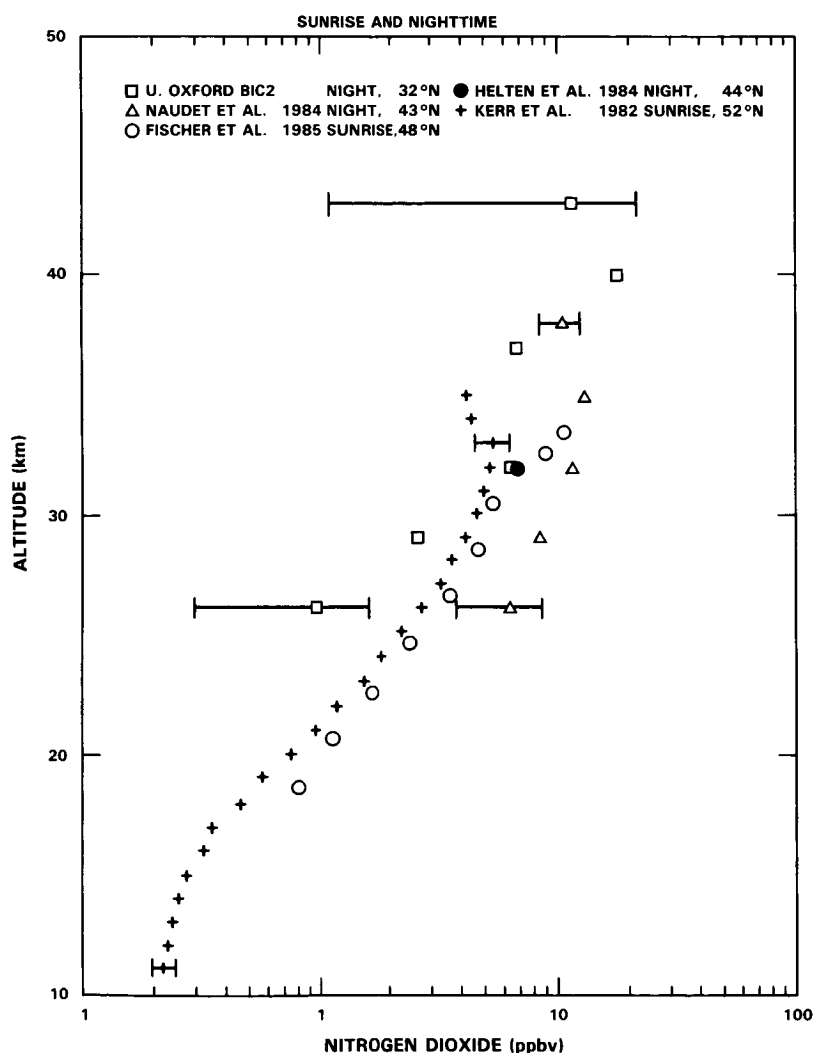
Figure 10-11. Nighttime and sunrise observations of NO_2 from all latitudes.
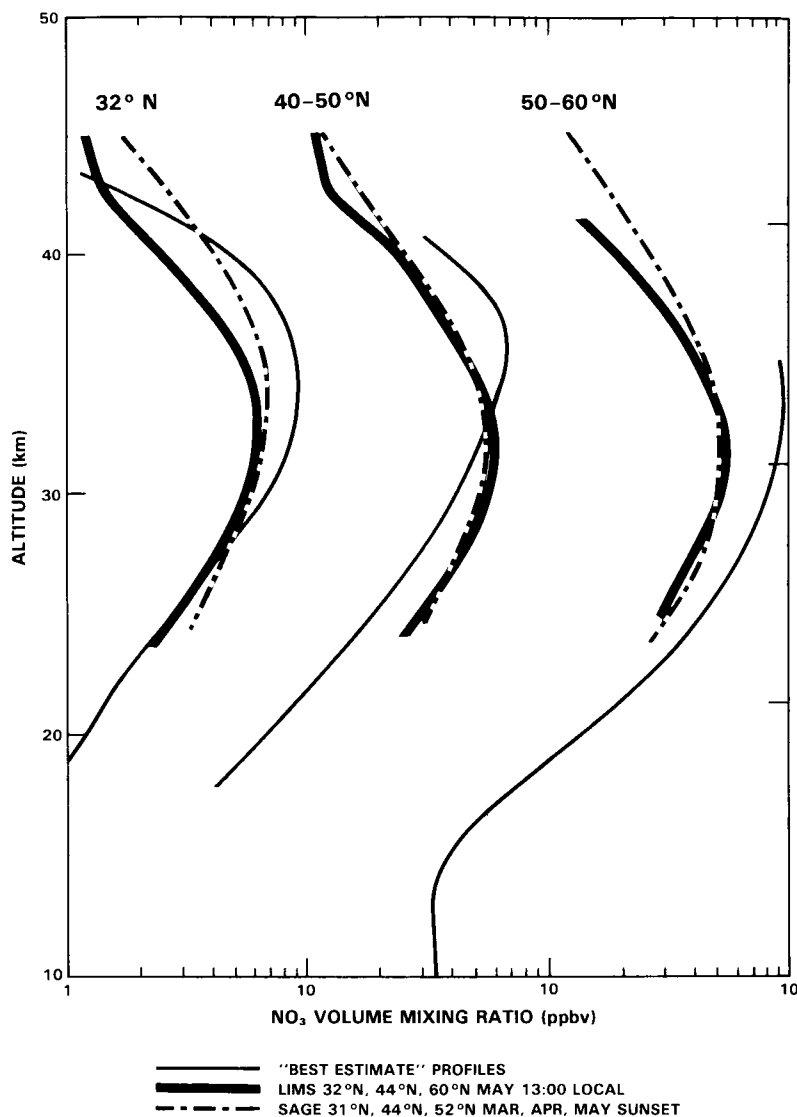
Figure 10-12. Best estimate of NO_2 profiles in three latitude ranges from non-satellite techniques compared with observations by the satellite-borne instruments LIMS and SAGE.

10.1.3 Nitric Acid (HNO₃)

A nearly complete listing of balloon-borne measurements of stratospheric HNO_3 profiles is given in Table 10-3. Most of the measurements have been performed with remote sounding instruments. The compilation also includes measurements with the filter collection and ion-sampling techniques. The list of University of Denver (DU) measurements and Atmospheric Environment Service (AES) measurements is not complete.

The two Balloon Intercomparison Campaigns (BIC) provided a good comparison for understanding instrumental differences. Firstly, some systematic errors were discovered. The profile measured by the ONERA grille spectrometer exhibits significantly greater concentrations in the lower stratosphere than those measured by other instruments (errors could be as large as 50%). The absence of spectroscopic

Table 10-3. Measurements of Profiles of HNO_3 from Balloons

| O = solar occultation | | SS = sunset | BIC 1 = Sep/Oct 82, 32°N, SS |
| E = thermal emission | | | BIC 2 = Jun 83, 32°N, SS |

Groups	Instrument	Flights	References
AES	Filter	Jul 74, 59°N	Evans *et al.* 1976
AES	radiometer,	Aug 76, 51°N	Ridley *et al.* 1984
AES	880cm⁻¹, E	Feb 77, 8, 9, 54°N	Ridley *et al.* 1984
AES	ascent	BIC 1+2	—
Denver U	ascent	May-Nov 70, 33°N	Murcray *et al.* 1973
Denver U	ascent	71-75, 64°N	Goldman *et al.* 1976
Denver U	Cooled spectr,	June 74, 33°N	Murcray *et al.* 1983
Denver U	880cm⁻¹,E,asc.	BIC 1+2	
NPL	Interfer, far IR	Sep 74, 44°N	Harries *et al.* 1976
NPL	Cooled spectr,	May 81, 32°N	Louisnard and Pollitt, 1985
NPL	880cm⁻¹,E	BIC 1+2	—
Wuppertal	Cooled spectr.	Sep 83, 44°N	Rippel 1984a, b
GHSW	880cm⁻¹,E		
Met Inst.	Filt radiometer	Feb 79, 32°N, SS	Fischer *et al.* 1985a
Munich	880cm⁻¹,O	May 79, 32°N, SS	Fischer *et al.* 1985a
NOAA	Spectrometer,	Jun 82, 32°N, SS	Weinreb *et al.* 1984
Washington	880cm⁻¹,O		
Denver U	Interferometer,	Mar 81, 33°N, SS	Goldman *et al.* 1984c
Denver U	880cm⁻¹,O	BIC 2	—
ONERA	Grille spectr,	May 78, 44°N, SS	Borghi *et al.* 1983
ONERA	1325 cm⁻¹,O	Apr 79, 32°N, SS	Girard and Louisnard, 1984
ONERA	1325 cm⁻¹,O	Sep 80, 44°N, SS	Louisnard *et al.* 1983
ONERA	1325 cm⁻¹,O	BIC 2	—
MPIH	Ion measure	Nov 77, Oct 82+3, 44°N	Arnold and Qui, 1984
MPIH	*in situ*	1984, 48-50°N	Knop and Arnold, 1985
NCAR	Cellulose	Spring 71, 34S-64°N	Lazrus and Gandrud, 1974
NCAR	filters,	Spring 72, 34S-64°N	Lazrus and Gandrud, 1974
NCAR	*in situ*	Spring 73, 34S-32°N	Lazrus and Gandrud, 1974

line parameters at 1320 cm⁻¹ is probably responsible for this discrepancy, since the temperature dependence of the absorption is unknown. The laboratory calibration which was used is now under reinvestigation. The AES group has improved their data evaluation procedure by taking into account the CFC-11 and CFC-12 absorption. This increased the HNO_3 mixing ratio retrieved below 20 km by 1×10^{-9}; above 20 km, the increase decreases linearly to zero at 30 km (Evans, private communication). All previous profiles published by the AES group must be similarly corrected. Secondly, after reanalysis,

the profiles measured by different instruments in the campaigns showed agreement within ± 30%. However, not all groups listed in Table 10-3 were able to participate in the BIC intercomparisons. Thus it is not clear how much of the remaining differences are caused by instrumental effects including data processing. As stated in WMO 1981 the *in situ* measurements of Lazrus and Gandrud (1974) yield lower HNO_3 values than the other techniques, in particular in the lower stratosphere. The reason for this discrepancy has still not been found.

Due to the known latitudinal variation of HNO_3, the balloon-borne measurements are divided into sets made in different latitude ranges. A large number of the profiles were measured at 32°N. Since no noticeable change in the HNO_3 concentration as a function of the time of the day has been observed and, since there is no evidence to support a significant seasonal variation at latitudes less than 40°N (Murcray *et al.*, 1975; Coffey *et al.*, 1981a), the balloon profiles measured at 32°N should be comparable. Several groups have measured similar HNO_3 profiles at 32°N at different times and in different years (e.g. NPL, Met Inst., Munich). Figure 10-13 shows a selection of typical profiles from different groups. The agreement between all of the profiles is good around 25 km. The high HNO_3 values of the ONERA profile below 24 km are suspect as discussed above. The University of Denver profile measured during BIC 2 is representative of profiles measured during this campaign and can therefore be used for comparison with the other results. Above 30 km most of the profiles show a rapidly decreasing HNO_3 concentration; only the NOAA group have deduced high values, but with large error bars (Weinreb *et al.*, 1984).

All measurements available for 40-50°N are presented in Figure 10-14. Most of them were measured in the autumn. The large discrepancy between remote sounding and filter collection results is obvious
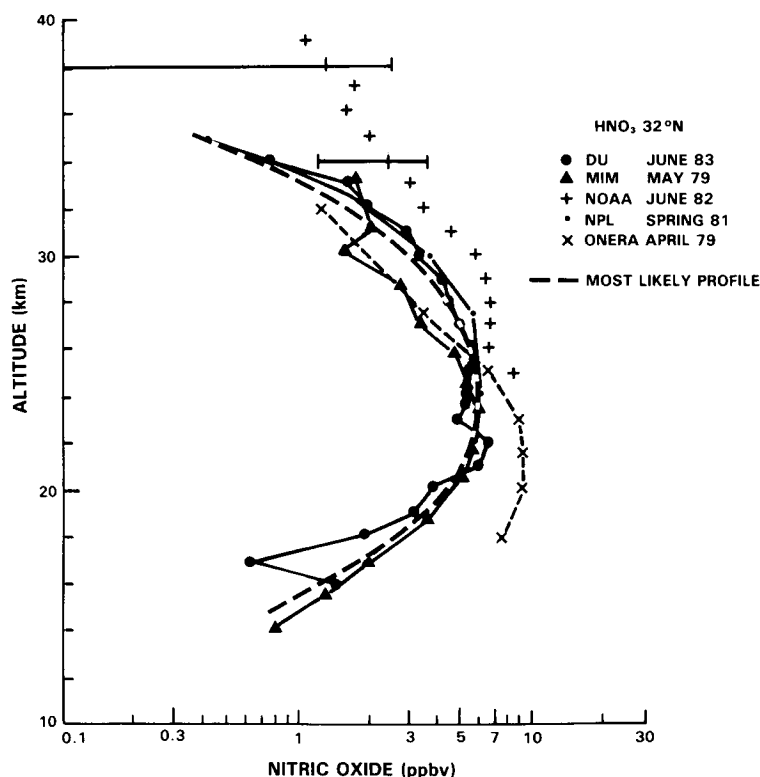
Figure 10-13. Observed HNO_3 profiles from a number of groups near 32°N latitude.

while the HNO_3 values evaluated from measurements with the ion technique agree with the remote sounding results. The Wuppertal measurements with a cooled grating spectrometer show relatively high HNO_3 mixing ratios at levels above 30 km; possibly because these measurements were made after the El Chichon eruption and the radiance measurements may be contaminated by aerosol emission.

A comparison between Figures 10-13 and 10-14 shows that the HNO_3 values at the maximum and in particular above the maximum are greater at 40-50°N than at 32°N. This was already noted by Louisnard *et al.* (1983, ONERA) who have carried out measurements at 32°N and 44°N.

At high latitudes, HNO_3 profiles have been measured by two groups, in the latitude belt between 50°N and 55°N by AES and around 64°N by University of Denver (Figure 10-15). A comparison between a summer profile at 51°N and a profile at 54°N averaged from two measurements in February 1978 and February 1979 shows clearly the seasonal variations at these latitudes (Ridley *et al.*, 1984). It should be recognized that the increase of the HNO_3 mixing ratios takes place at all altitudes. A similar picture of the seasonal changes is given by the averaged profiles at 64°N (D. Murcray, private communication). A comparison of the results of the two groups below the HNO_3 maximum shows a considerable difference (see Figure 10-15). The difference appears to be consistent with the rapid increase of the vertical column amount with increasing latitude.

Some of the spread in the HNO_3 profiles is due to atmospheric variability. This is illustrated by the results of several groups which have performed measurements at different times at the same location. Thermal emission measurements at different azimuth directions have shown significant differences around 29 km which lead to the conclusion that there is a mesoscale spatial variability in HNO_3 concentration (Pollitt, *et al.*, 1984).
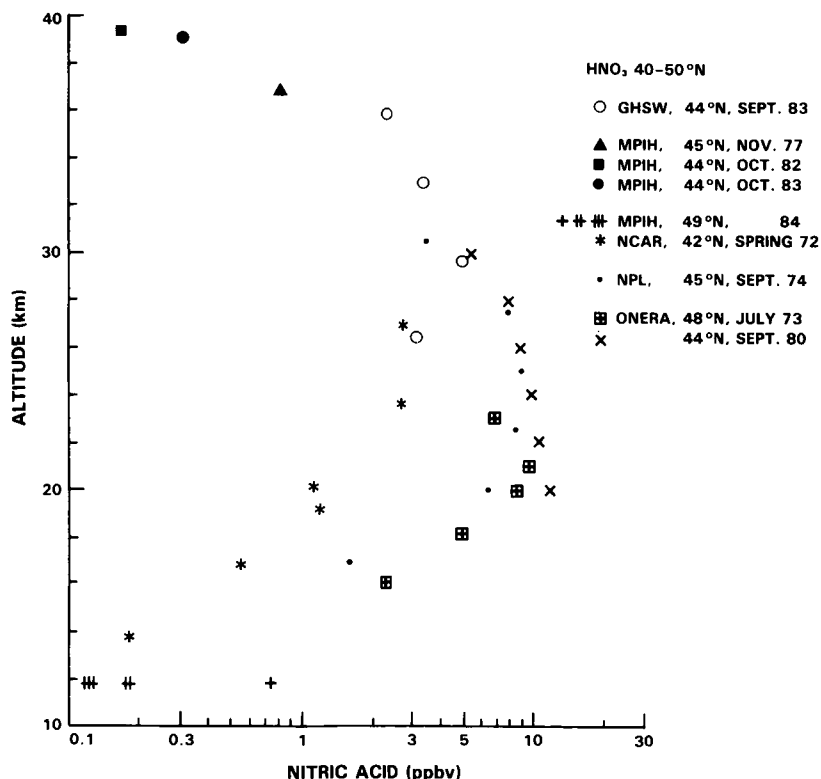
Figure 10-14. HNO_3 observations in the 40 to 50°N latitude range.

NITROGEN SPECIES

The most likely profile for HNO_3 at 32°N is deduced from the data presented in Figure 10-13, not taking into account the more suspicious points of the ONERA and the NOAA profiles.

Our knowledge of the HNO_3 profile has increased since the WMO assessment report of 1982. The balloon measurements have contributed to this in the following way:

1. Most of the more recent balloon measurements have confirmed that calculations overestimate HNO_3 concentrations above 25 km. The balloon measurements show HNO_3 mixing ratios above 32 km which are on average lower than the LIMS satellite measurements.

2. Taking into account our more recent experience about systematic errors in some of the balloon results, some features of the latitudinal variation in the HNO_3 profile become obvious. Between 32°N and 45°N the HNO_3 mixing ratios increase with latitude at and above the altitude of maximum mixing ratio. Between 45°N and 64°N there is a distinct increase of HNO_3 mixing ratios with latitude in the lower stratosphere.

3. The seasonal variation has been identified at latitudes above 50°N. The HNO_3 mixing ratios are larger at all altitudes in winter than in summer.

4. HNO_3 profiles show spatial variability at 32°N in the altitude region around 30 km.

5. Several HNO_3 profiles measured during ascent show a layered structure. At the moment it is not clear whether this structure is real or an artifact of the data evaluation.
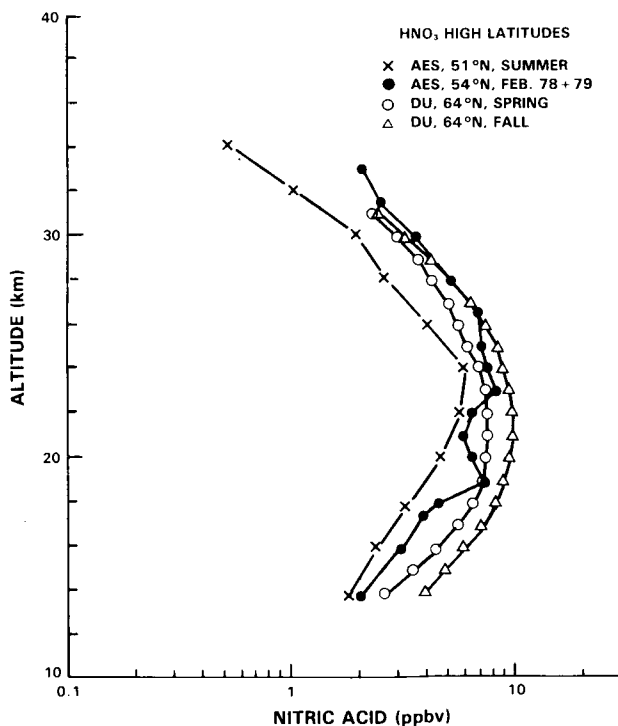
Figure 10-15. High latitude observations of stratospheric HNO_3.

520

10.1.4 Nitrous Oxide (N₂O)

Our understanding of the behavior of stratospheric N_2O has not changed substantially since the WMO 1981 assessment. There is a rapid decrease in mixing ratio with altitude and, at a given altitude above the tropopause, there is less N_2O at midlatitudes than at the equator. Figure 10-16 shows mean curves drawn through the observations represented in WMO 1981 for tropical and midlatitude conditions. Also shown in Figure 10-16 are the more recent measurements by an infrared grille spectrometer flown on Spacelab (Laurent *et al.*, 1983, Ackerman *et al.*, 1985). These solar occultation measurements, applicable to 43 °N latitude, support the rapid decrease in N_2O amount above about 20 km and extend the measurements to more than 50 km.
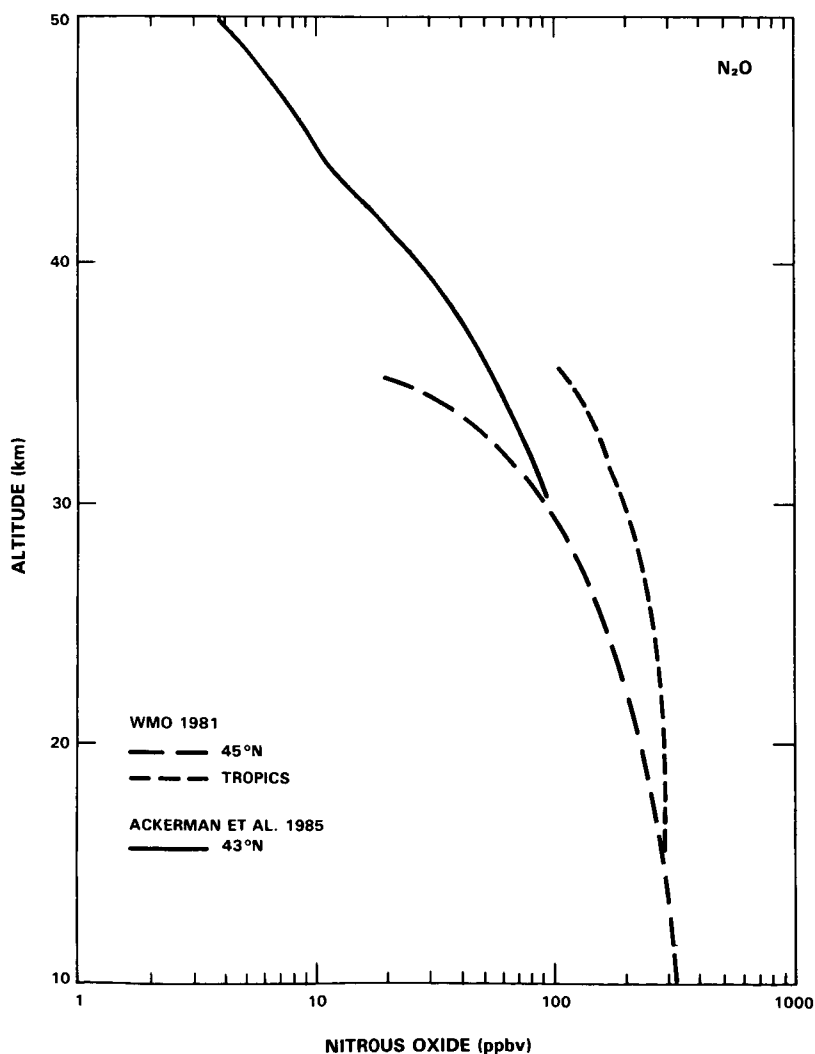
Figure 10-16. Observed stratospheric N_2O profiles.

10.1.5 Nitrogen Trioxide (NO₃)

Visible absorption spectroscopy near 600 nm with the moon or a star as a light source is used to measure NO_3 in the stratosphere. As there is still some uncertainty in the absorption cross section the results have been scaled to a value that is assumed to be temperature independent: 1.7×10^{-17} cm² given by Ravishankara and Wine (1983).

The total column abundance at night has been measured over a 5 year period at 40 °N from a ground-based station by Norton and Noxon (1985). They observed a maximum of stratospheric NO_3 in April/May and usually found it to be below their detection limit during the rest of the year. The latitudinal variation of the NO_3 column abundance (Norton and Noxon, 1985) is shown in Figure 10-17.

Nighttime profiles at 44 °N have been obtained from a balloon platform at 38.8 km in fall 1980, 1981, 1983 and in spring 1982 (Rigaud *et al.*, 1983; Pirre *et al.*, 1985) looking at the setting star Arcturus or at the rising planet Venus (Figure 10-18).
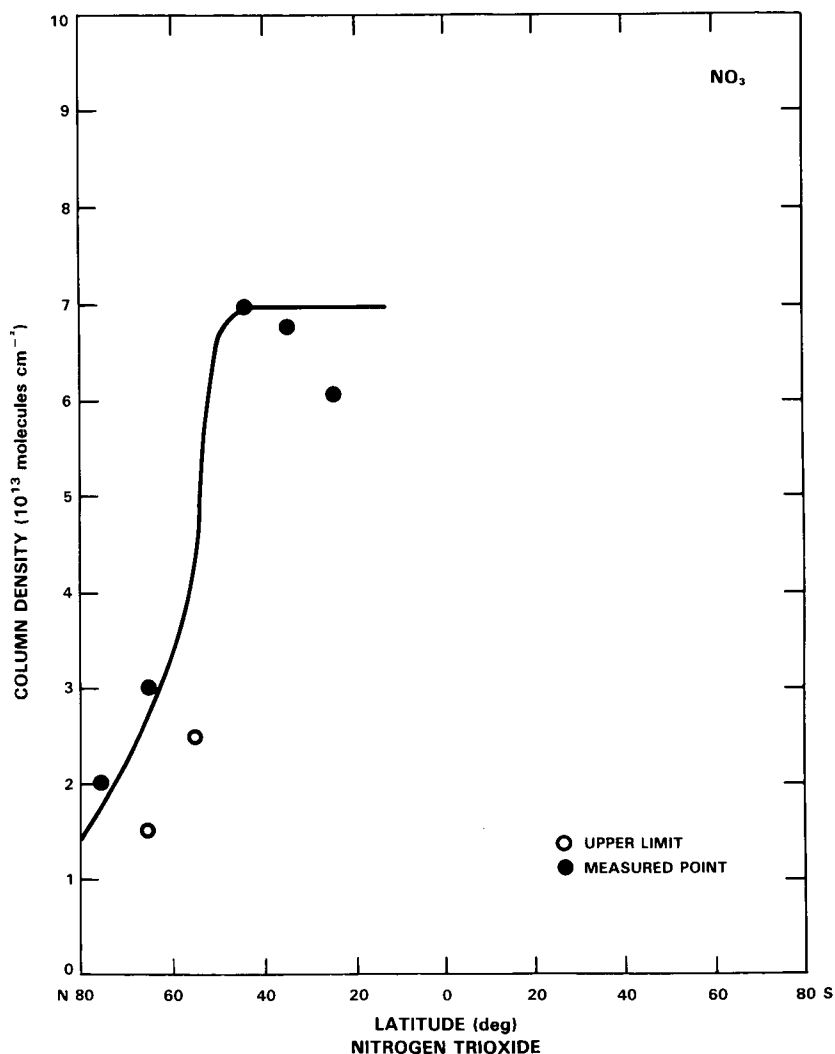
Figure 10-17. Latitude variation during Spring of column abundance of NO₃ from ground-based visible absorption spectroscopy.
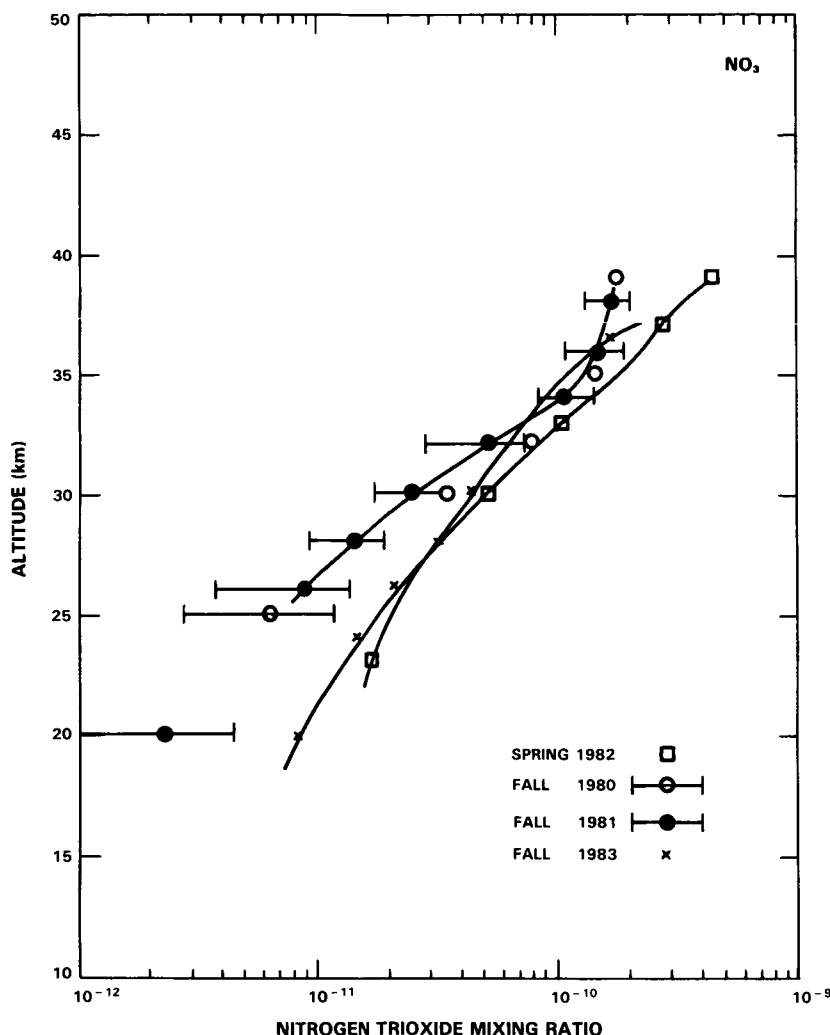
Figure 10-18. Nighttime profiles of NO₃ near 44°N.

In situ diurnal variations at sunrise have recently been measured by Helten *et al.* (1984b) using matrix isolation and electron spin resonance spectroscopy from a balloon platform at 32.7 km. The nighttime mixing ratio is 2×10^{-10}. About 30 minutes before sunrise the mixing ratio decreases to a value below 2×20^{-11} (the detection limit). These values tend to be about a factor of two larger than those from visible spectroscopy.

10.1.6 Dinitrogen Pentoxide (N₂O₅)

This important molecule still has not been definitively measured in quantitative manner in the stratosphere. A tentative measurement by Roscoe (1982) suggests a mixing ratio of $1.2 \pm 0.5 \times 10^{-9}$ at 32 km. Both the profile, shown in Figure 10-19 and the measured nighttime increase are fully consistent with predictions by the model of Fabian *et al.* (1982a). The recent first mission of the ATMOS spectrometer has yielded a clear detection of N_2O_5, though data are not available at the time of writing this report.

523
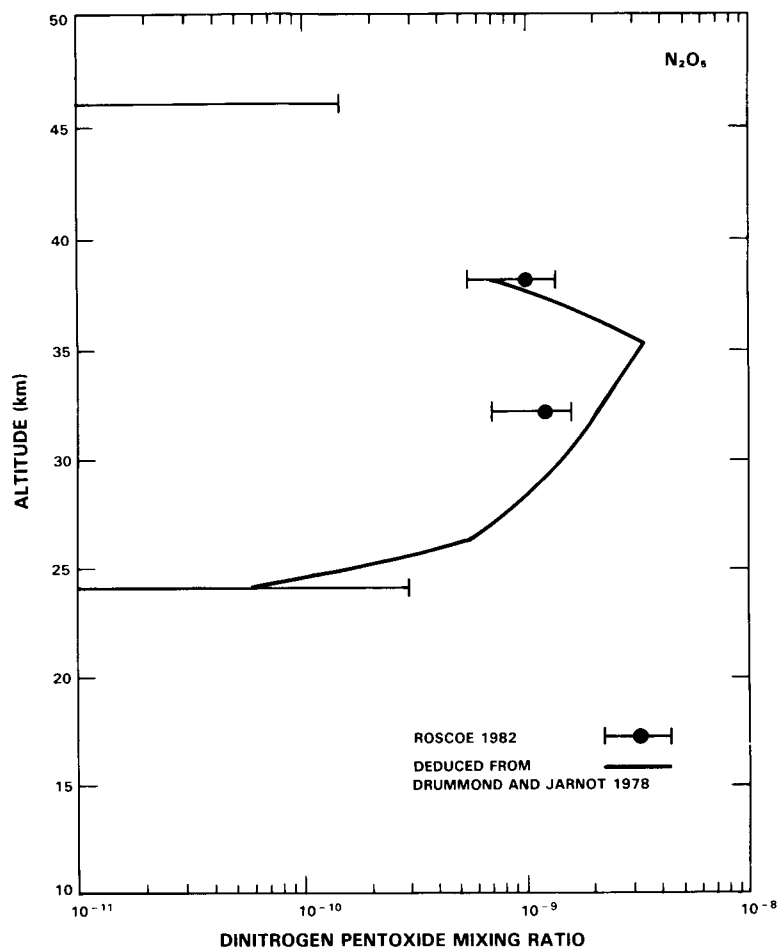
Figure 10-19. Tentative observation of stratospheric N_2O_5 near 32°N.

Fabian *et al.* (1982a) deduced N_2O_5 from the change of daytime [NO + NO_2] to nighttime [NO_2] measured by Drummond and Jarnot (1978). Although the deduced profile is fully consistent with that measured by Roscoe (1982), the error bar is large enough to encompass zero. Similarly, measurement of the nighttime decay of NO_2 by Roscoe *et al.* (1985b) is consistent with the N_2O_5 of Roscoe (1982), but again with a large error bar (see Section 10.2.2). For the purpose of deriving N_2O_5, measuring the change in NO_2 during the night should be more accurate than measuring the change in NO plus NO_2 across sunrise since the total error must be smaller.

The column of N_2O_5 can be deduced from changes in the columns of NO_2 and NO from sunrise to sunset. These have been measured by Coffey *et al.* (1981a), Ridley *et al.* (1984), and by Girard *et al.* (1983).

10.1.7 Chlorine Nitrate ($ClONO_2$)

This important stratospheric molecule still has not been definitively detected. However, tentative detections have been reported by the University of Denver group (Murcray *et al.*, 1979; Rinsland *et al.*, 1985b). If confirmed, these measurements would correspond to a mixing ratio of $1.1 \pm 0.7 \times 10^{-9}$ at 28 km. For a more detailed discussion, see Chapter 11, Section 11.3.

10.1.8 Peroxynitric Acid (HNO₄)

Although this molecule awaits a definitive detection in the stratosphere, the University of Denver group have observed a weak feature, just above noise level, at the frequency of one of its Q-branches near 802 cm^{-1} (D. G. Murcray, private communication). Assuming the line intensity measured by Molina (private communication) this would correspond to an upper limit of 0.5×10^{-9} at 28 km.

10.1.9 Hydrogen Cyanide (HCN)

Hydrogen cyanide is present in the stratosphere as a result of surface emission due to biomass burning and industrial activity (Cicerone and Zellner, 1983). According to the observations by Rinsland et al. (1982a), the tropospheric mixing ratio of HCN is of the order of $170 \pm 50 \times 10^{-12}$. The observations of Coffey et al. (1981b) and Carli et al. (1982) indicate a slightly lower mixing ratio in the stratosphere.

10.1.10 Methyl Cyanide (CH₃CN)

Methyl cyanide (or acetonitrile) has been postulated to be one of the ligands of positive stratospheric ions (Arnold et al., 1978; Arnold and Henschen, 1978) and should thus be present in the atmosphere. The stratospheric abundance of this molecule has been inferred from balloon and rocket borne ion mass spectrometric observations; the deduced mixing ratio is smaller than 10×10^{-12} above 25 km.

10.1.11 Latitudinal, Diurnal and Seasonal Variations

Most non-satellite observations of stratospheric NO_x reported since the 1981 WMO assessment have not substantially altered our understanding of latitudinal and seasonal variations in NO, NO_2, and HNO_3. An important exception to this general statement is provided by balloon data characterizing high latitude NO variations.

Observational techniques that lend themselves to latitudinal surveys or long term monitoring for seasonal variation are ground- and aircraft-based, and, more recently, the extensive temporal and spatial measurements by satellite-borne instruments. Various techniques are summarized in Table 10-4.

No *in situ* measurement surveys of NO versus latitude have been made since the 1981 WMO assessment. The measurements of Loewenstein et al. (1978b) reproduced in Figure 10-20 still represent our best understanding of the variation of NO concentration versus latitude at a pair of selected altitudes.

Figure 10-21 shows the column measurements of NO. Open symbols represent data reported at the time of WMO 1981; closed symbols represent measurements reported since the 1981 assessment. Measurements since 1981 were during summer or early autumn conditions and tend to support a nearly uniform distribution of the NO column between the equator and 70°N in summer with a value near 3×10^{15} molecules cm^{-2}.

The difference in magnitude between the NO column derived by Girard et al. and those derived by Coffey et al. is probably not significant, as their error bars overlap. Mean NO vertical profiles from summer and autumn measurements at three latitudes (Section 10.1.1) show no significant variation with latitude and indicate a symmetric distribution in the two hemispheres. One may integrate the mean profile, assuming no NO above 52 km to derive a vertical column. This yields a column amount of 3.95×10^{15} molecules cm^{-2}, and is plotted in Figure 10-21 at the three latitudes of those measurements; 38°N, 51°N and 34°S.

Table 10-4. Techniques for Observation of Latitudinal and Seasonal Variations of NO, NO_2 and HNO_3

Investigator	Technique	Molecule	Accuracy
Loewenstein et al. (1978b)	aircraft in situ chemiluminescence	NO 18.3, 21.3 km	±25%
Rinsland et al. (1984b)	ground-based	NO	
Noxon (1979a)	ground-based vis. absorption spectrometer	NO_2	±20%
McKenzie and Johnston (1982)	"	NO_2	±20%
Syed and Harrison (1981)	"	NO_2	±20%
Elansky et al. (1984)	"	NO_2	±20%
Coffey et al. (1981a)	aircraft IR Fourier transform spectrometer	NO NO_2 HNO_3	±20% ±20% ±20%
Girard et al. (1978/79)	aircraft IR Grille spectrometer	NO NO_2 HNO_3	±30% ±15% ±25%
Murcray et al. (1975)	aircraft IR emission	HNO_3	±25%

Profile measurements reported since the 1981 assessment for nitric oxide at high latitude in winter and summer (Ridley et al., 1984, to be published, 1986) have confirmed a decrease of NO mixing ratio in winter below 28 km. The 1981 interpretation of a decrease in NO column north of 50 to 60 degrees in winter remains unchanged.

Previous observations of the NO_2 column abundance established a diurnal variation from sunrise to sunset of about a factor of two (Noxon, 1979; Syed and Harrison, 1981), presumably due to photolysis of N_2O_5 and $ClONO_2$ formed at night. Since NO_2 and NO are in photochemical equilibrium in the sunlit atmosphere, a substantial diurnal increase in NO should also be anticipated.

The early measurements of Girard et al. (1978/79) showed no diurnal change in NO. Results for NO are not reported for subsequent flights of the Girard spectrometer in STRATOZ 1 and 2. Further comparison of NO columns measured by Coffey and Mankin confirms that NO increases by a factor of two between early morning and late afternoon. Note that their measurements, while close to sunrise or sunset,
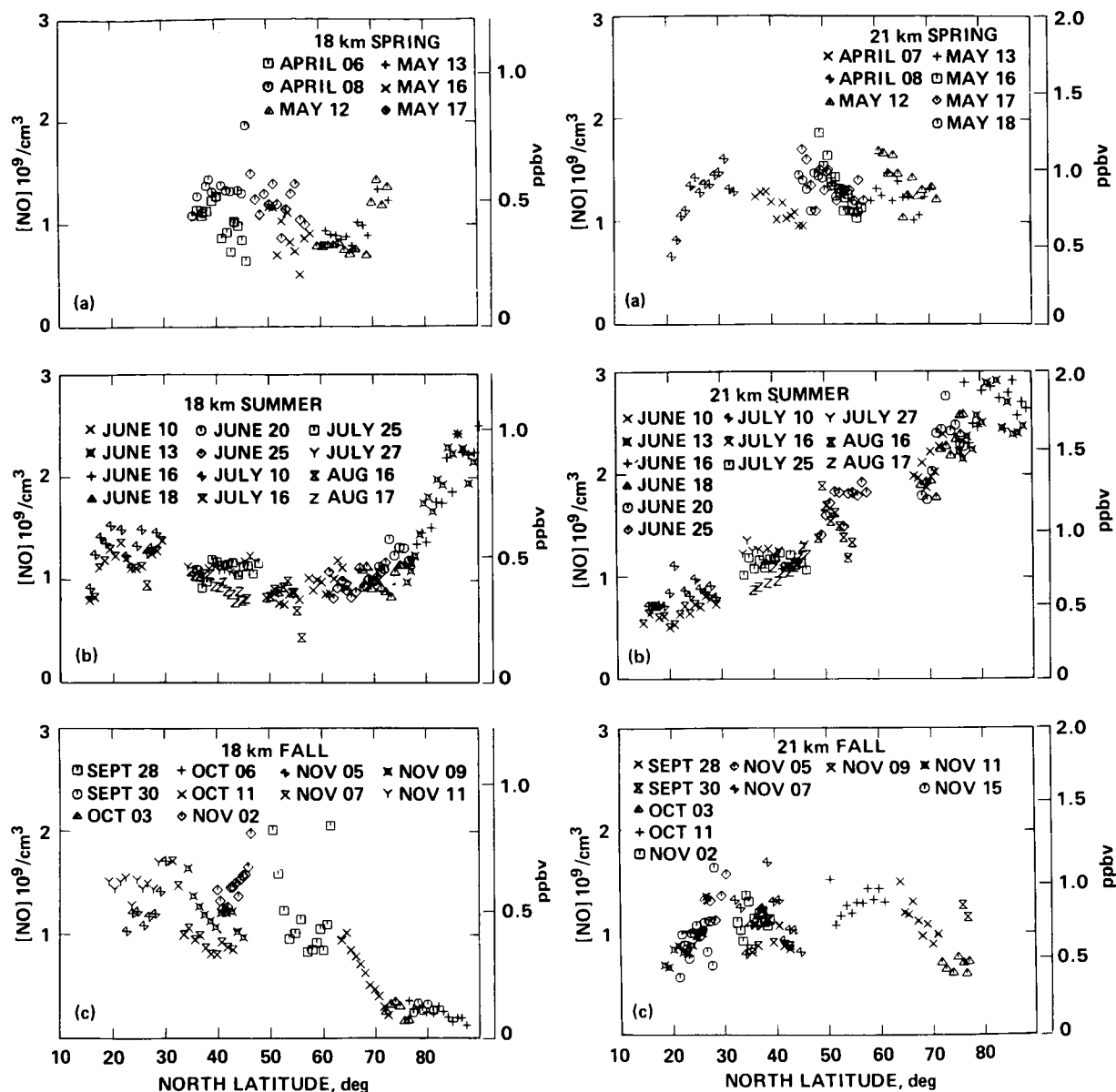
Figure 10-20. Variation of NO at 18 and 21 km versus latitude and season (Loewenstein *et al.,* 1978a, b).

are made when the solar zenith angle is in the range 75 to 85°. Roscoe *et al.* (1985a, b) have also observed diurnal changes in NO and NO_2 profiles, as discussed in section 10.3.2.

A number of important developments have occurred since the 1981 WMO assessment in the observation of stratospheric NO_2. Firstly, three exciting data sets have become available from satellite-borne limb viewing instruments, discussed in Section 10.2. Secondly, long term ground-based measurements of stratospheric NO_2 columns have been reported by Elansky *et al.* (1984) at 44°N, Syed and Harrison (1981) at 50°N and by McKenzie and Johnston (1982) at 45°S. Since the 1981 assessment further latitudinal measurements of NO_2 column amounts have been made by the aircraft mounted instruments of Girard *et al.* and Coffey *et al.*

527

NITROGEN SPECIES
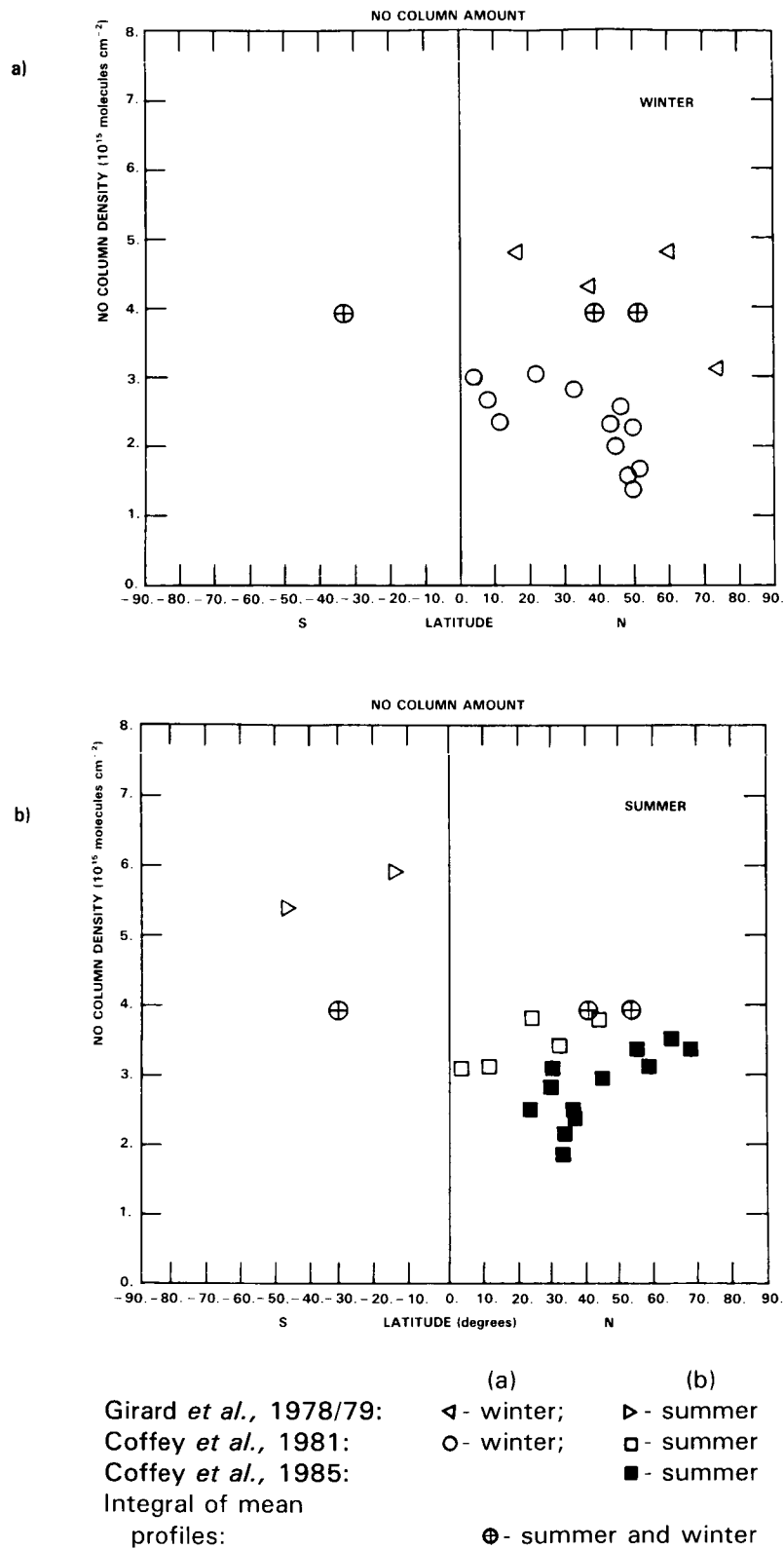
Figure 10-21. Vertical column of daytime stratospheric NO versus latitude.

The main features of the latitudinal distribution of NO_2 are not changed from that presented in WMO 1981. A general increase occurs with latitude in both hemispheres in winter and summer up to near 30 degrees of latitude. At higher latitudes a sharp decline is observed in winter NO_2 columns. Figure 10-22 shows NO_2 vertical columns for sunset conditions from a number of sources. Open symbols are from the 1981 WMO assessment, solid symbols are observations reported since 1981.

As has been observed by Noxon and others, the NO_2 vertical column may change by as much as a factor of two in the time span of a few days at a given location. This effect probably accounts for much of the spread of observed NO_2 columns between 40 and 60°N latitude in Figure 10-22.

Extensive ground-based measurements of NO_2 have been reported. Figure 10-23 shows the variation over a year for a number of latitudes. The pioneering work of Noxon has been supplemented by studies near 50°N (Syed and Harrison, 1981) and at 45°S (McKenzie and Johnston, 1982) latitudes. Column measurements at 43.7°N from 1979-1984 by Elansky et al. (1984) show a behavior very similar to the 40°N panel of Figure 10-23.

The behavior is consistent at all latitudes with a minimum column in winter and a maximum in summer with a less pronounced annual variation near the equator, as expected.

The basic features of the latitudinal and seasonal variations of HNO_3 are not substantially different from those described in WMO 1981. Since the 1981 assessment a wealth of data has become available from the infrared radiometer LIMS on the Nimbus 7 satellite, and is discussed in Section 10.2.

There is a strong increase in the vertical column of HNO_3 with increasing latitude in both hemispheres. Figure 10-24 shows the results from a number of investigations. The measurements indicate that there may be an asymmetry about the equator with a steeper increase with latitude in the Southern Hemisphere.

There appears to be a decreasing gradient in column HNO_3 at high latitudes in summer. Above about 50 degrees latitude in the Northern Hemisphere and 30 degrees latitude in the Southern Hemisphere, the summertime HNO_3 column amounts reported by Murcray et al. (1975, 1978) and Coffey et al. (1985) do not increase with latitude as they do in the lower latitudes and at higher latitudes in winter.

Aircraft and ground-based measurements have shown no evidence for a diurnal change in HNO_3 columns.

10.2 SATELLITE DATA

Introduction

Satellite observations of the global distributions of several of the nitrogen species are one of the major recent developments in the study of the stratosphere. Since 1981 there have been presentations of three sets of observations of NO_2, one of HNO_3 and one of N_2O. These must be regarded as major technical and scientific achievements, since these gases are present in concentrations from a few to a few hundred parts per billion by volume (ppbv). These observations provide a wealth of information on the temporal and spatial variations of these species that was not previously available.
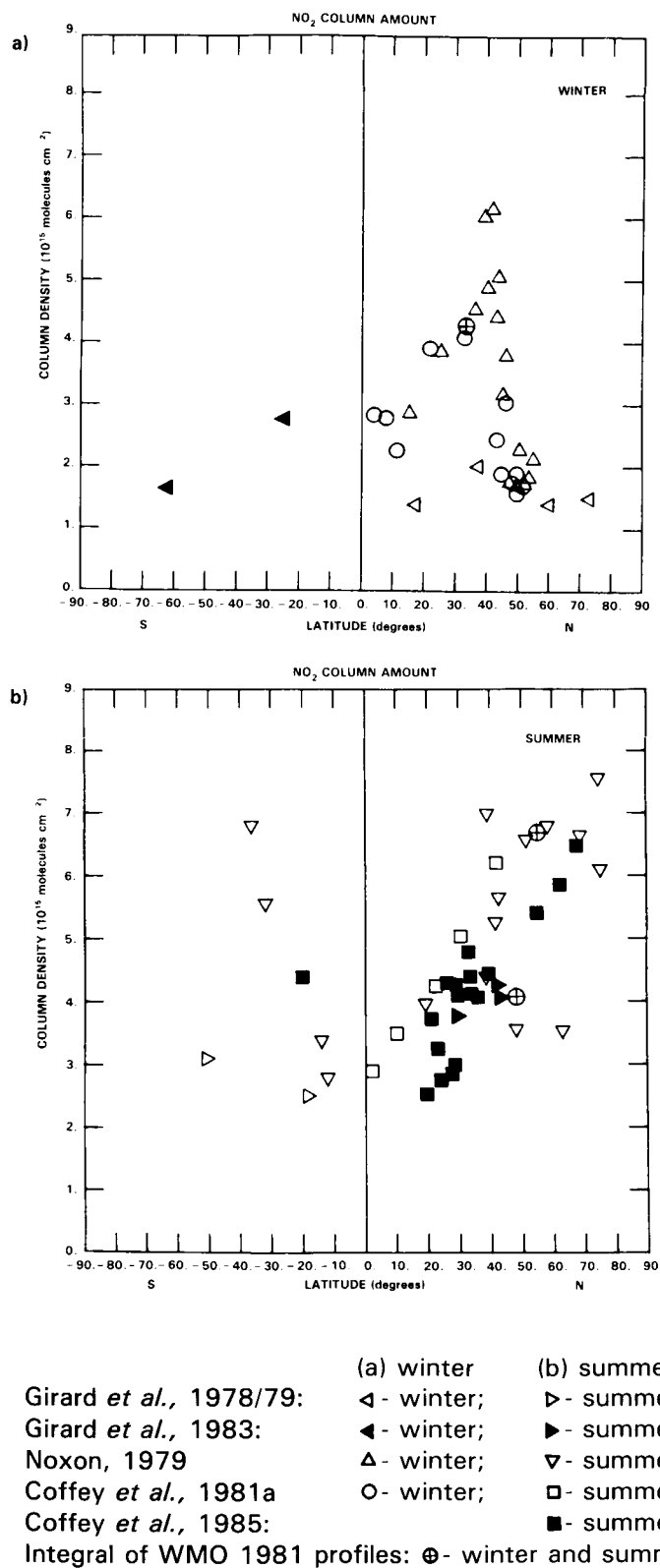
Figure 10-22. Vertical column of daytime NO_2 versus latitude.
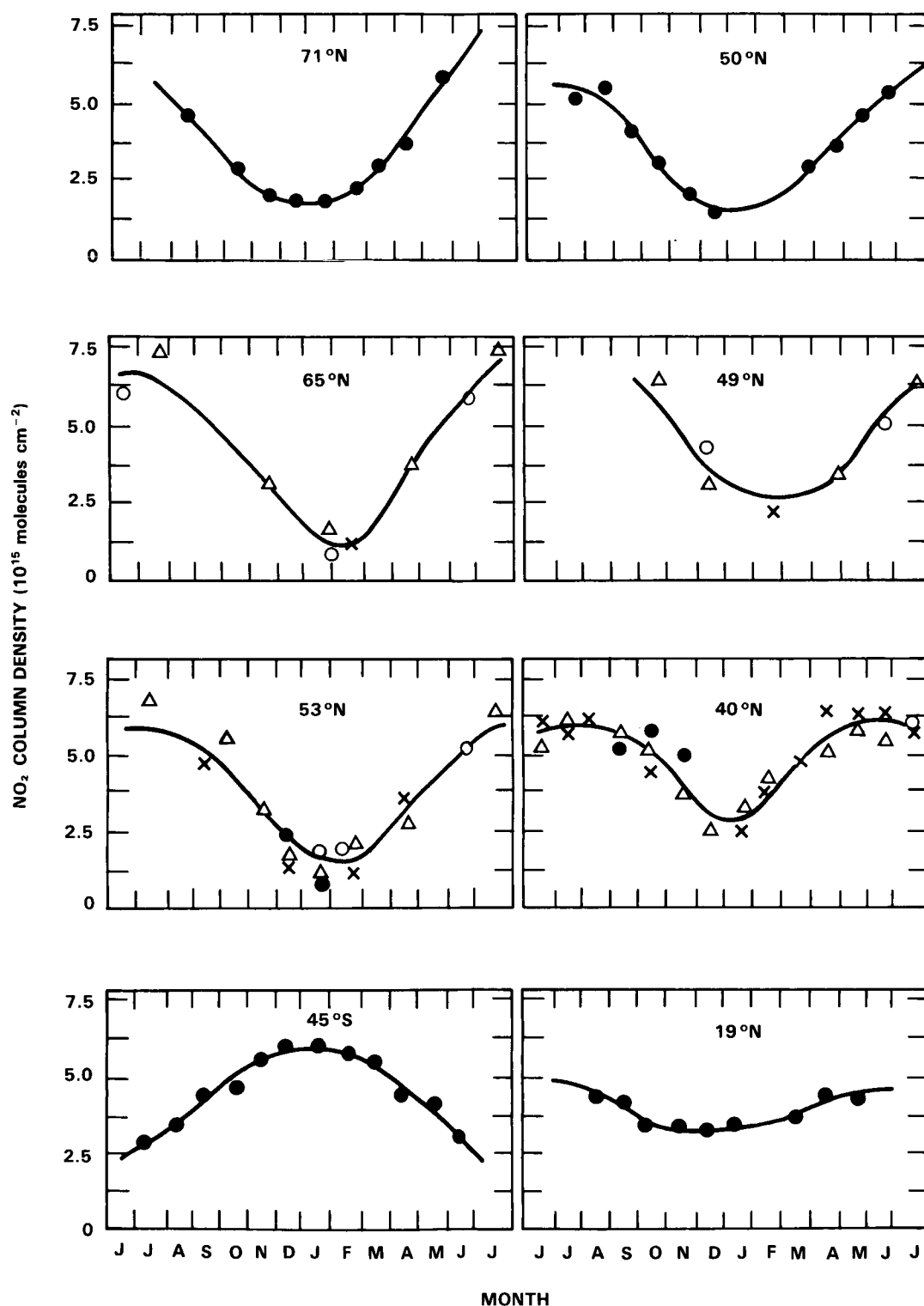
Figure 10-23. Variation over a year of the daytime NO_2 vertical column at various latitudes. Latitude 50°N is from Syed and Harrison (1981), 45°S is from McKenzie and Johnston (1982), all other latitudes are from Noxon (1979) and Noxon et al. (1983).

531
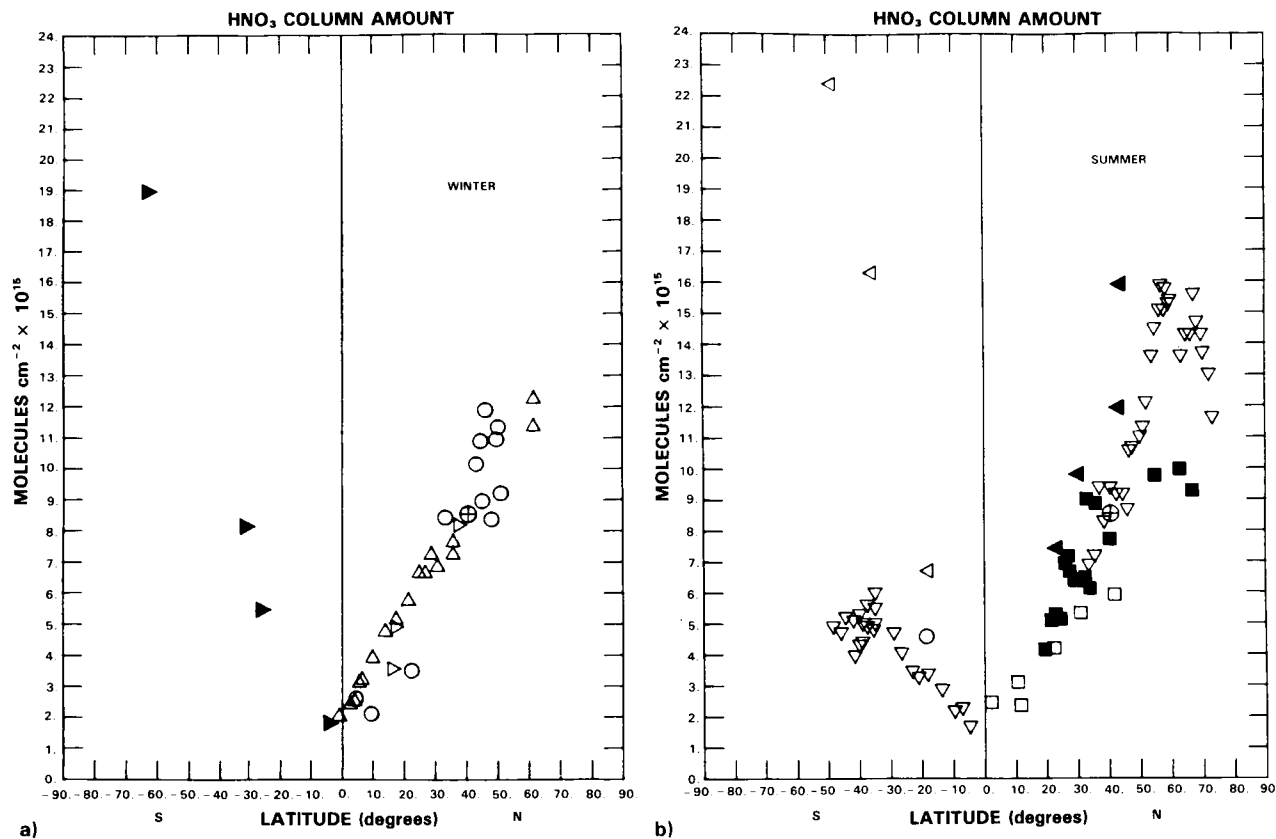
Figure 10-24. Vertical column of stratospheric HNO₃ versus latitude.

	(a) winter	(b) summer
Murcray *et al.*, 1975, 1978:	Δ - winter;	▽ - summer
Girard *et al.*, 1978/79:	▷ - winter;	◁ - summer
Girad *et al.*, 1983:	▶- winter;	◀ - summer
Coffey *et al.*, 1981a	O- winter;	□ - summer
Coffey *et al.*, 1985:		■ - summer
Integral of WMO 1981 profiles:	⊕- winter and summer	

In the following section, the experiments and the data validation are briefly described, since most of this has been published. The results of the measurements are then described, with emphasis on the scientific questions which they address, and the uses to which the data can be put.

10.2.1 Nitrogen Dioxide (NO₂)

Measurements of NO₂ have been obtained by three different instruments, LIMS, SAGE and SME, measurements being made at five different local times during the day, using three different techniques. Their results are described below. Because NO₂ varies with time of day, an intercomparison between the measurements is more easily done in conjunction with a model, and is discussed in the modelling section.

10.2.1.1 LIMS Measurements of Nitrogen Dioxide

The LIMS Experiment

The Limb Infrared Monitor of the Stratosphere (LIMS) has been described in the Special Introduction to Chapters 8, 9, 10 and 11. The instrument and its performance in orbit, the data reduction, and examples of the results, are described by Gille and Russell (1984). Earlier descriptions are given by Russell and Gille (1978) and Gille et al. (1980a).

Gille and House (1971) mentioned some of the advantages of limb viewing. These include the long horizontal path through the atmosphere, giving greater sensitivity to gases present in trace amounts, and the dark background behind the atmosphere, which aids in signal detection and interpretation. By making measurements in the thermal infrared, observations can in principle be obtained at any local time. The geometry also allows good vertical resolution, if a narrow field of view is used in the instrument and the sampling is sufficiently frequent in the vertical. Because clouds along the line of sight block any signal from the lower atmosphere, the long horizontal path also precludes the soundings from extending into the troposphere on a regular basis.

Two instrumental details affect the data discussed here. To achieve a high radiometric signal to noise ratio with narrow fields of view, the LIMS detectors were cooled to 63 K by a subliming solid methane cryogen. This was designed for a seven-month lifetime, resulting in a LIMS data span from 25 October 1978 to 28 May 1979.

To prevent sunlight from directly entering the LIMS aperture, the instrument viewed off the plane of the orbit. This resulted in latitudinal coverage from 64 °S to 84 °N. The local times of overpass were close to 1 PM and 11 PM over a wide range of latitudes, but changed rapidly at high latitudes near the terminator. These times are shown in Table 10-5.

Table 10-5. Tangent Point Local Time, as a Function of Latitude
(From Gille & Russell, 1984)

Latitude °N	Local time. Hours	
	Ascending Part of Orbit	Descending Part of Orbit
80	14.76	21.23
60	13.03	22.97
40	12.85	23.15
20	12.90	23.11
0	13.06	22.94
−20	13.38	22.62
−40	13.97	22.03
−60	15.77	20.24

NITROGEN SPECIES

Each retrieval provides a profile with a vertical resolution of about 3 km. Retrievals were performed every 4 degrees of latitude from 64 °S to 84 °N, resulting in about 1000 profiles per day for the life of the experiment. The results at each latitude were then treated as a time series, and Kalman filtered to provide an optimal estimate of the zonal mean and the amplitudes and phases of the first six harmonics around the latitude circle, as described by Rodgers (1977) and Kohri (1981). This procedure provides data smoothing, in that noise and small scale geophysical features are reduced, and explicitly provides a time interpolation to standard map times, which are taken to be 12 UT daily. These mapped data provide the basis for the data presentations that follow.

Evaluation of the NO₂ Results

The radiances, data reduction, and error assessment for the NO_2 observations are described in detail by Russell et al. (1984a). The methods by which the precision and accuracy were assessed are briefly summarised, and some particular features of these data are noted here.

The measured radiance decreases with altitude, eventually approaching the noise level, which sets the upper altitude limit of the retrievals. For single scans of the NO_2 channel, this occurs slightly below 1 mbar (48 km). However, by averaging scans together, altitudes as high as 70 km can be reached (Russell et al., 1984b). The lower limit can be set by clouds, but also by the large opacity in this spectral interval due to water vapour and the pressure induced absorption of molecular oxygen. A calculation of the NO_2 signal coming from a given pressure level indicates poor signal to noise ratio below 30 mbar. The operational retrieval is extended to 100 mbar and below, but these levels are strongly influenced by climatological NO_2 input profiles: data below 30 mbar will not be considered.

At 6.2 μm, the NO_2 channel is on the steep, high frequency end of the Planck function for atmospheric temperatures, and signal strength drops rapidly for low temperatures. During northern winter, the temperatures in the polar region were often so low that no retrievals of single profiles were attempted, resulting in some data loss under those conditions.

The precision (repeatability) has been estimated by a forward propagation of errors, and from the data themselves. Observationally, a series of 7 sequential radiance scans in a meteorologically undisturbed situation were retrieved independently, and the standard deviation calculated. This is a measure of the end-to-end repeatability of the retrievals, and resulted in values between 0.1 and 0.5 ppbv, depending on altitude. Numerical simulations, calculating the response of the retrievals to the random noise sources, radiometer noise, and random temperature errors (from Gille et al., 1984a), are in excellent agreement with the observations. The observational results do not depend to any great extent on the meteorological situation. The results are noted in Table 10-6 below.

The accuracy has been estimated by two complementary methods. Several sources of systematic errors were identified, and their magnitudes estimated. These included errors in the radiometric calibration, in the size of the field of view effects, uncertainties in their removal, errors in the LIMS temperatures and water vapour concentrations which enter into the NO_2 retrievals, and uncertainties in the spectral data for NO_2 and O_2. The effect of these errors on the results was estimated by numerical simulations; the results are shown in Table 10-6.

To make sure that no major source of error had been omitted, and to relate the LIMS results to other measurements which have been made in the past, four balloon underflights to measure NO_2 with spectroscopic instruments were made. All of the measurements were obtained as the sun set, which complicates

Table 10-6. LIMS NO₂ Channel Systematic Error Sensitivity Study

Error Parameter	NO₂ Mixing Ratio Error. %					
	50 mbar	30 mbar	10 mbar ($\approx$ 30 km)	5 mbar	3 mbar	1 mbar ($\approx$ 50 km)
1. Temperature profile. $\pm$ 2 K	36	22	14	12	7	8
2. O₂ absorption coefficient. $\pm$ 20%	68	37	5	1	0	0
3. H₂O mixing ratio. $\pm$ 30%	32	20	10	8	9	30
4. IFOV side lobe integrated area, $\pm$ 0.8%	1	2	4	1	2	1
5. NO₂ spectral parameters. $\pm$ 10%	10	10	10	10	10	10
6. Retrieval algorithm	5	5	5	5	5	5
7. RSS of 1 through 6 with 6% systematic radiometric error and 5% error due to IFOV removal	84	49	23	20	18	34

The random NO₂ error is estimated to be 10% for 25 mbar $<$ P $<$ 100 mbar; 5% for 3 mbar $<$ P $<$ 25 mbar; 30% for P $<$ 3 mbar

the comparison because of the large diurnal changes in NO₂ concentration. A model was used to adjust the sunset measurements to LIMS overpass times. The mean difference between LIMS and the correlative measurement data in the 5 to 30 mbar region is 15%, which is much smaller than the combined error bars of the balloon determinations and LIMS. The LIMS data were also shown to lie within the envelope of previous measurements presented in WMO 1981 (1982), and with the model results presented there.

Daytime Values

Zonal Cross Sections of NO₂

One of the most straight-forward ways to display the results is as latitude-altitude cross sections of the zonally averaged quantities. In these, the longitudinal variations are averaged out, but the larger variations with altitude and latitude are shown. Similarly, monthly averages are displayed to smooth out short period temporal variations. Distributions under both day and night conditions are presented.

Zonally averaged monthly mean cross-sections of the NO₂ measurements obtained for daytime conditions are presented in Figure 10-25 for the months, October, January, April and May (the closest to northern summer conditions available). Note that the latitudes in daylight vary as the terminator moves with the season.

The standard deviations (in per cent) of the daily cross section values are shown in Figure 10-26 for January and April. The day-to-day variations are $<$ 0.3 ppbv away from the terminator, or $<$ 5% in

NITROGEN SPECIES
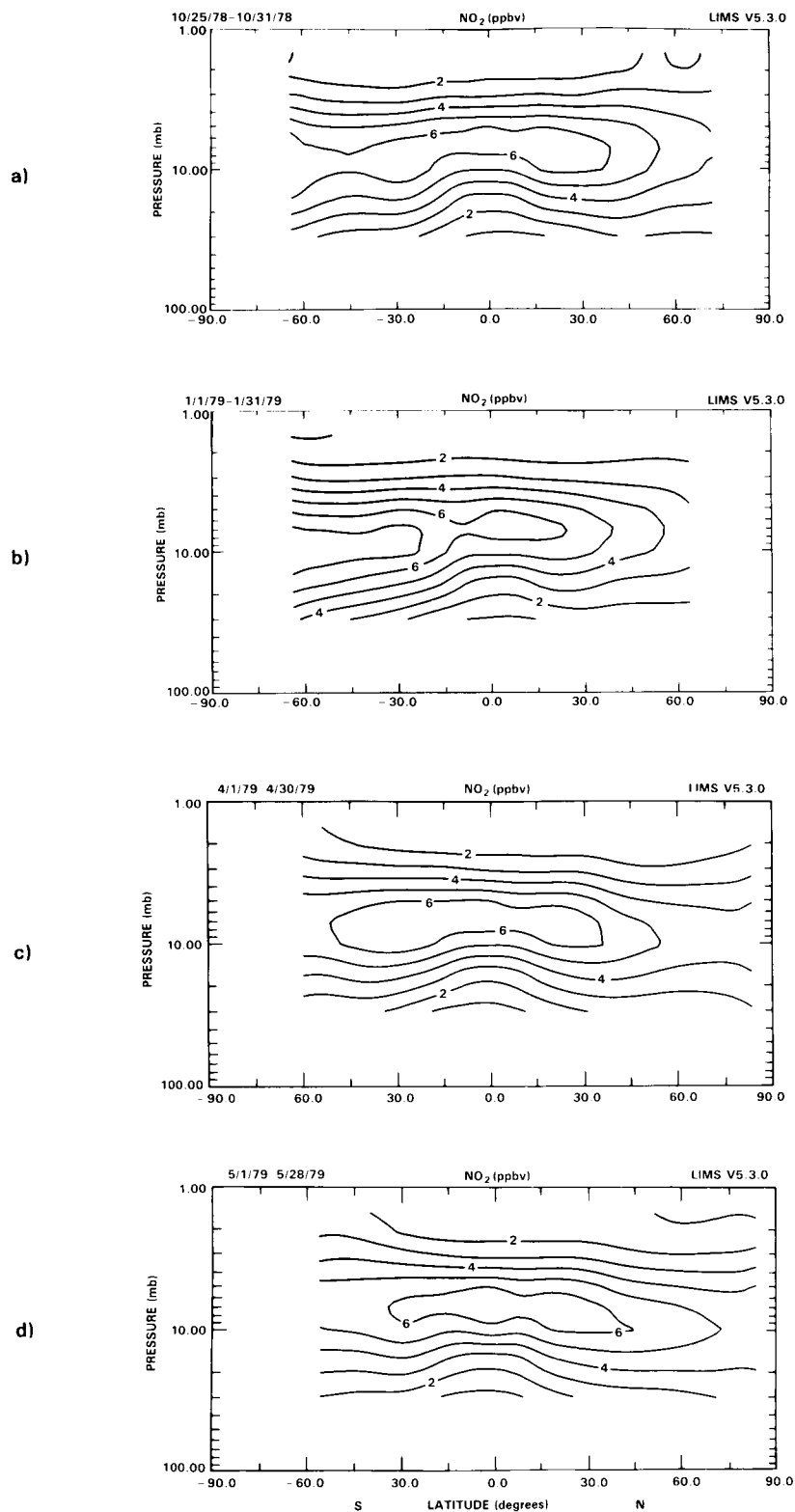
Figure 10-25. Monthly average zonal mean cross-sections of daytime NO_2 for (a) October (last 7 days), (b) January, (c) April and (d) May (first 28 days).
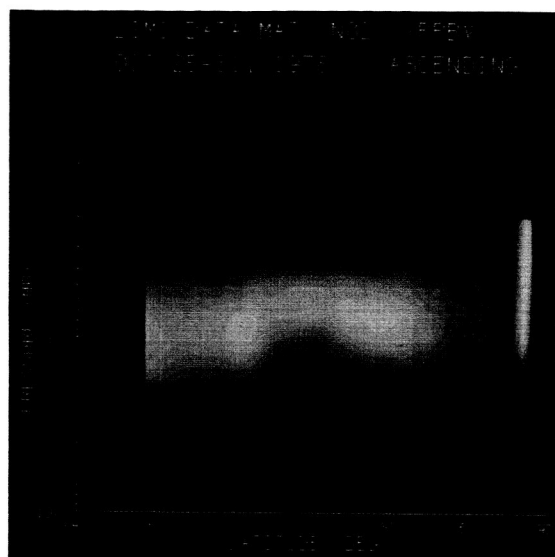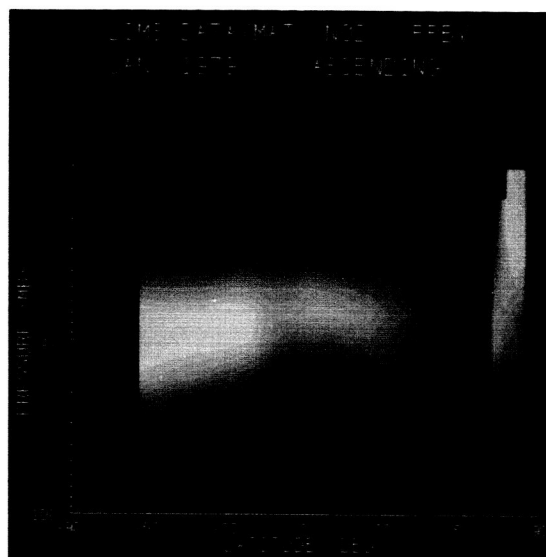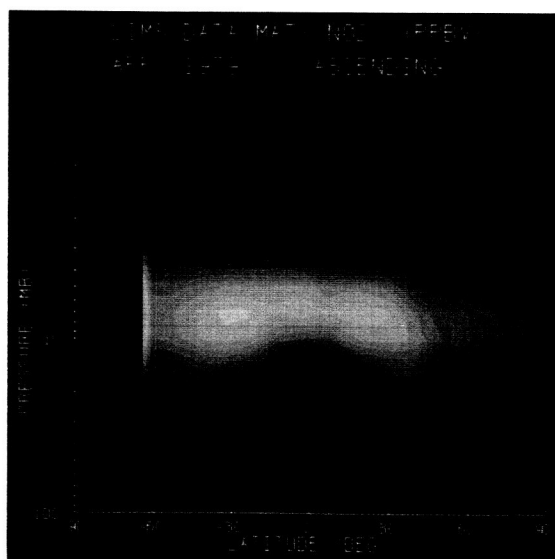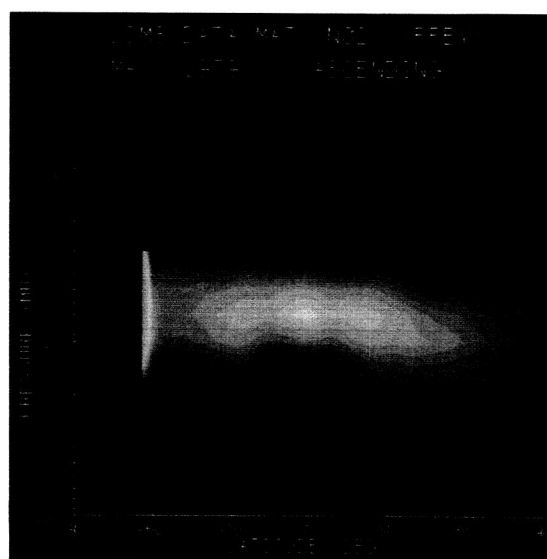
Figure 10-25. (Color) Monthly average zonal mean cross-sections of daytime NO_2 for (a) October (last 7 days), (b) January, (c) April and (d) May (first 28 days).

1/1/79–1/31/79   STANDARD DEVIATION FOR NO₂ (PERCENT)   LIMS V5.3.0

4/1/79–4/30/79   STANDARD DEVIATION FOR NO₂ (PERCENT)   LIMS V5.3.0
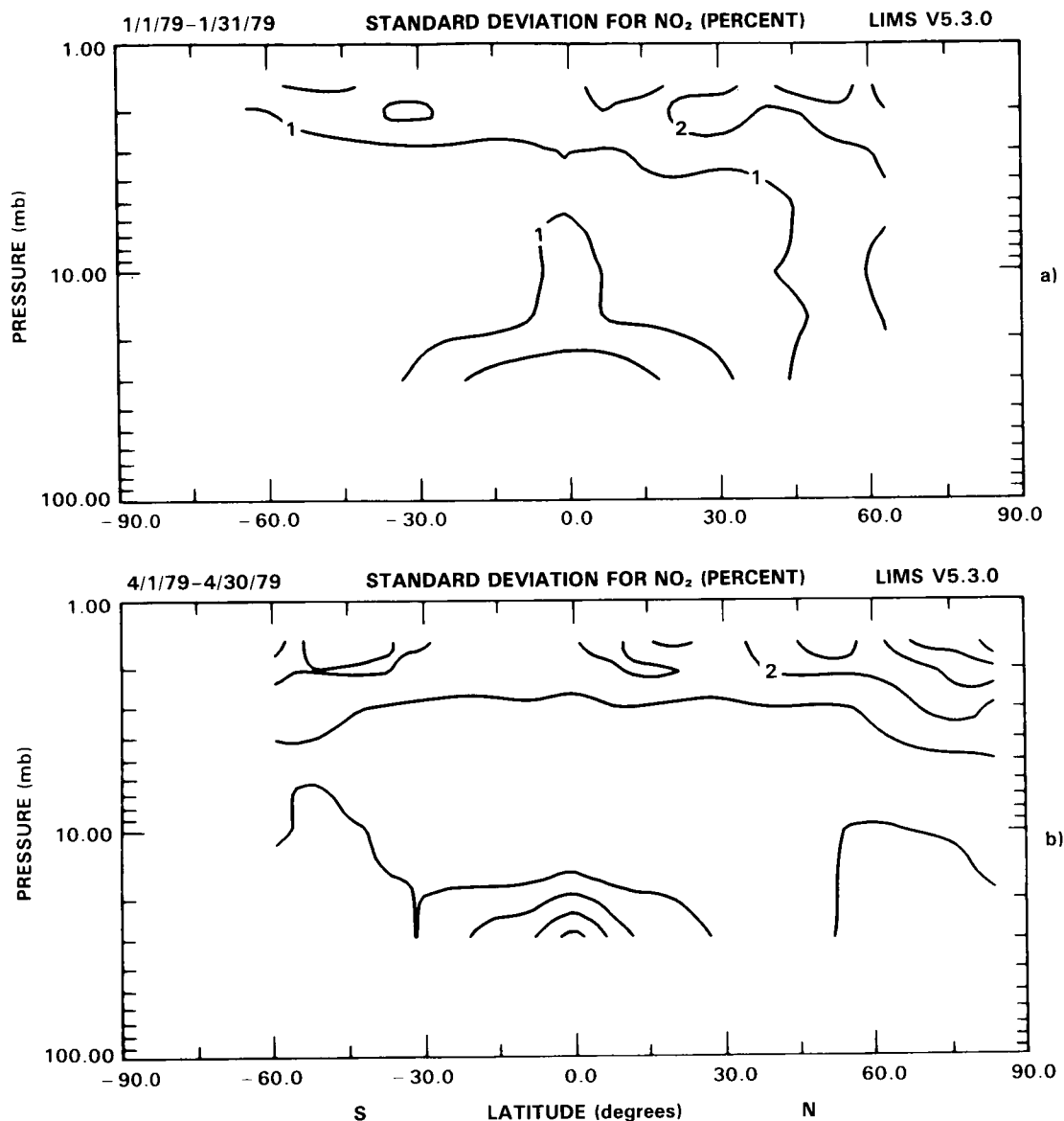
Figure 10-26. Standard deviation of daily values of daytime NO₂ cross-sections for (a) January and (b) April. Contour interval is 1 percent.

most cases, indicating that the means are quite stable, that the latitudinal and vertical structure is consistently present, and that the differences between months are statistically significant.

The general features of the NO₂ distribution can be seen in the January cross-section. There is a layered structure, with maximum values of 7 ppbv at 10 mbar in the summer hemisphere, decreasing toward the winter hemisphere, and toward the northern terminator. At lower altitudes there is a minimum in the tropics resulting from the injection of NO₂-poor air from the troposphere. As N_2O is oxidised in this upward moving air, the NO₂ concentration increases. Above the maximum, there is very little variation with latitude.

The distribution is the same in the other months, but becomes more symmetric with latitude in April and May. There is also a tendency for the level of maximum values to slope down towards the summer pole.

Vertical Profiles

Prior to the satellite observations, a large fraction of the available data were as vertical profiles obtained from balloon-borne measurements. The LIMS data can also be displayed in this way for comparison with balloon measurements most of which are made during the day (or at sunrise or sunset, which are also close to day conditions). This presentation clearly shows the seasonal variations, since the large number of observations allows the random error to be reduced to a very small value, and subtle changes to be seen.

As discussed in the introduction, formation and loss of N_2O_5 probably plays a major role in determining spatial and temporal variation in NO_2 densities, particularly at high latitudes. N_2O_5 is formed in large amounts in the lower stratosphere at night (destroying NO_2) and photolyzed slowly on a time scale of hours to days in the sunlit atmosphere (reforming NO_2). Thus the altitude and magnitude of the NO_2 maximum abundance should be expected to vary greatly between high latitude summer and winter, as the balance between the sunlit and dark portion of the day changes.

Monthly average zonal mean vertical profiles for 5 latitudes are shown in Figure 10-27. At 60 °S, the peak value increases from 7 to 8 ppbv from spring to summer but the levels of the distributions are quite similar. The peak value decreases in the fall, and the shape of the curve is altered, presumably due to the short length of day near the terminator. The summer maximum at the peak level can also be seen at 32 °S, again with larger values in the fall at the high levels. There is rather little seasonal variation at the equator, especially above and below the maximum.

The Northern Hemisphere latitudes show the same type of behaviour, shifted by 6 months. At 32 °N there is a winter minimum at the peak altitude, but not the usual behaviour above the maximum. At 60 °N the winter value is lower at the level of the maximum, which here is at a higher altitude than under summer conditions, again, presumably because of the shorter day and shorter span of time between sunrise and the measurement time. The values are larger and lower in late spring.
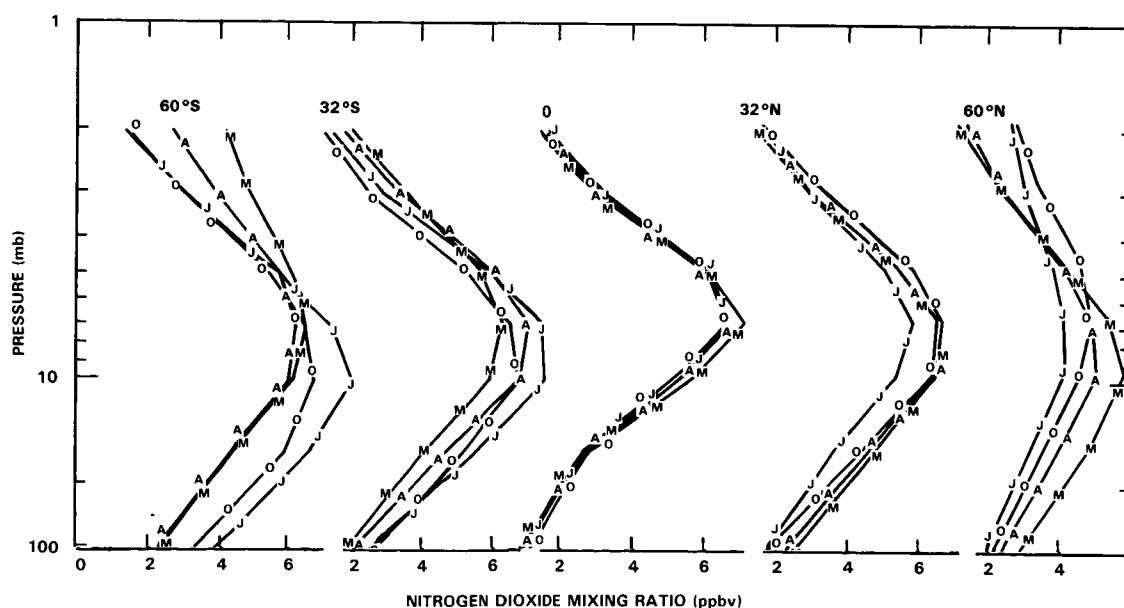
Figure 10-27. Vertical profiles of daytime NO_2 showing seasonal variation at several latitudes. O - October, J - January, A - April, M - May.

Figure 10-28. Map of NO₂ mixing ratio (ppbv) on the 10 mbar surface (~ 30 km altitude) for February 21, 1979.

It should be noted that the standard deviations about these profiles are rather small, indicating that in any month the zonal mean changes slowly. The question of variations at particular balloon launch sites is discussed below.

Overburden Measurements

The LIMS values can be vertically integrated to provide a measure of the total column amount of NO₂. Using a ground-based technique, Noxon (1979) observed very rapid decreases of NO₂ column amounts toward the pole during the winter, a phenomenon referred to as the Noxon "cliff". Figure 10-28 presents a map of the LIMS NO₂ mixing ratio on the 10 mbar surface for 21 February. This is during a sudden warming disturbance, and two regions of low mixing ratio can be seen near 60 °N, 90 °W and 70 °E. The column amount above 30 mbar (24 km) is shown as a function of latitude for 90 °W in Figure 10-29, where it is compared with the zonal average. The zonal average shows a small decrease from 30 °N to 60 °N, beyond which there is an increase near the terminator. Along 90 °W, there is a much steeper drop, by a factor of two, from 40 °N to 60 °N. There is a similar variation at 70 °E. This is not as steep as those
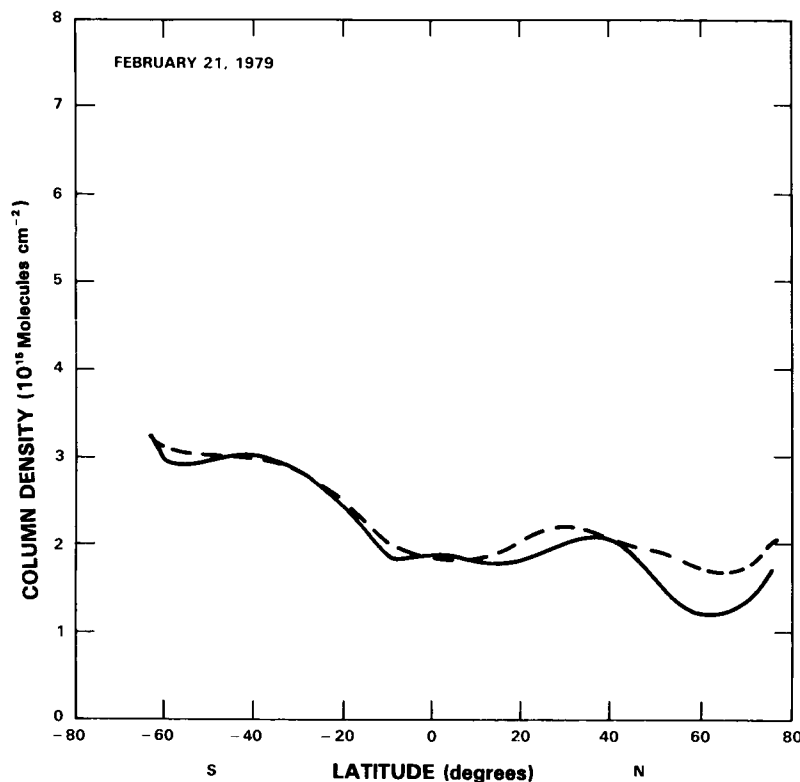
Figure 10-29. Total column amount of NO_2 above 30 mbar as a function of latitude for 90°W (solid line) and the zonal mean (dashed line), for February 21, 1979.

seen on some occasions by Noxon; the differences may be due to differences in the meteorological and measurement situation. Note that Noxon's measurements were obtained at sunset after the NO_x has built up over the entire day; which would be expected to result in a steeper gradient. Callis *et al.* (1983b) calculated larger gradients in the nighttime cliff observed by LIMS. These data show in some detail how the effect depends on the advection of air from the polar cap that is low in NO_2, as Noxon suggested.

Nighttime Values

Zonally Averaged Cross-Sections

The zonally averaged monthly mean values of NO_2 are displayed in Figure 10-30 for the same months as were shown for the daytime values. Regions which were in daylight for all or some of the days have been left blank.

The standard deviations of the daily values are shown in Figure 10-31. Although these are larger than for the daylight values, the percentages are again < 5% in most locations, indicating that there is rather little day-to-day variability, and that the means are quite stable.

The nighttime distribution also shows a layered structure, with maximum values of approximately 17-19 ppbv, now centred near 4-5 mb. There is a maximum over the equator in October, with a region of high values in the Southern Hemisphere near the southern terminator. In January the equatorial maximum has shifted appreciably toward the south, and the peak values are larger. At the same time, the
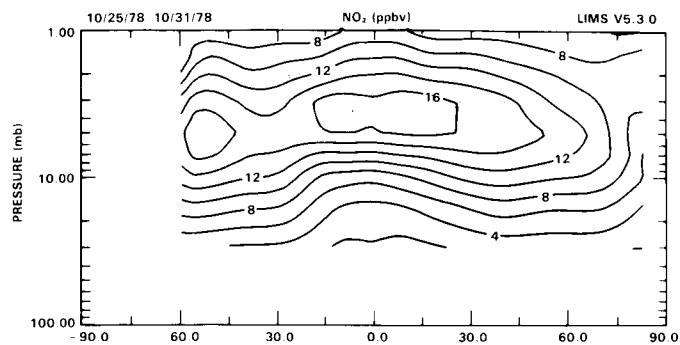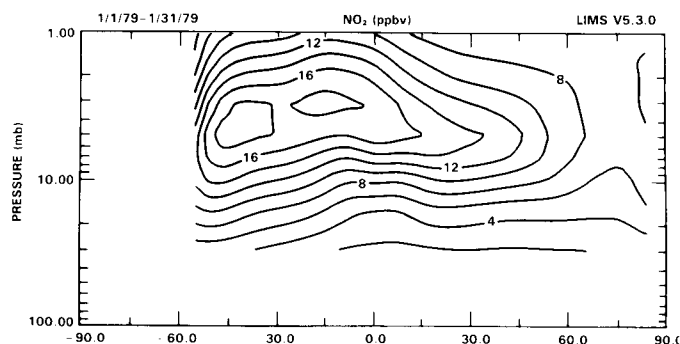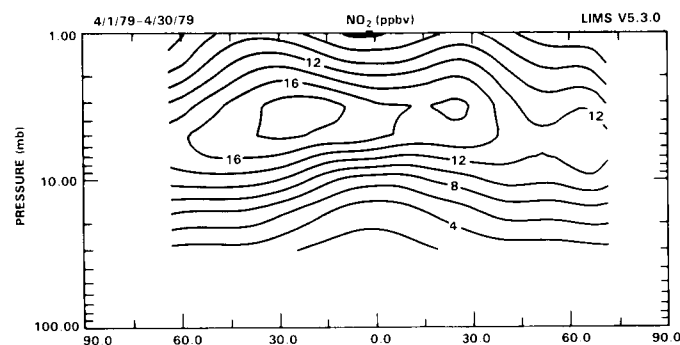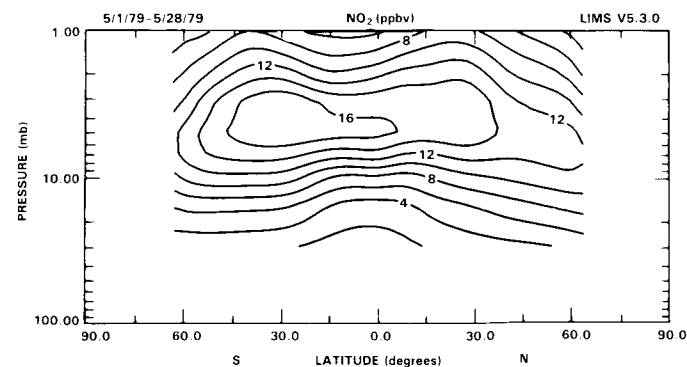
Figure 10-30. Monthly average zonal mean cross-sections of nighttime NO_2 for a) October (last 7 days), b) January, c) April, and d) May (first 28 days).

542
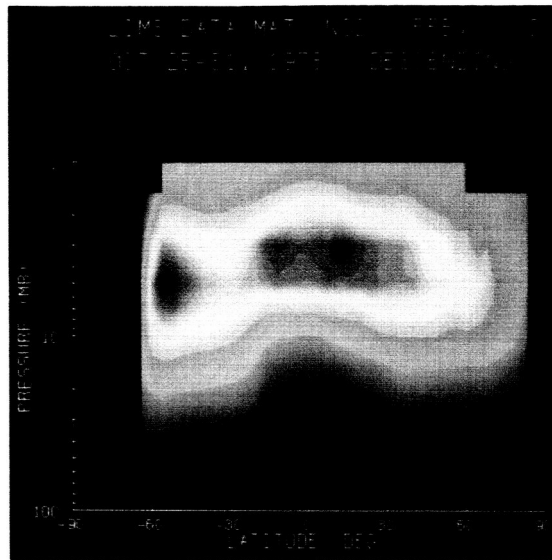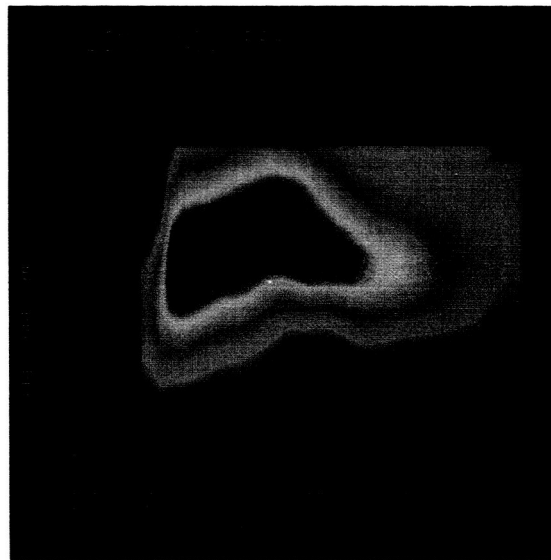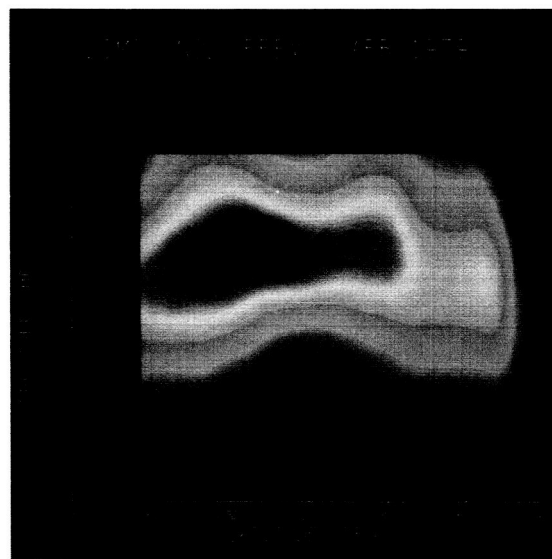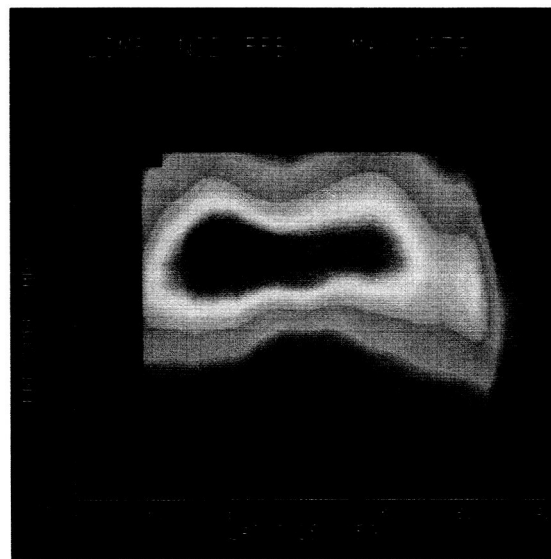
Figure 10-30. (Color) Monthly average zonal mean cross-sections of nighttime NO_2 for a) October (last 7 days), b) January, c) April, and d) May (first 28 days).
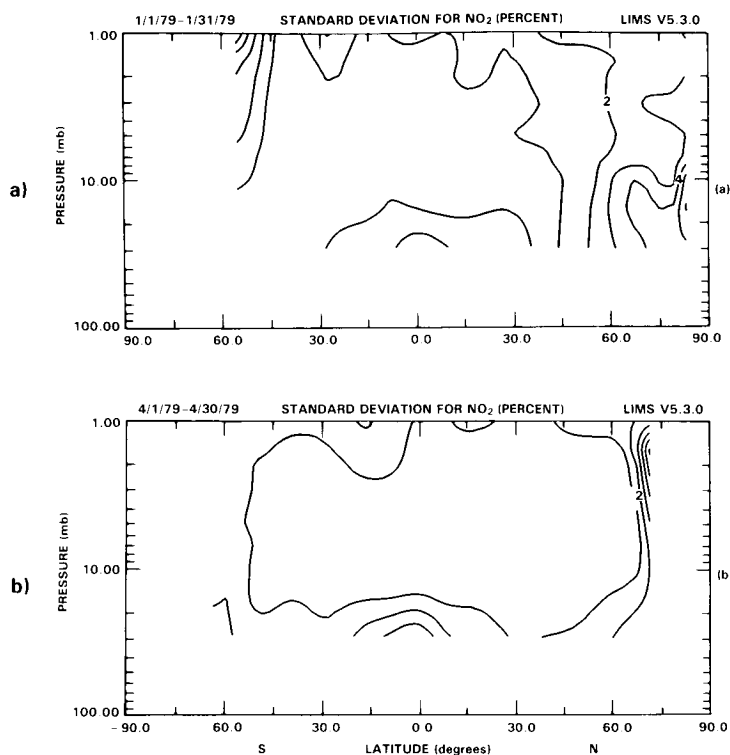
Figure 10-31. Standard deviation of daily values of nighttime NO₂ cross-sections for (a) January and (b) April. Contour interval is 1 percent.

values in the Northern Hemisphere polar night are quite low. April is characterised by a maximum still in the Southern Hemisphere, but a small local maximum in the Northern Hemisphere. These weaken in May. One feature that stands out in these plots is the tendency for there to be more NO_2 at the level of the maximum in the Southern Hemisphere night.

The interpretation of these data is in its early stages. However, it is clear that they should be invaluable in studies of the photochemistry of the nitrogen species, and their interactions with transport processes.

10.2.1.2 SAGE Measurements Nitrogen Dioxide

SAGE Instrument and Techniques

The Stratospheric Aerosol and Gas Experiment (SAGE) instrument has been described in the Special Introduction to Chapter 8, 9, 10 and 11, and is reported in McCormick *et al.* (1979) and Chu and McCormick (1979).

Measurement Errors and Validation

The estimated SAGE NO_2 measurement errors are tabulated in Table 10-7 for the altitude range from 25 to 45 km. Since the SAGE instrument measures the absorption due to atmospheric NO_2, noise in the measurement will directly affect the inferred number density of NO_2. Therefore, the estimated random

Table 10-7. SAGE NO_2 Profile Measurement Error Estimates

A. Systematic Errors

NO_2 Absorption Cross-section	10%
Instrument Wavelength Calibration	2%
Rayleigh Correction	4%

B. Random Error

	Altitude - km	Number Density molecules cm^{-3}
Noise (Measurement and inversion)	25	7×10^8
	30	5×10^8
	40	2×10^8
	45	1×10^8

errors for the SAGE NO_2 profiles are given as number density at selected altitudes. For a typical mid-latitude sunset observation, they correspond to approximately 25 percent error between 30 to 40 km altitude, and higher error above and below.

Since there were no correlative measurements of NO_2 during SAGE's lifetime, SAGE data have been compared with previous measurements of NO_2 from either balloon or aircraft platforms which have been summarised in the previous WMO assessment report, WMO 1981 (1982). Figures 10-32 (a) and (b) show some of the previously reported NO_2 profiles at sunset compared to the SAGE sunset measurements centered at latitude bands of 32 to 33°N and 45 to 50°N. The SAGE data are indicated by solid lines and are obtained by averaging all three year's observations during the spring season (March through May) over the corresponding latitude bands. The horizontal bars on the SAGE profile denote one standard deviation from the mean. As can be been in the figures, the agreement between SAGE observations and those of the balloon measurements is well within their respective uncertainties at these two latitude bands.

SAGE NO_2 Zonal Cross-Sections

Figure 10-33 shows the SAGE measured zonal mean NO_2 cross-sections. Data for the 34 months of SAGE NO_2 profiles have been grouped into 10-degree latitude bands for the four seasons to generate the zonal mean vertical cross-sections of NO_2 mixing ratio. The number of profiles in each latitude band varies from 40 to 500. The four seasons are represented by Northern Hemisphere winter (December through February), spring (March through May), summer (June through August), and fall (September through November). The SAGE data show that the NO_2 mixing ratio in the middle and upper stratosphere is at a maximum in equatorial regions and decreases towards high latitudes in both the northern and southern hemispheres for all four seasons. The maximum mixing ratio contour of 8 ppbv typically covers altitudes from about 32 to 36 km. The latitude of the peak mixing ratio shifts away from the equator with the sun and with the JJA peak located north of the equator while the DJF peak is located south of the equator. The NO_2 mixing ratio distribution for the spring and fall seasons is generally symmetric about the equator, while the summer and winter distributions show significantly less NO_2 in the local winter high latitude regions. An unusual feature of a MAM "bulge" at low latitudes above the peak can be seen.
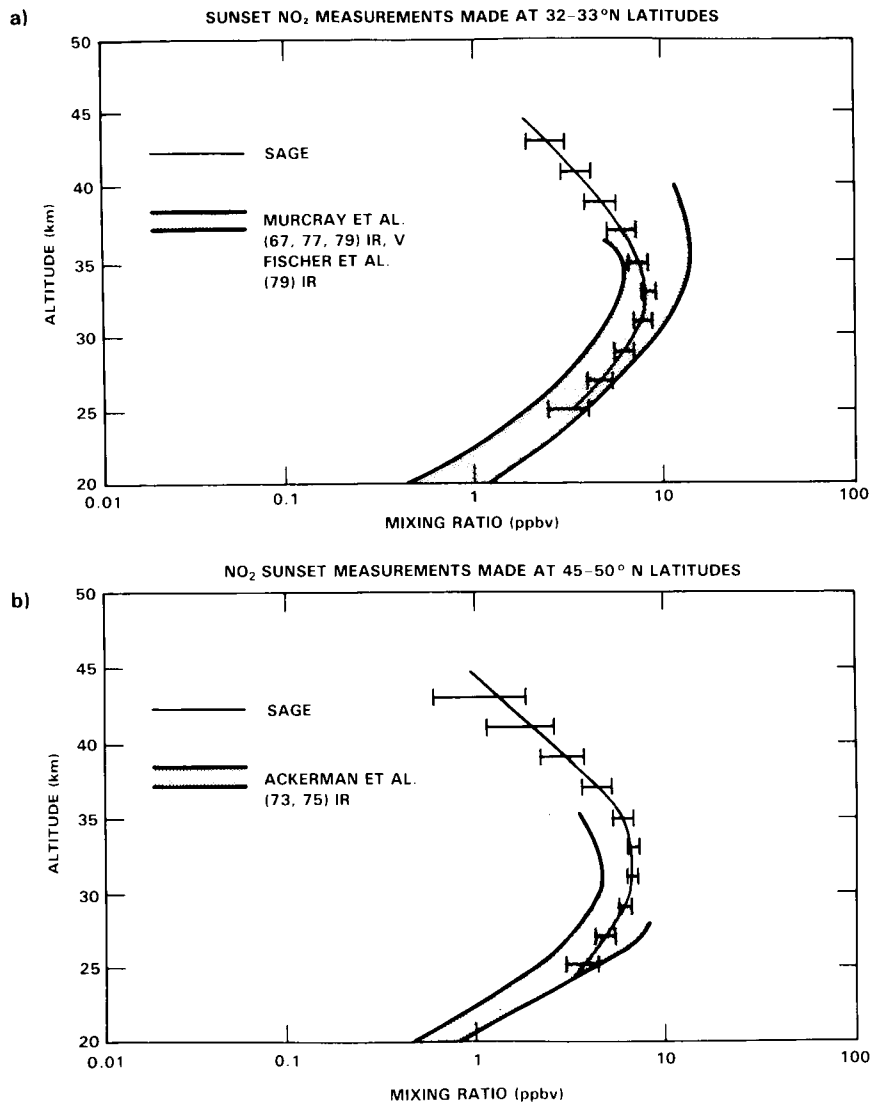
Figure 10-32. Comparison of some previous sunset measurements of NO₂ with sunset SAGE data, for (a) 32–33°N and (b) 45–50°N.

SAGE Total Column NO₂

Figure 10-34 shows the 1979 to 1981 averaged zonal mean column abundance of SAGE NO_2 integrated from 25 to 45 km altitude for the four seasons. The behaviour of the seasonal zonal mean column abundance is similar to that illustrated by the zonal mean mixing ratio cross-sections in Figure 10-33. Specifically, for all four seasons, there is a local minimum of NO_2 content in the equatorial region. The zonal mean column abundance distribution for the local winter versus summer season is significantly different. It shows a larger content in the local summer and a minimum in local winter with a rapid decrease to high latitudes in winter. As in the cross-sectional plots of Figure 10-33, the spring and fall column contents are almost symmetrical with indications of a double maximum, one near 30°N and the other near 20°S.
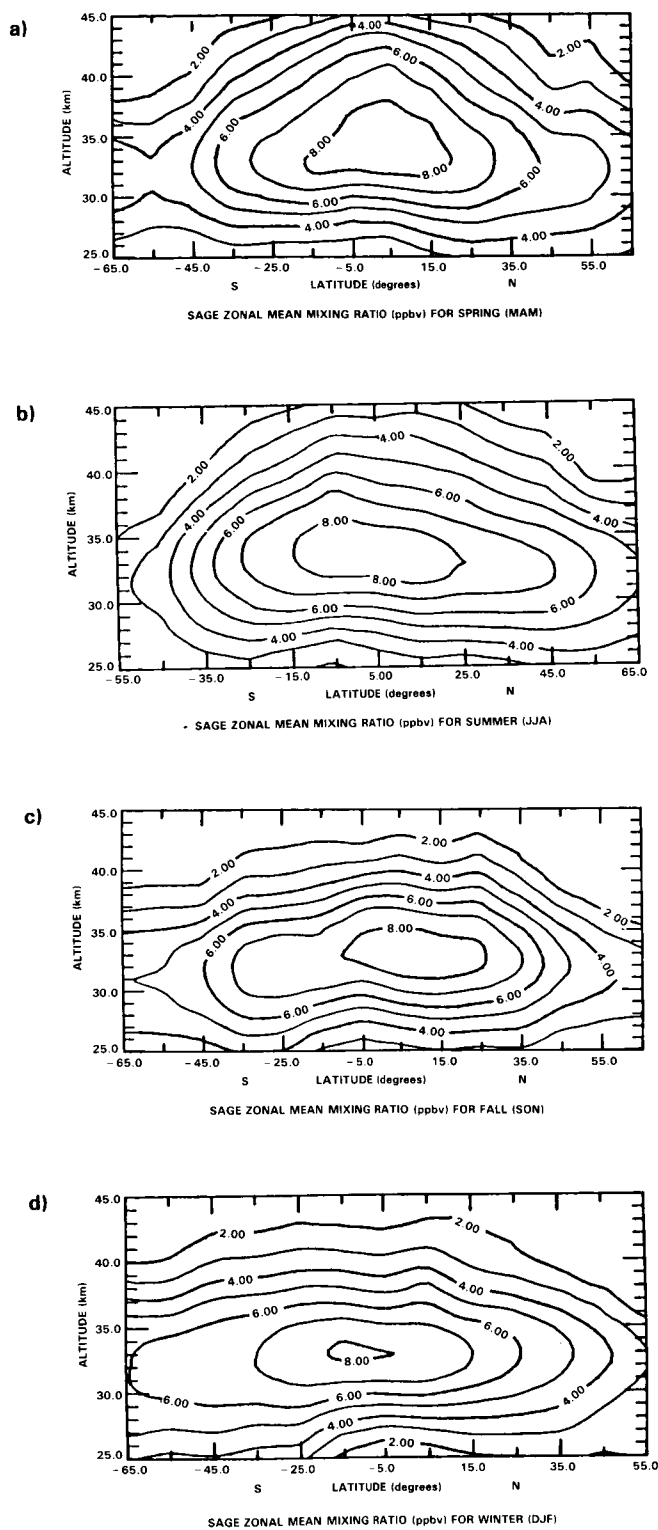
Figure 10-33. SAGE zonal mean cross-sections for NO₂ averaged for the 34 month lifetime of the experiment. (a) Spring (March, April, May); (b) Summer (June, July, August); (c) Fall (September, October, November); (d) Winter (December, January, February).
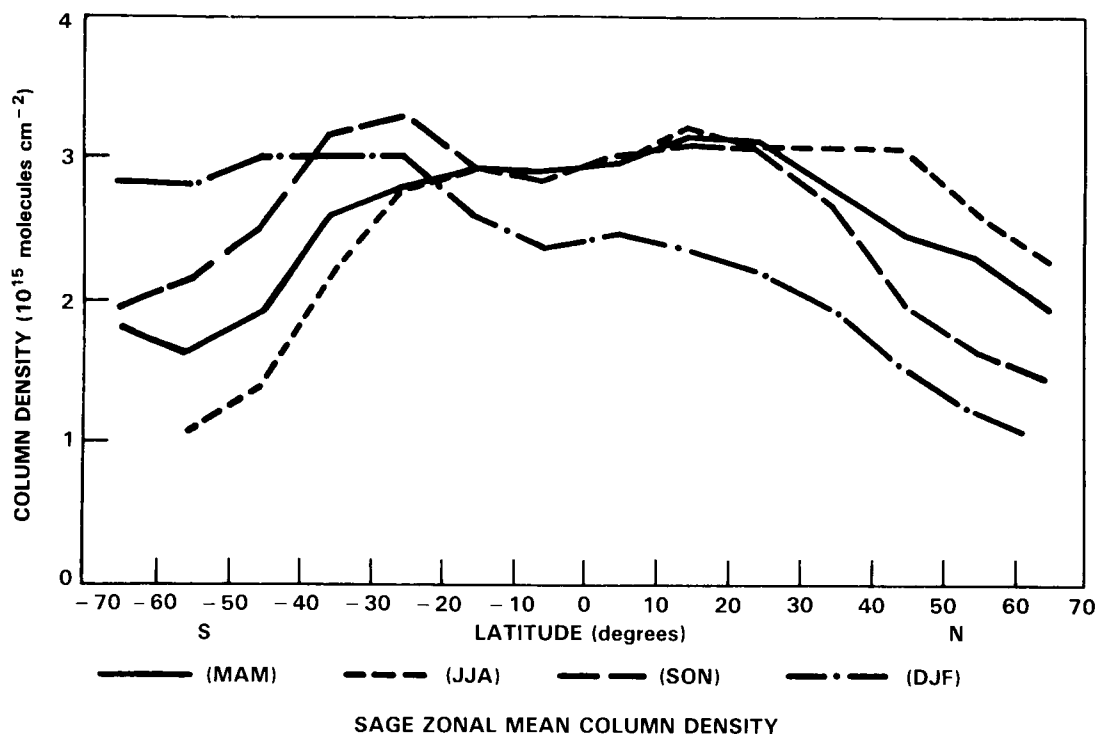
Figure 10-34. SAGE averaged zonal mean column abundance for NO_2 from 1979 to 1981, from 25 to 45 km, for the four seasons.

NO_2 Variability Near 31, 44 and 52°N

Figures 10-35 (a) through (c) show the SAGE zonal mean mixing ratio profiles for the spring season (March through May) averaged over the nearly 3 years of SAGE observations. Figure 10-35 (a) is for the latitude band from 26 to 36°N centered at 31°N. Figure (b) is for latitude band from 39 to 49°N centered at 44°N, and Figure (c) is for the latitude band from 47 to 57°N centered at 52°N. The bars denote one standard deviation from the mean. There is little variability below the peak from these northern latitudes between 31 and 52°N but significant difference above the peak for the 31°N plot which is higher in mixing ratio for all altitudes above the peak. Similar located profiles for winter (as shown in Figures 10-36 (a) through (c) show the located profiles for summer and fall (not included here) are all in between those shown in Figures 10-35 and 36.

Special Events: Noxon Cliff and Sudden Warmings

One of the most striking features of the behaviour of NO_2 is the observed sharp column density gradient (the "cliff") at high latitude during the winter season (Noxon *et al.*, 1979).

Even though the SAGE coverage does not usually penetrate into high latitudes during the winter season where cliffs are normally situated, there are occasions such as during a sudden warming event (where the polar vortex splits and/or moves to a lower latitude), when cliffs can be observed at more southerly locations. Figure 10-37 shows the SAGE observations on 23 February 1979 at 52°N. latitude during the
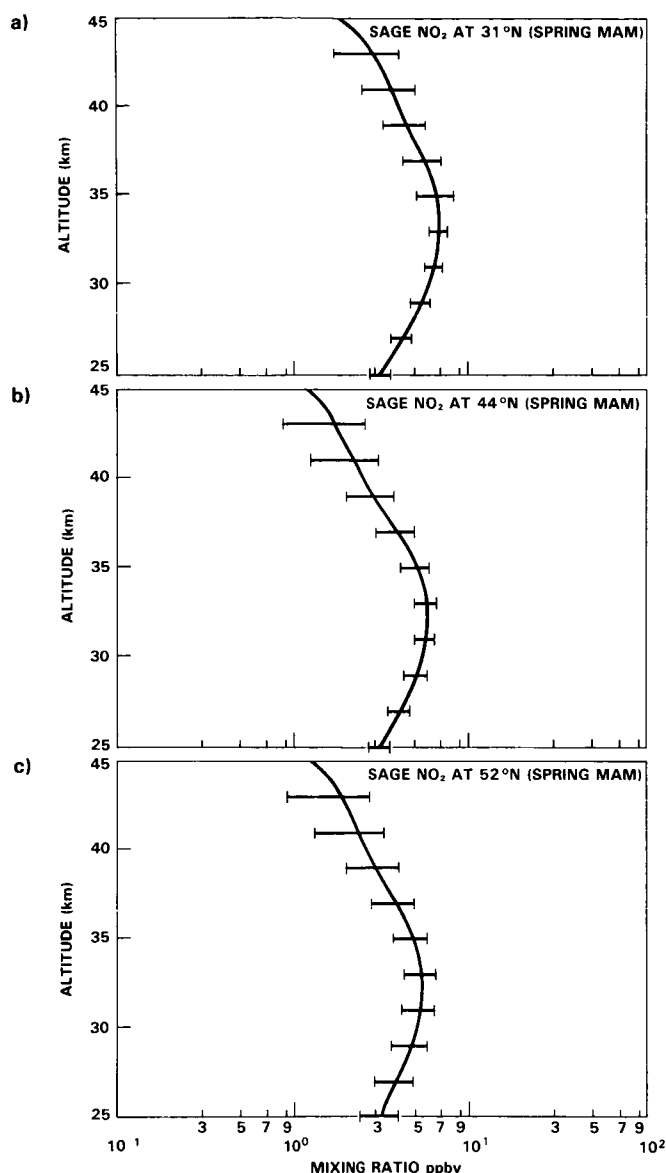
Figure 10-35. SAGE averaged zonal mean mixing ratio profiles for spring (MAM) at three latitudes, (a) 26-36°N centered at 31°N; (b) 39-49°N centered at 44°N; (c) 47-57°N centered at 52°N.

last phase of the sudden warming for this winter season. The normal single polar low was distorted and split into two lows approximately centered on the eastern and western hemispheres. Of the 13 sunrise SAGE NO_2 measurements, there are two distinct minima of NO_2 column. Positions A and B in Figure 10-37a show these on the 10 mbar isobaric height contour map. The locations of the SAGE measurement are illustrated by black dots and the heavy height contour lines around the two lows are the approximate boundaries of the two vortices based on calculations of the positions of the maximum wind field across the height contour levels. Figure 10-37b gives the corresponding SAGE NO_2 column content values. It is very clear that within the polar vortex there was significantly less NO_2 than observed outside the two vortices. These data demonstrate that one must consider dynamical as well as photochemical processes in understanding NO_2 distributions.

549
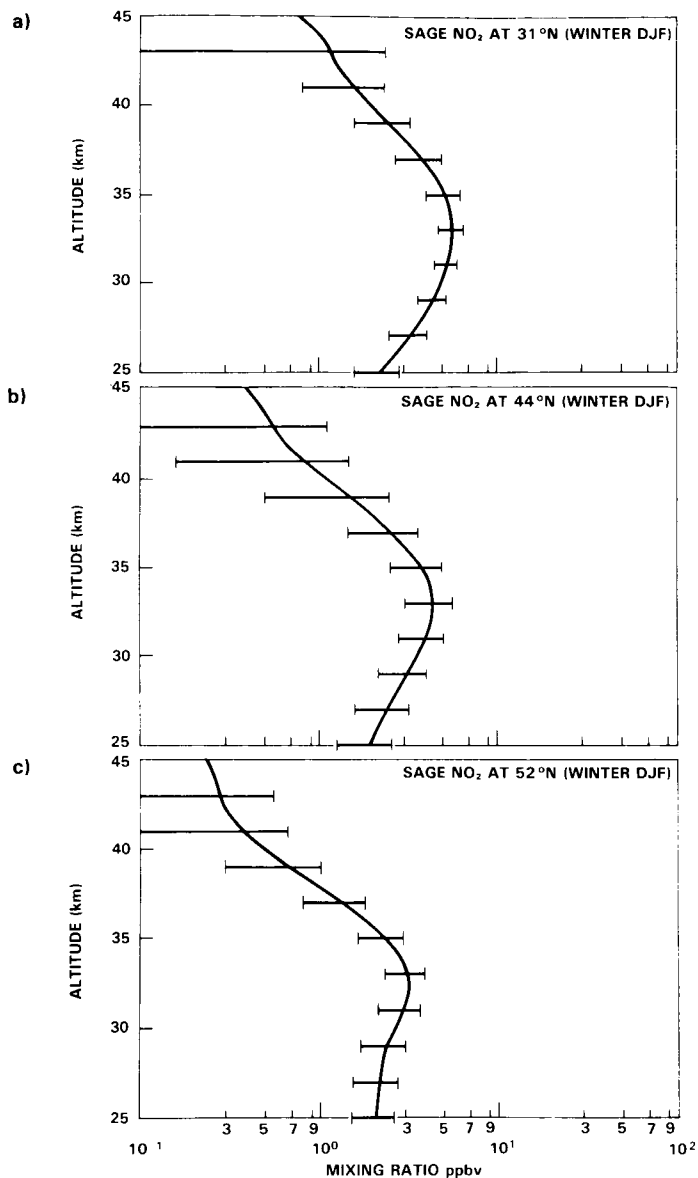
Figure 10-36. SAGE averaged zonal mean mixing ratio profiles for winter (DJF) season at three latitudes, (a) 26–36 °N centered at 31 °N; (b) 39–49 °N centered at 44 °N; (c) 47–57 °N centered at 52 °N.

10.2.1.3 SME Measurements of Nitrogen Dioxide

The Solar Mesosphere Explorer (SME) satellite measures stratospheric NO_2 in the 20-40 km altitude region. The instrument has been described in the Special Introduction. Detailed discussions of the measurements, which are based on the technique of Noxon (1979), are provided by Mount *et al.*, (1983, 1984).

Table 10-8 provides an estimate of the accuracy of the NO_2 observations. The largest error in determination of the NO_2 density profiles is caused by measurements of the altitude for the instrument field of view above the Earth's surface as a function of time. The absolute altitude determination is made to

550
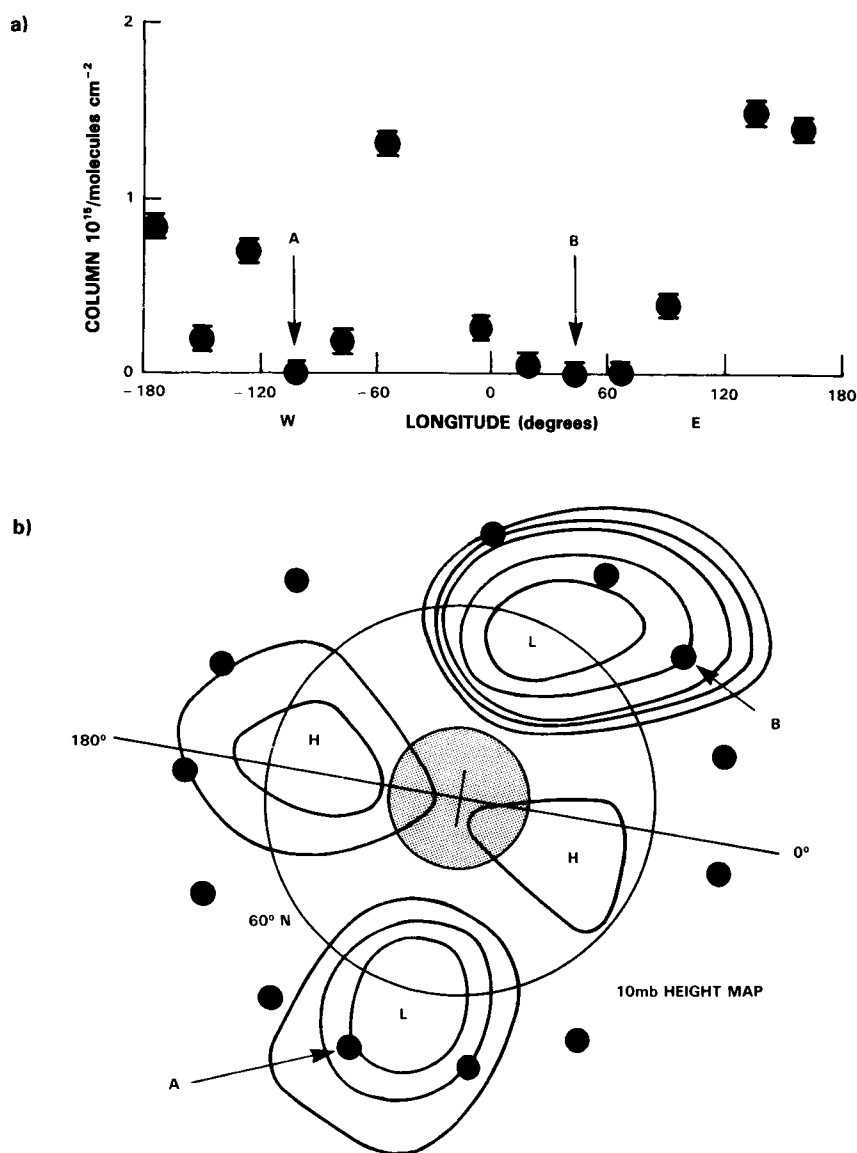
SAGE NO₂ COLUMN MEASUREMENTS ON FEB. 23, 1979

Figure 10-37. SAGE sunset measurements on February 23, 1979 at 59°N.
(a) SAGE column content integrated from 25 to 45 km.
(b) 10 mb height map. SAGE measurement locations shown by black dots.

an upper error limit of ± 1 km at the limb, and since the NO_2 scale height is about 4 km, this results in a significant error in NO_2 density determination. (See Table 10-8).

The primary NO_2 quantity measured by SME is the concentration or density (molecule/cm³). Because of an instrument failure on board the SME spacecraft, measurements of the atmosphere neutral density are not available, and the NO_2 observations can only be converted to mixing ratio by adopting a reference atmosphere (see, Mount *et al.*, 1984; Rusch *et al.*, 1984). This introduces an additional large error in the mixing ratio products displayed here which may be as much as 20%.

551

Table 10-8. SME Error Analysis

Type of Error	Error	Error in NO$_2$ Density	
		28 km	38 km
Altitude of field of view at limb	± 1 km	5%	50%
Random error in data numbers (noise)	± <1 DN	<5%	<25%
Determination of on board differencing amplification ratio	1%	<1%	10%
Determination of relative instrument polarization	1%	<1%	10%
Determination of diode "dead" time	<1%	<1%	<1%
Error in master null set used for subtraction	<0.2%	5%	25%
NO$_2$ cross section (relative error between wave-length pairs)	<10%	10%	10%
Ozone correction	×2	<15%	0%
Absolute placement of instrument on spacecraft	<30 arc sec	<5%	<10%
Determination of electronic background	± <1 DN	<5%	<5%
Total rms error (quadrature sum)		± 21%	±65%

The Solar Mesosphere Explorer began taking NO$_2$ observations in December 1981. The eruption of the El Chichon volcano on 4 April 1982 injected a large number of scattering particles into the atmosphere, interrupting NO$_2$ observations. We present here results only from the first winter of observations, 1981-1982 before the eruption. Coverage of the NO$_2$ data is restricted to about 4 orbits over North America on a daily basis, at a local time near 3 pm. There are no coincident correlative measurements of NO$_2$ available for this period. Figure 10-38 shows a comparison of NO$_2$ vertical profiles in January 1982, in the summer hemisphere compared to several observations performed in the Northern Hemisphere summer. The comparison reveals reasonable agreement.

Figure 10-39 presents monthly and zonally averaged NO$_2$ mixing ratio distributions from SME for January, February and March of 1982. The most striking feature in these distributions is the sharp gradient observed near the polar night terminator. The progression of NO$_2$ mixing ratio near 40-80 °N from January to March reveals that NO$_2$ must be converted to another reservoir NO$_y$ species during high latitude winter, as first suggested by Noxon (1978), and as shown in several other ground-based and aircraft studies (e.g. McKenzie and Johnston, 1982).

Figures 10-40 (a-c) show vertical profiles observed by SME at the equator, 35 and 55 °N. Because of the limited seasonal information, only a few statements regarding the profiles can be made. The altitude of maximum mixing ratio occurs near 30 ±1km in virtually all seasons and latitudes. The equatorial profile reveals a steep gradient below the peak, probably because of the predominance of upward transport in the tropical lower stratosphere. NO$_2$ abundances observed in winter at 55 °N are extremely low, and show only a very modest peak. A significant increase occurs in the peak values in March.

On many occasions, SME observed abrupt decreases in NO$_2$ abundances during winter in high latitudes at particular longitudes; this is the Noxon "cliff" phenomenon, discussed earlier. Note that the gradients
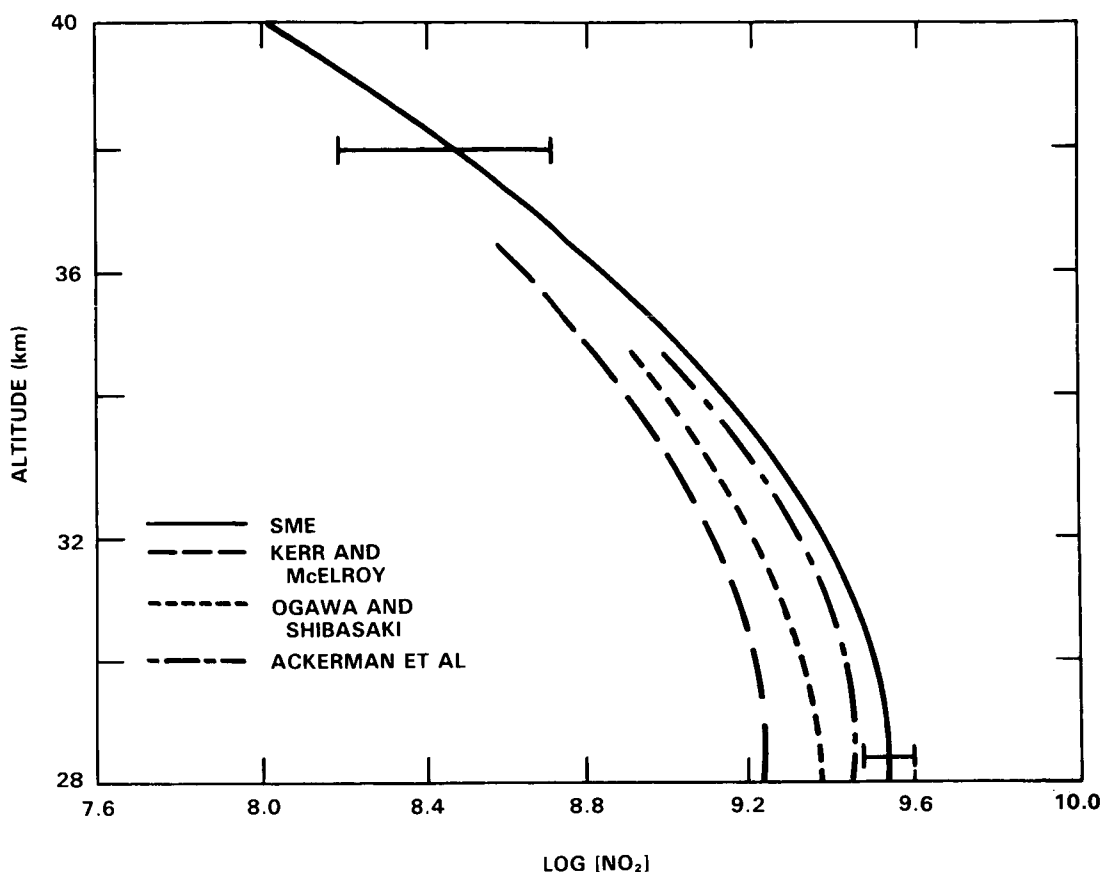
Figure 10-38. A typical NO_2 number density profile taken during January 1982 at 40 °S latitude compared with measured NO_2 profiles (summer mid-latitudes) of Kerr and McElroy (1976), Ackerman *et al.* (1975), and Ogawa and Shibasaki (1980). The agreement of both shape and absolute value is acceptable, considering the lack of temporal and geophysical coincidence. The comparison of the southern summer data taken in January to published northern summer data should be reasonable. The eruption of El Chichon in April 1982 prevents a direct comparison of northern summer data for SME.

at particular longitudes were much greater than those obtained in the zonal mean as shown in Figure 10-39. Figure 10-41a shows an example of the NO_2 density gradient observed at 10 mbar on day 40 of 1982 on a single orbit, showing a decrease of a factor of 4.5 in 20 degrees of latitude. A chemistry/trajectory model calculation is also shown (Figure 10-41b). The model calculation and its implications will be discussed in Section 10.3.

10.2.2 Nitric Acid (HNO₃)

The LIMS instrument, which was described above, also made observations of the global distribution of HNO_3.

Data Quality

The HNO_3 data are discussed and evaluated by Gille *et al.* (1984b), from which the following discussion is summarised. The vertical range is again set by the region of adequate signal to noise ratio, and
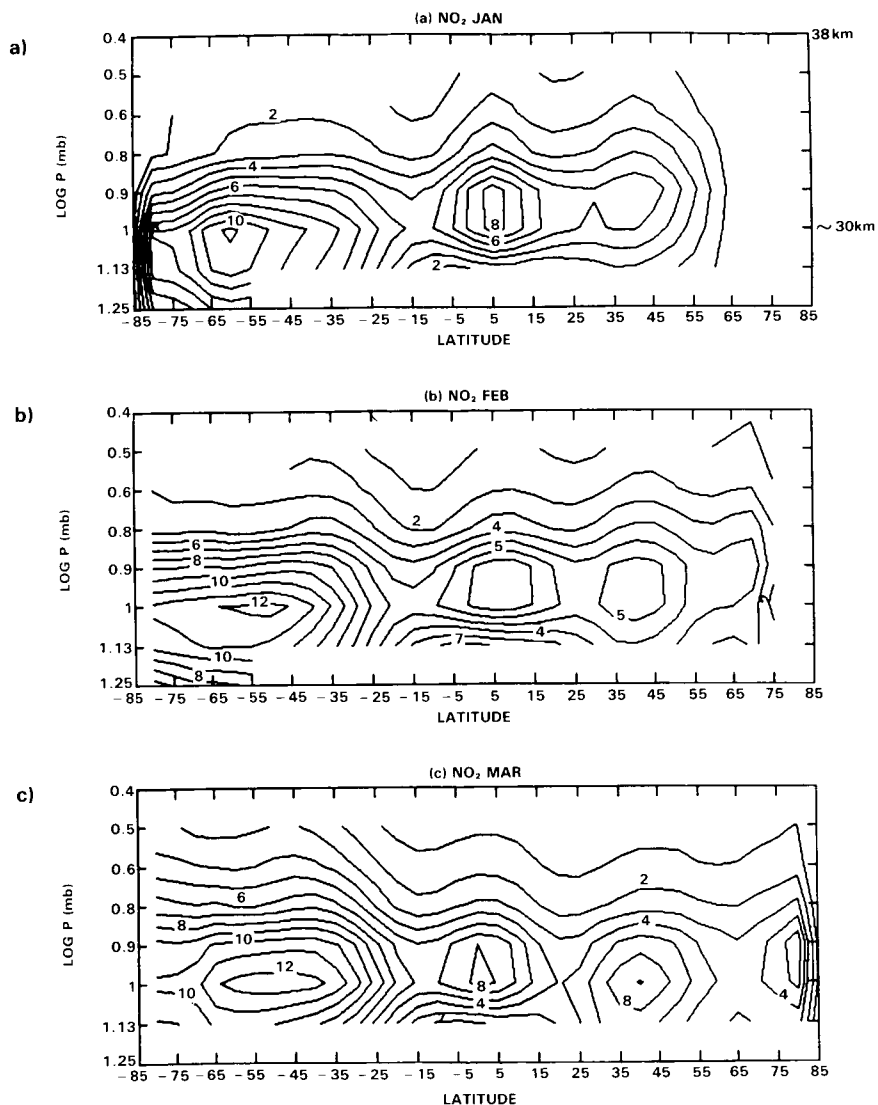
Figure 10-39. Monthly and zonally averaged NO₂ distributions from SME for (a) January, (b) February, and (c) March 1982.

at the bottom, by the frequent occurrence of clouds. For the HNO_3 signal, the upper limit occurred at about 2 mbar pressure level, or around 45 km altitude. Clouds usually interrupt the path at or above the 100 mbar pressure level in the tropics. Retrievals to lower altitude are possible at higher latitudes, but with rather small signal to noise ratios. In this discussion the lower boundary is usually taken to be 100 mbar.

The precision of the profiles or scan-to-scan repeatability, is about 0.05-0.1 ppbv in undisturbed regions, where atmospheric changes do not contribute much to the variations. This intrinsic precision is of the order of 2% up to 7 mbar rising to only 6% at 5 mbar. When natural atmospheric variability, which may incorporate real variations on scales smaller than the 100 km inter-scan spacing, is included, a repeatability at almost all latitudes and altitudes of 0.1 ppbv is found. These values are somewhat lower than the estimates presented in Table 10-9, which are based on calculations of the effects of known noise sources.
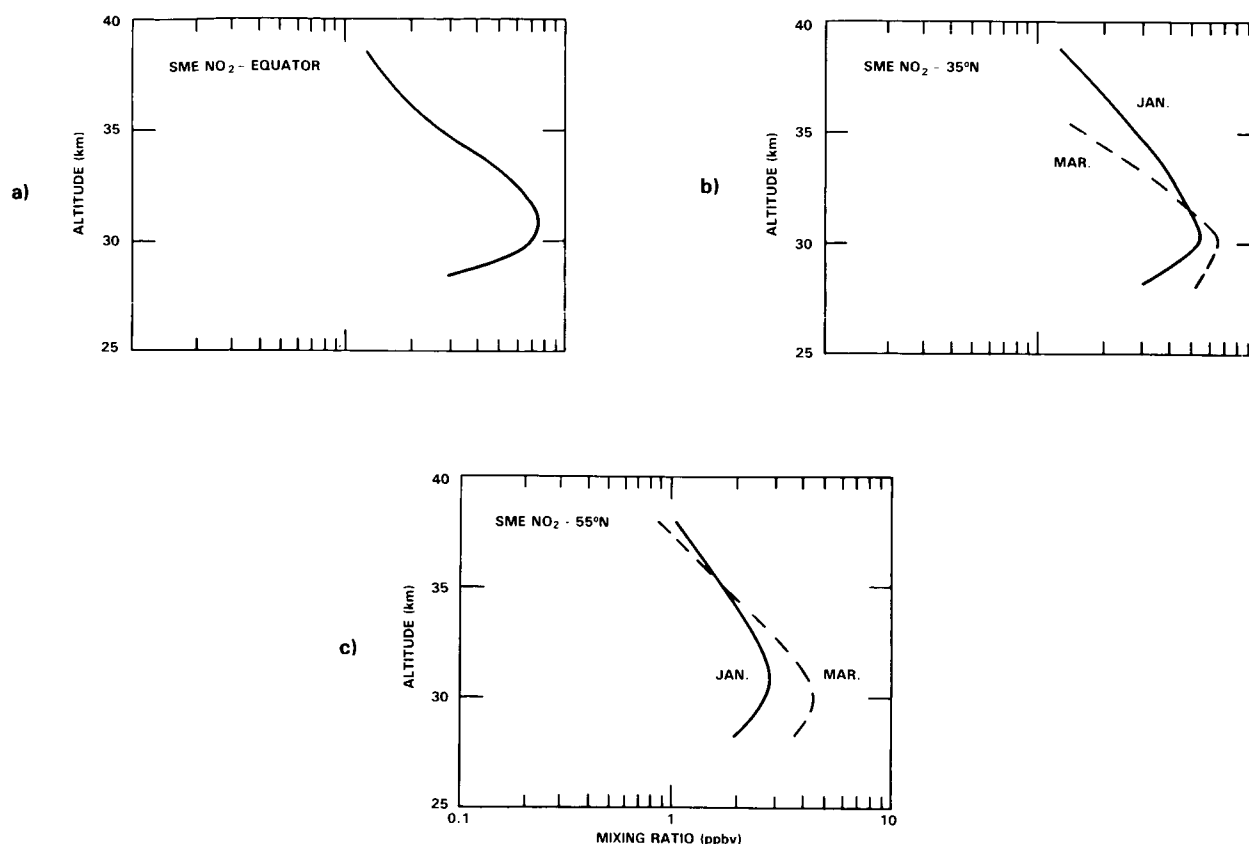
Figure 10-40. Vertical profiles of NO₂ observed by SME at (a) the equator, (b) 35°, and (c) 55°N, 1982.

The accuracy is much more difficult to establish. Table 10-9 also presents results of calculations of the effects of instrumental and data uncertainties. The errors are estimated to be 30–40% between 10 and 50 mbar rising to 65% at 3 mbar, where the signal is very close to the noise. These estimates, at least away from the top levels, are thought to be rather conservative. A second approach to estimating the accuracy is through comparison with other measurements. Mean differences of about ± 20% between LIMS measurements and 15 balloon-borne measurements were found from 100 to 10 mbar. These differences are approximately the errors associated with the balloon-borne measurements, and so form a lower limit to the differences that might be expected. However, the LIMS results become systematically larger than the correlative measurements with increasing altitude, e.g. by 7 mb the LIMS data is ~50% greater than the correlative data. There are reasons for thinking that such an effect could be due to an instrumental effect (Bailey *et al.*, in preparation). In addition, chemical consistency suggests that the original values are too large (Jackman *et al.*, 1986). Therefore, the values presented here for the upper levels should be considered as too large.

The Zonal Mean Distribution of Nitric Acid

Figure 10-42 presents monthly averaged values for the months October, January, April and May. The general features of the distribution are similar from month to month, but there are significant changes.

555

Table 10-9. Calculated Error Estimates for LIMS Nitric Acid Retrievals

Error Sources	Pressure Level, mbar				
	80	**50**	**30**	**10**	**3**
Random errors, ppbv					
Radiometer noise and jitter	0.25	0.27	0.29	0.16	0.09
Temperature noise	0.22	0.07	0.06	0.01	0.05
rss†	0.33	0.28	0.30	0.16	0.10
Systematic errors, %					
Calibration	1	—‡	2	1	7
Out of spectral band signal	29	29	20	7	45
Field of view side lobes	27	28	25	27	45
Temperature bias	9	1	4	1	8
Spectral data	5	5	5	5	5
Uncertainty in CFC contribution	8	1	—‡	1	1
rss†	42	41	33	28	65
Algorithm effects	5	5	5	5	5
rss†	42	41	33	29	65

†Root sum squared
‡Less than 0.5%

A knowledge of the variability of these cross-sections is necessary before they can be meaningfully discussed. Figure 10-43 presents the standard deviations of the daily values for January and April. January is the month with the largest temporal variability, which is associated with a major disturbance toward the end of the month. The standard deviation is less than 0.2 ppbv south of 45 °N, and reaches values of 1 ppbv only at the highest latitudes. The same results are presented as a percentage of the mean in Figure 10-44 which shows percentage variations for January less than 5 % except for a region at high latitude. The low altitude region at the equator is spurious, resultng from the incomplete removal of cloud effects, and the low mean values present there. For other months, e.g., April (Figure 10-44b), the variability is smaller. Thus, the values at a given location are quite stable from day-to-day, and means such as those in Figure 10-42 are representative.

The general features of the nitric acid distribution are illustrated by the October data. There is a broad saddle in the tropics, centered near 20 mbar and characterised by the values of 2-3 ppbv. Mixing ratios decrease slowly above and below this level, indicating a low and relatively uniform profile. Maximum values increase toward both poles, with the altitude of the maximum decreasing to the 30 mbar level at the highest latitudes. In the Northern Hemisphere (NH) the maximum of 3 ppbv at 20 mbar and 10 °N progresses to a maximum of 12 ppbv at 30 mbar and 84 °N. The variations are similar in the Southern Hemisphere (SH) as far as they can be seen. Note also that the isolines are relatively flat on the upper side of the layer, but have fairly steep slopes on the lower side. Finally, there is an indication of an increase at high northern latitudes and high altitudes.
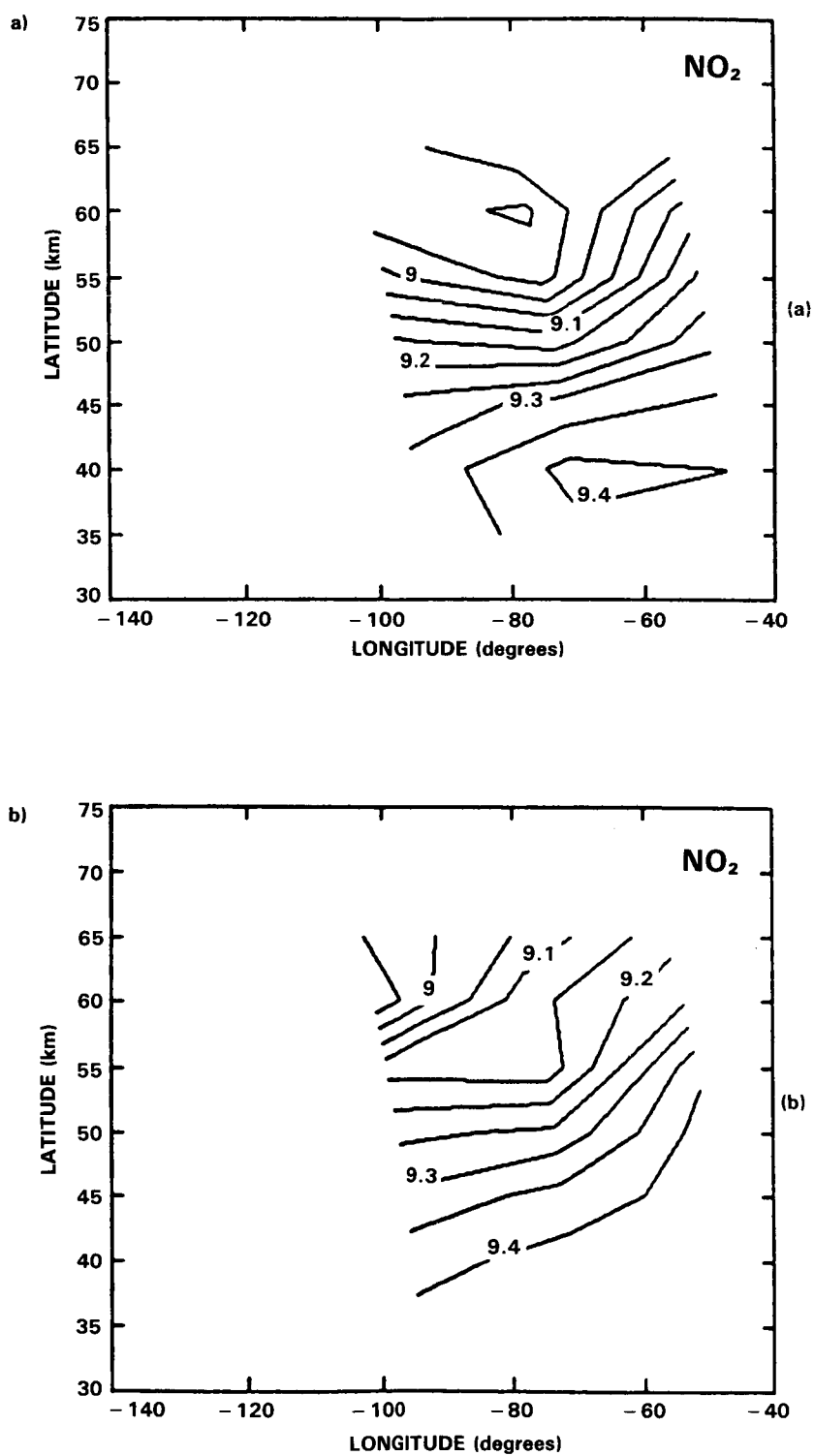
Figure 10-41. Logarithm of NO_2 density for day 40 (1982), at 10 mbar; (a) observed by SME; (b) from a 2-D coupled dynamical-chemical model.

557
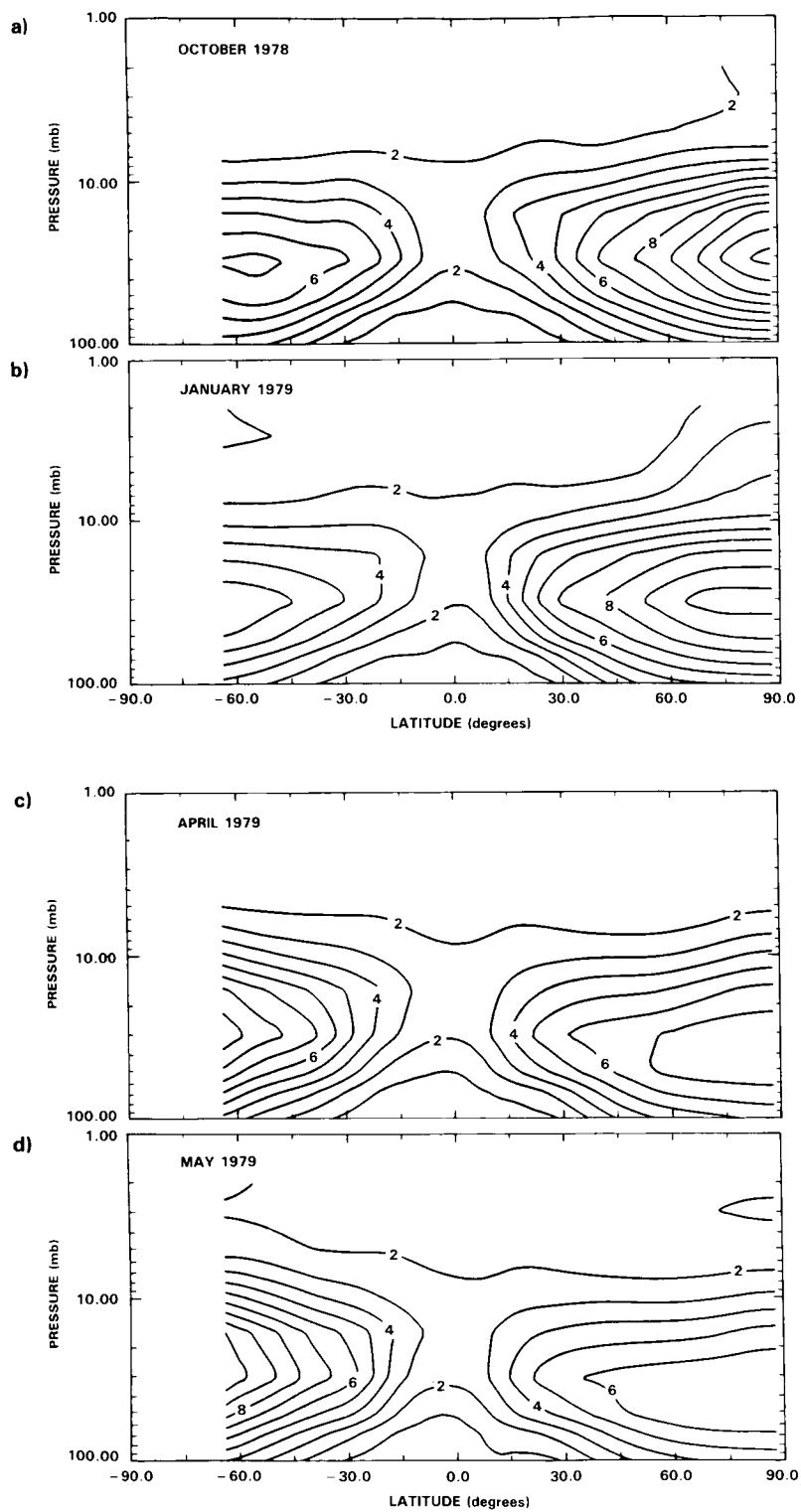
Figure 10-42. Monthly averaged zonal mean cross-sections of HNO_3 mixing ratio (ppbv) for (a) October (last 7 days), (b) January, (c) April, and (d) May (first 28 days). Note that values above 10 mb are probably somewhat too large.
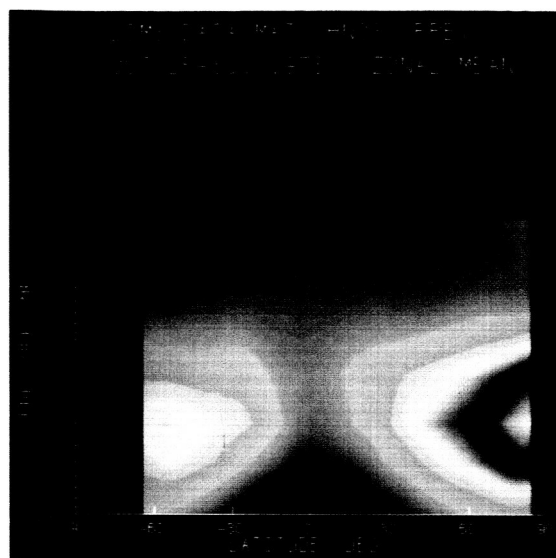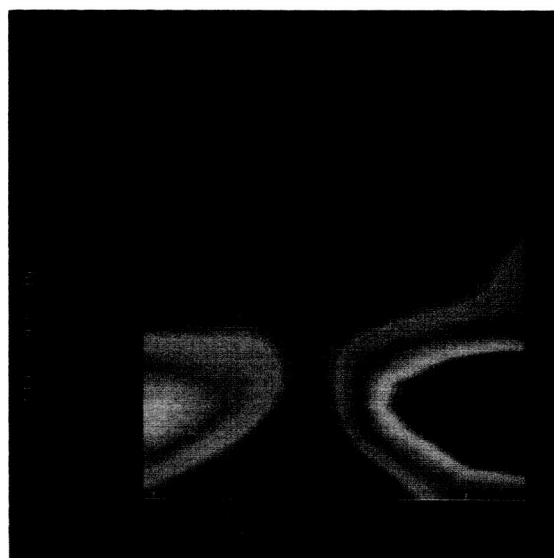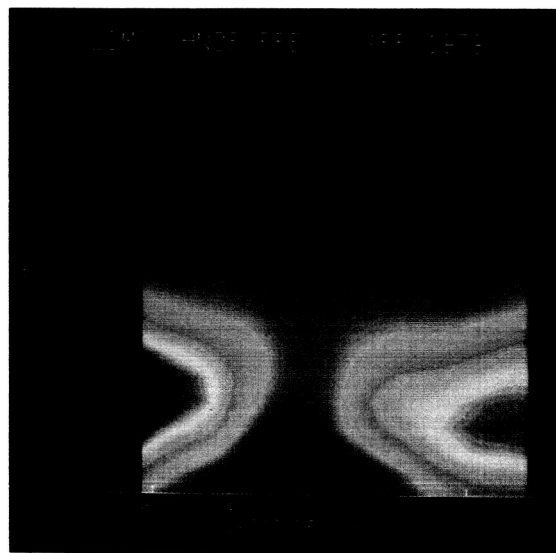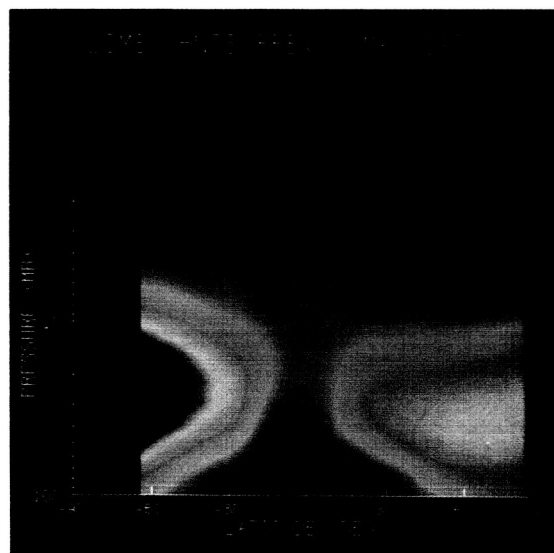
Figure 10-42. (Color) Monthly averaged zonal mean cross-sections of HNO_3 mixing ratio (ppbv) for (a) October (last 7 days), (b) January, (c) April, and (d) May (first 28 days). Note that values above 10 mbar are probably somewhat too large.
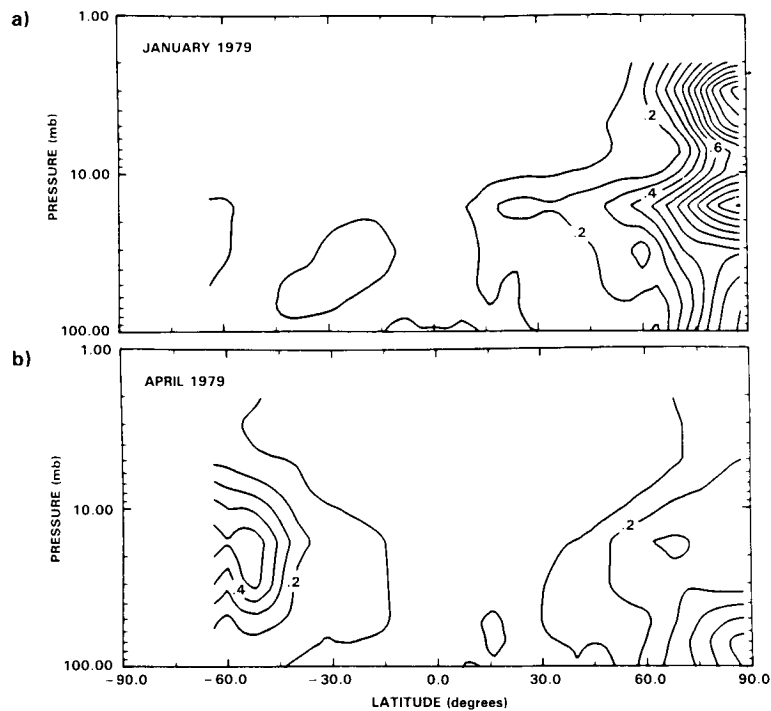
Figure 10-43. Standard deviation of daily zonal mean values of HNO$_3$ mixing ratio (ppbv) for (a) January and (b) April. Contour interval is 0.1 ppbv.
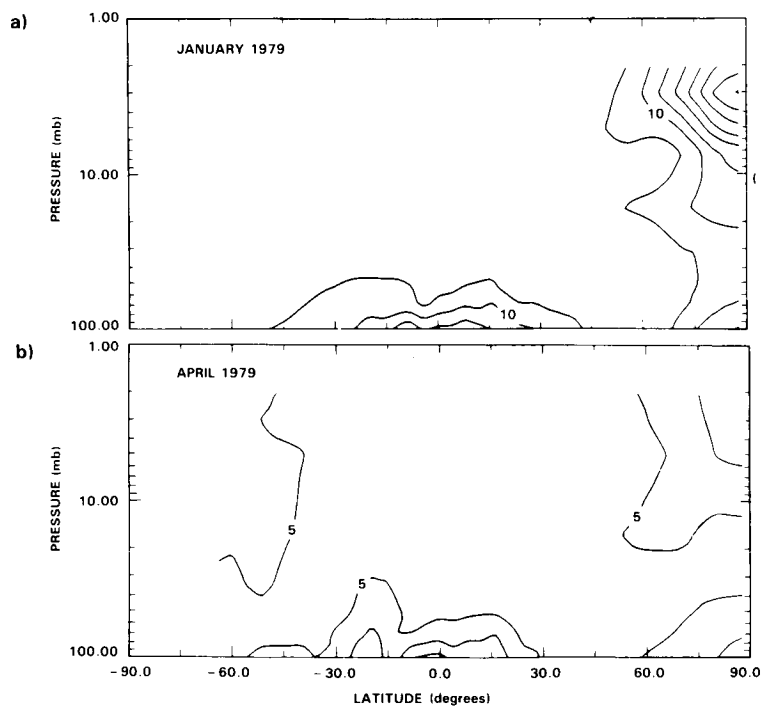
Figure 10-44. Standard deviation of daily zonal mean values of HNO$_3$ mixing ratio as a percent of the mean values, for (a) January and (b) April. Contour interval is 5%.

The monthly mean cross-sections in Figure 10-45 indicate that there are significant but regular changes with season. The NH maximum value at 30 mbar and 84 °N decreases from over 12 ppbv in the fall to about 7 ppbv in May. At the same time, the values in the SH are increasing. Above 10 mbar, the slope of the isolines reverses from October to May, along with the indication of higher concentrations at the winter pole.

Time-Height Cross-Sections

The temporal variation of the zonal mean is shown more explicitly by the time-height cross sections in Figure 10-45. There is an apparent semi-annual oscillation in the tropics, where the HNO₃ maxima are reached in December and (probably) June at 16 mbar, but somewhat earlier at 30 mbar and later at 10 mbar. The minimum at each level is close to the mid-point between the maxima.

At 32 °N there is an annual variation, which is approximately in anti-phase with that at 32 °S. The NH maximum occurs in late January, while the SH minimum occurs in February at 50 and 30 mbar, but somewhat earlier at higher altitudes. The patterns are similar above 30 mbar, but the spring values in the SH are larger than the NH maxima in February, suggesting a hemispheric asymmetry in the HNO₃ amounts. A striking feature is that the maximum appears to occur later at lower altitudes, as if propagating downward.

The characteristics are similar at 60 °N and S, but the NH maxima occur in January at 50 mbar, or in December at 30 mbar. This level also shows higher values in late autumn in the SH than in the NH. Again, there is a suggestion that the NH maximum occurs earlier than the SH minimum.

At 80 °N (for which a SH counterpart does not exist in the LIMS database), the maximum occurs in November. At 30 mbar the maximum of over 12.5 ppbv is reached in mid-November, after which the concentration decreases irregularly through the winter and more smoothly in the spring to a value just under 7 ppbv. The altitude of maximum values decreases from fall to winter, and rises again in the spring.

These plots clearly indicate that there are long term changes, probably due to a combination of transport and photochemical effects, and short period variations, especially during the winter, that are related to dynamical effects. There are marked decreases at high levels during the times of major disturbances in the stratosphere, which are to be expected when downward motions (which lead to stratospheric warming through adiabatic heating) bring down air that is poorer in HNO₃.

It is clear that the SH maxima and perhaps the minima have larger mixing ratios than those in the NH, indicating an asymmetry between the hemispheres in nitrogen compounds. This has also been seen in NO₂, and in estimates of the total odd nitrogen (Noxon, 1979; McKenzie and Johnston, 1982; Solomon *et al.*, 1983a; Gille, 1984b).

Vertical Profiles

Monthly and zonally averaged vertical profiles are shown in Figure 10-46 for 5 latitudes and the 4 months for which the cross-sections were discussed above. At 60 °S the largest mixing ratios are always at 30 mbar, with the lowest value in the summer, and maximum of over 10 ppbv in the late autumn. At 32 °S the values decrease from spring to summer, then increase into the autumn. There is very little seasonal variation at the equator, where the peak values are at 16 mbar. At 32 °N the seasonal variation is similar to that in the Southern Hemisphere. The smallest peak values are in the autumn, increasing into winter, and

(a) 60 °S

(b) 32 °S

(c) Equator

(d) 32 °N

(e) 60 °N

(f) 80 °N

Months

Months
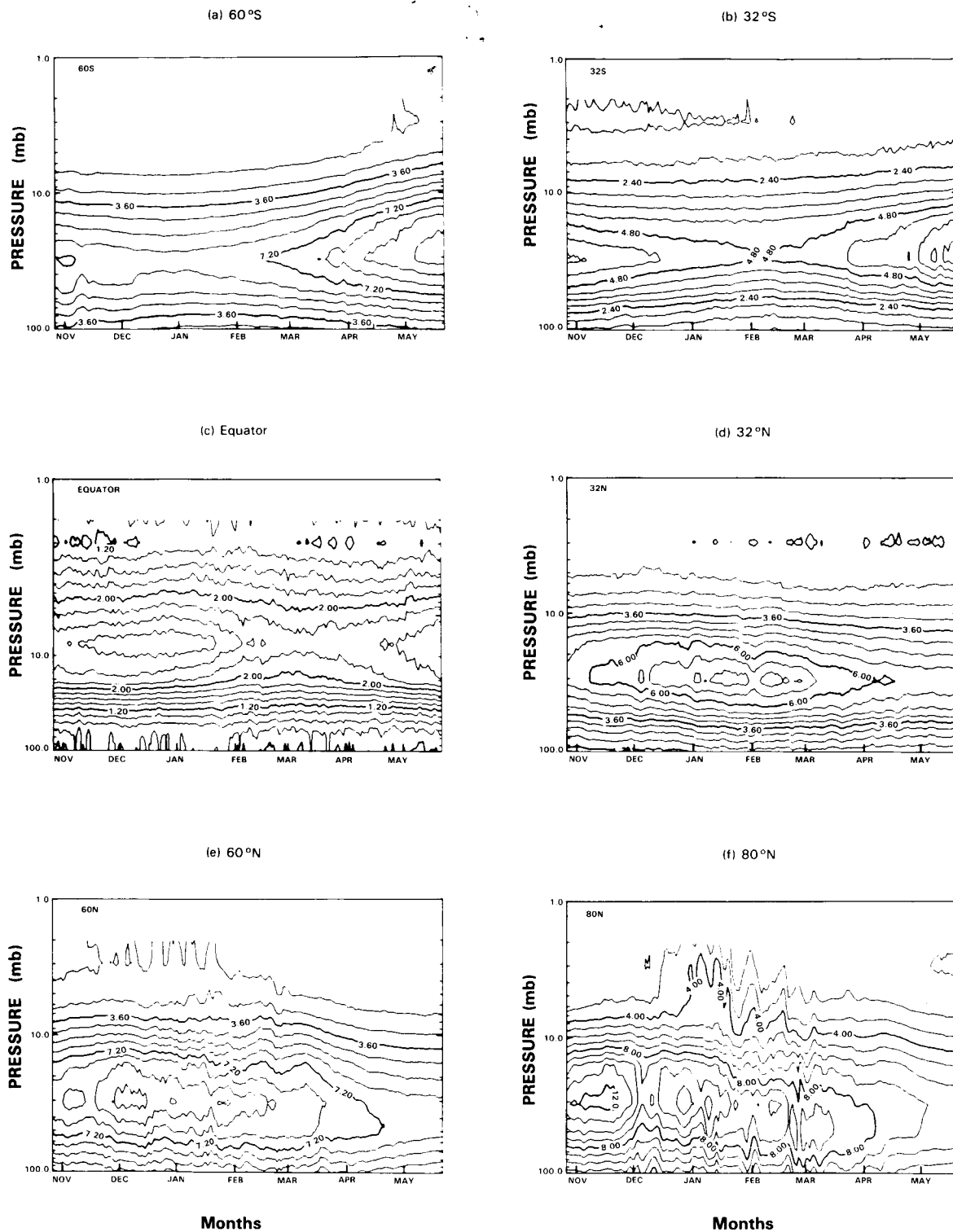
Figure 10-45. Time-height cross sections for HNO_3, for latitudes (a) 60 °S, (b) 32 °S, (c) Equator, (d) 32 °N, (e) 60 °N and (f) 80 °N.
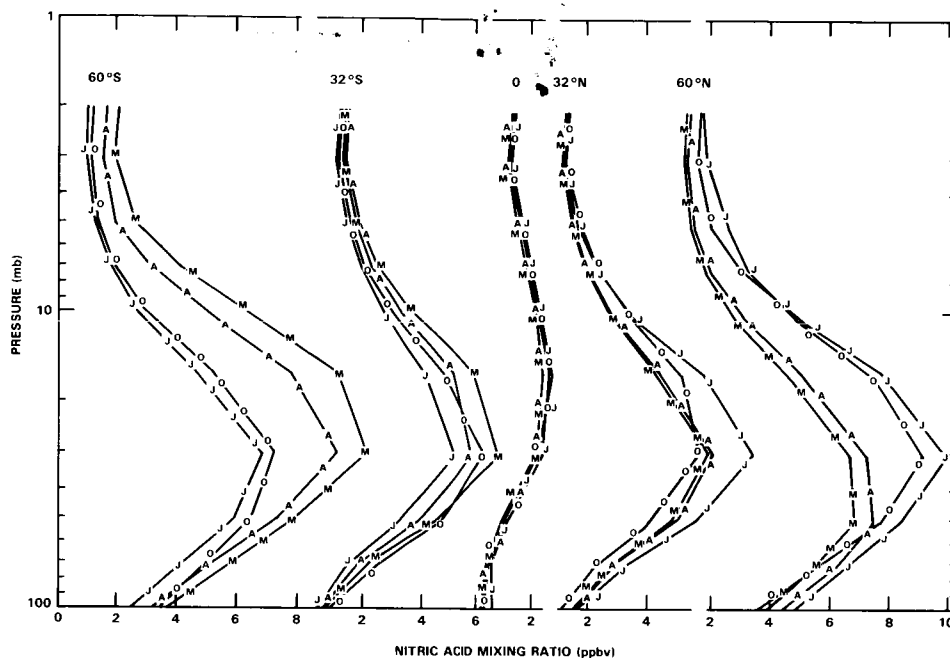
Figure 10-46. Vertical profiles of zonally and temporally averaged HNO₃ mixing ratios, at 5 latitudes for October, January, April and May. O-October, J-January, A-April, M-May.

dropping back in the spring. The same qualitative variations take place at 60 °N, but now the autumn values are almost as large as the winter value. At 84 °N the maximum value over 12 ppbv is reached in the autumn, with a continuous but irregular decrease to the late spring. Again, it should be noticed that the maximum values at 60 °S are larger than those at 60 °N, again indicating that the HNO₃ is not symmetric between the hemispheres.

10.2.3 Nitrous Oxide (N₂O)

10.2.3.1 Nitrous Oxide Mixing Ratio Measurements from SAMS

Introduction

The Stratospheric and Mesospheric Sounder (SAMS) instrument launched on the Nimbus 7 satellite in October 1978 is a multi-channel infrared limb-scanning radiometer using both "conventional" and pressure modulaton techniques to measure atmospheric temperature and the abundances of a number of minor atmospheric constituents. It is further described in the Special Introduction. In this section we present data from the nitrous oxide channel on SAMS.

Nitrous Oxide Data from SAMS

A detailed description of the SAMS instrument has been given by Drummond *et al.* (1980). Of relevance to the nitrous oxide measurements is the fact that the same optical chain is used by the methane channel on SAMS, which also shares a common detector. This meant that methane and nitrous oxide could not be measured simultaneously, and in practice this meant that measurements of the two gases were made

on alternate 24 hour periods. This, and the duty cycle of the SAMS instrument (3 days in every 4) meant that nitrous oxide measurements were made for approximately 40% of the time (approx. 12 days per month).

Details of the instrument radiometric calibration and the approach taken to deduce mixing ratio profiles from measured radiance profiles can be found in Wale and Peskett (1984) and Rodgers *et al.* (1984), respectively.

The signal-to-noise ratio of the radiances measured by the nitrous oxide channel was not in general sufficiently high to allow single profiles to be retrieved. The normal procedure was therefore to average radiances zonally before inversion. Corresponding zonal average temperature profiles were also produced by averaging the Planck function at 7.8μ (using SAMS derived temrperatures). The normal procedure was to average the radiances measured over a 24 hr. period over 10 degree latitude bands and 0.2 scale height (approx 1.4 km) intervals in the vertical. Zonal mean mixing ratio profiles were then derived from the zonally averaged quantities from which daily (and of course longer term) zonal mean cross-sections could be derived.

The SAMS instrument began operation in late October 1978 and functioned until the middle of 1983 except for a period between late September 1982 and mid-February 1983. Thus a continuous record spanning in excess of three years was obtained.

The Error Budget of the SAMS Nitrous Oxide Measurements

A detailed discussion of the error budget of the SAMS nitrous oxide budget may be found in Jones and Pyle (1984). A summary of this work is given below.

Systematic errors in the retrieved nitrous oxide fields fall broadly into four categories: Uncertainties in the spectroscopy of nitrous oxide and any contaminating gases (mainly methane), instrumental uncertainties, limitations and simplifications in the retrieval method and algorithm, and inaccurate knowledge of the state of the atmosphere (mainly of the temperature structure.)

To estimate the impacts of these various error sources a synthetic radiance profile was computed from assumed typical mixing ratio and temperature profiles with all the uncertain components set to their nominal values. The simulated data set was then retrieved with each uncertain parameter offset in turn to its limit of uncertainty and the retrieved mixing ratio profile was compared each time with the original.

In addition to the systematic error sources, even with the zonal averaging there remained a significant random component to the error budget due to radiance noise. The effects of this on the retrieved mixing ratio profiles was quantified during the retrieval by means of an error covariance matrix (see Rodgers *et al.*, 1984).

A summary of the error budget of the SAMS nitrous oxide measurements are shown at various pressure levels in Table 10-10.

A detailed discussion of the various error sources may be found in Jones and Pyle (1984) and it is necessary here merely to reinforce the main conclusions found there, namely that uncertainties in retrieved temperatures have maximum impact at the profile extremities (notably at lower levels) while effects such as uncompensated Doppler shifts (due to zonal winds) have pronounced effects at upper levels. The net RSS accuracy reaches around $\pm$ 50% at most levels and is lowest (approx 20%) near 7 mbar. The random

Table 10-10. Summary of the Error Budget for the SAMS Nitrous Oxide Measurements

Pressure Level	20 mbar	7 mbar	2 mbar	0.6 mbar
1. Spectroscopy	±7%	±7%	±5%	±5%
2. Field of view	±2%	±4%	±7%	±8%
3. Mean PMC pressure	±3%	±2%	±17%	±21%
4. Uncompensated Doppler shifts	±3%	±2%	±45%	±15%
5. Zonal averaging	±8%	±8%	±8%	±8%
6. Interference of CH_4	±8.5%	±2%	±5%	±25%
7. Temperature (± 2 K)	±50%	±15%	±10%	±20%
8. Line-of-sight attitude (± 0.0006)	±4%	±8%	±12%	±3%
9. RSS of latitude and time dependent error	±51%	±17%	±48%	±35%
10. RSS of bias errors	±9%	±7%	±20%	±24%
11. Net RSS accuracy	±52%	±20%	±50%	±43%
12. Precision of monthly mean cross section	±12-20%	±6-17%	±10-24%	±50-100%

noise on a monthly zonal mean nitrous oxide cross-section was generally 10–20% except above 2 mbar where it increased dramatically. It should be noted that the precision depends strongly on the mixing ratio and temperature structure, being lowest where both high mixing ratios and high temperatures are present.

Comparison of SAMS Nitrous Oxide with Other Measurements

As was pointed out above, only zonally averaged mixing ratio profiles were derived from SAMS data. Any comparison with individual *in situ* or balloon based measurements as a means of validating the SAMS data must be regarded as of limited value. Nevertheless, it is useful to compare the SAMS data with other available measurements.

Vertical profiles of N_2O have been measured on numerous occasions over the last decade, mainly by grab-sampling (see WMO 1982). These data do not have uniform spatial coverage and for nitrous oxide are strongly weighted to equatorial latitudes and 44 °N. The data show substantial variability, far in excess of the precision of 2-5% quoted by the various experimenters, and no clear seasonal variation is discernable. For these reasons the comparison with the SAMS data have been performed by comparing all the available non-satellite measurements at each latitude irrespective of season with the SAMS nitrous oxide annual mean profile for 1979 at that latitude. These comparisons are shown in Figures 10-47 (a) and (b). Also shown are the estimated accuracies of the SAMS observations (horizontal bars) and an envelope embracing the month-to-month variability of the SAMS data.

It can be seen that the SAMS data extend to much higher levels (approx 55 km) than the *in situ* data. The SAMS nitrous oxide data give mixing ratios of around 300 ppbv at around 30 km, falling off exponentially with height to below 10 ppbv at upper levels.

NITROGEN SPECIES

At equatorial latitudes (Figure 10-47 (a)) above 30 km the SAMS measurements agree well with other measurements both in terms of vertical gradient and absolute amount. Below 30 km the SAMS measurements are biased high, but nevertheless the two data sets are consistent to within their estimated accuracies. At 45 °N (Figure 10-47(b)), although the SAMS measurements reproduce the vertical gradient suggested by the *in situ* measurements, they again appear biased high, by 20-30% at 30 km and rather more below. It is conceivable that this discrepancy is exacerbated by inaccuracies relating the geometric height scale of the *in situ* data and the pressure scale of the SAMS data. A similar comparison except using data for the three year period 1979-1981 gives very similar results (see Jones, 1984).

Overall, the SAMS nitrous oxide measurements reproduce well the gross features of the other measurements, namely the low stratosphere low latitude mixing ratio maximum and the sharp fall-off of mixing ratio with height together with a somewhat slower decrease towards high latitudes.

The Data

In Figure 10-48(a-1) are shown monthly mean zonal cross-sections of nitrous oxide mixing ratio measured by SAMS for January to December 1979. The data extend from 50 °S to 70 °N and from around 20 mbar to 0.6 mbar, covering the stratosphere and low mesosphere. Note that each monthly mean in fact comprises only approximately 12 days per month.

The gross structure suggested by these data is of a low stratosphere low latitude maximum, with the mixing ratio of nitrous oxide decreasing from around 300 ppbv at low equatorial latitudes to between 5 and 10 ppbv at high levels. Closer inspection reveals substantial differences between the various months, as slow seasonal changes progress through the year.

In January 1979 (Figure 10-48a) the distribution of nitrous oxide mixing ratio shows a marked asymmetry about the equator, with a region of elevated mixing ratios extending throughout the stratosphere, tilting from the equator at approx 20 mbar into the Southern (summer) Hemisphere, reaching 10 °S by the stratopause. This gives rise to rather sharp latitudinal gradients at high southern latitudes, with somewhat slacker gradients in the Northern Hemisphere. In the Northern Hemisphere sharp vertical gradients exist at this time in the lower stratosphere, with a more uniformly mixed region above. During February (Figure 10-48b) a second maximum began to emerge in the Northern Hemisphere at high levels. During March and April (Figures 10-48c and d) the second maximum intensified while the Southern Hemisphere maximum subsided to give by May (Figure 10-48e) an almost symmetric pattern with, on a fixed pressure surface, two low latitude maxima separated by an equatorial minimum. This evolution continued, giving by July 1979 a single maximum extending into the Summer (now the Northern) Hemisphere. The pattern during July was essentially a reversal of that of January.

The structure seen during the second half of 1979 differed in many aspects from that of the first. During August and September throughout the middle stratosphere there existed a pronounced maximum at low northern latitudes. By October (Figure 10-48j) this maximum had subsided somewhat. A region of almost uniform mixing in the vertical persisted throughout August to October at high northern latitudes in the upper stratosphere. Interestingly, the "double-peak" structure evident during May that year was not repeated. In the final months of 1979 the maximum continued to subside giving, by December, an almost symmetric distribution (Figure 10-48).

It is obviously necessary to attempt to assess how credible the month-to-month changes observed in the data are, particularly in view of the substantial random and systematic errors which may be present
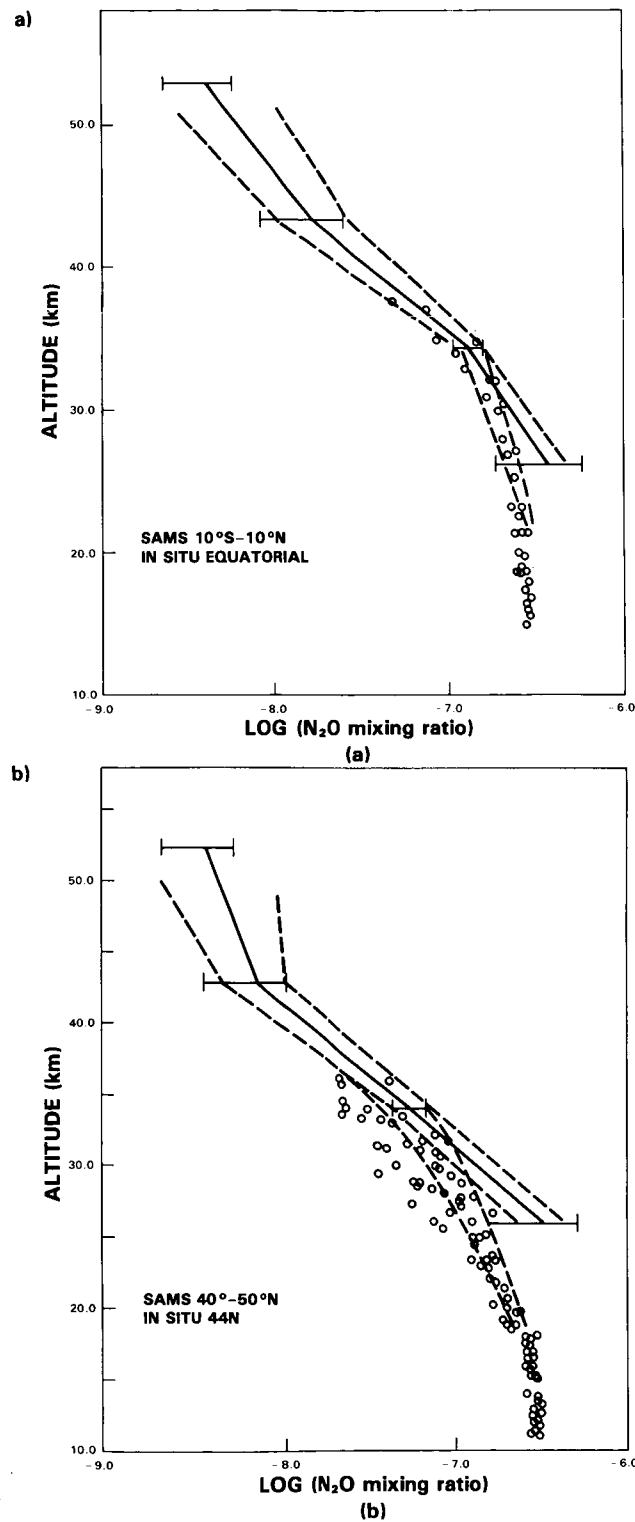
Figure 10-47. Comparison of the SAMS nitrous oxide 1979 annual mean profile (a) (Solid line) for 10°S–10°N with other measurements (circles, WMO 1982). The dashed envelope shows the standard deviation of the monthly mean profiles for the latitude band and the horizontal bars the estimated accuracy. (b) As for (a) except for 40–50°N.

567
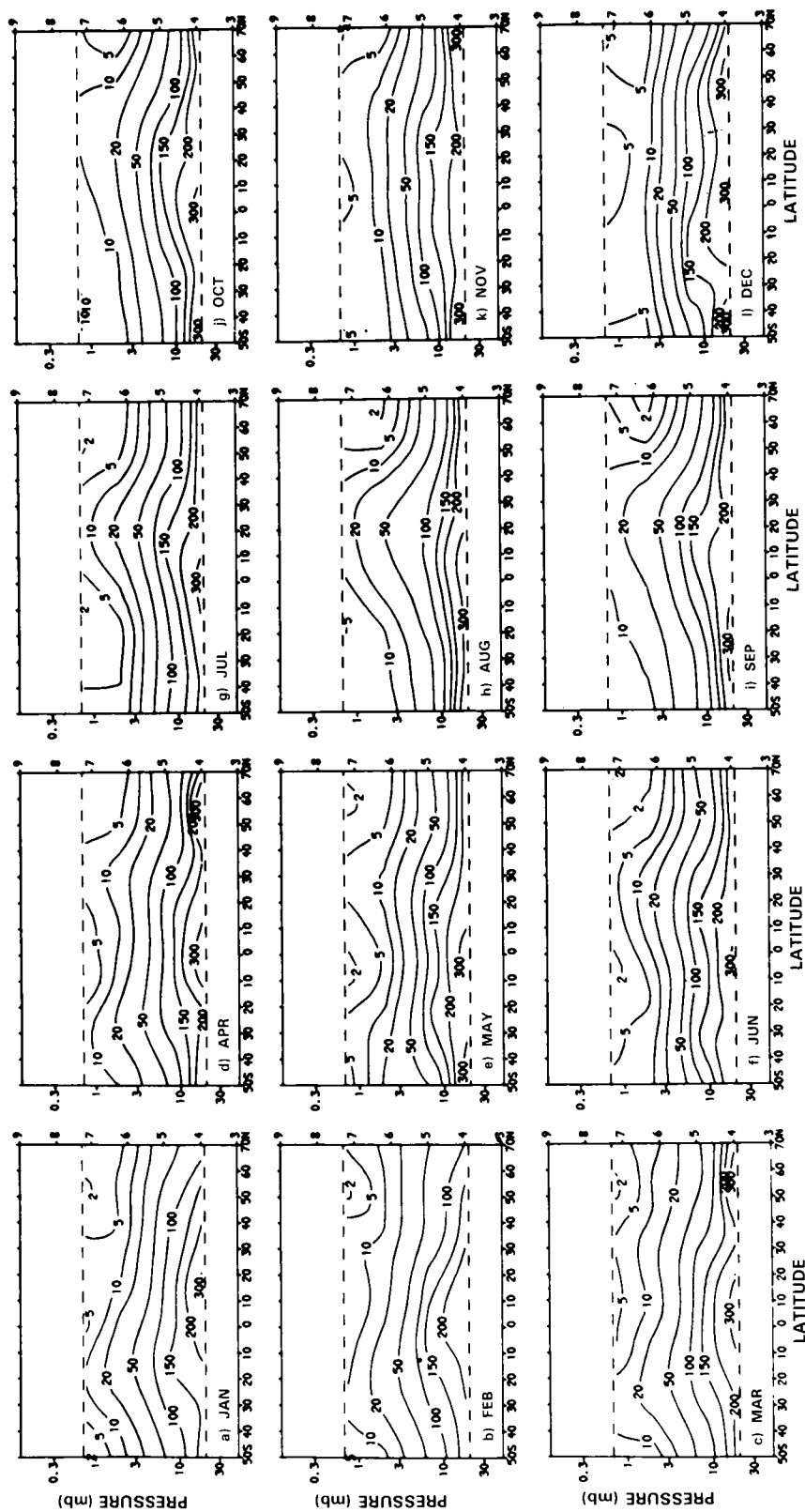
Figure 10-48. Monthly, zonal mean cross-sections of nitrous oxide (ppbv) for 1979 derived from SAMS observations.
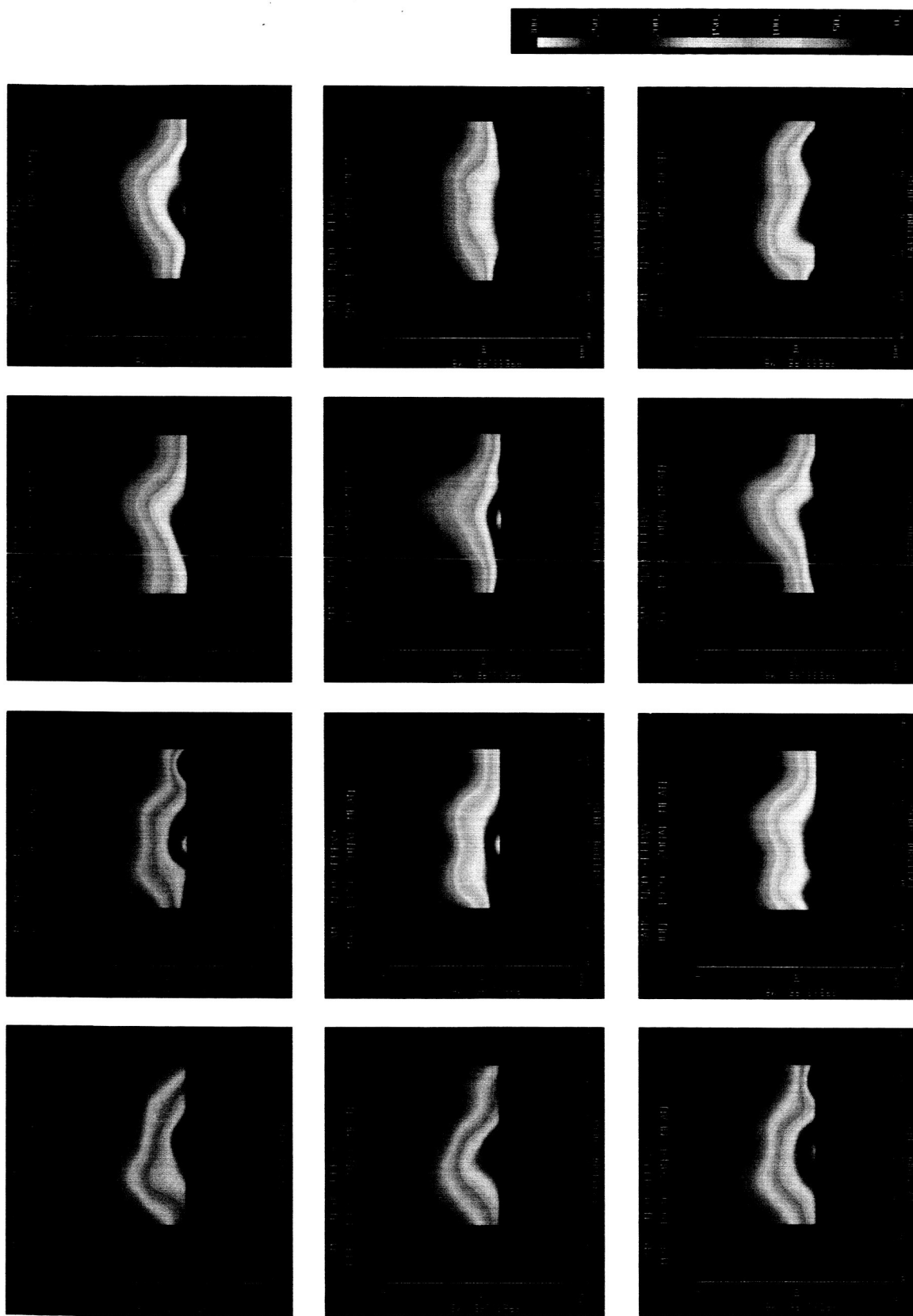
Figure 10-48. (Color) Monthly, zonal mean cross-sections of nitrous oxide (ppbv) for 1979 derived from SAMS observations.

in the data. From this point of view it it of great value to have essentially simultaneous measurements of methane made from the same instrument and in fact made using the same spectral region and optical chain. Because both methane and nitrous oxide originate in the troposphere and are destroyed with long photochemical time constants in the stratosphere, the distributions of both species are determined in large part of the same dynamical processes. The distributions, although not the gradients, of methane and nitrous oxide observed by SAMS are thus expected to be similar and this is in fact the case (Figure 10-49). Jones and Pyle (1984) argue that because of the much more rapid vertical fall-off of nitrous oxide mixing ratio, the errors required to introduce similar spurious features into the distributions of both species are quite different in percentage terms, while known error sources are very similar in percentage terms or do not influence the methane observations significantly. They suggest that the similarity of the methane and N_2O supports the thesis that features such as the "double-peak" are real and not artifacts of the retrieval method. In further support of this, it should be pointed out that independent measurements of another long lived tracer (water vapour) by the LIMS instrument on Nimbus 7 also shows many similar features including the branching seen at low latitudes at certain times of the year (see e.g. Jones et al., 1985).

An equally important question is to ask whether the features seen in the nitrous oxide distributions in 1979 would appear in a long term climatology of that gas. Over three complete years of SAMS nitrous oxide data have now been retrieved and it appears (Jones, 1984) that while there are minor differences from year to year, the seasonal changes are essentially unchanged. To illustrate this, in Figures 10-50 (a-j) are shown monthly mean cross-sections for January, April, July and October for the years 1979, 1980 and 1981. These months are chosen to best emphasise the contrast between the nitrous oxide distributions observed at different times of the year. It is immediately evident that the seasonal variation observed during 1979 is broadly reproduced in 1980 and 1981. There are differences between the years; for example while the July data for 1979 and 1981 closely correspond, those for 1980 appear rather different. Nonetheless, all three years show a mixing ratio maximum extending into the Southern (summer) Hemisphere in January, a "double peak" in April/May, the July distributions mirroring those of January and a rather more quiescent distribution by the end of the year. The fact that many of the features observed during 1979 do appear in the subsequent two years suggests that the SAMS nitrous oxide data are useful as a climatology of that gas.

10.2.4 Nitric Oxide (NO)

One channel on the stratospheric and mesospheric sounder (SAMS) instrument was devoted to measuring mixing ratio of NO in the stratosphere and low mesosphere. There were, however, a number of instrumental and interpretational problems with this channel which meant that unambiguous mixing ratio fields could not be obtained. A detailed exposition of the problems encountered is given by Kerridge (1985).

10.2.5 Intercomparison of NO₂ Satellite Data

This subsection describes an inter-comparison of the NO_2 satellite data presented earlier in this section.

Comparison of the SAGE and LIMS profiles are given in Figures 10-51 a-d which show general agreement, well within the stated accuracies and temporal variability of the measurements. The data compared are zonal means for the Palestine (32 °N) and Aire sur l'Adour (44 °N) latitudes. Sunset data from SAGE for the December, January, February (February 1979-November 1981) zonal average about 32 °N ±5 °, are compared with the LIMS 1 PM monthly average for January 1979 (Figure 10-51a). Likewise the March, April, May SAGE data for 34 months are compared with the May LIMS average in Figure 10-51b. For the 32 °N case, SAGE is, as expected, slightly higher in value (cf. Section 10.3 for diurnal effects) with about the same vertical shape except above about 35 km for the winter comparison, where SAGE tends
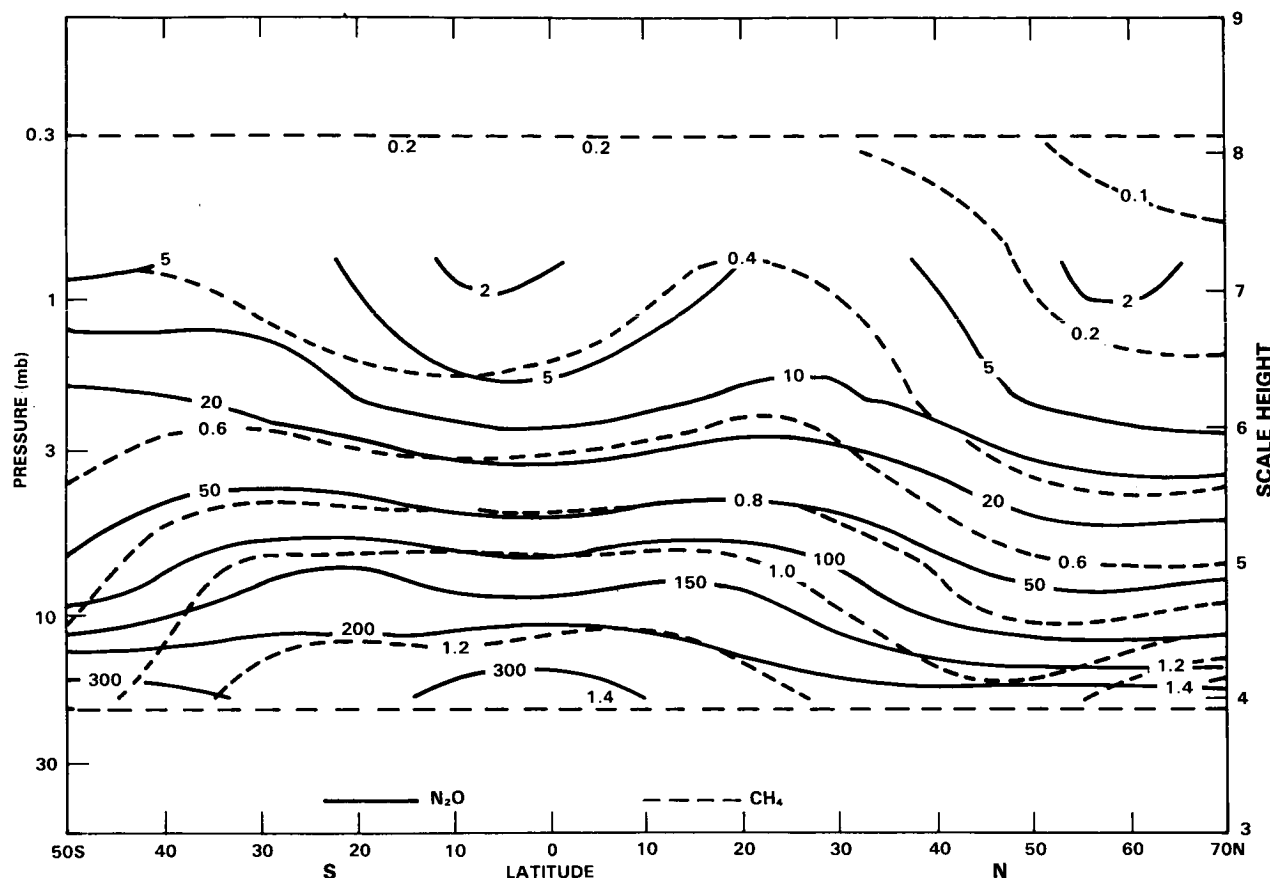
Figure 10-49. Cross-sections of methane (broken/ppmv) and nitrous oxide (solid/ppbv) for May 1979.

to be lower than LIMS which tends to turn upward. Both values are well within the accuracies of both measurements as well as within the variability shown in the three years of SAGE data.

Similarly, the data are compared for 44 °N. The comments above generally hold for this case, with the winter showing a larger difference above 35 km. The values at other altitudes and for May are very similar. Obviously, this comparison should be made for days when LIMS and SAGE were performing measurements at the same latitude. This detailed comparison is in progress.

Comparing the zonal mean cross sections show some similarities and differences but a meaningful comparison is again difficult to make due to diurnal differences (LIMS measurements are at 1 PM (Figure 10-25); SME at 3 PM (Figure 10-30); and SAGE at sunset (Figure 10-33)) and, in addition, due to temporal differences in the measurements. SME data presented in this report are for January, February, March, 1982 monthly averaged from the profiles over the U.S.; LIMS data are for the last 7 days in October, all of January and April, and the first 28 days of May 1979; and, SAGE data are for February 21, 1979 through November 1981 with data shown in this report averaged for the four seasons over three months each centered at January, April, July and October. Nevertheless it is useful to present these data and compare their gross features so that at a minimum a qualitative assessment of this new data set can be made.

All three data sets show the peak in NO_2 mixing ratio to be in the equatorial region centered at 30-36 km altitudes with the SME peak appearing slightly lower than the LIMS and SAGE peak. LIMS and SAGE

571
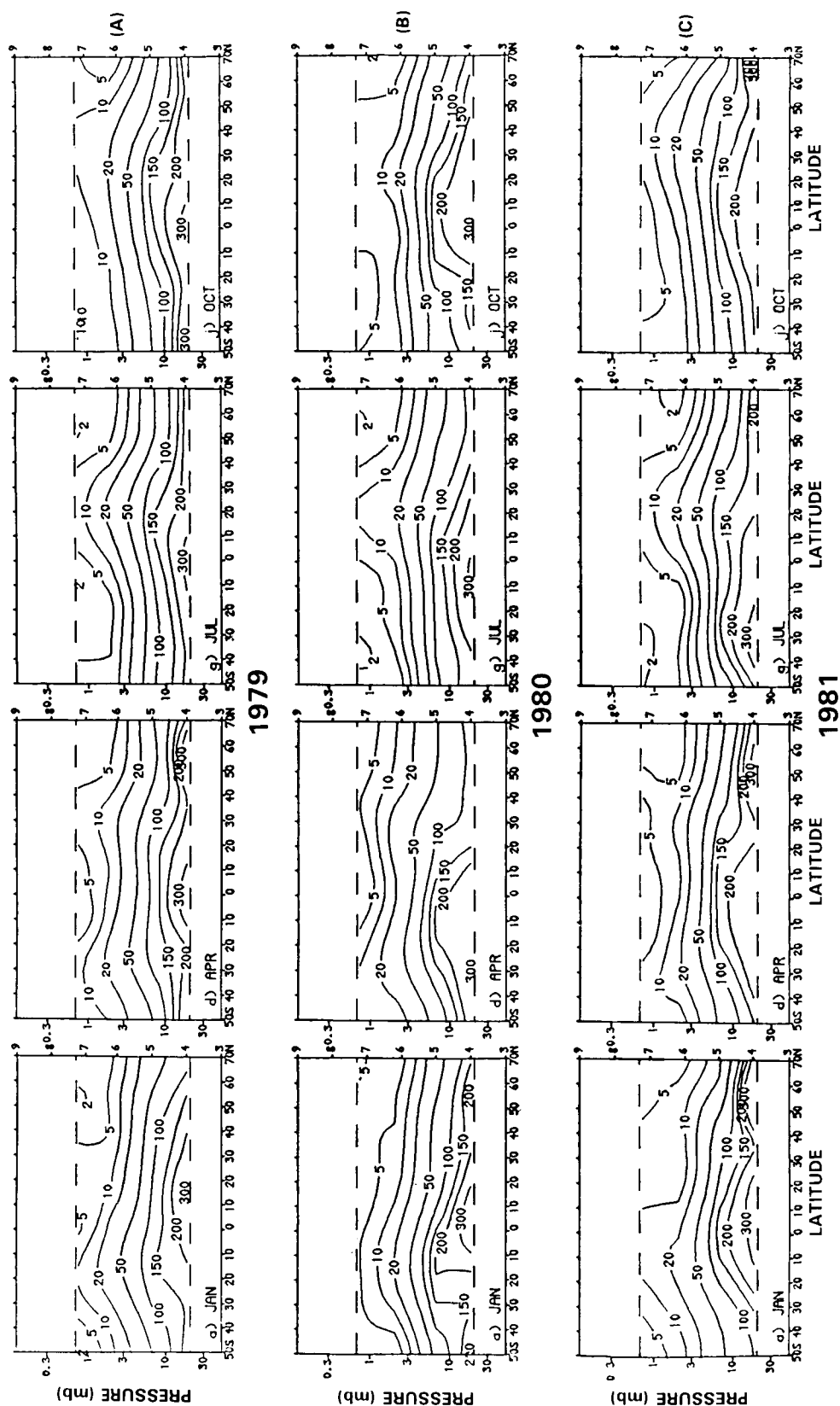
FIGURE 10-50. Monthly mean cross-sections of nitrous oxide (ppbv) for January, April, July and October, (A) is 1979, (B); 1980; (C) is 1981.
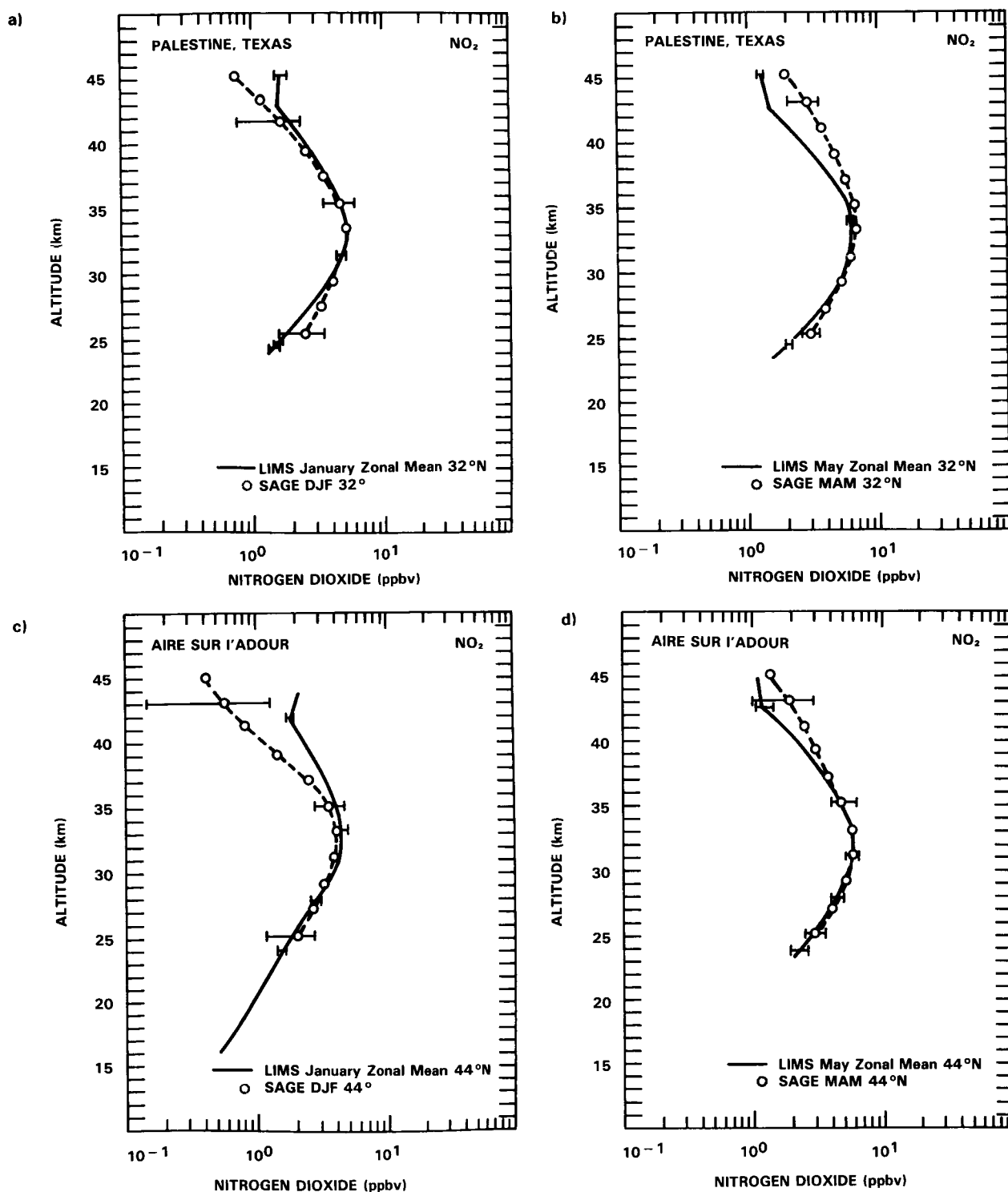
Figure 10-51. Comparison between monthly averaged LIMS profiles and seasonally (32 °N) and Aire sur l'Adour, France (44 °N), in January and May. Solid line LIMS, dashed line, SAGE. Bars indicate standard deviation over the averaging period. a) January, Palestine, Texas (32 °N), b) May, Palestine, Texas (32 °N), c) January, Aire sur l'Adour, France (44 °N), d) May, Aire sur l'Adour, France (44 °N).

573

both show decreases to higher latitudes north and south but SME shows a decrease only to the north. SME shows large peaks north and south of troughs to either side of the equatorial peak, with an especially strong peak at about 50°S at about 1 mbar. This feature in the Southern Hemisphere or the troughs are not seen in the SAGE or LIMS data. The LIMS contours seem to be flatter above the peak than does SAGE or LIMS. Possibly this difference is due to water vapour effects in the daytime measurements. The SAGE measurements show a strong bulge above the equatorial peak in northern spring (and somewhat in summer). This is not seen in the LIMS data.

Both SAGE and LIMS show the strong summer/winter difference in profile and column content of NO_2. The data clearly show high values of NO_2 during local summer compared to winter. All three data sets show the "cliff" phenomena at high northern latitudes as described in Section 10.3

Although much more detailed comparison work needs to be done, which considers diurnal variations and other effects, the similarity of the results from these three satellite sensors (especially LIMS and SAGE where more data have been compared) utilising completely different measurement techniques (limb emission, solar absorption, and limb scattering), very encouraging.

Comparisons of LIMS and SAGE data with balloon data are presented in Figure 10-12 and show good agreement below the peak value but the balloon data are higher above the peak.

10.2.6 Representativeness of Palestine and Aire sur l'Adour Launch Sites Compatibility between Satellite and Balloon Observations

Balloon data have provided a large amount of the past and present data on the vertical distributions of trace species. The largest number of these have been made at two locations — Palestine, Texas, USA (32°N, 95°W), and Aire sur l'Adour, France (44°N, 0°W). Two questions immediately arise, namely, are these locations typical of their latitudes, and secondly, what is the seasonal and short term variation of the results at these locations, as seen in satellite observations, and how does this compare with the results of large numbers of balloon measurements.

Figure 10-52a-d compare daytime NO_2 and HNO_3 results at Palestine and Aire sur l'Adour with the zonal average for those latitudes for January and May. Clearly, these locations are very representative of the zonal averages. These values in Figure 10-52a,b agree well with the mean values for balloon based observations at the same latitudes presented in Section 10.1. Since quite different techniques are used, this provides further information for assessing the absolute accuracy of the techniques, and supports the suggestion that the balloon and satellite results are reasonably compatible with each other.

They also show that the short term variations are larger during the winter than in May, but in both months are rather small. The seasonal changes shown in the January to May differences are therefore significant, although they are not large in an absolute sense. The satellite derived variations are considerably smaller than the flight to flight variations in the balloon soundings; the reasons for this are not clear at this time.

Similar results for HNO_3 are presented in Figure 10-52c,d. Again, Palestine represents the zonal average well in January and May. For Aire sur l'Adour, the October profile (highest during the LIMS period) is somewhat higher than the zonal average at 24 km, but the agreement in May is very close. The fall and winter variances are considerably larger than those in May. The seasonal differences again are not extremely large, but significant.

C-3
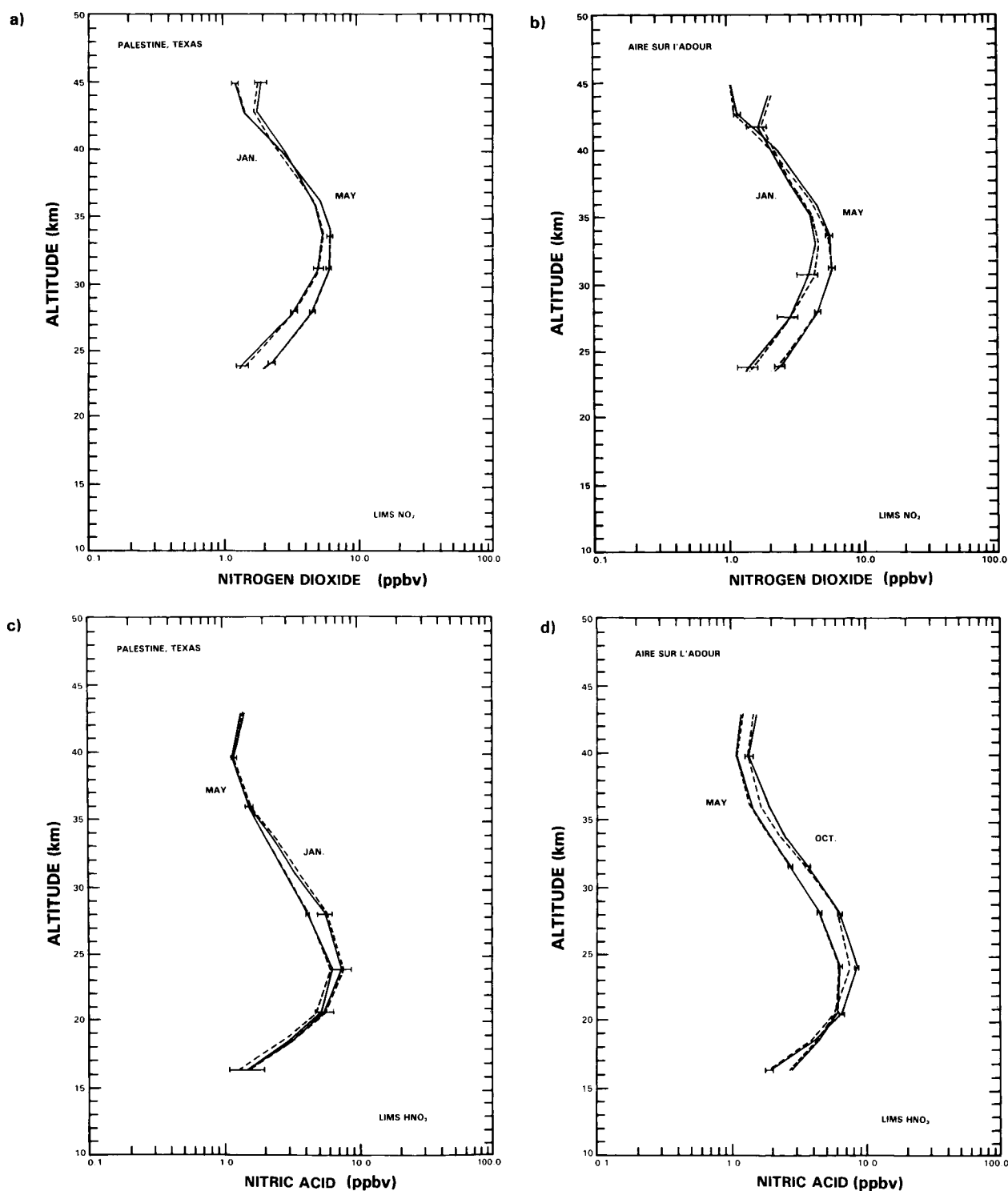
Figure 10-52. Mean profiles of daytime NO₂ and HNO₃ at the balloon launch sites at Palestine, Texas and Aire sur l'Adour, France (solid lines). These are compared to the zonal means (dashed line) at their latitudes, bars show standard deviations of the launch site profiles 32 °N and 44 °N respectively.
a) NO₂ at Palestine, Texas, b) NO₂ at Aire sur l'Adour, France. c) HNO₃ at Palestine, Texas, d. HNO₃ at Aire sur d'Adour.

Below 35 km these results are also in quite good agreement with the balloon data presented in Section 10.1. Above that they appear larger, as noted by Gille *et al.*, 1984b.

10.3 ODD NITROGEN MODELING

Odd nitrogen plays an important role in the photochemistry of ozone at stratospheric heights, and therefore a large number of observational studies have been devoted to characterizing the distributions of nitrogen compounds. Balloon and aircraft measurements have provided crucial information on the local concentrations, altitude profiles and latitudinal behavior of the column abundances of nitrogen species. In addition, simultaneous measurements of several species have been used to assess the completeness of model photochemical schemes. The direct comparison of model results and measured values provides a consistency check between model results and measurements. Attempts to resolve the discrepancies have resulted in better understanding of the mechanisms controlling many trace gas distributions and identification of the types of data needed for subsequent measurements.

Satellite data provides information on the temporal and spatial behavior of the trace constituents. In some cases, simultaneous measurements of several species are available. In addition to providing a large data base for intercomparison of model results and observations, these experimental and associated theoretical studies have revealed that the distributions of odd nitrogen constituents are controlled by close coupling with stratospheric dynamics. For example, study of the observed zonal mean distributions of N_2O and HNO_3 provides information on the balance between advection and eddy mixing in the zonally averaged transport of trace constituents (Guthrie *et al.*, 1984; Ko *et al.*, 1985). As a result, current interest in nitrogen species goes far beyond their photochemical properties and relationship to ozone; rather, it is now clear that a number of more fundamental atmospheric processes can be explored through observations and modeling of odd nitrogen. These will be the subject of this subsection.

10.3.1 Sources of Odd Nitrogen

10.3.1.1 Nitrous Oxide

The primary source of odd nitrogen in the stratosphere is believed to be the reaction

$$N_2O+O(^1D)\rightarrow 2NO \tag{7}$$

Recently satellite data on the distribution of N_2O have been obtained by the SAMS satellite experiment onboard NIMBUS 7. The global distribution of $O(^1D)$ can also be inferred using satellite data on ozone. Therefore, the distribution of the odd nitrogen source strength resulting from this reaction (assuming presently accepted photochemistry) can be well-characterized using available satellite data, as shown by Crutzen and Schmailzl (1983). Figure 10-53 presents the distribution of the calculated rate of odd nitrogen production through reaction (7) based on that study. The globally integrated rate of NO_y production was found to be about $1.1–1.9\times10^8$ molecule cm^{-2} s^{-1}. It is important to note that the region of primary NO_y production is found in the tropics, where the product of the densities of N_2O and $O(^1D)$ are maximum in the middle stratosphere (see 10.2.3).

The rate of production of NO_y is thus quite sensitive to the meridional distribution of N_2O. The satellite observations of this species exhibit larger abundances in the tropics than at middle and high latitudes,

NO$_x$ – PRODUCTION [molecule cm^{-3}s^{-1}], ANNUAL 24 hr. AV., O$_3$ LOW
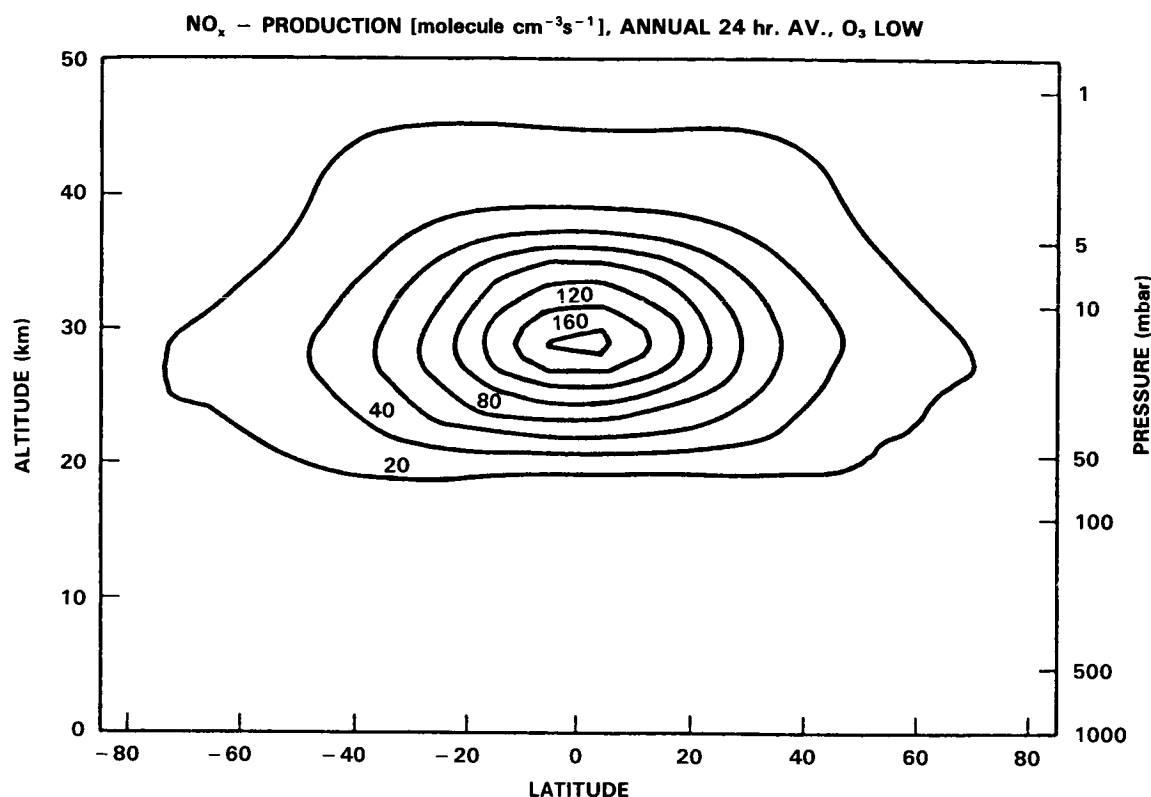
Figure 10-53. Diurnally and annually averaged NO production rate via the reaction O(^{1}D) with N$_2$O, using the N$_2$O distributions from SAMS data and the ozone distribution by Duetsch (1978). From Crutzen and Schmailzl, 1983.

roughly consistent with two-dimensional numerical model calculations by Jones and Pyle (1984), Guthrie *et al.* (1984), Ko *et al.* (1985), and Solomon and Garcia (1984b). The SAMS satellite data also exhibit important variations in the details of the N$_2$O distribution with season (Jones and Pyle, 1984). In particular, the observed distribution of N$_2$O exhibits a "double-peak" in the spring season, with a local minimum near the equator (Figure 10-48). Gray and Pyle (1985) have conducted detailed studies of the transport processes that are likely to be responsible for this feature, and have shown that momentum deposition associated with the westerly phase of the tropical semiannual oscillation in the zonal winds gives rise to a circulation that yields an N$_2$O distribution similar to that observed. Thus the distribution of the source of NO$_y$ is very sensitive to transport processes, and the nitrogen species N$_2$O provides an important test of the completeness of our understanding of stratospheric transport.

Balloon observations of N$_2$O and other long-lived trace species have revealed important information on local variability of these consitituents, at spatial resolution far beyond the reach of remote sensing instruments. In particular, Ehhalt *et al.* (1983a) have shown that observed vertical variations in N$_2$O can be characterized by an equivalent displacement height (EDH) relative to a reference profile. This variability is significantly larger than the measurement errors, and changes systematically with altitude for all the species examined. Hess and Holton (1985) have suggested that the observed variance may be related to the dynamical processes associated with stratospheric warmings, i.e., the variance introduced by breaking of large amplitude planetary waves.

While oxidation of N_2O is believed to be the principal source of stratospheric NO_y, other sources must also be considered. Thermospheric odd nitrogen production and its possible transport to the stratosphere will be the subject of the next subsection. Another known source of stratospheric NO_y is provided by galactic cosmic rays (Nicolet, 1975), which have their largest effects at high latitudes. Because of the large rate of NO_y production at low latitudes through reaction (7) and its subsequent transport, this added high latitude source is not very important to the global NO_y distribution. Another possible source of N_2O is associated with mesospheric charged particle precipitation (Zipf and Prasad, 1982) but this process has not yet been quantified insofar as its atmospheric importance is concerned. Finally, odd nitrogen is produced in lightning discharges in the troposphere and perhaps also in the lowest part of the stratosphere in overshooting cumulonimbus clouds (e.g., Tuck, 1976; Noxon, 1976; Logan, 1983). The quantitative importance of this source on a global scale in the stratosphere has also not yet been established.

10.3.1.2 Thermospheric Sources

Odd nitrogen is produced in large amounts at thermospheric heights, via a series of ion-molecule and secondary electron reactions such as

$$e^* + N_2 \rightarrow 2N(^4S, ^2D, ^2P) + e \tag{8}$$

as discussed, for example, by Strobel *et al.* (1970) and Oran *et al.* (1975).

The dissociation of N_2 proceeds rapidly above about 100 km, resulting in mixing ratios of NO near 100 km of the order of a few ppmv. Since the mixing ratios of NO_y in the stratosphere are only of the order of a few tens of ppbv, even a small flux of thermospheric NO_y to the stratosphere could be of potentially great importance to the stratospheric NO_y budget (see, e.g., Strobel *et al.*, 1970; Brasseur and Nicolet, 1973). On the other hand, NO_y is rapidly destroyed in the sunlit mesosphere via

$$NO + h\nu \rightarrow N(^4S) + O \tag{9}$$

followed by

$$N(^4S) + NO \rightarrow N_2 + O \tag{10}$$

which yields a minimum in the mesospheric NO_y mixing ratio of only a few ppbv near 70-80 km, and essentially destroys the downward flux of thermospheric NO_y. This process clearly requires the presence of sunlight, and, as such, does not occur in the polar night. Therefore, polar night represents a region where effective coupling between thermospheric and stratospheric NO_y may occur, if downward transport processes can act over the time scale of about a season. Theoretical studies by Brasseur (1982), Frederick and Orsini (1982) and Solomon *et al.* (1982) showed that the downward transport of thermospheric NO_y may be significant at high latitudes in winter. Solomon and Garcia (1984b) examined apparent solar cycle variations in BUV and SBUV ozone data, and concluded that transport of thermospheric NO_y to the upper stratosphere (roughly 40-55 km) appeared to be significant for latitudes poleward of about 50-60 °N in the winter season. The study by Russell *et al.* (1984b) employed LIMS data for nighttime NO_2 to show more directly that odd nitrogen transport to the upper stratosphere can clearly be detected in high latitude winter, as shown in detail in Figure 10-54. The large and rapidly increasing mixing ratios observed in the polar winter lower mesosphere are strongly indicative of downward transport from above. Further indications of a high latitude winter enhancement in lower mesospheric NO_y have resulted from observa-

a)
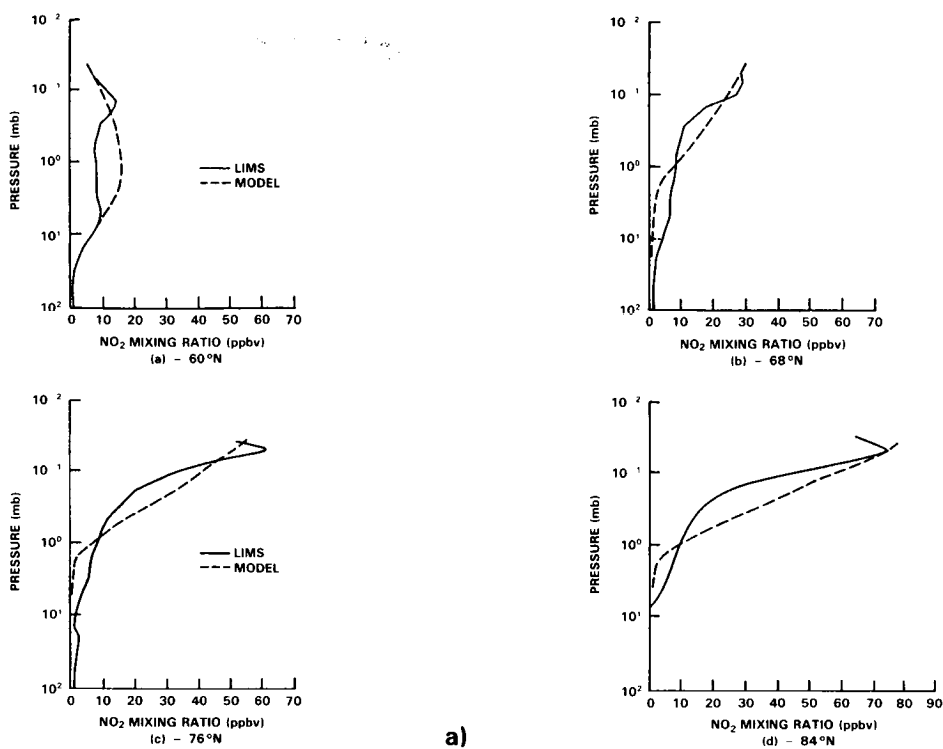
b)

Figure 10-54. (a) Comparison of LIMS zonal mean NO_2 measurements for January 5-9, 1979 with the 2-D model of Solomon and Garcia (1983a), at various latitudes. From Russell *et al.* (1984b); (b) Color plot of LIMS zonal mean NO_2 measurements for January 5-9, 1979.

tions of the NO column abundance above about 50 km as deduced from SBUV observations of NO resonant scattering (Frederick and Serafino, 1985).

A detailed intercomparison of odd nitrogen sources including polar proton events and other high altitude processes was presented by Jackman *et al.* (1980). While thermospheric sources are unlikely to be of importance to the globally averaged NO_y and ozone budgets, observations demonstrate that local ozone and NO_y densities in high latitude winter are substantially influenced by downward transport from the thermospheric source region. More importantly, these data provide excellent tracers for our understanding of mesospheric transport processes.

10.3.1.3 Modelling Studies of the Odd Nitrogen Budget

Although the distribution of N_2O is now relatively well known due to the availability of satellite data, and it is established that the principal stratospheric source of NO_y is likely to be reaction (7) above, the budget of NO_y in model calculations depends upon the transport formulation, and on the uncertainties in the photochemical processes (7), (9) and (10) above. Further, the strongly nonlinear latitudinal gradient in NO_y production via reaction (7) as shown in Figure 10-53 must be considered in the interpretation of one-dimensional globally averaged model profiles of NO_y and their comparison to data. An analysis of the NO_y budget in the one and two-dimensional models by AER (Ko and Sze, 1983; Ko *et al.*, 1985) provides important insight into these questions (see also, model formulation chapter).

Figure 10-55 shows the latitude-altitude cross section of the photochemical production and removal rates for NO_y for equinox conditions calculated from the AER two-dimensional model. Both the production and loss rates show a maximum in the tropics near 30 and 35 km, respectively. Note that the loss rate is about an order of magnitude smaller than the production rate in the tropical mid-stratosphere. Figure 10-56 shows the net photochemical source term (P-L) together with a vector plot of the transport fluxes for the annually averaged budget. Some of the NO_y produced in the tropical stratosphere is removed by photochemical reactions as it is transported to mid- and high latitudes. The rest is removed by transport into the troposphere, particularly in the extratropical regions. Figure 10-57 shows a more detailed accounting of the budget by dividing the atmosphere into boxes. Within each box, the burden, the chemical production and loss rates are given, along with the fluxes across the boundaries due to transport. Note that the transport fluxes are, with the exception of the equatorial stratosphere, significantly larger than the local photochemical terms, indicating the importance of transport in determining the NO_y distribution.

Considering the differences in formulation between one and two-dimensional models, there is no *a priori* reason to expect the calculated globally averaged concentrations of NO_y in a two-dimensional model to agree with the result from a one-dimensional model. However, it is important to discuss how one-dimensional models of NO_y can be interpreted in the context of two-dimensional models, since one-dimensional models are often used in assessment studies, and since NO_y plays an important role in modulating the effect of chlorine perturbations on ozone, especially at high chlorine levels. Figure 10-58 shows calculated NO_y profiles from the AER two-dimensional model compared with that of the AER one-dimensional model, using an identical treatment of radiation and photochemistry. The qualitative similarity between the two models may be explained in terms of the budget on a global basis. The budget from a one-dimensional model indicates a production and loss rate of 0.3mt/year (4.5×10^{26} molecules/sec) and 0.1 mt/year (1.2×10^{26} molecules/sec), respectively, with an export of 0.2 mt/year (3.3×10^{26} molecules/sec) into the troposphere. The ratio of these terms is similar to that in the two-dimensional model although the absolute magnitudes obtained in the one-dimensional model are somewhat smaller. This is to be ex-
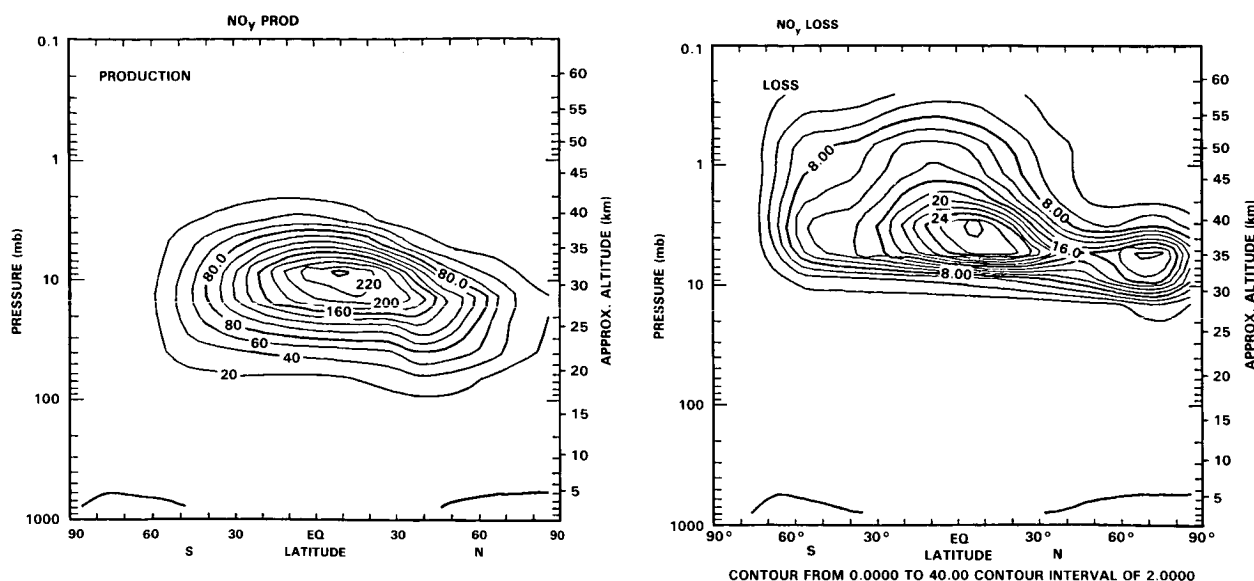
Figure 10-55. Calculated NO_y production and loss rates (molecule cm^{-3} s^{-1}) from the AER two dimensional model (Ko *et al.,* 1985).

pected since the one-dimensional model is adjusted to simulate the N_2O distribution at mid-latitudes (where the N_2O abundances are smaller than in the tropics) and the production rate is calculated using an equinox 30° degree sun angle. In spite of the similarities, one must also recognize the intrinsic differences between one and two dimensional models. The one-dimensional model cannot account for the covariance in the product of $O(^1D)$ and N_2O in calculating the global production rate (Tuck, 1979; Ko and Sze, 1982; Owens *et al.,* 1982a). The analysis in the AER two-dimensional model showed that this accounts for about 10-15% of the differences in the production rate. The one-dimensional model also cannot simulate the effect of horizontal transport, which is important in determining the latitudinal variations of the profiles in the two-dimensional model and will also modify the response of the two-dimensional model results to changes in production rates.

Comparison of the model results shows that the 1-D model result tends to underestimate the peak concentrations around 40 km. In the lower stratosphere, the 1-D simulated NO_y is higher than 2-D models using small eddy diffusion — and comparable to that simulated by 2-D models using large eddy coefficients (See e.g. Ko *et al.,* 1984).

In this section we will examine how uncertainty in rate data would affect the calculated NO_y profiles. A large part of the discrepancies among 1-D NO_y profiles can be explained in term of the treatment of the photodissociation rates for N_2O and NO. Since the balance of NO_y is, to a large extent, maintained by photochemical production and transport, in this section we will concentrate on the effect of the uncertainties in the rate data concerning the production rate.

A sensitivity study is performed using the DuPont 1-D model which analyses the response of the calculated NO_y concentrations to changes in the production rate from uncertainties in the rate data.

The study includes modification of the $O(^1D)$ concentrations by modifying the photolysis rate of O_3 and the quenching of $O(^1D)$. Specifically, the photolysis rate for O_3 and the $O(^1D)$ quenching rate are

MODEL $\left(\frac{dNO_y}{dt}\right)$ CHEMICAL AND DYNAMICAL FLUXES
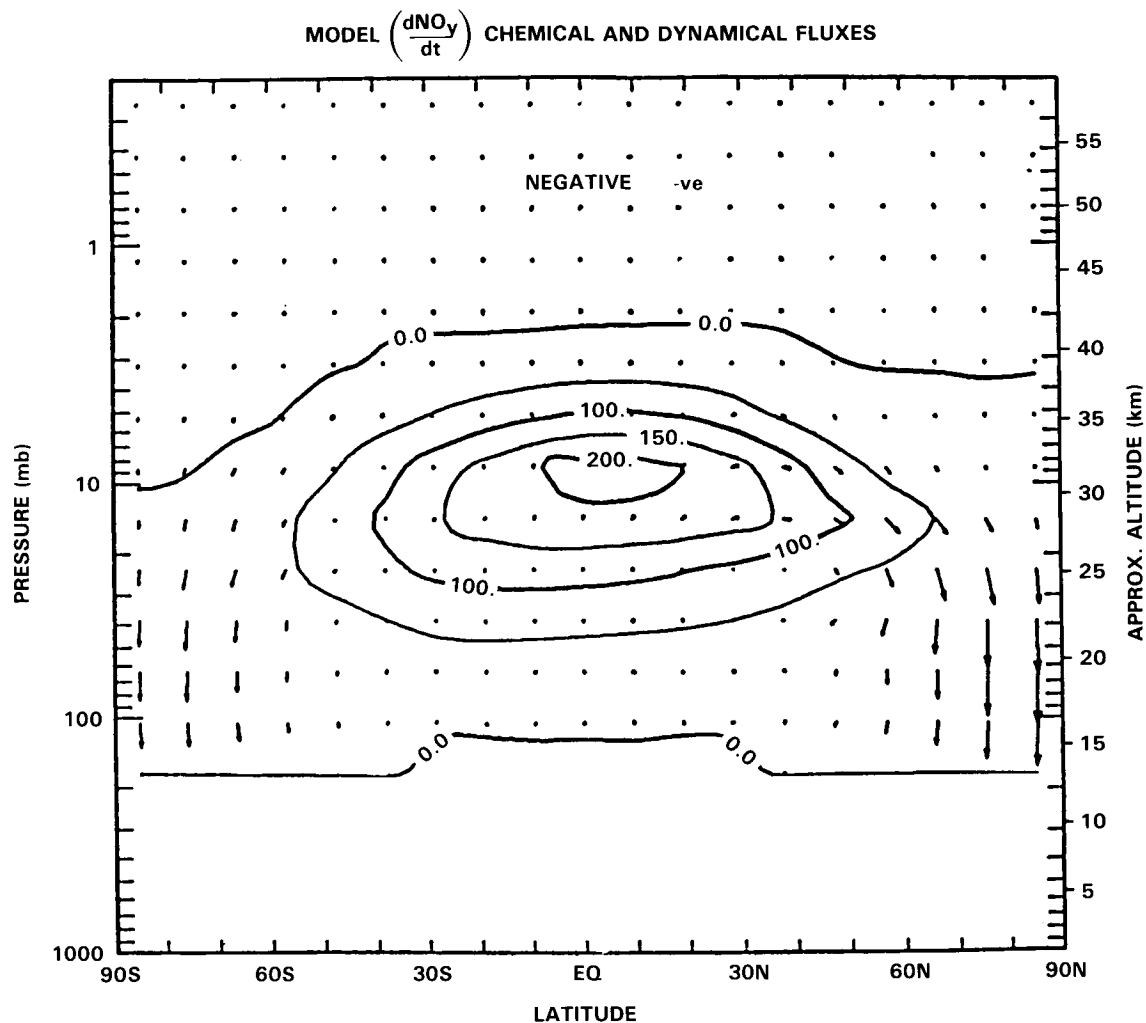
Figure 10-56. Net photochemical production/loss rate (P-L, including washout, (molecule $cm^{-3}\ s^{-1}$) for NO_y on an annually averaged basis. Also plotted indicating the transport fluxes. Note that transport is away from the net production region in the tropics and downward into the troposphere at extra-tropical latitudes (from the model of Ko et al., 1985).

varied by 40% and 30% respectively corresponding to the maximum uncertainties cited in the JPL publication. The effects of varying the rate constant of $O(^1D)$ and N_2O (by $\pm$ 50%) and N+NO (by $\pm$ 30%) are also evaluated. The result is summarised in Figure 10-59 which shows the ratio of the perturbed NO_y concentration to the standard 1-D profile. The response of the model is found to have a square root dependence around 40 km where the vertical transport is negligible. In the lower stratosphere, where photochemical production is balanced by vertical transport the response is linear in the production perturbation. In the upper stratosphere, the response to the production changes is small since the balance is between transport into the region and local photochemical losses.

The DuPont analysis shows there could be a factor of two uncertainties in the calculated production and loss rate if the maximum uncertainties in each rate are adopted to obtain the largest possible deviations. This should be reflected in a corresponding uncertainty in the calculated NO_y of about 40% at 40

30°S   30°N   60°N   90°N

50km

← 1.1
P = .056
L = 2.2
M = 1.4 × 10³³

→ 1.0
P = .006
L = .26
M = 3.1 × 10³²

→ .21
P = .001
L = .005
M = 9.8 × 10³¹

40km   ↑ 3.8   ↓ .06   ↓ .17

← 29
P = 45
L = 7.8
M = 2 × 10³⁴

→ 28
P = 5.2
L = 1.2
M = 7.7 × 10³³

→ 18
P = .64
L = .34
M = 3.3 × 10³³

24km   ↑ 23   ↓ 15   ↓ 19

→ 9.5
P = 12
L = 7.6
M = 1.2 × 10³⁴

← 9.3
P = 1.8
L = 0
M = 1.2 × 10³³

← 8.4
P = .025
L = 0
M = 7.7 × 10³²

10km   ↓   ↓   ↓

        .86   16   11

EQUATORIAL   MID-LAT.   HIGH LAT.

UNIT 10²⁵ MOLECULES/SEC
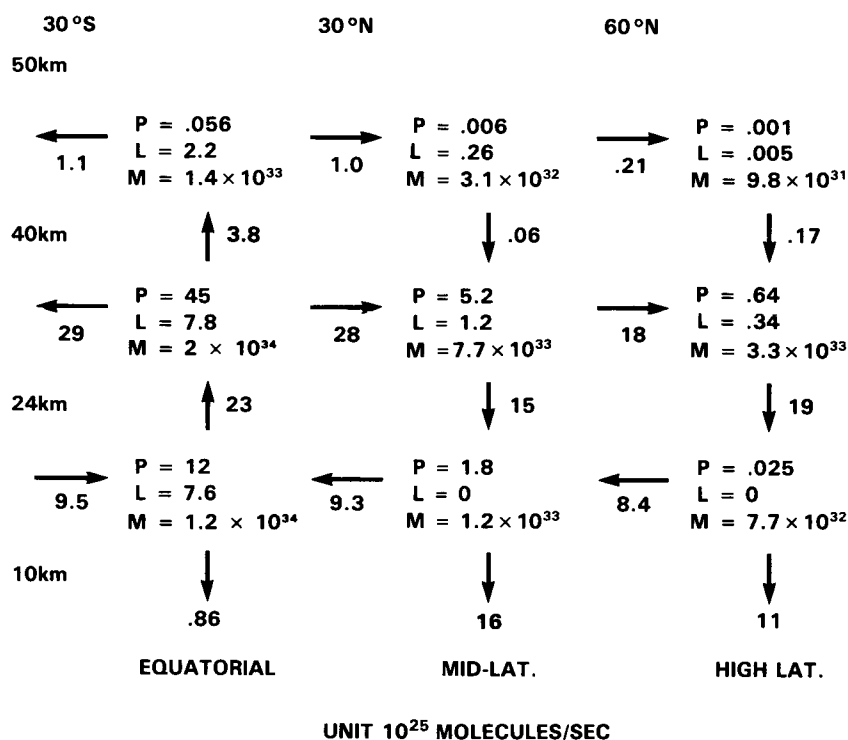
Figure 10-57. Box budget of NO_y from the model of Ko *et al.,* 1985. The atmosphere is divided into boxes covering the tropics, the mid-latitudes and the polar regions from 10-24 km, 24-40 km, and 40-50 km. Within each box, the NO_y burden, in 10^{25} molecules, is indicated. Photochemical loss and production rates, and transport across each boundary of each box, are also indicated in units of 10^{25} molecule s^{-1}

km and close to factor of two in the lower stratosphere. However, a more realistic estimate of the combined uncertainties should be of the order of about 30%.

The response of a 2-D model is expected to be somewhat different since horizontal transport plays an important role. We expect the response to be closer to linear in the stratosphere since transport is important everywhere. In particular, the calculated NO_y in the lower stratosphere should respond linearly to the production term since the concentration has to go up proportionally to maintain the transport out of the stratosphere to balance the excess.

Thus, in the lower stratosphere, where the concentration of NO_y plays a crucial role in modulating the effect of Cl_x on O_3, uncertainties in rate data could have a large impact.

10.3.2 Distributions and Comparisons to Data

Stratospheric odd nitrogen distributions can be examined in detail due to the availability of satellite data for NO_2 (from LIMS, SAGE, and SME), and HNO_3 (from LIMS), as well as ground based and aircraft data on the latitudinal variations of the distributions of these species, as presented in Sections 10.1 and 10.2. Indeed, a number of theoretical studies have been devoted to obtaining a fuller understanding of the observed variations in these constituents, and have led to significant progress in the conceptual basis for dynamical-chemical coupling.

583
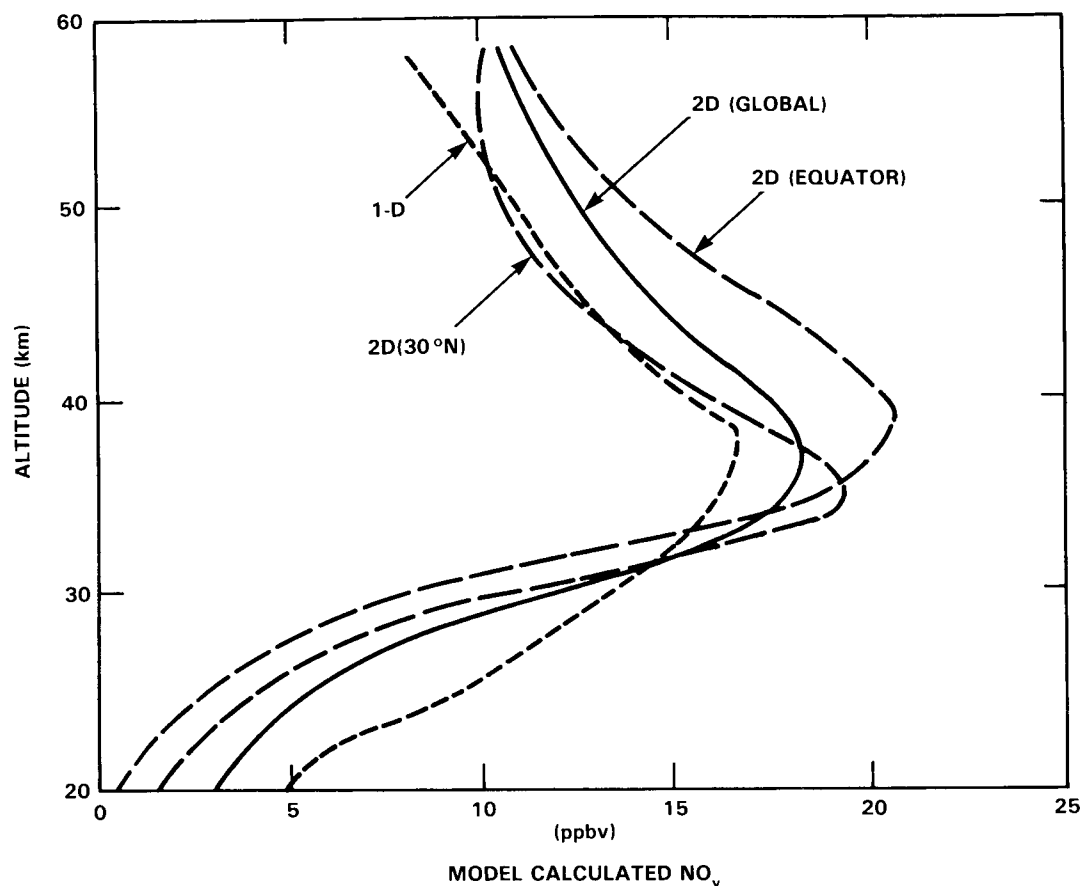
Figure 10-58. Comparison of model calculated NO_y profiles from the AER 1-D and 2-D models.

10.3.2.1 Local Variability in NO₂

Perhaps the most dramatic illustration of dynamical-chemical coupling is provided by observations of stratospheric NO_2. Ground-based studies, particularly those of Noxon (1978a, b, 1979), first presented evidence for this phenomenon. Noxon (1979) observed extremely large gradients in the total NO_2 column during February, 1977, and showed that the distribution of the total NO_2 column depends sensitively on dynamical processes. The unusually large gradient with latitude (see Figure 10-60) led to the observed phenomenon being called a Noxon "cliff" in NO_2. Knight *et al.* (1982) and Evans *et al.* (1982a) suggested that formation of N_2O_5 should be quite important in determining the distribution of NO_2 in high latitude winter. The details of the nature of the dynamical-chemical coupling remained a mystery, however, until laboratory measurements of the temperature dependence of the N_2O_5 absorption cross section were made by Yao *et al.* (1982). Solomon and Garcia (1983a, b) applied these laboratory data in photochemical/trajectory model calculations of the February, 1977 "cliff" observed by Noxon, and showed that the distribution of NO_2 in the cold, high-latitude region depends strongly on the photochemical history of air parcels. In particular NO_x can be largely converted to N_2O_5 at high latitudes in winter, where the number of sunlit hours in the day is small, and the temperatures are cold, leading to a depletion in the abundance of NO_2 in favor of N_2O_5. Rapid transport of these air parcels in the meridional direction (North-South) can occur in the presence of large scale planetary waves on a time scale faster than the photolysis time of N_2O_5, yielding very low NO_2 column abundances at mid-latitude. Such conditions occurred during the February, 1977 "cliff" observed by Noxon.
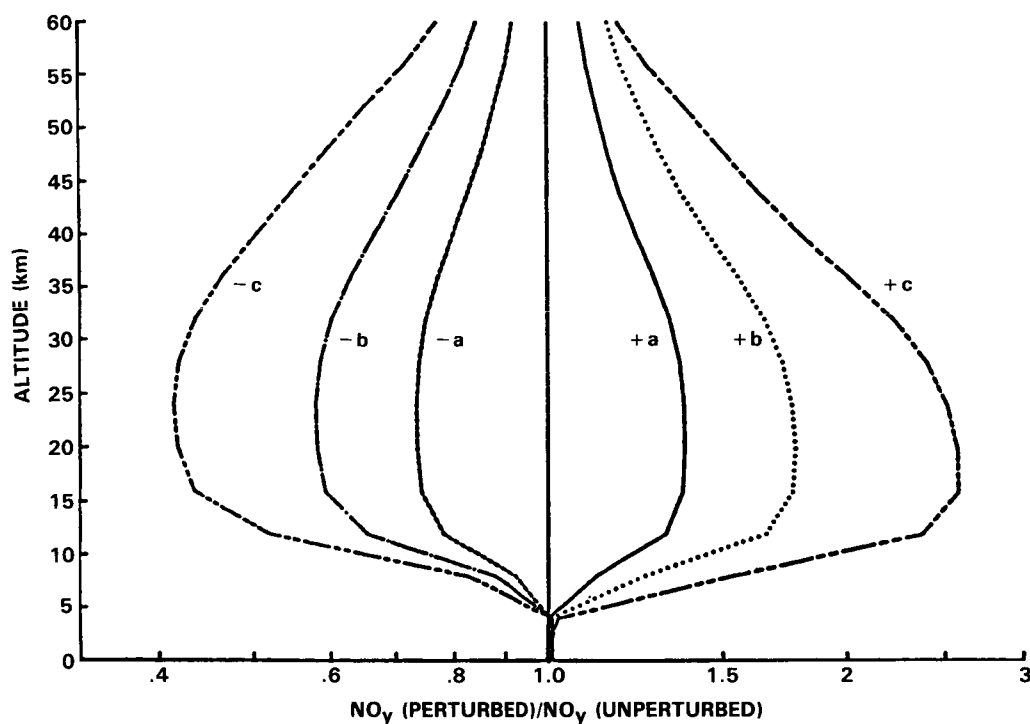
Figure 10-59. Sensitivity study of the response of the DuPont 1-D model profile of NO_y to uncertainties in the rate data. For each case, the reaction of photolysis rates are adjusted to the maximum and minimum values allowed by the uncertainties cited in the rate recommendation. Case a corresponds to adjustment of the photolysis of ozone by $\pm 40\%$. Case b corresponds to case a plus adjustment of the $O(^1D)$ quenching rate by $\pm 30\%$. Case c, corresponds to case b plus the uncertainties in the rates of $O(^1D) + N_2O$ ($\pm$ 50%), and $N + NO$ ($\pm$ 30%) are considered.

Additional insight into the behavior of odd nitrogen species under ''cliff'' conditions is available from the balloon chemiluminescent NO observations of Ridley *et al.* (1984). Figure 10-61 shows the NO profile observed by Ridley *et al.* on February 19, 1977 (i.e., for the same ''cliff'' observed by Noxon in that period), compared to a vertical profile observed at the same location under zonally symmetric (undisturbed) conditions. The profile obtained on February 19 is close to the normal profile near 30 km, but is dramatically different below about 28 km, where much lower NO densities were observed. Thus it is clear that NO_x is indeed reduced during ''cliff'' conditions, but this reduction is not uniform with altitude: rather, it is confined to the lower part of the stratosphere. Because of the altitude dependence of the N_2O_5 lifetime, this vertical variation in the perturbed profile supports the identification of N_2O_5 as the primary reservoir involved in the Noxon ''cliff'' phenomenon (Ridley *et al.*, 1984).

Section 10.2 presented satellite observations of Noxon ''cliffs'' from all three of the available NO_2 satellite data bases. A detailed study of the ''cliff'' observed by the LIMS satellite experiment during February 1979 was presented by Callis *et al.* (1983b). It was shown that a steep latitudinal gradient observed near 10 mbar was consistent with trajectory calculations during this period, as indicated in Figure 10-62.

An observational and theoretical study of the behavior of NO_2 and its reservoir in high latitude winter was conducted using the SME NO_2 data for the entire winter of 1982 (Zawodny, 1985a, b). The SME data show that large variations in NO_2 are observed not only as a function of latitude as shown in Figure
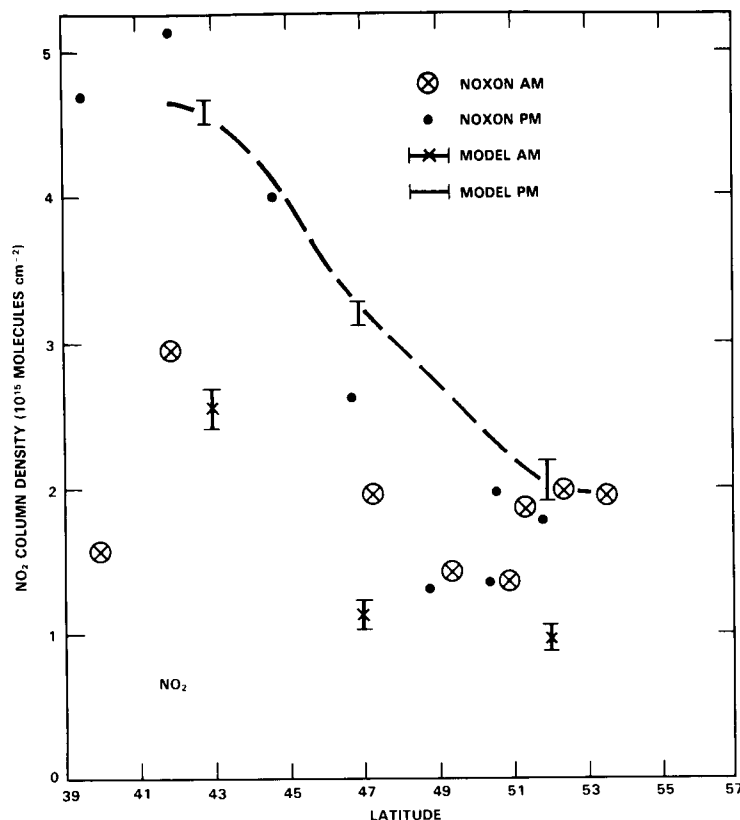
Figure 10-60. Total column abundances as a function of latitude observed by Noxon (1979) in February, 1977, compared to the model calculations of Solomon and Garcia (1983b).

10-60, but also as a function of longitude (i.e., on adjacent orbits). Unlike ground-based or aircraft studies, then, the strength of satellite data for this problem lies in the ability to examine the spatial behavior of NO_2 in several directions. Parcel trajectory calculations can be used to accurately estimate the time required for a moving air parcel in a stationary wave to pass from one orbit to the next. Typically, this time scale is on the order of a day or less for SME orbits over North America during wave displacements. Observed variations from one orbit to the next therefore provide very detailed information on the characteristics of the reservoir species presumably involved in the observed variability; i.e., the photochemical formation and destruction time scales for the reservoir are revealed by the changes in NO_2 between adjacent orbits. Figure 10-63a (see also Figure 10-41) displays a typical pattern of NO_2 variation at the 10 mbar level observed on day 40. The region of very low NO_2 on the westernmost side of the observations corresponds roughly to the location of the displaced polar vortex on this date. Figure 10-63b shows trajectory/chemistry model calculations for the same day, displaying a similar gradient with respect to latitude and longitude (see Zawodny, 1985a, b for details). The increase in NO_2 calculated by the model near 60°N from west to east is due to the photolysis of N_2O_5 formed principally in the polar night region in the days previous to the observations, and, most importantly, this increase occurs on a time scale of only a day or so. The similarities between model and measured NO_2 therefore suggest that the reservoir species must have a time scale for photochemical loss which is close to that for N_2O_5. This strongly suggests that the principal reservoir is likely to be N_2O_5, as it is in the model. Direct observations of N_2O_5, particularly in high latitude winter, are badly needed to confirm or refute the apparent role of N_2O_5 in determining the local variability of NO_2.
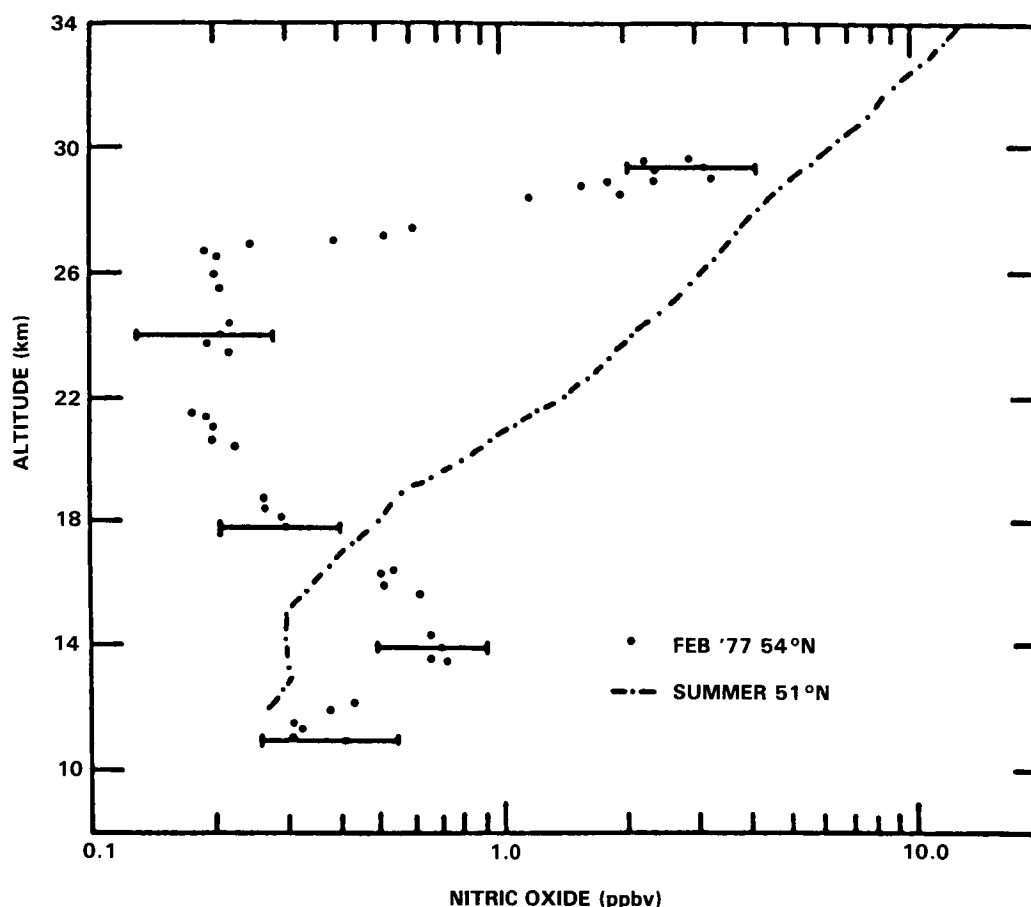
Figure 10-61. The NO distribution for February 19, 1977, compared with an average summer profile for 51°N. From Ridley *et al.* (1984).

10.3.2.2 Global Distributions of NO$_y$ Species

In addition to its importance in determining the dramatic local variations in NO$_2$ under zonally asymmetric conditions, N$_2$O$_5$ plays a major role in the annual cycle of NO$_2$ under averaged conditions (see Ko *et al.*, 1984). Figure 10-64 presents calculated distributions of NO$_2$ at midnight and noon from the model of Garcia and Solomon (1983), Solomon and Garcia (1983a, 1984a) for comparison with the distributions shown in Section 10.2 (satellite data). Note that the calculated distribution of NO$_2$ exhibits a minimum in high latitude winter (even in the zonal and monthly mean distribution shown here) due to the formation of N$_2$O$_5$, as discussed above. This feature is also reflected in the satellite and aircraft total column data. *In situ* observations at high latitudes also reveal a similar depletion in NO at altitudes below about 30 km in winter as compared to summer. Ridley *et al.* (1984) showed that NO vertical profiles obtained in summer at 54 °N contained systematically larger abundances than those measured in winter, and they attributed the differences between seasons to the enhanced abundance of N$_2$O$_5$ in the winter lower stratosphere.

Figure 10-64 also shows that the calculated nighttime NO$_2$ maximizes near 40 km in the tropics, similar to the observations by LIMS. This local maximum is related to the maximum in odd nitrogen production shown in Figure 10-53 above, and is closely tied to the N$_2$O distribution, as discussed above.

587
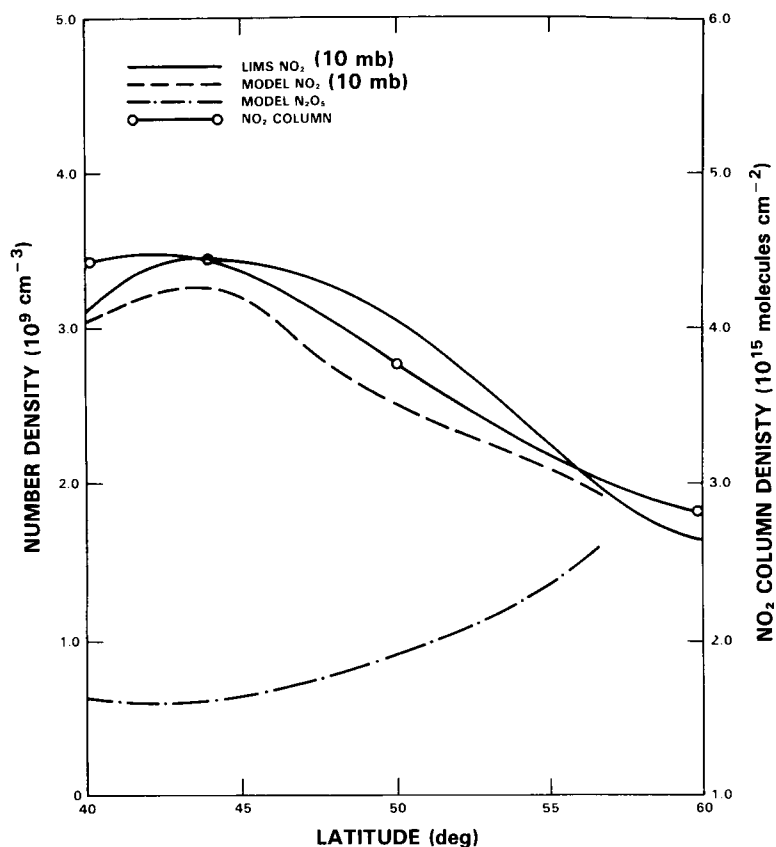
Figure 10-62. Latitudinal gradients in NO₂ observed by LIMS in January, 1979, compared to model calculations. From Callis *et al.* (1983b).

It should be emphasized that stratospheric NO_2 abundance decays during the night to form N_2O_5, which then photolyzes during the following day to yield a temporal increase in NO_2. This phenomenon is clearly reflected by the observed diurnal variation in total column and *in situ* observations of NO_2 and NO (see, e.g., Noxon *et al.*, 1979a; Ridley *et al.*, 1977; Kerr *et al.*, 1982). Therefore, since the available satellite data on NO_2 were obtained at different local times, their intercomparison can only be performed through photochemical modeling of the diurnal variability. Using the LIMS observations of O_3 and temperature, Solomon *et al.* (1985a) have studied the diurnal variations to be expected in NO_2. These calculations use the daytime LIMS measurement of NO_2 (near 1 pm) to constrain the amount of NO_y. Thus the daytime measurements by LIMS are assumed to be exact, but the calculated diurnal variations around this value depend strongly on photochemistry, and provide a means of comparing daytime LIMS data to SME (near 3 pm local time), to SAGE (sunrise and sunset), to the nighttime LIMS data, and to photochemical theory. Figure 10-65 presents a typical comparison of this type using the monthly and zonally averaged data from each satellite experiment. In general, the various satellite instruments were found to be in rather good agreement with one another, and with presently accepted theory controlling diurnal variations.

Available balloon data provide important, and somewhat more direct, information on NO_2 diurnal variations. During BIC 1 the Oxford University BPMR obtained measurements of NO_2 over both dawn and dusk, the flight covering nearly a 24 hour period (Roscoe *et al.* 1985a). Data from the upper levels
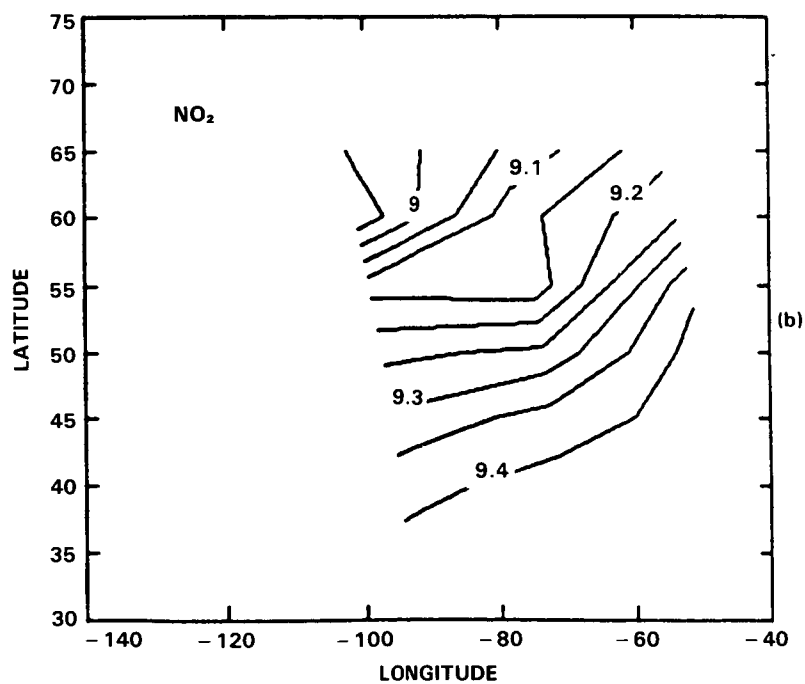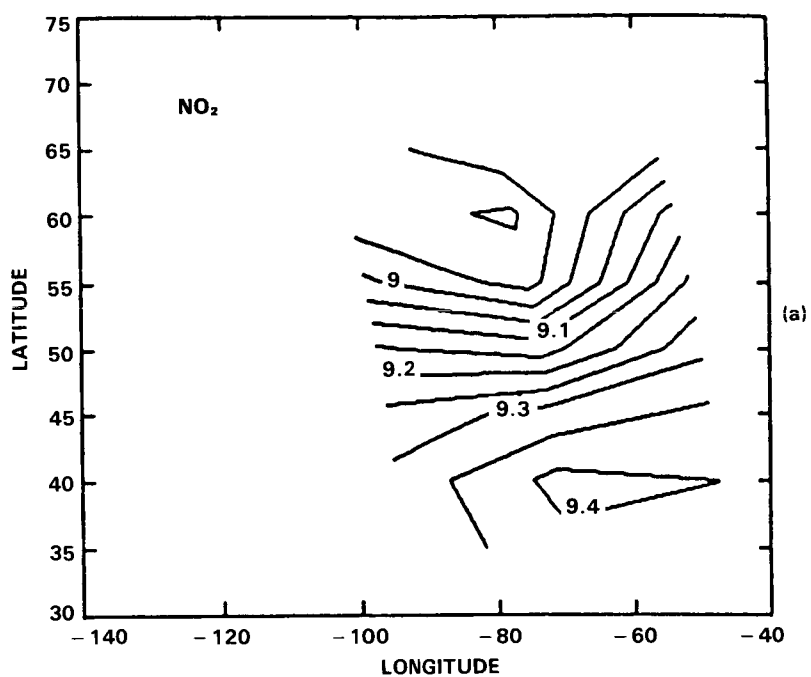
Figure 10-63. Latitudinal-longitude contours of the logarithm of NO_2 densities on day 40, 1982, (a) observed by SME and (b) calculated using the parcel trajectory method. See Zawodny, 1985a, b.

589
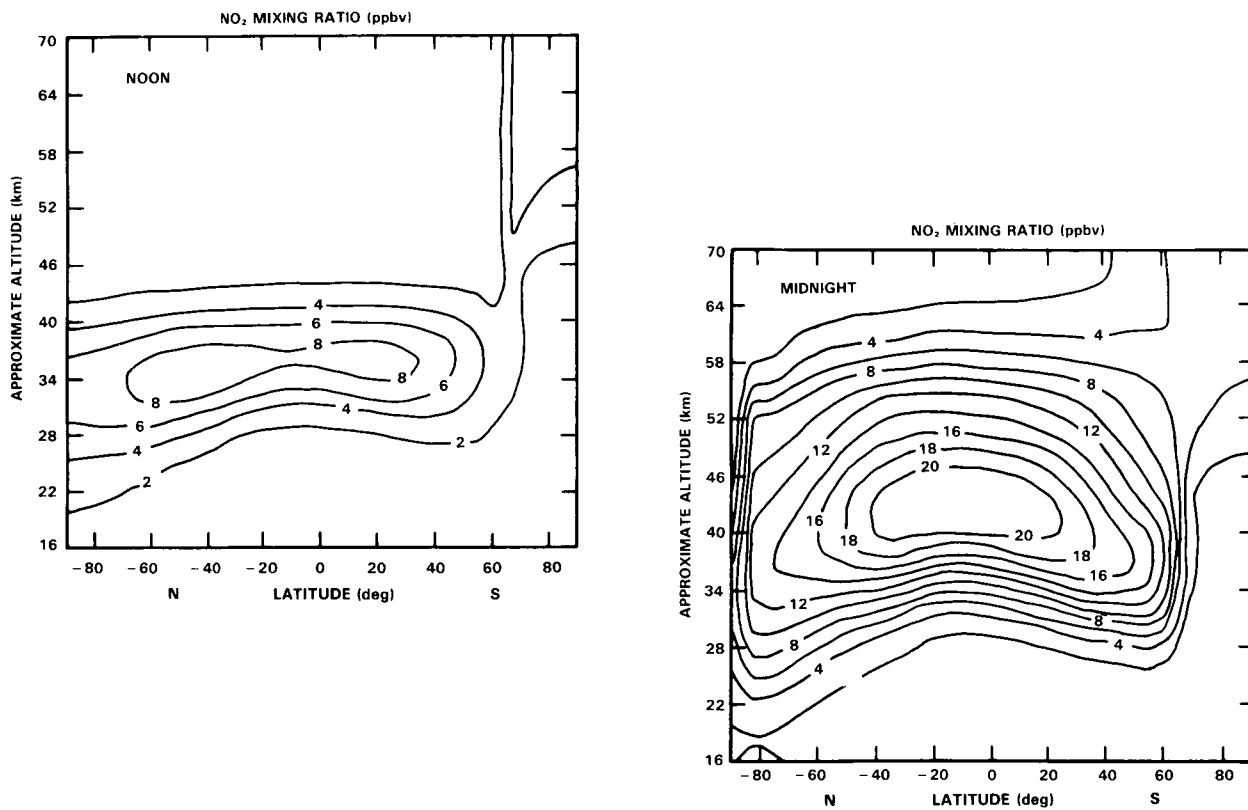
Figure 10-64. NO_2 mixing ratios at noon and midnight, from the model of Solomon and Garcia (1983a, 1984a).
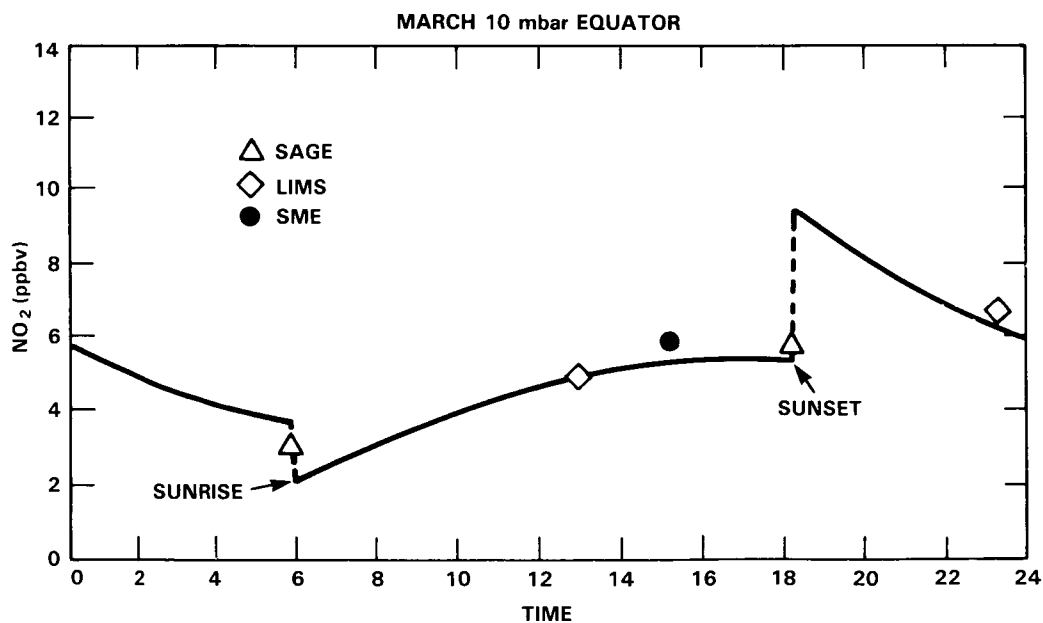
Figure 10-65. Comparison of monthly mean satellite NO_2 data 10 mbar at the Equator, and a model calculation.

at ~ 38 and 42 km are compared with a diurnal photochemical model in Figures 10-66 and 10-67 (data at lower levels were affected by the El Chichon volcano). The changes at dawn and dusk and the night-time decay of NO_2 are consistent with theory. Notice, for example, the slower night-time decay of NO_2 at ~ 42 km compared with ~ 38 km, consistent with a greater role of N_2O_5 formation at the lower altitude. Thus qualitatively the measurements confirm the theory.

Roscoe et al. (1985a) considered whether thé data might provide a more quantitative test. The night-time decay of NO_2 can be written:

$$\frac{d[NO_2]}{dt} = - 2k_1 \, [NO_2] \, [O_3] \tag{11}$$

where $NO_2 + O_3 \overset{k_1}{\rightarrow} NO_3 + O_2$ is followed rapidly by $NO_3 + NO_2 + M \overset{k_2}{\rightarrow} N_2O_5 + M$. The equation can be rewritten:

$$\frac{dln[NO_2]}{dt} = - 2k_1 \, [O_3] \tag{12}$$

to show the simple dependence of the night time decay on O_3. During BIC 1 there were a number of measurements of O_3 in the upper stratosphere, including measurements in the microwave (Robins et al. 1985) and the UV photometric measurements of Robbins (1985). Preliminary analyses show significant differences between these data. A good measurement of the night time variation of NO_2 could possibly distinguish the ozone value, using Equation (12).

Diurnal calculations were performed in which the model ozone values were replaced by, first, the microwave measurements and, second, the preliminary UV data. Figures 10-66 and 10-67 show the calculated diurnal variations at 38 and 42 km. However the standard error of the observed NO_2 decay (with only five points characterizing the period of darkness) is so large at both heights that the ozone data cannot be distinguished. Two conclusions may be reached. The NO_2 data, which represent probably the first measurements of a complete diurnal cycle, are of insufficient accuracy to be used to make a critical test of the photochemistry. (Nevertheless, physical insight suggests, for example that the role of N_2O_5 is confirmed by the measurements). A critical test requires measurements with higher precision. Second, a critical test will also require measurements of ozone to higher absolute accuracy. It must be regretted that the El Chichon aerosol cloud affected the results around 30 km since the signal-to-noise of the BPMR maximises at this height and it is here that the role of N_2O_5 is most important.

Since the distributions of nighttime NO_2 and HNO_3 are available from satellite data the distribution of NO_y can be obtained from data, at least in part (Callis et al., 1985a, b; Solomon et al., 1985a). A measurement of NO_2 and HNO_3 near 11 pm (as obtained by LIMS) does not, however, represent a direct measurement of total NO_y since production of N_2O_5 during the period from sunset to the measurement time must be an important process. This can be readily taken into account using diurnal photochemistry as shown in Figure 10-65, and a value for NO_y can therefore be inferred from the satellite data. Figure 10-68 presents a contour plot of the NO_y distribution derived from zonally and monthly averaged conditions in January (Solomon et al., 1985a). The inferred maximum abundance of NO_y is about 21 ppbv near 40 km, in good agreement with the two-dimensional photochemical models discussed in Chapters 12 and 13. At lower altitudes, however, the two-dimensional models exhibited large variations in calculated NO_y, depending on the transport processes and treatment of HNO_3 rainout imposed in the models.
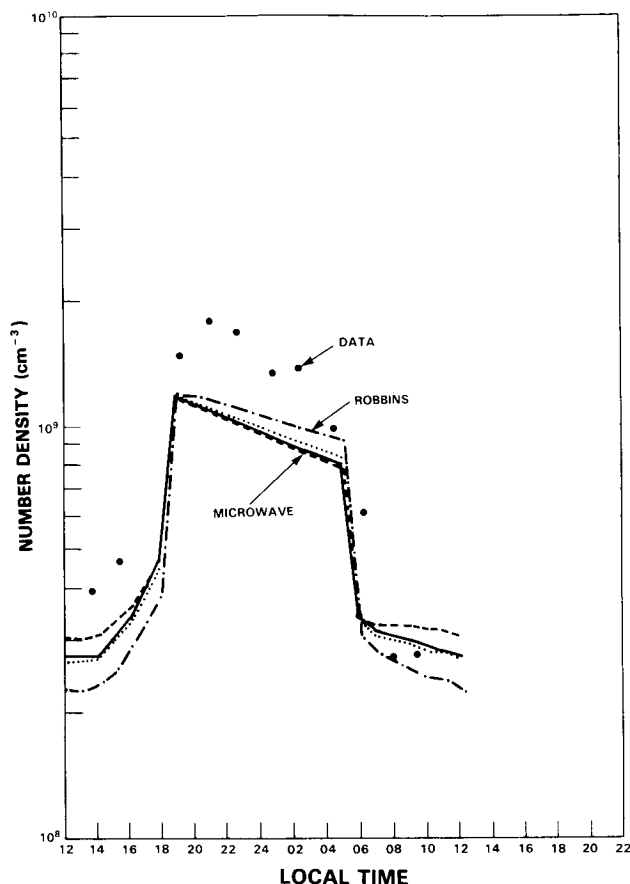
Figure 10-66. Observed diurnal variations in NO₂ at 38 km observed by Roscoe *et al.* (1985b), and model calculations including various ozone profiles (see text).

Figure 10-69 presents the latitude variation of NO_y inferred from the LIMS data at 3, 16 and 30 mbar compared to several two-dimensional models. Particularly in the tropical lower stratosphere most models tend to underestimate the inferred abundance of NO_y by a considerable margin. The magnitude of the gradient predicted by the residual Eulerian AER model is in good agreement with the observations, but the model is systematically low compared to the inferences drawn from LIMS. On the other hand, the classical Eulerian model of Pyle is much closer to the observations in the tropics, but exhibits a gradient that is somewhat shallower than the observed (see Chapter 12 on model formulation). Further observations of NO_y are badly needed to elucidate the causes of these discrepancies and to improve our understanding of odd nitrogen in the lower stratosphere.

A best estimate lower limit for a mid-latitude equinox NO_y profile can also be deduced directly from *in situ* data by summing the individual best estimate profiles for NO, NO_2, and HNO_3. This should be considered a lower limit, particularly at altitudes below 32 km, since no contribution from N_2O_5 or other reservoir species has been included. Figure 10-70 presents the lower limit profile derived from the *in situ* data compared to the total NO_y inferred from LIMS for April, 1979 at 32 °N. The two estimates are in good agreement.

An interesting problem in the chemistry of odd nitrogen in the stratosphere is the distribution of HNO_3 in winter. As shown above in the satellite subsection, the observed gradient of HNO_3 increases sharply
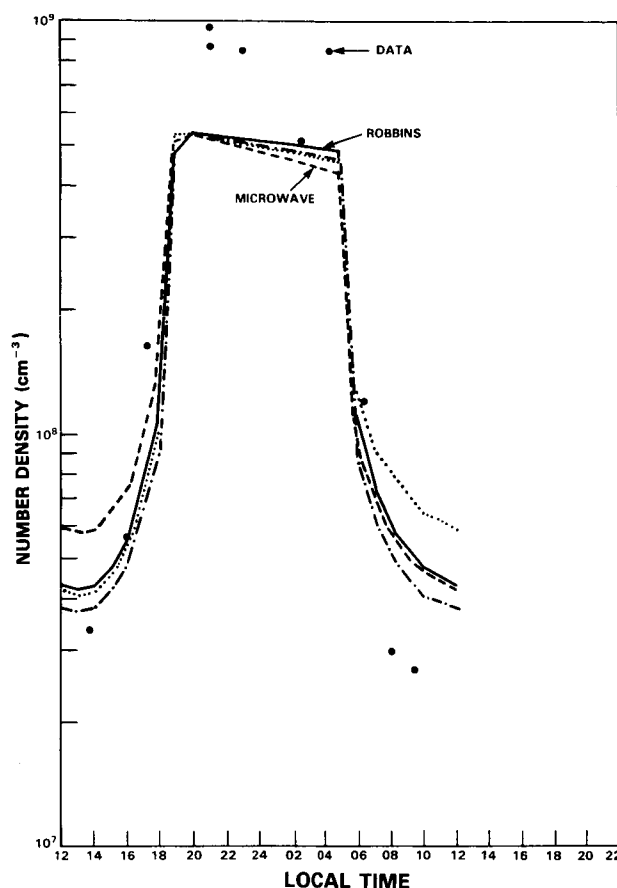
Figure 10-67. Same as Figure 10-66, but for 42 km.

with latitude inside the polar night region. Satellite observations of ozone and methane suggest that the circulation in high latitude winter must be directed downward and poleward in the zonal and seasonal mean. Such a circulation must then lead to downward transport of HNO_3 poor air from above, and a depletion of HNO_3 in high latitude winter, in contrast to trends in the data. Figure 10-71 presents a calculated contour distribution showing this feature. Comparison (for example) of Figures 10-42 and 10-71 suggest that our present understanding of HNO_3 chemistry may be incomplete during winter at high latitude. An additional source of HNO_3 during high latitude winter could resolve these discrepancies. More detailed studies by Austin *et al.* (1985b) using parcel trajectory methods along with LIMS data in the polar night strongly suggest that an additional source of HNO_3 must be present in high latitude winter.

10.3.2.3 Latitudinal Survey of HNO₃

The column abundance of HNO_3 has previously been reported by several investigators using aircraft platforms (Murcray *et al.*, 1975, Coffey *et al.*, 1981a and Girard *et al.*, 1982). The satellite observations (Gille *et al.*, 1984b) have been shown to be consistent with the data from the aircraft survey.

Since no significant diurnal variation is expected of HNO_3, the data are relatively easy to interpret as the exact local time at which the measurement is made is not crucial. The major contribution to the column abundance originates from the lower stratosphere below 25 km (about 90%) where the photochemical

JANUARY NO_y INFERRED FROM LIMS (ppbv)
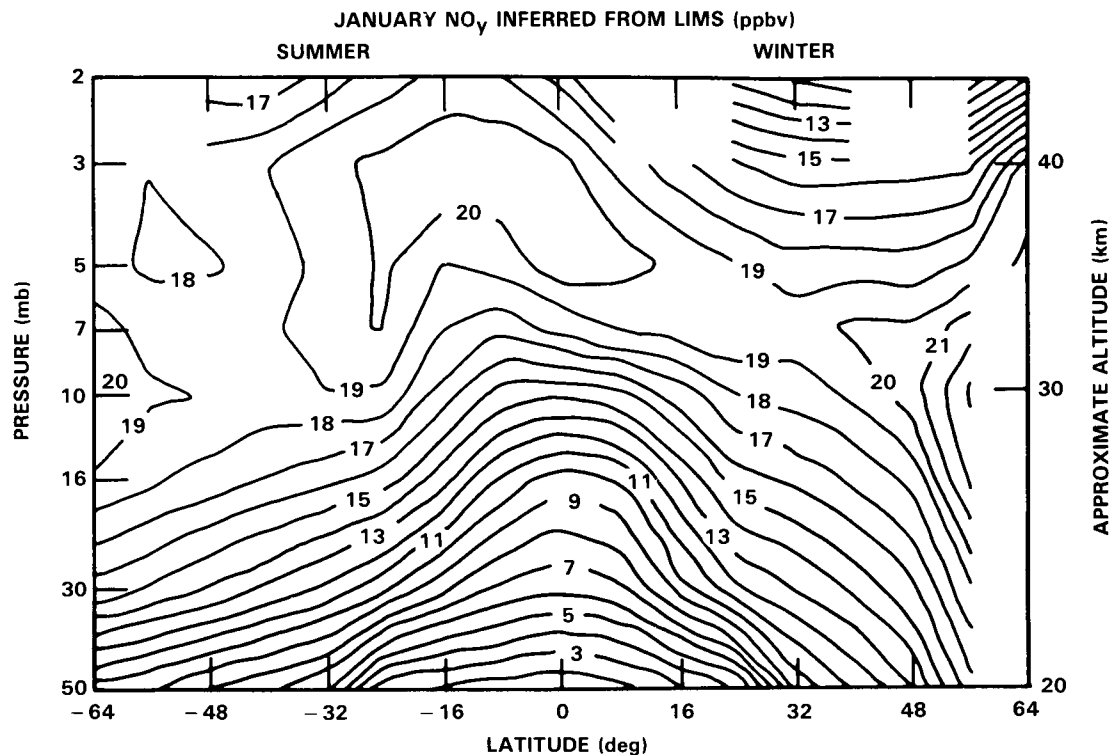
Figure 10-68. NO_y inferred from LIMS for January, 1979. See text.

lifetime of HNO_3 is comparable to or longer than transport time constants. The species HNO_3, which is one of the few downward diffusing species for which extensive observational data are available, is a useful tracer for diagnosing the transport of trace gases in the lower stratosphere.

The data show a factor of three increase in the column abundance from the equator to 45 degree latitude, and up to an order of magnitude increase from equator to pole. In addition, the abundance in the winter hemisphere is also higher in the high latitude regions. Since HNO_3 is produced in the stratosphere and removed rapidly in the troposphere by heterogenous processes, regions dominated by upwelling motion should have a lower concentration of HNO_3 than regions with subsiding motion. This observed latitudinal behaviour is consistent with what could be expected from models with diabatic circulation where upwelling in the tropics results in lower HNO_3 abundance. The seasonal variability is also related to possible photochemical exchanges with reserviour species such as N_2O_5 (Solomon and Garcia 1983a; Ko et al., 1984). The role of N_2O_5 is particularly important near the polar night region in the winter hemisphere where intrusion of air from the polar night may cause significant fluctuations of the observed HNO_3 at particular longitudes (Solomon and Garcia 1983b, Noxon et al., 1983).

Figure 10-72 shows calcuated column abundances of HNO_3 from different model groups. The results separate rather nicely into two groups with models using large eddy difficusion coefficients ($K_{yy} \sim 1 \times 10^{10}$ cm^2 s^{-1}, $K_{zz} \sim 1 \times 10^4 - 1 \times 10^5$ and those using small diffusion coefficients ($K_{yy} \sim 3 \times 10^9$ cm^2 s^{-1}). Models using large eddy coefficients (Ko et al. 1984) obtain results with smaller latitudinal contrast. In spite of the use of large diffusion coefficients, the DuPont model (Miller et al., 1981) produced a large contrast. This could be due to the choice of K_{zz} to stimulate the higher tropopause at the equatorial region.
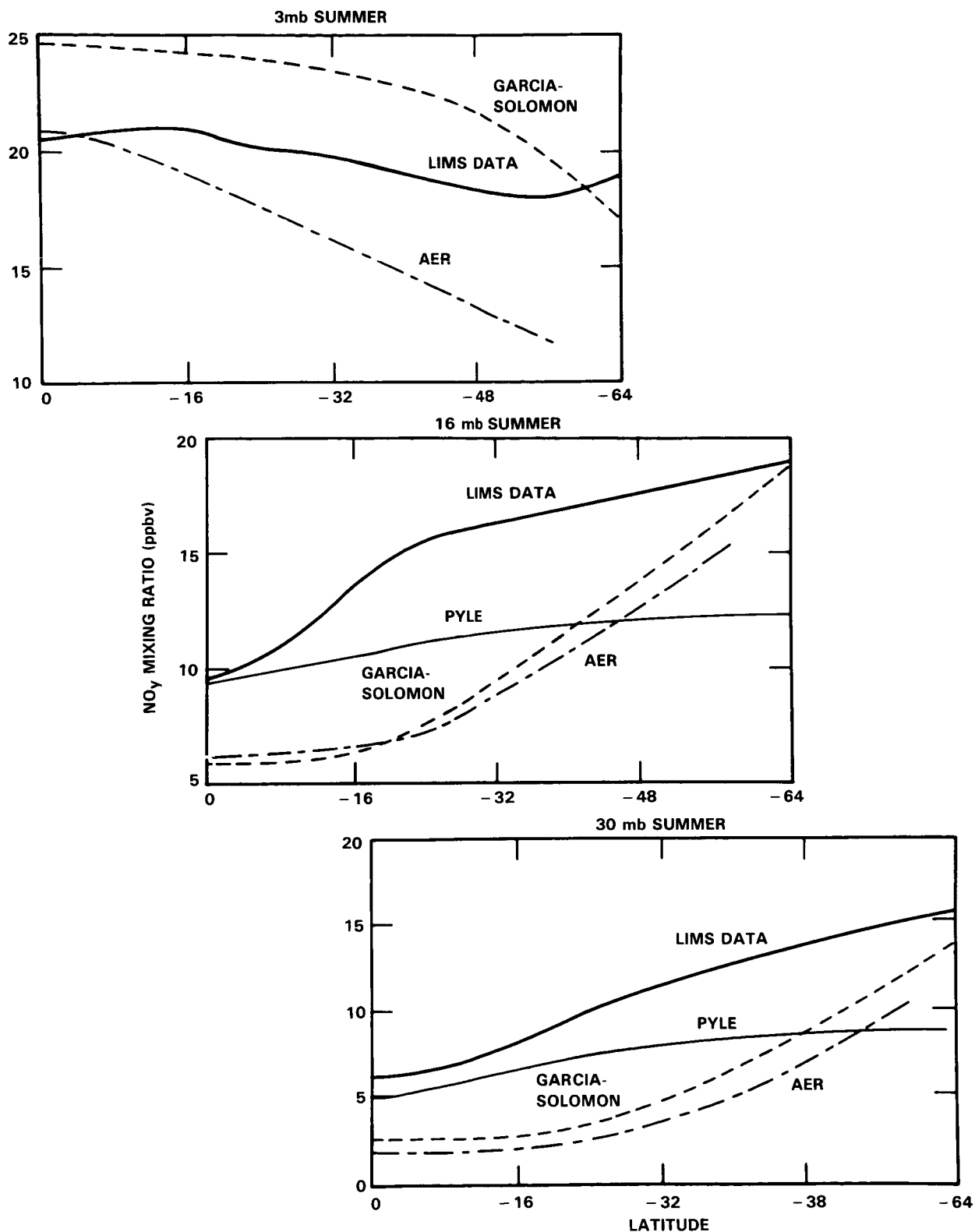
Figure 10-69. Latitudinal gradients in NO_y observed by LIMS, and calculated in various 2-D models, at the 3 mb, 16 mb, and 30 mb levels.
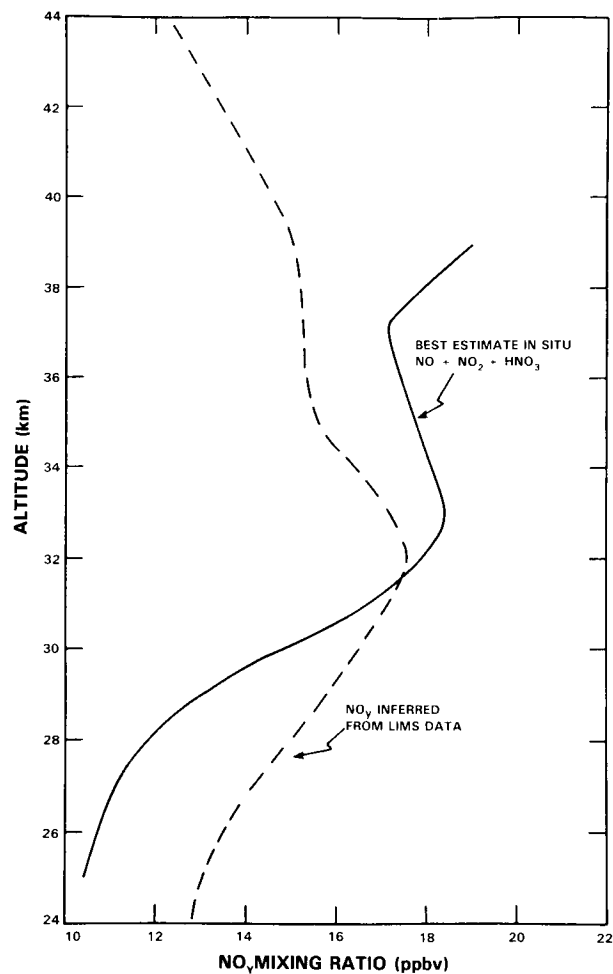
Figure 10-70. Best estimate of the sum of NO, NO₂, and HNO₃ at mid-latitudes in spring from in situ data, and the corresponding values from LIMS.
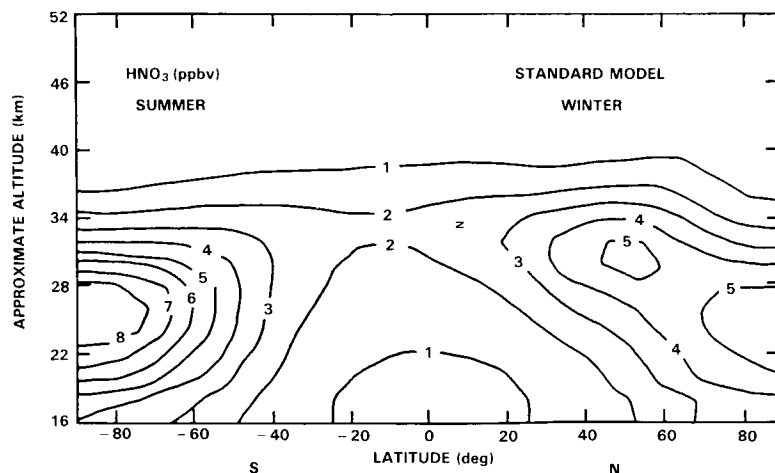
Figure 10-71. Model calculated HNO₃ distributions near winter solstice. From Austin *et al.* 1985a).

596
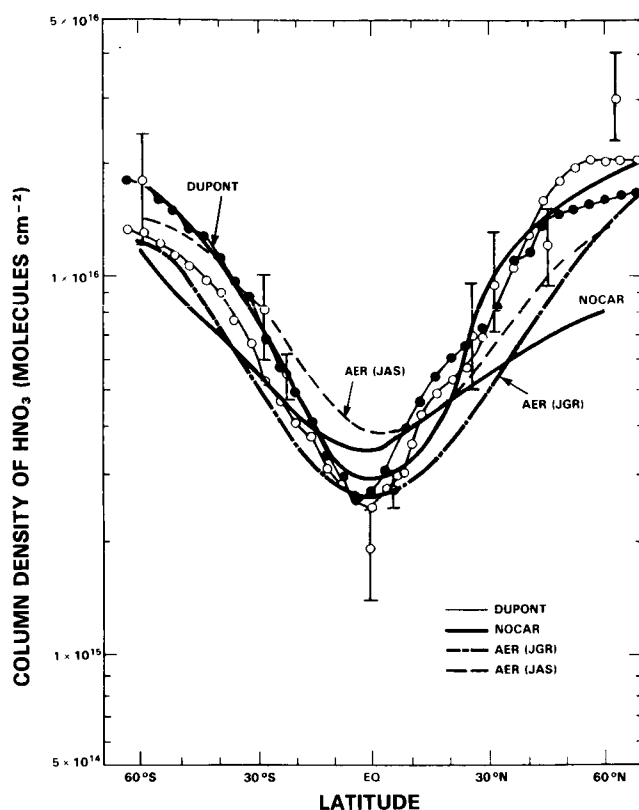
Figure 10-72. Column abundances of HNO₃ from a number of two-dimensional models, and from observations. See Ko *et al.* (1985).

The simulated abundances from models using small eddy coefficients (Solomon and Garcia 1983a; Ko *et al.*, 1985) show larger latitudinal gradients.

The model calculated column abundance of HNO₃ is sensitive to the dynamical treatment both in the mean circulation and eddy mixing in the lower stratosphere (Ko *et al.*, 1985). Further observations of the latitudinal variation of the column abundance of HNO₃ from satellite and aircraft platforms may help elucidate the appropriate parameterization for mixing processes in the lower stratosphere.

10.3.3 Photochemical Considerations

In this subsection, some of the photochemical processes influencing the distributions of the NO_x species will be discussed.

10.3.3.1 The NO/NO_2 Ratio in the Stratosphere.

Nitric oxide which is produced in the stratosphere by the oxidation of N_2O is rapidly converted to nitrogen dioxide mainly by ozone

$$NO + O_3 \rightarrow NO_2 + O_2 \tag{13}$$

but also by HO_2, CH_3O_2 and ClO through

$$NO + HO_2 \rightarrow NO_2 + OH \tag{14}$$

$$NO + CH_3O_2 \rightarrow NO_2 + CH_3O \tag{15}$$

$$NO + ClO \rightarrow NO_2 + Cl \tag{16}$$

During the day, it is destroyed either by photodissociation

$$NO_2 + h\nu \rightarrow NO + O \tag{17}$$

or by reaction with atomic oxygen

$$NO_2 + O \rightarrow NO + O_2 \tag{18}$$

Since the atmospheric attenuation near 400 nm (where NO_2 absorbs) is weak through the entire middle atmosphere, the photodissociation frequency of NO_2 keeps its optically thin value (about $1 \times 10^{-2} s^{-1}$ for an overhead Sun) to as low an altitude as 15 km, so that the lifetime of nitrogen dioxide is never larger than a few minutes during the day. Consequently NO_2 is in immediate photochemical equilibrium with NO during sunlight hours and the NO/NO_2 ratio is given by

$$\frac{[NO]}{[NO_2]} = \frac{J(NO_2) + k_{18}\,[O]}{k_{13}\,[O_3] + k_{14}\,[HO_2] + k_{15}\,[CH_3O_2] + k_{16}\,[ClO]} \tag{19}$$

A comparison of the various terms appearing in the above expression shows that the most effective transfer from NO to NO_2 is due to ozone (reaction 13) and that the other processes contribute for less than 25% in the whole stratosphere and for less than 10% below 30 km. Both photodissociation and reaction with atomic oxygen have to be considered in the conversion from NO_2 to NO, the first process being dominant below 42 km and the second one above this level. During the night, both of these reactions are inefficient and therefore nitric oxide is converted to NO_2 throughout the whole stratosphere.

The comparison between the NO/NO_2 ratio inferred from *in situ* observations and obtained by a full model calculation is an important test to validate our present knowledge of the odd nitrogen photochemistry. The accurate calculation of this ratio however is not straightforward since the parameters involved vary with geophysical conditions and may thus change for example during the period of a ballon flight. The value of the J_{NO_2} coefficient is very sensitive to the local albedo, i.e. to cloud coverage, and may also vary with atmospheric temperature (Madronich *et al.*, 1983). Model calculations show that the NO/NO_2 ratio can change by a factor of 2 with cloud coverage or surface conditions.

Further, extreme accuracy in temperature and ozone measurements is needed to test the ratio in a meaningful manner (Harries, 1982).

A recent comparison between the NO/NO_2 ratio derived from the measurements of McFarland *et al.*, (1985) at Gimli, Manitoba (50 °N) and Palestine, Texas (32 °N) and the calculated NO/NO_2 ratio between 20 and 30 km agrees within ±40% and suggest that the observations are, within the error bars, consistent with theory. However additional simultaneous measurements of NO and NO_2 together with the temperature and the J_{NO_2} coefficient are required to test this photochemistry more accurately.

10.3.3.2. HNO₃/NO₂

The photochemical time constant for HNO_3 is some hours in the sunlit upper stratosphere and equilibrium between HNO_3 and NO_2 can be assumed to a good approximation. Comparison of the measured and calculated HNO_3 to NO_2 has been used to test photochemical theory. In equilibrium:

$$\frac{[HNO_3]}{[NO_2]} = \frac{k_4[OH] \, [M]}{J(HNO_3) + k_6[OH]} \tag{20}$$

so that the ratio depends just on rate constants, a photolysis rate and the OH concentration.

Early investigation based on ballon data suggested that the observed ratio was low compared with models (Evans *et al.*, 1976, Harries 1978), and the measurements themselves, taken at different latitudes and local times, were also significantly different. The problem of modelling HNO_3 in the middle and upper stratosphere has been apparent for some time. Whether the problems with the ratio comparisons were simply due to this or, for example to a poor model description of OH was not clear.

Testing chemistry using such ratio measurements is particularly subject to systematic errors in the observation. Nevertheless the LIMS measurements of HNO_3 and NO_2 provide the opportunity for extensive study with nearly global coverage at a range of zenith angles. Pyle and Zavody (1985a) have used the LIMS data to test aspects of the photochemistry. Rather than comparing the modelled and observed HNO_3 to NO_2 ratios, they have derived OH using Equation 20 and compared this with the limited stratospheric measurements of OH to OH derived, again using the satellite data, by calculation of its sources and sinks. In this latter case H_2O, from LIMS data, and $O(^1D)$, assumed to be in photochemical steady state with LIMS O_3, define the source. Similarly, the sink terms are defined by using LIMS data and making certain photochemical steady state assumptions. The reader is referred to the HO_x chapter (9) for a detailed discussion of the use of satellite data in deriving OH. A detailed estimate was made of the likely error in the two derivations of OH. The derived values in low and middle latitudes agree within these estimated errors and are consistent with the few atmospheric measurements of OH.

Figure 10-73 shows a comparison of the derived OH at 32 °N including the estimated errors of the determinations due to errors in the rate constants and errors in the LIMS observations. The agreement between the two methods constitutes a modest positive test of this subset of NO_x -HO_x photochemistry and does not support the earlier suggestions of limitations in theory based on ballon measurements. Nevertheless, an anticipated bias in LIMS HNO_3 could change this conclusion. Note that the LIMS HNO_3 is systematically higher than ballon measurements, but less than models, above about 30 km (see below). Correspondingly in Figure 10-73 the OH derived using equation (20) is less than OH derived from its sources and sinks. The possibility remains of an unidentified sink for HNO_3, although note again that the error in derived OH and errors in the kinetic data are significant. For a satisfactory test, simultaneous measurements of OH, HNO_3 and NO_2 are urgently required.

10.3.3.3 Absolute Abundance of HNO₃ at Mid-Latitude in the Upper Stratosphere

The nitric acid concentration predicted by model calculations above 25-30 km is about a factor 1.5 to 2 larger than the values measured by ballon-borne instruments, but closer to the LIMS measurements. This discrepancy with *in situ* data cannot presently be explained by current uncertainties in the chemical parameters involved in the calculation. Predicted HNO_3 abundance depends on the total NO_y concentra-
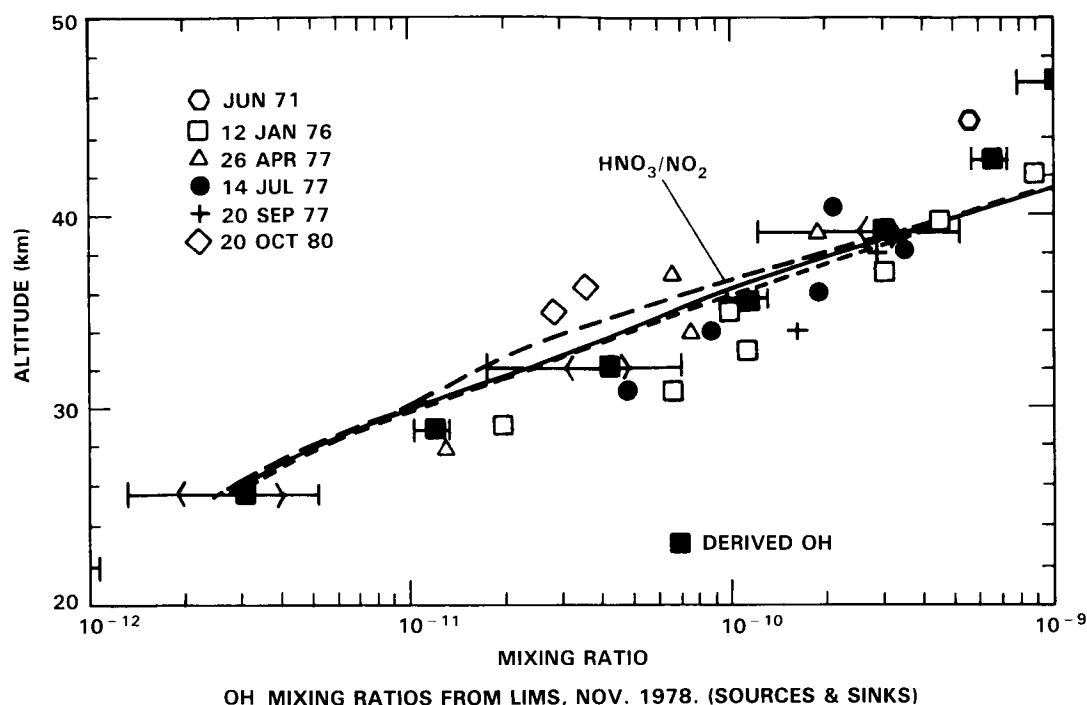
Figure 10-73. OH derived from LIMS data using the equilibrium between HNO_3 and NO_2 (dashed line) and by calculation of sources and sinks (solid line). Errors in the derivation due to estimated LIMS errors (↔) and due to estimated errors in kinetic and photochemical data (↔) are also shown. Based on Pyle and Zavody (1985a).

tion by which is calculated in the model. Most models however predict a NO_y mixing ratio close to 18-22 ppbv at 35 km in acceptable agreement with the values inferred from LIMS data. In any case, the 30% difference in NO_y among most models cannot explain a factor of 1.5 to 2 difference between observed and calculated HNO_3 amount.

Differences in the treatment of the diurnal averaging of the HNO_3 formation rate also lead to significant changes in the calculated concentration above 25 km. The use of a 24 hour average of the rate instead of the calculation of the rate with averaged OH and NO_2 concentrations reduces the resulting nitric acid abundance but does not entirely resolve the discrepancy.

Unless an important mechanism is omitted in the theoretical approach, it is more likely that the overestimation of the predicted HNO_3 concentration may be related to an improper calculation of the solar transmission in the Schumann-Runge bands and consequently of the HNO_3 photodissociation frequency. The use of smaller O_2 cross section in the Herzberg continuum has already brought the calculated HNO_3 concentration into closer agreement with observations (Froidevaux and Yung, 1982: Basseur et al., 1983).

10.3.3.4 NO₃ at Night

Perhaps the area of largest current discrepancy between odd nitrogen observations and photochemical theory lies in the observed behavior of NO_3 at night. NO_3 is formed by the reaction.

$$NO_2 + O_3 \rightarrow NO_3 + O_2 \tag{1}$$

and it is destroyed by reaction with NO_2 to form N_2O_5 in a three-body process. During the day, it also photolyses rapidly at visible wavelengths, so that the daytime abundance is expected to be extremely small. At night, however NO_3 is expected to build up to large abundances near 40 km or so. The rate of formation of NO_3 is particularly dependent on temperature through the strong negative temperature sensitivity of reaction (1) and the expected total column abundance should therefore be several times greater in summer at middle and high-latitudes than it is in the winter. NO_3 total column observations by Norton and Noxon (1985), however, show clearly that the observed abundances at 40°N in summer are no larger than they are in winter, and are many times smaller than model predictions. Therefore, Norton and Noxon (1985) conclude that a scavenger must exist for stratospheric NO_3. Nighttime NO_3 profiles are also available from the balloon measurements of Naudet *et al.* (1984). These data show greater abundances in spring than in fall near 40 km, whereas the opposite is predicted by photochemical theory using climatological mean observations of ozone and temperature for the latitude where the observations were obtained (Norton and Noxon, 1985). More extensive observations of NO_3 as a function of latitude and season are badly needed to characterize this discrepancy in greater detail, but the consistency of these observations suggests the existence of a gap in our understanding of odd nitrogen photochemistry.

10.4 SUMMARY AND CONCLUSIONS

This chapter has demonstrated that substantial progress in our understanding of stratospheric odd nitrogen has been achieved in the past few years. Indeed, a number of questions that might have been termed ''outstanding problems'' in 1980 have been largely resolved. Others remain subject for ongoing research, and with our improved understanding additional challenges have also emerged.

The availability of satellite data on NO_2 and HNO_3 has been a major achievement in stratospheric research, allowing us to quantify our knowledge of the temporal and spatial variations in NO_y to a remarkable extent. No less that five new techniques are also now used to detect NO_2 from balloons, enabling a much fuller understanding of NO_2 to be achieved. Intercomparison of balloonborne techniques for measuring NO_2 and NO has greatly added to the value of the existing dataset, and has led to firm knowledge of the detailed profiles of these species at mid-latitude. NO_3 has been observed both by ground-based and balloon methods, revealing an important inconsistency with photochemistical theory over much of the annual cycle. N_2O_5 and $ClONO_2$ have also been tentatively measured. Diurnal variations in NO_2 have been directly measured from a balloon, and are also revealed by the combination of available satellite data obtained at various local times. Both are in broad agreement with photochemical theory regarding the interchange between members of the NO_y family. Direct measurements of the important ratio between NO and NO_2 and are also available from balloons, and are consistent with theoretical predictions. Observations of NO_2 and HNO_3, and their ratio, are now available from satellites as well as balloons, yielding new information on HNO_3 chemistry and inferences about the OH content of the stratosphere. NO_2 observations following the eruption of the El Chichon volcano suggest that important changes in stratospheric photochemistry are associated with major eruptions.

The combination of available data on NO_2, HNO_3, and NO has greatly improved our knowledge of total NO_y. This information is particularly important both because it enables us to better understand the budget of the family as a whole, and because NO_y plays a major role in model predictions of ozone perturbations. It is important to emphasise that the NO_y derived from the data is in marked disagreement with two-dimensional model predictions below about 30 km. This suggests that boundary conditions or low-altitude NO_y sources are not properly treated in the models.

On the other hand, the derived NO_y above 30 km is in good agreement with model predictions. Here again, this good agreement is partly due to the availability of new data (principally from satellites), which has guided theoretical study. In particular, available satellite observations of N_2O have enabled a much more quantitative understanding of the sources of NO_y via N_2O oxidation to be achieved.

Satellite observations of NO_2 in the polar night region have also quantified our knowledge of thermospheric sources, providing the first observational evidence that thermospheric NO_y can be transported to the upper stratosphere. This possibility was first raised in about 1970, and has only now been addressed directly with observations.

The availability of improved data on N_2O has greatly enhanced our understanding of stratospheric transport processes. Satellite observations on N_2O have shown that tropical circulation patterns are likely to be strongly linked to the semi-annual oscillation. Further, balloon data for N_2O at higher vertical resolution than that resolved by the satellites has shown that vertical variability exists systematically, and on very fine spatial scales. These are yet to be completely understood theoretically, but the variance associated with stratospheric sudden warmings seems to play a significant role in this phenomenon.

Ground based, balloon, aircraft, and satellite data have all been used to address the variability of NO_2 at high latitude in winter in much more detail than previously possible. These data have greatly quantified our understanding of the distribution of N_2O_5 and its role in the Noxon "cliff" phenomena. Balloon data have shown that the "missing" NO_2 in the "cliff" region occurs at altitudes from about 15-30 km. Theoretical studies have revealed that the Noxon "cliff" is primarily due to meridional transport processes and combined photochemical effects in the presence of large-scale waves.

Studies of the latitudinal variations in HNO_3, both from aircraft and from satellites, have also to led to important insights into transport processes, showing in some detail how advection and dispersion compete in tropical latitudes.

In spite of these numerous advances, several outstanding problems must be considered unresolved. The ratio between HNO_3 and NO_2 remains imperfectly simulated by current models, although it should be emphasised that possible errors in kinetic data regarding OH reactions might resolve the apparent discrepancy. Another possibility is that the HNO_3 photolysis rate may be under estimated, particularly in the Schuman-Runge bands. Further laboratory kinetic studies, and *in situ* simultaneous observations of OH, NO_2 and HNO_3 could be used to address this question. Satellite data also suggests that an unknown chemical source of HNO_3 may be present in the high latitude winter stratosphere. Further observations are badly needed, and should include both Northern and Southern Hemisphere data.

Observations of the Noxon "cliff" also suggest that the temperature sensitivity of the N_2O_5 photolysis rate at the very cold temperatures of the Antarctic winter may not be completely well understood. Further observation of the "cliff" phenomenon in the arctic is needed, as well as laboratory studies. Direct measurements of N_2O_5 are also of the most critical importance to a fuller understanding of NO_2 variability. Other temporary reservoirs such as $ClONO_2$ and HNO_4 also require quantitative study as detailed functions of latitude and season.

Data on diurnal variations in NO_2 from balloons and satellites, while of considerable qualitative use, are not yet sufficiently accurate nor temporally detailed to definitively test photochemical theory. Highly accurate simultaneous observations of several species (i.e. NO, NO_2, and N_2O_5 as a minimum) are needed to address these issues.

Finally, the nighttime behaviour of total column NO_3 observed by Norton and Noxon shows that important mysteries remain present in the behaviour of stratospheric odd nitrogen species, and a dependence on only a few relatively well known parameters such as O_3 and temperature. Yet, the observations reveal seasonal variability that defies current interpretation.

In closing, we remark that continual research into the problems of stratospheric odd nitrogen must involve a variety of methods and tools. Theoretical studies should include multi-dimensional and simple box models. Laboratory kinetics remain of critical importance, and several areas have been mentioned as uncertain here. Satellite and aircraft data on temporal and spatial variations are needed, as well as high vertical and short time resolution data from balloons.

10.5 FUTURE RESEARCH

The review presented in this chapter has revealed that the study of NO_x is an active field of atmospheric research. A number of indications of future research requirements have emerged, and are summarised here.

The power of the new satellite data sets has been clearly demonstrated. Researchers (and funding agencies) should recognise the importance of continuing to exploit these sources of information to the maximum.

A problem remains with the explanation of the distribution of high altitude (>30 km) HNO_3. Current models show considerable excesses over both satellite (LIMS) and balloon measurements. Similarly, we do not currently understand the balance of HNO_3 at high latitudes: the suggestion that there is an unidentified source of high latitude HNO_3 needs to be tested.

There are several independent suggestions on the importance of N_2O_5 as a temporary reservoir under dark conditions. N_2O_5 has recently been reported as detected by the ATMOS experiment at night in mid-latitudes. Future work needs to identify and measure N_2O_5 at higher latitudes, and under polar night conditions. Furthermore, until N_2O_5 photolysis rates are better determined, we will not be able to adequately understand the time variation of exchange between NO, NO_2, HNO_3 and N_2O_5. Other temporary reservoirs such as $ClONO_2$ may be of lesser importance, but should be similarly studied.

Some of the most stringent tests of theory have come from measurements of diurnal variations. However, measurement accuracy and time resolution need to be increased substantially to allow a very "tight" comparison.

Considerably more work is needed to understand NO_3. The past 5 years have given us a valuable new set of observations of this species, but these have revealed that our understanding of the seasonal variation of NO_3 is not properly understood. Is there a summer-time "scavenger" of NO_3?

It is now a truism that we need more observations, particularly simultaneous observations of groups of species which might provide a "closed" test of some aspect of the chemistry or physics. Even so, it must be stressed that experimentalists must continue to generate ideas, and hardware, to permit such experiments, and to seek to achieve the highest accuracies possible. In connection with the present chapter, an example would be the simultaneous measurement of NO, NO_2, N_2O_5, HNO_3, and NO_3 at an absolute accuracy in the 5%-10% range, with a time resolution of ~5 minutes; height resolution is not so demanding: as much as 5 km would not be critical.

NITROGEN SPECIES

Finally, we recognise that, in the same way that Nimbus 7 (SAM, LIMS), SAGE, and SME have caused a minor revolution in the quantity and nature of the data available to us, the simultaneous measurements to be made by the instruments complement on the Upper Atmosphere Research Satellite (UARS) can be expected to have a major impact on our understanding on NO_x, and many other areas of atmospheric science. It is important that researchers prepare properly to exploit these data: it is also important that agencies ensure that facilities are in hand to ensure efficient distribution of the UARS results to the community.

CHAPTER **11**

HALOGENATED SPECIES
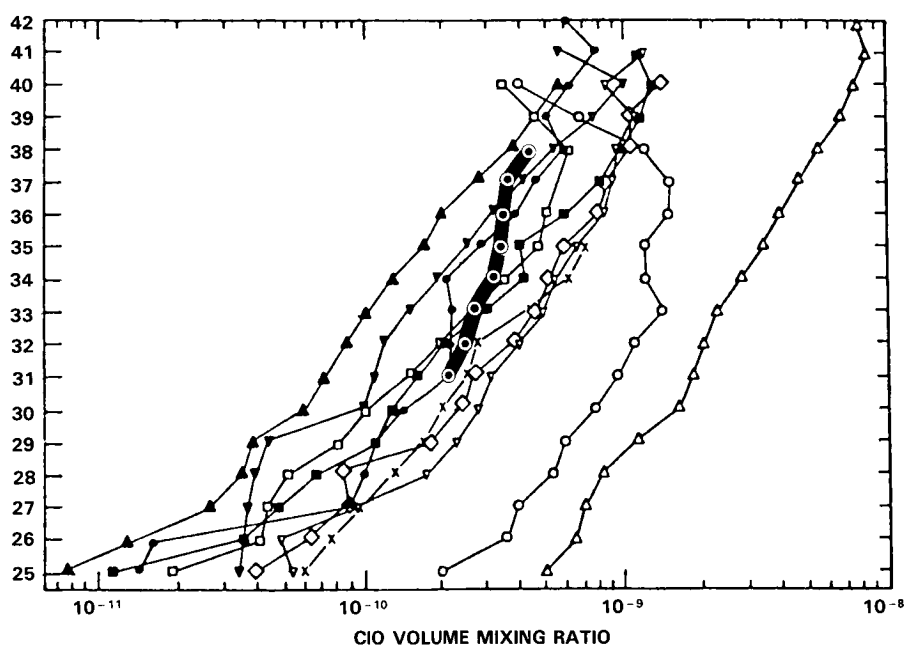
Panel Members

M.J. Molina, Chairman

R. deZafra   N.D. Sze
P. Fabian   J. Waters
C.B. Farmer   R.J. Zander
W.G. Mankin

CHAPTER 11

HALOGENATED SPECIES: OBSERVATIONS AND INTERPRETATION

TABLE OF CONTENTS

11.0 INTRODUCTION

In this chapter stratospheric measurements of halogen containing species are reviewed and compared with model predictions. Emphasis is placed here on new developments since the previous assessment [WMO Report -11, 1982].

The bulk of the chapter deals with chlorinated species. In fact, HF is the only inorganic compound containing a halogen other than chlorine for which there are measurements not already reported in the earlier 1979 assessment [NASA Reference Publication 1049]. There are, however, new stratospheric observations of organic source species containing bromine ($CBrClF_2$, $CBrF_3$ and CH_3Br).

The most important findings in the chapter are summarized in Section 7. Section 8--the final one--refers to future research needs involving stratospheric measurements of species within the chlorine family. These needs represent only a fraction of the research accomplishments required to significantly advance current understanding of stratospheric chlorine chemistry.

11.1 CHLORINE MONOXIDE (ClO)

11.1.1 Introduction

The principal fate of the chlorine atoms released in the stratosphere by photodecomposition of CFC's is reaction with ozone to form ClO, the chlorine monoxide radical, which in turn reacts with atomic oxygen to regenerate the chlorine atom, thereby completing a catalytic cycle which destroys ozone. Understanding of stratospheric ClO is thus crucial for prediction of stratospheric ozone depletion by CFC's.

First measurements of stratospheric ClO were made from *in-situ* resonance fluorescence detected by instrumentation on parachutes dropped from high-altitude balloons [Anderson *et al.*, 1977, 1980]. Tentative detection of millimeter-wavelength emission lines of ClO was made by aircraft-based instruments [Waters *et al.*, 1979], followed by definitive measurements from ground-based [Parrish *et al.*, 1981] and balloon-based [Waters *et al.* 1981] millimeter wavelength spectrometers. An early measurement of stratospheric ClO by balloon based infrared absorption spectroscopy was also reported [Menzies, 1979; amended, 1983]. The status of ClO measurements up to 1981 is summarized in the previous assessment report [WMO, 1982].

Since the 1981 assessment, the stratospheric ClO data base has been improved in the following ways:

1. The diurnal variability of ClO has been measured by both ground-based and balloon-based millimeter-wavelength techniques.

2. The time-base on measurements of the ClO column abundance has been extended, and observations have now been made at latitudes of 20°, 32°, and 42°N by ground-based millimeter-wavelength techniques.

3. Additional *in situ* profile measurements have been obtained from the recently developed reel down technique.

4. Balloon-borne infrared laser heterodyne results have been reevaluated, and are now generally consistent with other measurements.

5. Initial results from ground-based infrared heterodyne measurements failed to detect stratospheric ClO; preliminary results from more recent measurements, however, have indicated the presence of a ClO signal.

6. Observations of stratospheric ClO have been obtained from balloon-borne submillimeter measurements.

Continued refinements in theoretical modeling, adjustments in laboratory-measured rate constants and in uv solar flux, and improvement in the observational data base for ClO, including the 24-hour cycle of diurnal variation, have by now produced a state of reasonable agreement between theory and experiment in both the average altitude profile and diurnal behavior. On the other hand, existing experimental data is inadequate to measure seasonal and latitudinal variations or long term trends which are theoretically predicted. Also, simultaneous measurements of ClO at the same location by independent techniques have not yet been performed, although agreement in the mean value of measurements from various techniques appears good.

11.1.2 Midday ClO

11.1.2.1 Vertical Profile

Figure 11-1 summarizes existing measurements of the mid-day stratospheric ClO vertical profile. The *in situ* resonance fluorescence measurements, are (a) the average of eight profiles measured between
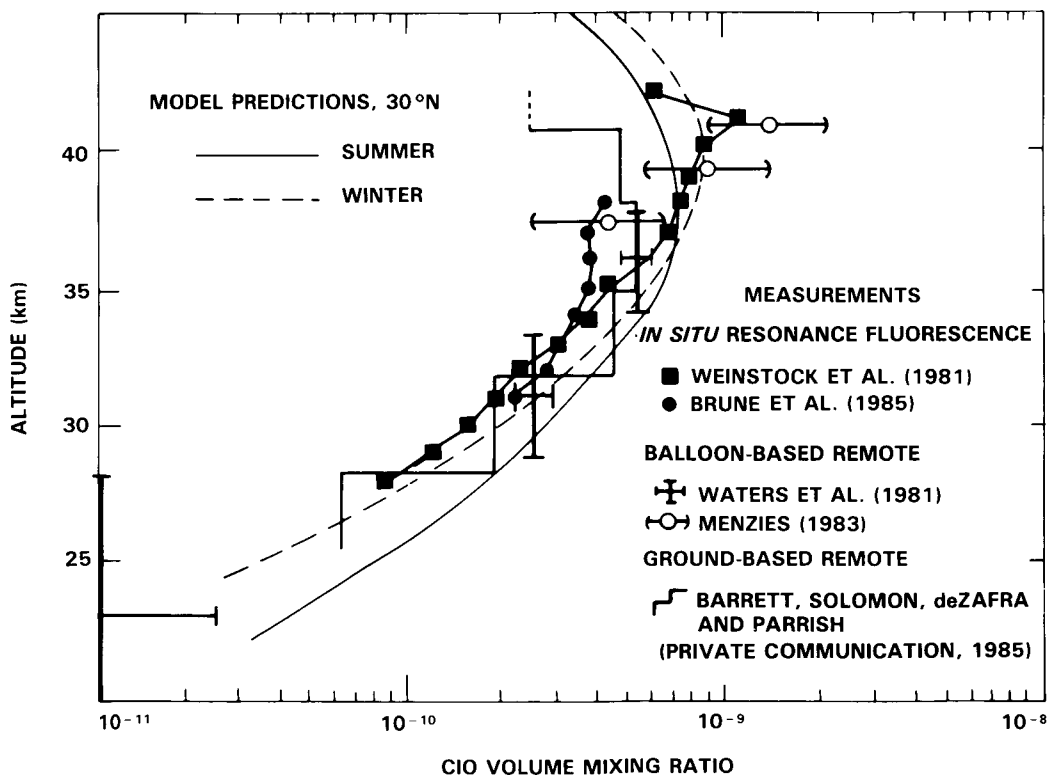
Figure 11-1. ClO vertical profiles from measurements and theoretical models. See text for details.

9 Dec. 1976 and 26 Sept. 1979; (with the omission of the anomalously high mixing ratio profiles measured on 28 July 1976 and 14 July 1977 [Weinstock et al., 1981]), and (b) a profile measured on 14 Sept. 1984 using an entirely reengineered fluorescence instrument in a repeatable reel-down mode [Brune et al., 1985]. The two anomalously high profiles measured in July of 1976 and 1977 are omitted since they have been previously discussed in the literature and represent data well outside the norm (and in the case of July 1977, exceeding the total accepted chlorine budget for the stratosphere). The points from Waters et al., [1981] were obtained from balloon-borne millimeter-wavelength heterodyne spectrometer measurements of limb thermal emission by the 204-GHz ClO line. The Menzies [1983] points are a reevaluation of earlier published data from balloon-borne infrared laser heterodyne spectrometer measurements of atmospheric absorption against the setting sun. The ground-based profile results from a deconvolution of the pressure broadened ClO spectral line shape obtained at Mauna Kea, Hawaii (20 °N) in December 1982 [Barrett et al., private communication 1985]. The data used to obtain this profile do not differ by more than 15 % from the mean of other data taken in 1982, 1983, and 1984 at Mauna Kea, although having a better overall signal/noise ratio. These data also do not differ qualitatively from line shapes obtained at 32 ° and 42 °N using the same technique and equipment. The measurements reported in Weinstock et al., Brune et al., Waters et al. and Menzies were all made at 32 °N.

Also shown in Figure 11-1 are two calculated noontime vertical profiles of ClO from the model of Ko and Sze [1984] with updated chemistry [see Appendix A]. These profiles were calculated for 30 °N latitude and solar declination angles + 20° (summer) and −20° (winter). Note the larger abundances near the peak and the shift of the profile to higher altitudes in the winter. The calculated midday ClO profiles appear to be in reasonably good agreement with the measurements as presented in Figure 11-1. Since 1981 there has been significant improvement in the agreement between measured and calculated ClO profiles, due to improved values for reaction rates.

11.1.2.2 Variations

The in situ resonance fluorescence measurements of 1976-1979 by Anderson and co-workers were reviewed in the previous Assessment Report [WMO, 1982] and in Weinstock et al., [1981]. With the exception of the anomalous data of 28 July 1976 and 14 July 1977, the remainder, all taken near local noon (whose average is given in Figure 11-1), show vertical profiles between 25 and 40 km which lie within a region whose bounds differ from the mean by about a factor of 2. According to Anderson [private communication, 1985], the standard deviation in calibration accuracy between the individual profiles evolved from about 30% in the earlier flights, to about 15% in the later ones. Table 11-1 gives statistics on the in situ ClO measurements reported in [Weinstock et al., 1981]. The standard deviation in these data, excluding the 28 July 1976 and 14 July 1977 measurements, varies from about 65% at 25 km to about 45% at 40 km. Accounting for the expected calibration uncertainty, as shown in the table, the residual standard deviation (which is the maximum that can be attributed to stratospheric ClO variability) varies between about 60% at 25 km, to 30-40% at 40 km. Figure 11-2 shows the in situ measurements from Weinstock et al., [1981] with those from the recent reel down [Brune et al., 1985] added. It is the opinion of Brune et al., that the rather different shape of the reel down profile is real and not an instrumental artifact related to the change of experimental methods.

Millimeter-wavelength ground-based measurements of ClO [Parrish et al., 1981; Solomon et al., 1984; de Zafra et al., 1985a] now extend from January 1980 to December 1984, and include data taken at 20°, 32°, and 42 °N, with observations near both the winter and summer solstices from the southernmost location.

Table 11-1. Statistics on the *in situ* ClO measurements given in Figure 2 of Weinstock *et al.,* [1981]. The mean μ and standard deviation σ are in units of ClO volume mixing ratio in ppbv. The quantity $(\sigma/\mu)_R$ is the residual relative variation after quadrature subtraction of a random calibration error having the indicated value.

		HEIGHT			
		25 km	**30 km**	**35 km**	**40 km**
WITHOUT 28 JULY 76 OR 14 JULY 77					
	mean μ	0.03	0.16	0.45	0.91
	std. dev. σ	0.02	0.08	0.20	0.40
	σ/μ	0.66	0.50	0.44	0.44
$(\sigma/\mu)_R(0.3)$	$\sqrt{(\sigma/\mu)^2-(0.3)^2}$	0.59	0.40	0.32	0.32
$(\sigma/\mu)_R(0.15)$	$\sqrt{(\sigma/\mu)^2-(0.15)^2}$	0.64	0.48	0.41	0.41
WITH 28 JULY 76 AND 14 JULY 77					
	mean μ	0.09	0.39	0.82	1.50
	std. dev. σ	0.15	0.54	0.95	2.14
	σ/μ	1.66	1.38	1.16	1.43
$(\sigma/\mu)_R(0.3)$	$\sqrt{(\sigma/\mu)^2-(0.3)^2}$	1.63	1.35	1.12	1.40
$(\sigma/\mu)_R(0.15)$	$\sqrt{(\sigma/\mu)^2-(0.15)^2}$	1.65	1.37	1.15	1.42

The results are summarized in Figure 11-3. No latitudinal or seasonal variations in column density above 30 km are discernable in these data at a level greater than ± 20% about the mean and the data set is not yet long enough in time to detect the expected 5% per year increase in ClO due to industrial chlorocarbon release. The two-dimensional model of Solomon and Garcia [1984b] predicts about ± 20% latitudinal variation in ClO concentration at the peak (~ 38 km) between the latitudes of the ground-based measurements at solstice. This model also predicts (at the peak of the mixing ratio profile) approximately 50% more ClO at 40° latitude in winter than in summer, and approximately 25% more in winter at 20° latitude. More ground-based millimeter-wavelength measurements at different latitudes and seasons would provide tests of these predictions.

A smaller overall variation exists in the ClO data base from the groundbased millimeter-wavelength technique than that from the *in situ* resonance fluorescence technique. This contrast in measured variability is illustrated in Figure 11-4 where the measured *in situ* profiles have been used to calculate millimeter-wavelength emission lines which are compared with the ground-based measurements. The origin of this difference in measured variability is not completely resolved at present, but it should be noted that the
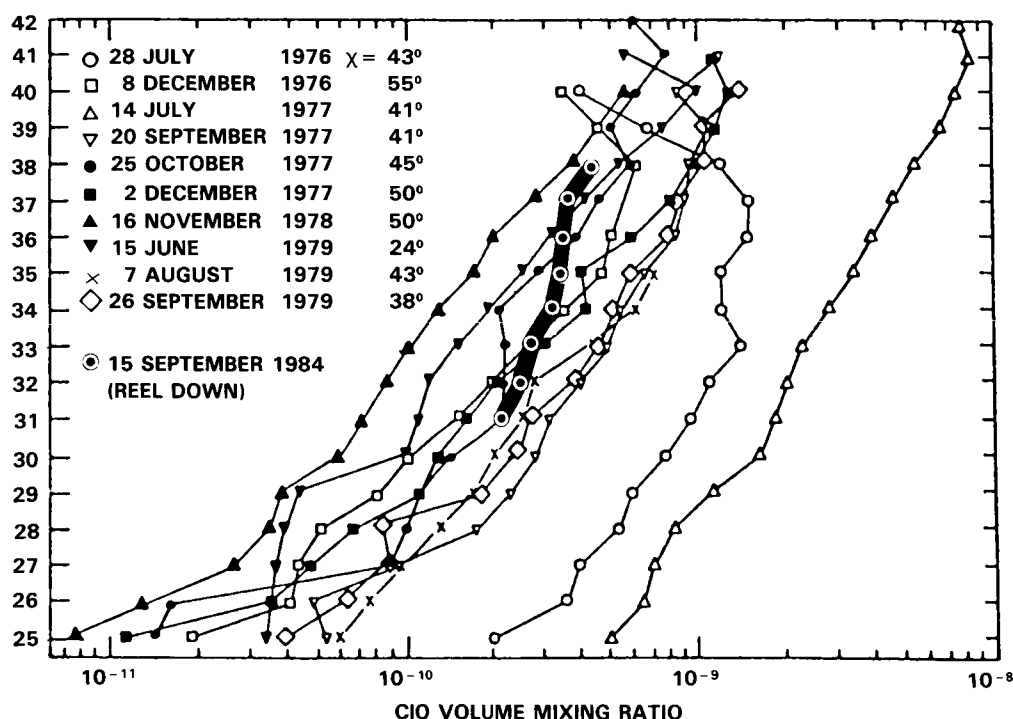
Figure 11-2. Comparison of the average reel down ClO profile of 15 September 1984 [Brune *et al.*, 1985] with earlier "fast" parachute drop profiles measured by *in situ* resonance fluorescence [Weinstock *et al.*, 1981]. Concentrations from the reel down measurement have been converted to mixing ratios using the 1976 U.S. Standard Atmosphere.

claimed accuracy for the ground-based technique is about twice that of the *in-situ*, (which is about the same as the ratio of variations in the *in situ* data set to that in the ground-based millimeter data set), and that the integration times for the two measurement techniques differ greatly. The *in situ* profile points are measured in less than a minute, whereas the ground-based millimeter wavelength measurements are averages over typical periods of several days or more.

Pyle and Zavody [1985a] and Solomon and Garcia [1984b] estimated the variability of ClO using LIMS and SAMS satellite data. Neither of these instruments made measurements of chlorine compounds. However, species which determine the partitioning among odd chlorine compounds were measured or can be derived the partitioning among odd chlorine compounds were measured or can be derived.

For example,

$$\frac{[HCl]}{[ClO]} \approx \frac{k_1 \, [CH_4] + k_2 \, [HO_2]}{k_3 \, [OH]} \times \frac{k_4[O] + k_5[NO]}{k_6 \, [O_3]}$$

$[O_3]$ and $[CH_4]$ were measured by LIMS and SAMS, respectively. $[OH]$, $[HO_2]$, $[NO]$ and $[O]$ can all be derived from LIMS and SAMS measurements of H_2O, CH_4, O_3 and NO_2 using photochemical steady-state arguments (see, for example, Pyle and Zavody [1985b]).

609
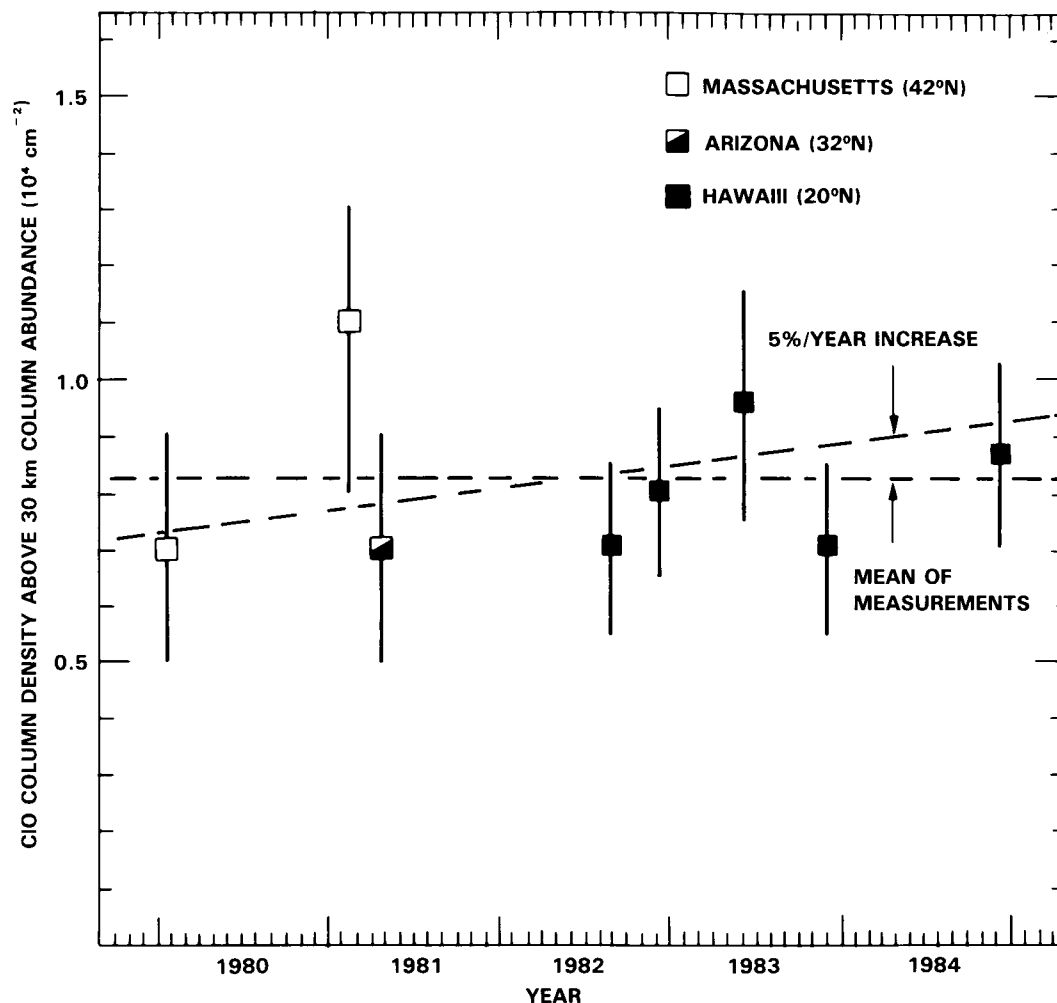
Figure 11-3. Midday ClO column abundances above 30km measured by ground-based millimeter-wavelength spectrometry [from de Zafra *et al.*, 1985a, with data for December 1984 added and a slight change in error bars on the February 1981 data]. The January-February measurements are from the 204 GHz ClO line; all others are from the 278 GHz ClO line.

Similar expressions can be used to derive the partitioning between all the odd chlorine species (Cl, ClO, HCl, HOCl and ClONO$_2$). Then, if an odd chlorine profile is specified, the partitioning can be computed for each sounding of the LIMS mission.

Taking satellite data at 32 °N, Pyle and Zavody [1985a] have estimated the variability of the derived ClO about the monthly zonal mean. Between 25 and 40 km the standard deviation of the monthly zonal mean is ~20% or less. Using all the LIMS data in 1979 (the five months from January to May) the variability of any one month about the five-month mean amounts to less than 10%.

These values are smaller than suggested by the measurements of Weinstock *et al.*, [1981] but agree well with estimates from the ground- based microwave measurements. It should perhaps be remembered
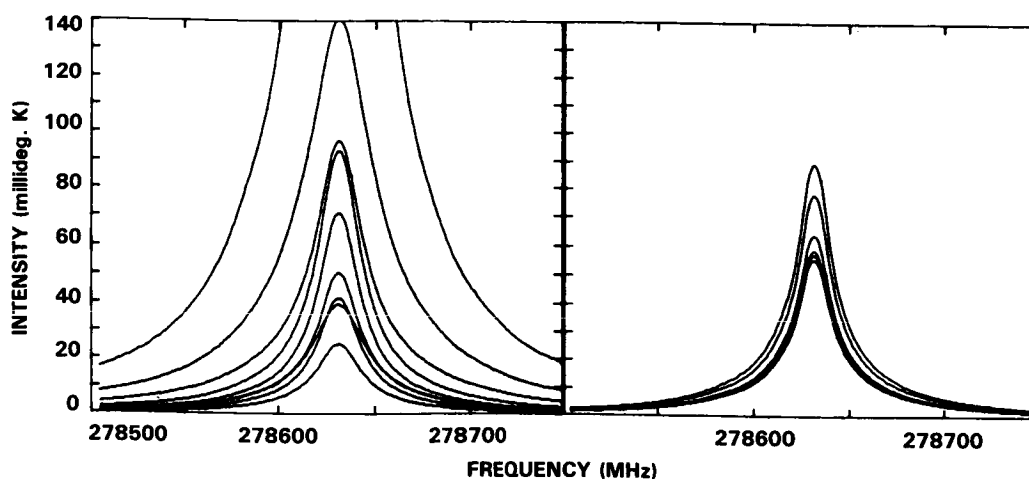
Figure 11-4.

Left: 278 GHz ClO emission lines calculated for ClO profiles measured by *in situ* resonance fluorescence between 1976 and 1979 and reported in Weinstock *et al.* [1981] (see Figure 11-2). The line of greatest intensity is for the *in situ* measurements of 14 July 1977 and the next highest is for 28 July 1976. All intensities shown here are somewhat lower than true intensities would be, because no allowance has been made for ClO above 40 km where there are no *in situ* measurements.

Right: 278 GHz ClO emission lines measured from the ground, covering observations from Massachusetts (Winter, 1980, 1981), Arizona (May 1981), and Hawaii (October, Dec. 1982, June 1983, Dec. 1983, and Dec. 1984). All lines are scaled to zenith-looking observations with no tropospheric absorption.

Essentially all of the contribution to the lines is from ClO above ~30 km, [from de Zafra *et al.,* 1985a with data for Dec. 1984 added].

that remotely sensed data are averages over a large volume of air so that small scale variability cannot be inferred. Short term local variations in methane, as indicated by balloon measurements [Ehhalt *et al.,* 1983] could possibly explain much of the variation in midday ClO observed by *in situ* resonance fluorescence [Solomon and Garcia, 1984b]. Given the scatter in the *in situ* data and calibration uncertainty, and the lack of simultaneous measurements of interacting species, however, it is at present difficult to assess the variability of stratospheric ClO from the *in situ* measurements.

11.1.2.3 Additional Results

11.1.2.3.1 Ground-Based Infrared Laser Heterodyne Measurements

An upper limit for stratospheric ClO obtained with a ground-based infrared heterodyne spectrometer measuring absorption against the sun was reported by Mumma, *et al.* [1983]. These measurements were made at the McMath solar telescope (Kitt Peak National Observatory 32 °N, 112 °W) in May and October of 1981. Three lines of ClO were searched for near 12μm (~856 cm^{-1}) with primary emphasis on the R9.5 line of ^{35}ClO at 856.50137 cm^{-1}. Measurements were made in early morning and late afternoon, to increase the absorption path length. The early morning measurements were made to establish the atmospheric spectral transmittance at a time when ClO was expected to be minimal. By comparing their

observed transmittance spectra with modelled spectra, the authors concluded that the absence of a detectable ClO line indicated the "stratospheric ClO abundance to be smaller by at least a factor of 7 than the currently accepted value" based on an average of all previous balloon-borne *in situ* measurements. This conclusion depends in part upon the assumption that the infrared line strengths and pressure broadening parameters for several nearby lines (primarily HNO_3, but also including NO_2 and OCS) are correctly known, as well as those for ClO, since the R9.5 line falls near the middle of an absorption minimum between two significantly stronger HNO_3 lines. Most of the molecular line parameters have been measured at doppler-limited spectral resolution [Maki *et al.*, 1982; Weaver *et al.*, 1983] and the early morning (no ClO) spectra are satisfactorily modelled using them.

Recently, these observations have been repeated [M. J. Mumma; J. Olivero, private communications], extending the observing period throughout the day. Preliminary analysis indicates the presence of a ClO signal in the new data, and a variation in this signal during the daylight hours when measurements were made. Hence, considering uncertainties, the ground-based infrared measurements no longer appear to be in significant conflict with all other observations as was initially thought.

11.1.2.3.2 Balloon-borne Submillimeter Measurements

Carli *et al.*, [1985] have recently reported balloon measurements of stratospheric ClO emission by the rotational transition J = 37/2 → 35/2 of ^{35}ClO located at 22.8976 cm^{-1} (686 GHz). The instrument is a Martin-Puplett type Fourier transform spectrometer [Carli *et al.*, 1984] observing thermal emission from the limb with 0.0033 cm^{-1} unapodized spectral resolution. Data were obtained from flights in April 1979 and November 1982. Assignment of the ClO feature in the spectra from these flights has recently been made possible by compilations of submillimeter spectral lines [Baldecchi *et al.*, 1984; Poynter and Pickett, 1984]. Results from analysis of this line indicate the observed ClO daytime profile is consistent with the mean of measurements discussed above to within the experimental uncertainty of approximately 50%, and also support diurnal variability in ClO as discussed below.

This submillimeter result at 686 GHz gives a total of four pure rotational lines of ClO which have now been either measured or tentatively detected in the stratospheric spectrum. Lines at 204 and 278 GHz have been measured with good signal to noise by ground [Parrish *et al.*, 1981; Solomon *et al.*, 1984; de Zafra *et al.*, 1985a] and, at 204 GHz, by balloon-based [Waters *et al.*, 1981] millimeter spectrometers. Tentative detection of an additional line at 241 GHz, as well as the 278 GHz line, were made by aircraft-based millimeter-wavelength spectrometers [Waters, *et al.*, 1979]. Results from all the rotational line measurements for stratospheric ClO are consistent to within the measurement accuracies. The positions and strengths [Poynter and Pickett, 1984], as well as the pressure broadening parameters for these transitions are known with sufficient accuracy so as to not limit the measurement interpretation. (Pure rotational line strengths can be accurately determined from the measured dipole moment and are not subject to the substantial uncertainties which often exist in experimental line or band strength values for vibrational and electronic transitions).

11.1.3 Diurnal Variation of ClO

Measurements of the diurnal variation in ClO provide a critical test of theoretical predictions of the coupling between chlorine and nitrogen/hydrogen chemistries in the stratosphere. Interpretation of such measurements is also relatively free from uncertainties caused by longer-term variations due to transport, which are more difficult to predict.

Results from ground-based millimeter-wavelength measurements of the stratospheric ClO diurnal variation [Solomon, *et al.*, 1984] are shown in Figure 11-5 and compared with predictions of theoretical models. These measurements were conducted from the Hawaii Mauna Kea Observatory (19.7 °N) during two observing periods in October and December of 1982. Approximately eight 24-hour cycles of measured emission from the 15/2→13/2 ClO rotational transition at 278.630 GHz were averaged to improve the signal to noise ratio, and the data were binned in two-hour time intervals to give the diurnal variation in ClO column density above ~30 km altitude which is shown in Figure 11-5. The observed day-to-night ratio of ClO column density is in reasonable agreement with predictions as shown in Table 11-2. However, current theory predicts approximately 50% more in the column above 30 km than measured. Agreement is also found with the predicted hour-by-hour variations except that a somewhat slower post-dawn increase in ClO is measured. The measured narrowing in the pressure-broadened line shape also qualitatively confirmed the predicted night-time disappearance of nearly all ClO below 35 km.

Data from the balloon-borne microwave limb sounder, which measures ClO by thermal emission from the J = 11/2→9/2 rotational transition at 204.352 GHz [Waters *et al.*, 1981 and 1984], have also been analyzed for the diurnal variability in ClO. The results, given in Figure 11-6, show the variation of ClO in a 4 km thick vertical layer centered at 30 km altitude, as a function of time with 1/2 hour temporal resolution, for noon through 7 p.m. on 20 February 1981 and for midnight through 11 a.m. on 12 May
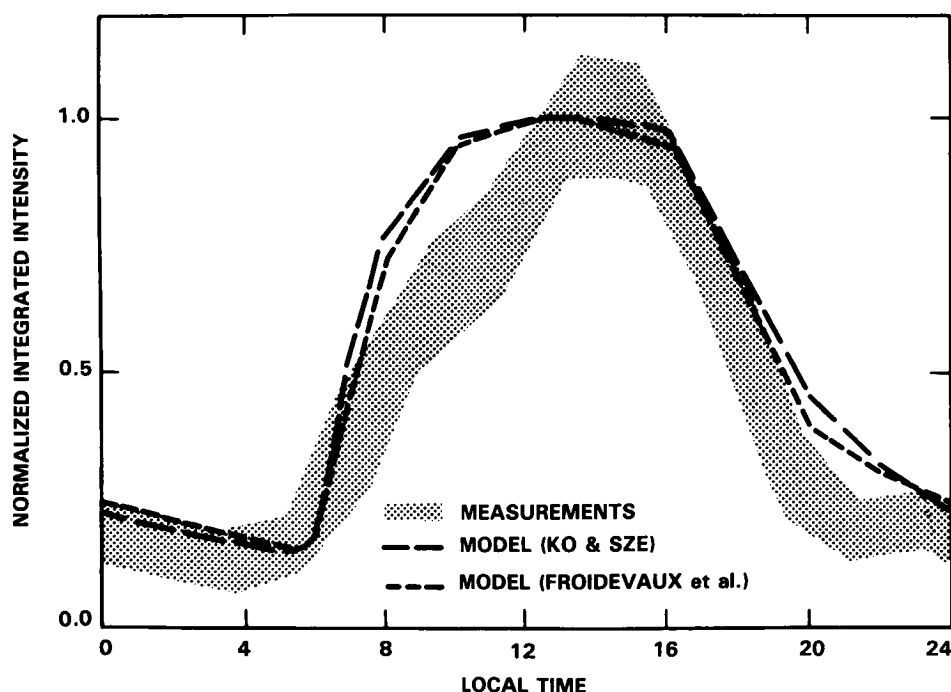
Figure 11-5. Diurnal variation of ClO measured by ground-based millimeter-wavelength spectroscopy and compared with theoretical predictions of Ko and Sze [1984] and Froidevaux *et al.* [1985a]. Measurements and predictions have both been normalized to unity at midday. Measurements were binned in two-hour intervals and smoothed; the shaded area represents estimated error limits about the mean. The measurements have been analyzed so that the normalized integrated intensity shown here is proportional to the ClO column density above ~30 km, although a small contribution from lower material is present. (From Solomon *et al.* [1984]).

Table 11-2. Day and night ClO column densities measured by ground-based millimeter measurements [Solomon et al., 1984, with correction of typographical error on quoted uncertainty for measured day column above 40 km] and calculated from the photochemical model of Ko and Sze [1984] with updated chemistry (see Appendix A). The measurements were made in October and December 1982 from Mauna Kea, Hawaii (20°N). The model results were also for winter 20°N.

	ClO column density		
	Day $(10^{13}cm^{-2})$	Night $(10^{13}cm^{-2})$	Day/Night ratio
Above 30 km			
Measurement (8–11 Oct 82)	7 ± 1	1.0 ± 0.2	7^{+3}_{-2}
Measurement (9–16 Dec 82)	7.5 ± 1	1.3 ± 0.3	5.7^{+3}_{-2}
Model	12	1.5	8
Above 40 km			
Measurement (8–11 Oct 82)	1.3 ± 0.6		
Measurement (9–16 Dec 82)	2.0 ± 0.6	1.0 ± 0.3	2.0^{+2}_{-1}
Model	2.1	1.1	1.9

1981. Comparisons with theoretical predictions show general agreement in the rate of decrease around sunset, but the observed increase after sunrise is slower than predicted. This result is similar to that from the ground-based millimeter-wavelength measurements discussed above, which cover a longer time period and a larger vertical layer.

The measured diurnal variation of ClO column density above 30 km and of local ClO around 30 km can be explained by exchange processes between ClOx (Cl + ClO) and $ClONO_2$ operating during the day (via photolysis of $ClONO_2$) and the night (via recombination of ClO with NO_2). The measured morning rise in ClO appears to be somewhat more gradual than predicted. Ko and Sze [1984] argue that this observed feature rules out the possiblity of any appreciable formation of $ClNO_3$ isomers such as $ClOONO$ or $OClONO$ which are expected to have shorter photolytic lifetimes than $ClONO_2$. Laboratory studies [Margitan, 1983; Cox et al., 1984] have recently demonstrated that $ClONO_2$ is the sole product from the recombination of ClO with NO_2. The apparent experimental evidence of a postdawn rise in ClO even slower than that predicted from photolysis of $ClONO_2$ may be, at least in part, an effect due to advection by stratospheric zonal winds across the day-night terminator [Ko and Sze, 1984].
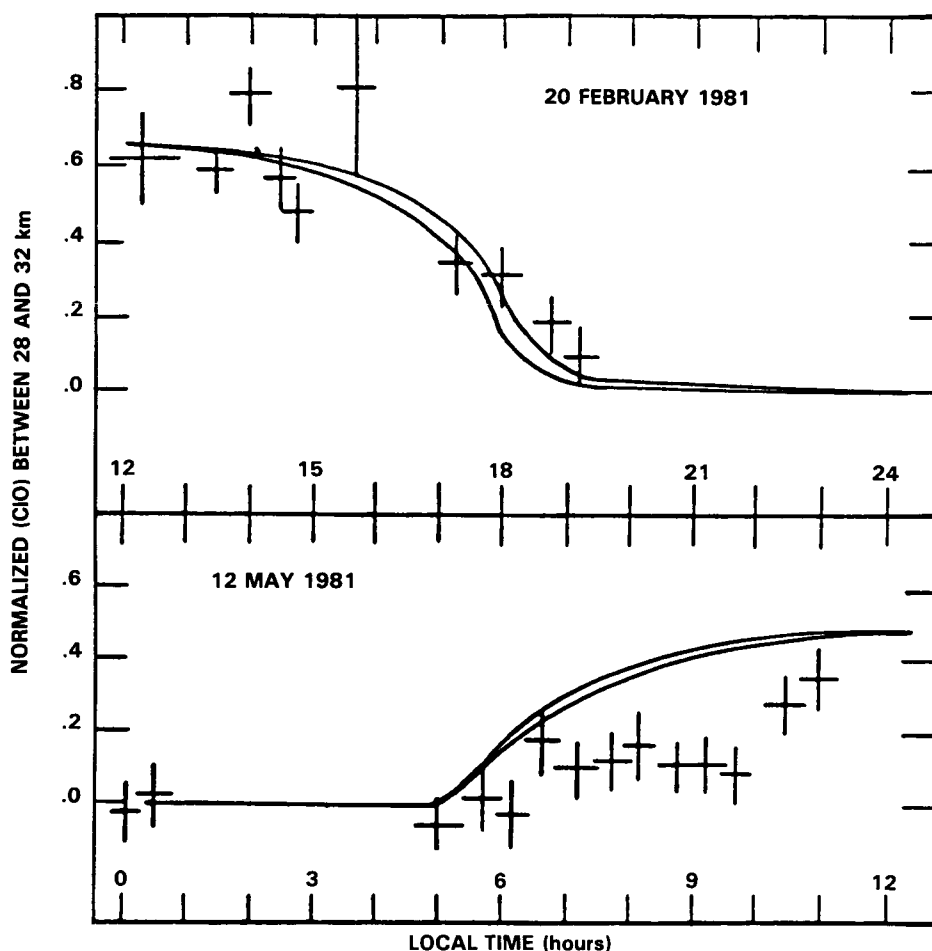
Figure 11-6. Diurnal variation in ClO measured by balloon-borne microwave limb sounding (crosses) on two flights (from Palestine, TX, 32°N) and compared with theoretical predictions (curves). The vertical scale is an average of the measured brightness temperature of the 204 GHz line which is proportional to the abundance of ClO between heights of approximately 28 and 32 km. The vertical bars on the measurements are ±one standard deviation of instrument noise. The two theoretical curves for each flight are normalized to noon and are for the same latitude and solar conditions as the measurements, but for 6 km thick layers centered, respectively, at 29 and 31 km altitude. [From Froidevaux *et al.*, 1985a].

The observed diurnal variation of about a factor of two (see Table 11-2) in ClO above 40 km, however, is not explained by $ClONO_2$ chemistry alone. Ko and Sze argue that formation of HOCl via the recombination of ClO with HO_2 can provide an additional nighttime sink for upper stratospheric ClO, while photolysis of HOCl can enhance daytime ClO above 40 km. These effects are included in the model whose results are given in Table 11-2.

Measurements of the diurnal variation in the *shape* of the ClO vertical profile, with better vertical resolution and coverage than is available in the diurnal data to date, would provide important additional tests of the theoretical models. The capability of such measurements now exists with the recently-developed *in situ* reel-down technique whose initial results are given by Brune *et al.*, [1985] and a 10x improvement

615

in the sensitivity of the balloon microwave limb sounder [Waters *et al.*, 1984] which was flown successfully in May 1985 obtaining data over a full diurnal cycle.

11.2 ATOMIC CHLORINE (Cl)

Chlorine atoms have been directly measured in the stratosphere only on two occasions (on July and December 1976), betwen ~35 km and 42 km altitude [Anderson *et al.*, 1977, 1980; NASA RP 1049, 1979]. The technique employed was *in situ* resonance fluorescence. The extremely low concentration of Cl make the observations very difficult. Current models (e.g., Ko and Sze [1984]) predict a Cl-atom concentration which is within a factor of two of these measurements, which can be considered as satisfactory agreement particularly in view of the sparcity of the data.

Indirect information on the Cl-atom profile below 35 km has been obtained from ethane (C_2H_6) measurements [Rudolph *et al.*, 1981], since the main stratospheric sink for this hydrocarbon is reaction with atomic chlorine. No new stratospheric ethane measurements have been reported since the time of the last assessment (1981). Figure 11-7 shows the existing C_2H_6 data together with a calculated profile, which was obtained by Ko and Sze [1984] with a 1-D model. The agreement is significantly better than with the older models [WMO, 1982] which overestimated the OH abundance in the lower stratosphere.

11.3 CHLORINE NITRATE ($ClONO_2$)

Chlorine nitrate ($ClONO_2$) is predicted to be a major temporary reservoir of chlorine in the middle stratosphere (25-35 km). It is formed by the recombination of ClO with NO_2 and removed in the daytime by photolysis. Chlorine nitrate plays several important roles in stratospheric chemistry. For instance, the observed diurnal variation of ClO (as discussed in the ClO section) is thought to be driven mainly by $ClONO_2$ chemistry. Formation of $ClONO_2$ also leads to strong coupling between the stratospheric chlorine
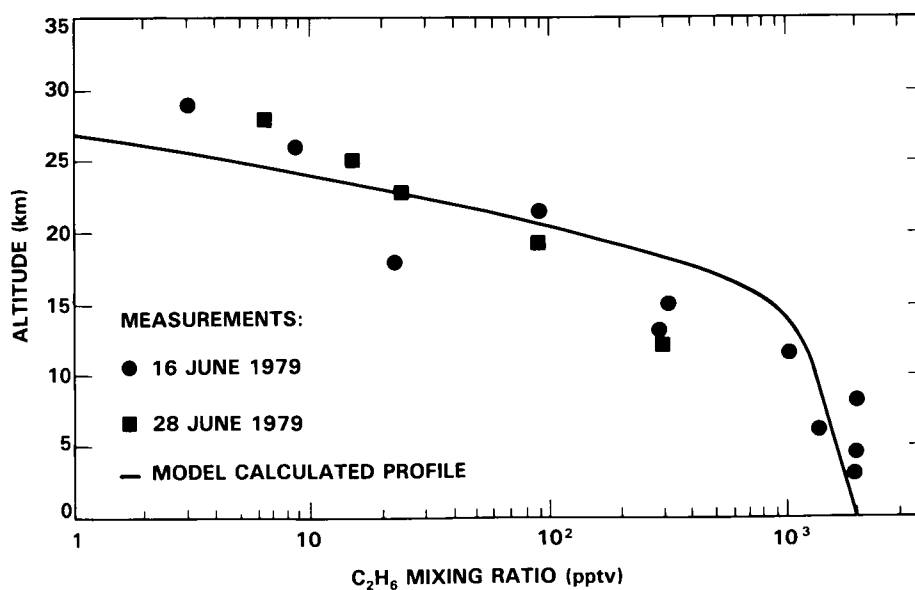
Figure 11-7. Comparison of C_2H_6 measurements [Rudolph *et al.*, 1981] with a one-dimensional calculation [Ko and Sze, 1983].

616

and nitrogen cycles. At high concentrations (> 12 ppbv) of stratospheric chlorine, this coupling involving $ClONO_2$ chemistry could lead to highly nonlinear response of ozone to chlorine perturbations (see Chapter 13 for a discussion of nonlinear chemistry). Measurements of $ClONO_2$ are not only important for better understanding of stratospheric chemistry, but also for the assessment of impacts on ozone of chlorine perturbations.

Evidence for the presence of chlorine nitrate ($ClONO_2$) in the lower stratosphere has improved during the period since the previous assessment report. The first claimed detection [Murcray et al., 1979] was based on measurements of the $ClONO_2$ band at 1292 cm^{-1}. This occurs in a spectral region of strong, closely spaced absorptions of several of the minor gases, making the positive identification and quantitative analysis of $ClONO_2$ very difficult. More recently, the same group has reported the results of balloon observations of the Q-branch of the longer wavelength band at 780 cm^{-1} [Rinsland et al., 1985b]. This feature, while still contaminated by weak absorptions of CO_2 and O_3, is generally more suitable for analysis. The necessary laboratory work to establish the frequencies and strengths of the interfering lines has been done, so as to allow the identification of residual $ClONO_2$ absorption to be made with confidence. The vertical distribution of $ClONO_2$ determined from these observations is reproduced here and found to be in reasonable agreement with model calculations (Figure 11-8).
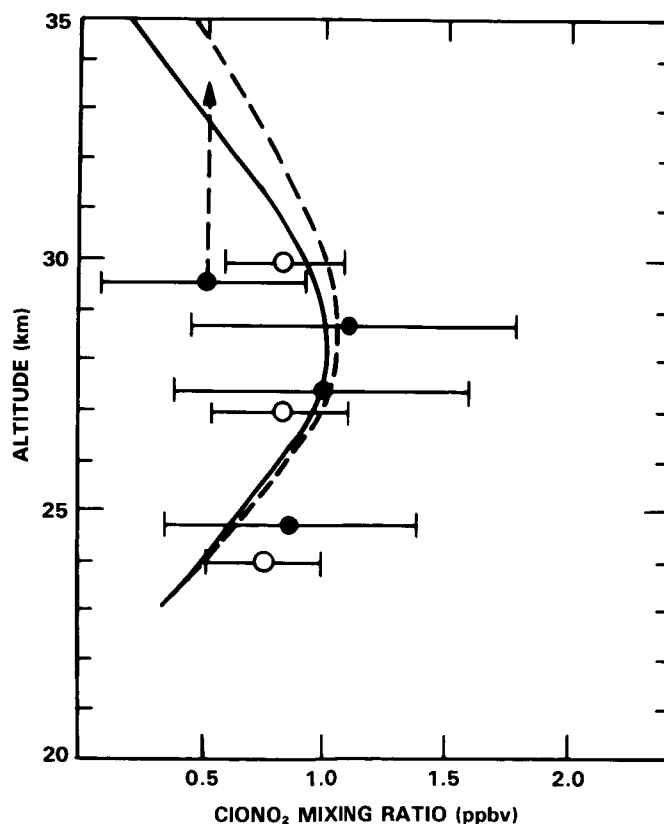
Figure 11-8. Mixing ratio profile of $ClONO_2$. The open circles are from Murcray et al. [1979] and the closed circles from Rinsland et al. [1985b]. Both sets of measurements were made at 33° N latitude. Model results corresponding to 30° N for noon (——) and sunset (— —) are from Ko and Sze [1984], calculated with updated chemistry (Appendix A).

617

The quantitative analysis of $ClONO_2$ at relative concentrations less than 10^{-9} by volume requires data of very high resolution and signal-noise ratio, and is hampered by the need to model the spectral structure of the Q-branch absorption from laboratory measurements which have been made under very different partial pressure conditions than occur in the stratosphere. Nevertheless within the realistic errors given with the profile derived by Rinsland *et al.* [1985b], it appears that the measured $ClONO_2$ distribution is in reasonable agreement with model predicitions. It is noted here that, at the time of writing, a preliminary examination of the ATMOS spectra obtained during the May 1985 Spacelab-3 flight confirms the presence of the $ClONO_2$ feature at 780.2 cm^{-1} [C. B. Farmer, private communication].

11.4 HYDROGEN CHLORIDE AND HYDROGEN FLUORIDE (HCl, HF)

11.4.1 Introduction

HCl has sources in both the troposphere and stratosphere; the principal tropospheric source is natural - the interaction between SO_4 and NO_3 ions and NaCl in ocean spray - although some tropospheric HCl originates from burning of plastics and from certain industrial processes. By contrast, the stratospheric source is primarily anthropogenic, (photolysis of halocarbons) with a minor fraction resulting from the reaction of OH with CH_3Cl released from the oceans and burning vegetation, and from direct injection of HCl into the stratosphere from volcanic eruptions. We thus expect HCl to show a characteristic vertical distribution having a minimum in the upper troposphere and lower stratosphere. The variability in this distribution might be expected to reflect the distribution of its surface sources, as modified by circulation and temperature, its sinks (primarily rainout) and perturbations to the stratospheric steady state chemistry resulting from volcanic activity.

HF, while in many ways the analog of HCl, differs from HCl in the respect that its source is stratospheric and (as far as is known) anthropogenic involving only the photolysis of halocarbons. HF has no known tropospheric source of significance. Thus monitoring the relative abundances of HCl and HF can provide the means for distinguishing between the man-made and the natural components of the stratospheric halogen burden and their variation with time. In addition, the ratio of HCl:HF provides an indirect check on stratospheric OH.

Almost all of the measurements of HCl and HF have been made by remote sensing spectroscopic methods, both at near IR wavelengths (by absorption) and, more recently, in the far infrared (by emission). Because the infrared spectrum of these gases is relatively simple and well understood, the techniques for their measurement have been developed to the point where a comparatively high level of precision and absolute accuracy can now be achieved. The situation regarding the shapes of the vertical distributions of HCl and HF, and the variability in their total column abundances, has improved considerably over the past three or four years. Current understanding of stratospheric HCl and HF is reviewed here under the headings of the vertical profile of concentration, latitude distribution, seasonal effects, temporal variation, and the effects of volcanic activity.

Measurements of stratospheric HCl have been made since 1975. Apart from the early *in situ* measurements of total acidic chlorine by filter collection techniques [Lazrus *et al.*, 1976], the available data have almost exclusively been obtained from spectroscopic observations of the 1-0 vibration-rotation band at around 3000 cm^{-1} (3 μm), with the recent addition of far infrared emission measurements of pure rotation lines in the frequency range from 40 to 160 cm^{-1}.

Since the time of the last assessment (1981) there have been a number of additional studies of HCl from the ground, from aircraft and from stratospheric balloons. These include the accumulation of data on the total HCl column density and its variability from ground-based sites, aircraft surveys of the latitude dependence of the stratospheric HCl component, and extensive profile and column measurements made at 32 °N latitude during the two international Balloon Intercomparison Campaigns (BIC-1 and -2) in 1982 and 1983.

The improvement in the experimental techniques and the corresponding data quality achieved during these more recent investigations have yielded results which are of sufficient precision to reveal variability over a variety of spectral and temporal scales, including a systematic latitude dependence. The data from the balloon observations of June 1983 (BIC-2) provide a stratospheric vertical concentration profile (for the particular latitude and season) with an estimated accuracy of $\pm$ 15% over most of the 18 to 40 km altitude range - a considerable advance over the confidence that could be attached to the mean HCl profile given in the previous assessment. This result includes agreement between the data obtained from five different experiments, three of which were carried on the same gondola, (i.e., observing the same airmass).

The magnitude of the variability of HCl, seen particularly in the total column data taken from the surface, is too large to allow a long-term trend in the total HCl abundance to be established with confidence. However, the groundbased and aircraft results are in apparent disagreement in this regard. These separate aspects of the current status of knowledge of HCl in the atmosphere are discussed in detail in the following sections.

11.4.2 Hydrogen Chloride (HCl)

11.4.2.1 Vertical Concentration Profile

The large uncertainties and the wide spread of possible values associated with the mean vertical mixing ratio profile in the 1981 assessment report resulted from the fact that the data were obtained from a variety of different experimental methods and that the observations were made at different latitudes and seasons. From the earliest ground-based measurements of the total column abundance of HCl [Farmer et al., 1976] and the aircraft observations of the column above about 12 km by Mankin and Coffey [1983] it was apparent that the HCl concentration is variable both temporally (on relatively short time scales) and spatially (i.e., latitudinally, see later). It was not known to what extent the large spread of data combined into the 1981 profile was due to this variability as opposed to systematic differences between the results of techniques which had not been carefully intercompared. It was for this reason, together with the importance of HCl in the overall knowledge of the characteristic properties of the present stratosphere, that HCl was chosen as one of the principal molecular species for inclusion in the international Balloon Intercomparison Campaigns (BIC), which were conducted in fall of 1982 and summer of 1983. Although there have been additional observations of the stratospheric mixing ratio profile of HCl in the time period under consideration here, it is from the BIC observations that significant progress in obtaining high precision and confidence in the stratospheric vertical distribution has been obtained and which, in turn, has allowed the effects of experimental uncertainty and natural variability to be separated.

Figure 11-9 shows the individual concentration profiles obtained from the BIC-2 measurements [Farmer et al., private communication 1985]; details of the instruments and their observation modes are given in the figure caption. Three of the five profiles were obtained from instruments carried on the same gondola (i.e., observing the same airmass); these were the near-IR absorption measurements of AES and ONERA, and the far infrared emission results of SAO. The remaining two BIC profiles (from the UL absorption
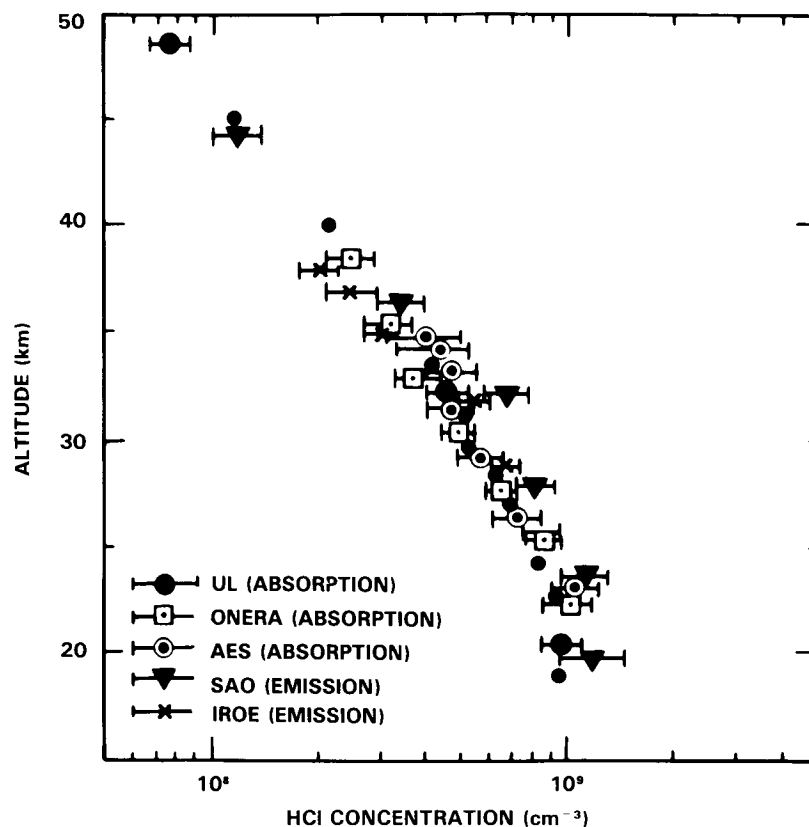
Figure 11-9. Results of measurements of the vertical distribution of HCl from BIC-2. The University of Liege (UL) and the Office National D'Etudes et de Recherches Aerospatiales (ONERA) data were obtained by absorption spectroscopy using grating instruments. The Atmospheric Environment Service, Canada, (AES) measurements were also by absorption, but used a Michelson Interferometer. The Smithsonian Astrophysical Observatory (SAO) and the Instituto di Ricerca sulle Onde Electromagnetiche (IROE) measurements were both made in the far infrared by emission, using high resolution Michelson Interferometers. The five instruments were carried on three separate flights (see text). The error bars represent the estimated errors from all sources except the uncertainty in the values of the molecular spectroscopic constants.

and the IROE emission measurements) were obtained on separate flights, one on the same day and one 3 days before the 3-instrument flight. The meteorological observations of the stratosphere made during the period of time covered by these flights indicate that all of the profile measurements sampled the same atmospheric parcel, so that differences between the profiles arising from any short-term or spatial variability are minimized.

The estimated final accuracies of the profiles are included in Figure 11-9. The weighted mean profile derived from the combination of all of the data is shown in Figure 11-10 together with the extreme values required to emcompass all of the estimated errors. The maximum uncertainty in the profile is not expected to exceed $\pm 15\%$. Figure 11-11 shows the same mean distribution in terms of volume mixing ratio together with the earlier (1981) profile for comparison. It should be noted that the observations of HCl made thus far have not been able to reach high enough altitudes to locate a maximum in the volume mixing ratio of HCl as a function of height.
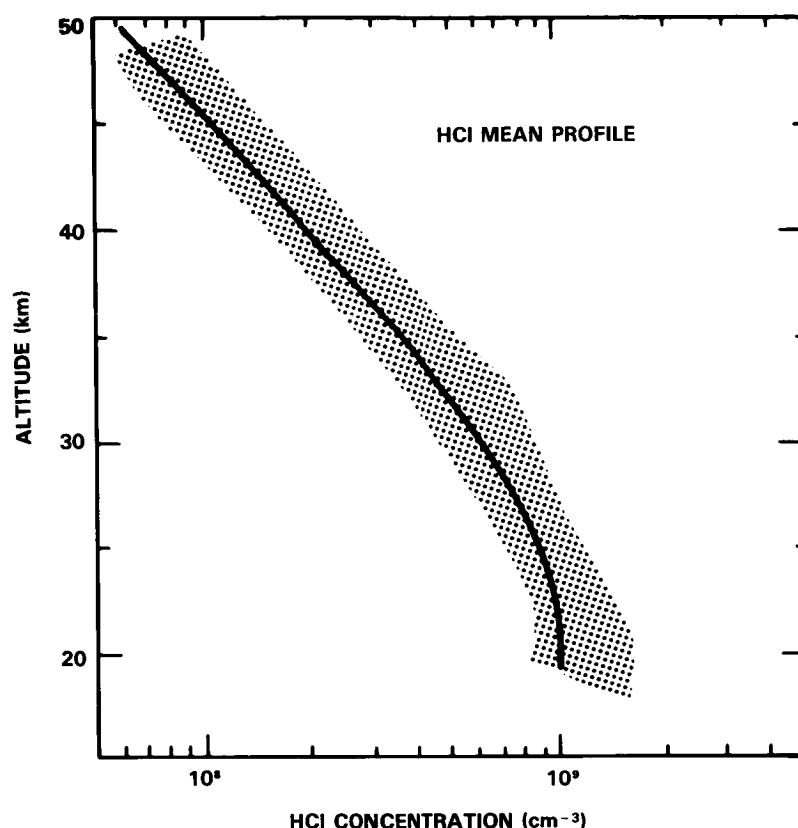
Figure 11-10. Weighted mean profile of concentration of HCl from data of Figure 11-9 (solid line). The hatched area represents the envelope of the estimated errors of all of the individual measurements.

The BIC-1 flights, which were made in late 1982 and involved some of the instruments used for BIC-2, gave profiles which were generally similar to the BIC-2 results but were associated with rather larger errors and uncertainties. The mean of the BIC-1 data gives a profile on the high side of the BIC-2 profile by about 20%, suggesting a marginally significant decrease from fall-winter of 1982 to the summer of 1983.

Observations of the vertical distributions of HCl are not only important for diagnosing certain key aspects of stratospheric chlorine chemistry, but also important for defining the stratospheric chlorine budget. The abundance of HCl in the upper stratosphere, for instance, is often taken as an approximate measure of total chlorine in the stratosphere. Since HCl is an inactive form (towards destruction of O_3) of stratospheric chlorine, its abundance relative to other active chlorine species (e.g., ClO) provides important clues to the efficiency of chlorine catalysis of ozone removal.

Plotted in Figure 11-11 is a theoretical profile of HCl calculated by Ko and Sze [1984] with updated rate data (see Appendix A). The model profile corresponds to summer conditions at 30 °N latitude. Comparing with the BIC data, the calculated concentration of HCl at around 30 km is about a factor of 2 lower. The agreement, however, is much better at around 20 and 40 km, where $ClONO_2$ is expected to be a minor form of chlorine. Interestingly, the observed HCl concentrations are closer to the sum of the calculated HCl and $ClONO_2$ concentrations. One possible interpretation of the HCl data is that models might have overestimated the abundance of stratospheric $ClONO_2$. However, $ClONO_2$ in amounts comparable to those
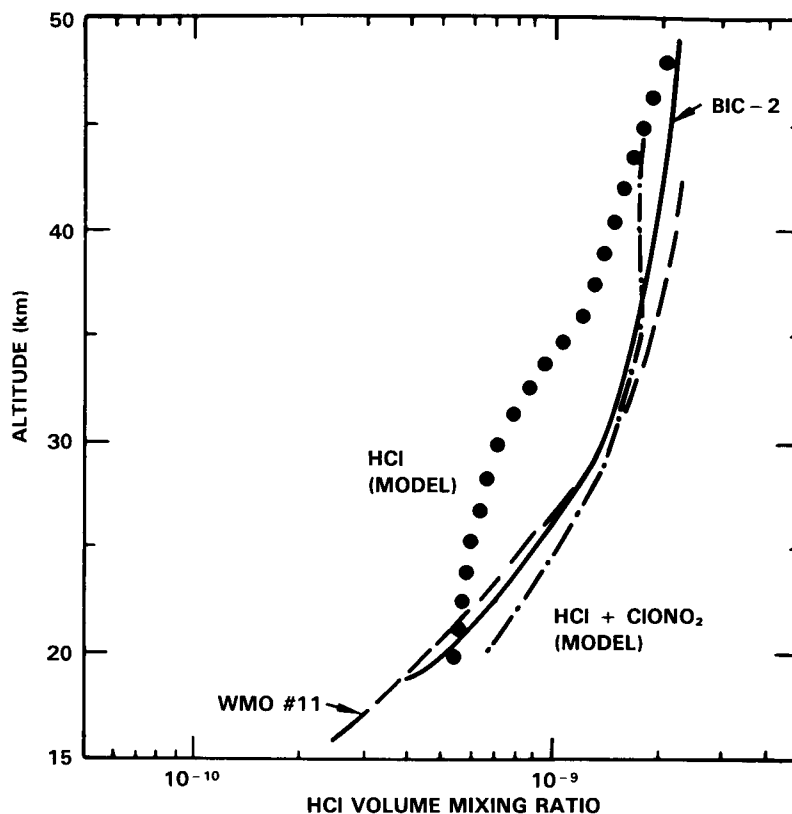
Figure 11-11. The weighted mean profile from Figure 11-9 reproduced as HCl mixing ratio by volume (——) BIC-2 and compared with the mean profile of the last assessment (---), and the model prediction of Ko and Sze [1984] for HCl (•••) and for HCl + ClONO₂ (·—·—).

predicted by models is needed to account for the observed diurnal variation of ClO (see Section 11.1.3). Another possible interpretation is that models might have underestimated the total stratospheric chlorine (Cl_x) burden. But higher total Cl_x would imply too much ClO in the model compared with observations (see Section 11.1.2). If this discrepancy persists, it could have serious implications for stratospheric chemistry and/or the chlorine budget. However, the discrepancy is not very significant at present, considering the lack of data on variability and on simultaneous observations for HCl, $ClONO_2$ and ClO.

11.4.2.2 Latitude Distribution of the Stratospheric Column

Whereas balloons have the advantage of altitude over other platforms for obtaining vertical profiles from limb scanning, they are generally not suitable for measurements of latitude distributions because they can be launched at only a few locations. Aircraft, on the other hand, can operate over a wide geographic range, and can cover a large range of latitude in a few days. Such measurements are extremely useful for understanding meridional transport. Aircraft observations, however, being made from below the bulk of the stratospheric HCl, are unable to obtain the detailed distribution of HCl in the stratosphere, although some information on the distribution is available in the variation of line of sight amount of absorber with observation angle. Since aircraft cannot reach altitudes at which the HCl concentration peaks, remote sensing methods from aircraft are required for measuring the latitudinal distribution of stratospheric column HCl.

Two groups, Girard and his colleagues [Girard *et al.*, 1978/79, 1982, 1983] and Mankin and Coffey [1983, 1984] have used spectrometers flown on aircraft to measure column HCl.

Girard *et al.*, made a series of nine flights in April and May of 1980, covering the latitude range from 62 °N. to 60 °S. They report the total vertical column of HCl and HF, along with several other trace gases, above, the flight altitude of 11.5 km. The analysis is based on measurements of the R2 line of $H^{35}Cl$ at 2944.92 cm^{-1}. Their results, which have an estimated precision of 15% and an estimated accuracy of 25%, show a minimum, below their detection limit of 0.8 x 10^{15} molec-cm^{-2}, at the equator, rising in both hemispheres. Their maximum value of 3.0 x 10^{15} is observed at 60 °N. [Girard *et al.*, 1983]. An earlier analysis of the same data [Girard *et al.*, 1982] was based on older values of the line parameters both for HCl and for interfering species, principally CH_4; these results have been superseded by the newer analysis and should be disregarded [N. Louisnard, private communication].

Mankin and Coffey [1983] made flights in both winter and summer over a five year period from 1978 through 1983, covering the Northern hemisphere only, from the equator to 70 °N. Their estimated precision and accuracy are 10% and 25% respectively. Generally their values are lower than those of Girard *et al.*, except that at 4.6 °N. they report a column of 0.54 x 10^{15} and at 6.1 °N. a value of 0.97 x 10^{15} molec-cm^{-2}. On average, their values are 45% lower than those of Girard *et al.* [1983]. The shape of the distribution is very similar to the findings of Girard *et al.*, Mankin and Coffey find that their data fit the equation

$$[HCl] = (3.41 - 2.77 \times \cos(\phi)) \times 10^{15} \text{ molecule cm}^{-2}$$

where ϕ the North latitude.

Figure 11-12 shows the aircraft measurements of the column amounts for both HCl and HF. In addition, the column amounts predicted by two different models are shown. There is good agreement between models and measurements for the shape of the latitude distribution, although there is still some question about the magnitudes of the values. We can conclude that the latitude distribution of HCl shows a minimum in the tropics and a strong latitude gradient to a value at 60-70° which is three or four times the tropical value. It is difficult to explain the difference in magnitude of the HCl column in the two similar experiments. Both experiments use a spectroscopic technique, Girard, a grille spectrometer and Mankin and Coffey a Fourier transform spectrometer; Mankin and Coffey have better spectral resolution (0.06 cm^{-1} as opposed to 0.15 cm^{-1}). Mankin and Coffey analyze two lines, R_1 and R_2, and both lines give comparable results. The differences in the two data sets are less than the errors in absolute accuracy, but many of the systematic errors should be common to both.

11.4.2.3 Temporal Variability of the Stratospheric Column

11.4.2.3.1 Seasonal Effects

The only data for stratospheric HCl obtained with a single instrument, which are extensive enough to allow any variation of HCl with season to be discerned, are the aircraft measurements of Mankin and Coffey [1983]. Their measurements were made in winter (December through early February) or in summer (late June and July) in the Northern hemisphere. There is some tendency for the summer measurements to be higher in total column, particularly at the higher latitudes, but the effect is small and it is difficult to distinguish the seasonal effects from the short-term variability. Zander (private communication, 1985)
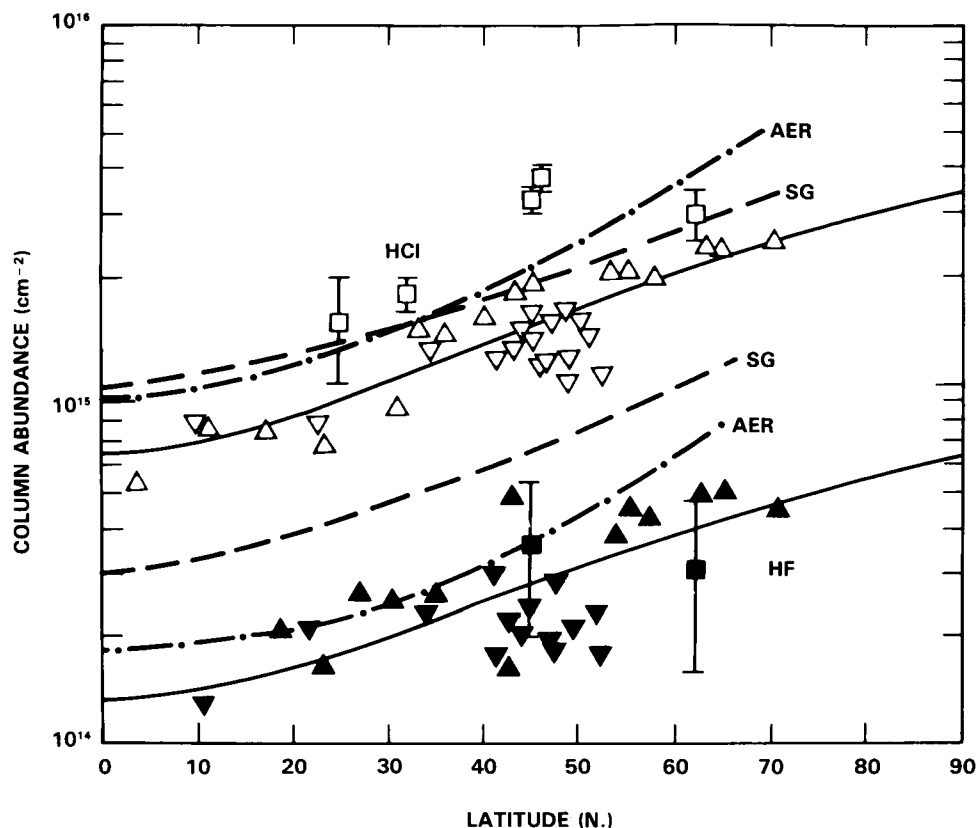
Figure 11-12. Latitude variation of the stratospheric column abundance of HCl and HF. The open and closed symbols correspond respectively to HCl and HF. The triangles are data from the aircraft measurements of Mankin and Coffey [1983], and the squares from Girard *et al.* [1983]. The solid lines are parametric fits to the Mankin and Coffey data (see text). The dashed lines are model predictions: AER from Ko *et al.* [1985], and SG from Solomon and Garcia [1984b].

has a long time series of observations of total column of HCl from the Jungfraujoch; here the stratospheric effects are somewhat obscured by variability in the tropospheric column (see discussion below), and no seasonal effects are clearly shown. Model calculations indicate that the HCl abundance should be smaller in the summer because of the larger amounts of OH corresponding to higher insolation. The seasonal variation should be small at equatorial latitudes and perhaps as large as 40% at high latitudes.

11.4.2.3.2 Short-Term Variability

When the aircraft data of Mankin and Coffey are corrected for the latitude dependence of the column amount above the cruising altitude of 12 km, the results show day-to-day differences which exceed the precision of the individual measurements, indicating some short-term variability of the stratospheric HCl burden. The authors note that, when interpreting their results in terms of both latitudinal and temporal variability, the residuals in the analysis are irregular; this may reflect monthly or seasonaly variability but will require further observations for a satisfactory description.

Figure 11-13 shows monthly means of the total HCl column content as deduced from observations carried out at the Jungfraujoch Station, Switzerland (3580 m altitude: 46.65° N; 8.0° E) between 1977 and 1984 [Zander, 1985]. Referring to that figure, the scatter of the arithmetic means (full points) is a direct indication of the variability of the total column of HCl on a monthly time scale. Furthermore, as the vertical bars between arrows correspond to the observational and analytical errors while their full amplitudes show the rms dispersions of the observations about the monthly arithmetic means, the differences between these two amplitudes are direct indications of the HCl variability on a day-to-day time scale. HCl column variations above the Jungfraujoch as large as 30% have been observed among measurements made during the same day.

Other, less extensive series of measurements from the ground-based sites have been made - e.g., at the Kitt Peak National Observatory, Tucson, Arizona, USA (hereafter KPNO: 2064 m altitude; 31.95° N; 111.60° W) and at the Observatoire de Haute Provence, Chiran, France (hereafter OHP: 1905 m altitude; 43.88° N; 6.18° E). The result of these measurements support variabilities of similar amplitudes as those observed above the Jungfraujoch [Zander and Johnson, private communication; Marche and Meunier, 1983].

In summary, the ground-based measurements show larger and more frequent changes in the total atmospheric content, on various time scales, than do the data for the stratosphere only. This result indicates that the tropospheric component of HCl is of significance relative to the total abundance both in quantity and in its variability.
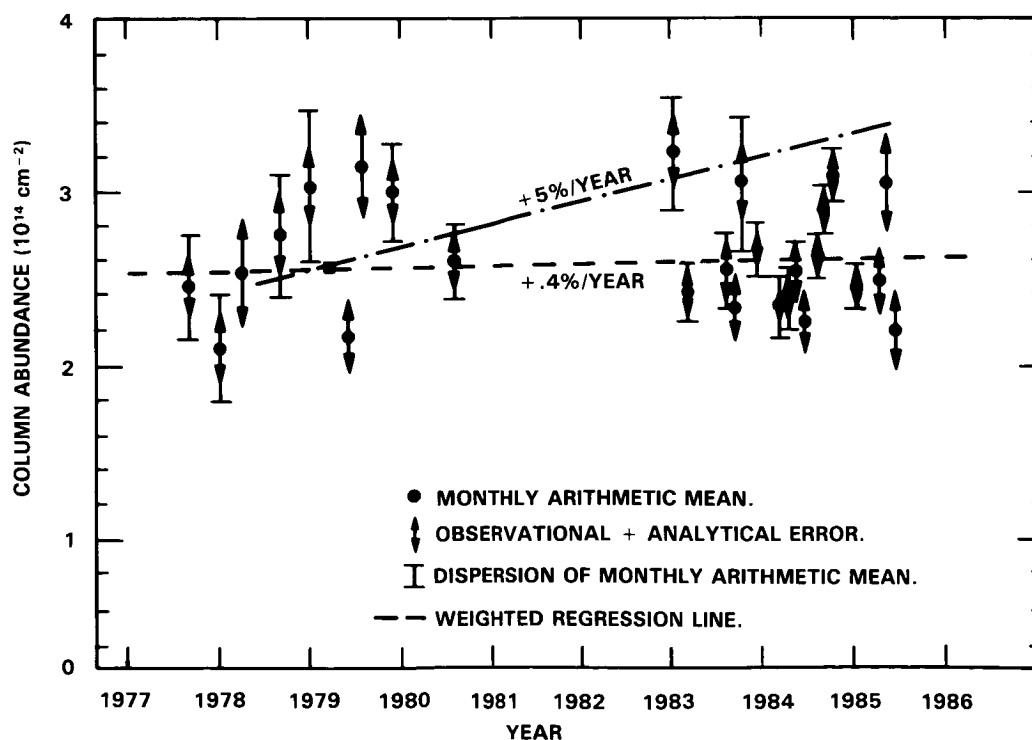
Figure 11-13. Observations of the total atmospheric column abundance of HCl over the Jungfraujoch Scientific Station from 1977 to 1984 (from Zander, [1985]).

The first measurements in which an attempt was made to separate the tropospheric and stratospheric components were those of Farmer *et al.* [1976]. Their results indicated (as expected) a small scale height for tropospheric HCl, coupled with day-to-day variability of as much as a factor of 2. Recently, Vierkorn-Rudolph *et al.*, [1984] have reported on vertical profiles of hydrogen chloride in the troposphere. Their paper gives an idea of the background values of gaseous HCl in the mid-troposphere, between 1 and 7 km altitude. The mean results deduced from their *in situ* samplings by airplane, at 3 different locations, are reproduced on Figure 11-14. Although the data are far from being representative, they show that mixing ratios of 50 to 100 pptv are not unusual over the whole 3 to 7 km range. In air masses not influenced by continental sources, below 3 km, the variations are larger, with maximum values of up to 500 pptv. It is worth noticing here that Marche and Meunier [1983], investigating variability observed over OHP during June 1981, suggest that the total HCl could be inversly correlated with the tropopause height.

TROPOSPHERIC HCl

O	TROMSO, NORWAY	09/06/81
□	TROMSO, NORWAY	09/08/81
△	TROMSO, NORWAY	09/10/81
◇	W. MEDITERRANEAN	12/06/81
○	ZARAGOZA, SPAIN	12/08/81

ALTITUDE (km)

HCl MIXING RATIO (ppbv)
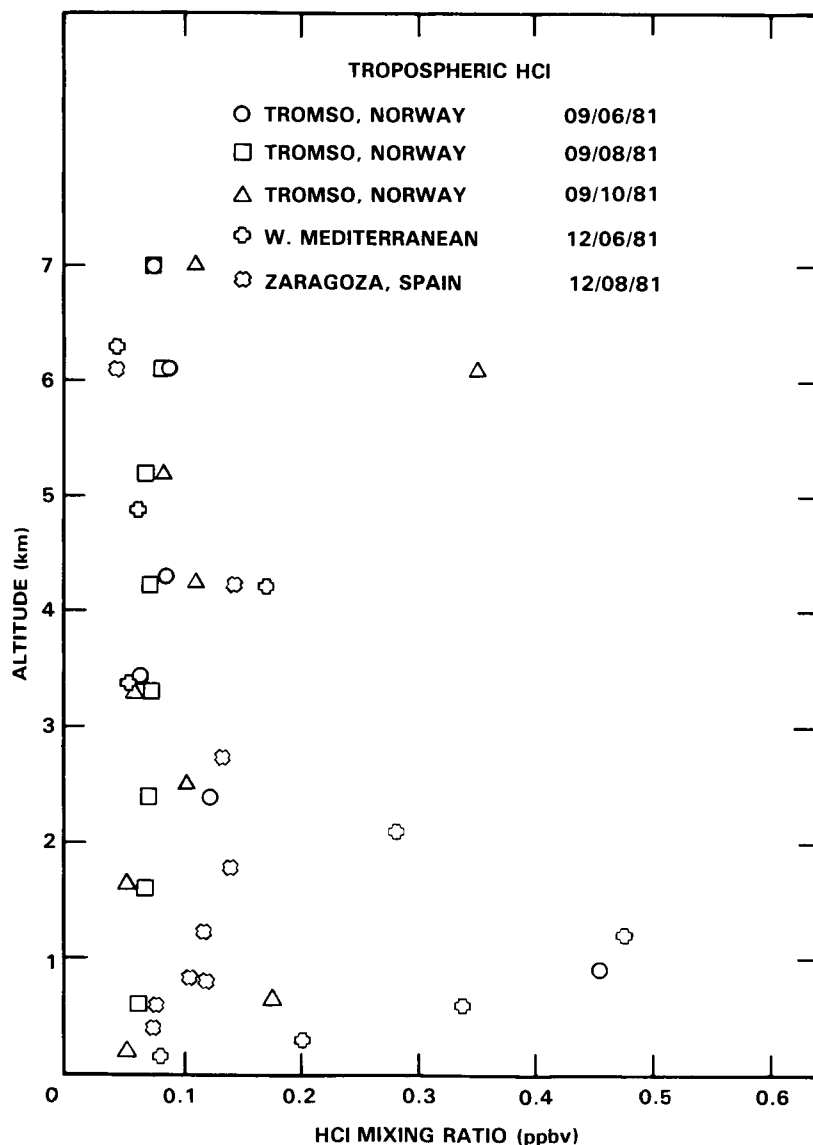
Figure 11-14. *In situ* measurements of the volume mixing ratio of tropospheric HCl at three locations (from Vierkorn-Rudolph *et al.* [1984]).

11.4.2.3.3 Long-Term Trend in HCl

On the basis of balloon observations carried out in May 1976, October 1978 and September 1979, Zander [1981] concluded that there was no significant change in the content of HCl above 30 km altitude, over the three year period covered by his flights up to that time. However, conflicting results deduced from the two most extensive series of observations available at the present time characterize the secular trend of hydrogen chloride; these are the airplane results from Mankin and Coffey [1983] and the ground-based observations from the Jungfraujoch.

From their airborne observations made between 1978 and 1982, Mankin and Coffey [1983] deduced a long-term trend in the integrated column of HCl above 12 km, amounting to an average increase of 5% per year. The conclusion was based on spectra in the latitude range 35-55° N, because that is the range with the largest number of observations, but the conclusion was the same if all of their data were included. The authors note that the fit of this rate of increase to their data leaves negative residuals for 1980 and positive residuals for earlier and later years. The measurements of Mankin and Coffey were made in four observation periods - winter 1978, summer 1978, winter 1979-80 and summer 1982. Measurements later in 1982 and 1983 were excluded from the fit because of the observation of a large amount of HCl injected into the stratosphere by the volcano El Chichon [Mankin and Coffey, 1984]. The summer 1982 observations were made at latitudes above 34° N where it is believed (based on lidar studies) that the volcanic debris had not yet reached. It is possible, however, that the HCl data in summer 1982, which have a strong effect on the magnitude of the fitted trend, were influenced by volcanic HCl.

Determination of the existence of a long-term trend is dependent upon the magnitude of any short-term variability that may be present. The available data base of aircraft measurements does not cover a long enough period, nor is it sampled frequently enough, to allow a long-term trend in the presence of substantial random variability to be determined. It is important that the aircraft program be continued in order to establish with certainty the secular trend of the HCl content of the stratosphere.

The weighted regression line drawn through the ensemble of monthly means from the Jungfraujoch observations, shown in Figure 11-13, indicates a linear increase in the total column of HCl of 0.4% per year. A sizable and highly variable portion of the HCl column measured from the Jungfraujoch is tropospheric, so the rate of increase of the stratospheric HCl could be significantly larger. Unfortunately, the magnitude of the tropospheric contribution is not known. It should be noted that if the fit had been restricted to observations up through July 1982 (as was the case with the data fit by Mankin and Coffey) the indicated trend would have been around 5% per year (dash dotted line in Figure 11-13). This illustrates the importance of a long time series in determining trends in the presence of short-term variability.

The KPNO observations carried out between 1977 and 1983 indicate a yearly increase in the total HCl content equal to about 1%. Measurements of the integrated column of HCl above Reims and OHP, published by Marche et al. [1980a,b] and Marche and Meunier [1983] covering the period 1979 to 1981, do not reveal any significant trend. The OHP results obtained in 1983 during the Map-Globus intercomparison campaign also support this conclusion [Marche, private communication].

While model calculations predict a trend in stratospheric HCl of 3 to 5% per year, it is not possible to draw any satisfactory conclusion as to its actual magnitude from the available observational data. Further measurements from aircraft and from the ground, made more frequently and with better coordination, are needed to provide a clear understanding of the variability and trend of the tropospheric and stratospheric components of the HCl burden.

11.4.2.4. Effects of Volcanos

In their original paper on the effects of chlorine on stratospheric chemistry, Stolarski and Cicerone [1974] considered volcanos as a possible source of stratospheric chlorine, concluding that they are probably one of the most important sources. Until recently, there was little evidence of significant volcanic input to the stratospheric chlorine budget. Johnston [1980] estimated from studies of the chlorine content of magma and ash, and from morphology of the volcanic plume, that the Augustine volcano in Alaska injected 84,000 to 180,000 tons of HCl into the stratosphere during its January 1976 eruptions. Mankin and Coffey, observing six months after the eruptions of El Chichon in March and April 1982, saw approximately 40% enhancements of the HCl column at latitudes where they were under the cloud of volcanic debris [Mankin and Coffey, 1984]. They estimated that the increased HCl amounted to 40,000 tons. These amounts are equivalent to a sizable fraction of the annual production of fluorocarbons. Thus, we conclude that volcanoes can occasionally be a substantial contributor to the stratospheric chlorine budget. Volcanic eruptions that inject a large amount of material into the stratosphere can perturb the ozone layer by a variety of chemical, radiative, and dynamical effects. The major eruptions, however, are infrequent events and their effects are transitory; they probably have a minor effect on the stratospheric ozone in the long term.

11.4.3 Hydrogen Fluoride (HF)

Hydrogen fluoride is the only sink for fluorine in the stratosphere. So far as is known, it does not actively participate in the chemistry of the stratosphere. It is quickly formed after the photolysis of fluorocarbons and is stable, ultimately diffusing to the troposphere where it is rained out. It has no known source except photodecomposition of fluorcarbons. Comparison of HCl and HF can give some indication of the relative abundances of natural and anathropogenic halogens in the stratosphere, since HCl has both natural and manmade sources.

HF has a strong infrared spectrum, both in the pure rotation region and the rotation-vibration fundamental near 4000 cm^{-1}. Both of these bands have been used for the measurement of HF from balloons, the near infrared in absorption against the sun and the far infrared in emission. The near infrared band includes lines that may be seen from the surface and both ground-based and aircraft observations have been used to measure the total column. Because there is very little tropospheric HF, the ground based measurements give essentially the stratospheric column.

11.4.3.1 Vertical Concentration Profile

Since the time of the last assessment, additional measurements of the vertical profile of HF have been made as part of the Balloon Inter-comparison Campaigns (BIC-1 in Sept. 1982, BIC-2 in June 1983). HF was a molecule of secondary importance for BIC, so there are comparatively few measurements.

The vertical profile from BIC-2 is shown in Figure 11-15. Measurements from three instruments are shown: vertical profiles from two far infrared interferometers and a single point from a near infrared grating spectrometer (open circle). The single point gives the total column above the 34 km float altitude, interpreted as a uniform mixing ratio above that altitude. The error bars are somewhat wider than for HCl because there are fewer measurements and less effort has been used in refining them. Also plotted in Figure 11-15 is a theoretical HF profile calculated by Ko and Sze [1984] with the updated kinetic data of Appendix A.
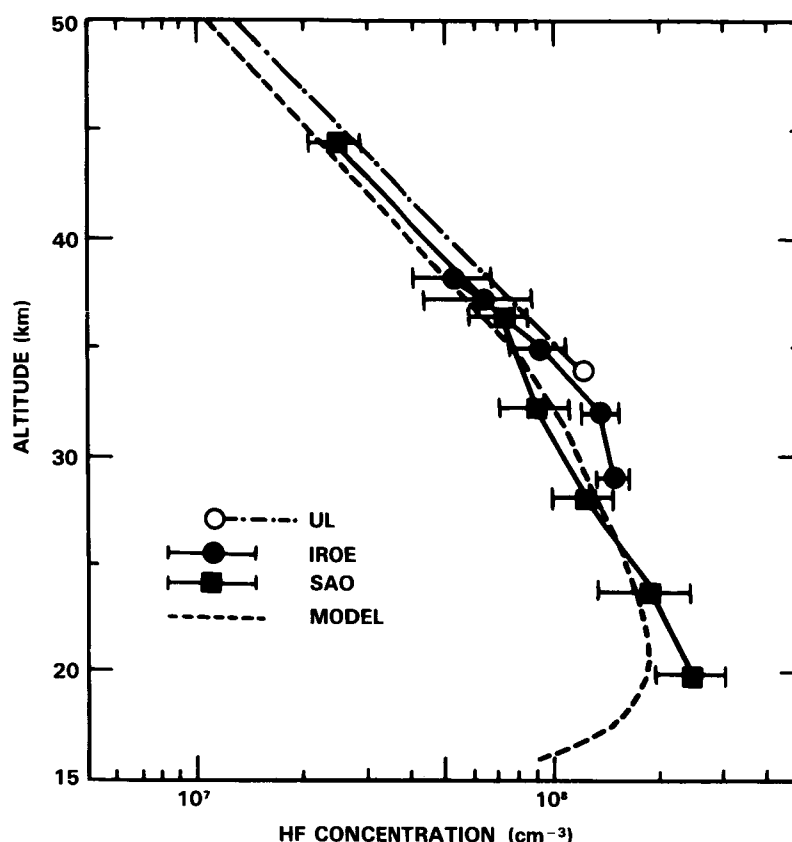
Figure 11-15. Results of measurements of the vertical distribution of HF from BIC-2. The flights on which the data were obtained are the same as for Figure 11-9. The dashed line is the model prediction of Ko and Sze [1984].

The BIC-1 results, from only two instruments, are similar in magnitude but show an intriguing difference in shape of the profile, with a mixing ratio minimum near 27 km. The aircraft and ground based measurements of the total column of HF are consistent with the integrated profiles from the balloons.

11.4.3.2 Latitude Distribution

Measurements of the total column of HF above 12 km as a function of latitude have been made from aircraft by two groups, on the same flights as those on which they measured the HCl columns. Girard et al. [1983] made a series of nine flights covering the range 62°S to 60°N. Mankin and Coffey [1983] report data from 26 flights from 10°N to 70°N. In the Northern Hemisphere, there is generally good agreement between the measurements of the two groups (see Figure 11-12), although Girard et al. report only upper limits for latitudes between 40°N and the equator.

The shapes of the distributions are very similar for HCl and HF. The Southern Hemisphere measurements of Girard et al. do not show any significant differences from the Northern Hemisphere measurements.

629

11.4.3.3 Temporal Variability

There is some evidence for short term temporal variability from measurements of the total column of HF. Figure 11-16 reproduces the monthly means of the total column amount as deduced from near-infrared solar observations made at the Jungfraujoch, between October 1976 and December 1984 [Zander, private communication, 1985]. The vertical scatter of the monthly arithmetic means (full points) gives an indication about variability of the total column of HF. As for HCl, the vertical bars between the arrows correspond to the observational errors, while their full amplitudes give the rms deviations of the means. The differences between these two amplitudes are indicative of the HF variability on a day-to-day time scale: the largest differences (e.g., March 1977, March 1978, Feb. 1984) occur when stratospheric polar air, enriched in HF, intrudes towards lower latitudes and lower altitudes. (The correlation with increasing ozone column amounts is striking on some occasions).

Between June and July 1981, Marche and Meunier [1983] observed a decrease of 13% in the monthly mean total HF content above Haute Provence. Observations carried out during 1982 at KPNO show monthly and daily variabilities exceeding 15% on many occasions [R. Zander and D. Johnson, private communication].

The aircraft measurements of Mankin and Coffey in the 40-50 °N range (containing the largest number of observations) provide further evidence of variability. The standard deviation of these points from their mean (corrected for the observed latitude variation) is 37%, substantially greater than the estimated precision of 10%. Part of this variance is doubtless due to a long term trend (see below), but a portion is clearly
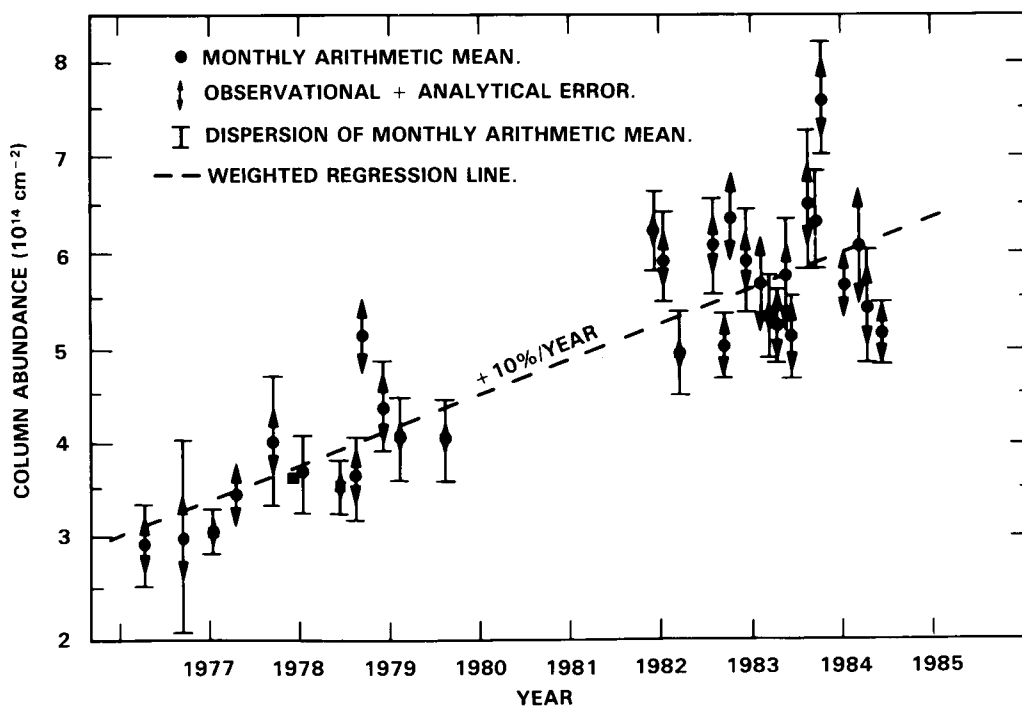
Figure 11-16. Observations of the total column of HF above the Jungfraujoch Station from 1976 through 1984 (from Zander private communication, 1985).

short term variation. Because the aircraft data set is less extensive than the ground based data set, it is not possible to establish as clearly from it the magnitude and time scale of the variability. There is no detectable seasonal variation in either the ground based or aircraft columns from the data availabe to date.

11.4.3.4 Trend in HF

There is good agreement among the various results deduced during recent years regarding the hydrogen fluoride secular increase in the atmosphere.

First, from their airplane observations at 12 km altitude, Mankin and Coffey [1983] have reported a linear temporal trend in the total column of HF above cruising altitude, equal to 12% per year for the period 1978-1982: that trend, because of the latitudinal variation of the HF content (discussed elsewhere), was based on data obtained between 35 and 55 °N, normalized to an effective latitude of 45 °N. Second, from the ground-based measurements of the total column of HF above the Jungfraujoch station, the weighted regression line drawn through the total set of the data (shown in Figure 11-16) leads to a linear increase of 10% per year between 1977 and 1984. Treating the data as two separate but representative groups of results, a cumulative increase of 9% per year between mid-1978 and the fall of 1983 is obtained.

The HF observations of Marche and Meunier [1983], obtained between 1979 and 1981, support a trend of 10% per year. The observations at KPNO, made between 1977 and 1984, confirm a yearly increase in the integrated amount of HF equal to ~10% [R. Zander, private communication].

The Jungfraujoch, data of Figure 11-16 gives HF column abundances which are almost a factor of two larger than the corresponding aircraft results (Figure 11-2), at the appropriate latitude and time. Although the discrepancy cannot be satisfactorily explained, much of it can be attributed to the intrinsic uncertainties associated with the measurement techniques themselves. It might be pointed out that a comparison of Figures 11-12 and 11-13 also indicates an apparent discrepancy in the HCl data, but in this case it can be attributed to the tropospheric HCl contribution, which can be 30–50% of the total column.

11.4.4 HCl/HF RATIO

While HF measurements can serve as an indicator for monitoring the quantities of chlorofluoromethanes destroyed by photolysis in the stratosphere, the concentrations of HCl provide insight into both the total chlorine budget of the stratosphere and the importance of competing reservoirs (such as HOCl and $ClONO_2$). Their relative long-term trends provide a test of the validity of the chemistry of the present models. Furthermore, HF and HCl measurements, when carried out simultaneously, may help in establishing the relative influence of natural versus anthropogenic sources of stratospheric chlorine. From the results reported in the previous paragraphs, the following HF/HCl ratios can be derived:

Mankin and Coffey [1983], using all their reported data for 1978 through 1982, and ignoring temporal variations, obtain an average HF/HCl ratio of 0.2 ± 0.08, with no significant latitude variation. This value corresponds to the mean time of their observations, i.e., 1980, and it is an average for the whole stratosphere above 12 km altitude.

Due to the variability seen in the total columns of both HF and HCl observed from the ground, an isolated measurement of the ratio will not be representative of the mean atmospheric content of these molecules above the point of observation. Therefore, the values of that ratio given below are averages of series of measurements made over selected time intervals.

631

When treating the Jungfraujoch results as two separate ensembles the following mean values for the HF/HCl ratio are obtained:

Group A (March, 1977 to September, 1978) HF/HCl = 0.15 ± 0.03
Group B (June, 1982 to December, 1984) HF/HCl = 0.22 ± 0.03

The HF/HCl ratio deduced from the results for Haute Provence [Marche and Meunier, 1983] is 0.29 ± 0.05. Marche and Meunier suspect the presence of a local source of hydrogen fluoride which enhances the tropospheric content of HF above OHP; while this possibility needs further assessment, it would explain the higher values of the HF/HCl ratios above central France. Above KPNO the mean HF/HCl ratio is 0.15 ± 0.04 for the period May 1977 through October 1979.

It should be noted that the Jungfraujoch as well as the Haute Provence data include tropospheric contributions, while the Mankin and Coffey results are for the stratosphere only. The theoretical HF/HCl ratio for the stratosphere estimated for the year 1982 by Ko and Sze [1984] is 0.18, a value which is in good agreement with observations.

11.5 STRATOSPHERIC DISTRIBUTION OF HALOCARBONS

Since 1980 stratospheric profiles of many halocarbons have become available. These include fully halogenated methanes, such as CCl_4, CCl_3F, CCl_2F_2, $CClF_3$, CF_4, $CBrClF_2$, and $CBrF_3$; fully halogenated ethanes, such as CCl_2FCClF_2, $CClF_2CClF_2$, $CClF_2CF_3$, and CF_3CF_3; and hydrohalocarbons whose overall atmospheric lifetimes are longer than 1 year: CH_3Cl, CH_3Br, $CHClF_2$, and CH_3CCl_3.

The origins and sources of halocarbons are discussed in Chapter 3. These compounds are transported into the stratosphere where they are photochemically decomposed to provide sources of chlorinated free radicals. The most important halocarbons are CCl_4, CCl_3F, CCl_2F_2, CH_3CCl_3 and CH_3Cl--all of which have a tropospheric abundance in excess of 100 pptv. These are also the halocarbons that have been included in most models used in the assessment of stratospheric ozone perturbations (see Chapter 13).

Knowledge about the vertical distributions of halocarbons is important for several reasons. First, the vertical gradients of these species provide important information regarding their photochemical removal rates, and also regarding transport processes. Second, stratospheric abundances of each halocarbon help define its relative contribution to the stratospheric chlorine or fluorine budget.

Most of the available data on the vertical distribution of halocarbons have resulted from the analysis of air samples collected aboard aircraft and balloon platforms. The analytical techniques employed, i.e., gas chromatography (GC) and mass spectrometry (MS), have been reviewed by Penkett [1981]. Both grab-sampling (with and without a compressor) and cryogenic sampling have been applied successfully. Only very few data have so far been obtained by means of other methods such as infrared spectroscopy. This section focuses on new stratospheric data, most of which have been obtained by cryogenic sampling experiments carried out in southern France (44 °N). Previous stratospheric data for CCl_3F, CCl_2F_2, and CH_3Cl have been compiled and reviewed in the WMO Report #11 [1982].

11.5.1 CCl₄ (FC-10)

Prior to 1980, aircraft samples provided scattered CCl_4 data for various latitudes and altitudes of the lower stratosphere [Lovelock, 1974; Robinson *et al.*, 1977; Seiler *et al.*, 1978; Tyson *et al.*, 1978; Rasmussen

and Khalil, 1980], and sampling aboard U2 aircraft provided data up to about 20 km [Krey *et al.*, 1977; Vedder *et al.*, 1978; Leifer *et al.*, 1979a, 1979b, 1981]. These early measurements are compiled in a review article by Fabian [1985].

The first stratospheric profile of CCl_4 was obtained by Borchers *et al.* [1983]. Stratospheric samples collected cryogenically on September 20, 1982, by means of the MPAE sampler were analyzed in turn at Max Planck Institut fur Aeronomie (MPAE) Lindau/Germany by GC with Electron Capture Detection (ECD) (profile "a" in Figure 11-17) and by gas chromatography mass spectrometry (GC-MS) at AERE Harwell, Great Britain (profile "b"). The precision of both sets of analyses was ± 10% or 0.1 pptv, whichever is greater. The absolute calibration by 2-step static dilution was made at AERE to better than ± 10%. The 4 lowest samples were used to determine the calibration factor for the MPAE profile.

Two data sets obtained from stratospheric samples collected with the cryogenic sampler of KFA Julich, on October 21, 1982, and on September 10, 1983 [Knapska *et al.*, 1985a] are also displayed in Figure 11-17 (c-f). The analyses of these samples were made at KFA by GC-ECD (c and e) and at AERE by GC-MS (d and f) in turn. The precision of both sets of analyses is given as ± 10% or ± 0.2 pptv, whichever is greater. The absolute calibration was performed to better than ± 5% against a Harwell standard.
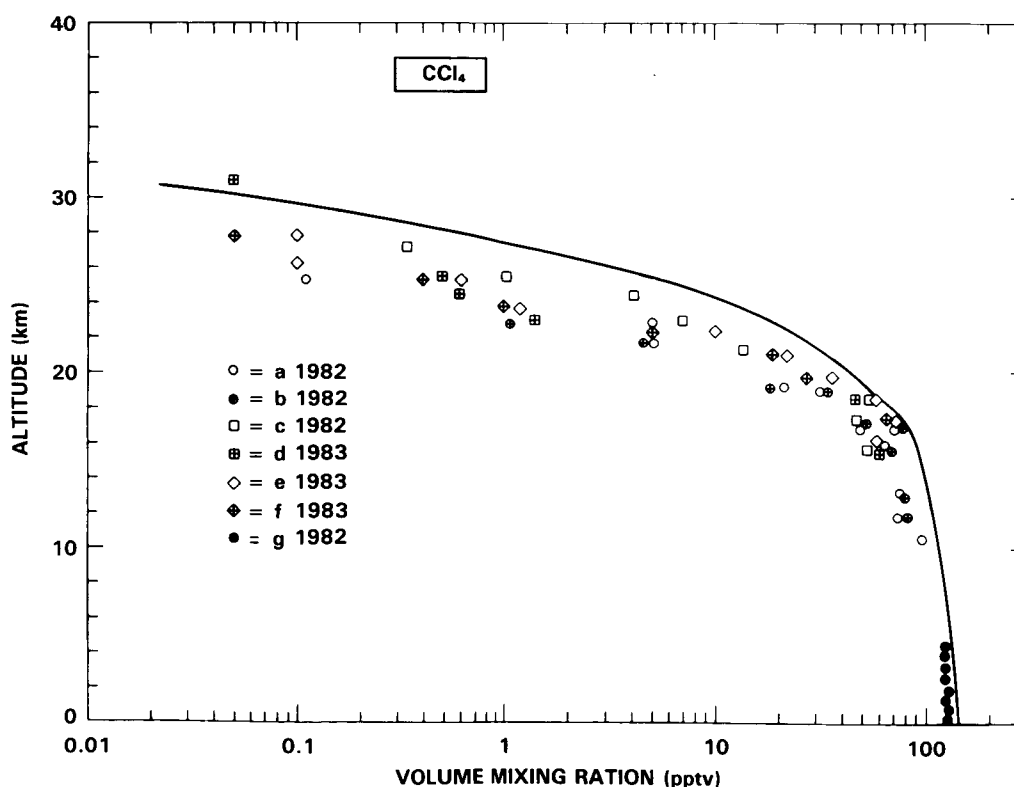
Figure 11-17. Vertical distribution of CCl_4 (FC-10) at northern midlatitudes.

a,b: [Borchers *et al.*, 1983]

c-f: [Knapska *et al.*, 1985a]

g: [Rasmussen and Khalil, 1983b]

The year of measurement is indicated in the figure. The solid line is for latitude 47°N calculated by a 2-D model [Ko *et al.*, 1985].

Although these published data sets appear to agree reasonably well, the data by Borchers *et al.* are generally lower than those by Knapska *et al.* On the other hand, the latter ones show larger discrepancies between the GC-ECD and GC-MS results as compared to Borchers *et al.* It should be noted again that both data sets are based on the same absolute calibration method. A tropospheric CCl_4 profile obtained by Rasmussen and Khalil [1983b], at about 70°N, is shown for comparison (profile "g"). It indicates CCl_4 mixing ratios of about (120 ± 2) pptv. This profile has been scaled down by a factor of 0.8 to take into account a recent recalibration of the measurements, as is the case for CH_3CCl_3 [Khalil and Rasmussen, 1984a].

The height dependence of the older aircraft data is consistent with the stratospheric profiles presented here (see Fabian [1985]), although absolute values were generally lower at that time. It appears reasonable to establish a mean 1982/83 profile of CCl_4, representative of northern midlatitude conditions, as an average of the data presented in Figure 11-1. The absolute scale of this profile may have an error of up to ± 10%.

11.5.2 CCl₃F (FC-11)

Stratospheric profiles of CCl_3F measured prior to 1980, at northern midlatitudes and in the tropics, are compiled in the WMO-Report #11 [1982]. New CCl_3F data from northern midlatitudes are displayed in Figure 11-18. The stratospheric data resulting from GC analyses of air samples collected with the MPAE
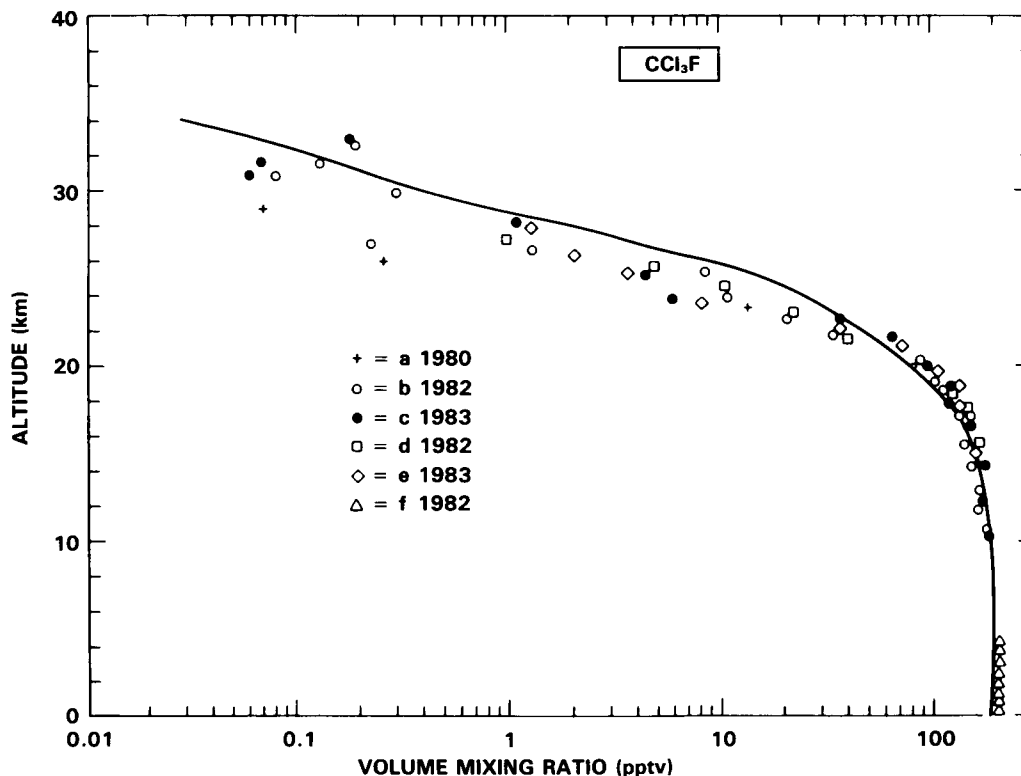
Figure 11-18. Vertical distribution of CCl_3F (FC-11) at northern midlatitudes.
  a: [Fabian *et al.*, 1981a]
  b: [Borchers and Fabian, private communication 1985]
  c,e: [Schmidt *et al.*, 1985a]
  d: [Schmidt *et al.*, 1984, Knapska *et al.*, 1985a]
  f: [Rasmussen and Khalil, 1983b]
  The solid line is for latitude 47°N calculated by a 2-D model [Ko *et al.*, 1985].

(profiles a-c) and KFA cryogenic samplers (profiles d and e) are supplemented by a tropospheric profile of (205±2) pptv measured at 70°N [Rasmussen and Khalil, 1983].

While profile "a" results from GC-MS analysis made at AERE Harwell with a precision of ± 15% [Fabian et al., 1981a], analyses of "b" and "c" were performed at MPAE Lindau by GC-ECD, with ± 5% precision [Borchers and Fabian, private communication 1985; Schmidt et al., 1985a], and "d" and "e" by GC-ECD at KFA Julich with ± 3% quoted precision [Schmidt et al., 1984, 1985b]. The detection limit was 0.1 pptv for all profiles, while the quoted error of the absolute calibration was ± 10% and ± 5% for a-c and d-e, respectively.

11.5.3   CCl₂F₂ (FC-12)

As CCl_2F_2 is usually analyzed along with CCl_3F, the data base of both halocarbons is almost identical. The new profiles a-f shown in Figure 11-19 refer to the same groups and techniques as those in Figure 11-18. The quoted precisions for CCl_2F_2 are ± 15% for a, ± 5% for b and c, and ± 3% for d and e. The detection limit was 0.2 pptv for a-e, while the absolute calibration was achieved to better than ± 10% and ± 5% for a-c and d-e, respectively. The tropospheric abundances of CCl_2F_2 as measured in May 1982, at 70°N (f), are (353 ± 3) pptv. As for CCl_3F, the slope of the profiles shown in Figure 11-19 is consistent with that of the older data compiled in the WMO-Report #11 [1982], while the absolute values are clearly higher indicating the growth of the CCl_2F_2 abundance with time.

11.5.4   CClF₃ (FC-13)

This halocarbon is used as a refrigerant either by itself or in an azeotropic mixture with CHF_3 (refrigerant 503) for very low temperature applications [Chou et al., 1978]. It was measured in the atmosphere for the first time in 1979: while Rasmussen and Khalil [1980] found (3.6 ± 0.7) pptv and (3.2 ± 0.5) pptv in clean tropospheric air of Antarctica, Penkett et al. [1981] measured 3 pptv for both hemispheres.

The first stratospheric profile of $CClF_3$ was obtained by GC-MS analysis of air samples collected On September 25, 1980, with the MPAE cryogenic sampler, at 44°N [Fabian et al., 1981a]. The analytical precision was ± 15% or ± 0.5 pptv, whichever is greater, while the absolute calibration was achieved to better than ± 10%.

$CClF_3$ data are shown in Figure 11-20. More measurements of this halocarbon, for which no data of global release rates are available, would be useful.

11.5.5   CF₄ (FC-14)

Atmospheric CF_4 is thought to originate from anthropogenic (aluminum production) and possibly natural sources (see reviews by Cicerone [1979] and Fabian [1985]). Its tropospheric abundance was first measured by Rasmussen et al. [1979] and Penkett et al. [1981] as (67 ± 10) pptv. In the stratosphere, CF_4 was first measured by Goldman et al. [1979], who determined a mixing ratio of 75 pptv at 25 km. A complete stratospheric profile (Figure 11-21) was obtained by GC-MS analysis of air samples collected on September 25, 1980 [Fabian et al., 1981a]. It confirms that CF_4 must have a very long atmospheric lifetime which had been estimated by Cicerone [1979] as more than 10,000 years. From the quoted precision of the stratospheric data given as ± 15%, it cannot be concluded whether or not the slight decrease from 72 pptv at 10 km to 60 pptv at 33 km is real; more measurements are needed to settle this question.

Figure 11-19. Vertical distribution of CCl_2F_2 (FC-12) at northern midlatitudes.

a: [Fabian *et al.*, 1981a]
b: [Borchers and Fabian, private communication 1985]
c,e: [Schmidt *et al.*, 1985a]
d: [Schmidt *et al.*, 1984, Knapska *et al.*, 1985a]
f: [Rasmussen and Khalil, 1983b]
The solid line is for latitude 47 °N calculated by a 2-D model [Ko *et al.*, 1985].

11.5.6 CBrClF₂ (FC-12B1)

This bromine-containing methane is used as fire extinguisher. Rasmussen and Khalil [1984c] report tropospheric abundances of (1.1 ± 0.1) pptv measured at 70 °N during 1983. A tropospheric profile resulting from GC-ECD analysis of aircraft samples collected at 70 °N, during May 1979, is shown in Figure 11-22.

Stratospheric profiles of $CBrClF_2$ were obtained for the first time by Lal *et al.* [1985] by GC-ECD analysis of samples collected with MPAE cryogenic samplers, on September 20, 1982, September 10, 1983, and October 1, 1984 (Figure 11-22). Thus, the vertical stratospheric distribution could be measured for 3 consecutive years, with an analytical precision of ± 5% or 0.03 pptv, whichever is greater. The absolute calibration was achieved by 2-step static dilution within ± 10% accuracy. Repetitive analyses
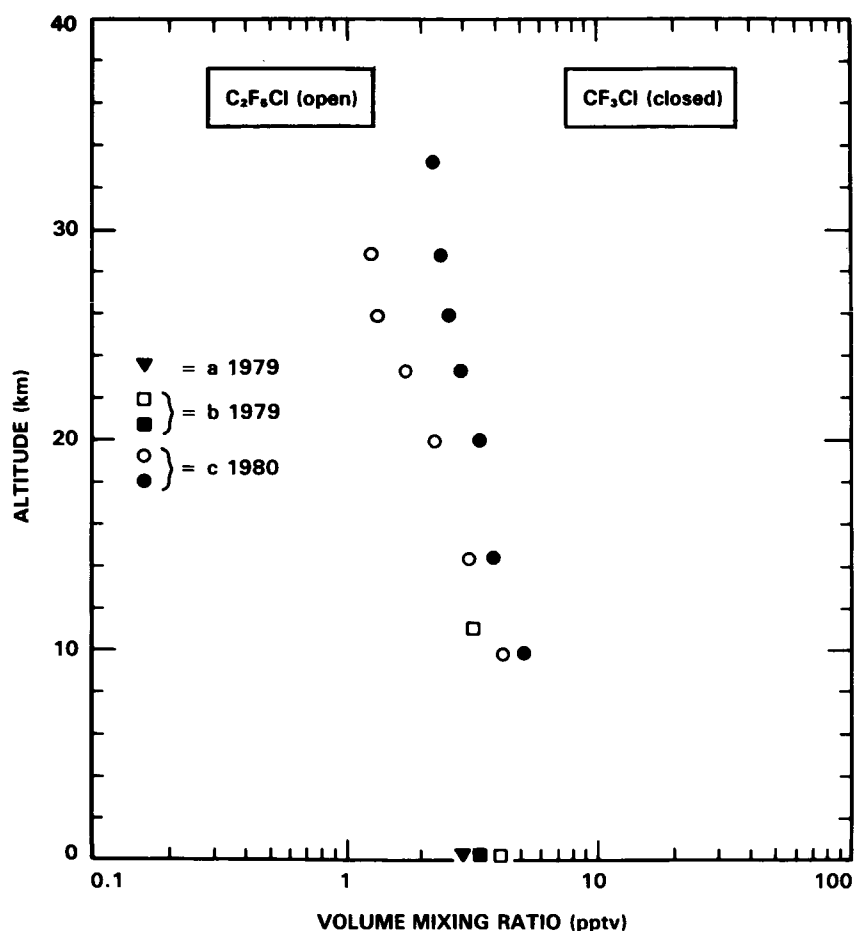
Figure 11-20. Vertical distribution of CF₃Cl (FC-13) and of CClF₂CF₃ (FC-115) at northern midlatitudes.

a: [Rasmussen and Khalil, 1980]
b: [Penkett *et al.,* 1981]
c: [Fabian *et al.,* 1981a]

and cross-checks were carried out to ensure that the rapid increase of $CBrClF_2$ mixing ratios observed in the lower stratosphere, which amounts to about 20%/year, is real [Lal *et al.*, 1985].

11.5.7   CBrF₃ (FC-13B1)

Like FC-12B1, this bromine-bearing halocarbon is used as fire extinguisher. In 1979, its tropospheric abundance was first measured by Penkett *et al.* [1981] as 0.7 pptv. The first stratospheric profile obtained by Fabian *et al.* [1981a] is shown in Figure 11-22. GC-MS analysis of samples collected on September 25, 1980, was made with a precision of ± 15%. The detection limit was about 0.05 pptv, and the absolute calibration was made to within ± 10%.

11.5.8   CCl₂FCClF₂ (FC-113)

FC-113 is used primarily as a solvent. According to Wuebbles [1983a] its global release rate into the atmosphere is 91 x 10³ tons/year. It was first measured in the atmosphere by Singh *et al.* [1979] who
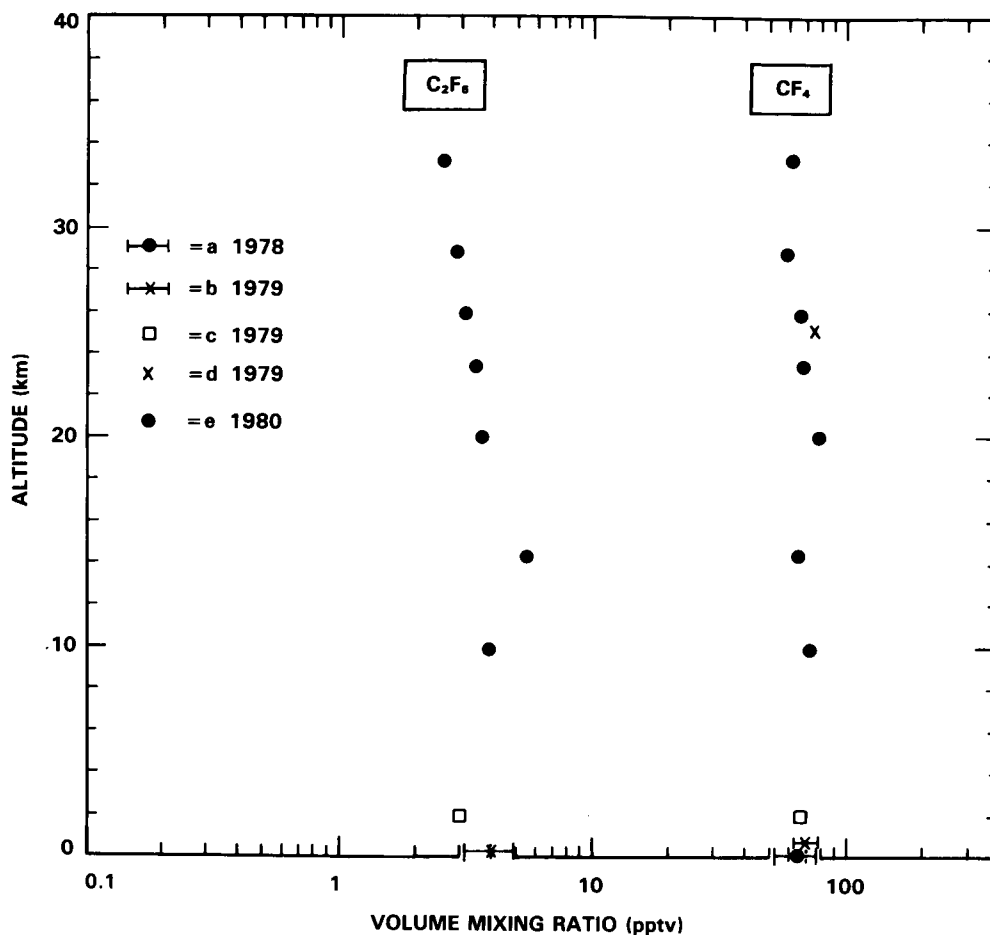
Figure 11-21. Vertical distribution of CF₄ (FC-14) and of CF₃CF₃ (FC-116) at northern
midlatitudes.
    a: [Rasmussen *et al.*, 1979]
    b: [Penkett *et al.*, 1981]
    c: [Rasmussen and Khalil, 1980]
    d: [Fabian *et al.*, 1981a]

found in 1975, (19 ± 3.5) pptv and (12 ± 1.9) pptv on the northern and southern hemispheres, respectively, on a latitudinal survey between 60 °N and 40 °S. Rasmussen and Khalil [1981c, 1982, 1983b] and Rasmussen *et al.* [1983] measured FC-113 abundances ranging between 13 and 23 pptv.

The first stratospheric profile was obtained by Fabian *et al.* [1981a] by GC-MS analysis (AERE Harwell) of samples collected with a MPAE sampler on September 25, 1980 (Figure 11-23). The analytical precision of these data points was ± 15% or ± 0.1 pptv, whichever is greater. The absolute calibration was achieved to better than ± 10%.

Two profiles resulting from GC-ECD analyses at KFA (b and d) and GC-MS analyses at AERE (c and e) of samples collected with the KFA sampler, on October 21, 1982 and September 10, 1983, showed a factor of 3 larger FC-113 mixing ratios [Knapska *et al.*, 1985a]. Their analytical precision against a
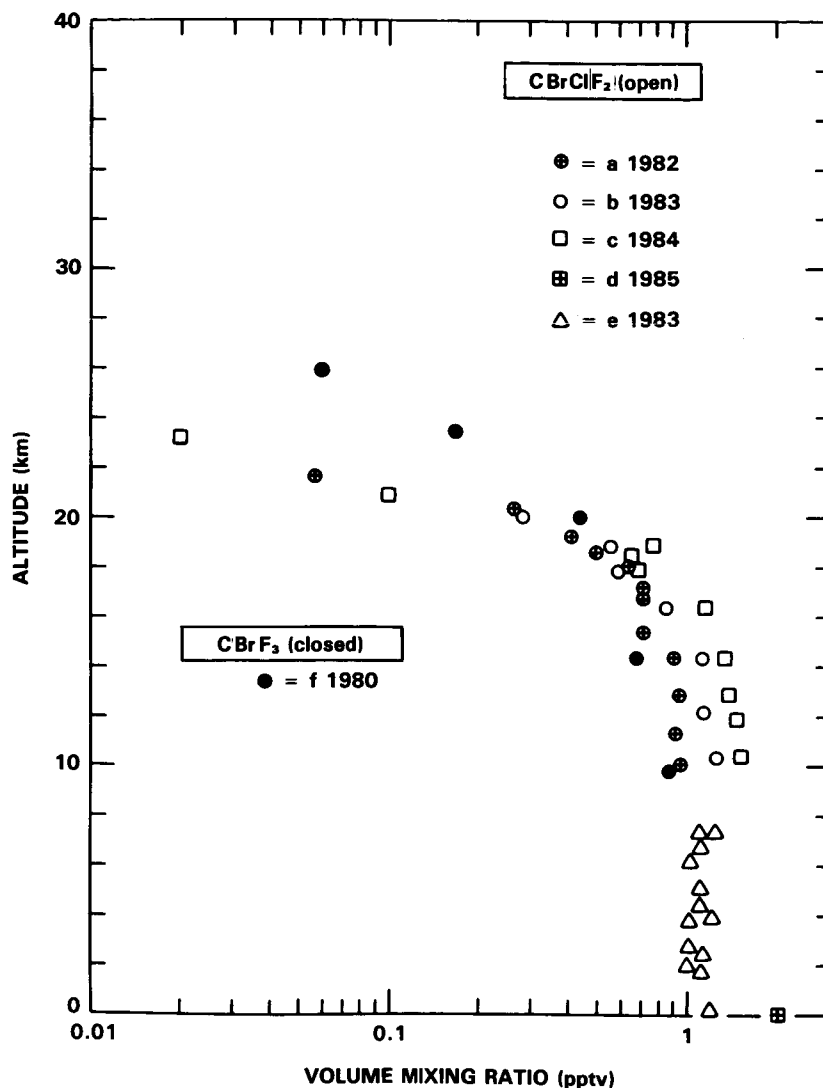
Figure 11-22. Vertical distribution of CBrClF₂ (FC-12B1) and CBrF₃ (FC-13B1) at northern midlatitudes.

a-d: [Lal *et al.*, 1985]
e: [Rasmussen and Khalil, 1983b]
f: [Fabian *et al.*, 1981a]

standard is quoted as ± 10% or ± 0.2 pptv, whichever is greater. The absolute calibration of this standard was made at AERE only.

Three FC-113 profiles (not presented in Figure 11-23) measured by MPAE during 1982, 1983 and 1984 showed that the first 1980 profile is certainly too low by a factor 2 [Borchers *et al.*, 1985]. They match the tropospheric profile of (23 ± 1) pptv measured by Rasmussen and Khalil [1983b] at 70 °N (profile "f" in Figure 11-23). This would imply that the KFA profiles b-e have to be reduced by about 30%. More measurements and intercalibrations are needed for FC-113 whose absolute calibration is extremely difficult to achieve.
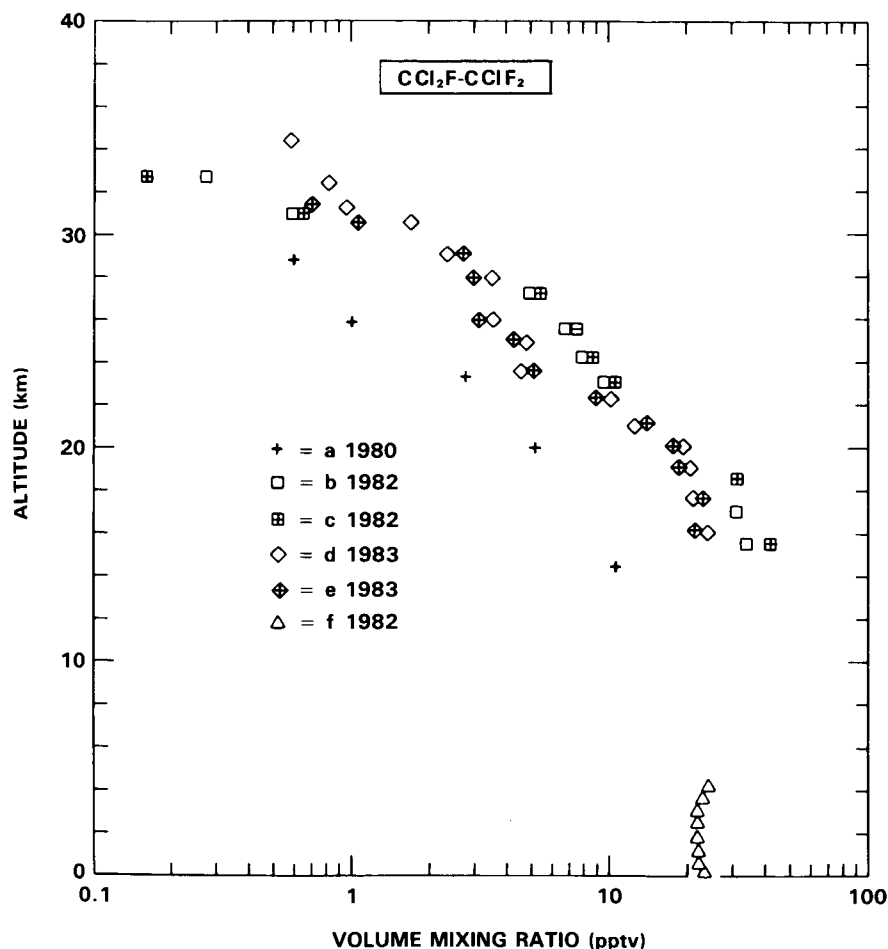
Figure 11-23. Vertical distribution of CCl₂FCClF₂ (FC-113) at northern midlatitudes.

  a: [Fabian *et al.*, 1981a]

  b-e: [Knapska *et al.*, 1985a]

  f: [Rasmussen *et al.*, 1983]

11.5.9 CCIF₂CCIF₂ (FC-114)

FC-114 is used as an aerosol propellant and as a refrigerant, with present global emission rates being estimated as 18 x 10³ tons/year [Wuebbles, 1983a]. This halocarbon was first measured in 1975 by Singh *et al.* [1979] who found (12 ± 1.9) pptv and (10 ± 1.3) pptv at sea level for the northern and southern hemispheres, respectively.

Figure 11-24 shows the first stratospheric profile of FC-114 [Fabian *et al.*, 1981a]. Samples collected on September 25, 1980 with the MPAE cryogenic sampler at 44 °N were analyzed by GC-MS at AERE Harwell. The precision was ± 15% or ±0.5 pptv, whichever is greater, and the error of the absolute calibration was within ± 10%. Three as yet unpublished profiles obtained by GC-ECD analysis of samples collected with the MPAE sampler on September 20, 1982, September 10, 1983, and October 1, 1984 are consistent with the profile shown in Figure 2-8 [Fabian and Borchers, private communication 1985].

640
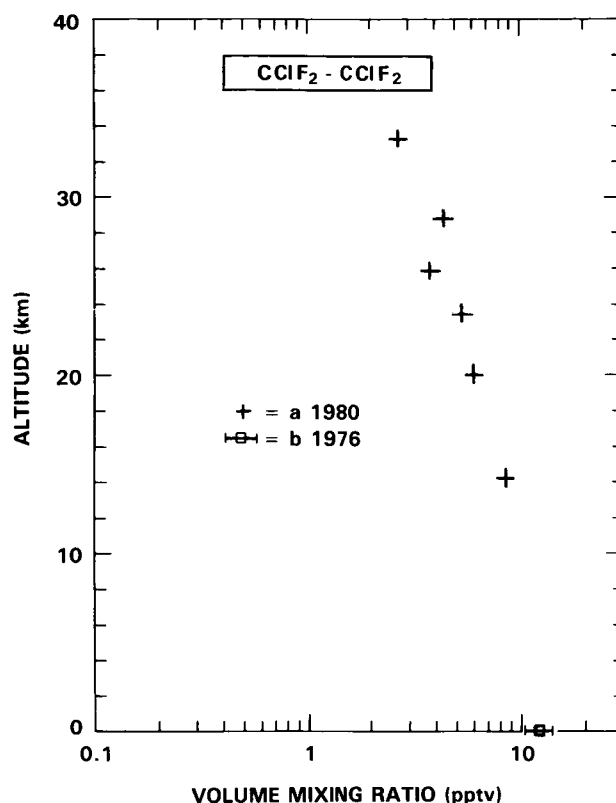
Figure 11-24. Vertical distribution of CCIF₂CCIF₂ (FC-114) at northern midlatitudes.
a: [Fabian *et al.*, 1981a]
b: [Singh, 1977]

11.5.10 CCIF₂CF₃ (FC-115)

This halocarbon is used as a propellant for foods dispensed from aerosols, and as a refrigerant either directly or in mixture with FC-22 in the azeotropic refrigerant 502. Its present global release rate into the atmosphere, as evaluated by Wuebbles [1983a], is 4.5×10^3 tons/year.

Penkett *et al.* [1981] measured the tropospheric abundance of FC-115 as 4.1 pptv in 1979. The first stratospheric profile, shown in Figure 11-20, was obtained by GC-MS analysis of cryogenically collected samples [Fabian *et al.*, 1981a]. The quoted precision was $\pm$ 15% with a detection limit of about 0.5 pptv, while the absolute calibration was made to within $\pm$ 10%.

11.5.11 CF₃CF₃ (FC-116)

Like CF_4, this halocarbon is thought to be released from aluminum plants. Its tropospheric abundance was measured to range between 3 and 5 pptv with no indication of latitudinal or hemispheric differences [Penkett *et al.*, 1981; Rasmussen and Khalil, 1980]. The first stratospheric profile obtained by GC-MS of cryogenically collected midlatitude samples [Fabian *et al.*, 1981a] shows a slight decrease from 4 pptv at 10 km to 2.5 pptv at 33 km (Figure 11-21). The precision of these data points was $\pm$ 15% with a detection limit of about 0.5 pptv. The absolute calibration was made with an error of $\pm$ 10%.

11.5.12 CH₃Cl (Methyl Chloride)

A first stratospheric midlatitude profile of methyl chloride, the most important natural halocarbon, was already presented in the WMO Report #11 [Penkett *et al.*, 1980]. More stratospheric data which have become available since then are presented in Figure 11-25, supplemented by a tropospheric profile measured at 70°N by Rasmussen and Khalil [1983b].

The profiles "a" and "b" result from analyzing cryogenically collected midlatitude samples of the MPAE sampler. For profile "a" [Fabian *et al.*, 1981a], GC-MS analysis was made at AERE, with a

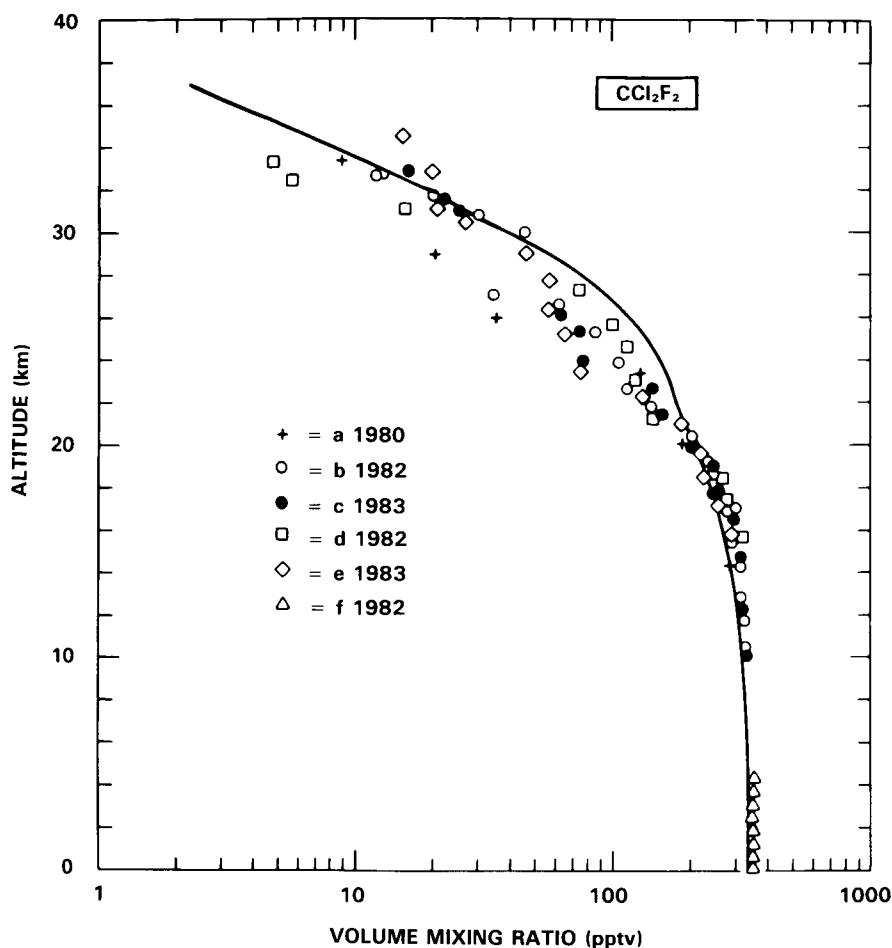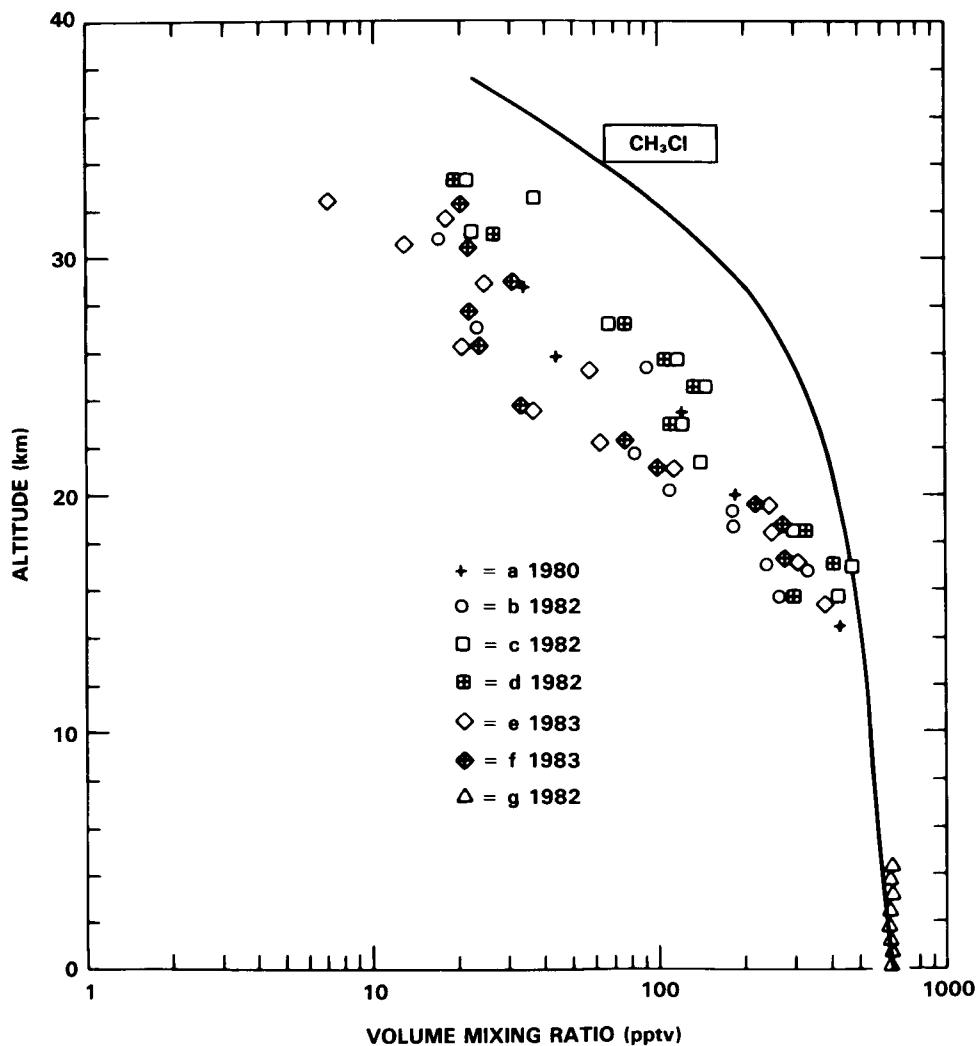**Figure 11-25.** Vertical distribution of CH₃Cl at northern midlatitudes.

a: [Fabian *et al.*, 1981a]
b: [Borchers and Fabian, private communication 1985]
c-f: [Knapska *et al.*, 1985a]
g: [Rasmussen and Khalil, 1983b]
The solid line is for latitude 47°N calculated by a 2-D model [Ko *et al.*, 1985].

precision of ± 15%, while profile "b" [Borchers and Fabian, private communication 1985] results from GC-MS analysis at MPAE with ± 10% precision. The detection limit was about 1 pptv, while the absolute calibration was performed to within ± 10% in both cases. The profiles c-f result from samples collected with the KFA sampler during two balloon flights in 1982 and 1983, respectively. The samples were analyzed both by GC-ECD and KFA (c and e) and GC-MS of AERE (d and f). The quoted precision was ± 15% and ± 10%, and the detection limits were about 10 pptv and 1 pptv for the GC-ECD and GC-MS analyses, respectively. The absolute calibration was made against an AERE standard calibrated to within ± 5%.

Some of the scatter noticeable in Figure 11-25 may reflect real variations due to large-scale advection. To a larger extent, however, this scatter is likely to be due to contamination and alteration of the samples during sampling in the presence of ozone, and to storage [Schmidt et al., 1985b].

11.5.13 CHClF$_2$ (FC-22)

This hydrohalocarbon has been used in refrigeration and as a foam blowing agent, and global release data have been assessed [Jesson, 1980]. Since FC-22 was first measured in 1979 by Rasmussen et al. [1980], an increase of its abundance of about 12%/year was found in both hemispheres [Khalil and Rasmussen, 1981].

For the lower stratosphere, the first profile was reported by Leifer et al. [1981], who found FC-22 mixing ratios decreasing from about 55 pptv at the tropopause to 35 pptv at 19 km. Goldman et al., [1981d] reported 100 pptv measured at 15 km by infrared spectroscopy.

Two complete midlatitude profiles up to 33 km were reported by Fabian et al. [1985]. They are shown in Figure 11-26 along with a tropospheric profile measured at 70°N [Rasmussen and Khalil, 1983b]. Cryogenically collected samples of two balloon flights, on September 20, 1982 and September 10, 1983 at 44°N, were analyzed by GC-MS. Samples of the first flight were analyzed at MPAE (a) and AERE (b) in turn, with a precision of ± 10% or ± 3 pptv, whichever is greater. The absolute calibration was made at Harwell to within ± 10%, and a calibration factor was applied to the MPAE data. The samples collected during the 1983 flight were analyzed at MPAE only, with a precision of ± 5% or ± 3 pptv, whichever is greater, the error of the absolute calibration being ± 10%.

This data base confirms that FC-22, although being decomposed in the troposphere by OH attack, is fairly stable in the stratosphere. Its mixing ratios decrease by a factor of 3 only, while those of its fully halogenated counterpart, CCl$_2$F$_2$ decrease by about a factor of 30, within the height range discussed here.

11.5.14 CH$_3$Br (Methyl Bromide)

Like methyl chloride, methyl bromide is mostly of natural origin. Singh [1977] and Singh et al. [1977, 1979] measured tropospheric background mixing ratios of 5 pptv or less, with values as high as 20 pptv in the marine environment. Rasmussen and Khalil [1980] reported CH$_3$Br mixing ratios varying between 5 and 25 pptv, while Penkett et al. [1981] found about 10 pptv in the upper troposphere. Rasmussen and Khalil [1984c] measured a tropospheric profile at 70°N up to 7 km yielding (10 ± 2) pptv. The first stratospheric measurement indicates that CH$_3$Br falls off rapidly above the tropopause: 1.2 pptv was measured at 14.4 km, while a sample collected at 20 km was already below the detection limit [Fabian et al., 1981a]. As these data are considered preliminary, more measurements are needed to establish a realistic profile.
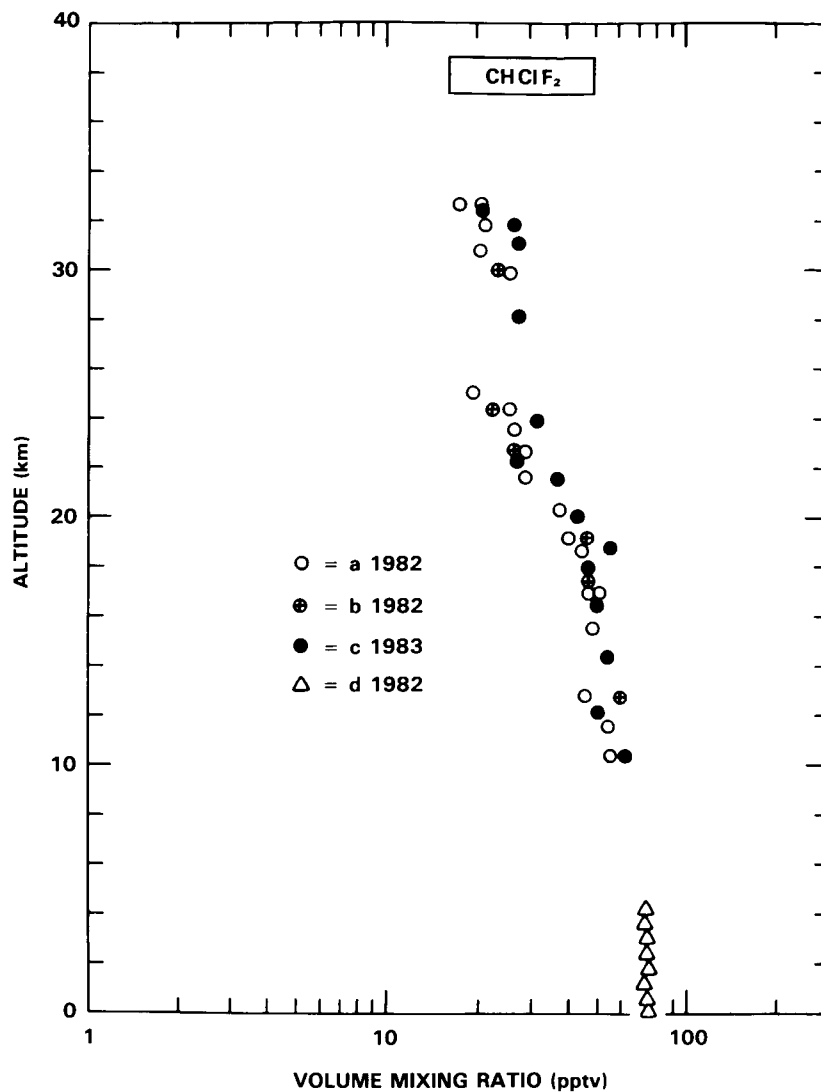
Figure 11-26. Vertical distribution of CHClF₂ (FC-22) at northern midlatitudes.
a-c: [Fabian *et al.*, 1985a]
d: [Rasmussen and Khalil, 1983b]

11.5.15 CH₃CCl₃ (Methyl Chloroform)

Tropospheric measurements of methyl chloroform were reviewed in the WMO Report #11 [1982], but no stratospheric data were available then. From analyses of air samples collected aboard aircraft some CH₃CCl₃ data for the lower stratosphere were obtained by Leifer *et al.* [1981], showing midlatitude mixing ratios decreasing from about 100 pptv at the tropopause to 30 pptv at 19 km.

A first complete stratospheric profile of CH₃CCl₃ was obtained by Borchers *et al.* [1983]. Samples collected on September 20, 1982, with an MPAE cryogenic sampler at 44 °N were analyzed by GC-ECD at MPAE and GC-MS at AERE Harwell. The results are plotted as profiles "a" and "b" in Figure 11-27.
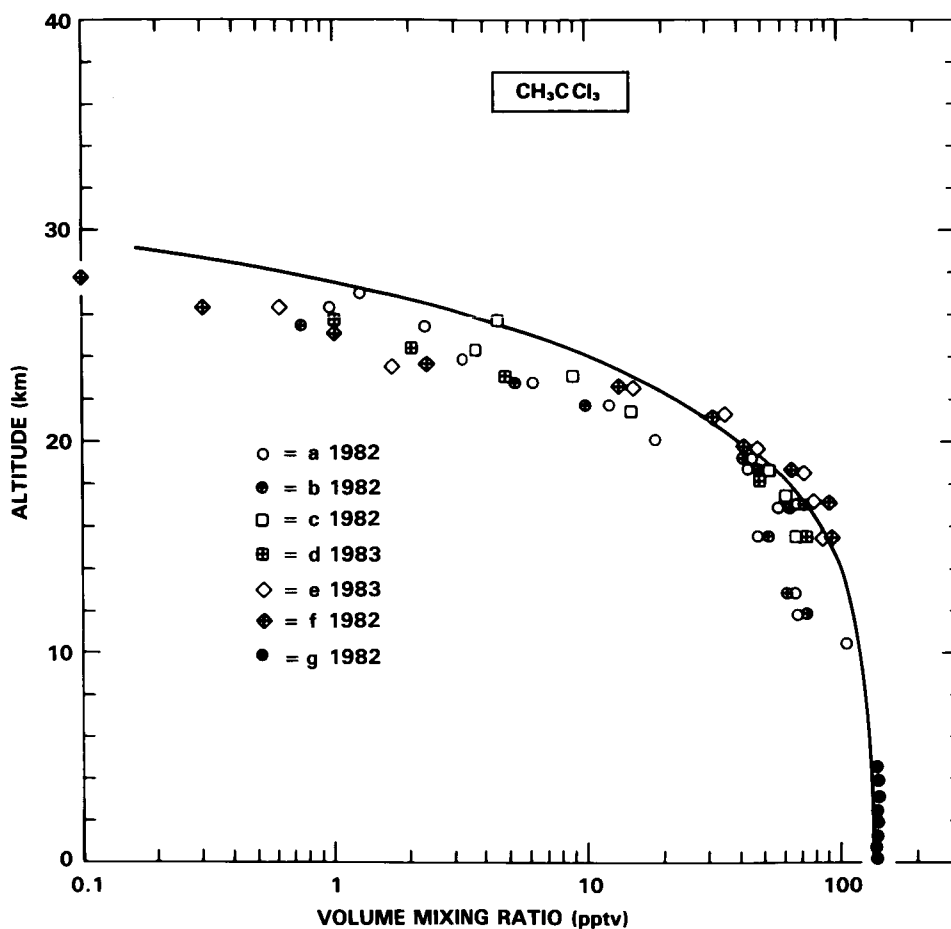
Figure 11-27. Vertical distribution of CH₃CCl₃ at northern midlatitudes.

a,b: [Borchers *et al.,* 1983]

c-f: [Knapska *et al.,* 1985a]

g: [Rasmussen and Khalil, 1983b; Khalil and Rasmussen, 1984a]

The solid line is for latitude 47°N calculated by a 2-D model [Ko *et al.,* 1985].

The quoted precision and detection limit was ± 10% and 0.1 pptv, respectively, for both data sets, while the absolute calibration was made at AERE to within ± 10%, with a calibration factor applied to the MPAE data points.

From samples collected during two flights of the KFA sampler, on October 21, 1982, and September 10, 1983, two more CH₃CCl₃ profiles were established [Knapska *et al.,* 1985a]. The analyses of these samples were made by GC-ECD at KFA (c and e) and by GC-MS at AERE (d and f), and the quoted analytical precision was ± 10% or ± 2 pptv, whichever is greater, for both data sets. All analyses were made against an AERE standard calibrated to within ± 5%. A tropospheric profile measured at 70°N, also shown in Figure 11-27, indicates (175 ± 2) pptv of CH₃CCl₃ in 1982. The data of Rasmussen and Khalil [1983b] have been scaled down by a factor of 0.8 to reflect a recent recalibration of the measurements [Khalil and Rasmussen, 1984a].

Although the data set presented in Figure 11-27 reveals some scatter which may, as in the case of CH_3Cl, reflect contamination effects, it appears reasonable to establish a mean profile representative of 1982/83 midlatitude conditions as an average of the data points presented here.

11.5.16 Comparison With Models

Among the various halocarbons discussed above, model profiles are only presented for the most abundant halocarbons, i.e., CCl_4, CCl_3F, CCl_2F_2, CH_3Cl and CH_3CCl_3. The stratospheric sinks for these species are reasonably well established, but the transport processes controlling their vertical distributions are less well characterized (see Chapter 12 for a discussion on the uncertainties in transport-related parameters).

Plotted in Figures 11-17, 11-18 and 11-19 are vertical profiles of CCl_4, CCl_3F and CCl_2F_2 at 47 °N latitude taken from AER's 2-D model calculations [Ko et al., 1985]. With the new O_2 cross section in the Herzberg continuum (see Chapter 6), the calculated profile of CCl_3F (Figure 11-18) is now in better agreement with observations, and the serious discrepancy noted earlier in the WMO Report #11 [1982] is now partially resolved.

The calculated concentration of CCl_4 (Figure 11-17) appears to be somewhat higher than observations. It should be noted, however, that because of the very steep vertical gradient of stratospheric CCl_4, the difference between model and observations may be attributed to a shift of as small as ~ 1 km in vertical scale. Such a shift may occur when the model profiles are transformed from pressure coordinates to height coordinates.

Figure 11-25 shows the calculated profile of CH_3Cl along with observations which indicate a much steeper vertical gradient. Unlike its fully halogenated counterparts, CH_3Cl is mainly removed by reaction with OH. The discrepancy between the calculated and observed profiles of CH_3Cl could be indicative of uncertainties in transport coefficients or higher OH in the lower stratosphere. However, more and better data will be required to establish the variability of CH_3Cl and to assess in more detail the discrepancy with model profiles.

Figure 11-27 shows the calculated profile of CH_3CCl_3 along with observations. The agreement appears to be quite satisfactory.

Two-dimensional model calculations have not been made for other halocarbons whose data are summarized in Figures 11-20 through 11-24, and 11-26 and whose UV absorption cross sections are listed in JPL Publication 85-37 [1985]. This body of data should provide an additional test for models in the future.

11.6 TOTAL CHLORINE

The total amount of chlorine is determined largely by the amount of organically bound chlorine in the troposphere, whose background concentration is estimated to be in the range 2.4 - 2.8 ppbv chlorine (see Chapter 3). Hence, an equivalent mixing ratio for total chlorine is expected in the stratosphere. Berg et al. [1980] have measured total halogens at ~ 20 km altitude and at various latitudes, using activated charcoal traps and neutron activation analysis, obtaining values ranging between 2.7 ± 0.9 and 3.2 ± 0.7 ppbv chlorine.

More recently, Gallagher et al. [1985] employed cryogenic whole air samplers to measure individual halogenated hydrocarbons, and filter samplers to measure acidic and particulate chlorine, in order to estimate

the total chlorine content (excluding possibly Cl and ClO) at altitudes between 15 and 30 km. They measured total chlorine mixing ratios that decreased from 2.6 ppbv at 15 km, to 2.2 - 2.5 ppbv for the higher altitudes. Hence, at present there appears to be no significant discrepancy between measured and calculated total stratospheric chlorine abundance.

11.7 CONCLUSIONS

11.7.1 Chlorine Monoxide (ClO)

Since 1981 the stratospheric ClO data base, measurement techniques and theoretical models have been considerably improved. Between altitudes of about 28 and 38 km there is now agreement within a factor of two between the mean of the measurements and model predictions. The ClO diurnal variation has now been monitored and is also in reasonable agreement with model predictions, although observations indicate a somewhat slower morning rise than expected. The existing data base, however, is not yet adequate to establish seasonal and latitudinal variations or long term increases in ClO which are all predicted by theoretical models. Furthermore, the experimental precision and accuracy need to be improved in order to assess with confidence the magnitude of the shorter term variations in midday ClO which might be caused by transport-induced fluctuations in CH_4, H_2O and NO_X.

11.7.2 Chlorine Nitrate (ClONO₂)

There is now improved evidence for the presence of the reservoir species $ClONO_2$ with measurements made in a second spectral region, and there is also indirect evidence coming from the observed diurnal behavior of ClO.

11.7.3 Hydrogen Chloride (HCl) and Hydrogen Fluoride (HF)

Several different remote sensing techniques for HCl and HF were carefully intercompared during the balloon intercomparisons carried out in 1982 and 1983. The vertical concentration profile of HCl, for which many more observations were made, can now be measured to 15% accuracy with confidence. Total column values from the surface (i.e., including the tropospheric component) can be determined with a precision approching 5%. Significant variability in the column amount of HCl in the stratosphere in space and in time has been established. Column values for the total HCl seen from the surface show even greater variation with time. The expected trend in stratospheric HCl is presumably masked by this variation and has not yet been observed. For HF the measured latitude variation and long-term trend are compatible with theoretical prediction.

11.7.4 Stratospheric Halocarbon Profiles

There is now general agreement between calculated and measured profiles for the halogen source molecules. Some differences remain, but these are most likely due to imperfections in the modeling of transport processes. The least satisfactory agreement occurs with CH_3Cl, a species removed predominantly by reaction with OH. However, CH_3Cl is among the halocarbons presenting greatest measurement difficulties.

The discrepancy in the previous assessment [WMO Report #11, 1982] between models and observations, most apparent in CCl_3F, has been partially resolved by the new O_2 absorption cross sections around 200 nm (Chapter 7).

11.8 FUTURE RESEARCH NEEDS

In summarizing the future needs for measurements of radiatively and chemically active trace species in the stratosphere, it should be mentioned that a new source of data, the Atmospheric Trace Molecule Spectroscopy (ATMOS) experiment had its first flight as part of the Spacelab-3 mission in May of 1985. Although the results of this flight cannot be made available in time for inclusion in the present assessment, it can be stated that the experiment was successful and that data pertaining to many of the molecular species discussed in this and other chapters were obtained. The results, which provide simultaneous measurements of a large number of species at various locations over the globe, are expected to satisfy several of the specific needs discussed here.

One of the higher priority research items should be the simultaneous measurements of chlorine-bearing species, mainly HCl, $ClONO_2$ and ClO. Such observations should resolve questions concerning the total chlorine budget and its spatial and temporal variability. Measurements of high altitude HCl, e.g., at 50 km (which are probably available from ATMOS) would also be very useful in this context, since at those altitudes chlorine is expected to be present predominantly as HCl.

A more stringent test of the models, related to the partitioning of chlorine among the various species, would be possible with simultaneous measurements of O_3, H_2O, CH_4, NO_X and temperature, besides HCl, ClO and $ClONO_2$.

It is important to continue monitoring stratospheric HCl and HF. The long term increase expected as a result of CFM release is apparent in the HF, but not in the HCl data so far. Also, the latitudinal variation of these two species in the stratosphere needs to be better established by continued measurements.

It appears that $ClONO_2$ can now be added to the list of species positively identified in the stratosphere. Given its relative abundance--next to HCl in the inorganic chlorine family--higher sensitivity measurements are now required in order to establish reliably a stratospheric concentration profile.

Measurements of stratospheric ClO have matured considerably since the first observations pioneered by Anderson and co-workers. An intercomparison of the several existing techniques is clearly needed at present. Furthermore, with state-of-the-art instrumentation it should now be possible to measure the diurnal, the seasonal and the latitudinal variation in ClO to about $\pm$ 15%. Also, measurements of the profile shape should be continued in order to better establish the behavior of this important species.

Techniques to measure HOCl to about 0.1 ppbv should be developed: detection of this species in the stratosphere is important in testing current knowledge of the chemistry of the chlorine family.

There are only two direct measurements of Cl-atoms, both by the in situ resonance fluorescence technique. Additional observations would be useful, particularly if coupled to measurements of other key species, as discussed above. Also, improved measurements of the shape of the C_2H_6 profile would provide important information on Cl-atom abundance in the lower stratosphere, where direct measurements are not practical due to the exceedingly small concentrations expected.

REFERENCES
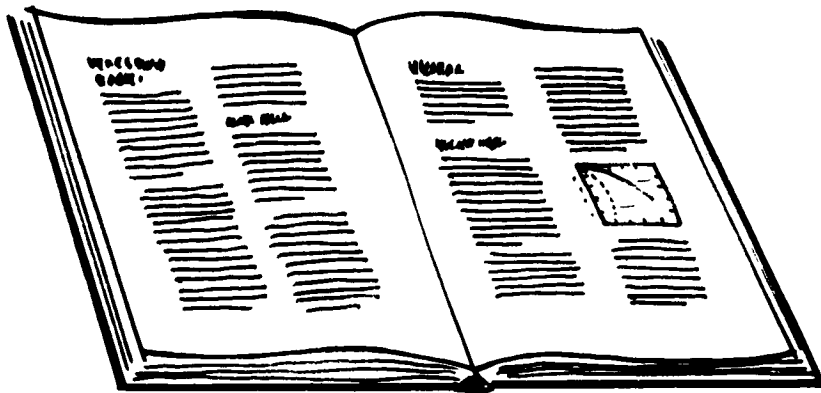
Research Panel

C. Meetre — Database Designer

M.A. Baldauf
K. Taylor

APPENDIX: REFERENCES

Abbas, M. M., T. Kostiuk, M. J. Mumma, D. Buhl, V. G. Kunde, and L. W. Brown, Stratospheric ozone measurement with an infrared heterodyne spectrometer, *Geophys. Res. Lett.*, *5*, 317-320, 1978.

Ackerman, M., Ultraviolet solar radiation related to mesospheric processes, in *Mesospheric Models and Related Experiments*, edited by G. Fiocco, pp. 149-159, D. Reidel, Dordrecht, 1971.

Ackerman, M., and C. Muller, Stratospheric methane and nitrogen dioxide from infrared spectra, *Pure Appl. Geophys.*, *106-108*, 1325-1335, 1973.

Ackerman, M., J. C. Fontanella, D. Frimout, A. Girard, N. Louisnard, and C. Muller, Simultaneous measurements of NO and NO_2 in the stratosphere, *Planet. Space Sci.*, *23*, 651-660, 1975.

Ackerman, M., D. Frimout, A. Girard, A. Gottignies, and C. Muller, Stratospheric HCl from infrared spectra, *Geophys. Res. Lett.*, *3*, 81-83, 1976.

Ackerman, M., D. Frimout, C. Muller, and D. J. Wuebbles, Stratospheric methane measurements and predictions, *Pure Appl. Geophys.*, *117*, 367-380, 1978/79.

Ackerman, M., C. Lippens, C. Muller, J. Vercheval, J. Besson, A. Girard, J. Laurent, and M. P. Lemaitre, Observations of middle atmosphere CH_4 and N_2O vertical distributions by the Spacelab one grille spectrometer, *Geophys. Res. Lett.*, submitted, 1985.

Ahlquist, J., Normal-mode global Rossby waves, theory and observations, *J. Atmos. Sci.*, *39*, 193-202, 1982.

Aikin, A. C., B. Woodgate, and H. J. P. Smith, Equatorial ozone profiles from the solar maximum mission - A comparison with theory, *Planet. Space Sci.*, *32*, 503-513, 1984.

Aimedieu, P., P. Rigaud, and J. Barat, The sunrise ozone depletion problem of the upper stratosphere, *Geophys. Res. Lett.*, *8*, 787-789, 1981.

Aimedieu, P., A. J. Krueger, D. E. Robbins, and P. C. Simon, Ozone profile intercomparison based on simultaneous observations between 20 and 40 km, *Planet. Space Sci.*, *31*, 801-807, 1983.

Al-Ajmi, D. N., R. S. Harwood, and T. Miles, A sudden warming in the middle atmosphere of the Southern Hemisphere, *Quart. J. Roy. Meteorol. Soc.*, *111*, 359-389, 1985.

Allam, R. J., and A. F. Tuck, Transport of water vapour in a stratosphere-troposphere general circulation model I. Fluxes, *Quart. J. Roy. Meteorol. Soc.*, *110*, 321-356, 1984a.

Allam, R. J., and A. F. Tuck, Transport of water vapour in a stratosphere-troposphere general circulation model II. Trajectories, *Quart. J. Roy. Meteorol. Soc.*, *110*, 357-392, 1984b.

Allam, R. J., K. S. Groves, and A. F. Tuck, Global OH distribution derived from general circulation model fields of ozone and water vapor, *J. Geophys. Res.*, *86*, 5303-5320, 1981.

Allen, D. C., J. D. Haigh, J. T. Houghton, and C. J. S. M. Simpson, Radiative cooling near the mesopause, *Nature*, *281*, 660-661, 1979.

Allen, D. C., T. Scragg, and C. J. S. M. Simpson, Low temperature fluorescence studies of the deactivation of the bend-stretch manifold of CO_2, *Chem. Phys.*, *51*, 279-298, 1980.

Allen, M., and J. E. Frederick, Effective photodissociation cross sections for molecular oxygen and nitric oxide in the Schumann-Runge bands, *J. Atmos. Sci.*, *39*, 2066-2075, 1982.

Allen, M., J. I. Lunine, and Y. L. Yung, The vertical distribution of ozone in the mesosphere and lower thermosphere, *J. Geophys. Res.*, *89*, 4841-4872, 1984.

Alpert, J. C., M. A. Geller, and S. K. Avery, The response of stationary planetary waves to tropospheric forcing, *J. Atmos. Sci.*, *40*, 2467-2483, 1983.

Altshuller, A. P., and J. J. Bufalini, Photochemical aspects of air pollution: A review, *Environ. Sci. Technol.*, *5*, 39-64, 1971.

Anderson, G. P., and L. A. Hall, Attenuation of solar irradiance in the stratosphere: Spectrometer measurements between 191 and 207 nm, *J. Geophys. Res.*, *88*, 6801-6806, 1983.

Anderson, J. G., The absolute concentration of OH $(X^2\pi)$ in the Earth's stratosphere, *Geophys. Res. Lett.*, *3*, 165-168, 1976.

REFERENCES

Anderson, J. G., Free radicals in the earth's stratosphere: A review of recent results, in *Proceedings of the NATO Advanced Study Institute on Atmospheric Ozone: Its Variation and Human Influences, Rep. FAA-EE-80-20*, edited by A. C. Aikin, pp. 233-251, DOT, FAA, Washington, DC, 1980.

Anderson, J. G., The past five years-the next five years, paper presented at the International Workshop on Current Issues in our Understanding of the Stratosphere and the Future of the Ozone Layer, BMFT, NASA, FAA, WMO, Feldafing, FRG, June 11-16, 1984.

Anderson, J. G., J. J. Margitan, and D. H. Stedman, Atomic chlorine and the chlorine monoxide radical in the stratosphere: Three in-situ observations, *Science, 198*, 501-503, 1977.

Anderson, J. G., H. J. Grassl, R. E. Shetter, and J. J. Margitan, Stratospheric free chlorine measured by balloon-borne in situ resonance fluorescence, *J. Geophys. Res., 85*, 2869-2887, 1980.

Anderson, J. G., H. J. Grassl, R. E. Shetter, and J. J. Margitan, HO_2 in the stratosphere: Three in situ observations, *Geophys. Res. Lett., 8*, 289-292, 1981.

Anderson, J. R., and R. D. Rosen, The latitude-height structure of 40-50 day variations in atmospheric angular momentum., *J. Atmos. Sci., 40*, 1584-1591, 1983.

Anderson, P. W., Pressure broadening in the microwave and infrared regions, *Phys. Rev., 76*, 647-661, 1949.

Andrews, D. G., and M. E. McIntyre, Planetary waves in horizontal and vertical shear: The generalized Eliassen-Palm relation and the mean zonal acceleration, *J. Atmos. Sci., 33*, 2031-2048, 1976.

Andrews, D. G., and M. E. McIntyre, Generalized Eliassen-Palm and Charney-Drazin theorems for waves on axisymmetric mean flows in compressible atmospheres, *J. Atmos. Sci., 35*, 175-185, 1978a.

Andrews, D. G., and M. E. McIntyre, An exact theory of nonlinear waves on a Lagrangian mean flow, *J. Fluid. Mech., 89*, 609-646, 1978b.

Andrews, D. G., J. D. Mahlman, and R. W. Sinclair, Eliassen-Palm diagnostics of wave-mean flow interaction in the GFDL "SKYHI" general circulation model, *J. Atmos. Sci., 40*, 2768-2784, 1983.

Angell, J. K., and J. Korshover, Recent rocketsonde-derived temperature variations in the Western Hemisphere, *J. Atmos. Sci., 35*, 1758-1764, 1978a.

Angell, J. K., and J. Korshover, Estimate of global temperature variations in the 100-30 mb layer between 1958 and 1977, *Mon. Weather Rev., 106*, 1422-1432, 1978b.

Angell, J. K., and J. Korshover, Global temperature variations in the troposphere and stratosphere, *Mon. Weather Rev., 111*, 901-921, 1983a.

Angell, J. K., and J. Korshover, Global variations in total ozone and layer-mean ozone: An update through 1981, *J. Clim. Appl. Meteor., 22*, 1611-1627, 1983b.

Angell, J. K., J. Korshover, and W. G. Planet, Ground-based and satellite evidence for a pronounced total-ozone minimum in early 1983 and responsible atmospheric layers, *Mon. Weather Rev., 113*, 641-646, 1985.

Apruzese, J., and D. F. Strobel, Radiative relaxation rates for individual 15-micron CO_2 lines in the upper stratosphere and lower mesosphere, *J. Geophys. Res., 89*, 7187-7194, 1984.

Apruzese, J. P., M. R. Schoeberl, and D. F. Strobel, Parameterization of IR cooling in a middle atmosphere dynamics model. 1. Effect on the zonally averaged circulation, *J. Geophys. Res., 87*, 8951-8966, 1982.

Arakawa, A., and W. H. Schubert, Introduction of cloud ensemble with the large scale environment, *J. Atmos. Sci., 31*, 674-701, 1974.

Arijs, E., D. Neverjans, and J. Ingles, Unambiguous mass determination of major stratospheric positive ions, *Nature, 288*, 684-686, 1980.

Arijs, E., D. Neverjans, and J. Ingels, Stratospheric positive ion composition measurements, ion abundances and related trace gas detection, *J. Atmos. Terr. Phys., 44*, 43-53, 1982.

Arnold, F., Multi-ion complexes in the stratosphere-Implications for trace gases and aerosol, *Nature, 284*, 610-611, 1980.

Arnold, F., Stratospheric trace gas detection by rocket-, balloon-, and aircraft-borne chemical ionization mass spectrometry, paper presented at the International Workshop on Current Issues in our Understanding of the Stratosphere and the Future of the Ozone Layer, BMFT, NASA, FAA, WMO, Feldafing, FRG, June 11-16, 1984.

Arnold, F., and G. Henschen, First mass analysis of stratospheric negative ions, *Nature*, *275*, 521-522, 1978.

Arnold, F., and S. Qiu, Upper stratosphere negative ion composition measurements and inferred trace gas abundances., *Planet. Space Sci.*, *32*, 169-177, 1984.

Arnold, F., H. Bohringer, and G. Henschen, Composition measurements of stratospheric positive ions, *Geophys. Res. Lett.*, *5*, 653-656, 1978.

Arnold, P. W., Losses of nitrous oxide from soil, *J. Soil*, *5*, 116-128, 1955.

Arrhenius, S., On the influence of carbonic acid in the air upon the temperature of the ground, *Philos. Mag.*, *41*, 237, 1896.

Arvesen, J. C., R. N. Griffin, and B. D. Pearson, Jr., Determination of extraterrestrial solar spectral irradiance from a research aircraft, *Appl. Optics*, *8*, 2215-2232, 1969.

Asai, K., T. Itabe, and T. Igarashi, Range-resolved measurements of atmospheric ozone using a differential-absorption CO_2 laser radar, *Appl. Phys. Lett.*, *35*, 60-62, 1979.

Atkinson, R., and A. C. Lloyd, Evaluation of kinetic and mechanistic data for modeling of photochemical smog, *J. Phys. Chem. Ref. Data*, *13*, 315-444, 1984.

Atkinson, R., S. M. Aschmann, A. M. Winer, and W. P. L. Carter, Rate constants for the gas-phase reactions of NO_3 with furan, thiophene and pyrole at 295 1 K and atmospheric pressure, *Environ. Sci. Technol.*, *19*, 87-90, 1985.

Atticks, M. G., and G. D. Robinson, Some features of the structure of the tropical tropopause, *Quart. J. Roy. Meteorol. Soc.*, *109*, 295-308, 1983.

Attmannspacher, W., and H. U. Duetsch, International ozone sonde intercomparison at the Observatory Hohenpeissenberg 5-20 April 1978, *Ber. Deutschen Wetterdienstes, Nr. 20*, 1970.

Attmannspacher, W., and H. U. Duetsch, Second international ozone sonde intercomparison at the Observatory Hohenpeissenberg 5-20 April 1978, *Ber. Deutschen Wetterdienstes, Nr. 157*, 1981.

Augustsson, T., and V. Ramanathan, A radiative-convective model study of the CO_2 climate problem, *J. Atmos. Sci.*, *34*, 448-451, 1977.

Ausloos, P., R. E. Rebbert, and L. Glasgow, Photodecomposition of chloromethane absorbed on silica surfaces, *J. of Res. of Nat. Bureau of Standards*, *82*, 1-8, 1977.

Austin, J., Comparison of stratospheric air parcel trajectories calculated from SSU and LIMS satellite data, *J. Geophys. Res.*, in press, 1985.

Austin, J., and A. F. Tuck, The calculation of stratospheric air parcel trajectories using satellite data, *Quart. J. Roy. Meteorol. Soc.*, *111*, 279-307, 1985.

Austin, J., R. R. Garcia, J. M. Russell III, S. Solomon, and A. F. Tuck, On the atmospheric photochemistry of nitric acid, *J. Geophys. Res.*, in press, 1985a.

Austin, J., R. C. Pallister, J. A. Pyle, A. F. Tuck, and A. M. Zarody, Photochemical model comparisons with LIMS observations in a stratospheric trajectory coordinate system, *Quart. J. Roy. Meteorol. Soc.*, in press, 1985b.

Azouit, M., and J. Vernin, Remote investigation of tropospheric turbulence by two dimensional analysis of stellar scintillation, *J. Atmos. Sci.*, *37*, 1550-1557, 1980.

Bacastow, R. B., C. D. Keeling, and T. P. Whorf, Seasonal amplitude increase in atmospheric CO_2 concentration at Mauna Loa, Hawaii, 1959-1982, *J. Geophys. Res.*, *90*, 10529-10540, 1985.

Baker, C. B., W. R. Kuhn, and E. Ryzner, Effects of the El Chichon volcanic cloud on direct and diffuse irradiances, *J. Clim. Appl. Meteor*, *23*, 449-452, 1984.

Baker-Blocker, A., T. M. Donahue, and K. H. Mancy, Methane flux from wetlands areas, *Tellus*, *29*, 245-250, 1977.

REFERENCES

Baldecchi, M. G., B. Carli, F. Mencaraglia, A. Bonetti, and M. Carlotti, Atlas of stratospheric submillimeter lines: 1. The 7-20 cm^{-1} interval, *J. Geophys. Res.*, *89*, 11689-11704, 1984.

Baldwin, A. C., and D. M. Golden, Heterogeneous atmospheric reactions-Sulphuric acid aerosols as tropospheric sinks, *Science*, *206*, 562-563, 1979.

Baldwin, A. C., J. R. Barker, D. M. Golden, and D. G. Hendry, Photochemical smog. Rate parameter estimates and computer simulation, *J. Phys. Chem.*, *81*, 2483-2492, 1977.

Ballard, H. N., A review of seven papers concerning the measurement of temperature in the stratosphere and mesosphere, *Tech. Rep. ECOM-5125*, 67 pp., U.S. Atmos. Sci. Lab., White Sands Missile Range, NM, 1967.

Balsley, B. B., and D. A. Carter, The spectrum of atmospheric velocity fluctuations at 8 km and 86 km, *Geophys. Res. Lett.*, *9*, 465-468, 1982.

Balsley, B. B., and A. C. Riddle, Monthly mean values of the mesospheric wind field over Poker Flat, Alaska, *J. Atmos. Sci.*, *41*, 2368-2375, 1984.

Baluteau, J. P., A. Marten, E. Bussoletti, M. Anderegg, J. E. Beckman, A. F. M. Moorwood, and N. Coron, High resolution infrared spectra of the Earth's atmosphere-II. Ground-based observations in the 500-570 cm^{-1} range, *Infrared Phys.*, *17*, 211-224, 1977.

Bamber, D. J., P. G. W. Healey, B. M. R. Jones, S. A. Penkett, A. F. Tuck, and G. Vaughan, Vertical profiles of tropospheric gases: Chemical consequences of stratospheric intrusions, *Atmos. Environ.*, *18*, 1759-1766, 1984.

Barat, J., Some characteristics of clear-air turbulence in the middle atmosphere, *J. Atmos. Sci.*, *39*, 2553-2564, 1982.

Barbe, A., P. Marche, C. Secroun, and P. Jouve, Measurements of tropospheric and stratospheric H_2CO by an infrared high resolution technique, *Geophys. Res. Lett.*, *6*, 463-465, 1979.

Barnes, I., K. H. Becker, E. H. Fink, A. Reimer, F. Zabel, and H. Niki, Rate constant and products of the reaction CS_2 + OH in the presence of O_2, *Int. J. Chem. Kinet.*, *15*, 631-645, 1983.

Barnes, R. A., A. R. Bandy, and A. T. Torres, ECC ozonesonde accuracy and precision, *J. Geophys. Res.*, *90*, 7881-7887, 1985.

Barnett, J. J., The mean meridional temperature behaviour of the stratosphere from November 1970 to November 1971 derived from measurements by the selective chopper radiometer on Nimbus 4, *Quart. J. Roy. Meteorol. Soc.*, *100*, 505-530, 1974.

Barnett, J. J., and M. Corney, Temperature comparisons between the NIMBUS 7 SAMS, rocket/radiosondes and the NOAA-6 SSU, *J. Geophys. Res.*, *89*, 5294-5302, 1984.

Barnett, J. J., and M. Corney, A middle atmosphere temperature reference model from satellite measurements, *Adv. Space Res.*, *5*, 125-134, 1984.

Barnett, J. J., J. T. Houghton, and J. A. Pyle, The temperature dependence of the ozone concentration near the stratopause, *Quart. J. Roy. Meteorol. Soc.*, *101*, 245-257, 1975a.

Barnett, J. J., R. S. Harwood, J. T. Houghton, C. G. Morgan, C. D. Rodgers, and E. J. Williamson, Comparison between radiosonde, rocketsonde and satellite observations of atmospheric temperatures, *Quart. J. Roy. Meteorol. Soc.*, *101*, 423-436, 1975b.

Barrett, E. W., P. M. Kuhn, and A. Shlanta, Recent measurements of the injection of water vapor and ozone into the stratosphere by thunderstorms, in *Proceedings of the 2nd Conference on the Climatic Impact Assessment Program*, *DOT-TSC-OST-73-4*, edited by A. J. Broderick, pp. 34-46, Transportation Systems Center, Cambridge, MA, 1973.

Barth, C. A., D. W. Rusch, R. J. Thomas, G. H. Mount, G. J. Rottman, G. E. Thomas, R. W. Sanders, and G. M. Lawrence, Solar Mesosphere Explorer: Scientific objectives and results, *Geophys. Res. Lett.*, *10*, 237-240, 1983.

Barton, I. J., Upper level cloud climatology from an orbiting satellite, *J. Atmos. Sci.*, *40*, 435-447, 1983.

Basco, N., and J. E. Hunt, Mutual combination of ClO radicals, *Int. J. Chem. Kin.*, *11*, 649-664, 1979.

Bass, A. M., and R. J. Paur, The ultraviolet cross sections of ozone: I. The measurements, in *Atmospheric Ozone*, edited by C. S. Zerefos and A. Ghazi, pp. 606-610, D. Reidel, Dordrecht, 1984.

Bates, D. R., Rayleigh scattering by air, *Planet. Space Sci.*, *32*, 785-790, 1984.

Bauer, E., A catalog of perturbing influences on stratospheric ozone, 1955-1975, *J. Geophys. Res.*, *84*, 6929-6940, 1979.

Baulch, D. L., R. A. Cox, R. F. Hampson, Jr., J. A. Kerr, J. Troe, and R. T. Watson, Evaluated kinetic and photochemical data for atmospheric chemistry, *J. Phys. Chem. Ref. Data*, *9*, 295-471, 1980.

Baulch, D. L., R. A. Cox, P. J. Crutzen, R. F. Hampson, J. A. Kerr, J. Troe, and R. T. Watson, Evaluated kinetic and photochemical data for atmospheric chemistry: Supplement I. CODATA Task Group on Chemical Kinetics, *J. Phys. Chem. Ref. Data*, *11*, 327-496, 1982.

Baulch, D. L., R. A. Cox, R. F. Hampson, Jr., J. A. Kerr, J. Troe, and R. T. Watson, Evaluated kinetic and photochemical data for atmospheric chemistry supplement II. CODATA Task Group on Gas Phase Chemical Kinetics, *J. Phys. Chem. Ref. Data*, *13*, 1259-1380, 1984.

Belmont, A. D., and D. G. Dartt, Semiannual variation in zonal wind from 20 to 65 kilometers, at 80°N-10°S, *J. Geophys. Res.*, *78*, 6373-6376, 1973.

Belmont, A. D., D. G. Dartt, and G. D. Nastrom, Periodic variations in stratospheric zonal winds from 20 to 65 km, at 80°N to 70°S, *Quart. J. Roy. Meteorol. Soc.*, *100*, 203-211, 1974.

Berg, W. W., and P. D. Sperry, Atmospheric bromine in the Arctic, *J. Geophys. Res.*, *88*, 6719-6736, 1983.

Berg, W. W., P. J. Crutzen, F. E. Grahek, S. N. Gitlen, and W. A. Sedlacek, First measurements of total chlorine and bromine in the lower stratosphere, *Geophys. Res. Lett.*, *7*, 937-940, 1980.

Berg, W. W., L. E. Heidt, W. Pollock, P. D. Sperry, R. J. Cicerone, and E. S. Gladney, Brominated organic species in the Arctic atmosphere, *Geophys. Res. Lett.*, *11*, 429-432, 1984.

Berner, W., H. Oeschger, and B. Stauffer, Information on the CO_2 cycle from ice-core studies, *Radiocarbon*, *22*, 227-235, 1980.

Betts, A. K., Parametric interpretation of trade wind cumulus budget studies, *J. Atmos. Sci.*, *32*, 1934-1945, 1975.

Bevilacqua, R. M., J. J. Olivero, P. R. Schwartz, C. J. Gibbins, J. M. Bologna, and D. L. Thacker, An observational study of water vapor in the mid-latitude mesosphere using ground-based microwave techniques, *J. Geophys. Res.*, *88*, 8523-8534, 1983.

Bevilacqua, R. M., W. J. Wilson, W. B. Ricketts, P. R. Schwartz, and R. J. Howard, Possible seasonal variability of mesospheric water vapor, *Geophys. Res. Lett.*, 12, 397-400, 1985.

Bhartia, P. K., K. F. Klenk, A. J. Fleig, C. G. Wellemyer, and D. Gordon, Intercomparison of Nimbus 7 Solar Backscattered Ultraviolet ozone profiles with rocket, balloon and Umkehr profiles, *J. Geophys. Res.*, *89*, 5227-5238, 1984a.

Bhartia, P. K., K. F. Klenk, C. K. Wong, D. Gordon, and A. J. Fleig, Intercomparison of the Nimbus 7 SBUV/TOMS total ozone data sets with Dobson and M83 results, *J. Geophys. Res.*, *89*, 5239-5248, 1984b.

Bhartia, P. K., D. F. Heath, and A. J. Fleig, Observation of anomalously small ozone densities in South Polar Stratosphere during October 1983 and 1984, paper presented at 5th General Assembly, IAGA Symposium, Prague, Czechoslovakia, July, 1985.

Blackmer, A. M., and J. M. Bremner, Potential of soil as a sink for atmospheric nitrous oxide, *Geophys. Res. Lett.*, *3*, 739-742, 1976.

Blackshear, W. T. W. L. Grose, and R. E. Turner, Simulated sudden stratospheric warmings: Synoptic evaluations, *Quart. J. Roy. Meteorol. Soc.*, in press, 1986.

Blake, A. J., An atmospheric absorption model for the Schumann-Runge bands of oxygen, *J. Geophys. Res.*, *84*, 3272-3282, 1979.

REFERENCES

Blake, A. J., S. T. Gibson, and D. G. McCoy, Photodissociation of $^{16}O^{18}O$ in the atmosphere, *J. Geophys. Res.*, *89*, 7277-7284, 1984.

Blake, D. R., Increasing concentrations of atmospheric methane, 1979-1983, Ph.D. thesis, 213 pp., U. of California, Irvine, CA, 1984.

Blake, D. R., and F. S. Rowland, World-wide increase in tropospheric methane, *J. Atmos. Chem.*, in press, 1985.

Blake, D. R., W. E. Mayer, S. C. Tyler, Y. Makide, D. C. Montaque, and F. S. Rowland, Global increase in atmospheric methane concentrations between 1978 and 1980, *Geophys. Res. Lett.*, *9*, 477-480, 1982.

Blake, D. R., V. H. Woo, S. C. Tyler and F. S. Rowland, Methane concentrations and source strengths in urban locations, *Geophys. Res. Lett.*, *11*, 1211-1214, 1984.

Blanchet, J. P., and R. List, On the optical properties of Arctic haze, in *Aerosols and Their Climate Effects*, edited by H. E. Gerber and A. Deepak, pp. 179-196, A. Deepak Publ., Hampton, VA, 1984.

Blatherwick, R. D., A. Goldman, D. G. Murcray, F. J. Murcray, G. R. Cook, and J. W. Van Allen, Simultaneous mixing ratio profiles of stratospheric NO and NO_2 as derived from balloon-borne infrared solar spectra, *Geophys. Res. Lett.*, *7*, 471-473, 1980.

Blatherwick, R. D., F. J. Murcray, F. H. Murcray, A. Goldman, and D. G. Murcray, Atlas of South Pole IR solar spectra, *Appl. Opt.*, *21*, 2658-2659, 1982.

Bloomfield, P., M. L. Thompson, and S. Zeger, A statistical analysis of Umkehr measurements of 32-46 km ozone, *J. Appl. Meteorol.*, *21*, 1828-1837, 1982.

Bloomfield, P., G. Oehlert, M. L. Thompson, and S. Zeger, A frequency domain analysis of trends in Dobson total ozone records, *J. Geophys. Res.*, *88*, 8512-8522, 1983.

Blumenthal, D. L., W. S. Keifer, and J. A. McDonald, Aircraft measurements of pollutants and meteorological parameters during the Sulphate Regional Experiment (SURE), *Rep. EPRI-EA-1909*, 230 pp., Meteorology Research, Santa Rosa, CA, 1981.

Bohringer, H., D. W. Fahey, F. C. Fehsenfeld, and E. E. Ferguson, The role of ion molecule reactions in conversion of N_2O_5 to HNO_3 in the stratosphere, *Planet. Space Sci.*, *31*, 185-191, 1983.

Bojkov, R. D., Some characteristics of the total ozone deduced from Dobson-spectrophotometer and filter-ozonometer data and their application to determination of the effectiveness of the ozone station network, *Ann. Geoph.*, *25*, 293-299, 1969.

Bojkov, R. D., Tropospheric ozone, its changes and possible radiative effect, *WMO Special Environment Report 16*, 1983.

Bojkov, R. D., and G. C. Reinsel, Trends in tropospheric ozone concentration, in *Atmospheric Ozone*, edited by C. S. Zerefos and A. Ghazi, pp. 775-781, D. Reidel, Dordrecht, 1984.

Bollinger, M. J., C. J. Hahn, D. D. Parrish, P. C. Murphy, D. L. Albritton, and F. C. Fehsenfeld, NOx measurements in clean continental air and analysis of the contributing meteorology, *J. Geophys. Res.*, *89*, 9623-9631, 1984.

Bonsang, B., and G. Lambert, Nonmethane HC in an oceanic atmosphere, *J. Atmos. Chem.*, *2*, 257-271, 1985.

Borchers, R., P. Fabian, and S. A. Penkett, First measurements of the vertical distribution of CCl_4 and CH_3CCl_3 in the stratosphere, *Naturwiss.*, *70*, 514-516, 1983.

Borchers, R., P. Fabian, B. C. Krueger, S. Lal, U. Schmidt, D. Knapska, and S. A. Penkett, The vertical distribution of CCl_2F-$CClF_2$ (CFC-113) and $CClF_2$-$CClF_2$ (CFC-114) in the stratosphere, paper presented at 5th General Assembly, International Association of Geomagnetism and Aeronomy, Prague, 5-17 August 1985.

Borden, T. R., and W. S. Hering, Ozonesonde observations over North America, Vol I, 525 pp., II, 286 pp., III, 266 pp., IV, 376 pp., *Report AFCRL-65-913*, Air Force Cambridge Res. Labs., Hanscom AFB, MA, 1964.

Borden, T. R., and W. S. Hering, Mean distributions of ozone density over North America 1963-1964, *Environmental Research Paper No. 162, Report AFCRL-65-913*, 28 pp., Air Force Cambridge Research Labs., Hanscom AFB, MA, 1965.

Borghi, R., D. Cariolle, A. Girard, J. Laurent, and N. Louisnard, Comparison entre les resultats d'un modele une dimensionnel et des resultats de mesures stratospheriques de CH_4, H_2O et des oxydes d'azote, *Rev. Phys. Appl.*, *18*, 229-237, 1983.

Borisenkov, Ye. P., and Yu. Ye. Kazakov, Effect of freons and halocarbons on the ozone layer of the atmosphere and climate, typed manuscript, USSR, 1977.

Borucki, W. J., and W. L. Chameides, Lightning: Estimates of the rates of energy dissipation of nitrogen fixation, *Res. Geophys. and Space Phys.*, *22*, 363-372, 1984.

Bossy, L., and M. Nicolet, On the variability of Lyman alpha with solar activity, *Planet. Space Sci.*, *29*, 907-914, 1981.

Bottenheim, J. W., K. A. Brice, and K. G. Anlauf, Discussion of a Lagrangian trajectory model describing long-range transport of oxides of nitrogen, the incorporation of PAN in the chemical mechanism, and supporting measurements of PAN and nitrate species at rural sites in Ontario, Canada, *Atmos. Environ.*, *18*, 2609-2619, 1984.

Boughner, R. E., The effect of increased carbon dioxide concentrations on stratospheric ozone, *J. Geophys. Res.*, *83*, 1326-1332, 1978.

Boughner, R. E., and V. Ramanathan, Climatic consequence of increasing CO_2: A study of the feedback mechanism between increasing CO_2 concentrations and the atmospheric ozone, water vapor, and thermal structure balance, paper presented at Second Conf. Atmospheric Radiation, Amer. Meteor. Soc., Arlington, VA, 29-31 October, 1975.

Boughner, R., J. C. Larsen, and M. Natarajan, The influence of NO and ClO variations at twilight on the interpretation of solar occultation measurements, *Geophys. Res. Lett.*, *7*, 231-234, 1980.

Bowman, K. P., and A. J. Krueger, A global climatology of total ozone from the Nimbus 7 Total Ozone Mapping Spectrometer (TOMS), *J. Geophys. Res.*, *90*, 7967-7976, 1985.

Boyd, J. P., The noninteraction of waves with the zonally averaged flow on a spherical Earth and the interrelationships of eddy fluxes of energy, heat and momentum, *J. Atmos. Sci.*, *33*, 2285-2291, 1976.

Bradford, C. M., F. H. Murcray, J. W. Van Allen, J. N. Brooks, D. G. Murcray, and A. Goldman, Ground level detection and feasibility for monitoring of several trace atmospheric constituents by high resolution infrared spectroscopy, *Geophys. Res. Lett.*, *3*, 387-390, 1976.

Bradshaw, J. D., and D. D. Davis, Sequential two-photon laser-induced fluorescence—A new method for detecting atmospheric trace levels of NO, *Optics Letters*, *7*, 224-226, 1982.

Bradshaw, J. D., S. KeSheng, M. O. Rodgers, S. T. Sandholm, and D. D. Davis, Measurements of tropospheric NO concentrations as part of the NASA GTE/CITE program, *Eos Trans. AGU*, *65*, 835, 1984.

Brasseur, G., *Physique et chimie de l'atmosphere moyenne*, Masson, Paris, 1982.

Brasseur, G., and M. Bertin, The action of chlorine on the ozone layer as given by a zonally averaged two-dimensional model, *Pure Appl. Geophys.*, *117*, 436-450, 1978/79.

Brasseur, G., and M. Nicolet, Chemospheric process of nitric oxide in the mesophere and stratosphere, *Planet. Space Sci.*, *21*, 939-961, 1973.

Brasseur, G., and P. C. Simon, Stratospheric chemical and thermal response to long-term variability in solar UV irradiance, *J. Geophys. Res.*, *86*, 7343-7362, 1981.

Brasseur, G., and S. Solomon, *Aeronomy of the Middle Atmosphere: Chemistry and Physics in the Stratosphere and Mesosphere*, 441 pp., D. Reidel, Dordrecht, 1984.

Brasseur, G., P. De Baets, and A. De Rudder, Solar variability and minor constituents in the lower thermosphere and in the mesosphere, *Space Sci. Rev.*, *34*, 377-385, 1983a.

REFERENCES

Brasseur, G., A. De Rudder, and P. C. Simon, Implication for stratospheric composition of a reduced absorption cross section in the Herzberg continuum of molecular oxygen, *Geophys. Res. Lett.*, *10*, 20-23, 1983b.

Brasseur, G., A. De Rudder, and C. Tricot, Stratospheric response to chemical perturbations, *J. Atmos. Chem.*, *3*, 261-288, 1985.

Bremner, J. M., and A. M. Blackmer, Nitrous oxide: Emission from soils during nitrification of fertilizer nitrogen, *Science*, *199*, 295-298, 1978.

Bremner, J. M., S. G. Robbins, and A. M. Blackmer, Seasonal variability in emission of nitrous oxide in soil, *Geophys. Res. Lett.*, *7*, 611-643, 1980.

Bretherton, F. P., Momentum transport by gravity waves, *Quart. J. Roy. Meteorol. Soc.*, *95*, 213-243, 1969.

Brewer, A. W., Evidence for a world circulation provided by the measurements of helium and water vapour distribution in the stratosphere, *Quart. J. Roy. Meteorol. Soc.*, *75*, 351-363, 1949.

Brewer, A. W., and J. R. Milford, The Oxford-Kew ozonesonde, *Proc. Roy. Soc. London A*, *256*, 470-495, 1960.

Brewer, A. W., and A. W. Wilson, The regions of formation of atmospheric ozone, *Quart. J. Roy. Meteorol. Soc.*, *94*, 249-265, 1968.

Brice, K. A., R. G. Derwent, A. E. J. Eggleton, and S. A. Penkett, Measurements of CCl_3F and CCl_4 at Harwell 1/75-6/81, *Atmos. Environ.*, *16*, 2543-2554, 1982.

Brice, K. A., S. A. Penkett, D. H. F. Atkins, F. J. Sandalls, D. J. Bamber, A. F. Tuck, and G. Vaughan, Atmospheric measurements of peroxyacetylnitrate (PAN) in rural, South-East England: Seasonal variations, Winter photochemistry, and long-range transport, *Atmos. Environ.*, *18*, 2691-2702, 1984.

Brietenbeck, G. A., A. M. Blackmer, and J. M. Bremner, Effects of different nitrogen fertilizers on emissions of nitrous oxide from soil, *Geophys. Res. Lett.*, *7*, 85-88, 1980.

Briggs, J., and W. T. Roach, Aircraft observations near jet streams, *Quart. J. Roy. Meteorol. Soc.*, *89*, 225-247, 1963.

Broadfoot, A. L., The solar spectrum 2100-3200 /, *Astrophys. J.*, *173*, 681-689, 1972.

Broecker, W. S., T. H. Peng, and R. Engh, Modeling the carbon system, *Radiocarbon*, *22*, 565-598, 1980.

Browell, E. V., A. F. Carter, and S. T. Shipley, An airborne lidar system for ozone and aerosol profiling in the troposphere and lower stratosphere, in *Proceedings of the Quadrennial International Ozone Symposium*, *Vol. I*, edited by J. London, pp. 99-107, IAMAP, NCAR, Boulder, CO, 1981.

Browell, E. V., A. F. Carter, S. T. Shipley, R. J. Allen, C. F. Butler, M. N. Mayo, J. H. Siviter, Jr, and W. M. Hall, NASA multi purpose airborne DIAL system and measurements of ozone and aerosol profiles, *Appl. Opt.*, *22*, 522-534, 1983.

Browell, E. V., S. Ismail, E. F. Danielsen, G. L. Gregory, and S. M. Beck, Airborne lidar and in situ measurements of a tropopause fold event, in press, 1985.

Bruehl, C. H., and P. J. Crutzen, A radiative-convective model to study the sensitivity of climate and chemical composition to a variety of human activities, *Stratosphere*, Proceedings of a working party meeting, Brussels, May 18, 1984, *Commission of European Communities*, edited by A. Ghazi, pp. 85-94, 1984.

Brune, W. H., E. M. Weinstock, J. J. Schwab, R. M. Stimpfle, and J. G. Anderson, Stratospheric ClO: Insitu detection with a new approach, *Geophys. Res. Lett.*, *12*, 441-444, 1985.

Bryan, K., F. G. Komro, S. Manabe, and M. J. Spelman, Transient climate response to increasing atmospheric carbon dioxide, *Science*, *215*, 56-58, 1982.

Bryan, K., F. G. Komro, and C. Rooth, The ocean's transient response to global surface temperature anomalies, in *Climate Processes and Climate Sensitivity, Geophysical Monograph 29*, Maurice Ewing Series Vol. 5, edited by J. E. Hanson and T. Takahashi, pp. 29-38, American Geophysical Union, Washington, DC, 1984.

Bufton, J. L., R. W. Stewart, and Chi Weng, Remote measurement of tropospheric ozone, *Appl. Opt.*, *18*, 3363-3364, 1979.

Buijs, H. L., G. L. Vail, G. Tremblay, and D. J. W. Kendall, Simultaneous measurements of the volume mixing ratio of HCl and HF in the stratosphere, *Geophys. Res. Lett.*, *7*, 205-208, 1980.

Burkhardt, E. G., C. A. Lambert, and C. K. N. Patel, Stratospheric nitric oxide: Measurements during daytime and sunset, *Science*, *188*, 1111-1113, 1975.

Burnett, C. R., and E. B. Burnett, Spectroscopic measurements of the vertical column abundance of hydroxyl (OH) in the Earth's atmosphere, *J. Geophys. Res.*, *86*, 5185-5202, 1981.

Burnett, C. R., and E. B. Burnett, Vertical column abundance of atmospheric OH at solar maximum from Fritz Peak, Colorado, *Geophys. Res. Lett.*, *9*, 708-711, 1982.

Burnett, C. R., and E. B. Burnett, OH PEPSIOS, *Appl. Opt.*, *22*, 2887-2892, 1983a.

Burnett, C. R., and E. B. Burnett, OH column abundance measurements from Boca Raton, FL, Fritz Peak, CO, and Poker Flat, AK, *Eos Trans. AGU*, *64*, 781, 1983b.

Burnett, C. R., and E. B. Burnett, Observational results on the vertical column abundance of atmospheric hydroxyl: Description of its seasonal behavior 1977-1982 and of the 1982 El Chichon perturbation, *J. Geophys. Res.*, *89*, 9603-9611, 1984.

Burnett, C. R., and E. B. Burnett, Atmospheric hydroxyl response to the partial solar eclipse of May 30, 1984, *Geophys. Res. Lett.*, *12*, 263-266, 1985.

Burnham, J., Atmospheric gusts-A review of the results of some recent research at the Royal Aircraft Establishment, *Mon. Weather Rev.*, *98*, 723-734, 1970.

Burrows, J. P., T. J. Wallington, and R. P. Wayne, Kinetics of the reaction of OH with ClO, *J. Chem. Soc. Faraday Trans. 2*, *80*, 957-971, 1984.

Burrows, J. P., D. W. T. Griffith, G. K. Moortgat, and G. S. Tyndall, Matrix isolation Fourier transform infrared study of the products of the reaction between ClO and NO_2, *J. Phys. Chem.*, 266-271, 1985.

Butchart, N., and E. E. Remsberg, The area of the stratospheric polar vortex as a diagnostic for tracer transport on an isentropic surface, *J. Atmos. Sci.*, in press, 1985.

Butchart, N., S. A. Clough, T. N. Palmer, and P. J. Trevelyan, Simulations of an observed stratospheric warming with quasi-geostrophic refractive index as a model diagnostic, *Quart. J. Roy. Meteorol. Soc.*, *108*, 475-502, 1982.

Butler, D. M., Earth observing system. Science and mission requirements. Working group report, Volume I, Part 2, *NASA Technical Memorandum 86129*, NASA Goddard Space Flight Center, Greenbelt, MD, 1984.

Cadle, R. D., and G. W. Grams, Stratospheric aerosol particles and their optical properties, *Reviews of Geophysics and Space Physics*, *13(4)*, 475-501, 1975.

Cadle, R. D., P. J. Crutzen, and D. H. Ehhalt, Heterogeneous chemical reactions in the stratosphere, *J. Geophys. Res.*, *80*, 3381-3385, 1975.

Cahen, C., J. Pelon, P. Flamant, and G. Megie, Mesure de la vapeur d'eau tropospherique par absorption differentielle laser, *C. R. Acad. Sci.*, Paris, *292*, 29, 1981.

Callis, L. B., and M. Natarajan, Stratospheric ozone and temperature perturbations: An examination of synergistic effects, in *Proceedings of the Quadrennial International Ozone Symposium, Vol. II*, edited by J. London, pp. 910-917, IAMAP, NCAR, Boulder, CO, 1981.

Callis, L. B., and M. Natarajan, Atmospheric carbon dioxide and chlorofluoromethanes: Combined effects on stratospheric ozone, temperature, and surface temperature, *Geophys. Res. Lett.*, *8*, 587-590, 1981.

Callis, L. B., M. Natarajan, and R. E. Boughner, On the relationship between the greenhouse effect, atmospheric photochemistry and species distribution, *J. Geophys. Res.*, *88*, 1401-1426, 1983a.

REFERENCES

Callis, L. B., J. M. Russell III, K. V. Haggard, and M. Natarajan, Examination of winter-time latitudinal gradients in stratospheric NO_2 using theory and LIMS observations, *Geophys. Res. Lett.*, *10*, 945-948, 1983b.

Callis, L. B., M. Natarajan, and J. M. Russell III, Estimates of the stratospheric distributions of odd nitrogen from the LIMS data, *Geophys. Res. Lett.*, *12*, 259-262, 1985a.

Callis, L. B., M. Natarajan, R. E. Boughner, J. M. Russell III, and J. D. Lambeth, Stratospheric photochemical studies using Nimbus 7 data, Part II: Development of infrared trace species distributions, *J. Geophys. Res.*, in press, 1985b.

Calvert, J. G., Test of the theory of ozone generation in Los Angeles atmosphere, *Environ. Sci. Technol.*, *10*, 248-256, 1976.

Camy-Peyret, C., J.-M. Flaud, L. Delbouille, G. Roland, J. W. Brault, and L. Testerman, Quadrupole transitions of the 1-0 band of N_2 observed in high resolution atmospheric spectrum, *J. Physique Lett.*, *42*, 279-283, 1981.

Camy-Peyret, C., J.-M. Flaud, J. Laurent, and G. M. Stokes, First infrared measurement of atmospheric NO_2 from the ground, *Geophys. Res. Lett.*, *10*, 35-38, 1983.

Cariolle, D., and D. Brard, The distribution of ozone and active stratospheric species: Results of a two-dimensional atmospheric model, in *Atmospheric Ozone*, edited by C. S. Zerefos and A. Ghazi, pp. 77-81, D. Reidel, Dordrecht, 1984.

Cariolle, D., and M. Deque, A GCM study of the transport of heat, momentum and ozone in the stratosphere, in *Atmospheric Ozone*, edited by C. S. Zerefos and A. Ghazi, pp. 24-27, D. Reidel, Dordrecht, 1984.

Carli, B., F. Mencaraglia, and A. Bonetti, Fourier spectroscopy of the stratospheric emission, *Int. J. Infrared mm Waves*, *1*, 253-276, 1980.

Carli, B., F. Mencaraglia, and A. Bonetti, New assignments in the submillimeter emission of the stratosphere, *Int. J. Infrared mm Waves*, *3*, 385-394, 1982.

Carli, B., F. Mencaraglia, A. Bonetti, B. M. Dinelli, and F. Forni, Submillimeter detection of stratospheric OH and further line assignments in the stratospheric emission spectrum, *Int. J. Infrared mm Waves*, *4*, 475-488, 1983.

Carli, B., F. Mencaraglia, and A. Bonetti, Submillimeter high resolution FT spectrometer for atmospheric studies, *Appl. Opt.*, *23*, 2534-2603, 1984.

Carli, B., F. Mencaraglia, A. Bonetti, M. Carlotti, and I. Nolt, Detection of atomic oxygen and further line assignments in the far infrared stratospheric spectrum, *Int. J. Infrared mm Waves*, *6*, 149-176, 1985a.

Carli, B. M. Carlotti, D. M. Dinelli, F. Mencaraglia, and I. Nolt, Further evidence of stratospheric chlorine monoxide, in press, 1985b.

Carney, T. A., and J. Fishman, An investigation of the vertical distribution of trace constituents in the troposphere with a one-dimensional photochemical model and a model of the trade-wind boundary layer, *Eos Trans. AGU*, *65*, 836, 1984.

Carroll, M. A., and B. A. Ridley, Tropospheric NOx measurements, *Eos Trans. AGU*, *65*, 834, 1984.

Carter, W. P. L., A. C. Lloyd, J. L. Sprung, and J. N. Pitts, Jr., Progress in the validation of a detailed mechanism for the photooxidation of propene and nebutane in photochemical smog, *Int. J. Chem. Kinet.*, *11*, 45-111, 1979.

Carver, J. H., B. H. Horton, and F. G. Burger, Nocturnal ozone distribution in the upper atmosphere, *J. Geophys. Res.*, *71*, 4189-4191, 1966.

Carver, J. H., H. P. Giess, T. H. Hobbs, B. R. Lewis, and J. H. McCoy, Temperature dependence of the molecular oxygen photoabsorption cross section near the H Lyman alpha line, *J. Geophys. Res.*, *82*, 1955-1960, 1977.

CDAC: See National Research Council, *Changing Climate*, Carbon Dioxide Assessment Committee.

Cess, R. D., Climatic change: An appraisal of atmospheric feedback mechanisms employing zonal climatology, *J. Atmos. Sci.*, *33*, 1831-1843, 1976.

Cess, R. D., and S. C. Chen, The influence of ethane and acetylene upon the thermal structure of the Jovian atmosphere, *Icarus*, *26*, 444-450, 1975.

Cess, R. D., and S. D. Goldenberg, The effect of ocean heat capacity upon global warming due to increasing atmospheric carbon dioxide, *J. Geophys. Res.*, *86*, 498-502, 1981.

Cess, R. D., and G. L. Potter, A commentary on the recent CO_2-climate controversy, *Climatic Change*, *6*, 365-376, 1984.

Cess, R. D., and L. S. Wang, A band absorptance formulation for nonisothermal gaseous radiation, *Int. J. Heat Mass Transfer*, *13*, 547-555, 1970.

Cess, R. D., B. P. Briegleb and M. S. Lian, Low-latitude cloudiness and climate feedback: Comparative estimates from satellite data, *J. Atmos. Sci.*, *39*, 53-59, 1982.

Cess, R. D., D. P. Kratz, S. J. Kim and J. Caldwell, Infrared band models for atmospheric methane, *J. Geophys. Res.*, in press, 1985.

Chamberlin, T. C., An attempt to frame a working hypothesis of the cause of glacial periods on an atmospheric basis, *J. Geol.*, *7*, 545, 1899.

Chameides, W. L., The photochemistry of a remote marine stratiform cloud, *J. Geophys. Res.*, *89*, 4739-4755, 1984.

Chameides, W. L., and D. D. Davis, The free radical chemistry of cloud droplets and its impact upon the composition of rain, *J. Geophys. Res.*, *87*, 4863-4877, 1982.

Chameides, W. L., and A. Tan, The two dimensional diagnostic model for tropospheric OH: An uncertainty analysis, *J. Geophys. Res.*, *86*, 5209-5223, 1981.

Chameides, W. L., and J. C. G. Walker, A photochemical theory of tropospheric ozone, *J. Geophys. Res.*, *78*, 8751-8760, 1973.

Chameides, W. L., D. H. Stedman, R. R. Dickerson, D. W. Rusch, and R. J. Cicerone, NOx production in lightning, *J. Atmos. Sci.*, *34*, 143-149, 1977a.

Chameides, W. L., S. C. Liu, and R. J. Cicerone, Possible variations in atmospheric methane, *J. Geophys. Res.*, *82*, 1795-1798, 1977b.

Chan, S. H., and C. L. Tien, Total band absorptance of nonisothermal infrared-radiating gases, *J. Quant. Spectrosc. Radiat. Transfer*, *9*, 1261-1271, 1969.

Chance, K. V., and W. A. Traub, An upper limit for stratospheric hydrogen peroxide, *J. Geophys. Res.*, *89*, 11655-11660, 1984.

Chance, K. V., and W. A. Traub, to be published under BIC I, BIC II, 1986.

Chance, K. V., J. C. Brasunas, and W. A. Traub, Far infrared measurement of stratospheric HCl, *Geophys. Res. Lett.*, *9*, 704-706, 1980.

Chandra, S., Solar-induced oscillations in the stratosphere: A myth or reality?, *J. Geophys. Res.*, *90*, 2331-2339, 1985.

Chang, C. P., Forcing of stratospheric Kelvin waves by tropospheric heat sources, *J. Atmos. Sci.*, *35*, 740-744, 1976.

Chang, J. S., A. C. Baldwin, and D. M. Golden, An explanation of the preferential formation of less stable isomers in threebody reactions: $Cl + NO_2 + M$, $ClO + NO_2 + M$, *J. Chem. Phys.*, *71*, 2021-2024, 1979.

Chanin, M. L., The Intercomparison Ozone Campaign held in France in June 1981: Description of the campaign, *Planet. Space Sci.*, *31*, 707-715, 1983a.

Chanin, M. L., The Ozone Intercomparison Campaign, 1981: Concluding remarks, *Planet. Space Sci.*, *31*, 811-812, 1983b.

Chanin, M. L., and A. Hauchecorne, Lidar observations of gravity and tidal waves in the middle atmosphere, *J. Geophys. Res.*, *86*, 9715-9721, 1981.

REFERENCES

Chao, W. C., and M. R. Schoeberl, On the linear approximation of gravity wave saturation in the mesosphere, *J. Atmos. Sci.*, *41*, 1893-1898, 1984.

Chapman, S., A theory of upper atmospheric ozone, *Mem. Roy. Met. Soc.*, *3*, 103-125, 1930.

Chapman, W., and G. Peckham, Spectral analysis of wave motions in the middle atmosphere, *Phil. Trans. Roy. Soc. London*, *A296*, 59-63, 1980.

Charlock, T. P., Cloud optical feedback and climate stability in a radiative-convective model, *Tellus*, *34*, 245-254, 1982.

Charney, J. G., The dynamics of long waves in a baroclinic westerly current, *J. Meteorol.*, *4*, 135-162, 1947.

Charney, J. G. (Chairman), *Carbon Dioxide and Climate: A Scientific Assessment*, 33 pp., National Academy Press, Washington, DC, 1979.

Charney, J. G., and P. G. Drazin, Propagation of planetary-scale disturbances from the lower into the upper atmosphere, *J. Geophys. Res.*, *66*, 83-109, 1961.

Charney, J. G., and M. E. Stern, On the stability of internal baroclinic jets in a rotating atmosphere, *J. Atmos. Sci.*, *19*, 159-172, 1962.

Chatfield, R. B., and P. J. Crutzen, Sulfur dioxide in remote oceanic air: Cloud transports of reactive precursors, *J. Geophys. Res.*, *89*, 7111-7132, 1984.

Chedin, A., and N. A. Scott, The impact of spectroscopic parameters on the comparison of the Jovian atmosphere discussed in connection with the recent laboratory, earth and planetary observation programs, *J. Quant. Spectrosc. Radiat. Transfer*, *32*, 453-461, 1984.

Chedin, A., N. Husson, N. A. Scott, I. Jobard, I. Cohen-Hallaleh, and A. Berroir, La Banque de donees GEISA, Description et logiciel d'utilisation, Laboratoire de Meteorologie Dynamique du C.N.R.S., *Internal Note 108*, Ecole Polytechnique, 91128 Palaiseau Cedex, France, October, 1980.

Chedin, A., N. Husson, N. A. Scott, I. Cohen-Hallaleh, and A. Berroir, The GEISA data bank: 1984 version, Laboratoire de Meteorologie Dynamique du C.N.R.S., *Internal Note 127*, Ecole Polytechnique, 91128 Palaiseau Cedex, France, February, 1985.

Chemical Manufacturers Association, CMA, *Effect of chlorofluorocarbons on the atmosphere, revision 17*, edited by B. P. Block, H. Magid, and R. B. Ward, 98 pp., Washington, DC, 1982.

Chemical Manufacturers Association, CMA, *Production, sales and calculated release of CFC 11 and CFC 12 through 1983*, October, 1984.

Chemical Manufacturers Association, CMA, *Production, sales and calculated release of CFC 11 and CFC 12 through 1984*, October, 1985.

Chemical Manufacturers Association-National Bureau of Standards, CMA-NBS, *Proceedings of CMA-NBS workshop on atmospheric spectra*, November 3-4, 1983, Gaithersburg, MD, edited by A. Weber, June, 1985.

Cheung, A.S.C., K. Yoshino, W. H. Parkinson, and D. E. Freeman, Herzberg continuum cross section of oxygen in the wavelength region 193.5-204.0 nm and band oscillator strengths of the (0,0) and (1,0) Schumann-Runge bands, *Can. J. Phys.*, *62*, 1752-1762, 1984a.

Cheung, A. S. C., K. Yoshino, W. H. Parkinson, and D. E. Freeman, Herzberg continuum cross-section of oxygen in the wavelength region 193.5-204 nm: New laboratory measurements and stratospheric implications, *Geophys. Res. Lett.*, *11*, 580-582, 1984b.

Chou, C. C., R. J. Milstein, W. S. Smith, H. Veraruiz, M. J. Molina, and F. S. Rowland, Stratospheric photodissociation of several saturated perhalo- chlorofluorocarbon compounds in current technological use (Fluorocarbons -13, -113, -114, and -115), *J. Phys. Chem.*, *82*, 1-7, 1978.

Chou, M.-D., L. Peng, and A. Arking, Climate studies with a multilayer energy balance model. Part III: Climatic impact of stratospheric volcanic aerosols, *J. Atmos. Sci.*, *41*, 759-767, 1984.

Chu, W. P., and M. P. McCormick, Inversion of stratospheric aerosol and gaseous constituents from spacecraft solar extinction data in the 0.38 - 1.0 μm wavelength region, *Appl. Opt.*, *18*, 1404-1413, 1979.

CIAP: See Climatic Impact Assessment Program.

Cicerone, R. J., Atmospheric carbon tetrafluoride: A nearly inert gas, *Science*, *206*, 59-61, 1979.

Cicerone, R. J., Methane in the atmosphere, in *Global Environment Problems*, edited by S. F. Singer, Paragon House, New York, in press, 1985.

Cicerone, R. J., and J. L. McCrumb, Photodissociation of isotopically heavy O_2 as a source of atmospheric O_3, *Geophys. Res. Lett.*, *7*, 251-254, 1980.

Cicerone, R. J., and J. D. Shetter, Sources of atmospheric methane: Measurements in rice paddies and a discussion, *J. Geophys. Res.*, *86*, 7203-7209, 1981.

Cicerone, R. J., and R. Zellner, The atmospheric chemistry of hydrogen cyanide, *J. Geophys. Res.*, *88*, 10689-10696, 1983.

Cicerone, R. J., S. Walters, and S. C. Liu, Non-linear response of stratospheric ozone column to chlorine injections, *J. Geophys. Res.*, *88*, 3647-3661, 1983a.

Cicerone, R. J., J. D. Shetter, and C. C. Delwiche, Seasonal variation of methane flux from a California rice paddy, *J. Geophys. Res.*, *88*, 11022-11024, 1983b.

Cieslik, S., and M. Nicolet, The aeronomic dissociation of nitric oxide, *Planet. Space Sci.*, *21*, 925-930, 1973.

Clancy, R. T., D. O. Muhleman, and G. L. Berge, Microwave spectra of terrestrial mesospheric CO, *J. Geophys. Res.*, *87*, 5009-5014, 1982.

Clark, J.H.E., and L. T. Morone, Mesospheric heating due to convectively excited gravity waves. A case study, *Mon. Weather Rev.*, *109*, 990-1001, 1981.

Clark, J.H.E., and T. G. Rogers, The transport of conservative trace gases by planetary waves, *J. Atmos. Sci.*, *35*, 2232-2235, 1978.

Clark, T. A., and D. J. W. Kendall, Far infrared emission spectrum of the stratosphere from balloon altitudes, *Nature*, *260*, 31-32, 1976.

Clark, T. A., and D. J. W. Kendall, Line positions and strengths of magnetic dipole transitions of molecular oxygen from stratospheric emission spectra, *J. Quant. Spectrosc. Radiat. Transfer*, *24*, 65-73, 1980.

Clark, T. A., D. A. Naylor, R. T. Boreiko, J. M. Hoogerdijk, B. Fitton, M. F. Kessler, and R. J. Emery, Downward flux of atmospheric 63)m emission from atomic oxygen at balloon altitudes, *Nature*, *313*, 206-207, 1985.

Climate Analysis Center, *Climate Diagnostics Bulletin*, Published monthly by the Climate Analysis Center, NOAA/NMC/NWS, Washington, DC, 1983.

Climate Analysis Center, *Climate Diagnostics Bulletin*, Published monthly by the Climate Analysis Center, NOAA/NMC/NWS, Washington, DC, 1984.

Climatic Impact Assessment Program, Report of findings: The effects of stratospheric pollution by aircraft, *DOT-TST-75-50*, edited by A. J. Grobecker, S. C. Coroniti, and R. H. Cannon, Jr., 551 pp., Department of Transportation, Washington, DC, 1974.

Clough, S. A., N. S. Grahame, and A. O'Neill, Potential vorticity in the stratosphere derived using data from satellites, *Quart. J. Roy. Meteorol. Soc.*, *111*, 335-358, 1985.

CMA: See Chemical Manufacturer's Association.

Coakley, J. A. Jr., and R. D. Cess, The effect of tropospheric aerosols on the earth's radiation budget: A parameterization for climate models, *J. Atmos. Sci.*, *40*, 116-138, 1983.

Coffey, M. T., W. G. Mankin, and A. Goldman, Simultaneous spectroscopic determination of the latitudinal, seasonal, and diurnal variability of stratospheric N_2O, NO, NO_2, and HNO_3, *J. Geophys. Res.*, *86*, 7331-7341, 1981a.

Coffey, M. T., W. G. Mankin, and R. J. Cicerone, Spectroscopic detection of stratospheric hydrogen cyanide, *Science*, *214*, 333-335, 1981b.

Coffey, M. T., W. G. Mankin, A. Goldman, C. P. Rinsland, G. A. Harvey, V. Malathy Devi, and G. M. Stokes, Infrared measurements of atmospheric ethane (C_2H_6) from aircraft and ground based solar absorption spectra in the 3000 cm^{-1} region, *Geophys. Res. Lett.*, *12*, 199-202, 1985.

REFERENCES

Coffey *et al.*, 1985: See Roscoe *et al.*, 1985.

Cohen, Y., and L. I. Gordon, Nitrous oxide in the oxygen minimum of the eastern tropical North Pacific: Evidence for its consumption during denitrification and possible mechanisms for its production, *Deep Sea Res.*, *6*, 509-524, 1978.

Cohen, Y., and L. I. Gordon, Nitrous oxide production in the ocean, *J. Geophys. Res.*, *84*, 347-353, 1979.

Cole, A. E., and A. J. Kantor, Air Force Reference Atmospheres, *Rep. AFGL-TR-78-0051*, 78 pp., Air Force Geophys. Lab., Hanscom AFB, MA, 1978.

Connell, P. S., D. J. Wuebbles, and J. S. Chang, Stratospheric hydrogen peroxide-The relationship of theory and observation, *J. Geophys. Res.*, *90*, 10726-10732, 1985.

Cook, J. W., G. E. Brueckner, and M. E. Van Hoosier, Variability of the solar flux in the far ultraviolet 1175-2100 Å, *J. Geophys. Res.*, *85*, 2257-2268, 1980.

Cornford, S. G., and C. S. Spavins, Some measurements of cumulonimbus tops in the pre-monsoon season in the north-east of India, *Met. Mag.*, *102*, 314-332, 1973.

COSPAR International Reference Atmosphere, CIRA, edited by A. C. Strickland, Akademie-Verlag, Berlin, 1972.

Cowley, J. R., and G. M. Lawrence, Earth Limb altitude determination for the Solar Mesosphere Explorer, paper presented at AIAA Aerospace Sciences Meeting, *AIAA Paper 83-0429*, 9 pp., Reno, Nevada, January 10-13, 1983.

Cox, R. A., and M. J. Coffey, Thermal decomposition of peroxyacetyl nitrate in the presence of NO, *Environ. Sci. Tech.*, *11*, 900-906, 1977.

Cox, R. A., and R. G. Derwent, Kinetics of chlorine oxide radical reactions using modulated photolysis, Part I, Disproportionation of ClO, *J. Chem. Soc. Far. I*, *75*, 1635-1647, 1979.

Cox, R. A., A.E.J. Eggleton, R. G. Derwent, J. E. Lovelock, and D. H. Pack, Long-range transport of photochemical ozone in north-western Europe, *Nature*, *255*, 118-121, 1975.

Cox, R. A., R. G. Derwent, A. E. J. Eggleton, and H. J. Reid, Kinetics of chlorine oxide radical reactions using modulated photolysis, Part 2, ClO and ClOO radical kinetics, *J. Chem. Soc. Far. I*, *75*, 1648-1666, 1979.

Cox, R. A., J. P. Burrows, and G. B. Coker, Product formation in the association reaction of ClO with NO_2 investigated by diode laser spectroscopy, *Int. J. Chem. Kinet.*, *16*, 445-467, 1984.

Coy, L., An unusually large westerly amplitude of the quasi-biennial oscillation, *J. Atmos. Sci.*, *36*, 174-176, 1979.

Coy, L., An unusually large westerly amplitude of the quasi-biennial oscillation, corrigendum, *J. Atmos. Sci.*, *37*, 913, 1980.

Coy, L., and M. Hitchman, Kelvin wave packets and flow acceleration: A comparison of modeling and observation, *J. Atmos. Sci.*, *41*, 1875-1880, 1984.

Craig, H., and C. C. Chou, Methane: The record in polar ice cores, *Geophys. Res. Lett.*, *9*, 1221-1224, 1982.

Craig, R. A., *The Upper Atmosphere: Meteorology and Physics*, 209 pp., Academic Press, New York, 1965.

Craig, R. L., R. A. Vincent, G. J. Fraser, and M. J. Smith, The quasi 2-day wave in the Southern Hemisphere mesosphere, *Nature*, *287*, 319-320, 1980.

Craig, R. L., R. A. Vincent, and R. A. Plumb, On the interaction between the quasi 2-day wave and the mean flow, in *Handbook for MAP, Vol. 18*, edited by S. Kato, pp. 76-79, SCOSTEP Secretariat, Univ. of Illinois, Urbana, 1985.

Crane, A. J., Uses of satellite data in studies of stratospheric dynamics, Ph.D. thesis, Oxford University, Oxford, 1977.

Crane, A. J., Aspects of the energetics of the upper stratosphere during the January-February 1973 major sudden warming, *Quart. J. Roy. Meteorol. Soc.*, *105*, 185-206, 1979.

Crane, A. J., J. D. Haigh, J. A. Pyle, and C. F. Rogers, Mean meridional circulations of the stratosphere and mesosphere, *Pure Appl. Geophys.*, *118*, 307-328, 1980.

Crutzen, P. J., discussion of "Absorption and emission by carbon dioxide in the mesosphere", *Quart. J. Roy. Meteorol. Soc.*, *96*, 767-769, 1970.

Crutzen, P. J., Ozone production rates in an oxygen, hydrogen, nitrogen-oxide atmosphere, *J. Geophys. Res.*, *76*, 7311-7327, 1971.

Crutzen, P. J., Gas phase nitrogen and methane chemistry in the atmosphere, in *Physics and Chemistry of Upper Atmospheres*, edited by B. M. McCormac, D. Reidel, Boston, MA, 1973a.

Crutzen, P. J., A discussion of the chemistry of some minor constituents in the stratosphere and troposphere, *Pure Appl. Geophys.*, *106-108*, 1385-1399, 1973b.

Crutzen, P. J., Photochemical reactions initiated by and influencing ozone in unpolluted tropospheric air, *Tellus*, *26*, 47-57, 1974.

Crutzen, P. J., The possible importance of CSO for the sulfate layer of the stratosphere, *Geophys. Res. Lett.*, *3*, 73-76, 1976.

Crutzen, P. J., The role of NO and NO_2 in the chemistry of the stratosphere and troposphere, *Ann. Rev. Earth Pl. Sci.*, *7*, 443-472, 1979.

Crutzen, P. J., Atmospheric interactions--Homogeneous gas reactions of C, N and S containing compounds, in *The Major Biogeochemical Cycles and Their Interactions*, edited by B. Bolin and R. Cook, pp. 67-112, Wiley, New York, 1983.

Crutzen, P. J., The role of the tropics in atmospheric chemistry, in *Geophysiology of Amazonia*, edited by R. Dickinson, Wiley, New York, in press, 1985.

Crutzen, P. J., and D. H. Ehhalt, Effects of nitrogen fertilizers and combustion on the stratospheric ozone layer, *Ambio*, *6*, 112-117, 1977.

Crutzen, P. J., and J. Fishman, Average concentrations of OH in the troposphere and the budgets of CH_4, CO, H_2, and CH_3CCl_3, *Geophys. Res. Lett.*, *4*, 321-324, 1977.

Crutzen, P. J., and L. T. Gidel, A two dimensional photochemical model of the atmosphere. 2. The tropospheric budgets of the anthropogenic chlorocarbons, CO, CH_4, CH_3Cl and the effect of various NO_x sources on tropospheric ozone, *J. Geophys. Res.*, *88*, 6641-6661, 1983.

Crutzen, P. J., and U. Schmailzl, Chemical budgets of the stratosphere, *Planet. Space Sci.*, *31*, 1009-1032, 1983.

Crutzen, P. J., and S. Solomon, Response of mesospheric ozone to particle precipitation, *Planet. Space Sci.*, *28*, 1147-1153, 1980.

Crutzen, P. J., I. S. A. Isaksen, and G. C. Reid, Solar proton events: Stratospheric sources of nitric oxide, *Science*, *189*, 457-459, 1975.

Crutzen, P. J., L. E. Heidt, J. P. Krasnec, W. H. Pollock, and W. Seiler, Biomass burning as a source of atmospheric gases CO, H_2, N_2O, NO, CH_3Cl and COS, *Nature*, *282*, 253-256, 1979.

Crutzen, P. J., W. Seiler, A. C. Delany, J. Greenburg, P. Haagensen, L. Heidt, R. Lueb, W. Pollock, A. Wartburg, and P. Zimmerman, Tropospheric chemical composition measurements in Brazil during the dry seasons, *J. Atmos. Chem.*, *2*, 233-256, 1983.

Cunnold, D., Fluorocarbon lifetime and releases from 5 years of ALE data, paper presented at CSIRO symposium, The Scientific Application of Baseline Observations of Atmospheric Composition, Aspendale, Australia, 7-9 November, 1984.

Cunnold, D., F. N. Alyea, N. Phillips, and R. G. Prinn, A three-dimensional dynamical chemical model of atmospheric ozone, *J. Atmos. Sci.*, *32*, 170-194, 1975.

Cunnold, D. M., F. N. Alyea, and R. G. Prinn, Relative effects on atmospheric ozone of latitude and altitude of supersonic flight, *AIAA Journal*, *15*, 337-345, 1977.

REFERENCES

Cunnold, D. M., F. N. Alyea, and R. G. Prinn, Preliminary calculations concerning the maintenance of the zonal mean ozone distribution in the Northern Hemisphere, *Pure Appl. Geophys.*, *118*, 329-354, 1980.

Cunnold, D. M., R. G. Prinn, R. A. Rasmussen, P. G. Simmonds, F. N. Alyea, C. A. Cardelino, A. J. Crawford, P. J. Fraser, and R. D. Rosen, The atmospheric lifetime experiment, 3, Lifetime methodology and application to 3 years of $CFCl_3$ data, *J. Geophys. Res.*, *88*, 8379-8400, 1983a.

Cunnold, D. M., R. G. Prinn, R. A. Rasmussen, P. G. Simmonds, F. N. Alyea, C. A. Cardelino, and A. J. Crawford, The atmospheric lifetime experiment, 4, Results for CF_2Cl_2 based on 3 years of data, *J. Geophys. Res.*, *88*, 8401-8414, 1983b.

Curtis, P. D., J. T. Houghton, G. D. Peskett, and C. D. Rodgers, The pressure modulator radiometer for Nimbus F, *Proc. Roy. Soc. London A*, *337*, 135-150, 1974.

Dacey, J., and M. J. Klug, Methane efflux from lake sediments through water lilies, *Science*, *203*, 1253-1255, 1979.

Danielsen, E. F., Trajectories: Isobaric, Isentropic and Actual, *J. Meteorol.*, *18*, 479-493, 1961.

Danielsen, E. F., *Project Springfield Report*, Defense Atomic Support Agency, DASA 1517, Washington, DC, 1964.

Danielsen, E. F., Transport and diffusion of stratospheric radioactivity based on synoptic hemispheric analyses of potential vorticity, Final report, *Report NYO-3317-3*, 97 pp., Pennsylvania State University, University Park, PA, 1967.

Danielsen, E. F., Stratospheric-tropospheric exchange based on radioactivity, ozone and potential vorticity, *J. Atmos. Sci.*, *25*, 502-518, 1968.

Danielsen, E. F., The relationship between severe weather, major dust storms and rapid large-scale cyclogenesis (II), in *Subsynoptic Extratropical Weather Systems: Observations, Analysis, Modeling, and Prediction, Notes from a colloquium, Summer, 1974, Volume II: Seminars and workshops,*, *Report PB-247286/8*, pp. 226-241, NCAR, Boulder, CO, 1974.

Danielsen, E. F., An objective method for determining the generalized transport tensor for two-dimensional Eulerian models, *J. Atmos. Sci.*, *38*, 1319-1339, 1981.

Danielsen, E. F., Statistics of cold cumulonimbus anvils based on enhanced infrared photographs, *Geophys. Res. Lett.*, *9*, 601-604, 1982.

Danielsen, E. F., Meteorological context for Global Tropospheric Experiments' instruments tests, paper presented to American Geophysical Union, San Francisco, California, December 3-7, 1984, *Eos Trans. AGU*, *65*, 834, 1984.

Danielsen, E. F., and R. S. Hipskind, Stratospheric-tropospheric exchange at polar latitudes in summer, *J. Geophys. Res.*, *85*, 393-400, 1980.

Danielsen, E. F., and D. Kley, A tropical cumulonimbus source for correlated water vapor and ozone minima in extratropical stratosphere, *J. Geophys. Res.*, in press, 1985.

Danielsen, E. F., and V. A. Mohnen, Project Dustorm Report: Ozone transport, in situ measurements and meteorological analyses of tropopause folding, *J. Geophys. Res.*, *82*, 5867-5877, 1977.

Danielson, E. F., R. Bleck, J. Shedlovsky, A. Wartburg, P. Haagensen and W. Pollock, Observed distribution of radioactivity, ozone and potential vorticity associated with tropopause folding, *J. Geophys. Res.*, *75*, 2353-2361, 1970.

Dave, J. V., J. J. DeLuisi, and C. L. Mateer, Results of a comprehensive theoretical examination of the optical effects of aerosols on the Umkehr measurements, *Spec. Environ. Rep. 14*, pp. 15-22, WMO, Geneva, 1979.

Davies, R. W., Many body treatment of pressure shifts associated with collisional broadening, *Phys. Rev.*, *A12*, 927-946, 1975.

Dawson, G. A., Nitrogen fixation by lightning, *J. Atmos. Sci.*, *37*, 174-178, 1980.

De La Noe, J., A. Baudry, M. Perault, P. Dierich, N. Monnanteuil, and J. M. Colmont, Measurements of the vertical distribution of ozone by ground-based microwave techniques at the Bordeaux Observatory during the June 1981 intercomparison campaign, *Planet. Space Sci.*, *31*, 737-741, 1983.

De More: See DeMore.

De Muer, D., Vertical ozone distributions over Uccle, Belgium from six years of soundings, *Beit. Phys. Atmos.*, *49*, 1-16, 1976.

De Rudder, A., and G. Brasseur, Ozone in the 21st century: Increase or decrease?, in *Atmospheric Ozone*, edited by C. S. Zerefos and A. Ghazi, pp. 92-96, D. Reidel, Dordrecht, 1984.

De Rudder, A., and G. Brasseur, A model calculation of the ozone response to the increase in the atmospheric emission of several gases, *Internal Report*, Inst. Aeronomie Spatiale de Belgique, Brussels, 1985.

de Zafra, R. L., A. Parrish, P. M. Solomon, and J. W. Barrett, A measurement of stratospheric HO_2 by ground-based millimeter-wave spectroscopy, *J. Geophys. Res.*, *89*, 1321-1326, 1984.

de Zafra, R. L., A. Parrish, P. M. Solomon, and J. W. Barrett, Quantitative observations of stratospheric chlorine monoxide as a function of latitude and season during the period 1980-1983, in *Atmospheric Ozone*, edited by C. S. Zerefos and A. Ghazi, pp. 206-209, D. Reidel, Dordrecht, 1985a.

de Zafra, R. L., A. Parrish, J. Barrett, and P. Solomon, An observed upper limit on stratospheric hydrogen peroxide, *J. Geophys. Res.*, *90*, 13087-13090, 1985b.

Deguchi, S., and D. O. Muhleman, Mesospheric water vapor, *J. Geophys. Res.*, *87*, 1343-1346, 1982.

Delany, A. C., P. J. Crutzen, P. Haagensen, S. Walters, and A. F. Wartburg, Photochemically produced ozone in the emission from large-scale tropical vegetation fires, *J. Geophys. Res.*, *90*, 2425-2429, 1985.

Delany, A. C., D. R. Fitzjarrald, D. Pearson, D. H. Lenschow, G. J. Wendel, and B. Woodruff, Direct measurements of fluxes of oxides of nitrogen and of ozone over grasslands, *J. Atmos. Chem.*, in press, 1986.

Delbouille, L., G. Roland, J. W. Brault, and L. Testerman, Photometric atlas of the solar spectrum from 1850 to 10,000 cm^{-1}, preliminary data, Kitt Peak National Observatory, 1981.

Delmas, R. J., J. M. Ascencia, and M. Legrand, Polar ice evidence that atmospheric CO_2 20,000 B.P. was 50% of present, *Nature*, *284*, 155-157, 1980.

DeLuisi, J. J., Umkehr vertical ozone profile errors caused by the presence of stratospheric aerosols, *J. Geophys. Res.*, *84*, 1766-1770, 1979.

Demerjian, K. L., J. A. Kerr, and J. G. Calvert, Mechanism of photochemical smog formation, *Adv. Environ. Sci. Technol.*, *10*, 1-262, 1974.

Demerjian, K. L., K. L. Schere, and J. T. Peterson, Theoretical estimates of active (spherically integrated) flux and photolytic rate constants of atmospheric species in the lower troposphere, *Adv. Environ. Sci. Technol.*, *10*, 369-459, 1980.

DeMore, W. B., Rate constants for the reactions of hydroxyl and hydroperoxyl radicals with ozone, *Science*, *180*, 735-737, 1973.

DeMore, W. B., Rate constant and possible pressure dependence of the reaction $OH + HO_2$, *J. Phys. Chem.*, *86*, 121-126, 1982.

DeMore, W. B., and O. Raper, Hartley band extinction coefficients of ozone in the gas phase and in liquid nitrogen, carbon monoxide and argon, *J. Phys. Chem.*, *68*, 412-414, 1964.

DeMore, W. B., M. J. Molina, R. T. Watson, D. M. Golden, R. F. Hampson, M. J. Kurylo, C. J. Howard, and A. R. Ravishankara, Chemical kinetics and photochemical data for use in stratospheric modeling, Evaluation number 6, *JPL Publication 83-62*, 219 pp., Jet Propulsion Lab., Pasadena, CA, 1983.

DeMore, W. B., J. J. Margitan, M. J. Molina, R. T. Watson, D. M. Golden, R. F. Hampson, M. J. Kurylo, C. J. Howard, and A. R. Ravishankara, Chemical kinetics and photochemical data for use in stratospheric modeling, Evaluation Number 7, *JPL Publication 85-37*, 226 pp., Jet Propulsion Lab., Pasadena, CA, 1985.

REFERENCES

Derwent, D. G., Two-dimensional model studies of the impact of aircraft emission on tropospheric ozone, *Atmos. Environ.*, *16*, 1997-2007, 1982.

Derwent, R. G., and A. E. J. Eggleton, Two dimensional model studies of methyl chloroform in the troposphere, *Quart. J. Roy. Meteorol. Soc.*, *107*, 231-242, 1981.

Derwent, R. G., and H. N. M. Steward, Elevated ozone levels in the air of central London, *Nature*, *241*, 342-343, 1973.

Dickerson, R. R., Measurements of reactive nitrogen compounds in the free troposphere, *Atmos. Chem.*, *18*, 2585-2593, 1984.

Dickenson, R. E., Planetary Rossby waves propagating vertically through weak westerly wind wave guides, *J. Atmos. Sci.*, *25*, 984-1002, 1968.

Dickinson, R. E., Theory of planetary wave-zonal flow interaction, *J. Atmos. Sci.*, *26*, 73-81, 1969.

Dickinson, R. E., Infrared radiative heating and cooling in the Venusian mesosphere, 1, Global mean radiative equilibrium, *J. Atmos. Sci.*, *29*, 1551-1556, 1972.

Dickinson, R. E., Method of parameterization for infrared cooling between altitudes of 30 and 70 kilometers, *J. Geophys. Res.*, *78*, 4451-4457, 1973.

Dickinson, R. E., Energetics of the stratosphere, *J. Atmos. Terr. Phys.*, *37*, 855-864, 1975.

Dickinson, R. E., Modeling climate changes due to carbon dioxide increases, in *Carbon Dioxide Review*, edited by W. C. Clark, pp. 101-133, Clarendon Press, New York, 1982.

Dickinson, R. E., Infrared radiative cooling in the mesosphere and lower thermosphere, *J. Atmos. Terr. Phys.*, *46*, 995-1008, 1984.

Dickinson, R. E., Modeling of future climate. WMO/ICSU/UNEP international assessment of the impact of an increased atmospheric concentration of carbon dioxide on the environment, in press, 1985.

Dickinson, R. E., S. C. Liu, and T. M. Donahue, Effect of chlorofluoromethane infrared radiation on zonal atmospheric temperature, *J. Atmos. Sci.*, *35*, 2142-2152, 1978.

Ditchburn, R. W., and P. A. Young, The absorption of molecular oxygen between 1850 and 2500 Å, *J. Atmos. Terr. Phys.*, *24*, 127-139, 1962.

Dobson, G. M. B., Origin and distribution of polyatomic molecules in the atmosphere, *Proc. Roy. Soc. London*, *A236*, 187-193, 1956.

Dobson, G. M. B., The laminated structure of the ozone in the atmosphere, *Quart. J. Roy. Meteorol. Soc.*, *99*, 599-607, 1973.

Dobson, G. M. B., D. N. Harrison, and J. Lawrence, Measurements of the amount of ozone in the Earth's atmosphere and its relation to other geophysical conditions: Part III, *Proc. Roy. Soc. London*, *A122*, 456-486, 1929.

Dobson, G. M. B., A. W. Brewer, and B. M. Cwilong, Meteorology of the lower stratosphere, *Proc. Roy. Soc. London*, *A185*, 144-175, 1946.

Dodge, M. C., Combined effects of organic reactivity and NMHC/NOx ratio on photochemical oxidant formation--a modeling study, *Atmos. Environ.*, *18*, 1657-1665, 1984.

Dognon, A. M., F. Caralp, and R. Lesclaux, Reactions of chlorofluoromethyl peroxy radicals with NO: A kinetic study in the temperature range 230-430K, *J. Chem. Phys. Phys. Biol.*, in press, 1985.

Doherty, G. M., R. E. Newell, and E. F. Danielsen, Radiative heating rates near the stratospheric fountain, *J. Geophys. Res.*, *89*, 1380-1384, 1984.

Donner, L. J., and H.-L. Kuo, Radiative forcing of stationary planetary waves, *J. Atmos. Sci.*, *41*, 2849-2868, 1984.

Donner, L. J., and V. Ramanathan, Methane and nitrous oxide: Their effects on the terrestrial climate, *J. Atmos. Sci.*, *37*, 119-124, 1980.

Dopplick, T. G., Radiative heating of the global atmosphere: Corrigendum, *J. Atmos. Sci.*, *36*, 1812-1817, 1979.

C-4

Douglass, A. R., R. B. Rood, and R. S. Stolarski, Interpretation of ozone temperature correlations, 2. Analysis of SBUV ozone data, *J. Geophys. Res.*, *90*, 10693-10708, 1985.

Drayson, S. R., Calculation of long-wave radiative transfer in planetary atmospheres, Ph.D. thesis, *Rep. 07584-1-T*, 110 pp., College of Engineering, University of Michigan, Ann Arbor, MI, 1967.

Drayson, S. R., P. L. Bailey, H. Fischer, J. C. Gille, A. Girard, L. L. Gordley, J. E. Harries, W. G. Planet, E. E. Remsberg, and J. M. Russell, III, Spectroscopy and transmittances for the LIMS experiment, *J. Geophys. Res.*, *89*, 5141-5146, 1984.

Drummond, J. R., and R. F. Jarnot, Infrared measurements of stratospheric composition II. Simultaneous NO and NO_2 measurements, *Proc. Roy. Soc. London A*, *364*, 237-254, 1978.

Drummond, J. R., J. T. Houghton, G. D. Peskett, C. D. Rodgers, M. J. Wale, J. Whitney, and E. J. Williamson, The stratospheric and mesospheric sounder on Nimbus 7, *Phil. Trans. Roy. Soc. London*, *A296*, 219-241, 1980.

Drummond, J. W., J. M. Rosen, and D. J. Hofmann, Balloon borne chemiluminescent measurement of NO to 45 km, *Nature*, *265*, 319-320, 1977.

Drummond, J. W., A. Volz, and D. H. Ehhalt, An optimized chemiluminescence detector for tropospheric NO measurements, *J. Atmos. Chem.*, *2*, 287-306, 1985.

Duce, R. A., V. A. Mohnen, P. R. Zimmerman, D. Grosjean, W. Cautreels, R. Chatfield, R. Jaenicke, J. A. Ogren, E. D. Pellizzari, and G. T. Wallace, Organic material in the global troposphere, *Revs. Geophys. Space Phys.*, *21*, 921-952, 1983.

Duetsch, H. U., Two years of regular ozone soundings over Boulder, Colorado, *NCAR Tech. Note No. 10*, 449 pp., NCAR, Boulder, CO, 1966.

Duetsch, H. U., Vertical ozone distribution on a global scale, *Pure Appl. Geophys.*, *116*, 511-529, 1978.

Duetsch, H. U., Total ozone trend in the light of ozone soundings, The impact of El Chichon, in *Atmospheric Ozone*, edited by C. S. Zerefos and A. Ghazi, pp. 263-268, D. Riedel, Dordrecht, 1985.

Duetsch, H. U., C. Ling, and W. Zuellig, Regular ozone observation at Thalwill, Switzerland and at Boulder, Colorado, *Rept. LAPETH-1*, 279 pp., Eidgenoessische Technische Hochschule, Zurich, 1970.

Dunkerton, T. J., On the mean meridional mass motions of the stratosphere and mesosphere, *J. Atmos. Sci.*, *35*, 2325-2333, 1978.

Dunkerton, T. J., On the role of Kelvin waves in the westerly phase of the semi-annual zonal wind oscillation, *J. Atmos. Sci.*, *36*, 32-41, 1979.

Dunkerton, T. J., Stochastic parameterization of gravity wave stresses, *J. Atmos. Sci.*, *39*, 1711-1725, 1982a.

Dunkerton, T. J., Theory of the mesopause semi-annual oscillation, *J. Atmos. Sci.*, *39*, 2681-2690, 1982b.

Dunkerton, T. J., Laterally-propagating planetary waves in the easterly phase of the quasi-biennial oscillation, *Atmosphere-Ocean*, *21*, 55-68, 1983a.

Dunkerton, T. J., Modification of stratospheric circulation by trace constituent changes?, *J. Geophys. Res.*, *88*, 10831-10836, 1983b.

Dunkerton, T. J., and N. Butchart, Propagation and selective transmission of internal gravity waves in a sudden warming, *J. Atmos. Sci.*, *41*, 1443-1460, 1984.

Dunkerton, T. J., and D. P. Delisi, Climatology of the equatorial lower stratosphere, *J. Atmos. Sci.*, *42*, 376-396, 1984.

Dunkerton, T. J., C. P. F. Hsu, and M. E. McIntyre, Some Eulerian and Lagrangian diagnostics for a model stratospheric warming, *J. Atmos. Sci.*, *38*, 819-843, 1981.

Dutton, J. A., *The Ceaseless Wind*, 579 pp., McGraw-Hill, New York, 1976.

Duxbury, J. M., D. R. Bouldin, R. E. Terry, and R. L. Tate, Emissions of nitrous oxide from soils, *Nature*, *298*, 462-464, 1982.

Dvoryashina, Y. V., V. I. Dianov-Klokov, and L. N. Yurganov, On the variations of atmospheric total column carbon monoxide abundance for 1970-1982, *Phys. Atmos. Oceans*, *20*, 40-47, 1984.

Eady, E. T., Long waves and cyclone waves, *Tellus*, *1*, 35-42, 1949.

REFERENCES

Eastman, J. A., and D. H. Stedman, A fast response sensor for eddy-correlation flux measurement, *Atmos. Environ.*, *11*, 1209-1211, 1977.

Eaton, F., and G. Wendler, Some environmental effects of forest fires in interior Alaska, *Atmos. Environ.*, *17*, 1331-1337, 1983.

Edmon, Jr., H. J., B. J. Hoskins, and M. E. McIntyre, Eliassen-Palm cross sections for the troposphere, *J. Atmos. Sci.*, *37*, 2600-2616, 1980.

Edmonds, J. A., J. Reilly, J. R. Trabalka, and D. E. Reichle, An analysis of possible future atmospheric retention of fossil fuel CO_2, *DOE/OR-21400/1*, 169 pp., Institute for Energy Analysis, Washington, DC, 1984.

Edwards, D. K., and S. J. Morizumi, Scaling of vibration-rotation band parameters for nonhomogeneous gas radiation, *J. Quant. Spectrosc. Radiat. Transfer*, *10*, 175-188, 1970.

Ehhalt, D. H., The atmospheric cycle of methane, *Tellus*, *26*, 58-70, 1974.

Ehhalt, D. H., and J. W. Drummond, The tropospheric cycle of NOx, in *Chemistry of the Unpolluted and Polluted Troposphere*, edited by H. W. Georgii and W. Jaeschke, D. Reidel, Hingham, MA, 1982.

Ehhalt, D. H., and J. Rudolph, On the importance of light hydrocarbons in multiple atmospheric systems, in *Berichte der Kernforschungsanlage*, Julich GMbH, Juli, 1984.

Ehhalt, D. H., and U. Schmidt, Sources and sinks of atmospheric methane, *Pure Appl. Geophys.*, *116*, 452-464, 1978.

Ehhalt, D. H., and A. Toennissen, Hydrogen and carbon compounds in the stratosphere, in *Proceedings of the NATO Advanced Study Institute on Atmospheric Ozone: Its Variation and Human Influences*, *Rep. No. FAA-EE-80-20*, edited by A. C. Aikin, pp. 129-151, DOT, FAA, Washington, DC, 1980.

Ehhalt, D. H., L. E. Heidt, R. H. Lueb, and E. A. Martell, Concentrations of CH_4, CO, CO_2, H_2, H_2O, and N_2O in the upper stratosphere, *J. Atmos. Sci.*, *32*, 163-169, 1975.

Ehhalt, D. H., E. P. Roeth, and U. Schmidt, On the temporal variance of stratospheric trace gas concentrations, *J. Atmos. Chem.*, *1*, 27-51, 1983a.

Ehhalt, D. H., R. J. Zander, and R. A. Lamontagne, On the temporal increase of tropospheric CH_4, *J. Geophys. Res.*, *88*, 8442-8446, 1983b.

Ehhalt, D. H., J. Rudolph, F. Meixner, and U. Schmidt, Measurements of selected C_2-C_5 hydrocarbons in the background troposphere: Vertical and latitudinal variations, *J. Atmos. Chem.*, *3*, 29-52, 1985.

Elansky, N. F., A. Ya. Arabov, A. S. Elskhov, and I. A. Senik, Spatial and temporal variability of the NO_2 total content based on annual observation data in *Atmospheric Ozone*, edited by C. S. Zerefos and A. Ghazi, pp., 157-162, D. Reidel, Dordrecht, 1984.

Eliasen, E., and B. Machenhauer, A study of the fluctuations of atmospheric planetary flow patterns represented by spherical harmonics, *Tellus*, *17*, 220-238, 1965.

Eliasen, E., and B. Machenhauer, On the observed large-scale atmospheric wave motions, *Tellus*, *21*, 149-165, 1969.

Eliassen, A., On the vertical circulation in frontal zones, *Geofys. Pub.*, *24 (4)*, 147-160, 1962.

Eliassen, A., and E. Palm, On the transfer of energy in stationary mountain waves, *Geofys. Publ.*, *22, No. 3*, 1-23, 1961.

Elkins, J. W., S. C. Wofsy, M. B. McElroy, C. E. Kolb, and W. A. Kaplan, Aquatic sources and sinks for nitrous oxide, *Nature*, *275*, 602-606, 1978.

Ellingson, R. G., and G. N. Serafino, Observations and calculations of aerosol heating over the Arabian Sea during MONEX, *J. Atmos. Sci.*, *41*, 575-589, 1984.

Elliott, W. P., L. Machta and C. D. Keeling, An estimate of the biotic contribution to the atmospheric CO_2 increase based on direct measurements at Mauna Loa Observatory, *J. Geophys. Res.*, *90*, 3741-3746, 1985.

Ellis, P., G. Holah, J. T. Houghton, T. S. Jones, G. Peckham, G. D. Peskett, D. R. Pick, C. D. Rodgers, H. K. Roscoe, R. Sandwell, The selective chopper radiometer for Nimbus 5, *Proc. Roy. Soc. London A, 334,* 149-170, 1973.

Ellsaesser, H. W., Sources and sinks of stratospheric water vapor, in *Proceedings of the NATO Advanced Study Institute on Atmospheric Ozone: Its Variation and Human Influences, Rep. FAA-EE-80-20,* edited by A. C. Aikin, pp. 283-300, DOT, FAA, Washington,DC, 1980.

Ellsaesser, H. W., J. E. Harries, D. Kley and R. Penndorf, Stratospheric H_2O, *Planet Space Sci., 28,* 827-835, 1980.

Enting, I. G., Preliminary studies with a two-dimensional model using transport fields derived from a GCM, *J. Atmos. Chem.,* in press, 1985.

National air pollutant emission estimates, 1940-1983, *EPA-450/4-84-028,* Environmental Protection Agency, Research Triangle Park, NC, 1984.

EPA: See National Air Pollutant Estimates.

Ertel, H., Ein neuer hydrodynamischer wirbelsatz, *Meteor. Z., 59,* 277-281, 1942.

Evans, W. F. J., C. I. Lin, and C. L. Midwinter, The altitude distribution of nitric acid at Churchill, *Atmosphere, 14,* 172-179, 1976.

Evans, W. F. J., J. B. Kerr, C. T. McElroy, R. S. O'Brien, and J. C. McConnell, Measurements of NO_2 and HNO_3 during a stratospheric warming at 54 degrees N. in February, 1979, *Geophys. Res. Lett., 9,* 493-496, 1982a.

Evans, W. F. J., C. T. McElroy, J. B. Kerr, and J. C. McConnell, Simulations of the October 23, 1980 stratoprobe flight, *Geophys. Res. Lett., 9,* 223-226, 1982b.

Fabian, P., Halogenated hydrocarbons in the atmosphere, in *The Handbook of Environmental Chemistry, Vol. 4,* Springer-Verlag, Heidelberg, in press, 1985.

Fabian, P., and C. E. Junge, Global rate of ozone destruction at the earth's surface, *Arch. Met. Geophys. Bioklim., A19,* 161-172, 1970.

Fabian, P., J. A. Pyle, and R. J. Wells, The August 1972 solar proton event and the atmospheric ozone layer, *Nature, 277,* 458-460, 1979.

Fabian, P., R. Borchers, S. A. Penkett, and N. J. D. Prosser, Halocarbons in the stratosphere, *Nature, 294,* 733-735, 1981a.

Fabian, P., R. Borchers, G. Flentje, W. A. Matthews, W. Seiler, H. Giehl, K. Bunse, F. Muller, U. Schmidt, A. Volz, A. Khedim, and F. J. Johnen, The vertical distribution of stable trace gases at mid-latitudes, *J. Geophys. Res., 86,* 5179-5184, 1981b.

Fabian, P., J. A. Pyle, and R. J. Wells, Diurnal variation of minor constituents in the stratosphere modeled as a function of latitude and season., *J. Geophys. Res., 87,* 4981-5000, 1982.

Fabian, P., R. Borchers, B. C. Krueger, S. Lal, and S. A. Penkett, The vertical distribution of $CHClF_2$ (CFC-22) in the stratosphere, *Geophys. Res. Lett., 12,* 1-3, 1985a.

Fabian, P., G. Flentje, and W. A. Mathews, Stratospheric NO profiles from simultaneous measurements of two chemiluminescent balloon-borne sondes, *Planet. Space Sci.,* in press, 1985b.

Fabian, P., R. Borchers, B. C. Krueger, and S. Lal, The vertical distribution of CFC-114 ($CClF_2$-$CClF_2$) in the atmosphere, *J. Geophys. Res., 90,* 13091-13093, 1985c.

Falls, A. H., and J. H. Seinfeld, Continued development of a kinetic mechanism for photochemical smog, *Environ. Sci. Technol., 12,* 1398-1400, 1978.

Farman, J. C., B. G. Gardiner, and J. D. Shanklin, Large losses of total ozone in Antarctica reveal seasonal ClO_x/NO_x interaction, *Nature, 315,* 207-210, 1985.

Farmer, C. B., and O. F. Raper, The HF:HCl ratio in the 14-38 km region of the stratosphere, *Geophys. Res. Lett., 4,* 527-529, 1977.

REFERENCES

Farmer, C. B., O. F. Raper, and R. H. Norton, Spectroscopic detection and vertical distribution of HCl in the troposphere and stratosphere, *Geophys. Res. Lett.*, *3*, 13-16, 1976.

Farmer, C. B., O. F. Raper, B. D. Robbins, R. A. Toth, and C. Mueller, Simultaneous spectroscopic measurements of stratospheric species: O_3, CH_4, CO, CO_2, N_2O, HCl, and HF at northern and southern mid-latitudes, *J. Geophys. Res.*, *85*, 1621-1632, 1980.

Farmer, C. B., B. Carli, A. Bonetti, M. Carlotti, B. M. Dinelli, H. Fast, N. Louisnard, C. Alamichel, W. Mankin, M. Coffey, I. G. Nolt, D. G. Murcray, A. Goldman, G. Stokes, D. Johnson, W. Traub, K. Chance, R. Zander, L. Delbouille, and G. Roland, Balloon Intercomparison Campaigns: Results of remote sensing measurements of HCl, to be published, 1986.

Fast, H., W.F.J. Evans, G. L. Vail, and H. L. Buijs, A measurement of the stratospheric HCl profile at 82 °N on November 8, 1978, *J. Geophys. Res.*, in press, 1985.

FCM: See *The National plan for stratospheric ozone monitoring*.

Feely, H. W., and J. Spar, Tungsten-185 from nuclear bomb tests as a tracer for stratospheric meteorology, *Nature*, *188*, 1062-1064, 1960.

Fehsenfeld, F. C., E. E. Ferguson, G. E. Streit, and D. L. Albritton, Stratospheric ion chemistry and the 11-year variation in polar ozone, *Science*, *194*, 544-545, 1976.

Fels, S. B., Simple strategies for inclusion of Voigt effects in infrared cooling rate calculations, *Appl. Opt.*, *18*, 2634-2637, 1979.

Fels, S. B., A parameterization of scale dependent radiative damping rates in the middle atmosphere, *J. Atmos. Sci.*, *39*, 1141-1152, 1982.

Fels, S. B., The radiative damping of short vertical scale waves in the mesosphere, *J. Atmos. Sci.*, *41*, 1755-1764, 1984.

Fels, S. B., Radiative-dynamical interactions in the middle atmosphere, in *Issues in Atmospheric and Oceanic Modeling*, edited by B. Saltzman, Advances in Geophysics 28, Part A, in press, 1985.

Fels, S. B., and L. D. Kaplan, A test of the role of longwave radiative transfer in a general circulation model, *J. Atmos. Sci.*, *33*, 779-789, 1975.

Fels, S. B., and M. D. Schwartzkopf, An efficient, accurate algorithm for calculating CO_2 15 μm band cooling rates, *J. Geophys. Res.*, *86*, 1205-1232, 1981.

Fels, S. B., J. D. Mahlman, M. D. Schwarzkopf, and R. W. Sinclair, Stratospheric sensitivity to perturbations in ozone and carbon dioxide: Radiative and dynamical response, *J. Atmos. Sci.*, *37*, 2265-2297, 1980.

Fiedler, B. H., An integral closure model for the vertical turbulent flux of a scalar in a mixed layer, *J. Atmos. Sci.*, *41*, 674-680, 1984.

Finger, F. G., M. E. Gelman, F. J. Schmidlin, R. Leviton, and B. Kennedy, Compatibility of meteorological rocketsonde data as indicated by International Comparison Tests, *J. Atmos. Sci.*, *32*, 1705-1714, 1975.

Firestone, M. K., and J. M. Tiedje, Temporal change in nitrous oxide and dinitrogen following the onset of an aerobiosis, *Appl. Environ. Microbiol.*, *38*, 673-679, 1979.

Firestone, M. K., M. S. Smith, R. B. Firestone, and J. M. Tiedje, The influence of nitrate, nitrite and oxygen on the gaseous products of denitrification in soil, *Soil Sci. Soc. Am. J.*, *43*, 1140-1144, 1979.

Fischer, H., F. Fergg, D. Rabus, and P. Burkert, Stratospheric H_2O and HNO_3 profiles derived from solar occultation measurements, *J. Geophys. Res.*, *90*, 3831-3835, 1985a.

Fischer, H., E. Redemann, F. Fergg, and D. Rabus, Measurements of stratospheric NO_2 profiles using a gas correlation radiometer in the solar occultation mode, *J. Atmos. Chem.*, in press, 1985b.

Fishman, J., Ozone in the troposphere, in *Ozone in the Free Atmosphere*, edited by R. C. Whitten and S. S. Prasad, pp. 161-194, Van Nostrand Reinhold, New York, 1985.

Fishman, J., and T. A. Carney, A one-dimensional photochemical model of the troposphere with planetary boundary-layer parameterization, *J. Atmos. Chem.*, 351-376, 1984.

Fishman, J., and P. J. Crutzen, The origin of ozone in the troposphere, *Nature*, *274*, 855-858, 1978.

Fishman, J., and W. Seiler, Correlative nature of ozone and carbon monoxide in the troposphere: Implications for the tropospheric ozone budget, *J. Geophys. Res.*, *88*, 3662-3670, 1983.

Fishman, J., V. Ramanathan, P. J. Crutzen, and S. C. Liu, Tropospheric ozone and climate, *Nature*, *282*, 818-820, 1979a.

Fishman, J., S. Solomon, and P. J. Crutzen, Observational and theoretical evidence in support of a significant in-situ photochemical source of tropospheric ozone, *Tellus*, *31*, 432-446, 1979b.

Fishman, J., W. Seiler, and P. Haagensen, Simultaneous presence of O_3 and CO bands in the troposphere, *Tellus*, *32*, 456-463, 1980.

Fitzjarrald, D. R., and M. Garstang, Boundary-layer growth over the tropical ocean, *Mon. Weather Rev.*, *109*, 1762-1772, 1981.

Fitzjarrald, D. R., and D. H. Lenschow, Mean concentration and flux profiles for chemically reactive species in the atmospheric surface layer, *Atmos. Environ.*, *17*, 2505-2512, 1983.

Flaud, J.-M., C. Camy-Peyret, and L. S. Rothman, Improved ozone line parameters in the 10- and 4.8 μm regions, *Appl. Opt.*, *19*, 655, 1980.

Flaud, J.-M., C. Camy-Peyret, D. Cariolle, J. Laurent, and G. M. Stokes, Daytime variations of atmospheric NO_2 from ground-based infrared measurements, *Geophys. Res. Lett.*, *10*, 1104-1107, 1983.

Fleig, A. J., K. F. Klenk, P. K. Bhartia, K. D. Lee, C. G. Wellemeyer, and V. G. Kaveeshwar, Vertical ozone profile results from Nimbus 4 data, in *Proc. 4th Conf. Atmos. Radiation*, pp. 20-26, AMS, Toronto, Canada, 1981.

Fleig, A. J., K. F. Klenk, P. K. Bhartia, D. Gordon, and W. H. Schneider, Users guide for the Solar Backscattered Ultraviolet (SBUV) instrument first-year ozone-S data set, *NASA Ref. Publ. 1095*, 72 pp., NASA Goddard Space Flight Center, Greenbelt, MD, 1982.

Fontanella, J., A. Girard, L. Gramont, and N. Louisnard, Vertical distribution of NO, NO_2, and HNO_3 as derived from stratospheric absorption infrared spectra, *Appl. Opt.*, *14*, 825-839, 1975.

Foot, J. S., Aircraft measurements of the humidity in the lower stratosphere from 1977 to 1980 between 45°N and 60°N, *Quart. J. Roy. Meteorol. Soc.*, *110*, 303-320, 1984.

Forbes, J. M., Middle atmosphere tides, *J. Atmos. Terr. Phys.*, *46*, 1049-1067, 1984.

Fouquart, Y., B. Bonnel, G. Brogniez, A. Cerf, M. Chaovi, L. Smith, and J. C. Vanhootte, Size distribution and optical properties of Saharan aerosols during Eclats, in *Aerosols and their Climate Effects*, edited by H. E. Gerber and A. Deepak, pp. 35-62, A. Deepak Publ., Hampton, VA, 1984.

Frank, W. M., The cumulus parameterization problem, *Mon. Weather Rev.*, *111*, 1859-1871, 1983.

Fraser, P. J., M. A. K. Khalil, R. A. Rasmussen, and A. J. Crawford, Trends of atmospheric methane in the Southern Hemisphere, *Geophys. Res. Lett.*, *8*, 1063-1066, 1981.

Fraser, P. J., G. I. Pearman, and P. Hyson, The global distribution of atmospheric CO_2: II. A review of provisional background observations 1978-1980, *J. Geophys. Res.*, *88*, 3591-3598, 1982.

Fraser, P. J., P. Hyson, I. G. Enting, and G. I. Pearman, Global distribution and Southern Hemisphere trend of atmospheric CCl_3F, *Nature*, *302*, 692-695, 1983a.

Fraser, P. J., M. A. K. Khalil, R. A. Rasmussen, and L. P. Steele, Tropospheric methane in the mid-latitudes of the Southern Hemisphere, *J. Atmos. Chem.*, *1*, 125-135, 1983b.

Fraser, P. J., P. Hyson, M. A. K. Khalil, and R. A. Rasmussen, Conference on Scientific Application of Baseline Observations on Atmospheric Composition, Aspendale, Australia, 7-9 November, 1984.

Frederick, J. E., Solar corpuscular emission and neutral chemistry in the Earth's middle atmosphere, *J. Geophys. Res.*, *81*, 3179-1976, 1976.

Frederick, J. E., Radiative-photochemical response of the mesosphere to dynamical forcing, *J. Geophys. Res.*, *86*, 5224-5230, 1981.

Frederick, J. E., and R. J. Cicerone, Dissociation of metastable O_2 as a potential source of atmospheric odd oxygen, *J. Geophys. Res.*, *90*, 10733-10738, 1985.

REFERENCES

Frederick, J. E., and A. R. Douglass, Atmospheric temperatures near the tropical tropopause: Temporal variations, zonal asymmetry and implications for stratospheric water vapor, *Mon. Weather Rev.*, *111*, 397-1403, 1983.

Frederick, J. E., and R. D. Hudson, Predissociation linewidths and oscillator strengths for the 2-0 to 13-0 Schumann-Runge bands of O_2, *J. Molec. Spectrosc.*, *74*, 247-258, 1979a.

Frederick, J. E., and R. D. Hudson, Predissociation of nitric oxide in the mesosphere and stratosphere, *J. Atmos. Sci.*, *36*, 737-745, 1979b.

Frederick, J. E., and R. D. Hudson, Dissociation of molecular oxygen in the Schumann-Runge bands, *J. Atmos. Sci.*, *37*, 1099-1106, 1980a.

Frederick, J. E., and R. D. Hudson, Atmospheric opacity in the Schumann-Runge bands and the aeronomic dissociation of water vapor, *J. Atmos. Sci.*, *37*, 1088-1098, 1980b.

Frederick, J. E., and J. E. Mentall, Solar irradiance in the stratosphere: Implications for the Herzberg continuum absorption of O_2, *Geophys. Res. Lett.*, *9*, 461-464, 1982.

Frederick, J. E., and N. Orsini, The distribution and variability of mesospheric odd nitrogen: A theoretical investigation, *J. Atmos. Terr. Phys.*, *44*, 479-1982, 1982.

Frederick, J. E., and G. N. Serafino, Satellite observations of the nitric oxide dayglow: Implications for the behavior of mesospheric and lower thermospheric odd nitrogen, *J. Geophys. Res.*, *90*, 3821-3830, 1985.

Frederick, J. E., R. D. Hudson, and J. E. Mentall, Stratospheric observations of the attenuated solar irradiance in the Schumann-Runge band absorption region of molecular oxygen, *J. Geophys. Res.*, *86*, 9885-9890, 1981.

Frederick, J. E., A. J. Blake, D. E. Freeman, R. W. Nicholls, T. Ogawa, and P. C. Simon, MSG-7: Molecular absorption processes related to the penetration of ultraviolet solar radiation into the middle atmosphere, in *Handbook for MAP*, *Vol. 8*, edited by C. F. Sechrist, Jr., pp. 53-74, SCOSTEP Secretariat, Univ. of Illinois, Urbana, 1983a.

Frederick, J. E., F. T. Huang, A. R. Douglass, and C. A. Reber, The distribution and annual cycle of ozone in the upper stratosphere, *J. Geophys. Res.*, *88*, 3819-3828, 1983b.

Frederick, J. E., G. N. Serafino, and A. R. Douglass, An analysis of the annual cycle in upper stratospheric ozone, *J. Geophys. Res.*, *89*, 9547-9555, 1984.

Fredriksson, K., B. Galle, K. Nystrom, and S. Svanberg, Lidar system applied in atmospheric pollution monitoring, *Appl. Optics*, *18*, 2998-2998, 1979.

Freeman, D. E., K. Yoshino, J. R. Esmond, and W. H. Parkinson, High resolution absorption cross section measurements of ozone at 195 K in the wavelength region 240-350 nm, *Planet. Space Sci.*, *32*, 239-248, 1984.

Freney, J. R., O. T. Denmead, and J. R. Simpson, Nitrous oxide emissions from soils at low moisture contents, *Soil Biol. Biochem.*, *11*, 167-173, 1979.

Frerking, M. A., and D. J. Muehlner, Infrared heterodyne spectroscopy of atmospheric ozone, *Appl. Opt.*, *16*, 526-528, 1977.

Friedl, R. R., W. H. Brune, and J. G. Anderson, Kinetics of SH with NO_2, O_3, O_2, and H_2O_2, *J. Phys. Chem.*, *89*, 5505-5510, 1985.

Friedli, H., E. Moore, H. Oeschger, U. Siegenghaler, and B. Stauffer, $^{13}C/^{12}C$ ratios in CO_2 extracted from antarctic ice, *Geophys. Res. Lett.*, *11*, 1145-1148, 1984.

Fritts, D. C., Gravity wave saturation in the middle atmosphere: A review of theory and observations, *Rev. Geophys. and Space Phys.*, *22*, 275-308, 1984.

Fritts, D. C., and T. J. Dunkerton, Fluxes of heat and constituents due to convectively unstable gravity waves, *J. Atmos. Sci.*, *42*, 549-556, 1985.

Fritz, B., and R. Zellner, Reaction rate and equilibrium constant for $ClO + O_2 \rightarrow OClOO$, presented at CMA Chemistry Workshop, Goettingen, 1984.

Froidevaux, L., Photochemical modeling of the earth's stratosphere, Ph.D. thesis, 275 pp., California Institute of Technology, Pasadena, CA, 1983.

Froidevaux, L., and Y. L. Yung, Radiation and chemistry in the stratosphere: Sensitivity to O_2 absorption cross-sections in the Herzberg continuum, *Geophys. Res. Lett.*, 9, 854-857, 1982.

Froidevaux, L., M. Allen, and Y. L. Yung, A critical analysis of ClO and O_3 in the mid-latitude stratosphere, *J. Geophys. Res.*, 90, 12999-13030, 1985a.

Froidevaux, L., M. Allen, S. Berman, and A. Daughton, Analysis of LIMS observations in the upper stratosphere and lower mesosphere, I. The mean O_3 profile and its temperature sensitivity at mid-latitudes in May, 1979, in press, 1985b.

Funk, J. P., and G. J. Garnham, Australian ozone observations and a suggested 24-month cycle, *Tellus*, 14, 378-382, 1962.

Gage, K. S., and B. B. Balsley, MST radar studies of wind and turbulence in the middle atmosphere, *J. Atmos. Terr. Phys.*, 46, 739-753, 1984.

Galbally, I. E., Emission of fixed nitrogen compounds to the atmosphere in remote areas, in *Biogeochemical Cycling of Sulfur and Nitrogen in Remote Areas*, edited by J. N. Galloway, D. Reidel, Dordrecht, in press, 1985.

Galbally, I. E., and C. R. Roy, Loss of fixed nitrogen from soils by nitric oxide exhalation, *Nature*, 275, 734-735, 1978.

Galbally, I. E., and C. R. Roy, Destruction of ozone at the earth's surface, *Quart. J. Roy. Meteorol. Soc.*, 106, 599-620, 1980.

Galbally, I. E., and C. R. Roy, Ozone and nitrogen oxides in the Southern Hemisphere troposphere, in *Proceedings of the Quadrennial International Ozone Symposium*, *Vol. I*, edited by J. London, pp. 431-438, IAMAP, NCAR, Boulder, CO, 1981.

Galbally, I. E., C. R. Roy, R. S. O'Brien, B. A. Ridley, D. R. Hastie, W. F. J. Evans, C. T. McElroy, J. B. Kerr, P. Hyson, W. Knight, and J. E. Laby, Measurements of the trace composition of the Austral stratosphere: Chemical and meteorological data, *Technical Paper No. 1*, CSIRO, Div. of Atmos. Res., Australia, 1983.

Galindo, I., Anthropogenic aerosols and their regional scale climatic effects, in *Aerosols and their Climatic Effects*, edited by H. E. Gerber and A. Deepak, pp. 245-260, A. Deepak Publ., Hampton, VA, 1984.

Gallagher, C. C., C. A. Forsberg, A. S. Mason, B. W. Gandrud, and M. Janghorbani, Total chlorine content in the lower stratosphere, *J. Geophys. Res.*, 90, 10747-10752, 1985.

Gamache, R. R., and R. W. Davies, Theoretical N_2-, O_2-, and air broadened halfwidths of O_3 calculated by quantum Fourier transform theory with realistic collision dynamics, *J. Molec. Spec.*, 109, 283-299, 1985.

Gamlen, P. H., B. C. Lane, P. M. Midgley, and J. J. Steed, The production and release to atmosphere of $CHCl_3$ and CCl_2F_2, *Atmos. Environ.*, in press, 1985.

Gammon, R. H., and W. D. Komhyr, Response of the global atmospheric CO_2 distribution to the atmospheric/oceanic circulation perturbation in 1982, in *IUGG Symposium 19 (Oceans and CO_2 Climate Response)*, *Vol. 2*, 828 pp., Hamburg, FRG, 1983.

Gammon, R. H., W. D. Komhyr, L. Waterman, T. Conway, K. Thoning, and D. Gillette, The 1982/83 ENSO event: Response of the global atmospheric CO_2 distribution, paper presented at Conference on Scientific Application of Baseline Observations of Atmospheric Composition, CSIRO, Aspendale, Australia, 7-9 November, 1984.

Gammon, R. H., E. T. Sandquist, and P. J. Fraser, History of carbon dioxide in the atmosphere, *U.S. Department of Energy State-of-the-Art Report on the Global Carbon Cycle (DOE)*, Chapter 3, in press, 1985a.

REFERENCES

Gammon, R. H., W. D. Komhyr, and J. T. Peterson, The global atmospheric CO_2 distribution 1968-83: Interpretation of the results of the NOAA/GMCC measurement program, in *The Global Carbon Cycle: Analysis of the Natural Cycle and Implications of Anthropogenic and Alterations for the Next Century*, edited by J. R. Trabalka and D. E. Reichle, Springer-Verlag, New York, in press, 1985b.

Garcia, R. R., and J. Geisler, Stochastic forcing of small amplitude oscillations in the stratosphere, *J. Atmos. Sci.*, *38*, 2187-2197, 1981.

Garcia, R. R., and S. Solomon, A numerical model of the zonally averaged dynamical and chemical structure of the middle atmosphere, *J. Geophys. Res.*, *88*, 1379-1400, 1983.

Garcia, R. R., and S. Solomon, The effect of breaking gravity waves on the dynamics and chemical composition of the mesosphere and lower thermosphere, *J. Geophys. Res.*, *90*, 3850-3868, 1985.

Garcia, R. R., S. Solomon, R. G. Roble, and D. W. Rusch, A numerical response of the middle atmosphere to the 11-year solar cycle., *Planet. Space Sci.*, *32*, 411-423, 1984.

Garland, J. A., and S. A. Penkett, Absorption of peroxyacetyl nitrate and ozone by natural surfaces, *Atmos. Environ.*, *10*, 1127-1131, 1976.

Garland, J. A., A. W. Elzerman, and F. A. Penkett, The mechanism for dry deposition of ozone to sea water surfaces, *J. Geophys. Res.*, *85*, 7488-7492, 1980.

Gates, W. L., Modeling the ice-age climate, *Science*, *191*, 1138-1144, 1976.

Gates, W. L., K. H. Cook, and M. E. Schlesinger, Preliminary analysis of experiments on the climatic effects of increased CO_2 with an atmospheric general circulation model and a climatological ocean, *J. Geophys. Res.*, *86*, 6385-6393, 1981.

Geisler, J. E., and R. E. Dickinson, The five-day wave on the sphere with realistic zonal winds, *J. Atmos. Sci.*, *33*, 632-641, 1976.

Geller, M. A., Dynamics of the middle atmosphere, *Space Sci. Rev.*, *34*, 359-375, 1983.

Geller, M. A., Modelling the middle atmosphere circulation, in *Dynamics of the Middle Atmosphere*, edited by J. R. Holton and T. Matsuno, pp. 467-500, Terrapub, Tokyo, 1984.

Geller, M. A., and J. C. Alpert, Planetary wave coupling between the troposphere and the middle atmosphere as a possible sun-weather mechanism, *J. Atmos. Sci.*, *37*, 1197-1215, 1980.

Geller, M. A., M. F. Wu, and M. E. Gelman, Troposphere-stratosphere (Surface-55 km) monthly winter general circulation statistics for the Northern Hemisphere-four year averages, *J. Atmos. Sci.*, *40*, 1334-1352, 1983.

Geller, M. A., M. F. Wu, and M. E. Gelman, Troposphere-stratosphere (Surface-55 km) monthly winter general circulation statistics for the Northern Hemisphere-interannual variations, *J. Atmos. Sci.*, *41*, 1726-1744, 1984.

Gelman, M. E., A. J. Miller, R. M. Nagatani, and H. D. Bowman II, Mean zonal wind and temperature structure during the PMP-1 winter periods, *Adv. Space Res.*, *10*, 159-162, 1983.

Geophysical Monitoring for Climatic Change: See Harris, J. M.

Georgii, H.-W., and F. X. Meixner, Measurement of the tropospheric and stratospheric SO_2 distribution, *J. Geophys. Res.*, *85*, 7433-7438, 1980.

Ghazi, A., *Atlas der Globalverteilung des Gesamtozonbetrages nach Satellitenmessungen (April 1970-Mai 1972).*, Mitteilungen aus dem Institut fuer Geophysik and Meteorologie der Universitat zu Koln, 1980.

Ghazi, A., and J. J. Barnett, Ozone behavior and stratospheric thermal structure during Southern Hemispheric spring, *Contr. to Atmos. Phys.*, *53*, 1-13, 1980.

Ghazi, A., A. Ebel, and D. F. Heath, A study of satellite observations of ozone and stratospheric temperatures during 1970-1971, *J. Geophys. Res.*, *81*, 5365-5373, 1976.

Ghazi, A., V. Ramanathan, and R. E. Dickinson, Acceleration of upper stratospheric radiative damping: Observational evidence, *Geophys. Res. Lett.*, *6*, 437-440, 1979.

Ghazi, A., R. H. Wang, and M. P. McCormick, A study on radiative damping of planetary waves utilizing stratospheric observations, *J. Atmos. Sci.*, *42*, 2032-2042, 1985.

Gibbins, C. J., P. R. Schwartz, D. L. Thacker, and R. M. Bevilacqua, The variability of mesospheric water vapor, *Geophys. Res. Lett.*, *9*, 131-134, 1982.

Gidel, L. T., Cumulus cloud transport of transient tracers, *J. Geophys. Res.*, *88*, 6587-6599, 1983.

Gidel, L. T., and M. A. Shapiro, The role of clear air turbulence in the production of potential vorticity in the vicinity of upper tropospheric jetstream-frontal systems., *J. Atmos. Sci.*, *36*, 2125-2138, 1979.

Gidel, L. T., and M. A. Shapiro, General circulation model estimates of the net vertical flux of ozone in the lower stratosphere and the implications for the troposheric ozone budget, *J. Geophys. Res.*, *85*, 4049-4058, 1980.

Gidel, L. T., P. J. Crutzen, and J. Fishman, A two-dimensional photochemical model of the atmosphere. 1: Chlorocarbon emissions and their effect on stratospheric ozone, *J. Geophys. Res.*, *88*, 6622-6640, 1983.

Gill, A. E., *Atmosphere-Ocean Dynamics*, 662 pp., Academic Press, New York, 1982.

Gill, P. S., T. E. Graedel, and C. J. Weschler, Organic films on atmospheric aerosol particles, fog droplets, cloud droplets, raindrops and snowflakes, *Rev. Geophys. Space Phys.*, *21*, 903-920, 1983.

Gille, J. C., and F. B. House, On the inversion of Limb radiance measurements, I, Temperature and thickness., *J. Atmos. Sci.*, *28*, 1427-1442, 1971.

Gille, J. C., and L. V. Lyjak, An overview of wave-mean flow interactions during the winter of 1978-1979 derived from LIMS observations, in *Dynamics of the Middle Atmospere*, edited by J. R. Holton and T. Matsuno, pp. 289-306, Terrapub, Tokyo, 1984.

Gille, J. C., and J. M. Russell III, The Limb Infrared Monitor of the Stratosphere: Experiment description, performance, and results, *J. Geophys. Res.*, *89*, 5125-5140, 1984.

Gille, J. C., P. L. Bailey, R. A. Craig, F. B. House, and G. P. Anderson, Sounding the stratosphere and mesosphere by infrared Limb scanning from space, *Science*, *208*, 397-399, 1980a.

Gille, J. C., P. L. Bailey, and J. M. Russell III., Temperature and composition measurements from the LRIR and LIMS experiments on Nimbus 6 and 7, *Phil. Trans. Roy. Soc. London*, *A296*, 205-218, 1980b.

Gille, J. C., P. L. Bailey, L. V. Lyjak, and J. M. Russell III, Results from the LIMS experiment for the PMP-1 winter 1978/79, *Adv. in Space Res.*, *2*, 163-167, 1983.

Gille, J. C., J. M. Russell III, P. L. Bailey, L. L. Gordley, E. E. Remsberg, J. H. Lienesch, W. G. Planet, F. B. House, L. V. Lyjak, and S. A. Beck, Validation of the temperature retrievals obtained by the Limb Infrared Monitor of the Stratosphere (LIMS) experiment on NIMBUS 7, *J. Geophys. Res.*, *89*, 5147-5160, 1984a.

Gille, J. C., J. M. Russell III, P. L. Bailey, E. E. Remsberg, L. L. Gordley, W. F. J. Evans, H. Fischer, B. W. Gandrud, A. Girard, J. E. Harries, and S. A. Beck, Accuracy and precision of the nitric acid concentrations determined by the Limb Infrared Monitor of the Stratosphere experiment on NIMBUS 7, *J. Geophys. Res.*, *89*, 5179-5190, 1984b.

Gille, J. C., C. M. Smythe, and D. F. Heath, Observed ozone response to variations in solar ultraviolet radiation, *Science*, *225*, 315-317, 1984c.

Giorgi, F., and W. L. Chameides, The rainout parameterization in a photochemical model, *J. Geophys. Res.*, *90*, 7872-7880, 1985.

Girard, A., and N. Louisnard, Stratospheric water vapor, nitrogen dioxide, nitric acid and ozone measurements deduced from spectroscopic observations, *J. Geophys. Res.*, *89*, 5109-5114, 1984.

Girard, A., J. Besson, R. Giraudet, and L. Gramont, Correlated seasonal and climatic variations of trace constituents in the stratosphere, *Pure Appl. Geophys.*, *117*, 381-393, 1978/79.

Girard, A., L. Gramont, N. Louisnard, S. Le Boiteux, and G. Fergant, Latitudinal variation of HNO_3, HCl, and HF vertical column density above 11.5 km, *Geophys. Res. Lett.*, *9*, 135-138, 1982.

Girard, A., G. Ferganti, L. Gramont, O. Lado-Bordowsky, J. Laurent, S. LeBoiteux, M. P. Lemaitre, and N. Louisnard, Latitudinal distribution of ten stratospheric species deduced from simultaneous spectroscopic measurements, *J. Geophys. Res.*, *88*, 5377-5392, 1983.

REFERENCES

GMCC: See Harris, J. M.

Godson, W. L., Total ozone in the middle stratosphere over Arctic and sub-Arctic areas in winter and spring, *Quart. J. Roy. Meteorol. Soc.*, *86*, 301-317, 1960.

Goldan, P. D., W. C. Kuster, D. L. Albritton, and A. L. Schmeltekopf, Stratospheric $CFCl_3$, CF_2Cl_2, and N_2O height profile measurements at several latitudes, *J. Geophys. Res.*, *85*, 413-423, 1980.

Goldman, A., D. G. Murcray, F. H. Murcray, W. J. Williams, and F. S. Bonomo, Identification of the ν_3 NO_2 band in the solar spectrum observed from a balloon-borne spectrometer, *Nature*, *225*, 443-444, 1970.

Goldman, A., R. N. Stocker, D. Rolens, W. J. Williams, and D. G. Murcray, Stratospheric HNO_3 distributions from balloon-borne infrared atmospheric emission measurements from 1970-75, *Scientific Report*, University of Denver, Denver, CO, 1976.

Goldman, A., F. G. Fernald, W. J. Williams, and D. G. Murcray, Vertical distribution of NO_2 in the stratosphere as determined from balloon measurements of solar spectra in the 4500 Å region, *Geophys. Res. Lett.*, *5*, 257-260, 1978.

Goldman, A., D. G. Murcray, F. J. Murcray, G. R. Cook, J. W. Van Allen, F. S. Bonomo, and R. D. Blatherwick, Identification of the ν_3 vibration rotation band of CF_4 in balloon-borne infrared solar spectra, *Geophys. Res. Lett.*, *6*, 609-612, 1979.

Goldman, A., D. G. Murcray, F. J. Murcray, and E. Niple, High resolution IR balloon-borne solar spectra and laboratory spectra in the HNO_3 1720 cm^{-1} region: An analysis, *Appl. Opt.*, *19*, 3721-3724, 1980.

Goldman, A., F. J. Murcray, R. D. Blatherwick, J. R. Gillis, F. S. Bonomo, F. H. Murcray, D. G. Murcray, and R. J. Cicerone, Identification of acetylene (C_2H_2) in infrared atmospheric absorption spectra, *J. Geophys. Res.*, *86*, 12143-12146, 1981a.

Goldman, A., J. Reid, and L. S. Rothman, Identification of electric quadrupole O_2 and N_2 lines in the infrared atmospheric absorption spectrum due to the vibration-rotation fundamentals, *Geophys. Res. Lett.*, *8*, 77-78, 1981b.

Goldman, A., F. J. Murcray, J. R. Gillis, and D. G. Murcray, Identification of new solar OH lines in the 10-12 micron region, *Astrophys. J.*, *248*, L133-L135, 1981c.

Goldman, A., F. J. Murcray, R. D. Blatherwick, F. S. Bonomo, F. H. Murcray, and D. G. Murcray, Spectroscopic identification of $CHClF_2$ (F-22) in the lower stratosphere, *Geophys. Res. Lett.*, *8*, 1012-1014, 1981d.

Goldman, A., R. D. Blatherwick, F. J. Murcray, J. W. Van Allen, F. H. Murcray, and D. G. Murcray, *New Atlas of Stratospheric Infrared Absorption Spectra*, Univ. of Denver, Denver, CO, 1982.

Goldman, A., F. G. Fernald, F. J. Murcray, F. H. Murcray, and D. G. Murcray, Spectral least squares quantification of several atmospheric gases from high resolution infrared solar spectra obtained at the South Pole, *J. Quant. Spectrosc. Radiat. Transfer*, *29*, 189-204, 1983a.

Goldman, A., D. G. Murcray, D. L. Lambert, and J. F. Dominy, The pure rotation spectrum of the hydroxyl radical and the solar oxygen abundance, *Mon. Not. R. Astr.*, *203*, 767-776, 1983b.

Goldman, A., F. H. Murcray, D. G. Murcray, and C. P. Rinsland, A search for formic acid in the upper troposphere: A tentative identification of the 1105 cm^{-1} $\nu6$ band Q branch in high-resolution balloon-borne solar absorption spectra, *Geophys. Res. Lett.*, *11*, 307-310, 1984a.

Goldman, A., C. P. Rinsland, F. J. Murcray, D. G. Murcray, M. T. Coffey, and W. G. Mankin, Balloon-borne and aircraft infrared measurements of ethane (C_2H_6) in the upper troposphere and lower stratosphere, *J. Atmos. Chem.*, *2*, 211-221, 1984b.

Goldman, A., J. R. Gillis, C. P. Rinsland, F. J. Murcray, and D. G. Murcray, Stratospheric HNO_3 quantification from line-by-line nonlinear least-squares analysis of high-resolution balloon-borne solar absorption spectra in the 870 cm^{-1} region, *Appl. Opt.*, *23*, 3252-3255, 1984c.

Golombek, A., A global three-dimensional model of the circulation and chemistry of long-lived atmospheric species, Ph.D. thesis, 201 pp., Dept. of Meteor. and Phys. Oceanography, MIT, Cambridge, MA, 1982.

Goody, R. M., A statistical model for water vapor absorption, *J. Meteorol.*, *78*, 165-169, 1952.

Goody, R. M., *Atmospheric Radiation*, 436 pp., Oxford University Press, London, 1964.

Goreau, T. J., The biogeochemistry of nitrous oxide, Ph.D. thesis, Harvard Univ., Boston, MA, 1981.

Goreau, T. J., and W. Z. DeMello, Effects of deforestation on sources and sinks of atmospheric carbon dioxide, nitrous oxide and methane from some Amazonian biota and soils, in press, 1985.

Goreau, T. J., W. A. Kaplan, S. C. Wofsy, M. B. McElroy, F. W. Valois, and S. W. Watson, Production of NO_2 and N_2O by nitrifying bacteria at reduced concentrations of oxygen, *Appl. Environ. Microbiology*, *40*, 526-532, 1985.

Gotz, F. W. P., A. R. Meetham, and G. M. B. Dobson, The vertical distribution of ozone in the atmosphere, *Proc. Roy. Soc. London*, *A145*, 416-446, 1934.

Graedel, T. E., and J. R. McRae, On the possible increase of the atmospheric methane and carbon monoxide concentrations during the last decade, *Geophys. Res. Lett.*, *7*, 977-979, 1980.

Grant, K. E., P. S. Connell, and D. J. Wuebbles, Monte Carlo uncertainty analysis of atmosphere ozone concentrations from large trace gas perturbations, in press, 1985.

Gray, L. J., and J. A. Pyle, Semi-annual oscillation and equatorial tracer distributions, *Quart. J. Roy. Meteorol. Soc.*, in press, 1986.

Gray, W. M., Global view of the origin of tropical disturbances and storms, *Mon. Weather Rev.*, *26*, 653-700, 1968.

Gray, W. M., Cumulus convection and large-scale circulations, Part I: Broadscale and mesoscale considerations, *Mon. Weather Rev.*, *101*, 839-855, 1973.

Greenberg, J. P., and P. R. Zimmerman, Nonmethane HC in remote tropical, continental, and marine atmospheres, *J. Geophys. Res.*, *89*, 4767-4778, 1984.

Greenberg, J. P., P. R. Zimmerman, L. Heidt, and W. Pollock, Hydrocarbons and carbon monoxide emissions from biomass burning in Brazil, *J. Geophys. Res.*, *89*, 1350-1354, 1984.

Grevesse, N., A. J. Sauval, and E. F. Van Dishoeck, An analysis of vibration-rotation lines of OH in the solar infrared spectrum, *Astron. Astrophys.*, *141*, 10-16, 1984.

Griffing, G. W., Ozone and nitrogen oxides production during thunderstorms, *J. Geophys. Res.*, *82*, 943-950, 1977.

Griggs, M., Absorption coefficients of ozone in the ultraviolet and visible regions, *J. Chem. Phys.*, *49*, 857-859, 1968.

Grose, W. L., Recent advances in understanding stratospheric dynamics and transport processes: Application of satellite data to their interpretation, *Adv. in Space Res.*, *4*, 19-28, 1984.

Grose, W. L., and J. M. Russell III, The use of isentropic potential vorticity in conjunction with quasi-conserved species in the study of stratospheric dynamics and transport, in press, 1985.

Grose, W. L., R. E. Turner, and J. E. Nealy, Transport processes in the stratosphere: Model simulations and comparisons with satellite observations, in *Proceedings of the International Middle Atmosphere Symposium*, Kyoto, Japan, in press, 1984.

Grose, W. L., R. E. Turner, and J. E. Nealy, Coupling between photochemistry and transport: Simulations with a 3-D model, *J. Atmos. Terr. Phys.*, in press, 1985.

Grosjean, D., Atmospheric reactions of ortho cresol: Gas phase and aerosol products, *Atmos. Environ.*, *18*, 1641-1652, 1984.

Groves, G. V., Seasonal and latitudinal models of atmospheric temperature, pressure and density, 25 to 100 km, *AFCRL-70-0261*, 78 pp., Air Force Cambridge Research Labs., Hanscom AFB, MA, 1970.

Groves, G. V., and J. M. Forbes, Equinox tidal heating of the upper atmosphere, *Planet. Space Sci.*, *32*, 447-436, 1984.

REFERENCES

Guedalia, D., C. Estournel, and R. Vehil, Effects of Sahel dust layers upon nocturnal cooling of the atmosphere, *ECLATS Experiment*, 644-650, 1984.

Guicherit, R., and H. Van Dop, Photochemical production of ozone in Western Europe (1971-1978) and its relation to meteorology, *Atmos. Environ.*, *11*, 145-155, 1977.

Guthrie, P. D., C. H. Jackman, J. R. Herman, and C. J. McQuillan, A diabatic circulation experiment in a two-dimensional photochemical model, *J. Geophys. Res.*, *89*, 9589-9602, 1984.

Hack, W., and H. Kurzke, The production of H-atoms in the energy transfer reaction of O_2 ($^1\Delta g$) with HO_2 (X^2A''), *Chem. Phys. Lett.*, *104*, 93-96, 1984.

Hack, W., and H. Kurzke, Kinetic study of the elementary chemical reaction $H(^2S) + O_2(^1\Delta g) \rightarrow OH$ ($^2\pi$) $+ O(^3P)$ in the gas phase, *J. Phys. Chem.*, in press, 1985.

Haggard, K. V., and W. L. Grose, Numerical simulation of a sudden stratospheric warming with a three-dimensional spectral, quasi-geostrophic model, *J. Atmos. Sci.*, *38*, 1480-1497, 1981.

Hahn, J., and P. J. Crutzen, The role of fixed nitrogen in atmospheric photochemistry, *Phil. Trans. Roy. Soc. London*, *B296*, 521-541, 1982.

Haigh, J. D., and J. A. Pyle, Ozone perturbation experiments in a two-dimensional circulation model, *Quart. J. Roy. Meteorol. Soc.*, *108*, 551-574, 1982.

Haigh, J. D., Radiative heating in the lower stratosphere and the distribution of ozone in a two-dimensional model, *Quart. J. Roy. Meteorol. Soc.*, *110*, 167-185, 1984.

Hall, C. A. S., C. A. Ekdahl, and D. E. Wartenberg, A fifteen-year record of biotic metabolism in the Northern Hemisphere, *Nature*, *255*, 136-138, 1975.

Hameed, S., and R. D. Cess, The impact of a global warming on biospheric sources of methane and its climatic consequences, *Tellus*, *35*, 1-7, 1983.

Hameed, S., J. P. Pinto, and R. W. Stewart, Sensitivity of the predicted CO-OH-CH_4 perturbation to tropospheric NO_x concentrations, *J. Geophys. Res.*, *84*, 763-768, 1979.

Hameed, S., R. D. Cess, and J. S. Hogan, Response of the global climate to changes in atmospheric chemical composition due to fossil fuel burning, *J. Geophys. Res.*, *85*, 7537-7545, 1980.

Hamilton, K., Studies of wave-mean flow interaction in the stratosphere, mesophere and lower thermosphere, Ph.D. thesis, Princeton University, Princeton, NJ, 1981a.

Hamilton, K., The vertical structure of the quasi-biennial oscillation and its theory, *Atmos.-Ocean*, *19*, 236-250, 1981b.

Hamilton, K., Rocketsonde observation of the mesospheric semiannual oscillation at Kwajalein, *Atmos.-Ocean*, *20*, 281-286, 1982a.

Hamilton, K., Some features of the climatology of the Northern Hemisphere stratosphere revealed by NMC upper atmosphere analyses, *J. Atmos. Sci.*, *39*, 2737-2749, 1982b.

Hamilton, K., Diagnostic study of the momentum balance in the Northern Hemisphere winter stratosphere, *Mon. Weather Rev.*, *111*, 1434-1441, 1983a.

Hamilton, K., Aspects of wave behavior in the mid and upper troposphere of the Southern Hemisphere, *Atmos.-Ocean*, *21*, 40-54, 1983b.

Hamilton, K., Mean wind evolution through the quasi-biennial cycle in the tropical lower stratosphere, *J. Atmos. Sci.*, *41*, 2113-2125, 1984.

Hampson, J., Chemiluminescent emissions observed in the stratosphere and mesosphere, in *Les Problemes Meteorologiques de la Stratosphere et de la Mesosphere*, edited by CNES, Presses Universitaires de France, Paris, 1965.

Handwerk, V., and R. Zellner, Laboratory study of the reaction $ClO + O_2(^1\Delta) \rightarrow$ products, Final report to CMA, 1984.

Hanel, R. A., B. J. Conrath, V. G. Kunde, C. Prabhakara, I. Revah, V. V. Salomonson, and G. Wolford, The Nimbus 4 infrared spectroscopy experiment 1. Calibrated thermal emission spectra, *J. Geophys. Res.*, *77*, 2629-2641, 1972.

Hansen, J., D. Johnson, A. Lacis, S. Lebedeff, P. Lee, D. Rind, and G. Russell, Climate impact of increasing atmospheric carbon dioxide, *Science, 213*, 957-966, 1981.

Hansen, J., A. Lacis, D. Rind, G. Russell, P. Stone, I. Fung, R. Ruedy, and J. Lerner, Climate sensitivity: Analysis of feedback mechanisms, in *Climate Processes and Climate Sensitivity*, Maurice Ewing Series 5, edited by J. E. Hansen and T. Takasashi, 368 pp., American Geophysical Union, Washington, DC, 1984.

Hao, W. M., Sources of N_2O from combustion, Ph.D. thesis, Harvard University, Boston, MA, 1985.

Harries, J. E., Ratio of HNO_3 to NO_2 concentrations in daytime stratosphere, *Nature, 274*, 235, 1978.

Harries, J. E., Stratospheric composition measurements as tests of photochemical theory, *J. Atmos. Terr. Phys., 44*, 591-597, 1982.

Harries, J. E., D. G. Moss, N. R. W. Swann, G. F. Neill, and P. Gildwarg, Simultaneous measurements of H_2O, NO_2, and HNO_3 in the daytime stratosphere from 15 to 35 km, *Nature, 259*, 300-302, 1976.

Harries, R. C., D. I. Sebacher, and F. P. Day, Methane flux in the Great Dismal Swamp, *Nature, 297*, 673-674, 1982.

Harris, J. M. and B. A. Bodhaine (Eds.), *Geophysical Monitoring for Climatic Change, Summary Report 1982*, 160 pp., NOAA Air Resources Laboratory, Boulder, CO, 1983.

Harris, J. M., and E. C. Nickerson (Eds.), *Geophysical Monitoring for Climatic Change, No. 12, Summary Report, 1983*, 199 pp., NOAA Air Resources Laboratory, Boulder, CO, 1984.

Harshvardhan, A. Arking, M. D. King and M.-D. Chou, Impact of the El Chichon stratospheric aerosol layer on N. H. temperatures, paper presented at WMO(CAS)/IAMAP Workshop on Aerosols and Their Climatic Effects, Williamsburg, VA, 28-30 March 1983.

Hartmann, D. L., The structure of the stratosphere in the Southern Hemisphere during late winter 1973 as observed by satellite, *J. Atmos. Sci., 33*, 1141-1154, 1976a.

Hartmann, D. L., The dynamical climatology of the stratosphere in the Southern Hemisphere during late winter 1973, *J. Atmos. Sci., 33*, 1789-1802, 1976b.

Hartmann, D. L., A note concerning the effect of variable extinction on radiative-photochemical relaxation, *J. Atmos. Sci., 35*, 1125-1130, 1978.

Hartmann, D. L., Barotropic instability of the polar night jet stream, *J. Atmos. Sci., 40*, 817-835, 1983.

Hartmann, D. L., and R. R. Garcia, A mechanistic model of ozone transport by planetary waves in the stratosphere, *J. Atmos. Sci., 36*, 350-364, 1979.

Hartmann, D. L., C. R. Mechoso, and K. Yamazaki, Observations of wave mean-flow interaction in the Southern Hemisphere, *J. Atmos. Sci., 41*, 351-362, 1984.

Harwood, R. S., The temperature structure of the Southern Hemisphere stratosphere: August-October, 1971, *Quart. J. Roy. Meteorol. Soc., 102*, 757-770, 1975.

Harwood, R. S., and J. A. Pyle, A two-dimensional mean circulation model for the atmosphere below 80 km, *Quart. J. Roy. Meteorol. Soc., 101*, 723-747, 1975.

Harwood, R. S., and J. A. Pyle, Studies of the ozone budget using a zonal mean circulation model and linearized photochemistry, *Quart. J. Roy. Meteorol. Soc., 103*, 319-343, 1977.

Harwood, R. S., and J. A. Pyle, The dynamical behaviour of a two-dimensional model of the stratosphere, *Quart. J. Roy. Meteorol. Soc., 106*, 395-420, 1980.

Hasebe, F., Interannual variations of global total ozone revealed from Nimbus 4 BUV and ground-based observations, *J. Geophys. Res., 88*, 6819-6834, 1983.

Hasebe, F., The global structure of the total ozone fluctuations observed on the time scales of two to several years, in *Dynamics of the Middle Atmosphere*, edited by J. R. Holton and T. Matsuno, pp. 445-464, Terrapub, Tokyo, 1984.

Hashimoto, L. K., W. A. Kaplan, S. C. Wofsy, and W. B. McElroy, Transformations of fixed nitrogen in the Cariaco Trench, *Deep Sea Res., 30*, 575-590, 1983.

REFERENCES

Hasson, V., and R. W. Nicholls, Absolute spectral absorption measurements in molecular oxygen from 2640-1920Å: II. Continuum measurements 2430-1920Å, *J. Phys. B.: Atom. Mol. Phys.*, *4*, 1789-1797, 1971.

Hastie, D. R., and M. D. Miller, A balloon-borne tunable diode laser absorption spectrometer for multi-species trace gas measurements in the stratosphere, *Appl. Opt.*, in press, 1985.

Hayashi, Y., A theory of large-scale equatorial waves generated by condensation heat and accelerating the zonal wind, *J. Meteorol. Soc. Japan*, *48*, 140-160, 1970.

Hayashi, Y., Spectral analysis of tropical disturbances appearing in a GFDL general circulation model, *J. Atmos. Sci.*, *31*, 180-218, 1974.

Hayashi, Y., Non-singular resonance of equatorial waves under the radiation condition, *J. Atmos. Sci.*, *33*, 183-201, 1976.

Hayashi, Y., D. Golder, and J. Mahlman, Stratospheric and mesospheric Kelvin waves simulated by the GFDL "SKYHI" general circulation model, *J. Atmos. Sci.*, *41*, 1971-1984, 1984.

Hayashi, Y., and D. Golder, Transient planetary waves simulated by GFDL spectral general circulation models. Part I: Effects of mountains, *J. Atmos. Sci.*, *40*, 941-950, 1983.

Hayashi, Y., D. Golder, and J. Mahlman, Stratospheric and mesospheric Kelvin waves simulated by the GFDL "SKYHI" general circulation model, *J. Atmos. Sci.*, *41*, 1971-1984, 1984.

Heaps, W. S., and T. J. McGee, Balloon borne lidar measurements of the stratospheric hydroxyl radical, *J. Geophys. Res.*, *88*, 5281-5285, 1983.

Heaps, W. S., and T. J. McGee, Progress in stratospheric hydroxyl measurement by balloon-borne lidar, *J. Geophys. Res.*, *90*, 7913-7922, 1985.

Heaps, W. S., T. J. McGee, R. D. Hudson, and L. O. Caudill, Stratospheric ozone and hydroxyl radical measurements by balloon-borne lidar, *Applied Opt.*, *21*, 2265-2274, 1982.

Hearn, A. G., The absorption of ozone in the ultraviolet and visible regions of the spectrum, *Proc. Phys. Soc. (London)*, *78*, 932-940, 1961.

Heaseman, C. H., Satellite observations of mesospheric wind structure, Ph.D. thesis, Oxford University, Oxford, 1981.

Heastie, H., and P. M. Stephenson, Upper winds over the world, *Geophys. Mem.*, No. 103, London: HMSO, *13*, 1-217, 1960.

Heath, D. F., A review of observational evidence for short and long term ultraviolet flux variability of the sun, in *Proceedings of the International Conference on Sun and Climate*, Centre National d'Etudes Spatiales, Toulouse, Sept. 30-Oct. 3, 445-450, 1980.

Heath, D. F., and B. M. Schlesinger, Temporal variability of the UV solar spectral irradiance from 160-400 nm over periods of the evolution and rotation of active regions from maximum to minimum phases of the sunspot cycle, in press, 1985.

Heath, D. F., A. J. Krueger, H. A. Roeder, and B. D. Henderson, The solar backscatter ultraviolet and total ozone mapping spectrometer (SBUV/TOMS) for Nimbus G, *Opt. Eng.*, *14*, 323-331, 1975.

Heath, D. F., A. J. Krueger, and P. J. Crutzen, Solar proton event: Influence on stratospheric ozone, *Science*, *197*, 886-889, 1977.

Heath, D. F., T. P. Repoff, and R. F. Donnelly, Nimbus-7 SBUV observations of solar UV spectral irradiance variations caused by solar rotation and active-region evolution for the period November 7, 1978-November 1, 1980, *NOAA-TM-ERL-ARL-129*, 78 pp., NOAA Air Resources Laboratory, Rockville, MD, September, 1984.

Heicklen, J., *Atmospheric Chemistry*, 406 pp., Academic Press, New York, 1976.

Heidt, L. E., J. P. Krasnec, R. A. Lueb, W. H. Pollack, B. E. Henry, and P. J. Crutzen, Latitudinal distributions of CO and CH_4 over the Pacific, *J. Geophys. Res.*, *85*, 7329-7336, 1980.

Heikes, B., and A. M. Thompson, Effects of heterogeneous processes on NO_3, HONO, and HNO_3 chemistry in the troposphere, *J. Geophys. Res.*, *10*, 10883-10895, 1983.

Helas, G., and P. J. Warneck, Background NO_x mixing ratios in air masses over the North Atlantic Ocean, *J. Geophys. Res.*, *86*, 7283-7290, 1981.

Held, I. M., Stationary and quasi-stationary eddies in the extratropical troposphere: Theory, in *Large-scale Dynamical Processes in the Atmosphere*, edited by B. J. Hoskins and R. Pearce, pp. 127-168, Academic Press, New York, 1983.

Helten, M., W. Patz, M. Trainer, H. Fark, E. Klein, and D. H. Ehhalt, Measurements of stratospheric HO_2 and NO_2 by matrix isolation and ESR spectroscopy, *J. Atmos. Chem.*, *2*, 191-202, 1984a.

Helten, M., W. Patz, D. H. Ehhalt, and E. P. Roeth, Measurements of nighttime NO_3 and NO_2 in the stratosphere by matrix isolation and ESR spectroscopy, in *Atmospheric Ozone*, edited by C. S. Zerefos and A. Ghazi, pp. 196-200, D. Reidel, Dordrecht, 1984b.

Hendry, D. G., and R. A. Kenley, Chapter 7, in *Atmospheric chemistry of perioxynitrates, nitrogen air pollutants: Chemical and biological implications*, edited by D. Grosjean, Ann Arbor Science, Ann Arbor, MI, 1979.

Hering, W. S. and T. R. Borden: See Borden, T. R. and W. S. Hering.

Herman, J. R., and C. J. McQuillan, Atmospheric chlorine and stratospheric ozone nonlinearities and trend detection, *J. Geophys. Res.*, *90*, 5721-5732, 1985.

Herman, J. R., and J. E. Mentall, O_2 absorption cross sections (187-225 nm) from stratospheric solar flux measurements, *J. Geophys. Res.*, *87*, 8967-8975, 1982a.

Herman, J. R., and J. E. Mentall, The direct and scattered solar flux within the stratosphere, *J. Geophys. Res.*, *87*, 1319-1330, 1982b.

Hess, P. H., and J. R. Holton, The origin of temporal variance in long-lived trace constituents in the summer stratosphere, *J. Atmos. Sci.*, *42*, 1455-1463, 1985.

Hicks, B. B., M. L. Wesely, and J. L. Durham, *Critique of Methods to Measure Dry Deposition*, 83 pp., Environmental Sciences Research Laboratory, Office of Research and Development, U. S. Environmental Protection Agency, Research Triangle Park, NC, 1980.

Hidalgo, H., and P. J. Crutzen, The tropospheric and stratospheric composition perturbed by NO_x emissions of high-altitude aircraft, *J. Geophys. Res.*, *82*, 5833-5866, 1977.

Hide, R., and P. J. Mason, Sloping convection in a rotating fluid, *Advances in Physics*, *24*, 47-100, 1975.

Hill, W. J., P. N. Sheldon, and J. J. Tiede, Analyzing worldwide total ozone for trends, *Geophys. Res. Lett.*, *4*, 21-24, 1977.

Hills, A. J., and C. J. Howard, Rate coefficient temperature dependence and branching ratio for the OH + ClO reaction, *J. Chem. Phys.*, *81*, 4458-4465, 1984.

Hilsenrath, E., and B. M. Schlesinger, Total ozone seasonal and interannual variations derived from the 7 year Nimbus 4 data, *J. Geophys. Res.*, *86*, 12087-12096, 1981.

Hilsenrath, E., T. Seiden, and P. Goodman, An ozone measurement in the mesosphere and stratosphere by means of a rocketsonde, *J. Geophys. Res.*, *71*, 1385-1397, 1969.

Hilsenrath, E., J. Ainsworth, A. Holland, J. Mentall, A. Torres, W. Attmannspacher, A. Bass, W. Evans, W. Komhyr, K. Mauersberger, A. J. Miller, M. Proffitt, D. Robbins, S. Taylor, and E. Weinstock, Results from the balloon ozone intercomparison campaign (BOIC), in *Atmospheric Ozone*, edited by C. S. Zerefos and A. Ghazi, pp. 454-459, D. Reidel, Dordrecht, 1985.

Hilsenrath, E., J. Ainsworth, W. Attmannspacher, A. Bass, W. F. J. Evans, A. Holland, W. Komhyr, K. Mauersberger, J. Mentall, M. Proffitt, D. Robbins, S. Taylor, A. Torres, and E. Weinstock, Results from the Balloon Ozone Intercomparison Campaign (BOIC), to be published, 1986.

Hines, C. O., Dynamical heating of the upper atmosphere, *J. Geophys. Res.*, *70*, 177-183, 1965.

REFERENCES

Hinteregger, H. E., Representations of solar EUV fluxes for aeronomical applications, in *The Mesosphere and Thermosphere*, edited by G. Schmidtke and K. S. W. Champion, pp. 39-52, Pergamon Press, Oxford, 1981.

Hirooka, T., and I. Hirota, Normal mode Rossby waves observed in the upper stratosphere. Part II. Second antisymmetric and symmetric modes of zonal wavenumbers 1 and 2, *J. Atmos. Sci.*, 42, 536-548, 1985.

Hirota, I., Seasonal variation of planetary waves in the stratosphere observed by the Nimbus 5 SCR, *Quart. J. Roy. Meteorol. Soc.*, 102, 757-770, 1976.

Hirota, I., Equatorial waves in the upper stratosphere and mesosphere in relation to the semi-annual oscillation of the zonal wind, *J. Atmos. Sci.*, 35, 714-722, 1978.

Hirota, I., Kelvin waves in the equatorial middle atmosphere observed by the Nimbus-5 SCR, *J. Atmos. Sci.*, 36, 217-222, 1979.

Hirota, I., Observational evidence of the semiannual oscillation in the tropical middle atmosphere-A review, *Pure Appl. Geophys.*, 118, 217-238, 1980.

Hirota, I., Climatology of gravity waves in the middle atmosphere, *J. Atmos. Terr. Phys.*, 46, 767-773, 1984.

Hirota, I., and T. Hirooka, Normal mode Rossby waves observed in the upper stratosphere. Part I: First symmetric modes of wavenumbers 1 and 2, *J. Atmos. Sci.*, 41, 1253-1267, 1984.

Hirota, I., and Y. Sato, Periodic variation of the winter circulation and intermittent vertical propagation of planetary waves, *J. Meteorol. Soc. Japan*, 47, 390-402, 1969.

Hirota, I., T. Hirooka, and M. Shiotani, Upper stratospheric circulation in the two hemispheres observed by satellites, *Quart. J. Roy. Meteorol. Soc.*, 109, 443-454, 1983a.

Hirota, I., Y. Maekawa, S. Fukao, K. Fukuyama, M. P. Sulzer, J. L. Fellous, T. Tsudo, and S. Kato, Fifteen-day observation of mesospheric and lower thermospheric motions with the aid of the Arecibo UHF radar, *J. Geophys. Res.*, 88, 6835-6842, 1983b.

Hitchman, M. H., An observational study of wave-mean flow interaction in the equatorial middle atmosphere, Ph.D. thesis, 360 pp., Dept. of Atmospheric Sciences, University of Washington, Seattle, WA, 1985.

Hitchman, M. H., and C. B. Leovy, Evolution of the zonal mean state in the equatorial middle atmosphere during October, 1978-May, 1979, *J. Atmos. Sci.*, 43, in press, 1986.

Hocking, W. K., Mesospheric turbulence intensities measured with a HF radar at 35° S - II, *J. Atmos. Terr. Phys.*, 45, 103-114, 1983.

Hocking, W. K., Turbulence in the region 80-120 km, in *Handbook for MAP, Vol. 16*, edited by K. Labitzke, J. J. Barnett, and B. Edwards, pp. 290-304, SCOSTEP Secretariat, Univ. of Illinois, Urbana, 1985.

Hodges, Jr., R. R., Generation of turbulence in the upper atmosphere by internal gravity waves, *J. Atmos. Sci.*, 72, 3455-3458, 1967.

Hoell, J. M., C. N. Harward, and B. S. Williams, Remote infrared heterodyne radiometer measurements of atmospheric ammonia profiles, *Geophys. Res. Lett.*, 7, 313-316, 1980.

Hoell, J. M., G. L. Gregory, M. A. Carroll, M. McFarland, B. A. Ridley, D. D. Davis, J. Bradshaw, M. O. Rodgers, A. L. Torres, G. W. Sachse, G. F. Hill, E. P. Condon, R. A. Rasmussen, M. C. Campbell, J. C. Farmer, J. C. Sheppard, C. C. Wang, and L. I. Davis, An intercomparison of carbon monoxide, nitric oxide, and hydroxyl measurement techniques: Overview of results, *J. Geophys. Res.*, 89, 11819-11825, 1984.

Hoffert, M. I., A. J. Callegari, and C. T. Hsieh, The role of deep sea storage in the secular response to climate forcing, *J. Geophys. Res.*, 85, 6667-6679, 1980.

Hoffman-Sievert, R., and A. W. Castleman, The reaction of SO_3 with water clusters and the formation of H_2SO_4, *J. Phys. Chem.*, 88, 3329-3333, 1984.

Hofmann, D. J., and J. M. Rosen, Balloon-borne observations of stratospheric aerosol and condensation nuclei during the year following the Mt. St. Helens eruption, *Geophys. Res. Lett.*, 87, 11039-11061, 1982.

Hofmann, D. J., and J. M. Rosen, Sulfuric acid droplet formation and growth in the stratosphere after the 1982 eruption of El Chichon, *Science*, *222*, 325-327, 1983.

Holland, A. J., T. D. Keenan, and G. D. Crane, Observations of a phenomenal temperature perturbation in tropical cyclone Kerry (1979), *Mon. Weather Rev.*, *112*, 1074-1082, 1984.

Holstein, K. J., E. H. Fink, J. Wildt, R. Winter, and F. Zabel, Mechanisms of $HO_2(A2A')$ excitation in various chemical systems, *J. Phys. Chem.*, *87*, 3943-3948, 1983.

Holton, J. R., Waves in the equatorial stratosphere generated by tropospheric heat sources, *J. Atmos. Sci.*, *29*, 368-375, 1972.

Holton, J. R., A note on the frequency distribution of atmospheric Kelvin waves, *J. Atmos. Sci.*, *30*, 499-501, 1973.

Holton, J. R., *The Dynamical Meteorology of the Stratosphere and Mesosphere*, 216 pp., American Meteorological Society, Boston, MA, 1975.

Holton, J. R., Wave propagation and transport in the middle atmosphere, *Phil. Tran. Roy. Soc. London*, *A296*, 73-85, 1980.

Holton, J. R., An advective model for two-dimensional transport of stratospheric trace species, *J. Geophys. Res.*, *86*, 11989-11994, 1981.

Holton, J. R., The role of gravity wave induced drag and diffusion in the momentum budget of the mesosphere, *J. Atmos. Sci.*, *39*, 791-799, 1982.

Holton, J. R., The influence of gravity wave breaking in the circulation of the middle atmosphere, *J. Atmos. Sci.*, *40*, 2497-2507, 1983.

Holton, J. R., The generation of mesospheric planetary waves by zonally asymmetric gravity wave breaking, *J. Atmos. Sci.*, *41*, 3427-3430, 1984a.

Holton, J. R., Troposphere-stratosphere exchange of trace constituents: The water vapor puzzle, in *Dynamics of the Middle Atmosphere*, edited by J. R. Holton and T. Matsuno, pp. 369-385, Terrapub, Tokyo, 1984b.

Holton, J. R., A dynamically based transport parameterization for one-dimensional photochemical models, in *Handbook for MAP, Vol. 18*, edited by S. Kato, Chap. 4, SCOSTEP Secretariat, Univ. of Illinois, Urbana, 1985.

Holton, J. R., A dynamically based transport parameterization for one-dimensional photochemical models of the stratosphere, *J. Geophys. Res.*, in press, 1986.

Holton, J. R., and R. S. Lindzen, An updated theory of the quasi-biennial oscillation of the tropical stratosphere, *J. Atmos. Sci.*, *29*, 1076-1080, 1972.

Holton, J. R., and H. C. Tan, The influence of the equatorial quasi-biennial oscillation on the global circulation at 50 mb, *J. Atmos. Sci.*, *37*, 2200-2208, 1980.

Holton, J. R., and H. C. Tan, The quasi-biennial oscillation in the Northern Hemisphere lower stratosphere, *J. Meteorol. Soc. Japan*, *60*, 140-148, 1982.

Holton, J. R., and W. M. Wehrbein, The role of forced planetary waves in the annual cycle of zonal mean circulation of the middle atmosphere, *J. Atmos. Sci.*, *37*, 1968-1983, 1980a.

Holton, J. R., and W. M. Wehrbein, A numerical model of the zonal mean circulation of the middle atmosphere, *Pure Appl. Geophys.*, *118*, 284-306, 1980b.

Holton, J. R., and X. Zhu, A further study of gravity wave induced drag and diffusion in the mesosphere, *J. Atmos. Sci.*, *41*, 2653-2662, 1984.

Hood, L. L., The temporal behavior of upper stratospheric ozone at low latitudes: Evidence from Nimbus 4 BUV data for short-term responses to solar ultraviolet variability, *J. Geophys. Res.*, *89*, 9557-9568, 1984.

Hopkins, R. H., Evidence of polar-tropical coupling in upper stratospheric zonal wind anomalies, *J. Atmos. Sci.*, *32*, 712-719, 1975.

REFERENCES

Horvath, J. J., J. E. Frederick, N. Orsini, and A. R. Douglass, Nitric oxide in the upper stratosphere: Measurements and geophysical interpretation, *J. Geophys. Res.*, *88*, 10809-10817, 1983.

Hoskins, B. J., Non-Boussinesq effects and further development in a model of upper troposheric frontogenesis, *Quart. J. Roy. Meteorol. Soc.*, *98*, 532-541, 1972.

Hoskins, B. J., The role of potential vorticity in symmetric stability and instability, *Quart. J. Roy. Meteorol. Soc.*, *100*, 480-482, 1974.

Hoskins, B. J., The geostrophic momentum approximation and the semi-geostrophic equations, *J. Atmos. Sci.*, *32*, 233-242, 1975.

Hoskins, B. J., Modelling of the transient eddies and their feedback on the mean flow, in *Large-scale Dynamical Processes in the Atmosphere*, edited by B. J. Hoskins and R. Pearce, pp. 169-199, Academic Press, New York, 1983.

Hoskins, B. J., and I. Draghici, The forcing of ageostrophic motion according to the semi-geostrophic equations and in an isentropic coordinate model, *J. Atmos. Sci.*, *34*, 1859-1867, 1977.

Hoskins, B. J., and W. A. Heckley, Baroclinic waves and frontogenesis in a non-uniform potential vorticity semi-geostrophic model, *J. Atmos. Sci.*, *39*, 1999-2016, 1982.

Hoskins, B. J., I. Draghici, and H. C. Davies, A new look at the omega equation, *Quart. J. Roy. Meteorol. Soc.*, *104*, 31-38, 1978.

Hoskins, B. J., M. E. McIntyre, and A. W. Robertson, On the use and significance of isentropic potential vorticity maps, *Quart. J. Roy. Meteorol. Soc.*, *111*, 877-946, 1985.

Houghton, J. T., *The Physics of Atmospheres*, 203 pp., Cambridge University Press, Cambridge, 1977.

Houghton, J. T., The stratosphere and mesosphere, *Quart. J. Roy. Meteorol. Soc.*, *104*, 1-30, 1978.

Houghton, J. T., F. W. Taylor, and C. D. Rodgers, Remote sounding of atmospheres, *Cambridge Planetary Science Series No. 5*, 343 pp., Cambridge University Press, Cambridge, 1984.

Houze, Jr., R. A., Cloud clusters and long-scale vertical motions in the tropics, *J. Meteorol. Soc. Japan*, *60*, 396-409, 1982.

Houze, R. A., and A. K. Betts, Convection in GATE, *Rev. Geophys. Space Phys.*, *19*, 541-576, 1981.

Houze, R. A., S. G. Geotis, F. D. Marks, and A. K. West, Winter monsoon convection in the vicinity of North Borneo. Part I: Structure and time evolution of the clouds and precipitation, *Mon. Weather Rev.*, *109*, 1595-1614, 1981.

Hov, O., S. A. Penkett, I. S. A. Isaksen, and A. Semb, Organic gases in the Norwegian Arctic, *Geophys. Res. Lett.*, *11*, 425-428, 1984.

Hoyt, S. D., The air-sea exchange of carbonyl sulfide (OCS) and halocarbons, Ph.D. thesis, Oregon Graduate Center, Beaverton, Oregon, 1982.

Hsu, C. P. F., Air parcel motions during a numerically simulated sudden stratospheric warming, *J. Atmos. Sci.*, *37*, 2768-2792, 1980.

Hubler, G., D. Perner, U. Platt, A. Tonnissen, and D. H. Ehhalt, Ground-level OH radical concentrations: New measurements by optical absorption, *J. Geophys. Res.*, *89*, 1309-1319, 1984.

Huddleston, R. K., and E. Weitz, A laser-induced fluorescence study of energy transfer between the symmetric stretching and bending modes of CO_2, *Chem. Phys. Lett.*, *83*, 174-179, 1981.

Hudson, R. D., Critical review of ultraviolet photoabsorption cross sections for molecules of astrophysical and aeronomic interest, *Rev. Geophys. Space Phys.*, *9*, 305-406, 1971.

Hudson, R. D. (Ed.), *The Stratosphere 1981. Theory and Measurements*, WMO Global Ozone Research and Monitoring Project Report No. 11, 516 pp., WMO, Geneva, 1982.

Hudson, R. D., and S. H. Mahle, Photodissociation rates of molecular oxygen in the mesosphere and lower thermosphere, *J. Geophys. Res.*, *77*, 2902-2914, 1972.

Hudson, R. D., and E. I. Reed (Eds.), *The Stratosphere: Present and Future*, NASA Reference Publication 1049, 432 pp., NASA Goddard Space Flight Center, Greenbelt, MD, 1979.

Huebert, B. J., The dry deposition of nitric acid to grass, *J. Geophys. Res.*, *90*, 2085-2090, 1985.

Huebert, B. J., and A. L. Lazrus, Tropospheric gas-phase and particulate nitrate measurements, *J. Geophys. Res.*, *85*, 7322-7328, 1980.

Hungate, R. E., *The Rumen and Its Microbes*, 533 pp., Academic Press, New York, 1960.

Hunt, B. G., Experiments with a stratospheric general circulation model. III. Large-scale diffusion of ozone including photochemistry. *Mon. Weather Rev.*, *97*, 287-306, 1969.

Hunt, B. G., The maintenance of the zonal mean state of the upper atmosphere as represented in a three-dimensional general circulation model extending to 100 km, *J. Atmos. Sci.*, *38*, 2172-2186, 1981.

Hunt, B. G., The impact of gravity wave drag and diurnal variability on the general circulation of the middle atmosphere, *J. Atmos. Sci.*, in press, 1985.

Hunt, B. G., and S. Manabe, Experiments with stratospheric general circulation model, II. Large-scale diffusion of tracers in the stratosphere, *Mon. Weather Rev.*, *96*, 503-539, 1968.

Hunten, D., The philosophy of one-dimensional modeling, in *Proceedings Fourth Conference Climatic Impact Assessment Program*, DOT-TSC-OST-75-38, edited by T. M. Hard and A. J. Broderick, pp. 147-155, Transportation Systems Center, Cambridge, MA, 1975.

Huntress, W. T. Jr., Upper Atmosphere Research Satellite Program—to study the chemistry, energetics, and dynamics, Final Report, *JPL Publ. 78-54*, 62 pp., Jet Propulsion Lab., Pasadena, CA, 1978.

Husson, N., A. Chedin, N. A. Scott, I. Cohen-Hallaleh, and A. Berroir, La Banque de donnees GEISA. Mise a jour no. 3, Laboratoire de Meteorologie Dynamique du C.N.R.S., *Internal Note 116*, Ecole Polytechnique, 91128 Palaiseau Cedex, France, July 1982.

Husson, N., A. Chedin, N. A. Scott, D. Bailly, G. Graner, N. Lacome, A. Levy, C. Rossetti, G. Tarrago, C. Camy-Peyret, J. M. Flaud, A. Bauer, J. M. Colmont, N. Monnanteuil, J. C. Hilico, G. Pierre, M. Loete, J. P. Champion, L. S. Rothman, L. R. Brown, G. Orton, P. Varanasi, C. P. Rinsland, M. A. H. Smith, and A. Goldman, The GEISA spectroscopic line parameters data bank in 1984, *Annales Geophysicae*, Fasc. 2, Series A, 1986.

Hutchinson, G. E., and A. R. Mosier, Nitrous oxide emissions from an irrigated cornfield, *Science*, *205*, 1125-1127, 1976.

Hyson, P., Stratospheric water vapor over Australia, *Quart. J. Roy. Meteorol. Soc.*, *109*, 285-294, 1983.

Idso, S. B., The climatological significance of a doubling of earth's atmospheric carbon dioxide concentration, *Science*, *207*, 1462-1463, 1980.

Iman, R. L., and M. J. Shortencarier, A Fortran 77 program and user's guide for the generation of Latin hypercube and random samples for use with computer models, *SAND 83-2365*, Sandia National Laboratories, Albuquerque, NM, 1984.

Iman, R. L., J. C. Helton, and J. E. Campbell, An approach to sensitivity analysis of computer models: Part I-Introduction, Input variable selection and preliminary variable assessment, *J. Quality Tech.*, *13*, 174-183, 1981.

Imbrie, J., and K. P. Imbrie, *Ice Ages, Solving the Mystery*, 224 pp., Enslow Pub., Short Hills, NJ, 1979.

Inn, E. C. Y., and Y. Tanaka, Absorption coefficient of ozone in the ultraviolet and visible regions, *J. Opt. Soc. Am.*, *43*, 870-873, 1953.

Inst. fur Met. des Frei Universiteit Berlin, Meteorologische Abhandlungen, Tagliche Hohenkarten der 30-Mbar-flache sowie monatliche mittelkarten fur das jahr 1980, Verlag Von Dietuch Reiner, Berlin, 1980.

Isaksen, I. S. A., Tropospheric ozone budget and possible man made effects, in *Quadrennial International Ozone Symposium, Vol. II*, edited by J. London, pp. 845-852, IAMAP, NCAR, Boulder, CO, 1981.

Isaksen, I. S. A., and O. Hov, Calculations of trends in the tropospheric concentration of O_3, OH, CO, CH_4 and NO_x, in press, 1985.

REFERENCES

Isaksen, I. S. A., and F. Stordal, Ozone perturbations by enhanced levels of CFCs, N_2O and CH_4: A two-dimensional diabatic circulation study including uncertainty estimates, *J. Geophys. Res.*, in press, 1985.

Ishiwata, T., I. Fujiwara, Y. Naruge, K. Obi, and I. Tanaka, Study of NO_3 by laser induced fluorescence, *J. Phys. Chem.*, 87, 1349-1352, 1983.

Itoh, H., The response of equatorial waves to thermal forcing, *J. Meteorol. Soc. Japan*, 55, 222-239, 1977.

Jackman, C. H., and P. D. Guthrie, Sensitivity of N_2O, $CFCl_3$ and CF_2Cl_2 two-dimensional distributions to O_2 absorption cross sections, *J. Geophys. Res.*, 90, 3919-3923, 1985.

Jackman, C. H., and R. D. McPeters, The response of ozone to solar proton events during solar cycle 21: A theoretical interpretation, *J. Geophys. Res.*, 42, 90, 7955-7966, 1985.

Jackman, C. H., J. E. Frederick, and R. S. Stolarski, Production of odd nitrogen in the stratosphere and mesosphere: An intercomparison of source strengths, *J. Geophys. Res.*, 85, 7495-7505, 1980.

Jackman, C. H., J. A. Kaye, and P. D. Guthrie, LIMS HNO_3 data above 5 mbar: Corrections based on simultaneous observations of other species, *J. Geophys. Res.*, 90, 7923-7930, 1985.

Jackman, C. H., R. S. Stolarski, and J. A. Kaye, Two-dimensional monthly average ozone balance from Limb Infrared Monitor of the stratosphere and stratospheric and mesospheric sounder data, *J. Geophys. Res.*, 91, 1103-1116, 1986.

Jesson, J. P., Release of industrial halocarbons and tropospheric budget, in *Proceedings of the NATO Advanced Study Institute on Atmospheric Ozone: Its Variation and Human Influences*, Rep. FAA-EE-80-20, edited by A. C. Aikin, pp. 373-396, DOT, FAA, Washington, DC, 1980.

Johansson, C., Field measurements of emission of nitric oxide from fertilized and unfertilized forest soils in Sweden, *J. Atmos. Chem.*, 1, 429-442, 1984.

Johansson, C., and L. Granat, Emission of nitric oxide from arable land, *Tellus*, 36B, 25-37, 1984.

Johnson, D. R., Systematic stratospheric-tropospheric exchange through quasi-horizontal transport within active baroclinic waves, in *The Long-Range Transport of Pollutants and its Relation to General Circulation including Stratospheric/Tropospheric Exchange Processes—Conference Proceedings*, WMO No. 538, pp. 401-408, WMO, Geneva, 1979.

Johnson, D. R., A generalized transport equation for use with meteorological coordinate systems, *Mon. Weather Rev.*, 108, 733-745, 1980.

Johnson, D. R., On the forcing and maintenance of the isentropic zonally averaged circumpolar vortex, paper presented at *IAMAP-WMO Symposium on Maintenance of the Quasi-Stationary Components of the Flow in the Atmosphere and in Atmospheric Models*, pp 19-22, WMO, Geneva, Paris, August 30-September 2, 1983.

Johnson, D. R., On the global distribution of heat sources and sinks and their relation to mass and energy transport, paper presented at WMO Proceedings of the FGGE Tropics Seminar, Tallahassee, Florida, October 8-12, 1984a.

Johnson, D. R., The global circulation during the FGGE year: On the balance of mass, energy, and angular momentum within isentropic and isobaric coordinates as revealed by different FGGE data sets, paper presented at *WMO Proceedings of the Global Weather Experiment Scientific Seminar*, Helsinki, Finland, August 29-31, 1984b.

Johnson, D. R., and W. K. Downey, Azimuthally averaged transport and budget equations for storms: Quasi-Lagrangian diagnostics 1, *Mon. Weather Rev.*, 103, 967-979, 1975.

Johnson, D. R., and R. D. Townsend, Diagnostics of the heat sources and sinks of the Asiatic monsoon and the thermally-forced planetary scale response, M. S. thesis, AD-A119755, 72 pp., Wisconsin Univ., Madison, WI, 1981.

Johnson, D. R., R. D. Townsend, and M-Y Wei, The thermally forced responses of the planetary scale circulation to the global distribution of heat sources and sinks, *Tellus*, 37A, 106-125, 1985.

Johnson, F. S., J. D. Purcell, R. Tourey, and K. Watanabe, Direct measurements of the vertical distribution of atmospheric ozone to 70 kilometers altitude, *J. Geophys. Res.*, *57*, 157-176, 1952.

Johnson, J. E., The role of the oceans in the atmospheric cycle of carbonyl sulfide, Ph.D. thesis, University of Washington, Seattle, WA, 1985.

Johnson, K. W., and M. E. Gelman, Trends in the upper stratospheric temperatures as observed by rocket-sondes (1965-1983), in *Handbook for MAP, Vol. 18*, edited by S. Kato, pp. 24-27, SCOSTEP Secretariat, Univ. of Illinois, Urbana, 1985.

Johnson, R. H., and D. C. Kriete, Thermodynamic circulation characteristics of winter monsoon tropical mesoscale convection, *Mon. Weather Rev.*, *110*, 1898-1911, 1982.

Johnston, D. A., Volcanic contribution of chlorine to the stratosphere: More significant to ozone than previously estimated?, *Science*, *209*, 491-493, 1980.

Johnston, H. S., Reduction of stratospheric ozone by nitrogen oxide catalysts from supersonic transport exhaust, *Science*, *173*, 517-522, 1971.

Johnston, H. S., Human effects on the global atmosphere, *Ann. Rev. Phys. Chem.*, *35*, 481-505, 1984.

Johnston, H. S., and J. Podolske, Interpretations of stratospheric photochemistry, *Rev. Geophys. Space Phys.*, *16*, 491-519, 1978.

Johnston, H. S., D. Kattenhorn, and G. Whitten, Use of excess carbon 14 data to calibrate models of stratospheric ozone depletion by supersonic transports, *J. Geophys. Res.*, *78*, 368-380, 1976.

Johnston, H. S., M. Paige, and F. Yao, Oxygen absorption cross sections in the Herzberg continuum and between 206 and 326 K, *J. Geophys. Res.*, *89*, 11661-11665, 1984.

Johnston, H. S., C. A. Cantrell, and J. G. Calvert, Unimolecular decomposition of NO_3 to NO and O_2, *J. Geophys. Res.*, in press, 1985.

Jones, B. M. R., J. P. Burrows, R. A. Cox, and S. A. Penkett, OCS formation in the reaction of OH with CS_2, *Chem. Phys. Lett.*, *88*, 372-376, 1982.

Jones, B. M. R., R. A. Cox, and S. A. Penkett, Atmospheric chemistry of carbon disulfide, *J. Atmos. Chem.*, *1*, 65-86, 1983.

Jones, R. L., Satellite measurements of atmospheric composition: Three years' observations of CH_4 and N_2O, *Adv. Space Res.*, *4*, 121-130, 1984.

Jones, R. L., and J. A. Pyle, Observations of CH_4 and N_2O by the Nimbus 7 SAMS: A comparison with in-situ data and two-dimensional numerical model calculations, *J. Geophys. Res.*, *89*, 5263-5279, 1984.

Jones, R. L., J. A. Pyle, J. E. Harries, A. M. Zavody, J. M. Russell III, and J. C. Gille, The water vapour budget of the stratosphere studied using LIMS and SAMS satellite data, *Quart. J. Roy. Meteorol. Soc.*, in press, 1985.

Joseph, J. H., The sensitivity of a numerical model of the global atmosphere to the presence of desert aerosols, Dept. of Geophysics and Planetary Sciences, Tel-Aviv Univ., Ramat Aviv, Israel, 6997, 1983.

JPL: See DeMore, et al. and NASA-JPL listings.

Junge, C., W. Seiler, and P. Warneck, The atmospheric ^{12}CO and ^{14}CO budget, *J. Geophys. Res.*, *76*, 2866-2879, 1971.

Junge, C. E., Global ozone budget and exchange between stratosphere and troposphere, *Tellus*, *14*, 363-377, 1962.

Junge, C. E., *Air chemistry and radioactivity*, 380 pp., Academic Press, New York, 1963.

Just, T., and J. Troe, Theory of two-channel unimolecular reactions. 1. General formulation, *J. Phys. Chem.*, *84*, 3068-3072, 1980.

Kagann, R. H., J. W. Elkins, and R. L. Sams, Absolute band strengths of halocarbons F-11 and F-12 in the 8 to 16μm region, *J. Geophys. Res.*, *88*, 1427-1432, 1983.

Kanzawa, H., The behavior of mean zonal wind and planetary-scale disturbances in the troposphere and stratosphere during the 1973 sudden warming, *J. Meteorol. Soc. Japan*, *58*, 329-356, 1980.

REFERENCES

Kanzawa, H., Eliassen-Palm flux diagnostics and the effect of the mean zonal wind on planetary wave propagation for an observed sudden stratospheric warming, *J. Meteorol. Soc. Japan*, *60*, 1063-1073, 1982.

Kanzawa, H., Four observed sudden warmings diagnosed by the Eliassen-Palm flux and refractive index, in *Dynamics of the Middle Atmosphere*, edited by J. R. Holton and T. Matsuno, pp. 307-331, Terrapub, Tokyo, 1984.

Karoly, D. J., and B. J. Hoskins, Three dimensional propagation of planetary waves, *J. Meteorol. Soc. Japan*, *60*, 109-123, 1982.

Katz, M., *Methods of Air Sampling and Analysis*, edited by M. Katz, pp. 549-555, American Public Health Assoc., Washington, DC, 1977.

Kawahira, K., A quasi-one-dimensional model of the ozone transport by planetary waves in the winter stratosphere, *J. Meteorol. Soc. Japan*, *60*, 831-849, 1982.

Keating, G. M., The response of ozone to solar activity variations. A review, *Solar Physics*, *74*, 321-347, 1981.

Keating, G. M., and D. F. Young, Interim reference ozone models for the middle atmosphere, in *Handbook for MAP*, *Vol. 16*, edited by K. Labitzke, J. J. Barnett, and B. Edwards, pp. 205-229, SCOSTEP Secretariat, Univ. of Illinois, Urbana, 1985.

Keating, G. M., G. P. Brasseur, J. Y. Nicholson III, and A. De Rudder, Detection of the response of ozone in the middle atmosphere to short-term solar ultraviolet variations, *Geophys. Res. Lett.*, *12*, 449-452, 1985.

Keeling, C. D., The Global Carbon Cycle: What we know and could know from atmospheric, biospheric, and oceanic observations, in *Proceedings of the CO_2 Research Conference: Carbon Dioxide, Science and Consensus*, *DOE CONF-820970*, pp. II.3-II.62, U.S. Dept. of Energy, Washington, DC, 1983.

Keeling, C. D., A. F. Carter, and W. G. Mook, Seasonal, latitudinal and secular variations in the abundance and isotopic ratios of atmospheric CO_2, *J. Geophys. Res.*, *89*, 4615-4628, 1984.

Keenan, T. D., and J. I. Templeton, A comparison of tropical cyclone, hurricane and typhoon mass and moisture structure, *Mon. Weather Rev.*, *111*, 320-327, 1983.

Keller, M., T. J. Goreau, S. C. Wofsy, W. A. Kaplan, and M. B. McElroy, Production of nitrous oxide and consumption of methane by forest soils, *Geophys. Res. Lett.*, *10*, 1156-1159, 1983.

Keller, M., W. A. Kaplan, and S. C. Wofsy, Emissions of N_2O, CH_4 and CO from tropical forest soils, in press, 1985.

Kelly, P. M., P. D. Jones, T. M. L. Wigley, R. S. Bradley, H. F. Diaz, and C. M. Goodess, The extended Northern Hemisphere surface air temperature record: 1851-1984, *Proceedings, AMS Conference on Climate Variations*, Boston, MA, 190 pp., 1984.

Kendall, D. J. W., and H. L. Buijs, Stratospheric NO_2 and upper limits of CH_3Cl and C_2H_6 from measurements at 3.4 μm, *Nature*, *303*, 221-222, 1983.

Kendall, D. J. W., and T. A. Clark, Balloon-borne far infrared atmospheric emission studies, *Infrared Phys.*, *18*, 803-813, 1978.

Kendall, D. J. W., and T. A. Clark, The pure rotational atmospheric lines of hydroxyl, *J. Quant. Spectrosc. Radiat. Transfer*, *21*, 511-526, 1979.

Kendall, D. J. W., and T. A. Clark, Detection of minor constituents of the stratosphere by far infrared emission spectroscopy, *Int. J. Infrared mm Waves*, *3*, 783-808, 1981.

Kennedy, P. J., and M. A. Shapiro, The energy budget in a clear air turbulence zone as observed by aircraft, *Mon. Weather Rev.*, *111*, 650-993, 1975.

Kennedy, P. J., and M. A. Shapiro, Further encounters with clear air turbulence in research aircraft, *J. Atmos. Sci.*, *37*, 986-993, 1980.

Kerr, J. B., and C. T. McElroy, Measurement of stratospheric nitrogen dioxide from the AES stratospheric balloon program, *Atmosphere*, *14*, 166-171, 1976.

Kerr, J. B., C. L. Mateer, C. T. McElroy, and D. I. Wardle, Intercomparison of the Dobson and grating ozone spectrophotometers, in *Proc. Joint Symp. on Atm. Ozone, Vol. 1*, pp. 109-120, Dresden, GDR, 1976.

Kerr, J. B., C. T. McElroy, and W. F. J. Evans, Mid-latitude summertime measurements of stratospheric NO_2, *Can. J. Phys.*, *60*, 196-200, 1982.

Keyser, L. F., High pressure flow kinetics. A study of the OH + HCl reaction from 2 to 100 torr, *J. Phys. Chem.*, *88*, 4759-4759, 1984.

Khalil, M. A. K., and R. A. Rasmussen, Increase of $CHClF_2$ in the earth's atmosphere, *Nature*, *292*, 823-824, 1981.

Khalil, M. A. K., and R. A. Rasmussen, Secular trends of methane, *Chemosphere*, *12*, 877-883, 1982.

Khalil, M. A. K., and R. A. Rasmussen, Gaseous tracers of Arctic haze, *Environ. Sci. and Tech.*, *17*, 157-164, 1983a.

Khalil, M. A. K., and R. A. Rasmussen, Increase and seasonal cycles of nitrous oxide in the Earth's atmosphere, *Tellus*, *35B*, 161-169, 1983b.

Khalil, M. A. K., and R. A. Rasmussen, Sources, sinks and seasonal cycles of atmospheric methane, *J. Geophys. Res.*, *88*, 5131-5144, 1983c.

Khalil, M. A. K., and R. A. Rasmussen, Termites and methane, *Nature*, *302*, 355, 1983d.

Khalil, M. A. K., and R. A. Rasmussen, The atmospheric lifetime of methylchloroform (CH_3CCl_3), *Tellus*, *36B*, 317-332, 1984a.

Khalil, M. A. K., and R. A. Rasmussen, Global increase of carbon monoxide, in *Transactions of the APCA Specialty Conference on Environmental Impacts of Natural Emissions*, edited by V. P. Aneja, 1984b.

Khalil, M. A. K., and R. A. Rasmussen, Carbon monoxide in the Earth's atmosphere: Increasing trend, *Science*, *224*, 54-56, 1984c.

Khalil, M. A. K., and R. A. Rasmussen, Causes of increasing atmospheric methane: Depletion of hydroxyl radicals and the rise of emissions, *Atmos. Environ.*, *19*, 397-407, 1985a.

Khalil, M. A. K., and R. A. Rasmussen, Global sources, lifetimes and mass balances of carbonyl sulfide (OCS) and carbon disulfide (CS_2) in the earth's atmosphere, *Atmos. Environ.*, *18*, 1805-1813, 1985b.

Khalil, M. A. K., and R. A. Rasmussen, The trend of bromodifluoromethane ($CBrClF_2$) and the concentration of other bromine containing gases at the South Pole, *Antarctic Journal of the U.S.*, in press, 1985c.

Khalil, M. A. K., and R. A. Rasmussen, Trichlorotrifluoroethane (F-113) trends at Pt. Barrow, Alaska, in *Geophysical Monitoring for Climate Change, No. 13, Summary Report 1984*, U.S. Department of Commerce, ERL/NOAA, Boulder, CO, in press, 1985d.

Khalil, M. A. K., and R. A. Rasmussen, Atmospheric carbon tetrafluoride (CF_4): Sources and trends, *Geophys. Res. Lett.*, *12*, 671-672, 1985e.

Khalil, M. A. K., and R. A. Rasmussen, Interannual variability of atmospheric methane, *Science*, in press, 1985f.

Khalil, M. A. K., R. A. Rasmussen, and S. D. Hoyt, Atmospheric chloroform ($CHCl_3$): Ocean-air exchange and global mass balance, *Tellus*, *35B*, 266-274, 1983.

Kiang, C. S., D. Stauffer, V. J. Mohnen, J. Bricard, and D. Vigla, Heteromolecular nucleation theory applied to gas-to-particle conversion, *Atmos. Environ.*, *7*, 1279-1283, 1973.

Kida, H., A numerical investigation of the atmospheric general circulation and stratospheric-tropospheric mass exchange. I. Long-term integration of a simplified general circulation model. II. Lagrangian motion of the atmosphere, *J. Meteorol. Soc. Japan*, *55*, 52-88, 1977.

Kida, H., General circulation of air parcels and transport characteristics from a hemispheric GCM, Part 1. A determination of advective mass flow in the lower stratosphere, *J. Meteorol. Soc. Japan*, *61*, 171-188, 1983a.

REFERENCES

Kida, H., General circulation of air parcels and transport characteristics derived from a hemispheric GCM. Part 2. Very long-term motions of air parcels in the troposphere and stratosphere, *J. Meteorol. Soc. Japan*, *61*, 510-523, 1983b.

Kida, H., A numerical experiment on the general circulation of the middle atmosphere with a three-dimensional model explicitly representing internal gravity waves and their breaking, *Pure Appl. Geophys.*, *122*, 731-746, 1985.

Kiehl, J. T., The effect of aerosols on radiative damping rates in the stratosphere, paper presented at *Proceedings of the International Radiation Symposium*, Perugia, Italy, Aug. 21-26, 1984.

Kiehl, J. T., The results cited under this citation refer to calculations performed by J. T. Kiehl employing the narrow band model described in Ramaswamy, V. and J. T. Kiehl, Sensitivities of the radiative forcing due to large loadings of smoke and dust aerosols, *J. Geophys. Res.*, *90*, 5597-5613, 1985.

Kiehl, J. T., and V. Ramanathan, CO_2 radiative parameterization used in climate models: Comparison with narrow band models and with laboratory data, *J. Geophys. Res.*, *88*, 5191-5202, 1983.

Kiehl, J. T., and S. Solomon, On the radiative balance of the stratosphere, *J. Atmos. Sci.*, *43*, in press, 1986.

Kircher, C., and S. P. Sander, Kinetics and mechanism of HO_2 and DO_2 disproportionations, *J. Phys. Chem.*, *88*, 2082-2091, 1984.

Kleinschmidt, E., Dynamic meteorology, in *Handbuch der Physik*, edited by A. Eliassen and E. Kleinschmidt, pp. 1-154, 1957.

Kley, D., $Ly(\alpha)$ absorption cross section of H_2O and O_2, *J. Atmos. Chem.*, *2*, 203-210, 1984.

Kley, D., and E. J. Stone, A measurement of water vapor in the stratosphere by photodissociation with Ly (α) (1216Å) light, *Rev. Sci. Instrum.*, *49*, 691-697, 1978.

Kley, D., E. J. Stone, W. R. Henderson, J. W. Drummond, W. Harrop, A. L. Schmeltekopf, and T. L. Thompson, In situ measurements of the mixing ratio of water vapor in the stratosphere, *J. Atmos. Sci.*, *36*, 2513-2534, 1979.

Kley, D., J. W. Drummond, and A. L. Schmeltekopf, On the structure and microstructure of stratospheric water vapor, in *Atmospheric Water Vapor* edited by A. Deepak, T. D. Wilkinson, and L. H. Ruhke. pp. 315-327, Academic Press, New York, 1980.

Kley, D., J. W. Drummond, M. McFarland, and S. C. Liu, Tropospheric profiles of NO_x, *J. Geophys. Res.*, *86*, 3153-3161, 1981.

Kley, D., A. L. Schmeltekopf, K. Kelley, R. H. Winkler, T. L. Thompson, and M. McFarland, Transport of water vapor through the tropical tropopause, *Geophys. Res. Lett.*, *9*, 617-620, 1982.

Kley, D., A. L. Schmeltekopf, K. Kelly, R. H. Winkler, T. L. Thompson, and M. McFarland, The U2 Lyman-alpha hygrometer results from the 1980 Panama experiment, in *The 1980 Stratospheric-Tropospheric Exchange Experiment, NASA Tech Memo 84297*, edited by A. Margozzi, NASA Ames Research Center, Moffett Field, CA, 425 pp., 1983.

Knapska, D., U. Schmidt, C. Jebsen, G. Kulessa, J. Rudolph and S. A. Penkett, Vertical profiles of chlorinated source gases in the mid-latitude stratosphere, in *Atmospheric Ozone*, edited by C. S. Zerefos and A. Ghazi, pp. 117-121, D. Reidel, Dordrecht, 1985a.

Knapska, D., U. Schmidt, C. Jebsen, F. J. Johnen, A. Khedim, and G. Kulessa, A laboratory test of cryogenic sampling of long lived trace gases under simulated stratospheric conditions, in *Atmospheric Ozone*, edited by C. S. Zerefos and A. Ghazi, pp. 122-128, D. Reidel, Dordrecht, 1985b.

Knight, W., D. R. Hastie, and B. A. Ridley, Measurements of nitric oxide during a stratospheric warming, *Geophys. Res. Lett.*, *9*, 489-492, 1982.

Knittel, J., Ein Beitrag zur Klimatologi der Stratosphaere der Suedhalbkugel, *Meteor. Abh. der F.U.*, Berlin, A2, Nr.1, 1976.

Knollenberg, R. G., A. J. Dasher, and D. Huffman, Measurements of the aerosol and ice crystal population in tropical stratospheric cumulonimbus anvils, *Geophys. Res. Lett.*, *9*, 613-616, 1982.

Knop, G., and F. Arnold, Nitric acid vapor measurements in the troposphere and lower stratosphere by chemical ionization mass spectrometry, *Geophys. Res. Lett.*, in press, 1985.

Ko, M. K. W., and N. D. Sze, A 2-D model calculation of atmospheric lifetimes for N_2O, CFC-11 and CFC-12, *Nature*, *297*, 317-319, 1982.

Ko, M. K. W., and N. D. Sze, Effect of recent data revisions on stratospheric modeling, *Geophys. Res. Lett.*, *10*, 341-344, 1983.

Ko, M. K. W., and N. D. Sze, Diurnal variation of ClO: Implications for the stratospheric chemistries of $ClONO_2$, HOCl, and HCl, *J. Geophys. Res.*, *89*, 11619-11632, 1984.

Ko, M. K. W., N. D. Sze, M. Livshits, M. B. McElroy, and J. A. Pyle, The seasonal and latitudinal behavior of trace gases and O_3 as simulated by a two-dimensional model of the atmosphere, *J. Atmos. Sci.*, *41*, 2381-2408, 1984.

Ko, M. K. W., K. K. Tung, D. K. Weinstein, and N. D. Sze, A zonal-mean model of stratospheric tracer transport in isentropic coordinates: Numerical simulations for nitrous oxide and nitric acid, *J. Geophys. Res.*, *90*, 2313-2329, 1985.

Kobayashi, J., and Y. Toyama, On various methods of measuring the vertical distribution of atmospheric ozone 2, *Papers in Meteor. and Geoph.*, *17*, 97-112, 1966.

Kobayashi, J., M. Kyozuka, and H. Muamatsu, On various methods of measuring the vertical distribution of atmospheric ozone 1, *Papers in Meteor. and Geoph.*, *17*, 76-96, 1966.

Kohno, J., Stratospheric ozone transport due to transient large-amplitude planetary waves, *J. Meteorol. Soc. Japan*, *62*, 413-439, 1984.

Kohri, W. J., LRIR observations of the structure and propagation of the stationary planetary waves in the Northern Hemisphere during December 1975, Ph.D. thesis, *Cooperative Thesis No. 63*, Drexel Univ. and National Center for Atmospheric Research, Boulder, CO, 1981.

Komhyr, W. D., A carbon-iodine sensor for atmospheric soundings, paper presented at *Proc. Ozone Symp.*, Albuquerque, NM, pp. 26-30, 1965.

Komhyr, W. D., Electrochemical concentration cells for gas analysis, *Ann. Geoph.*, *25*, 203-210, 1969.

Komhyr, W. D., R. H. Gammon, J. Harriss, L. W. Waterman, T. J. Conway, W. R. Taylor, and K. W. Thoning, Global atmospheric CO_2 distribution and variation from 1968-1982 NOAA/GMCC flask sample data, *J. Geophys. Res.*, *90*, 5567-5596, 1985.

Kondo, Y., W. A. Matthews, A. Iwata, and M. Takagi, Measurements of nitric oxide from 7 to 32 km and its diurnal variation in the stratosphere, *J. Geophys. Res.*, *90*, 3813-3820, 1985.

Koyama, T., Gaseous metabolism in lake sediments and paddy soils and the production of atmospheric methane and hydrogen, *J. Geophys. Res.*, *68*, 3971-3973, 1963.

Koyama, T., Biogeochemical studies on lake sediments and paddy soils and the production of atmospheric methane and hydrogen, in *Recent Researches in the Fields of Hydrosphere, Atmosphere and Nuclear Geochemistry*, edited by Y. Miyake and T. Koyama, Water Research Laboratory, Nagoya University, Nagoya, Japan, 1964.

Krey, P. W., R. J. Lagomarsino, and L. E. Toonkel, Gaseous halogens in the atmosphere in 1975, *J. Geophys. Res.*, *82*, 1753-1766, 1977.

Krishnamurti, T. N., The subtropical jet stream of winter, *J. Meteorol.*, *18*, 172-191, 1961.

Krueger, A. J., Rocket measurements of ozone over Hawaii, *Ann. Geoph.*, *25*, 307-311, 1969.

Krueger, A. J., and R. A. Minzner, A mid-latitude ozone model for the 1976 U.S. standard atmosphere, *J. Geophys. Res.*, *81*, 4477-4481, 1976.

Krueger, A. J., B. Guenther, A. J. Fleig, D. F. Heath, E. Hilsenrath, R. McPeters, and C. Prabakhara, Satellite ozone measurements, *Phil. Trans. Roy. Soc. London*, *A296*, 191-204, 1980a.

Krueger, A. J., A. J. Fleig, J. A. Gatlin, D. F. Heath, P. K. Bhartia, V. G. Kaveeshwar, K. F. Klenk, and P. M. Smith, First results from the Nimbus 7 total ozone mapping spectrometer, in *Proceedings*

REFERENCES

Quadrennial International Ozone Symposium, Vol. I, edited by J. London, pp. 322-327, IAMAP, NCAR, Boulder, CO, 1981.

Krumins, M. V., and W. C. Lyons, Corrections for the upper atmosphere temperatures using a thin-film loop mount, *Tech. Rep. NOLTR 72-152*, 46 pp., U.S. Nav. Ordnance Lab., White Oak, MD, 1972.

Kuhn, W. R., and J. London, Infrared radiative cooling in the middle atmosphere (30-110 km), *J. Atmos. Sci.*, *26*, 189-204, 1969.

Kulcke, W., and H. K. Paetzold, Uber eine radiosonde zur bestimmung der vertikalen ozonverteilung, *Ann. Meteorol.*, *8*, 47-53, 1957.

Kunde, V., B. Conrath, R. Hanel, J. Herman, D. Jennings, W. Maguire, J. Brasunas, H. Buijs, J. Berike, and J. McKinnon, Measurement of lower stratosphere gaseous constituents with a balloon-borne cryogenic spectrometer, *J. Geophys. Res.*, in press, 1985.

Kurzeja, R. J., The transport of trace chemicals by planetary waves in the stratosphere. Part 1: Steady waves, *J. Atmos. Sci.*, *38*, 2779-2788, 1981.

Kurzeja, R. J., K. V. Haggard, and W. L. Grose, Numerical experiments with a general circulation model concerning the distribution of ozone in the stratosphere, *J. Atmos. Sci.*, *41*, 2029-2051, 1984.

Kutepov, A. A., and G. M. Shved, Radiative transfer in the 15 μm CO_2 band with non-LTE in the Earth's atmosphere, *Izves. Atmos. and Ocean. Phys.*, *14*, 28-43, 1978.

Labitzke, K., The interaction between stratosphere and mesosphere in winter, *J. Atmos. Sci.*, *29*, 1395-1399, 1972.

Labitzke, K., The temperature in the upper stratosphere: Differences between hemispheres, *J. Geophys. Res.*, *79*, 2171-2175, 1974.

Labitzke, K., Comparison of the stratospheric temperature distribution over Northern and Southern Hemispheres, *COSPAR Space Research*, *XVII*, 159-165, 1977.

Labitzke, K., The major stratospheric warming during January/February 1979, *Beilage zur Berliner Wetterkarte*, *8.5*, 1979.

Labitzke, K., Stratospheric-mesospheric midwinter disturbances: A summary of observed characteristics, *J. Geophys. Res.*, *86*, 9665-9678, 1981.

Labitzke, K., On the interannual variability of the middle stratosphere during the northern winters, *J. Meteorol. Soc. Japan*, *60*, 124-139, 1982.

Labitzke, K., A survey over the PMP-1 winters 1978/79-1981/82 in comparison with earlier winters, *Adv. Space Res.*, *2*, 149-157, 1983.

Labitzke, K., On the interannual variability of the middle atmosphere during winter, in *Handbook for MAP, Vol. 18*, edited by S. Kato, pp. 1-9, SCOSTEP Secretariat, Univ. of Illinois, Urbana, 1985.

Labitzke, K., and J. J. Barnett, Review of climatological information obtained from remote sensing of the stratosphere and mesosphere, *Space Res.*, *19*, 97-106, 1979.

Labitzke, K., and B. Naujokat, On the variability and on trends of temperature in the middle stratosphere, *Beitr. Phys. Atmosph.*, *56*, 495-507, 1983.

Labitzke, K., and B. Naujokat, An update of the observed QBO of the stratospheric temperatures over the Northern Hemisphere, *Geophys. Res. Lett.*, in press, 1986.

Labitzke, K., R. Lenschow, B. Naujokat, and K. Petzoldt, The second winter of PMP-1: 1979/80, *Beilage zur Berliner Wetterkarte*, *2.4*, 1980.

Labitzke, K., R. Lenschow, and B. Naujokat, The third winter of PMP-1: 1980/81, *Beilage zur Berliner Wetterkarte*, *16.7*, 1981.

Labitzke, K., B. Naujokat, and M. P. McCormick, Temperature effects on the stratosphere of the April 4, 1982 eruption of El Chichon, Mexico, *Geophys. Res. Lett.*, *10*, 24-26, 1983.

Labitzke, K., J. J. Barnett and B. Edwards (Eds.), *Draft of a New Reference Middle Atmosphere, Handbook for MAP, Vol. 16*, 318 pp., SCOSTEP Secretariat, Univ. of Illinois, Urbana, 1985.

Labitzke, K., G. Brasseur, B. Naujokat, and A. de Rudder, Long-term temperature trends in the stratosphere: Possible influence of antropogenic gases, *Geophys. Res. Lett.*, *13*, 1152-1155, 1986.

Lacis, A., Chlorofluorocarbons and stratospheric ozone, in *Global Environmental Problems*, edited by S. F. Singer, Paragon House, New York, in press, 1985.

Lacis, A. A., and J. E. Hansen, A parameterization for the absorption of solar radiation in the Earth's atmosphere, *J. Atmos. Sci.*, *31*, 118-133, 1974.

Lacis, A., J. Hansen, P. Lee, T. Mitchell, and S. Lebedeth, Greenhouse effect of trace gases, *Geophys. Res. Lett.*, *8*, 1035-1038, 1981.

Lacome, N., A. Levy, and C. Boulet, Air broadened line width of nitrous oxide: An improved calculation, *J. Mol. Spectrosc.*, *97*, 139-153, 1983.

Lal, S., R. Borchers, P. Fabian, and B. C. Krueger, Increasing abundance of $CBrClF_2$ in the atmosphere, *Nature*, *316*, 135-136, 1985.

Lau, K-M, and P. H. Chan, Short term climate variability and atmospheric teleconnections from satellite-observed outgoing longwave radiation. Part I: Simultaneous relationships, *J. Atmos. Sci.*, *40*, 2735-2750, 1983.

Laurent, J., M. P. Lemaitre, C. Lippens, and C. Muller, *L'Aeronautique et l'Astronautique*, *98*, 60-61, 1983.

Laurent, J., M. P. Lemaitre, J. Besson, A. Girard, C. Lippens, C. Muller, J. Vercheval, and M. Ackerman, Middle atmosphere NO and NO_2 observed by means of the Spacelab 1 grille spectrometer, *Nature*, in press, 1985.

Lazrus, A. L., and B. W. Gandrud, Distribution of stratospheric nitric acid vapor, *J. Atmos. Sci.*, *31*, 1102-1108, 1974.

Lazrus, A. L., B. W. Gandrud, R. N. Woodard, and W. A. Sedlacek, Direct measurements of stratospheric chlorine and bromine, *J. Geophys. Res.*, *81*, 1067-1090, 1976.

Lean, J. L., Estimating the variability of the solar flux between 200 and 300 nm, *J. Geophys. Res.*, *89*, 1-9, 1984.

Lean, J. L., and A. Skumanich, Variability of the Lyman alpha flux with solar activity, *J. Geophys. Res.*, *88*, 5751-5759, 1983.

Lean, J. L., O. R. White, W. C. Livingston, D. F. Heath, R. F. Donnelly, and A. Skumanich, A three component model of the variability of the solar ultraviolet flux: 145-200 nm, *J. Geophys. Res.*, *87*, 10307-10317, 1982.

Leifer, R., R. Larsen, and L. Toonkel, Stratospheric distributions and inventories of trace gases in the Northern Hemisphere for 1976, *Report EML-349, I-211*, Environmental Measurements Lab., New York, 1979a.

Leifer, R., L. Toonkel, and R. Larsen, Project airstream, trace gases in the stratosphere, *Report EML-349, II-107*, Environmental Measurements Lab., New York, 1979b.

Leifer, R., K. C. Sommers, and S. F. Guggenheim, Atmospheric trace gas measurements with a new clean air sampling system, *Geophys. Res. Lett.*, *8*, 1079-1081, 1981.

Leighton, H., Influence of Arctic haze on the solar radiation budget, *Atmos. Environ.*, *17*, 2065-2068, 1983.

Leighton, P. A., *Photochemistry of Air Pollution*, Academic Press, New York, 1961.

Lemaitre, M. P., J. Laurent, J. Besson, A. Girard, C. Lippens, C. Muller, J. Vercheval, and M. Ackerman, Sample performance of the grille spectrometer, *Science*, *225*, 171-172, 1984.

Lenoble, J., A general survey of the problem of aerosol climatic impact, in *Aerosols and Their Climatic Effects*, edited by H. E. Gerber and A. Deepak, pp. 279-294, A. Deepak Publ., Hampton, VA, 1984.

Lenoble, J., D. Tanre, P. Y. Deschamps, and M. Hessman, A simple method to compute the change in earth-atmosphere radiative balance due to a stratospheric aerosol layer, *J. Atmos. Sci.*, *39*, 2565-2576, 1982.

REFERENCES

Lenschow, D. H., R. Pearson, Jr., and B. B. Stankov, Measurements of ozone vertical flux to ocean and forest, *J. Geophys. Res.*, *87*, 8833-8837, 1982.

Leone, J. A., and J. H. Seinfeld, Analysis of the characteristics of complex chemical reaction mechanisms: Application to photochemical smog chemistry, *Environ. Sci. Technol.*, *18*, 280-287, 1984a.

Leone, J. A., and J. H. Seinfeld, Updated chemical mechanism for atmospheric photooxidation of toluene, *Int. J. Chem. Kinet.*, *16*, 159-193, 1984b.

Leovy, C. B., Simple models of thermally driven mesospheric circulations, *J. Atmos. Sci.*, *21*, 327-341, 1964a.

Leovy, C. B., Radiative equilibrium of the mesosphere, *J. Atmos. Sci.*, *21*, 238-248, 1964b.

Leovy, C. B., and P. J. Webster, Stratospheric long waves: Comparison of thermal structure in the northern and southern hemispheres, *J. Atmos. Sci.*, *33*, 1624-1638, 1976.

Leovy, C. B., C. R. Sun, M. H. Hitchman, E. E. Remsberg, J. M. Russell III, L. L. Gordley, J. C. Gille, and L. V. Lyjak, Transport of ozone in the middle stratosphere: Evidence for planetary wave breaking, *J. Atmos. Sci.*, *42*, 230-244, 1985.

Lesclaux, R., and F. Caralp, Determination of the rate constants for the reactions of $CFCl_2O_2$ radical with NO and NO_2 by laser photolysis and time resolved mass spectrometry, *Int. J. Chem. Kinet.*, *16*, 1117-1128, 1984.

Leu, M. T., Kinetics of the reaction $O + ClO \rightarrow Cl + O_2$, *J. Phys. Chem.*, *88*, 1394-1398, 1984.

Levine, J. S., C. P. Rinsland, and G. M. Tennille, The photochemistry of methane and carbon monoxide in the troposphere in 1950 and 1985, *Nature*, *318*, 254-257, 1985.

Levine, S. Z., and S. E. Schwartz, In-cloud and below-cloud scavenging of nitric acid vapor, *Atmos. Environ.*, *16*, 1725-1734, 1982.

Levy II, H., Normal atmosphere: Large radical and formaldehyde concentrations predicted, *Science*, *173*, 141-143, 1971.

Levy II, H., Photochemistry of the lower troposphere, *Planet. Space Sci.*, *20*, 919-935, 1972.

Levy II, H., J. D. Mahlman, and W. J. Moxim, A preliminary report on the numerical simulation of the three-dimensional structure and variability of atmospheric N_2O, *Geophys. Res. Lett.*, *6*, 155-158, 1979.

Levy II, H., J. D. Mahlman, and W. J. Moxim, A stratospheric source of reactive nitrogen in the unpolluted troposphere, *Geophys. Res. Lett.*, *7*, 441-444, 1980.

Levy II, H. B., J. D. Mahlman, W. J. Moxim, and S. C. Liu, Tropospheric ozone: The role of transport, *J. Geophys. Res.*, *90*, 3753-3771, 1985.

Lewis, B. R., I. M. Vardavas, and J. H. Carver, The aeronomic dissociation of water vapor by H Lyman alpha radiation, *J. Geophys. Res.*, *88*, 4935-4940, 1983.

Lilly, D. K., D. E. Waco, and S. I. Adelfang, Stratospheric mixing estimated from high-altitude turbulence measurements, *J. Appl. Meteorol.*, *13*, 488-493, 1974.

Lin, B. D., The behavior of winter stationary planetary waves forced by topography and diabatic heating, *J. Atmos. Sci.*, *39*, 1206-1226, 1982.

Lindzen, R. S., Some speculations on the roles of critical level interactions between internal gravity waves and mean flows, in *Acoustic-Gravity Waves in the Atmosphere-Symposium Proceedings*, edited by T. M. Georges, Environmental Science Services Administration, Boulder, CO, 427 pp., 1968.

Lindzen, R. S., Turbulence and stress owing to gravity and tidal breakdown, *J. Geophys. Res.*, *86*, 9707-9714, 1981.

Lindzen, R. S., and J. R. Holton, A theory of the quasi-biennial oscillation, *J. Atmos. Sci.*, *25*, 1095-1107, 1968.

Lindzen, R. S., and C. Y. Tsay, Wave structure of the tropical stratosphere over the Marshall Islands area during 1 April-1 July 1958, *J. Atmos. Sci.*, *22*, 2008-2021, 1975.

Lindzen, R. S., D. M. Straus, and B. Katz, An observational study of large-scale atmospheric Rossby waves during FGGE, *J. Atmos. Sci.*, *41*, 1320-1335, 1984.

Ling, X., and J. London, A theoretical study of the quasi-biennial oscillation in the tropical stratosphere, in *Atmospheric Ozone*, edited by C. S. Zerefos and A. Ghazi, pp. 53-58, D. Reidel, Dordrecht, 1985.

Lippens, C., and C. Muller, Atmospheric nitric acid and chlorofluoromethane 11 from interferometric spectra obtained at the Observatoires du Pic du Midi, *J. Optics (Paris)*, *12*, 331-336, 1981.

Lippens, C., C. Muller, J. Vercheval, M. Ackerman, J. Laurent, M. P. Lemaitre, J. Besson, and A. Girard, Trace constituents measurements deduced from spectrometric observations onboard Spacelab, *Adv. Space Res.*, *4*, 75-79, 1984.

Lipschultz, F., O. C. Zafiriou, S. C. Wofsy, M. B. McElroy, F. W. Valois, and S. W. Watson, Production of NO and N_2O by soil nitrifying bacteria: A source of atmospheric nitrogen oxides, *Nature*, *294*, 641-643, 1981.

Liu, S. C., and G. C. Reid, Sodium and other minor constituents of meteoric origin in the atmosphere, *Geophys. Res. Lett.*, *6*, 283-286, 1979.

Liu, S. C., T. M. Donahue, R. J. Cicerone, and W. L. Chameides, Effect of water vapor on the destruction of ozone in the stratosphere perturbed by Cl_x or NO_x pollutants, *J. Geophys. Res.*, *81*, 3111-3118, 1976.

Liu, S. C., D. Kley, M. McFarland, J. D. Mahlman, and H. Levy II, On the origin of tropospheric ozone, *J. Geophys. Res.*, *85*, 7546-7552, 1980.

Liu, S. C., M. McFarland, D. Kley, O. Zafiriou, and B. J. Huebert, Tropospheric NO_x and O_3 budgets in the equatorial Pacific, *J. Geophys. Res.*, *88*, 1360-1368, 1983.

Loewenstein, M., W. J. Starr, and D. G. Murcray, Stratospheric NO and HNO_3 observations in the Northern Hemisphere for three seasons, *Geophys. Res. Lett.*, *5*, 531-534, 1978a.

Loewenstein, M., W. J. Borucki, H. F. Savage, J. G. Borucki, and R. C. Whitten, Geographical variations of NO and O_3 in the lower stratosphere, *J. Geophys. Res.*, *83*, 1874-1882, 1978b.

Logan, J. A., Nitrogen oxides in the troposphere: Global and regional budgets, *J. Geophys. Res.*, *88*, 10785-10807, 1983.

Logan, J. A., Tropospheric ozone: Seasonal behavior, trends and anthropogenic influence, *J. Geophys. Res.*, *90*, 10463-10482, 1985.

Logan, J. A., M. J. Prather, S. C. Wofsy, and M. B. McElroy, Atmospheric chemistry: Response to human influence, *Phil. Trans. Roy. Soc. London*, *A290*, 187-234, 1978.

Logan, J. A., M. J. Prather, S. C. Wofsy, and M. B. McElroy, Tropospheric chemistry: A global perspective, *J. Geophys. Res.*, *86*, 7210-7254, 1981.

London, J., Radiative energy sources and sinks in the stratosphere and mesosphere, in *Proceedings of the NATO Advanced Study Institute on Atmospheric Ozone: Its Variation and Human Influences*, *Rep. FAA-EE-80-20*, edited by A. C. Aikin, pp. 703-721, DOT, FAA, Washington, DC, 1980a.

London, J., The observed distribution and variations of total ozone, in *Proceedings of the NATO Advanced Study Institute on Atmospheric Ozone: Its Variation and Human Influences*, *Report FAA-EE-80-20*, edited by A. C. Aikin, pp. 31-44, DOT, FAA, Washington, DC, 1980b.

London, J., and J. Park, Application of general circulation models to the study of stratospheric ozone, *Pure Appl. Geophys.*, *106-108*, 1611-1617, 1973.

London, J., and J. Park, The interaction of ozone photochemistry and dynamics in the stratosphere: A three-dimensional stratospheric model, *Can. J. Chem.*, *62*, 1599-1609, 1974.

London, J., B. D. Bojkov, S. Oltmans, and J. F. Kelly, Atlas of the global distribution of total ozone, July 1957-July 1967, *Tech. Note NCAR/TN/113* + STR, Nat. Center for Atmos. Res., Boulder, CO, Jan., 1976.

REFERENCES

London, J., J. E. Frederick, and G. P. Anderson, Satellite observations of the global distribution of stratospheric ozone, *J. Geophys. Res.*, *82*, 2543-2556, 1977.

London, J., G. G. Bjarnason, and G. J. Rottman, 18 months of UV irradiance observations from the Solar Mesosphere Explorer, *Geophys. Res. Lett.*, *11*, 54-56, 1984.

Lorenc, A. C., The evolution of the planetary scale 200 mb divergent flow during the FGGE year, *Quart. J. Roy. Meteorol. Soc.*, *110*, 427-441, 1984.

Lorenz, E. N., The nature and theory of the general circulation of the atmosphere, *WMO No 218, WMO*, 1967.

Louis, J. F., A two-dimensional transport model of the atmosphere, Ph.D. thesis, Univ. of Colorado, Boulder, CO, 1974.

Louisnard, N., and O. Lado-Bordowsky, Spectroscopic measurements of carbon monoxide in the stratosphere, *J. Geophys. Res.*, *88*, 3781-3797, 1983.

Louisnard, N., and S. Pollitt, Measurements of neutral constituents using infrared and visible remote sensing, in *Handbook for MAP, Vol. 15*, edited by D. G. Murcray, pp. 37-70, SCOSTEP Secretariat, Univ. of Illinois, Urbana, 1985.

Louisnard, N., A. Girard, and G. Eichen, Mesures du profil vertical de concentration de la vapeur d'eau stratospherique, *C. R. Acad. Sc. Paris*, *290*, 385-388, 1980.

Louisnard, N., G. Fergant, A. Girard, L. Gramont, O. Lado-Bordowsky, J. Laurent, S. Le Boiteau, and M. P. Lemaitre, Infrared absorption spectroscopy applied to stratospheric profiles of minor constituents, *J. Geophys. Res.*, *88*, 5365-5376, 1983.

Lovelock, J. E., Atmospheric halocarbons and stratospheric ozone, *Nature*, *252*, 292-294, 1974.

Lovelock, J. E., Methyl chloroform in the troposphere as an indicator of OH radical abundance, *Nature*, *267*, 32, 1977.

Ludlam, F. H., *Clouds and Storms, Chapter 8*, Pennsylvania State University Press, University Park, PA, 1980.

Luther, F., Commentary on climatic effects of minor atmospheric constituents, in *Carbon Dioxide Review*, edited by W. C. Clark, pp. 290-294, Clarendon Press, New York, 1982.

Luther, F. M., and Y. Fouquart, *WMO Report WCP-93*, 37 pp., Geneva, 1984.

Luther, F., D. J. Wuebbles, and J. S. Chang, Temperature feedback in a stratospheric model, *J. Geophys. Res.*, *82*, 4935-4942, 1977.

Madden, R. A., Oscillations in the winter stratosphere. 2: The role of horizontal heat transport and the interaction of transient and stationary planetary-scale waves, *Mon. Weather Rev.*, *103*, 717-719, 1975.

Madden, R. A., Evidence for large-scale regularly propagating waves in a 73-year data set, in *Extended Summaries of Contributions*, IAGA/IAMAP, Seattle, Washington, International Assoc. for Atmos. Phys., NCAR, Boulder, CO, 1977.

Madden, R. A., Further evidence of traveling planetary waves, *J. Atmos. Sci.*, *35*, 1605-1618, 1978.

Madden, R. A., The effect of the interference of traveling and stationary waves on time variations of the large-scale circulation, *J. Atmos. Sci.*, *40*, 1110-1125, 1983.

Madden, R. A., and P. R. Julian, Detection of a 40-50 day oscillation in the zonal wind in the tropical Pacific, *J. Atmos. Sci.*, *28*, 702-708, 1971.

Madden, R. A., and P. R. Julian, Descriptions of global scale circulation cells in the tropics with a 40-50 period, *J. Atmos. Sci.*, *29*, 1109-1123, 1972a.

Madden, R. A., and P. Julian, Further evidence of global-scale 5-day pressure waves, *J. Atmos. Sci.*, *29*, 1464-1469, 1972b.

Madden, R. A., and P. Julian, Reply to comments by R. Deland, *J. Atmos. Sci.*, *30*, 935-940, 1973.

Madden, R. A., and K. Labitzke, A free Rossby wave in the troposphere and stratosphere during January 1979, *J. Geophys. Res.*, *86*, 1247-1254, 1981.

Madronich, S., D. R. Hastie, B. A. Ridley, and H. I. Schiff, Measurement of the photodissociation coefficient of NO_2 in the atmosphere, I. Method and surface measurements, *J. Atmos. Chem.*, *1*, 3-25, 1983.

Mahlman, J. D., Relation of stratospheric-tropospheric mass exchange mechanisms to surface radioactivity peaks, *Arch. Met. Geoph. Biokl. A.*, *15*, 1-25, 1965.

Mahlman, J. D., Long-term dependence of surface fallout fluctuations upon tropopause-level cyclogenesis, *Arch. Met. Geoph. Biokl. A.*, *18*, 299-311, 1969a.

Mahlman, J. D., Heat balance and mean meridional circulations in the polar stratosphere during the sudden warming of January 1958, *Mon. Weather Rev.*, *97*, 534-540, 1969b.

Mahlman, J. D., On the maintenance of the polar front jet stream, *J. Atmos. Sci.*, *30*, 544-557, 1973.

Mahlman, J. D., Some fundamental limitations of simplified transport models as implied by results from a three-dimensional general circulation/tracer model, in *Proceedings Fourth Conference Climatic Impact Assessment Program, DOT-TSC-OST-75-38*, edited by T. M. Hard and A. J. Broderick, pp. 132-146, Transportation Systems Command, Cambridge, MA, 1975.

Mahlman, J. D., Coupling in atmospheric observations with comprehensive numerical models, *Proc. of ICMUA Sessions and IUGG Symposium 18*, XVII IUGG General Assembly, Canberra, Australia, *18*, pp. 253-259, 1980.

Mahlman, J. D., "Strategies for equatorial lower stratospheric measurements" and "The status of stratospheric general circulation models", papers presented at International Workshop on Current Issues in our Understanding of the Stratosphere and the Future of the Ozone Layer, BMFT, NASA, FAA, WMO, Feldafing, FRG, June 11-16, 1984.

Mahlman, J. D., Mechanistic interpretation of stratospheric tracer transport, *Issues in Atmos. and Oceanic Modelling*, J. Smagorinsky Comm. Vol., 1985.

Mahlman, J. D., and W. J. Moxim, Tracer simulation using global circulation model: results from a midlatitude instantaneous source experiment, *J. Atmos. Sci.*, *35*, 1340-1374, 1978.

Mahlman, J. D., and R. W. Sinclair, Recent results from the GFDL troposphere-stratosphere-mesosphere general circulation model, *Proc. of ICMUA Sessions and IUGG Symposium 18*, XVII IUGG General Assembly, Canberra, Australia, 11-18, 1980.

Mahlman, J. D., and L. J. Umscheid, Dynamics of the middle atmosphere: Successes and problems of the GFDL "SKYHI" general circulation model, in *Dynamics of the Middle Atmosphere*, edited by J. R. Holton and T. Matsuno, pp. 501-525, Terrapub, Tokyo, 1984.

Mahlman, J. D., H. B. Levy II, and W. J. Moxim, Three-dimensional tracer structure and behavior as simulated in two ozone precursor experiments, *J. Atmos. Sci.*, *37*, 655-685, 1980.

Mahlman, J. D., D. G. Andrews, H. U. Duetsch, D. L. Hartmann, T. Matsuno, R. J. Murgatroyd, and J. F. Noxon, Transport of trace constituents in the stratosphere, in *Handbook for MAP, Vol. 3*, edited by C. F. Sechrist, Jr., pp. 14-43, SCOSTEP Secretariat, Univ. of Illinois, Urbana, 1981.

Mahlman, J. D., D. G. Andrews, D. L. Hartmann, T. Matsuno, and R. G. Murgatroyd, Transport of trace constituents in the stratosphere, in *Dynamics of the Middle Atmosphere*, edited by J. R. Holton and T. Matsuno, pp. 387-416, Terrapub, Tokyo, 1984.

Mahlman, J. D., H. B. Levy II, and W. J. Moxim, Three dimensional simulations of stratospheric N_2O: Predictions for other trace constituents, *J. Geophys. Res.*, in press, 1985.

Maier, E. J., A. C. Aikin, and J. E. Ainsworth, Stratospheric nitric oxide and ozone measurements using photoionization mass spectrometry and UV absorption, *Geophys. Res. Lett.*, *5*, 37-40, 1978.

Maki, A. G., F. J. Lovas, and W. B. Olson, Infrared frequency measurements on the ClO fundamental band, *J. Mol. Spectros.*, *92*, 410-418, 1982.

Makide, Y., and F. S. Rowland, Tropospheric concentrations of methyl chloroform, CH_3CCl_3, in January 1978 and estimates of atmospheric residence times for hydrocarbons, *Proceedings Natl. Acad. Sci., USA*, 5933-5937, 1981.

REFERENCES

Malcolm, K. W., K. O. Nien, and D. A. K. Sze, A 2-D model calculation of atmospheric lifetimes for N_2O, CFC-11 and CFC-12, *Nature*, *297*, 317-319, 1982.

Malko, M. W., and J. Troe, Analysis of the unimolecular reaction $N_2O_5 + M \rightarrow NO_2 + NO_3 + M$, *Int. J. Chem. Kinet.*, *14*, 399-416, 1982.

Malkmus, W., Random Lorentz band model with exponential tailed S^{-1} line-intensity distribution, *J. Opt. Soc. Amer.*, *57*, 323-329, 1967.

Malkus, J. S., Large-scale interactions, in *The Sea, Vol. 1*, edited by M. N. Hill, Interscience Publishers, New York, 1962.

Manabe, S., and B. G. Hunt, Experiments with a stratospheric general circulation model: I. radiative and dynamic effects, *Mon. Weather Rev.*, *96*, 477-539, 1968.

Manabe, S., and J. D. Mahlman, Simulation of seasonal and interhemispheric variations in the stratospheric circulation, *J. Atmos. Sci.*, *33*, 2185-2217, 1976.

Manabe, S., and R. J. Stouffer, Sensitivity of a global climate model to an increase of CO_2 concentration in the atmosphere, *J. Geophys. Res.*, *85*, 5529-5554, 1980.

Manabe, S., and R. T. Wetherald, Thermal equilibrium of the atmosphere with a given distribution of relative humidity, *J. Atmos. Sci.*, *24*, 241-259, 1967.

Manabe, S., and R. T. Wetherald, The effects of doubling the CO_2 concentration on the climate of a general circulation model, *J. Atmos. Sci.*, *32*, 3-15, 1975.

Manabe, S., and R. T. Wetherald, On the distribution of climate change resulting from an increase in CO_2-content of the atmosphere, *J. Atmos. Sci.*, *37*, 99-118, 1980.

Mankin, W. G., and M. T. Coffey, Latitudinal distributions and temporal changes of stratospheric HCl and HF, *J. Geophys. Res.*, *88*, 10776-10784, 1983.

Mankin, W. G., and M. T. Coffey, Increased stratospheric hydrogen chloride in the El Chichon cloud, *Science*, *226*, 170-172, 1984.

Mankin, W. G., M. T. Coffey, D. W. T. Griffith, and S. R. Drayson, Spectroscopic measurement of carbonyl sulfide (OCS) in the stratosphere, *Geophys. Res. Lett.*, *6*, 853-856, 1979.

Mankin, W. G., M. T. Coffey, K. V. Chance, W. A. Traub, B. Carli, A. Bonetti, I. G. Nolt, R. Zander, D. W. Johnson, G. Stokes, and C. B. Farmer, Intercomparison of measurements of stratospheric hydrogen fluoride, to be published, 1986.

Manson, A. H., C. E. Meek, and J. G. Gregory, Winds and waves (10 min - 30 days) in the mesosphere and lower thermosphere at Saskatoon (32°N, 107°W, L=4.3) during the year October 1979 to July 1980, *J. Geophys. Res.*, *86*, 9615-9625, 1981.

Marche, P., and C. Meunier, Atmospheric trace species measured above Haute-Provence Observatory, *Planet. Space Sci.*, *31*, 731-733, 1983.

Marche, P., A. Barbe, C. Secroun, J. Corr, and P. Jouve, Ground based spectroscopic measurements of HCl, *Geophys. Res. Lett.*, *7*, 869-872, 1980a.

Marche, P., A. Barbe, C. Secroun, J. Corr, and P. Jouve, Mesures des acides fluorhydrique et chlorhydrique dans l'atmosphere par spectroscopie infrarouge a partir du sol, *C. R. Acad. Sc. Paris*, *290B*, 369-371, 1980b.

Marche, P., C. Meunier, A. Barbe, and P. Jouve, Total atmospheric ozone measured by ground based high resolution infrared spectra-comparison with Dobson measurements, *Planet. Space Sci.*, *31*, 723-727, 1983.

Margitan, J. J., Chlorine nitrate: The sole product of the $ClO + NO_2 + M$ recombination, *J. Geophys. Res.*, *88*, 5416-5420, 1983.

Margitan, J. J., Kinetics of the reaction $O + ClO \rightarrow Cl + O_2$, *J. Phys. Chem.*, *88*, 3638-3643, 1984a.

Margitan, J. J., Mechanisms of the atmospheric oxidation of sulfur dioxide catalysis by hydroxyl radicals, *J. Phys. Chem.*, *88*, 3314-3318, 1984b.

Maroulis, P. J., A. I. Torres, and A. R. Bandy, Atmospheric concentrations of carbonyl sulfide in the southwestern and eastern United States, *Geophys. Res. Lett.*, *4*, 510-512, 1977.

Martin, L. R., H. S. Judeikis, and M. Wu, Heterogeneous reactions of Cl and ClO in the stratosphere, *J. Geophys. Res.*, *85*, 5511-5518, 1980.

Maruyama, T., Long-term behavior of Kelvin waves and mixed Rossby-gravity waves, *J. Meteorol. Soc. Japan*, *47*, 245-254, 1969.

Mason, C. J., and J. J. Horvath, The direct measurement of nitric oxide concentration in the upper atmosphere by a rocket-borne chemiluminescent detector, *Geophys. Res. Lett.*, *3*, 391-394, 1976.

Massman, W. J., An investigation of gravity waves on a global scale using TWERLE data, *J. Geophys. Res.*, *86*, 4072-4082, 1981.

Mastenbrook, H. J., Water vapor distribution in the stratosphere and high troposphere, *J. Atmos. Sci.*, *25*, 299-311, 1968.

Mastenbrook, H. J., and S. J. Oltmans, Stratospheric water vapor variability for Washington, DC/Boulder, CO: 1964-82, *J. Atmos. Sci.*, *40*, 2157-2165, 1983.

Mateer, C. L., and I. A. Asbridge, On the appropriate haze correction for direct sun total ozone measurements with the Dobson spectrophotometer, in *Proceedings of the Quadrennial International Ozone Symposium*, *Vol. I*, edited by J. London, pp. 236-242, IAMAP, NCAR, Boulder, CO, 1981.

Mateer, C. L., and J. J. DeLuisi, The estimation of the vertical distribution of ozone by the short Umkehr method, in *Proceedings of the Quadrennial International Ozone Symposium*, *Vol. I*, edited by J. London, pp. 64-73, IAMAP, NCAR, Boulder, CO, 1981.

Mateer, C. L., and H. U. Duetsch, Uniform evaluation of Umkehr observations from the World Ozone Network: Part 1, Proposed standard Umkehr evaluation technique, Nat'l Center for Atmos. Res., Boulder, Colorado, 1964.

Mathews, E. I. Fung, and S. Ross, Atmospheric methane: Global distributions of biogenic source locations, in press, 1986.

Matson, M., Eruptions of El Chichon volcano, in *Radiative Effects of the El Chichon Volcanic Eruption: Preliminary Results Concerning Remote Sensing, NASA Tech. Memo. 84959*, edited by W. R. Bandeen and R. S. Fraser, 103 pp., NASA Goddard Space Flight Center, Greenbelt, MD, 1982.

Matsuno, T., Vertical propagation of stationary planetary waves in the winter Northern Hemisphere, *J. Atmos. Sci.*, *27*, 871-883, 1970.

Matsuno, T., A dynamical model of the stratospheric sudden warming, *J. Atmos. Sci.*, *28*, 1479-1494, 1971.

Matsuno, T., Lagrangian motion of air parcels in the stratosphere in the presence of planetary waves, *Pure Appl. Geophys.*, *118*, 189-216, 1980.

Matsuno, T., A quasi one-dimensional model of the middle atmosphere circulation interacting with internal gravity waves, *J. Meteorol. Soc. Japan*, *60*, 215-226, 1982.

Mattingly, S. R., The contribution of extratropical severe storms to the stratospheric water vapour budget, *Met. Mag.*, *106*, 256-262, 1977.

Mayer, E. W., D. R. Blake, S. C. Tyler, Y. Makide, D. C. Montague, and F. S. Rowland, Methane: Interhemispheric concentration gradient and atmospheric residence time, *Proc. Nat. Acad. Sci., USA*, *79*, 1366-1370, 1982.

McClatchey, R. S., R. W. Fenn, J. E. A. Selby, F. E. Volz, and J. S. Garing, Optical properties of the atmosphere, *AFCRC-71-0279*, 85 pp., Air Force Cambridge Res. Lab., Bedford, MA, 1971.

McClatchey, R. A., W. S. Benedict, S. A. Clough, D. E. Burch, R. F. Calfee, K. Fox, L. S. Rothman, and J. S. Garing, AFCRL atmospheric absorption line parameters compilation, *AFCRL-TR-73-0096*, 83 pp., Air Force Cambridge Research Laboratory Report, Hanscom AFB, MA, 1973.

McCormick, M. P., and T. J. Swissler, Stratospheric aerosol mass and latitudinal distribution of the El Chichon eruption cloud for October 1982, *Geophys. Res. Lett.*, *10*, 877-880, 1983.

REFERENCES

McCormick, M. P., P. Hamill, T. J. Pepin, W. P Chu, T. J. Swissler, and L. R. McMaster, Satellite studies of the stratospheric aerosol, *Bull. Amer. Meteor. Soc.*, *60*, 1038-1046, 1979.

McCormick, M. P., H. M. Steele, P. Hamill, W. P. Chu, and T. J. Swissler, Polar stratospheric cloud sightings by SAM II, *J. Atmos. Sci.*, *39*, 1387-1397, 1982.

McCormick, M. P., T. J. Swissler, E. Hilsenrath, A. J. Krueger, and M. T. Osborn, Satellite and correlative measurements of stratospheric ozone; Comparison of measurements made by SAGE, ECC balloons, chemiluminescent and optical rocketsondes, *J. Geophys. Res.*, *89*, 5315-5320, 1984.

McCormick, M. P., T. J. Swissler, W. H. Fuller, W. H. Hunt, M. T. Osborn, Airborne and ground-based lidar measurements of the El Chichon stratospheric aerosol from 90N to 56S, *Geof. Int.*, *23-2*, 187-221, 1984.

McElroy, M. B., Chemical processes in the solar system, in *Chemical Kinetics*, edited by D. R. Hersehbach, pp. 127-211, Int. Review of Science, Butterworths, London, 1976.

McElroy, M. B., and S. C. Wofsy, Tropical forests: Interactions with the atmosphere, in *Symposium volume on 'Tropical Forests and World Atmospheres'*, edited by G. T. Prance, in press, 1985.

McElroy, M., S. C. Wofsy, J. Penner and J. McConnell, Atmospheric ozone: Possible impact of stratospheric aviation, *J. Atmos. Sci.*, *31*, 287-303, 1974.

McElroy, M. B., S. C. Wofsy, and Y. L. Yung, The nitrogen cycle: Perturbations due to man and their impact on atmospheric N_2O and O_3, *Phil. Trans. Roy. Soc. London*, *A277*, 159-181, 1977.

McFarland, J., D. Kley, J. W. Drummond, A. L. Schmeltekopf, and R. H. Winkler, Nitric oxide measurements in the Equatorial Pacific region, *Geophys. Res. Lett.*, *6*, 605-608, 1979.

McFarland, M., B. A. Ridley, M. Profitt, and D. L. Albritton, Simultaneous in-situ measurements of stratospheric O_3, NO_2, and NO, in press, 1985.

McGregor, J., and W. A. Chapman, Stratospheric temperatures and geostrophic winds during 1973-1974, *Quart. J. Roy. Meteorol. Soc.*, *105*, 241-261, 1979.

McInturff, R. M. (Ed.), Stratospheric warmings: Synoptic, dynamic and general-circulation aspects, *NASA Ref. Publ. 1017*, 166 pp., NASA, Washington, DC, 1978.

McIntyre, M. E., Towards a Lagrangian-mean description of stratospheric circulations and chemical transports, *Phil. Trans. Roy. Soc. London*, *A296*, 129-148, 1980a.

McIntyre, M. E., An introduction to the generalized Lagrangian-mean description of wave, mean-flow interaction, *Pure Appl. Geophys.*, *118*, 152-176, 1980b.

McIntyre, M. E., How well do we understand the dynamics of stratospheric warmings?, *J. Meteorol. Soc. Japan*, *60*, 37-65, 1982.

McIntyre, M. E., and T. N. Palmer, Breaking planetary waves in the stratosphere, *Nature*, *305*, 593-600, 1983.

McIntyre, M. E., and T. N. Palmer, The 'surf zone' in the stratosphere, *J. Atmos. Terr. Phys.*, *46*, 825-850, 1984.

McKay, M. D., R. J. Beckman, and W. J. Conover, A comparison of three methods for selecting values of input variables in the analysis of output from a computer code, *Technometrics*, *21*, 239-245, 1979.

McKenney, D. J., D. L. Wade, and W. I. Findlay, Rates of N_2O evolution from N fertilized soil, *Geophys. Res. Lett.*, *5*, 777-780, 1978.

McKenney, D. J., K. F. Shuttleworth, J. R. Vriesacker, and W. T. Findlay, Production and loss of nitric oxide from denitrification in anaerobic Brookstone clay, *Appl. Env. Microbiol.*, *43*, 534-541, 1982.

McKenzie, R. L., and P. V. Johnston, Seasonal variation in stratospheric NO_2 at 45 degrees S, *Geophys. Res. Lett.*, *9*, 1255-1258, 1982.

McMahon, T. A., and P. J. Denison, Empirical atmospheric deposition parameters—A survey, *Atmos. Environ.*, *13*, 571-585, 1979.

McMillin, L. M., and C. Dean, Evaluation of a new operational technique for producing clear radiances, *J. Appl. Meteorol.*, *21*, 1005-1014, 1982.

McPeters, R. D., and C. H. Jackman, The response of ozone to solar proton events during solar cycle 21: The observations, *J. Geophys. Res.*, 90, 7945-7954, 1985.

McPeters, R. D., C. H. Jackman, and E. G. Stassinopoulos, Observations of ozone depletion associated with solar proton events, *J. Geophys. Res.*, *86*, 12071-12081, 1981.

McPeters, R. D., D. F. Heath, and P. K. Bhartia, Average ozone profiles for 1979 from the NIMBUS 7 SBUV instrument, *J. Geophys. Res.*, *89*, 5199-5214, 1984.

McPherson, R. D., K. H. Bergman, R. E. Kistler, G. E. Rasch, and D. S. Gordon, The NMC operational global data assimilation system, *Mon. Weather Rev.*, *107*, 1445-1461, 1979.

Mechoso, C. R., M. J. Suarez, K. Yamazaki, J. Spahr, and A. Arakawa, A study of the sensitivity of numerical forecasts to an upper boundary condition in the lower stratosphere, *Mon. Weather Rev.*, *110*, 1984-1993, 1982.

Mechoso, C. R., K. Yamazaki, A. Kitch, and A. Arakawa, Numerical forecasts of stratospheric warming events during the winter of 1979, *J. Atmos. Sci.*, in press, 1985.

Meek, C. E., I. M. Reid, and A. H. Manson, Observations of mesospheric wind velocities. I. Gravity wave horizontal scale and phase velocities determined from spaced wind observations, *Rad. Sci.*, in press, 1985a.

Meek, C. E., I. M. Reid, and A. H. Manson, Observations of mesospheric wind velocities. II. Cross sections of power spectral density for 48-8h, 8-1h, 1h-10 min over 60-110 km for 1981, *Rad. Sci.*, in press, 1985b.

Megie, G., and J. E. Blamont, Laser sounding of atmospheric sodium, Interpretation in terms of global atmospheric parameters, *Planet. Space Sci.*, *25*, 1093-1109, 1977.

Megie, G., and R. T. Menzies, Complementarity of UV and IR differential absorption lidar for global measurements of atmospheric species, *Appl. Optics*, *19*, 1173-1183, 1980.

Megie, G., J. Y. Allain, M. L. Chanin, and J. E. Blamont, Vertical profile of stratospheric ozone by lidar sounding from the ground, *Nature*, *270*, 329-331, 1977.

Meier, R. R., D. E. Anderson, Jr., and M. Nicolet, Radiation field in the troposphere and stratosphere from 240-1000 nm - I. General analysis, *Planet. Space Sci.*, *30*, 923-933, 1982.

Mentall, J. E., J. E. Frederick, and J. R. Herman, The solar irradiance from 200-330 nm, *J. Geophys. Res.*, *86*, 9881-9884, 1981.

Mentall, J. E., B. Guenther, and D. Williams, The solar spectral irradiance between 150 and 200 nm, *J. Geophys. Res.*, *90*, 2265-2272, 1985.

Menzies, T., Remote measurement of ClO in the stratosphere, *Geophys. Res. Lett.*, *6*, 151-154, 1979.

Menzies, T., A re-evaluation of laser heterodyne radiometer ClO measurements, *Geophys. Res. Lett.*, *10*, 729-732, 1983.

Michalsky, J. J., B. M. Herman and N. R. Larson, Mid-latitude stratospheric aerosol layer enhancement by El Chichon: The first year, *Geophys. Res. Lett.*, *11*, 76-79, 1984.

Mihelic, D., D. H. Ehhalt, G. F. Kulessa, J. Klomfass, M. Trainer, U. Schmidt, and H. Rohrs, Measurements of free radicals in the atmosphere by matrix isolation and electron paramagnetic resonance, *Pure Appl. Geophys.*, *116*, 530-536, 1978.

Miles, T., and W. A. Chapman, Intercomparison of planetary-scale diagnostics derived from seperate satellite and radiosonde time-mean temperature fields, *Quart. J. Roy. Meteorol. Soc.*, *110*, 1003-1021, 1984.

Miller, A. J., Periodic variation of atmospheric circulation at 14-16 days, *J. Atmos. Sci.*, *31*, 720-726, 1974.

Miller, A. J., T. G. Rogers, R. M. Nagatani, D. F. Heath, A. J. Krueger, W. Planet, and D. Crosby, Preliminary comparisons of daily total ozone fields derived from SBUV, TOMS and HIRS-2 satellite

REFERENCES

instruments, in *Proc. XVII General Assembly of the International Union of Geodesy and Geophysics*, pp. 153-164, 1979.

Miller, A. J., R. M. Nagatani, T. G. Rogers, A. J. Fleig, and D. F. Heath, Total ozone variations 1970-1974 using Backscattered Ultraviolet (BUV) and ground-based observations, *J. Appl. Meteorol.*, *21*, 621-630, 1982.

Miller, A. J., R. M. Nagatani and J. E. Frederick, Ozone-temperature relationships in the stratosphere, in *Proceedings of the International Ozone Symposium*, pp. 321-324, Thessaloniki, Greece, D. Reidel, Dordrecht, 1985.

Miller, C., D. L. Filken, A. J. Owens, J. M. Steed, and J. P. Jesson, A two-dimensional model of stratospheric chemistry and transport, *J. Geophys. Res.*, *86*, 12039-12065, 1981.

Mitchell, J. F. B., The seasonal response of a general circulation model to changes in CO_2 and sea temperatures, *Quart. J. Roy. Meteorol. Soc.*, *109*, 113-152, 1983.

Mitchell, J. M., El Chichon: Weather-maker of the century?, *Weatherwise*, *35*, 252-261, 1982.

Miyahara, S., A numerical simulation of the zonal mean circulation of the middle atmosphere including effects of solar diurnal tidal waves and internal gravity waves; solstice condition, in *Dynamics of the Middle Atmosphere*, edited by J. R. Holton and T. Matsuno, pp. 271-287, Terrapub, Tokyo, 1984.

Miyahara, S., Suppression of stationary planetary waves by internal gravity waves in the mesosphere, *J. Atmos. Sci.*, *42*, 100-107, 1985.

Miyahara, S., Y. Hayashi, and J. D. Mahlman, Interactions between gravity waves and planetary scale flow simulated by GFDL "SKYHI" general circulation model, *J. Atmos. Sci.*, in press, 1985.

Miyakoda, K., R. F. Strickler, and G. D. Hembree, Numerical simulation of the breakdown of a polar-night vortex in the stratosphere, *J. Atmos. Sci.*, *27*, 139-154, 1970.

Moeng, C.-H., and J. C. Wyngaard, Statistics of conservative scalars in the convective boundary layer, *J. Atmos. Sci.*, *41*, 3161-3169, 1984.

Molina, L. T., M. J. Molina, and F. S. Rowland, Ultraviolet absorption cross sections of several brominated methanes and ethanes of atmospheric interest, *J. Phys. Chem.*, *86*, 2672-2676, 1982.

Molina, L. T., M. J. Molina, R. A. Stachnik and R. D. Tom, An upper limit to the rate of $HCl + ClONO_2$ reaction, *J. Phys. Chem.*, *89*, 3779-3781, 1985.

Molina, M. J., and F. S. Rowland, Stratospheric sink for chlorofluoromethanes: chorine atom catalyzed destruction of ozone, *Nature*, *249*, 810-814, 1974.

Molina, M. J., L. T. Molina, and T. Ishiwata, Kinetics of the $ClO + NO_2 + M$ reaction, *J. Phys. Chem.*, *84*, 3100-3104, 1980.

Molina, M. J., L. T. Molina, and C. A. Smith, The rate of the reaction of OH with HCl, *Int. J. Chem. Kinet.*, *16*, 1151-1160, 1984.

Mook, W. M., M. Koopermans, A. F. Carter, and C. D. Keeling, Seasonal, latitudinal, and secular variations in the abundance and isotopic ratios of atmospheric carbon dioxide (1): Results from land stations, *J. Geophys. Res.*, *88*, 915-933, 1983.

Morel, O., R. Simonaitis, and J. Heicklen, Ultraviolet absorption spectra of HO_2NO_2, $CCl_3O_2NO_2$, $CCl_2FO_2NO_2$ and $CH_3O_2NO_2$, *Chem. Phys. Lett.*, *73*, 38-42, 1980.

Mount, G. H., and G. J. Rottman, The solar spectral irradiance 1200-3184Å near solar maximum: 15 July 1980, *J. Geophys. Res.*, *86*, 9193-9198, 1981.

Mount, G. H., and G. J. Rottman, Solar absolute spectral irradiance 1150-3173Å: May 17, 1982, *J. Geophys. Res.*, *88*, 5403-5410, 1983a.

Mount, G. H., and G. J. Rottman, The solar absolute spectral irradiance at 1216Å and 1800-3173Å: January 12, 1983, *J. Geophys. Res.*, *88*, 6807-6811, 1983b.

Mount, G. H., and G. J. Rottman, The solar absolute spectral irradiance 118-300 nm: July 25, 1983, *J. Geophys. Res.*, *90*, 13031-13036, 1985.

Mount, G. H., G. J. Rottman, and J. G. Timothy, The solar spectral irradiance 1200-2550Å at solar maximum, *J. Geophys. Res.*, *85*, 4271-4274, 1980.

Mount, G. H., D. W. Rusch, J. M. Zawodny, J. F. Noxon, C. A. Barth, G. J. Rottman, R. J. Thomas, G. E. Thomas, R. W. Sanders, and G. M. Lawrence, Measurements of NO_2 in the Earth's stratosphere using a Limb scanning visible light spectrometer, *Geophys. Res. Lett.*, *10*, 265-268, 1983.

Mount, G. H., D. W. Rusch, J. F. Noxon, J. M. Zawodny, and C. A. Barth, Measurements of stratospheric NO_2 from the solar mesosphere explorer satellite, 1. An overview of the results, *J. Geophys. Res.*, *89*, 1327-1340, 1984.

Moxim, W. J., and J. D. Mahlman, Evaluation of the various total ozone sampling networks using the GFDL 3-D tracer model, *J. Geophys. Res.*, *85*, 4527-4539, 1980.

Mozurkewich, M., and S. Benson, Negative activation energies and curved Arrhenius plots. I. Theory of reaction over potential wells, *J. Phys. Chem.*, *88*, 6429-6435, 1984.

Mueller, P. K., and G. M. Hidy, The sulfate regional experiment: Report of findings, *EPRI-EA-1901*, Electric Power Research Institute, Palo Alto, CA, March, 1983.

Muller, C., J. Vercheval, M. Ackerman, C. Lippens, J. Laurent, M. P. Lamaitre, J. Besson, and A. Girard, Observations of middle atmospheric CH_4 and N_2O vertical distributions by the Spacelab 1 grille spectrometer, *Geophys. Res. Lett.*, *12*, 667-670, 1985.

Muller, H. G., Long period meteor wind oscillations, *Phil. Trans. Roy. Soc. London*, *A271*, 585-598, 1972.

Muller, H. G., G. A. Whitehurst, and A. O'Neill, Stratospheric warmings and their effects on the winds in the upper atmosphere during the winter of MAP/WINE 1983-1984, *J. Atmos. Terr. Phys.*, in press, 1985.

Mumma, M. J., J. D. Rogers, T. Kostiuk, D. Deming, J. J. Hillman, and D. Zipoy, Is there any chlorine monoxide in the stratosphere?, *Science*, *221*, 268-271, 1983.

Murad, E., W. Swider, and S. W. Benson, Possible role for metals in stratospheric chlorine chemistry, *Nature*, *289*, 273-275, 1981.

Murakami, T., Equatorial stratospheric waves induced by diabatic heat sources, *J. Atmos. Sci.*, *29*, 1129-1137, 1972.

Murcray, D. G., T. G. Kyle, F. H. Murcray, and W. J. Williams, Nitric acid and nitric oxide in the lower stratosphere, *Nature*, *218*, 78-79, 1968.

Murcray, D. G., A. Goldman, A. Csoeke-Poeckh, F. H. Murcray, W. J. Williams, and R. N. Stocker, Nitric acid distribution in the stratosphere, *J. Geophys. Res.*, *78*, 7033-7038, 1973.

Murcray, D. G., D. B. Barker, J. N. Brooks, A. Goldman, and W. J. Williams, Seasonal and latitudinal variations of the stratospheric concentration of HNO_3, *Geophys. Res. Lett.*, *6*, 223-225, 1975.

Murcray, D. G., A. Goldman, C. M. Bradford, G. R. Cook, J. W. Van Allen, F. S. Bonomo, and F. H. Murcray, Identification of the ν_2 vibration-rotation band of ammonia in ground level solar spectra, *Geophys. Res. Lett.*, *5*, 527-530, 1978.

Murcray, D. G., A. Goldman, F. H. Murcray, F. J. Murcray, and W. J. Williams, Stratospheric distribution of $ClONO_2$, *Geophys. Res. Lett.*, *6*, 857-859, 1979.

Murcray, D. G., F. J. Murcray, A. Goldman, F. H. Murcray, and J. J. Kosters, Balloon-borne remote sensing of stratospheric constituents, *22*, 2629-2640, 1983.

Murcray, D. G., A. Goldman, J. Kosters, R. Zander, W. Evans, N. Louisnard, C. Alamichel, M. Bangham, S. Pollitt, B. Carli, B. Dinelli, S. Piccioli, A. Volboni, W. Traub, and K. Chance, Intercomparison of stratospheric water vapor profiles obtained during the balloon intercomparison campaign, in *Atmospheric Ozone*, edited by C. S. Zerefos and A. Ghazi, pp. 144-148, D. Riedel, Dordrecht, 1985a.

Murcray, D. G., L. S. Rottman, G. A. Vanasse, F. H. Murcray, F. J. Murcray, and A. Goldman, Atmospheric emission spectra from the stratospheric cryogenic interferometer balloon experiment, paper presented at the Ninth colloquium on High Resolution Molecular Spectroscopy, Riccione, Italy, 1985b.

REFERENCES

Murcray, D. G., A. Goldman, J. Kosters, R. Zander, W. F. J. Evans, N. Louisnard, D. Alamichel, M. Bangham, S. Pollitt, B. Carli, B. Dinelli, S. Piccioli, A. Volboni, W. Traub, and K. Chance, Intercomparison of stratospheric water vapor profiles obtained during the balloon intercomparison campaign, to be published, 1986.

Murcray, F. J., A. Goldman, D. G. Murcray, G. R. Cook, J. W. Van Allen, and R. D. Blatherwick, Identification of isolated NO lines in balloon-borne infrared solar spectra, *Geophys. Res. Lett.*, 7, 673-676, 1980.

Murgatroyd, R. J., Recent progress in studies of the stratosphere, *Quart. J. Roy. Meteorol. Soc.*, 108, 271-312, 1982.

Murgatroyd, R. J., and R. M. Goody, Sources and sinks of radiative energy from 30 to 90 km, *Quart. J. Roy. Meteorol. Soc.*, 84, 225-234, 1958.

Murgatroyd, R. J., and F. Singleton, Possible meridional circulations in the stratosphere and mesosphere, *Quart. J. Roy. Meteorol. Soc.*, 87, 125-135, 1961.

Murray, E. R., Remote measurement of gases using discretely tunable infrared lasers, *Opt. Eng.*, 16, 284-290, 1977.

Myers, R. J. K., J. R. Simpson, R. Wetselaar, and G. T. McKinney, Problems in modelling the environmental aspects of the nitrogen cycle in agro-ecosystems, SCOPE workshop on "Dynamic Aspects of Nitrogen Cycling in the Australian Ecosystems," Aspendale, Vic., Australia, 1979.

Nagata, T., T. Tohmatsu, and T. Ogawa, Sounding rocket measurement of atmospheric ozone density, 1965-1970, *Space Res.*, 11, 849-855, 1971.

NAS: See National Academy of Sciences.

NASA, Man's impact on the troposphere: Lectures in tropospheric chemistry, *NASA Reference Publication 1022*, edited by J. S. Levine and D. R. Schryer, Hampton, VA, Sept. 1978.

NASA, *The Stratosphere: Present and Future*, NASA Reference Publication 1049, edited by R. D. Hudson and E. I. Reed, 432 pp., NASA Goddard, Greenbelt, MD, 1979.

NASA-JPL, Chemical kinetics and photochemical data for use in stratospheric modeling, Evaluation No. 7, NASA Panel for Data Evaluation, *JPL Publication 85-37*, Jet Propulsion Laboratory, Pasadena, CA, 1982.

Nastrom, G. D., B. B. Balsley, and D. A. Carter, Mean meridional winds in the mid- and high-latitude summer mesosphere, *Geophys. Res. Lett.*, 9, 139-142, 1982.

Nastrom, G. D., W. L. Ecklund, and K. S. Gage, Direct measurements of synoptic scale vertical velocities using clear air radars, *Mon. Weather Rev.*, 113, 708-718, 1985.

Natarajan, M., L. B. Callis, and J. E. Nealy, Solar UV variability: Effects on stratospheric ozone, trace constituents and thermal structure, *Pure Appl. Geophys.*, 119, 750-779, 1980/81.

National Academy of Sciences, NAS, *Halocarbons: Effect on Stratospheric Ozone*, National Academy Press, Washington, DC, 1976.

The National plan for stratospheric ozone monitoring and early detection of change, 1981-1986, *FCM-P17-1982*, 79 pp., Federal Coordinator for Meteorological Services and Supporting Research, NOAA, Rockville, MD, 1982.

National Research Council, *Environmental Impact of Stratospheric Flight*, National Academy of Sciences, Washington, DC, 1975.

National Research Council, *Effects on Stratospheric Ozone*, National Academy of Sciences, Washington, DC, 1976.

National Research Council, *Stratospheric Ozone Depletion by Halocarbons: Chemistry and Transport*, National Academy of Sciences, Washington, DC, 1979.

National Research Council, *Protection Against Depletion of Stratospheric Ozone by Chlorofluorocarbons*, Committee on Impacts of Stratospheric Change, 392 pp., National Academy of Sciences, Washington, DC, 1979.

National Research Council, *Changing Climate: Report of the Carbon Dioxide Assessment Committee*, CDAC, 496 pp., National Academy Press, Washington, DC, 1983.

National Research Council, *Causes and Effects of Changes in Stratospheric Ozone: Update 1983*, National Academy Press, Washington, DC, 1984.

National Research Council, *Global Tropospheric Chemistry, A Plan for Action*, National Academy Press, Washington, DC, 1984.

Naudet, J. P., P. Rigaud, and D. Huguenin, Stratospheric NO_2 at night from balloons, *J. Geophys. Res.*, *89*, 2583-2587, 1984.

Naudet, J. P., P. Rigaud, and D. Huguenin, Variabilite temporelle du NO_3 stratospherique, in *Atmospheric Ozone*, edited by C. S. Zerefos and A. Ghazi, pp. 201-205, D. Reidel, Dordrecht, 1985.

Naujokat, B., Long-term variations in the stratosphere of the Northern Hemisphere during the last two sunspot cycles, *J. Geophys. Res.*, *86*, 9811-9816, 1981.

Naujokat, B., An update of the observed QBO of the stratospheric winds over the tropics, *J. Atmos. Sci.*, in press, 1986.

Nava, D. F., J. V. Michael, and L. J. Stief, Rate constant for the reaction of atomic bromine with formaldehyde from 223 to 480K, *J. Phys. Chem.*, *85*, 1896-1899, 1981.

Naylor, D. A., T. A. Clark, and R. T. Boreiko, Determination of stratospheric H_2O and O_3 column densities from balloon altitude far infrared absorption spectra by a curve of growth method, *Infrared Phys.*, *21*, 271-281, 1981.

Naylor, D. A., R. T. Boreiko, T. A Clark, R. J. Emery, B. Fitton, and M. F. Kessler, Atmospheric emission in the 20 μm window from Mauna Kea, *Pub. Astron. Soc. Pacific*, *96*, 167-173, 1984.

Naylor, D. A., J. M. Hoogerdijk, R. T. Boreiko, T. A. Clark, B. Fitton, M. F. Kessler, and R. J. Emery, Observations of 63 micron atomic oxygen emission in the earth's atmosphere from balloon altitudes: Astronomical implications, in press, 1985.

Neckel, H., and D. Labs, Improved data of solar spectral irradiance from 0.33 to 1.25 μm, *Solar Physics*, *74*, 231-249, 1981.

Neckel, H., and D. Labs, The solar radiation between 3300 and 12500 Å, *Solar Physics*, *90*, 205-258, 1984.

Neftel, A., H. Oeschger, J. Schwander, B. Stauffer, and R. Zumbrunn, Ice core measurements give atmospheric CO_2 content during the past 40,000 years, *Nature*, *295*, 220-223, 1982.

Neftel, A., E. Moor, H. Oeschger, and B. Stauffer, Evidence from polar ice cores for the increase in atmospheric CO_2 in the past two centuries, *Nature*, *315*, 45-47, 1985.

Nelson, H. H., L. Pasternack, and J. R. McDonald, Laser-induced excitation and emissions spectra of NO_3, *J. Phys. Chem.*, *87*, 1286-1266, 1983.

Newell, R. E., The general circulation of the atmosphere and its effects on the movement of trace substances, *J. Geophys. Res.*, *68*, 3949-3962, 1963a.

Newell, R. E., The general circulation of the stratosphere above 60 km, *Meteor. Monogr.*, Amer. Meteor. Soc., Boston, *31*, 98-113, 1963b.

Newell, R. E., Further ozone transport calculations and the spring maximum in ozone amount, *Pure Appl. Geophys.*, *59*, 191-206, 1964.

Newell, R. E., and T. G. Dopplick, Questions concerning the possible influence of anthropogenic CO_2 on atmospheric temperature, *J. Appl. Meteor.*, *18*, 822-825, 1979.

Newell, R. E., and S. Gould-Stewart, A stratospheric fountain?, *J. Atmos. Sci.*, *38*, 2789-2796, 1981.

Newell, R. E., J. W. Kidson, D. G. Vincent, and G. J. Boer, *The General Circulation of the Tropical Atmosphere, Vol. 1*, MIT Press, Cambridge, MA, 1969.

Newell, R. E., J. W. Kidson, D. G. Vincent, and G. J. Boer, *The General Circulation of the Tropical Atmosphere, Vol. 2*, MIT Press, Cambridge, MA, 1974.

REFERENCES

Newell, R. E., E. P. Condon, and H. G. Reichle, Measurements of CO and CH_4 in the troposphere over Saudi Arabia, India and the Arabian Sea during the 1979 International Summer Monsoon Experiment (MONEX), *J. Geophys. Res.*, *86*, 9833-9838, 1981.

Newman, P. A., M. R. Schoeberl, and R. A. Plumb, A computation of the horizontal mixing coefficients calculated from NMC data, *Geophys. Res. Lett.*, in press, 1986.

Newson, R. L., An experiment with a tropospheric and stratospheric three-dimensional general circulation model, in *Proceedings Third Conference on the Climatic Impact Assessment Program, DOT-TSC-OST-74-15*, edited by A. J. Broderick and T. M. Hard, pp. 461-474, Dept. of Transp., Washington, DC, 1974.

Newton, C. W., and E. Palmen, Kinematic and thermal properties of a large amplitude wave in the westerlies, *Tellus*, *15*, 99-119, 1963.

Newton, C. W., and A. Trevisan, Clinogenesis and frontogenesis in jet stream waves. Part I: Analytical relation, *J. Atmos. Sci.*, *41*, 2717-2734, 1984.

Nicolet, M., On the production of nitric oxide by cosmic rays in the mesosphere and stratosphere, *Planet. Space Sci.*, *23*, 637-649, 1975.

Nicolet, M., The solar spectral irradiance and its action in the atmospheric photodissociation processes, *Planet. Space Sci.*, *29*, 951-974, 1981.

Nicolet, M., The influence of solar radiation on atmospheric chemistry, *Annales Geophysicae*, *1*, 493-502, 1983.

Nicolet, M., On the molecular scattering in the terrestrial atmosphere: An empirical formula for its calculation in the homosphere, *Planet. Space Sci.*, *32*, 1467-1468, 1984a.

Nicolet, M., On the photodissociation of water vapor in the mesophere, *Planet. Space Sci.*, *32*, 871-880, 1984b.

Nicolet, M., Aeronomical aspects of mesospheric photodissociation: Processes resulting from the H Lyman-alpha line, *Planet. Space Sci.*, *33*, 69-80, 1985.

Nicolet, M., and S. Cieslik, The photodissociation of nitric oxide in the mesosphere and stratosphere, *Planet. Space Sci.*, *28*, 105-115, 1980.

Nicolet, M., and W. Peetermans, Atmospheric absorption in the O_2 Schumann-Runge band spectral region and photodissociation rates in the stratosphere and mesosphere, *Planet. Space Sci.*, *28*, 85-103, 1980.

Nicolet, M., R. R. Meier, and D. E. Anderson, Jr., Radiation field in the troposphere and stratosphere. II. Numerical analysis, *Planet. Space Sci.*, *30*, 935-983, 1982.

Niki, H., P. D. Maker, C. M. Savage, and L. P. Breitenbach, Fourier transform IR spectroscopic observation of pernitric acid formed via $HOO + NO_2 \rightarrow HOONO_2$, *Chem. Phys. Lett.*, *45*, 564-566, 1977.

Niki, H., P. D. Maker, C. M. Savage, and L. P. Breitenbach, A fourier transform infrared study of the kinetics and mechanisms for the reaction $HO + CH_3OOH$, *J. Phys. Chem.*, *87*, 2190-2193, 1983.

Niple, E., W. G. Mankin, A. Goldman, D. G. Murcray, and F. J. Murcray, Stratospheric NO_2 and H_2O mixing ratio profiles from high resolution infrared solar spectra using nonlinear least squares, *Geophys. Res. Lett.*, *7*, 489-492, 1980.

Nitta, T., Response of cumulus updraft and downdraft to GATE A/B-scale motion systems, *J. Atmos. Sci.*, *34*, 1163-1186, 1977.

Nordhaus, W. D., and G. W. Yohe, Future paths of energy and carbon dioxide emissions, in *Changing Climate*, pp. 87-153, National Academy of Sciences, Washington, DC, 1983.

North, G. R., R. F. Cahalan and J. A. Coakley, Energy-balance climate models, *Rev. Geophys. Space Phys.*, *19*, 91-122, 1981.

Norton, R. B., and J. F. Noxon, The dependence of stratospheric NO_3 upon latitude and season, *J. Geophys. Res.*, in press, 1985.

Noxon, J. F., Atmospheric nitrogen fixation by lightning, *Geophys. Res. Lett.*, *3*, 463-465, 1976.

Noxon, J. F., Stratospheric NO_2 in the Antarctic winter, *Geophys. Res. Lett.*, *5*, 1021-1022, 1978a.

Noxon, J. F., Tropospheric NO_2, *J. Geophys. Res.*, *83*, 3051-3057, 1978b.

Noxon, J. F., Stratospheric NO_2, 2, Global behavior, *J. Geophys. Res.*, *84*, 5067, 1979.

Noxon, J. F., Tropospheric NO_2 (Correction), *J. Geophys. Res.*, *85*, 4560-4561, 1981a.

Noxon, J. F., NO_x in the mid-Pacific troposphere, *Geophys. Res. Lett.*, *8*, 1223-1226, 1981b.

Noxon, J. F., NO_3 and NO_2 in the mid-Pacific troposphere, *J. Geophys. Res.*, *88*, 11017-11021, 1983.

Noxon, J. F., R. B. Norton, and W. R. Henderson, Observation of atmospheric NO_3, *Geophys. Res. Lett.*, *5*, 675-678, 1978.

Noxon, J. F., E. C. Whipple Jr., and R. S. Hyde, Stratospheric NO_2 1. Observational method and behavior at mid-latitude, *J. Geophys. Res.*, *84*, 5047-5065, 1979a.

Noxon, J. F., E. Marovich, and R. B. Norton, Effect of a major warming upon stratospheric NO_2, *J. Geophys. Res.*, *84*, 7883, 1979b.

Noxon, J. F., R. B. Norton, and E. Marovich, NO_3 in the troposphere, *Geophys. Res. Lett.*, *7*, 125-128, 1980.

Noxon, J. F., W. R. Henderson, and R. B. Norton, Stratospheric NO_2, 3. The effects of large scale horizontal transport, *J. Geophys. Res.*, 88, 5240-5248, 1983.

NRC: See National Research Council.

Oeschger, H., The contribution of ice core studies to the understanding of environmental processes, in *Green Ice Core: Geophysics, Geochemistry, and the Environment, American Geophysical Union Monograph No. 33*, edited by C. C. Langway, H. Oeschger, and W. Dansgaard, pp. 9-17, *33*, 1985.

Oeschger, H., U. Siegenthaler, U. Schotterer and A. Gugelmann, A box diffusion model to study the carbon dioxide exchange in nature, *Tellus*, *27*, 168-192, 1975.

Ogawa, M., Absorption cross sections of O_2 and CO_2 continua in the Schumann and far-UV regions, *J. Chem. Phys.*, *54*, 2550-2556, 1971.

Ogawa, T., K. Shibasaki, and K. Suzuki, Balloon observation of the stratospheric NO_2 profile by visible absorption spectroscopy, *J. Meteorol. Soc. Japan*, *59*, 410-416, 1981.

Oltmans, S. J., and J. London, The quasi-biennial oscillation in atmospheric ozone, *J. Geophys. Res.*, *87*, 8981-8989, 1982.

O'Neill, A., and C. Youngblut, Stratospheric warmings diagnosed using the transformed Eulerian-mean equations and the effect of the mean state on wave propagation, *J. Atmos. Sci.*, *39*, 1370-1386, 1982.

O'Neill, A., R. L. Newson, and R. J. Murgatroyd, An analysis of the large-scale features of the upper troposphere and the stratosphere in a global, three-dimensional, general circulation model, *Quart. J. Roy. Meteorol. Soc.*, *108*, 25-53, 1982.

Ongstad, A. P., and J. W. Birks, Studies of reactions of importance in the stratosphere. V. Rate constants for the reactions $O + NO_2 \rightarrow NO + O_2$ and $O + ClO \rightarrow Cl + O_2$ at 298K, *J. Chem. Phys.*, *81*, 3922-3930, 1984.

Oort, A. H., Global Atmospheric Statistics, 1958-1973, *NOAA Professional Paper*, *14*, 1983.

Ooyama, K., On the stability of the baroclinic circular vortex: A sufficient criterion for instability, *J. Atmos. Sci.*, *23*, 43-53, 1966.

Oran, E. S., P. S. Julienne, and D. F. Strobel, The aeronomy of odd nitrogen in the thermosphere, *J. Geophys. Res.*, *80*, 3068-3076, 1975.

Orton, G. S., and A. G. Robiette, A line parameter list for the ν_2 and ν_4 bands of $^{12}CH_4$ and $^{13}CH_4$, extended to $J^1 = 25$ and its application to planetary atmospheres, *J. Quant. Spectrosc. Radiat. Transfer*, *24*, 81-95, 1980.

Ostlund, H. G., H. G. Dorsey and R. Brescher, GEOSECS Atlantic radiocarbon and tritium results, *Report No. 5*, Univ. Miami Tritium Laboratory Data, 1976.

REFERENCES

Owens, A. J., J. M. Steed, D. L. Filkin, C. Miller, and J. P. Jesson, The potential effects of increased methane on atmosphere ozone, *Geophys. Res. Lett.*, *9*, 1105-1108, 1982a.

Owens, A. J., J. M. Steed, C. Miller, D. L. Fillim, and J. P. Jesson, The atmospheric lifetime of CFC-11 and CFC-12, *Geophys. Res. Lett.*, *9*, 700-703, 1982b.

Owens, A. J., C. H. Hales, D. L. Filkin, C. Miller, and M. McFarland, Multiple scenario ozone change calculations: The subtractive perturbation approach, in *Atmospheric Ozone*, edited by C. S. Zerefos and A. Ghazi, pp. 82-86, D. Reidel, Dordrecht, 1985a.

Owens, A. J., C. H. Hales, D. L. Filken, C. Miller, J. M. Steed, and J. P. Jesson, A coupled one-dimensional radiative-convective, chemistry-transport model of the atmosphere 1. Model structure and steady-state perturbation calculations, *J. Geophys. Res.*, *90*, 2283-2311, 1985b.

Paetzold, H. K., New experimental and theoretical investigation on the atmospheric ozone layer, *J. Atmos. Terr. Phys.*, *7*, 128-140, 1955.

Pallister, R. C., and A. F. Tuck, The diurnal variation of ozone in the upper stratosphere as a test of photochemical theory, *Quart. J. Roy. Meteorol. Soc.*, *109*, 271-284, 1983.

Palmen, E., and C. W. Newton, *Atmospheric Circulation Systems*, 603 pp., Academic Press, New York, 1969.

Palmer, T. N., Diagnostic study of wavenumber-2 stratospheric sudden warming in a transformed Eulerian mean formalism, *J. Atmos. Sci.*, *38*, 844-855, 1981a.

Palmer, T. N., Aspects of stratospheric sudden warmings studied from a transformed Eulerian-mean viewpoint, *J. Geophys. Res.*, *86*, 9679-9687, 1981b.

Palmer, T., and C. Hsu, Stratospheric sudden coolings and the role of nonlinear wave interactions in preconditioning the circumpolar flow, *J. Atmos. Sci.*, *40*, 909-928, 1983.

Park, J. H., D. J. W. Kendall, and H. L. Buijs, Stratospheric HF mixing ratio profiles in the Northern and Southern Hemispheres, *J. Geophys. Res.*, *89*, 11645-11653, 1984.

Parker, D. E., and J. L. Brownscombe, Stratospheric warming following the El Chichon volcanic eruption, *Nature*, *301*, 406-408, 1983.

Parrish, A., R. L. De Zafra, P. M. Solomon, J. W. Barrett, and E. R. Carlson, Chlorine oxide in the stratospheric ozone layer: Ground-based detection and measurement, *Science*, *211*, 1158-1161, 1981.

Patel, C. K. N., E. G. Burkhardt, and C. A. Lambert, Spectroscopic measurements of stratospheric nitric oxide and water vapor, *Science*, *184*, 1173-1176, 1974.

Patrick, R., J. R. Barker, and D. M. Golden, Computational study of the $HO_2 + HO_2$ and $DO_2 + DO_2$ reactions, *J. Phys. Chem.*, *88*, 128-136, 1984.

Patterson, E. M., B. T. Marshall and K. A. Rahn, Radiative properties of the Arctic aerosol, *Atmos. Environ.*, *16*, 2967-2977, 1982.

Paur, R. J., and A. M. Bass, The ultraviolet cross sections of ozone II. Results and temperature dependence, in *Atmospheric Ozone*, edited by C. S. Zerefos and A. Ghazi, pp. 611-616, D. Reidel, Dordrecht, 1985.

Payne, W. J., *Denitrification*, 214 pp., Wiley, New York, 1983.

Pearman, G. I., P. Hyson, and P. J. Fraser, The global distribution of atmospheric carbon dioxide: I. Aspects of observation and modelling, *J. Geophys. Res.*, *88*, 3581-3590, 1983.

Pearman, G. I., D. Etheridge, F. deSilva, and P. J. Fraser, Evidence of changing concentrations of atmospheric CO_2, N_2O and CH_4 from air bubbles in antarctica, *Nature*, 1985.

Pearman, G. I., and P. Hyson, Activities of the global biosphere as reflected in atmospheric CO_2 records, *J. Geophys. Res.*, *85*, 4457-4467, 1980.

Pearson, Jr., R., and D. H. Stedman, Instrumentation for fast response ozone measurements from aircraft, *Atmos. Techn.*, National Center for Atmospheric Research, Boulder, CO, *12*, 51-55, 1980.

Pelon, J., and G. Megie, Ozone monitoring in the troposphere and lower stratosphere: Evaluation and operation of a ground based lidar station, *Geoph. Res.*, *87*, 4947-4955, 1982a.

Pelon, J., and G. Megie, Ozone vertical distribution and total content using a ground-based active remote sensing technique, *Nature*, *299*, 137-139, 1982b.

Pelon, J., and G. Megie, Ozone monitoring in the troposphere and lower stratosphere: Evaluation and operation of a ground-based lidar station, *J. Geophys. Res.*, *87*, 4947-4955, 1982c.

Pelon, J., and G. Megie, Lidar measurements of the vertical ozone distribution during the June 1981 intercomparison campaign GAP/OHP, *Planet. Space Sci.*, *31*, 717-721, 1983.

Penkett, S. A., The application of analytical techniques to the understanding of chemical processes occurring in the atmosphere, *Toxicol. Environ. Chem.*, *3*, 291-321, 1981.

Penkett, S. A., R. G. Derwent, P. Fabian, R. Borchers, and U. Schmidt, Methyl chloride in the stratosphere, *Nature*, *283*, 58-60, 1980.

Penkett, S. A., N. J. D. Prosser, R. A. Rasmussen, and M. A. K. Khalil, Atmospheric measurements of CF_4 and other fluorocarbons containing the CF_3 grouping, *J. Geophys. Res.*, *86*, 5172-5178, 1981.

Penn, S., A case study using ozone to determine structure and air motions at the tropopause, *J. Appl. Meteorol.*, *3*, 581-586, 1964.

Perner, D., D. H. Ehhalt, H. W. Paetz, U. Platt, E. P. Roeth, and A. Volz, OH radicals in the lower troposphere, *Geophys. Res. Lett.*, *3*, 466-468, 1976.

Perry, R., Kinetics of the reactions of NCO radicals with H_2, NO and O_2 using laser photolysis-laser induced fluorescence, paper presented at 16th Informal Conference on Photochemistry, *Abstract T-12*, Cambridge, MA, August, 1984.

Perry, R. A., R. Atkinson, and J. N. Pitts, Jr., Kinetics and mechanism of the gas phase reactions of OH radicals with aromatic hydrocarbons over the temperature range 296 - 435K, *J. Phys. Chem.*, *82*, 296-304, 1977.

Philbrick, C. R., Measurements of structural features in profiles of mesospheric density, in *Handbook for MAP*, *Vol. 2.* edited by S. K. Avery, pp. 333-340, SCOSTEP Secretariat, Univ. of Illinois, Urbana, 1981.

Pick, D. R., and J. L. Brownscombe, Early results based on the stratospheric channels of TOVS on the TIROS-N series of operational satellites, *Adv. in Space Res.*, *1*, 247-260, 1981.

Pickett, H. M., D. E. Brinza, and E. A. Cohen, Pressure broadening of ClO by nitrogen, *J. Geophys. Res.*, *86*, 7279-7282, 1981.

Pierotti, D., and R. A. Rasmussen, Combustion as a source of nitrous oxide in the atmosphere, *Geophys. Res. Lett.*, *3*, 265-267, 1976.

Pierotti, D., and R. A. Rasmussen, The atmosphere distribution of nitrous oxide, *J. Geophys. Res.*, *82*, 5823-5832, 1977.

Pirre, M., P. Rigaud, and D. Huguenin, New in-situ measurements of the absorption cross section of O_2 in the Herzberg continuum, *Geophys. Res. Lett.*, *11*, 1199-1202, 1984.

Pirre, M., P. Rigaud, and D. Huguenin, Mesure de l'absorption par la haute atmosphere dans le domame de hugeus donde de la fenetre atmosphenigue an voisinage de 200 nm, in *Atmospheric Ozone*, edited by C. S. Zerefos and A. Ghazi, pp. 630-634, G. Reidel, Dordrecht, 1985.

Pitari, G., and G. Visconti, Two-dimensional tracer transport: Derivation of residual mean circulation and eddy transport tensor from a 3-D model data set, *J. Geophys. Res.*, *90*, 8019-8032, 1985.

Pittock, A. B., Climatology of the vertical distribution of ozone over Aspendale, *Quart. J. Roy. Meteorol. Soc.*, *103*, 575-584, 1977.

Planet, W. G., D. S. Crosby, J. H. Lienesch, and M. L. Hill, Determination of total ozone amounts from TIROS radiance measurements, *J. Clim. and Appl. Meteor.*, *23*, 308-316, 1984.

REFERENCES

Platt, C. M. R., Cirrus clouds in tropical Australia, *Weatherwise*, *36*, 132-133, 1983.

Platt, U., and D. Perner, Direct measurements of atmospheric CH_2O, HNO_2, O_3, NO_2, and SO_2 by differential optical absorption in the near UV, *J. Geophys. Res.*, *85*, 7453-7458, 1980.

Platt, U., D. Perner, G. W. Harris, A. M. Winer, and J. N. Pitts, Jr., Observations of nitrous acid in an urban atmosphere by differential optical absorption, *Nature*, *285*, 312-314, 1980a.

Platt, U., D. Perner, A. M. Winer, G. W. Harris, and J. N. Pitts, Jr., Detection of NO_3 in the polluted troposphere by differential optical absorption, *Geophys. Res. Lett.*, *7*, 89-92, 1980b.

Platt, U., D. Perner, J. Schroder, C. Kessler, and A. Toennissen, The diurnal variation of NO_3, *J. Geophys. Res.*, *86*, 11965-11970, 1981.

Platt, U. F., A. M. Winer, H. W. Biermann, R. Atkinson, and J. H. Pitts, Jr., Measurement of nitrate radical concentrations in continental air, *Environ. Sci. Technol.*, *18*, 365-369, 1984.

Plumb, R. A., The interaction of two internal waves with the mean flow: Implications for the theory of the quasi-biennial oscillation, *J. Atmos. Sci.*, *34*, 1847-1858, 1977.

Plumb, R. A., Eddy fluxes of conserved quantities by small-amplitude waves, *J. Atmos. Sci.*, *36*, 1699-1704, 1979.

Plumb, R. A., Instability of the distorted polar night vortex: A theory of stratospheric warmings, *J. Atmos. Sci.*, *38*, 2514-2531, 1981.

Plumb, R. A., The circulation of the middle atmosphere, *Aus. Meteorol. Mag.*, *30*, 107-121, 1982.

Plumb, R. A., Baroclinic instability of the summer mesosphere: A mechanism for the quasi-two-day-wave?, *J. Atmos. Sci.*, *40*, 262-270, 1983a.

Plumb, R. A., A new look at the energy cycle, *J. Atmos. Sci.*, *40*, 1669-1688, 1983b.

Plumb, R. A., The quasi-biennial oscillation, in *Dynamics of the Middle Atmosphere*, edited by J. R. Holton and T. Matsuno, pp. 217-251, Terrapub, Tokyo, 1984.

Plumb, R. A., and R. C. Bell, A model of the quasi-bienniel oscillation on an equatorial beta-plane, *Quart. J. Roy. Meteorol. Soc.*, *108*, 335-352, 1982.

Plumb, R. A., and J. D. Mahlman, The zonally-averaged transport characteristics of the GFDL general circulation/tracer model, *J. Atmos. Sci.*, in press, 1986.

Plumb, R. A., and A. D. McEwan, The instability of a forced standing wave in a viscous stratified fluid: A laboratory analogue of the quasi-biennial oscillation, *J. Atmos. Sci.*, *35*, 1827-1839, 1978.

Pollack, J. B., and T. P. Ackerman, Possible effects of the El Chichon volcanic cloud on the radiation budget of the northern tropics, *Geophys. Res. Lett.*, *10*, 1057-1060, 1983.

Pollack, J. B., and C. P. McKay, The impact of polar stratospheric clouds on the heating rates of the winter polar stratosphere, *J. Atmos. Sci.*, *42*, 245-262, 1985.

Pollitt, S., M. Coffey, W. Evans, A. Goldman, J. J. Kosters, N. Louisnard, W. G. Mankin, D. G. Murcray, and W. J. Williams, Intercomparative measurements of stratospheric nitric acid, in *Atmospheric Ozone*, edited by C. S. Zerefos and A. Ghazi, pp. 151-156, D. Reidel, Dordrecht, 1985.

Pollitt, S., D. G. Murcray, A. Goldman, J. J. Kosters, W. J. Williams, N. Louisnard, W. F. J. Evans, M. Coffey, W. G. Mankin, R. Zander, D. W. Johnson, G. Stokes, and R. K. Seals, BIC nitric acid intercomparison, to be published, 1986.

Pollock, W., L. E. Heidt, R. Lueb, and D. H. Ehhalt, Measurement of stratospheric water vapor by cryogenic collection, *J. Geophys. Res.*, *85*, 5555-5568, 1980.

Pommereau, J. P., Observation of NO_2 diurnal variation in the stratosphere, *Geophys. Res. Lett.*, *9*, 850-853, 1982.

Porch, W. M., and M. C. MacCracken, Parametric study to the effects of Arctic soot on solar radiation, *Atmos. Environ.*, *16*, 1365-1371, 1982.

Posey, J., J. Sherwell, and M. Kaufman, Kinetics of the reactions of atomic bromine with HO_2 and H_2O_2, *Chem. Phys. Lett.*, *77*, 476-479, 1981.

Poulet, G., G. Laverdet, and G. Le Bras, Discharge flow-mass spectrometric determination of the rate coefficient for the reactions of formaldehyde with bromine atoms and chlorine atoms, *J. Phys. Chem.*, *85*, 1891-1895, 1981.

Poulet, G., G. Laverdet, and G. Le Bras, Kinetics of the reactions of atomic bromine with HO_2 and HCO at 298K, *J. Chem. Phys.*, *80*, 1922-1928, 1984.

Poulet, G., G. Laverdet, and G. LeBras, Rate constant and branching ratio for the reaction of OH with ClO, *J. Phys. Chem.*, in press, 1985.

Poynter, R. L., and H. M. Pickett, Submillimeter, millimeter, and microwave spectral line catalogue, *JPL Publication 80-23, Revision 1*, 151 pp., Jet Propulsion Laboratory, California Institute of Technology, Pasadena, CA, 1981.

Poynter, R. L., and H. M. Pickett, Submillimeter, millimeter, and microwave spectral line catalogue, *JPL Publication 80-23, Revision 2*, 171 pp., Jet Propulsion Laboratory, California Institute of Technology, Pasadena, CA, 1984.

Prabhakara, C., Effects of non-photochemical processes on the meridional distribution and total amount of ozone in the atmosphere, *Mon. Weather Rev.*, *91*, 411-431, 1963.

Prasad, S. S., Possible existence and chemistry of $ClO.O_2$ in the stratosphere, *Nature*, *285*, 152-154, 1980.

Prata, A., The 4-day wave, *J. Atmos. Sci.*, *41*, 150-155, 1984.

Prather, M. J., Ozone in the upper stratosphere and mesosphere, *J. Geophys. Res.*, *86*, 5325-5338, 1981.

Prather, M. J., Continental sources of halocarbons and nitrous oxide, *Nature*, *317*, 221-225, 1985.

Prather, M. J., M. B. McElroy, and S. C. Wofsy, Reductions in ozone at high concentrations of stratospheric halogens, *Nature*, *312*, 227-231, 1984.

Prinn, R. G., P. G. Simmonds, R. A. Rasmussen, R. D. Rosen, F. N. Alyea, C. A. Cardelino, A. J. Crawford, D. M. Cunnold, P. J. Fraser, and J. E. Lovelock, The atmospheric lifetime experiment, 1, Introduction, instrumentation and overview, *J. Geophys. Res.*, *88*, 8353-8367, 1983a.

Prinn, R. G., R. A. Rasmussen, P. G. Simmonds, F. N. Alyea, D. M. Cunnold, B. C. Lane, C. A. Cardelino, and A. J. Crawford, The atmospheric lifetime experiments, 5, Results for CH_3CCl_3 based on three years of data, *J. Geophys. Res.*, *88*, 8415-8426, 1983b.

Pugh, L. A., and K. N. Rao, Intensities from infrared spectra, *Mol. Spectros., Mod. Res.*, *2*, 165-225, 1976.

Pyle, J. A., A calculation of the possible depletion of ozone by chlorofluorocarbons using a two-dimensional model, *Pure Appl. Geophys.*, *118*, 355-377, 1980.

Pyle, J. A., and C. F. Rogers, A modified diabatic circulation model for stratospheric tracer transport, *Nature*, *287*, 711-714, 1980a.

Pyle, J. A., and C. F. Rogers, Stratospheric transport by stationary planetary waves: The importance of chemical processes, *Quart. J. Roy. Meteorol. Soc.*, *106*, 421-446, 1980b.

Pyle, J. A., and C. F. Rogers, Modelling tracer budgets in the stratosphere, *Quart. J. Roy. Meteorol. Soc.*, *110*, 1097-1106, 1984.

Pyle, J. A., and A. M. Zavody, The derivation of near-global fields of hydrogen containing radical concentrations from satellite data sets, *Quart. J. Roy. Meteorol. Soc.*, in press, 1985a.

Pyle, J. A., and A. M. Zavody, The variability of stratospheric radicals, paper presented at the 5th General Assembly, International Association of Geomagnetism and Aeronomy, Prague, 5-17 August 1985b.

Pyle, J. A., A. M. Zavody, J. E. Harries, and P. H. Moffat, Derivation of OH concentration from satellite infrared measurements of NO_2 and HNO_3, *Nature*, *305*, 690-692, 1983.

Quinn, T. H., K. A. Wolf, W. E. Mooz, J. K. Hammitt, T. W. Chesnutt and S. Sarma, Projected use, emissions, and banks of potential ozone depleting substances, *N-2282-EPA*, Rand Corp., Santa Monica, CA, 1985.

Quiroz, R. S., Stratospheric temperatures during solar cycle 20, *J. Geophys. Res.*, *84*, 2415-2420, 1979a.

Quiroz, R. S., Tropospheric-stratospheric interaction in the major warming event of January-February 1979, *Geophys. Res. Lett.*, *6*, 645-648, 1979b.

REFERENCES

Quiroz, R. S., The isolation of stratospheric temperature change due to the El Chichon volcanic signals, *J. Geophys. Res.*, *88*, 6773-6780, 1983a.

Quiroz, R. S., The climate of the "El Nino" winter of 1982-83. A season of extraordinary climatic anomalies, *Mon. Weather Rev.*, *111*, 1685-1706, 1983b.

Quiroz, R. S., and M. E. Gelman, An evaluation of temperature profiles from falling sphere soundings, *J. Geophys. Res.*, *81*, 406-412, 1976.

Quiroz, R. S., A. J. Miller, and R. M. Nagatani, A comparison of observed and simulated properties of sudden stratospheric warmings, *J. Atmos. Sci.*, *32*, 1723-1736, 1975.

Ramanathan, V., Greenhouse effect due to chlorofluorocarbons: Climatic implications, *Science*, *190*, 50-52, 1975.

Ramanathan, V., Radiative transfer within the Earth's troposphere and stratosphere: A simplified radiative-convective model, *J. Atmos. Sci.*, *33*, 1330-1346, 1976.

Ramanathan, V., Climatic effects of anthropogenic trace gases, in *Energy/Climate Interactions*, pp. 269-280, D. Reidel, Dordrecht, 1980.

Ramanathan, V., The role of ocean-atmosphere interactions in the CO_2 climate problem, *J. Atmos. Sci.*, *38*, 918-930, 1981.

Ramanathan, V., and J. A. Coakley, Jr., Climate modeling through radiative-convective models, *Rev. Geophys. Space Phys.*, *16*, 465-490, 1978.

Ramanathan, V., and R. E. Dickinson, The role of stratospheric ozone in the zonal and seasonal radiative energy balance of the earth-troposphere system, *J. Atmos. Sci.*, *36*, 1084-1104, 1979.

Ramanathan, V., and P. Downey, A non-isothermal emissivity and absorptivity formulation for water vapor, *J. Geophys. Res.*, *91*, in press, 1986.

Ramanathan, V., L. B. Callis and R. E. Boughner, Sensitivity of atmospheric and surface temperature to perturbations in the stratospheric concentration of ozone and nitrogen dioxide, *J. Atmos. Sci.*, *33*, 1092-1112, 1976.

Ramanathan, V., M. S. Lian and R. D. Cess, Increased atmospheric CO_2: Zonal and seasonal estimates of the effect on the radiation energy balance and surface temperature, *J. Geophys. Res.*, *84*, 4949-4958, 1979.

Ramanathan, V., E. J. Pitcher, R. C. Malone and M. L. Blackmon, The response of a spectral general circulation model to refinements in radiative processes, *J. Atmos. Sci.*, *40*, 605-630, 1983.

Ramanathan, V., R. J. Cicerone, H. B. Singh and J. T. Kiehl, Trace gas trends and their potential role in climate change, *J. Geophys. Res.*, *90*, 5547-5566, 1985.

Ramaswamy, V., and A. Detwiler, Interdependence of radiation and microphysics in cirrus clouds, *J. Atmos. Sci.*, *43*, in press, 1985.

Ramaswamy, V., and J. T. Kiehl, Sensitivities of the radiative forcing due to large loadings of smoke and dust aerosols, *J. Geophys. Res.*, *90*, 5597-5613, 1985.

Randal, W. J., and J. L. Stanford, Structure of medium-scale atmospheric waves in the Southern Hemisphere summer, *J. Atmos. Sci.*, *40*, 2312-2318, 1983.

Randhawa, J. S., Ozonesonde for rocket flight, *Nature*, *213*, 53-54, 1967.

Rao, M. S. V., Retrieval of worldwide precipitation and allied parameters from satellite microwave observations, in *Advances in Geophysics, Vol. 26*, edited by B. Saltzman, pp. 1238-1336, Academic Press, New York, 1984.

Rao (Vupputuri), R. K., Numerical experiment on the steady state meridional structure and ozone distribution in the stratosphere, *Mon. Weather Rev.*, *101*, 510-527, 1973.

Raper, O. F., C. B. Farmer, R. A. Toth, and B. D. Robbins, The vertical distribution of HCl in the stratosphere, *Geophys. Res. Lett.*, *4*, 531-534, 1977.

Rasmussen, R. A., and M. A. K. Khalil, Atmospheric halocarbons: Measurements and analyses of selected trace gases, in *Proceedings of the NATO Advanced Study Institute on Atmospheric Ozone: Its Variation and Human Influences*, Rep. FAA-EE-80-20, edited by A. C. Aikin, pp. 209-231, DOT, FAA, Washington, DC, 1980.

Rasmussen, R. A., and M. A. K. Khalil, Global atmospheric distribution and trend of methylchloroform (CH_3CCl_3), *Geophys. Res. Lett.*, 8, 1005-1007, 1981a.

Rasmussen, R. A., and M. A. K. Khalil, Atmospheric methane (CH_4); Trends and seasonal cycles, *J. Geophys. Res.*, 86, 9826-9832, 1981b.

Rasmussen, R. A., and M. A. K. Khalil, Differences in the concentrations of atmospheric trace gases in and above tropical boundary layer, *Pure Appl. Geophys.*, 119, 990-997, 1981c.

Rasmussen, R. A., and M. A. K. Khalil, Increase in the concentration of atmospheric methane, *Atmos. Environ.*, 15, 883-886, 1981d.

Rasmussen, R. A., and M. A. K. Khalil, Latitudinal distributions of trace gases in and above the boundary layer, *Chemosphere*, 11, 227-235, 1982.

Rasmussen, R. A., and M. A. K. Khalil, Natural and anthropogenic trace gases in the lower troposphere of the Arctic, Dept. of Environ. Sci., Beaverton, OR, 1983a.

Rasmussen, R. A., and M. A. K. Khalil, Atmospheric fluorocarbons and methyl chloroform at the South Pole, *1982 Annual Issue of the Antarctic Journal of the United States*, 17, 203-205, 1983b.

Rasmussen, R. A., and M. A. K. Khalil, Global production of methane by termites, *Nature*, 301, 700-702, 1983c.

Rasmussen, R. A., and M. A. K. Khalil, Natural and anthropogenic trace gases in the lower troposphere in the arctic, *Chemosphere*, 12, 371-375, 1983d.

Rasmussen, R. A., and M. A. K. Khalil, Trace gases at Point Barrow and Arctic haze, in *Geophysical Monitoring for Climatic Change Annual Report 10*, edited by B. A. Bodhaine and J. M. Harris, NOAA/ERL, U.S. Dept. of Commerce, Boulder, CO, 1983e.

Rasmussen, R. A., and M. A. K. Khalil, Rare trace gases at the South Pole: $CHClF_2$, CH_3I, $CHCl_3$ and SF_6, 1984a.

Rasmussen, R. A., and M. A. K. Khalil, Atmospheric methane in recent and ancient atmospheres: Concentrations, trends and interhemispheric gradients, *J. Geophys. Res.*, 89, 11599-11605, 1984b.

Rasmussen, R. A., and M. A. K. Khalil, Gaseous bromine in the Arctic and Arctic haze, *Geophys. Res. Lett.*, 11, 433-436, 1984c.

Rasmussen, R. A., S. A. Penkett, and N. Prosser, Measurements of carbontetrafluoride in the atmosphere, *Nature*, 277, 549-550, 1979.

Rasmussen, R. A., L. E. Rasmussen, M. A. K. Khalil, and R. W. Dalluge, Concentration distribution of methyl chloride in the atmosphere, *J. Geophys. Res.*, 85, 7350-7356, 1980.

Rasmussen, R. A., M. A. K. Khalil, and R. W. Dalluge, Atmospheric trace gases in Antarctica, *Science*, 211, 285-287, 1981.

Rasmussen, R. A., M. A. K. Khalil, A. J. Crawford, and P. J. Fraser, Natural and anthropogenic trace gases in the Southern Hemisphere, *Geophys. Res. Lett.*, 9, 704-707, 1982a.

Rasmussen, R. A., M. A. K. Khalil, R. Gunawardena, and S. D. Hoyt, Atmospheric methyl iodide (CH_3I), *J. Geophys. Res.*, 87, 3086-3090, 1982b.

Rasmussen, R. A., M. A. K. Khalil, and R. J. Fox, Altitudinal and temporal variations of hydrocarbons and other gaseous tracers of Arctic haze, *Geophys. Res. Lett.*, 10, 144-147, 1983.

Ravishankara, A. R., and P. H. Wine, Absorption cross sections for HNO_3 between 565 and 673 nm, *Chemical Physics Letters*, 101, 73-78, 1983.

Ravishankara, A. R., P. H. Wine, A. Torabi, C. A. Smith, and R. Wells, Photodissociation of N_2O_5, *J. Phys. Chem.*, in press, 1985.

REFERENCES

Rayez, J. C., B. Veyret, and R. Lesclaux, Thermodynamical and structural data of free radicals of atmospheric interest calculated by MNDO-CI, paper presented at XVth Int. Symp. on Free Radicals, Lauzelle-Ottignies, Belgium, 1983.

Raynaud, D., and J. M. Barnola, An Antarctica ice core reveals atmospheric CO_2 variations over the past few centuries, *Nature, 315*, 309-311, 1985.

Reagan, J. B., R. E. Meyerott, R. W. Nightingale, R. C. Gunton, R. G. Johnson, J. E. Evans, W. L. Imhof, D. F. Heath, and A. J. Krueger, Effects of the August 1972 solar particle events on stratospheric ozone, *J. Geophys. Res., 86*, 1473-1494, 1981.

Reber, C. A., Upper Atmosphere Research Satellite (UARS) Mission, *NASA Goddard Space Flight Center Publication 430-1003-001*, NASA Goddard Space Flight Center, Greenbelt, MD, 1985.

Reck, R. A., Stratospheric ozone effects on temperature, *Science, 192*, 557-559, 1976.

Reck, R. A., Atmospheric temperature calculated for ozone depletion, *Nature, 263*, 116-117, 1976.

Reck, R. A., Thermal effect of stratospheric ozone depletion at 85° latitude as influenced by airborne particles, *Geophys. Res. Lett., 5*, 361-364, 1978.

Reck, R. A., and D. L. Fry, The direct effect of chlorofluoromethanes on the atmospheric surface temperature, *Atmos. Environ., 12*, 2501-2503, 1978.

Reck, R. A., and J. R. Hummel, Influence of aerosol optical properties on surface temperatures computed with a radiative-convective model, *Atmos. Environ., 15*, 1727-1731, 1981.

Reed, R. J., The role of vertical motions in ozone-weather relationships, *J. Meteorol., 7*, 263-267, 1950.

Reed, R. J., A study of a characteristic type of upper level frontogenesis, *J. Meteorol., 12*, 226-237, 1955.

Reed, R. J., The structure and dynamics of the 26-month oscillation, paper presented at 40th anniv. meeting of the Amer. Met. Soc., Boston, 1960.

Reed, R. J., Evidence of geostrophic motion in the equatorial stratosphere, *Quart. J. Roy. Meteorol. Soc., 88*, 324-327, 1962.

Reed, R. J. A tentative model of the 26-month oscillation in tropical latitudes, *Quart. J. Roy. Meteorol. Soc., 90*, 441-466, 1964.

Reed, R. J., The quasi-biennial oscillation of the atmosphere between 30 and 50 km over Ascension Island, *J. Atmos. Sci., 22*, 331-333, 1965.

Reed, R. J., Zonal wind behaviour in the equatorial stratosphere and lower mesosphere, *J. Geophys. Res., 71*, 4223-4233, 1966.

Reed, R. J., and E. F. Danielson, Fronts in the vicinity of the tropopause, *Arch. Met. Geophys. Bioklim., 11*, 1-17, 1959.

Reed, R. J., and K. E. German, A contribution to the problem of stratospheric diffusion by large-scale mixing, *Mon. Weather Rev., 93*, 313-321, 1965.

Reed, R. J., and C. L. Vlcek, The annual temperature variation in the lower tropical stratosphere, *J. Atmos. Sci., 26*, 163-167, 1969.

Reed, R. J., D. C. Norquist, and E. F. Recker, The structure and properties of African wave disturbances as observed during Phase III of GATE, *Mon. Weather Rev., 105*, 317-333, 1977.

Regener, V. H., Vertical flux of atmospheric ozone, *J. Geophys. Res., 62*, 221-228, 1957.

Regener, V. H., Measurement of ozone with the chemiluminescent method, *J. Geophys. Res., 69*, 3795-3800, 1964.

Reid, G. C., and K. S. Gage, A relation between the height of the tropical tropopause and the global angular momentum of the atmosphere, *Geophys. Res. Lett., 11*, 840-842, 1984.

Reinsel, G., G. C. Tiao, M. N. Wang, R. Lewis, and D. Nychka, Statistical analysis of stratospheric ozone data for the detection of trend, *Atmos. Environ., 15*, 1569-1577, 1981.

Reinsel, G., G. C. Tiao, R. Lewis, and M. Bobkoski, Analysis of upper stratospheric ozone profile data from the ground-based Umkehr method and the Nimbus-4 BUV satellite experiment, *J. Geophys. Res., 88*, 5393-5403, 1983.

Reinsel, G. C., G. C. Tiao, J. L. De Luisi, C. L. Mateer, A. J. Miller, and J. E. Frederick, Analysis of upper stratospheric Umkehr ozone profile data for trends and the effects of stratospheric aerosols, *J. Geophys. Res.*, *89*, 4833-4840, 1984.

Reiter, E. R., Atmospheric transport processes. Part 1: Energy transfers and transformation, *USAEC Report TID-24868*, 253 pp., Colorado State Univ., Fort Collins, CO, 1968.

Reiter, E. R., Atmospheric transport processes. Part 2: Chemical tracers, *USAEC Report TID-25314*, 382 pp., Colorado State Univ., Fort Collins, CO, 1971.

Reiter, E. R., Atmospheric transport processes. Part 3: Hydrodynamic tracers, *USAEC Report TID-25731*, 212 pp., Colorado State Univ., Fort Collins, CO, 1972.

Reiter, E. R., Stratospheric-tropospheric exchange processes, *Rev. Geophys. Space Phys.*, *13*, 459-474, 1975.

Reiter, E. R., Tropospheric-stratospheric transport processes: Indications of their interannual variability, paper presented at WMO Symp. on Long Range Transport of Pollutants and its Relation to General Circulation including Stratosphere/Troposphere Exchange Processes, *WMO No. 538*, pp. 393-400, 1979.

Reiter, E. R., and H. J. Kanter, Time behavior of CO_2 and O_3 in the lower troposphere based on recordings from neighbouring mountain stations between 0.7 and 3.0 km ASL including the effects of meteorological parameters, *Arch. Met. Geoph. Biokl. Ser. B*, *30*, 191-225, 1982.

Reiter, E. R., and J. D. Mahlman, A case study of mass transport from stratosphere to troposphere not associated with surface fallout, in *Atmospheric Science Paper No. 70*, pp. 54-83, Colorado State University, Ft. Collins, CO, 1971.

Reiter, E. R., and M. P. McCormick, SAGE-European ozonesonde comparison, *Nature*, *300*, 337-339, 1982.

Reiter, E. R., and A. Nania, Jet stream structure and clear air turbulence (CAT), *J. Appl. Meteorol.*, *3*, 247-260, 1963.

Reiter, E. R., M. E. Glasser, and J. D. Mahlman, The role of the tropopause in stratospheric-tropospheric processes, *Pure Appl. Geophys.*, *75*, 185-218, 1969.

Remsberg, E. E., and L. L. Gordley, Analysis of differential absorption lidar from the Space Shuttle, *Appl. Optics*, *17*, 624-630, 1978.

Remsberg, E. E., J. M. Russell III, J. C. Gille, L. L. Gordley, P. L. Bailey, W. G. Planet, and J. E. Harries, The validation of Nimbus 7 LIMS measurements of ozone, *J. Geophys. Res.*, *89*, 5161-5178, 1984a.

Remsberg, E. E., J. M. Russell III, L. L. Gordley, J. C. Gille, and P. L. Bailey, Implications of stratospheric water vapor distribution as determined from the Nimbus 7 LIMS experiment, *J. Atmos. Sci.*, 2934-2945, 1984b.

Ridley, B. A., and D. R. Hastie, Stratospheric odd nitrogen: NO measurements at 51 °N in summer, *J. Geophys. Res.*, *86*, 3162-3166, 1981.

Ridley, B. A., and H. I. Schiff, Stratospheric odd nitrogen: Nitric oxide measurements at 32 °N in autumn, *J. Geophys. Res.*, *86*, 3167-3172, 1981.

Ridley, B. A., J. T. Bruin, H. I. Schiff, and J. C. McConnell, Altitude profile and sunset decay measurements of stratospheric nitric oxide, *Atmosphere*, *14*, 180-188, 1976.

Ridley, B. A., M. McFarland, J. T. Bruin, H. I. Schiff, and J. C. McConnell, Sunrise measurements of stratospheric nitric oxide, *Can. J. Phys.*, *55*, 212-221, 1977.

Ridley, B. A., S. H. Luu, D. R. Hastie, H. I. Schiff, J. C. McConnell, W. F. J. Evans, C. T. McElroy, J. B. Kerr, H. Fast, and R. S. O'Brien, Stratospheric odd nitrogen: Measurements of HNO_3, NO, NO_2 and O_3 near 54° N. in winter, *J. Geophys. Res.*, *89*, 4797-4820, 1984.

Riehl, H., *Climate and Weather in the Tropics*, Academic Press, New York, 611 pp., 1979.

Rigaud, P., J. P. Naudet, and D. Huguenin, Simultaneous measurements of vertical distribution of stratospheric NO_3 and O_3 at different periods of the night, *J. Geophys. Res.*, *88*, 1463-1467, 1983.

REFERENCES

Rind, D., and S. Lebedeff, Potential climatic impacts of increasing atmospheric CO_2 with emphasis on water availability and hydrology in the United States, *NASA-TM-87479*, 106 pp., NASA Goddard Space Flight Center, Greenbelt, MD, 1984.

Rind, D., R. Suozzo, A. Lacis, G. Russell, and J. Hansen, 21 layer troposphere-stratosphere climate model, *Mon. Weather Rev.*, in press, 1985.

Rinsland, C. P., and J. S. Levine, Free tropospheric carbon monoxide concentrations in 1950 and 1951 deduced from infrared total column amount measurements, *Nature*, *318*, 250-254, 1985.

Rinsland, C. P., M. A. H. Smith, J. M. Russell, J. H. Park, and C. B. Farmer, Stratospheric measurements of continuous absorption near 2400 cm⁻¹, *Appl. Opt.*, *20*, 4167-4171, 1981.

Rinsland, C. P., M. A. H. Smith, P. L. Rinsland, A. Goldman, J. W. Brault, and G. M. Stokes, Ground-based infrared spectroscopic measurements of atmospheric hydrogen cyanide, *J. Geophys. Res.*, *87*, 1119-1124, 1982a.

Rinsland, C. P., M. A. H. Smith, R. K. Seals, Jr., A. Goldman, F. J. Murcray, D. G. Murcray, J. C. Larsen, and P. L. Rarig, Stratospheric measurements of collision-induced absorption by molecular oxygen, *J. Geophys. Res.*, *87*, 3119-3122, 1982b.

Rinsland, C. P., A. Goldman, F. J. Murcray, D. G. Murcray, M. A. H. Smith, R. K. Seals, Jr., J. C. Larsen, and P. L. Rinsland, Stratospheric N_2O mixing ratio profile from high-resolution balloon-borne solar absorption spectra and laboratory spectra near 1880 cm⁻¹, *Appl. Opt.*, *21*, 4351-4355, 1982c.

Rinsland, C. P., R. E. Boughner, J. C. Larsen, G. M. Stokes, and J. W. Brault, Diurnal variations of atmospheric nitric oxide: Ground-based infrared spectroscopic measurements and their interpretation with time-dependent photochemical model calculations, *J. Geophys. Res.*, *89*, 9613-9622, 1984a.

Rinsland, C. P., A. Goldman, V. M. Devi, B. Fridovich, D. G. S. Snyder, G. D. Jones, F. J. Murcray, D G. Murcray, M. A. H. Smith, R. K. Seals, Jr., M. T. Coffey, and W. G. Mankin, Simultaneous stratospheric measurements of H_2O, HDO, and CH_4 from balloon-borne and aircraft infrared solar absorption spectra and tunable diode laser laboratory spectra of HDO, *J. Geophys. Res.*, *89*, 7259-7266, 1984b.

Rinsland, C. P., R. E. Boughner, J. C. Larsen, A. Goldman, F. J. Murcray, and D. G. Murcray, Stratospheric NO and NO_2 profiles at sunset from analysis of high resolution balloon-borne infrared solar absorption spectra obtained at 33 °N. and calculations with a time-dependent photochemical model, *NASA Tech. Memo 86285*, 46 pp., NASA Langley Research Center, Hampton, VA, 1984c.

Rinsland, C. P., J. S. Levine, and T. Miles, Concentration of methane in the troposphere deduced from 1951 solar spectra, *Nature*, *318*, 245-249, 1985a.

Rinsland, C. P., A. Goldman, D. G. Murcray, F. J. Murcray, F. S. Bonomo, R. D. Blatherwick, V. M. Devi, M. A. H. Smith, and P. L. Rinsland, Tentative identification of the 780 cm⁻¹ v_4 band Q branch of chlorine nitrate in high-resolution solar absorption spectra of the stratosphere, *J. Geophys. Res.*, *90*, 7931-7943, 1985b.

Rinsland, C. P., V. M. Devi, J.-M. Flaud, C. Camy-Peyret, M. A. H. Smith, and G. M. Stokes, Identification of ¹⁸O-isotopic lines of ozone in infrared ground-based solar absorption spectra, *J. Geophys. Res.*, *90*, 10719-10725, 1985c.

Rinsland, C. P., A. Goldman, and G. M. Stokes, Identification of atmospheric C_2H_2 lines in the 3230-3340 cm⁻¹ region of high resolution solar absorption spectra recorded at the National Solar Observatory, *Appl. Opt.*, *24*, 2044-2046, 1985d.

Rippel, H., A helium cooled balloon experiment for measuring infrared emission from stratospheric gases, Ph.D. Thesis, Univ. Wuppertal, Dept. of Atmospheric Physics, W. Germany, 1984a.

Rippel, H., Ein Heliumgekuhltes Ballonexperiment zur Messung der Infrarotemissionen stratospharischer Spurengase., Ph.D. Thesis, University of Wuppertal, F.R.G., 1984b.

Roach, W. T., Aircraft observations in the lower sub-arctic stratosphere in winter, *Meteorological Research Committee Paper 121*, (available at National Meteorological Library, UK Meteorological Office), 1962.

Roach, W. T., and B. F. James, A climatology of the potential vertical extent of giant cumulonimbus clouds in some selected areas, *Met. Mag.*, *101*, 161-181, 1973.

Robbins, D., W. Evans, N. Louisnard, S. Pollitt, W. Traub, and J. Waters, Ozone intercomparisons from the balloon intercomparison campaign, in *Atmospheric Ozone*, edited by C. S. Zerefos and A. Ghazi, pp. 465-469, D. Reidel, Dordrecht, 1985.

Robbins, D., J. Waters, P. Zimmermann, R. Jarnot, J. Hardy, H. Pickett, S. Pollitt, W. Traub, K. Chance, N. Louisnard, W. F. J. Evans, and J. Kerr, Ozone measurements during the balloon intercomparison campaign, to be published, 1986.

Robbins, R. C., L. A. Cavanagh, and L. J. Salas, Analysis of ancient atmospheres, *J. Geophys. Res.*, *78*, 5341-5344, 1973.

Robert, D., and J. Bonamy, Short range force effects in semiclassical molecular line broadening calculations, *Jl. de Physique*, *40*, 923-943, 1979.

Robertson, J. P., and J. M. Tiedje, Denitrification and nitrous oxide production in successful and old growth Michigan forests, *Soil Sci. Soc. Am. J.*, *48*, 383-389, 1984.

Robinson, E., and R. C. Robbins, Sources, abundance and fate of gaseous atmospheric pollutants, *Res. Proj. PR-6755*, Suppl. rep., Stanford Res. Inst., Menlo, CA, 1969.

Robinson, E., R. A. Rasmussen, J. Krasnec, D. Pierotti, and M. Jakubovic, Halocarbon measurements in the Alaskan troposphere and lower stratosphere, *Atmos. Environ.*, *11*, 215-218, 1977.

Roche, A. E., *UARS Spectroscopy Requirements: Report of the UARS Spectroscopy Working Group*, in press, 1985.

Rodgers, C. D., The radiative heat budget of the troposphere and lower stratosphere, Planet. Circ. Project, MIT Dept. Meteorol., *Rep. #A2*, 1967.

Rodgers, C. D., Evidence for the five-day wave in the upper stratosphere, *J. Atmos. Sci.*, *33*, 710-711, 1976a.

Rodgers, C. D., Retrieval of atmospheric temperature and composition from remote measurements of thermal radiation, *Rev. Geophys. Space Phys.*, *14*, 609-624, 1976b.

Rodgers, C. D., Statistical principles of inversion theory., in *Inversion Methods in Atmospheric Remote Sounding*, edited by A. Deepak, pp. 117-138, Academic Press, New York, 1977.

Rodgers, C. D. (Ed.), Coordinated Study of the Behavior of the Middle Atmosphere in Winter (PMP-1), *Handbook for MAP*, *Vol. 12*, 154 pp., SCOSTEP Secretariat, Univ. of Illinois, Urbana, 1984.

Rodgers, C. D., and W. L. Grose, PMP-1 Data Comparison Workshop, Part II, in *Handbook for MAP*, SCOSTEP Secretariat, Univ. of Illinois, Urbana, in press, 1985.

Rodgers, C. D., and A. J. Prata, Evidence for a travelling 2-day wave in the middle atmosphere, *J. Geophys. Res.*, *86*, 9661-9664, 1981.

Rodgers, C. D., and C. D. Walshaw, The computation of infra-red cooling rate in planetary atmospheres, *Quart. J. Roy. Meteorol. Soc.*, *92*, 67-92, 1966.

Rodgers, C. D., R. L. Jones, and J. J. Barnett, Retrieval of temperature and composition from Nimbus 7 SAMS measurements, *J. Geophys. Res.*, *89*, 5280-5286, 1984.

Rogers, C. F., and J. A. Pyle, Stratospheric tracer transport: A modified diabatic circulation model, *Quart. J. Roy. Meteorol. Soc.*, *110*, 219-237, 1984.

Rood, R. B., and A. R. Douglass, Interpretation of ozone temperature correlations 1. Theory, *J. Geophys. Res.*, *90*, 5733-5743, 1985.

Roscoe, H., Tentative observation of stratospheric N_2O_5, *Geophys. Res. Lett.*, *9*, 901-902, 1982.

Roscoe, H. K., J. R. Drummond, and R. F. Jarnot, Infrared measurements of stratospheric composition III. The daytime changes of NO and NO_2., *Proc. Roy. Soc. London A*, *375*, 507-528, 1981.

Roscoe, H. K., B. J. Kerridge, S. Pollitt, M. Bangham, N. Louisnard, C. Alamichel, J. P. Pommereau, T. Ogawa, N. Iwagami, M. T. Coffey, W. Mankin, J. M. Fland, C. Camay-Peret, F. J. Murcray,

REFERENCES

A. Goldman, W. F. J. Evans, and T. McElroy, Intercomparison of stratospheric measurements of NO and NO$_2$, in *Atmospheric Ozone*, edited by C. S. Zerefos and A. Ghazi, pp. 149-156, D. Reidel, Dordrecht, 1985a.

Roscoe, H. K., B. J. Kerridge, J. A. Pyle, L. J. Gray, and R. J. Wells, Simultaneous measurements of stratospheric NO and NO$_2$ and their comparison with model predictions, *J. Geophys. Res.*, in press, 1985b.

Roscoe, H. K., B. J. Kerridge, S. Pollitt, M. Bangham, N. Louisnard, C. Alamichel, J. M. Flaud, C. Camy-Peyret, J. R. Pommereau, T. Ogawa, N. Iwagami, M. T. Coffey, W. Mankin, F. J. Murcray, A. Goldman, W. F. J. Evans, T. McElroy, and J. Kerr, Intercomparison of remote measurements of stratospheric NO and NO$_2$, to be published, 1986.

Rose, K., and G. Brasseur, Ozone during sudden stratospheric warmings: A three-dimensional simulation, in *Atmospheric Ozone*, edited by C. S. Zerefos and A. Ghazi, pp. 28-32, D. Reidel, Dordrecht, 1985.

Rothman, L. S., *AFGL atmospheric absorption line parameters compilation: 1985 Edition*, in press, 1985.

Rothman, L. S., A. Goldman, J. R. Gillis, R. R. Gamache, H. M. Pickett, R. L. Poynter, N. Husson, and A. Chedin, AFGL trace gas compilation: 1982 version, *Appl. Opt.*, *22*, 1616-1627, 1983a.

Rothman, L. S., R. R. Gamache, A. Barbe, A. Goldman, J. R. Gillis, L. R. Brown, R. A. Toth, J. M. Flaud, and C. Camy-Peyret, AFGL atmospheric absorption line parameters compilation: 1982 Edition, *Appl. Opt.*, *22*, 2247-2256, 1983b.

Rothman, L. S., G. A. Vanasse, Murcray, D. G., F. H. Murcray, F. J. Murcray, and A. Goldman, Atmospheric emission spectra from the stratospheric cryogenic interferometer balloon experiment, in *Ninth Colloquium on High Resolution Molecular Spectroscopy*, pp. 19, University Press, Bologna, Italy, 1985.

Rottger, J., Structure and dynamics of the stratosphere and mesosphere revealed by VHF radar investigations, *Pure Appl. Geophys.*, *118*, 494-527, 1980.

Rottman, G. J., 27-day variations observed in solar ultraviolet (120-300 nm) irradiance, *Planet. Space Sci.*, *31*, 1001-1007, 1983.

Rowe, B. R., A. A. Viggiano, F. C. Fehsenfeld, D. W. Fahey, and E. E. Ferguson, Reactions between neutrals clustered on ions, *J. Chem. Phys.*, *76*, 742-743, 1982.

Rowland, F. S., and M. J. Molina, Chlorofluoromethanes in the environment, *Rev. of Geophys. Space Phys.*, *13*, 1-36, 1975.

Rowland, F. S., and P. J. Rogers, Upper stratospheric photolysis of NaCl and KCl, *Proc. Natl. Acad. Sci. USA*, *79*, 2737-2739, 1982.

Rowland, F. S., E. W. Mayer, D. R. Blake and Y. Makide, Trends in atmospheric methane concentrations since 1978, paper presented at Proc. Symp. Composition of the Non-urban Troposphere, Williamsburg, VA, 25-28 May 1982.

Rowland, F. S., D. R. Blake, and E. W. Mayer, World-wide increase in concentration of atmospheric methane since 1978, in *Symposium Proceedings* of WMO Technical Conference on Observation and Measurement of Atmospheric Contaminants, in press, 1984.

Roy, C. R., I. E. Galbally, and B. A. Ridley, Measurements of nitric oxide in the stratosphere of the Southern Hemisphere, *Quart. J. Roy. Meteorol. Soc.*, *106*, 887-894, 1980.

Ruderman, M. A., H. M. Folet, and J. W. Chamberlain, Eleven-year variation in polar ozone and stratospheric-ion chemistry, *Science*, *192*, 555-557, 1976.

Rudolph, J., and D. H. Ehhalt, Measurements of C$_2$-C$_5$ hydrocarbons over the North Atlantic, *J. Geophys. Res.*, *86*, 11959-11964, 1981.

Rudolph, J., D. H. Ehhalt, and A. Toennissen, Vertical profiles of ethane and propane in the stratosphere, *J. Geophys. Res.*, *86*, 7267-7272, 1981.

Rundel, R. D., D. M. Butler, and R. S. Stolarski, Uncertainty propagation in a stratospheric model 1. Development of a concise stratospheric model, *J. Geophys. Res.*, *83*, 3063-3072, 1978.

Rusch, D. W., and R. S. Eckman, Implications of the comparison of ozone abundances measured by the Solar Mesosphere Explorer to model calculations, *J. Geophys. Res.*, *90*, 12991-12998, 1985.

Rusch, D. W., J. C. Gerard, S. Solomon, P. J. Crutzen, and G. C. Reid, The effect of particle precipitation on the neutral and ion chemistry of the middle atmosphere—I. Odd nitrogen, *Planet. Space Sci.*, *29*, 767-774, 1981.

Rusch, D. W., G. H. Mount, C. A. Barth, G. J. Rottman, R. J. Thomas, G. E. Thomas, R. W. Sanders, G. M. Lawrence, and R. S. Eckman, Ozone densities in the lower mesosphere measured by a Limb Scanning Ultraviolet Spectrometer, *Geophys. Res. Lett.*, *10*, 241-244, 1983.

Rusch, D. W., G. H. Mount, C. A. Barth, and M. Callan, Global measurements of ozone in the 1.0 to 0.1 mb region by an ultraviolet spectrometer on the Solar Mesosphere Explorer, *J. Geophys. Res.*, *89*, 11677-11687, 1984.

Rusch, D. W., R. J. Thomas, and E. Hilsenrath, Satellite-rocket ozone profile comparisons over Natal, *J. Geophys. Res.*, in press, 1985.

Russell III, J. M., Global distribution and variability of stratospheric constituents measured by LIMS, *Adv. Space Res.*, *4*, 107-116, 1984.

Russell III, J. M, and J. C. Gille, The Limb Infared Monitor of the Stratosphere (LIMS) experiment, in *The Nimbus 7 Users' Guide*, edited by C. R. Madrid, pp. 71-103, NASA Goddard Space Flight Center, Greenbelt, MD, 1978.

Russell III, J. M., J. C. Gille, E. E. Remsberg, L. L. Gordley, P. L. Bailey, S. R. Drayson, J. Fischer, A. Girard, J. E. Harries, and W. F. J. Evans, Validation of nitrogen dioxide results measured by the Limb Infrared Monitor of the Stratosphere (LIMS) experiment on Nimbus 7, *J. Geophys. Res.*, *89*, 5099-5107, 1984a.

Russell III, J. M., S. Solomon, L. L. Gordley, E. E. Remsberg, and L. B. Callis, The variability of stratospheric and mesospheric NO_2 in the polar winter night observed by LIMS, *J. Geophys. Res.*, *89*, 7267-7275, 1984b.

Russell III, J. M., J. C. Gille, E. M. Remsberg, L. L. Gordley, P. L. Bailey, H. Fischer, A. Girard, S. R. Drayson, W. F. J. Evans, and J. E. Harries, Validation of water vapor results measured by the Limb Infrared Monitor of the Stratosphere experiment on NIMBUS 7, *J. Geophys. Res.*, *89*, 5115-5124, 1984c.

Russell III, J. M., S. Solomon, M. P. McCormick, A. J. Miller, D. W. Rusch, and J. J. Barnett, Middle atmosphere composition revealed by satellite observations, in *Handbook for MAP*, in press, 1986.

Ryden, J. C., N_2O exchange between grassland and the atmosphere, *Nature*, *292*, 235-237, 1981.

SRI International, *Chemical Economics Handbook Product Review: Fluorocarbons*, August, 1982.

Salby, M. L., Rossby normal modes in nonuniform background configurations. I: Simple fields, *J. Atmos. Sci.*, *38*, 1803-1826, 1981a.

Salby, M. L., Rossby normal modes in nonuniform background configurations. II: Equinox and solstice conditions, *J. Atmos. Sci.*, *38*, 1827-1840, 1981b.

Salby, M. L., The 2-day wave in the middle atmosphere—Observations and theory, *J. Geophys. Res.*, *86*, 9654-9660, 1981c.

Salby, M. L., A ubiquitous wavenumber-5 anomaly in the Southern Hemisphere during FGGE, *Mon. Weather Rev.*, *110*, 1712-1720, 1982a.

Salby, M. L., Sampling theory for asynoptic satellite observations. Part I. Space-time spectra, resolution and aliasing. Part II. Fast Fourier synoptic mapping, *J. Atmos. Sci.*, *39*, 2577-2614, 1982b.

Salby, M. L., Survey of planetary-scale traveling waves: The state of theory and observations, *Rev. Geophys. Space. Phys.*, *22*, 209-236, 1984a.

REFERENCES

Salby, M. L., Transient disturbances in the stratosphere: Implications for theory and observing systems, *J. Atmos. Terr. Phys.*, 46, 1009-1047, 1984b.

Salby, M. L., and R. Garcia, Vacillations induced by interference of stationary and traveling waves, in *Handbook for MAP, Vol. 18*, edited by S. Kato, pp. 170-174, SCOSTEP Secretariat, Univ. of Illinois, Urbana, 1985.

Salby, M. L., and R. G. Roper, Long-period oscillations in the meteor region, *J. Atmos. Sci.*, *37*, 237-244, 1980.

Salby, M. L., D. L. Hartmann, P. L. Bailey, and J. C. Gille, Evidence for equatorial Kelvin modes in Nimbus-7 LIMS, *J. Atmos. Sci.*, *41*, 220-235, 1984.

Samain, D., and P. C. Simon, Solar flux determination in the spectral range 150-210 nm, *Solar Physics*, *49*, 33-41, 1976.

Sandalls, F. J., and S. A. Penkett, Measurements of carbonyl sulfide and carbon disulfide in the atmosphere, *Atmos. Environ.*, *11*, 197-199, 1977.

Sander, S. P., and M. Peterson, Kinetics of the reaction $HO_2 + NO_2 + M \rightarrow HO_2NO_2 + M$, *J. Phys. Chem.*, *88*, 1566-1571, 1984.

Sanheuza, E., and J. Heicklen, Chlorine atom sensitized oxidation of dichloromethane and chloromethane, *J. Phys. Chem.*, *79*, 7-11, 1975.

Sato, T., and R. F. Woodman, Fine altitude resolution observations of stratospheric turbulent layers by the Arecibo 430 MHz radar, *J. Atmos. Sci.*, *39*, 2546-2552, 1982.

Savoie, D. L., and J. M. Prospero, Particle size distribution of nitrate and sulfate in the marine atmosphere, *Geophys. Res. Lett.*, *9*, 1207-1210, 1982.

Sawyer, J. S., The vertical circulation at meteorological fronts and its relation to frontogenesis, *Proc. Roy. Soc. London*, *A234*, 346-362, 1956.

Schenkel, A., and B. Broder, Interference of some trace gases with ozone measurements by the KI method, *Atmos. Environ.*, *16*, 2187-2190, 1982.

Schlesinger, M. E., A review of climate model simulations of CO_2-induced climatic change, *Rep. No. 41*, 135 pp., Climatic Research Institute, Oregon State University, Corvalalis, OR, 1983.

Schlesinger, M. E., Climate model simulation of CO_2-induced climatic change, in *Advances in Geophysics*, *26*, edited by B. Saltzman, pp. 141-235, Academic Press, New York, 1984.

Schlesinger, M. E., and Y. Mintz, Numerical simulation of ozone production, transport and distribution with a global general circulation model, *J. Atmos. Sci.*, *36*, 1325-1361, 1979.

Schlesinger, M. E., and J. F. B. Mitchell, Model projections of equilibrium climate response to increased CO_2, edited M. C. MacCracken and F. M. Luther, U.S. Department of Energy, in press, 1985.

Schlesinger, M. E., W. L. Gates, and Y. J. Han, The role of the ocean in CO_2-induced climate change: Preliminary results from the OSU coupled atmosphere-ocean general circulation model, in *Coupled Ocean Atmosphere Models*, edited by J. C. Nichol, pp. 447-478, Elsevier Science, New York, 1985.

Schmailzl, U., and P. J. Crutzen, Budgets of stratospheric trace gases from 2-D-model calculations and satellite observations, in *Atmospheric Ozone*, edited by C. S. Zerefos and A. Ghazi, pp. 43-47, D. Reidel, Dordrecht, 1985.

Schmeisser, M., and K. Brandle, Halogennitrate und ihre Reaktionen, *Angew. Chem.*, *73*, 388-393, 1961.

Schmidt, U., G. Kulessa, A. Khedim, D. Knapska, and J. Rudolph, Sampling of long lived trace gases in the middle and upper stratosphere, in *Sixth ESA Symposium on European Rocket and Balloon Programmes and Related Research—Conferences, ESA SP-183*, edited by W. R. Burke, pp. 141-145, European Space Agency, Paris, 1983.

Schmidt, U., A. Khedim, D. Knapska, G. Kulessa, and F. J. Johnen, Stratospheric trace gas distributions observed in different seasons, *Adv. Space Res.*, *4*, 131-134, 1984.

Schmidt, U., D. Knapska, and S. A. Penkett, A study of the vertical distribution of methyl chloride (CH_3Cl) in the midlatitude stratosphere, *J. Atmos. Chem.*, in press, 1985a.

Schmidt, U., P. Fabian, and R. Borchers, Intercomparison of balloon-borne cryogenic whole air samplers during the MAP/Globus campaign, *Planet. Space Sci.*, in press, 1985b.

Schneider, S. H., On the carbon dioxide-climate confusion, *J. Atmos. Sci.*, 32, 2060-2066, 1975.

Schneider, S. H., and S. L. Thompson, Atmospheric CO_2 and climate: Importance of the transient response, *J. Geophys. Res.*, 86, 3135-3147, 1981.

Schneider, W. H., P. K. Bhartia, K. F. Klenk, and C. L. Mateer, An optimum statistical technique for ozone profile retrieval from backscattered UV radiances, paper presented at Fourth Conference on Atmospheric Radiation, Am. Meteorol. Soc., Toronto, Ontario, Canada, June 16-18, 1981.

Schoeberl, M. R., Stratospheric warmings: Observations and theory, *Rev. Geophys. Space Phys.*, 16, 521-538, 1978.

Schoeberl, M. R., Medium-scale disturbances in total ozone during Southern Hemisphere summer, *Bull. Amer. Meteorol. Soc.*, 64, 1358-1365, 1983.

Schoeberl, M. R., On the penetration of mountain waves into the middle atmosphere, *J. Atmos. Sci.*, 42, 2856-2864, 1985.

Schoeberl, M. R., and M. A. Geller, A calculation of the structure of stationary planetary waves in winter, *J. Atmos. Sci.*, 34, 1235-1255, 1977.

Schoeberl, M. R., and D. F. Strobel, The response of the zonally averaged circulation to stratospheric ozone reductions, *J. Atmos. Sci.*, 35, 1751-1757, 1978a.

Schoeberl, M. R., and D. F. Strobel, The zonally averaged circulation of the middle atmosphere, *J. Atmos. Sci.*, 35, 577-591, 1978b.

Schoeberl, M. R., and D. F. Strobel, Nonzonal gravity wave breaking in the winter mesosphere, in *Dynamics of the Middle Atmosphere*, edited by J. R. Holton and T. Matsuno, pp. 45-64, D. Reidel, Dordrecht, 1984.

Schoeberl, M. R., D. F. Strobel, and J. Apruzese, A numerical model of gravity wave breaking and stress in the mesosphere, *J. Geophys. Res.*, 88, 5249-5259, 1983.

Schryer, D. R., *Heterogeneous Atmospheric Chemistry, Geophysical Monograph 26*, American Geophysical Union, Washington, DC, 1982.

Schwab, J. J., D. W. Toohey, W. H. Brune, and J. G. Anderson, Reaction kinetics of O + ClO → Cl + O_2 between 252-347K, *J. Geophys. Res.*, 89, 9581-9587, 1984.

Schwartz, P. R., C. L. Croskey, R. M. Bevilacqua, and J. J. Olivero, Microwave spectroscopy of H_2O in the stratosphere and mesosphere, *Nature*, 305, 294-295, 1983.

Schwartz, S. E., Gas- and aqueous-phase chemistry of HO_2 in liquid-water clouds, paper presented at the meeting of the American Chemical Society, Division of Environmental Chemistry, Washington, DC, September, 1983.

Secroun, C., A. Barbe, P. Jouve, P. Arcas, and E. Arie, Intensity of the $\nu3$ band of ozone from a study of its anomalous dispersion at 10 μm, *J. Molec. Spectrosc.*, 85, 8-15, 1981.

Sehmel, G. A., Particle and gas dry deposition: A review, *Atmos. Environ.*, 14, 983-1011, 1980.

Seiler, W., The cycle of carbon monoxide in the atmosphere, in *Proceedings of the ICESA Conference*, Vol. 2, I.E.E.E., New York, 1976.

Seiler, W., Contributions of biological processes to the global budget of CH_4 in the atmosphere, in *Current Perspectives in Microbial Ecology*, American Soc. for Microbiology, Washington, DC, edited by M. J. Klug and C. A. Reddy, 710 pp., 1984.

Seiler, W., and R. Conrad, Field measurements of natural and fertilizer-induced N_2O release rates from soils, *APCA Journal*, 31, 767-772, 1981.

REFERENCES

Seiler, W., and R. Conrad, Contributions of tropical ecosystems to the global budgets of trace gases, especially CH_4, H_2, CO and N_2O, in *Geophysiology of Amazonia*, edited by R. Dickinson, Wiley, New York, in press, 1985.

Seiler, W., and P. Crutzen, Estimates of the gross and net flux of carbon between the biosphere and the atmosphere from biomass burning, *Climate Change*, 2, 207-247, 1980.

Seiler, W., and J. Fishman, The distribution of carbon monoxide and ozone in the free troposphere, *J. Geophys. Res.*, 86, 7255-7265, 1981.

Seiler, W., and U. Schmidt, New aspects of CO and H_2 cycles in the atmosphere, in *Proceedings of the Int'l Conf. on the Structure, Composition, and Gen'l Circulation of the Upper and Lower Atmospheres and Possible Anthropogenic Perturbations*, pp. 192-222, IAMAP, Melbourne, 1974.

Seiler, W., F. Muller, and H. Oeser, Vertical distribution of chlorofluoromethanes in the upper troposphere and lower stratosphere, *Pure Appl. Geophys.*, 116, 554-566, 1978.

Seiler, W., A. Holzafel-Pschorn, R. Conrad, and D. Scharffe, Methane emissions from rice paddies, *J. Atmos. Chem.*, 1, 241-268, 1984a.

Seiler, W., H. Giehl, E. Brunke, and E. Halliday, The seasonality of CO abundance in the Southern Hemisphere, *Tellus*, 36B, 219-231, 1984b.

Seiier, W., R. Conrad, and D. Scharffe, Field studies of CH_4 emissions from termite nests into the atmosphere and measurements of CH_4 uptake by tropical soils, *J. Atmos. Chem.*, 1, 171-187, 1984c.

Seinfeld, J. H., *Air Pollution: Physical and Chemical Fundamentals*, 523 pp., McGraw-Hill Book Co., New York, 1975.

Senum, G. I., Y. N. Lee, and Gaffrey, Ultraviolet absorption spectrum of peroxyacetyl nitrate and peroxypropionyl nitrate, *J. Phys. Chem.*, 88, 1269-1270, 1984.

Sexstone, A. J., N. P. Reusbeck, T. B. Parkin, and J. M. Tiedje, Direct measurement of oxygen profiles and denitrification rates in soil aggregates, *Soil Sci. Am. J.*, 49, 645-651, 1985.

Sexton, K. and H. Westberg, Nonmethane HC composition of urban and rural atmospheres, *Atmos. Environ.*, 18, 1125-1132, 1984.

Shapiro, M. A., A multiple-structured frontal zone-jet stream system as revealed by meteorologically instrumented aircraft, *Mon. Weather Rev.*, 102, 244-253, 1974.

Shapiro, M. A., Simulation of upper level frontogenesis with a 20-level isentropic coordinate primitive equation model, *Mon. Weather Rev.*, 103, 591-604, 1975.

Shapiro, M. A., The role of turbulent heat flux in the generation of potential vorticity in the vicinity of upper level jetstream systems, *Mon. Weather Rev.*, 102, 892-896, 1976.

Shapiro, M. A., Further evidence of the mesoscale and turbulent structure of upper jet stream-frontal zone systems, *Mon. Weather Rev.*, 106, 1101-1111, 1978.

Shapiro, M. A., Turbulent mixing within tropopause folds as a mechanism for exchange of chemical constituents between the stratosphere and troposphere, *J. Atmos. Sci.*, 37, 994-1004, 1980.

Shapiro, M. A., Frontogenesis and geostrophically forced secondary circulations in the vicinity of jetstream-frontal zone systems, *J. Atmos. Sci.*, 38, 954-973, 1981.

Shapiro, M. A., E. R. Reiter, R. D. Cadle, and W. A. Sedlacek, Vertical mass and trace constituent transports in the vicinity of jet streams, *Arch. Met. Geoph. Biokl.*, B28, 193-206, 1980.

Shapiro, M. A., A. J. Krueger, and P. J. Kennedy, Nowcasting the position and intensity of jet streams using a satellite-borne total ozone mapping spectrometer, in *Nowcasting*, edited by K. A. Browning, pp. 137-145, Academic Press, New York, 1982.

Shapiro, M. A., R. C. Schnell, F. P. Parungo, S. J. Oltmans, and B. A. Bodhaine, El Chichon volcanic debris in an Arctic tropopause fold, *Geophys. Res. Lett.*, 11, 421-424, 1984.

Shardanand, and A. D. Prasad Rao, Collision induced absorption of O_2 in the Herzberg continuum, *J. Quant. Spectrosc. Radiat. Transfer*, 17, 433-439, 1977.

Sharma, R. D., and R. M. Nadile, Carbon dioxide (v2) radiative results using a new non-equilibrium model, *AIAA 81-0426*, paper presented at AIAA 19th Aerospace Sciences meeting, St. Louis, MO, 1981.

Shaw, Napier Sir, *Manual of Meteorology, The Physical Processes of Weather, Vol. III*, 445 pp., Cambridge University Press, Cambridge, 1942.

Shiotani, M., and I. Hirota, Planetary wave-mean flow interaction in the stratosphere: A comparison between the Northern and Southern Hemisphere, *Quart. J. Roy. Meteorol. Soc.*, *111*, 309-334, 1985.

Siegenthaler, U., and H. Oeschger, Transient temperature changes due to increasing CO_2 using simple models, *Ann. of Glaciology*, *5*, 153-159, 1984.

Silver, J. A., and C. E. Kolb, Measurement of molecular sodium species in the upper atmosphere, *Report No. ARI-RP-199*, Aerodyne Research, Inc., Billerica, MA, May, 1985.

Silver, J. A., A. C. Stanton, M. S. Zahniser, and C. E. Kolb, Gas phase reaction rate of sodium hydroxide with hydrochloric acid, *J. Phys. Chem.*, *88*, 3123-3129, 1984a.

Silver, J. A., M. S. Zahniser, A. C. Stanton, and C. E. Kolb, Temperature dependent thermolecular reaction rate constants for potassium and sodium superoxides formation, paper presented at 20th Symposium (International) on Combustion, Ann Arbor, MI, August, 1984b.

Simmonds, P. G., F. N. Alyea, C. A. Cardelino, A. J. Crawford, D. M. Cunnold, B. C. Lane, J. E. Lovelock, R. G. Prinn, and R. A. Rasmussen, The atmospheric lifetime experiment, 6, Results for carbon tetrachloride based on 3 years data, *J. Geophys. Res.*, *88*, 8427-8441, 1983.

Simmons, A. J., and R. Struefing, Numerical forecasts of stratospheric warming events using a model with a hybrid vertical coordinate, *Quart. J. Roy. Meteorol. Soc.*, *109*, 81-111, 1983.

Simon, P. C., Balloon measurements of solar fluxes between 1960 and 2300 A, in *Proceedings of the Third Conference on the Climatic Impact Assessment Program, DOT-TSC-OST-74-15*, edited by A. J. Broderick and T. M. Hard, pp. 137-140, Dept. of Transp., Washington, DC, 1975.

Simon, P. C., Solar irradiance between 120 and 400 nm and its variations, *Solar Physics*, *74*, 273-291, 1981.

Simon, P. C., and G. Brasseur, Photodissociation effects of solar UV radiation, *Planet. Space Sci.*, *31*, 987-999, 1983.

Simon, P. C., R. Pastiels, and D. Nevejans, Balloon observations of solar ultraviolet irradiance at solar minimum, *Planet. Space Sci.*, *30*, 68-71, 1982.

Simonaitis, R., Oxidation of the CH_3 radical and some halomethyl and haloethyl radicals of atmospheric interest, in *Proceedings of the NATO Advanced Study Institute on Atmospheric Ozone, Rep. FAA-EE-80-20*, edited by A. C. Aikin, pp. 501-515, DOT, FAA, Washington, DC, 1980.

Simonaitis, R., and J. Heicklen, Temperature dependence of the reactions of HO_2 with NO and NO_2, *Int. J. Chem. Kinet.*, *10*, 67-87, 1978.

Simons, J. W., R. J. Paur, H. A. Webster III, and E. J. Bair, Ozone ultraviolet photolysis. VI. The ultraviolet spectrum, *J. Chem. Phys.*, *59*, 1203-1208, 1973.

Singh, H. B., Atmospheric halocarbons: Evidence in favour of reduced average hydroxyl radical concentration in the troposphere, *Geophys. Res. Lett.*, *4*, 101-104, 1977a.

Singh, H. B., Preliminary estimates of average tropospheric OH concentrations in the Northern and Southern Hemispheres, *Geophys. Res. Lett.*, *4*, 453-456, 1977b.

Singh, H. B., and L. J. Salas, Measurement of selected light hydrocarbons over the Pacific Ocean: Latitudinal and seasonal variations, *Geophys. Res. Lett.*, *9*, 842-845, 1982.

Singh, H. B., and L. J. Salas, Methodology for the analysis of peroxyacetyl nitrate (PAN) in the unpolluted troposphere, *Atmos. Environ.*, *17*, 1507-1516, 1983a.

Singh, H. B., and L. J. Salas, Peroxyacetylnitrate in the free troposphere, *Nature*, *302*, 326-328, 1983b.

Singh, H. B., L. J. Salas, H. Shigeishi, and A. Crawford, Urban-nonurban relationships of halocarbons, SF_6, N_2O and other atmospheric trace constituents, *Atmos. Environ.*, *11*, 819-823, 1977.

Singh, H. B., L. J. Salas, H. Shigeishi, and E. Scibner, Atmospheric halocarbons, hydrocarbons, and sulfur hexafluride: Global distributions, sources, and sinks, *Science*, *203*, 899-903, 1979.

REFERENCES

Singh, H. B., L. J. Salas, and R. E. Stiles, Methyl halides in and over the eastern Pacific (40°N-32°S), *J. Geophys. Res.*, *88*, 3684-3690, 1983a.

Singh, H. B., L. J. Salas, and R. E. Stiles, Selected man-made halogenated chemicals in the air and oceanic environment, *J. Geophys. Res.*, *88*, 3675-3683, 1983b.

Singh, H. B., L. J. Salas, B. A. Ridley, J. Shetter, N. M. Donahue, F. C. Fehsenfeld, D. W. Fahey, D. D. Parrish, E. J. Williams, S. C. Liu, G. Hubler, P. C. Murphy, Relationship between peroxyacetyl nitrate (PAN) and nitrogen oxides in the clean troposphere, in press, 1985.

Slemr, F., and W. Seiler, Field measurements of NO and NO_2 emissions from fertilized and unfertilized soils, *J. Atmos. Chem.*, *2*, 1-24, 1984.

Smagorinsky, J. (Chairman), *Carbon Dioxide and Climate: A Second Assessment*, 92 pp., National Academy Press, Washington, DC, 1982.

Smagorinsky, J., S. Manabe, and J. L. Holloway Jr., Numerical results from a nine-level general circulation model of the atmosphere, *Mon. Weather Rev.*, *93*, 727-788, 1965.

Smith, A. K., An observational study of planetary wave propagation in the winter stratosphere, Ph.D. thesis, 71 pp., Washington Univ., Seattle, WA, 1982.

Smith, A. K., Observations of wave-wave interactions in the stratosphere, *J. Atmos. Sci.*, *40*, 2484-2496, 1983.

Smith, A. K., and L. V. Lyjak, An observational estimate of gravity wave drag from the momentum balance in the middle atmosphere, *J. Geophys. Res.*, *90*, 2233-2241, 1985.

Smith, A. K., J. C. Gille, and L. V. Lyjak, Wave-wave interactions in the stratosphere: Observations during quiet and active wintertime periods, *J. Atmos. Sci.*, *41*, 363-373, 1984.

Smith, C. J., R. D. DeLaure, and W. H. Patrick, Jr., Nitrous oxide emission from Gulf Coast wetlands, *Geochim. Cosmochim. Acta*, *47*, 1805-1814, 1983.

Smith, M. A. H. (Ed.), Review of spectroscopic parameters for upper atmospheric measurements, *NASA Conference Publication 2396*, 28 pp., NASA, Langley Research Center, Hampton, VA, 1985.

Smith, M. A. H., and C. P. Rinsland, Spectroscopic measurements of atmospheric HCN at northern and southern latitudes, *Geophys. Res. Lett.*, *12*, 5-8, 1985.

Smith, M. A. H., C. P. Rinsland, D. Frieourch and K. Narahari Rao, Intensities and collision broadening parameters from infrared spectra, in *Molecular Spectroscopy in Modern Research*, *Vol. 3*, pp. 111-248, Academic Press, New York, 1985.

Smith, P. L., H. E. Griesinger, J. H. Black, K. Yoshino, and D. E. Freeman, Interstellar O_2. II. VUV oscillator strengths of Schumann-Runge lines and prospects for space telescope observations, *Astrophys. J.*, *277*, 569-575, 1984.

Smith, R. M., A preview of the detection of mass return flow of air and water into the stratosphere using tritium as a tracer, *Tellus*, *20*, 76-81, 1968.

Smith, W. L., H. M. Woolf, C. M. Hayden, D. Q. Wark, and L. M. McMillin, The TIROS-N operational vertical sounder, *Bull. Amer. Meteor. Soc.*, *60*, 1177-1187, 1979.

Solomon, P. M., R. L. de Zafra, A. Parrish, and J. W. Barrett, Diurnal variation of stratospheric chlorine monoxide: A critical test of chlorine chemistry in the ozone layer, *Science*, *224*, 1210-1214, 1984.

Solomon, S., and P. J. Crutzen, Analysis of the August 1972 solar proton event including chlorine chemistry, *J. Geophys. Res.*, *86*, 1140-1146, 1981.

Solomon, S., and R. R. Garcia, On the distribution of nitrogen dioxide in the high-latitude stratosphere, *J. Geophys. Res.*, *88*, 5229-5239, 1983a.

Solomon, S., and R. R. Garcia, Simulation of NO_x partitioning along isobaric parcel trajectories, *J. Geophys. Res.*, *89*, 5497-5501, 1983b.

Solomon, S., and R. R. Garcia, Transport of thermospheric NO to the upper stratosphere, *Planet. Space Sci.*, *32*, 399-409, 1984a.

Solomon, S., and R. R. Garcia, On the distribution of long-lived tracers and chlorine species in the middle atmosphere, *J. Geophys. Res.*, *89*, 11633-11644, 1984b.

Solomon, S., D. W. Rusch, J.-C. Gerard, G. C. Reid, and P. J. Crutzen, The effect of particle precipitation events on the neutral and ion chemistry of the middle atmosphere: II. Odd hydrogen, *Planet. Space Sci.*, *29*, 885-892, 1981.

Solomon, S., P. J. Crutzen, and R. G. Roble, Photochemical coupling between the thermosphere and the lower atmosphere 1. Odd nitrogen from 50 to 120 km, *J. Geophys. Res.*, *87*, 7206-7220, 1982.

Solomon, S., D. W. Rusch, R. J. Thomas, and R. S. Eckman, Comparison of mesospheric ozone abundances measured by the Solar Mesosphere Explorer and model calculations, *Geophys. Res. Lett.*, *10*, 249-252, 1983a.

Solomon, S., G. C. Reid, D. W. Rusch, and R. J. Thomas, Mesospheric ozone depletion during the solar proton event of July 13, 1983, Part II. Comparison between theory and measurements, *Geophys. Res. Lett.*, *10*, 257-260, 1983b.

Solomon, P. M., R. de Zafra, A. Parrish and J. W. Barrett, Diurnal variation of stratospheric chlorine oxide: A critical test of chlorine chemistry in the ozone layer, *Science*, *224*, 1210-1214, 1984.

Solomon, S., J. M. Russell III, M. P. McCormick, D. W. Rusch, and J. M. Zawodny, Intercomparison of satellite datasets for NO_2 and odd nitrogen photo-chemistry, in press, 1985a.

Solomon, S., R. R. Garcia, and F. Stordal, Transport processes and ozone perturbations, *J. Geophys. Res.*, *90*, 12981-12990, 1985b.

Solomon, S., J. T. Kiehl, R. R. Garcia, and W. Grose, Tracer transport by the diabatic circulation deduced from satellite observations, *J. Atmos. Sci.*, in press, 1986.

Somerville, R. C. J., and L. A. Remer, Cloud optical thickness feedbacks in the CO_2 climate problem, *J. Geophys. Res.*, *89*, 9668-9672, 1984.

Spelman, M. J., and S. Manabe, Influence of oceanic heat transport upon the sensitivity of a model climate, *J. Geophys. Res.*, *89*, 571-586, 1984.

Speth, P., and R. Madden, Space-time spectral analyses of Northern Hemisphere geopotential heights, *J. Atmos. Sci.*, *40*, 1086-1100, 1983.

Spicer, C. W., M. W. Holdren, and C. W. Keigley, The ubiquity of peroxyacetyl nitrate in the continental boundary layer, *Atmos. Environ.*, *17*, 1055-1058, 1983.

Sridharan, U. C., L. X. Qui, and F. Kaufman, Kinetics and product channels of the reactions of HO_2 with O and H atoms at 296K, *J. Phys. Chem.*, *86*, 4569-4574, 1982.

Sridharan, U. C., L. X. Qui, and F. Kaufman, Rate constant of the OH + HO_2 reaction from 252 to 420K, *J. Phys. Chem.*, *88*, 1281-1282, 1984.

St. John, D., W. H. Bailey, W. H. Fellner, J. M. Minor, and R. D. Sull, Time series analysis of stratospheric ozone, *Commun. Statist. Theory Methods*, *11*, 1293-1333, 1982.

Staff, Upper Air Branch National Weather Service, Synoptic analyses, 5-, 2-, and 0.4-millibar surfaces for July 1974 through June 1976, *NASA Ref. Publ. 1023*, 330 pp., National Weather Service, Camp Springs, MD, 1978.

Staffensen, F. L., S. Kikkawa, and R. G. Phibbs, Meteorological rocket data processor and results from the solar eclipse of 7 March 1970, *J. Appl. Meteorol.*, *11*, 722-730, 1972.

Staley, D. O., Evaluation of potential vorticity changes near the tropopause and the related vertical motions, vertical advection of vorticity, and transfer of radioactive debris from stratosphere to troposphere, *J. Meteorol.*, *17*, 591-620, 1960.

Staley, D. O., On the mechanism of mass and radioactivity transport from stratosphere to troposphere, *J. Atmos. Sci.*, *19*, 450-467, 1962.

Starr, W. L., R. A. Craig, M. Loewenstein, and M. E. McGhan, Measurements of NO, O_3, and temperature at 19.8 km during the total solar eclipse of 26 February 1979, *Geophys. Res. Lett.*, *7*, 553-555, 1980.

REFERENCES

Stauffer, B., A. Neftel, H. Oeschger, and J. Schwander, CO_2 concentrations in air extracted from Greenland ice samples, in *Greenland Ice Core: Geophysical Geochemistry, and the Environment*, American Geophysical Union Monograph No. 33, edited by C. C. Langway, H. Oeschger, and W. Dansgaard, pp. 83-89, Washington, DC, 1985.

Stedman, D. H., and J. O. Jackson, The photostationary state in photochemical smog, *Int. J. Chem. Kinetics Symposium*, 1, 493-501, 1975.

Steed, J. M., A. J. Owens, C. D. Miller, D. L. Filkin, and J. P. Jesson, Two-dimensional model calculations of potential ozone perturbation by chlorofluorocarbons, *Nature*, 295, 308-311, 1982.

Steele, L. P., P. J. Fraser, R. A. Rasmussen, M. A. K. Khalil, T. J. Conway, A. J. Crawford, R. H. Gammon, K. A. Masarie, and K. W. Thoning, The global distribution of methane in the troposphere, *J. Atmos. Chem.*, in press, 1985.

Stelson, A. W., and J. H. Seinfeld, Relative humidity and temperature dependence of the ammonium nitrate dissociation constant, *Atmos. Environ.*, 16, 983-993, 1982.

Stephens, G. L., and P. J. Webster, Sensitivity of radiative forcing to variable cloud and moisture, *J. Atmos. Sci.*, 36, 1450-1466, 1979.

Stephens, G. L., S. Ackerman and E. A. Smith, A shortwave parameterization revised to improve cloud absorption, *J. Atmos. Sci.*, 41, 687-690, 1984.

Stern, A. C., *Air Pollution, Vol. III*, Academic Press, New York, 1977.

Stevens, C. M., and A. Engelkemeir, *J. Geophys. Res.*, in press, 1986.

Stockwell, W. R., and J. G. Calvert, The mechanism of the $HO-SO_2$ reaction, *Atmos. Environ.*, 17, 2231-2235, 1983.

Stolarski, R. S., Impact of large amounts of chlorine on stratospheric ozone, paper presented at the International Workshop on Current Issues in our Understanding of the Stratosphere and the Future of the Ozone Layer, BMFT, NASA, FAA, WMO, Feldafing, FRG, June 11-16, 1984.

Stolarski, R. S., and R. J. Cicerone, Stratospheric chlorine: A possible sink for ozone, *Can. J. Chem.*, 52, 1610-1615, 1974.

Stolarski, R. S., and A. R. Douglass, Parameterization of the photochemistry of stratospheric ozone including catalytic loss processes, *J. Geophys. Res.*, 90, 10709-10718, 1985.

Stolarski, R. S., D. M. Butler, and R. D. Rundel, Uncertainty propagation in a stratospheric model. 2. Monte Carlo analysis of imprecisions due to reaction rates, *J. Geophys. Res.*, 83, 3074-3078, 1978.

Stordal, F., I. S. A. Isaksen, and K. Horntveth, A diabatic circulation two-dimensional model with photochemistry: Simulations of ozone and ground released tracers, *J. Geophys. Res.*, 90, 5757-5776, 1985.

Stout, J., E. B. Rogers, and E. Nunez, abst, 16th Conf. Hurricanes and Tropical Meteorol 14-17 May 1985, Houston, Texas., 1985.

STRAC, Chlorofluorocarbons and their effects on stratospheric ozone, *Pollution Paper No 15, HMSO*, 1979.

Stratospheric Analysis Group, *Meteor. Abh. Met. Inst. Berlin*, 1980.

Strickland, A. C. (Ed.), *COSPAR International Reference Atmosphere*, Akademie-Verlag, Berlin, 1972.

Strobel, D. F., Parameterization of the atmospheric heating from 15-120 km due to O_2 and O_3 absorption of solar radiation, *J. Geophys. Res.*, 83, 6225-6230, 1978a.

Strobel, D. F., Photochemical radiative damping and instability in the stratosphere, II. Numerical results, *Geophys. Res. Lett.*, 5, 523-525, 1978b.

Strobel, D. F., D. M. Hunten, and M. B. McElroy, Production and diffusion of nitric oxide, *J. Geophys. Res.*, 75, 4307-4321, 1970.

Susskind, J., and J. E. Searl, Atmospheric absorption near 2400 cm^{-1}, *J. Quant. Spectrosc. Radiat. Transfer*, 18, 581-589, 1977.

Swanson, D., K. Brian, and H. S. Johnston, NO_3 quantum yield from N_2O_5 photolysis, *J. Phys. Chem.*, 88, 3115-3115, 1984.

Swider, W., and T. J. Keneshea, Decrease of ozone and atomic oxygen in the lower mesosphere during a PCA event, *Planet. Space Sci.*, *21*, 1969-1973, 1973.

Swider, W., T. J. Keneshea, and C. I. Foley, An SPE-distributed D-region model, *Planet. Space Sci.*, *26*, 883-892, 1978.

Syed, M. Q., and A. W. Harrison, Ground based observations of stratospheric nitrogen dioxide, *J. Canad. Phys.*, *58*, 788-802, 1980.

Syed, M. Q., and A. W. Harrison, Seasonal trend of stratospheric NO_2 over Calgary, *Can. J. Phys.*, *59*, 1278-1279, 1981.

Sze, N. D., Anthropogenic CO emissions: Implications for the atmospheric $CO-OH-CH_4$ cycle, *Science*, *195*, 673-675, 1977.

Sze, N. D., paper presented at CMA Workshop on Stratospheric Chemistry, Gottingen, FRG, October, 1984.

Sze, N. D., and M. K. Ko, CS_2 and COS in the stratospheric sulfur budget, *Nature*, *280*, 308-310, 1979.

Sze, N. D., M. K. W. Ko, W. Swider, and E. Murad, Atmospheric sodium chemistry. 1. The altitude region 70-100 km, *Geophys. Res. Lett.*, *9*, 1187-1190, 1982.

Sze, N. D., M. K. W. Ko, M. Livshits, W. C. Wang, P. B. Ryan, R. E. Specht, M. B. McElroy, and S. C. Wofsy, *Annual Report on the Atmospheric Chemistry, Radiation and Dynamics Program*, Atmospheric and Environmental Research, Inc., Cambridge, MA, 1983.

Taine, J., and F. LePoutre, A photoacoustic study of the collisional deactivation of the first vibrational levels of CO_2 by N_2 and CO, *Chem. Phys. Lett.*, *65*, 554-558, 1979.

Takahashi, M., A two-dimensional numerical model of the semi-annual zonal wind oscillation, in *Dynamics of the Middle Atmosphere*, edited by J. R. Holton and T. Matsuno, pp. 253-269, Terrapub, Tokyo, 1984.

Tang, I. N., On the equilibrium partial pressures of nitric acid and ammonia in the atmosphere, *Atmos. Environ.*, *14*, 819-828, 1980.

Telegades, K., The seasonal stratospheric distribution and inventory of excess carbon-14 from March 1955 to July 1969, *Rep. 243*, Health and Safety Lab., U.S. Atomic Energy Comm., Washington, DC, 1971.

Tenenbaum, J., Integrated and spectral energetics studies of the GLAS general circulation model, *Mon. Weather Rev.*, *110*, 962-980, 1982.

Terry, R. E., R. L. Tate, and J. M. Duxbury, Nitrous oxide emissions from drained, cultivated organic soils of S. Florida, *J. Air Poll. Control Assoc.*, *31*, 1173-1176, 1981.

Thacker, D. L., C. J. Gibbins, P. R. Schwartz, and R. M. Bevilacqua, Ground-based microwave observations of mesospheric H_2O in January, April, July, and September, 1980, *Geophys. Res. Lett.*, *8*, 1059-1062, 1981.

Theon, J. S., W. Nordberg, C. B. Katchen, and J. J. Horvath, Some observations on the thermal behavior of the mesosphere, *J. Atmos. Sci.*, *24*, 428-438, 1967.

Thomas, M. E., and R. J. Nordstrum, The N_2-broadened water vapor absorption line shape and infrared continuum absorption, I. Theoretical development, *J. Quant. Spectrosc. Radiat. Transfer*, *28*, 81-101, 1982.

Thomas, R. J., C. A. Barth, G. J. Rottman, D. W. Rusch, G. H. Mount, G. M. Lawrence, R. W. Sanders, G. E. Thomas, and L. E. Clemens, Ozone density distribution in the mesosphere (50-90 km) measured by the SME Limb Scanning Near Infared Spectrometer, *Geophys. Res. Lett.*, *10*, 245-248, 1983a.

Thomas, R. J., C. A. Barth, G. J. Rottman, D. W. Rusch, G. H. Mount, G. M. Lawrence, R. W. Sanders, G. E. Thomas, and L. E. Clemens, Mesospheric ozone depletion during the solar proton event of July 13, 1982, Part I-Measurement, *Geophys. Res. Lett.*, *10*, 253-255, 1983b.

Thomas, R. J., C. A. Barth, D. W. Rusch, and R. W. Sanders, Solar Mesosphere Explorer Near Infrared Spectrometer: Measurements of 1.27 μm radiances and the inference of mesospheric ozone, *J. Geophys. Res.*, *89*, 9569-9580, 1984a.

REFERENCES

Thomas, R. J., C. A. Barth, and S. Solomon, Seasonal variations of ozone in the upper mesosphere and gravity waves, *Geophys. Res. Lett.*, *11*, 673-676, 1984b.

Thompson, A. M., and D. H. Lenschow, Mean profiles of trace reactive species in the unpolluted marine surface layer, *J. Geophys. Res.*, *89*, 4788-4796, 1984.

Thompson, A. M., and O. C. Zafiriou, Air-sea fluxes of transient atmospheric species, *J. Geophys. Res.*, *88*, 6696-6708, 1983.

Tolson, R. H., Spatial and temporal variations of monthly mean total columnar ozone derived from 7 years of BUV data, *J. Geophys. Res.*, *86*, 7312-7330, 1981.

Tomatsu, K., Spectral energetics of the troposphere and lower stratosphere, *Advances in Geophysics*, *21*, 189-205, 1979.

Torabi, A., An investigation of the kinetics and excited state dynamics of the nitrate free radical, Ph.D. thesis, Georgia Institute of Technology, Atlanta, Georgia, 1985.

Torres, A. L., Tropospheric nitric oxide measurements during GTE/CITE, *Eos Trans. AGU*, *65*, 835, 1984.

Torres, A. L., and A. R. Bandy, Performance characteristics of the electrochemical concentration cell ozonesondes, *J. Geophys. Res.*, *83*, 5501-5504, 1978.

Torres, A. L., P. J. Maroulis, A. B. Goldberg, and A. R. Bandy, Atmospheric OCS measurements on Project Gametag, *J. Geophys. Res.*, *85*, 7357-7360, 1980.

Townsend, R. D., A diagnostic study of the zonally-averaged global circulation in isentropic coordinates. Ph.D. thesis, 221 pp., University of Wisconsin, Madison, 1980.

Townsend, R. D., and D. R. Johnson, The mass and angular momentum balance of the zonally averaged general circulation, paper presented at Int. Conf. Prelim. FGGE Data Anal. Res., pp. 542-552, Bergen, 23-27 June 1980.

Townsend, R. D., and D. R. Johnson, A diagnostic study of the isentropic zonally-averaged mass circulation during the first GARP global experiment, *J. Atmos. Sci.*, *42*, 1565-1579, 1985.

Traub, W. A., "An upper limit for stratospheric hydrogen peroxide" and "Measurements of OH from 18 to 48 km", papers presented at the International Workshop on Current Issues in our Understanding of the Stratosphere and the Future of the Ozone Layer, BMFT, NASA, FAA, WMO, Feldafing, FRG1, June 11-16, 1984.

Traub, W. A., and K. V. Chance, Stratospheric HF and HCl observations, *Geophys. Res. Lett.*, *8*, 1075-1077, 1981.

Traub, W. A., K. V. Chance, J. C. Brasunas, J. M. Vrtilek, and N. P. Carleton, Use of a Fourier Transform spectrometer on a balloon borne telescope and at the MMT, in *Proc. Soc. Photo-Opt. Instrum. Eng. Instrumentation in Astronomy IV*, *331*, 209-218, 1982.

Tsao, C. J., and B. Curnutte, Line widths of pressure broadened spectral lines, *J. Quant. Spectrosc. Radiat. Transfer*, *2*, 41-91, 1962.

Tsay, C. Y., Analysis of large scale wave disturbances simulated by an NCAR global circulation model, *J. Atmos. Sci.*, *31*, 330-339, 1974.

Tuazon, E. C., R. Atkinson, C. N. Plum, A. M. Winer, and J. N. Pitts, The reaction of gas phase N_2O_5 with water vapor, *Geophys. Res. Lett.*, *10*, 953-956, 1983.

Tuazon, E. C., A. M. Winer, and J. N. Pitts, Jr., Trace pollutant concentrations in a multiday smog episode in the California South Coast air basin by long path length fourier transform infrared spectroscopy, *Environ. Sci. Technol.*, *15*, 1232-1237, 1981.

Tuazon, E. C., R. Atkinson, H. MacLeod, H. W. Biermann, A. M. Winer, W. P. L. Carter, and J. N. Pitts, Jr., Yields of glyoxal and methylglyoxal from the NOx-air photooxidations of toluene and m- and p- xylene, *Environ. Sci. Technol.*, *18*, 981-984, 1984.

Tuck, A. F., Production of nitrogen oxides by lightning discharges, *Quart. J. Roy. Meteorol. Soc.*, *102*, 749-755, 1976.

Tuck, A. K., A comparison of one- two- and three-dimensional model representations of stratospheric gases, *Phil. Trans. Roy. Soc. London*, *A290*, 477-494, 1979.

Tucker, B. J., P. J. Maroulis, and A. R. Bandy, Free tropospheric measurements of CS_2 over a 45°N to 45°S latitude range, *Geophys. Res. Lett.*, *12*, 9-11, 1983.

Tucker, C. J., I. Y. Fung, C. D. Keeling, and R. H. Gammon, The relationship of global spectral vegetation indices to atmospheric CO_2 concentrations, *Nature*, in press, 1985.

Tung, Ka Kit, On the two-dimensional transport of stratospheric trace gases in isentropic coordinates, *J. Atmos. Sci.*, *39*, 2330-2355, 1982.

Tung, Ka Kit, Modeling of tracer transport in the middle atmosphere, in *Dynamics of the Middle Atmosphere*, edited by J. R. Holton and T. Matsuno, pp. 417-444, Terrapub, Tokyo, 1984.

Tung, Ka Kit, and R. S. Lindzen, A theory of stationary long waves. Part II: Resonant Rossby waves in the presence of realistic vertical shears, *Mon. Weather Rev.*, *107*, 735-750, 1979.

Turco, R. P., R. C. Whitten, O. B. Toon, J. B. Pollack, and P. Hamill, OCS stratospheric aerosols and climate, *Nature*, *283*, 283-286, 1980.

Turco, R. P., O. B. Toon, R. C. Whitten, R. G. Keesee, and P. Hamill, Importance of heterogeneous processes to tropospheric chemistry: Studies with a one-dimensional model, in *Heterogeneous Atmospheric Chemistry, Geophysical Monograph 26*, edited by David R. Schryer, pp. 231-240, American Geophysical Union, Washington, DC, 1982.

Turner, N. C., S. Rich, and P. E. Waggoner, Removal of ozone by soil, *J. Environ. Qual.*, *2*, 259-264, 1973.

Turner, N. C., P. E. Waggoner, and S. Rich, Removal of ozone from the atmosphere by soil and vegetation, *Nature*, *250*, 486-489, 1974.

Twomey, S. A., M. Piepgrass and T. L. Wolfe, An assessment of the impact of pollution on global albedo, *Tellus*, *36B*, 356-366, 1984.

Tyndall, J., On radiation through the Earth's atmosphere, *Philos. Mag.*, *4*, 200, 1863.

Tyson, B. J., J. C. Arvesen, and D. O'Hara, Interhemispheric gradients of CF_2Cl_2, $CFCl_3$, CCl_4, and N_2O, *Geophys. Res. Lett.*, *5*, 535-538, 1978b.

Uccellini, L. W., and D. R. Johnson, The coupling of upper and lower tropospheric jet streaks and implications for the development of severe convective storms, *Mon. Weather Rev.*, *107*, 682-702, 1979.

Uchino, O., M. Maeda, and M. Hirono, Applications of excimer lasers to laser-radar observations of the upper atmosphere, *IEEE J. Quant. Elec.*, *QE-15*, 1094-1107, 1979.

U.S. Dept. of HEW, Public Health Service, *Air Quality Criteria for Photochemical Oxidants*, *NAPCA-PUB-AP-63*, 202 pp., National Air Pollution Control Administration, Arlington, VA, 1970.

U.S. Standard Atmosphere Supplements, Superintendent of Documents, 289 pp., U.S. Government Printing Office, Washington, DC, 1966.

U.S. Standard Atmosphere, 1976, U.S. Government Printing Office, Washington, DC, 1976.

van Loon, H. K., K. Labitzke, and R. L. Jeene, Half-yearly wave in the stratosphere, *J. Geophys. Res.*, *77*, 3846-3855, 1972.

van Loon, H., C. S. Zerefos, and C. C. Repapis, Evidence of the southern oscillation in the stratosphere, *Publication No.3*, Academy of Athens, Research Center for Atmospheric Physics and Climatology, Athens, 1981.

Varanasi, P., and F. K. Ko, Intensity and transmission measurements in the nu-3 fundamental of N_2O at low temperatures, *J. Quant. Spectros. Radiat. Transfer*, *18*, 465-470, 1977.

Varanasi, P., L. P. Giver, and F. P. J. Valero, Intensity measurements in the V_4-fundamental of $^{13}CH_4$ at planetary atmospheric temperatures, *J. Quant. Spectros. Radiat. Transfer*, *30*, 491-495, 1983.

Vassy, A., Radiosonde speciale pour la mesure de la repartition verticale de l'ozone atmospherique, *J. Sci. Meteorol.*, *10*, 63-75, 1958.

Vaughan, G., and A. F. Tuck, Aircraft measurements near jet streams, in *Atmospheric Ozone*, edited by C. S. Zerefos and A. Ghazi, pp. 572-579, D. Reidel, Dordrecht, 1985.

REFERENCES

Vedder, J. F., B. J. Tyson, R. B. Brewer, C. A. Boitnott, and E. C. Y. Inn, Lower stratospheric measurements of variation with latitude of CF_2Cl_2, $CFCl_3$, CCl_4, and N_2O profiles in the Northern Hemisphere, *Geophys. Res. Lett.*, *5*, 33-36, 1978.

Venne, D., The horizontal structure of traveling planetary-scale waves in the upper stratosphere, *J. Geophys. Res.*, 1984.

Venne, D., and J. Stanford, An observational study of high-latitude stratospheric planetary waves in winter, *J. Atmos. Sci.*, *39*, 1026-1084, 1982.

Veryard, R. G., and R. A. Ebdon, Fluctuations in tropical stratospheric winds, *Meteor. Mag.*, *90*, 125-143, 1961.

Vienkorn-Rudolph, B., K. Bachmann, and B. Schwartz, Vertical profiles of hydrogen chloride in the troposphere, *J. Atmos. Chem.*, *2*, 47-63, 1984.

Vigroux, E., Contribution a l'etude experimentale de l'absorption de l'ozone, *Ann. Phys.*, *8*, 709-762, 1953.

Vincent, D. G., Mean meridional circulation in the Northern Hemisphere lower stratosphere during 1964 and 1965, *Quart. J. Roy. Meteorol. Soc.*, *94*, 333-349, 1968.

Vincent, R. A., Gravity wave motions in the mesosphere, *J. Atmos. Terr. Phys.*, *46*, 119-128, 1984a.

Vincent, R. A., MF/HF radar measurements of the dynamics of the mesopause region-A review, *J. Atmos. Terr. Phys.*, *46*, 961-974, 1984b.

Vincent, R. A., Planetary and gravity waves in the mesosphere and lower thermosphere, in *Handbook for MAP, Vol. 16*, edited by K. Labitzke, J. J. Barnett, and B. Edwards, pp. 269-277, SCOSTEP Secretariat, Univ. of Illinois, Urbana, 1985.

Vincent, R. A., and I. M. Reid, HF Doppler measurements of mesospheric gravity wave momentum fluxes, *J. Atmos. Sci.*, *40*, 1321-1333, 1983.

Volz, A., U. Schmidt, J. Rudolph, D. H. Ehhalt, F. J. Johnen, and A. Khedim, Vertical profiles of trace gases at mid latitudes, *Jul-Report 1742*, Kernforschungsanlage Julich GmbH, D-5170 Julich, FRG, 1981.

Vukovich, F. M., J. Fishman and E. V. Browell, The reservoir of ozone in the boundary layer of the eastern United States and its potential impact on the global tropospheric ozone budget, *J. Geophys. Res.*, *90*, 5687-5690, 1985.

Vupputuri, R. K. R., The structure of the natural stratosphere and the impact of chlorofluoromethanes on the ozone layer investigated in a 2-D time dependent model, *Pure Appl. Geophys.*, *117*, 448-485, 1978/79.

Vupputuri, R. K. R., Study the effect of El Chichon volcanic cloud on the stratospheric temperature structure and ozone distribution in a 2-D model, in *Atmospheric Ozone*, edited by C. S. Zerefos and A. Ghazi, pp. 59-60, D. Reidel, Dordrecht, 1985.

Vyas, N., Numerical modelling of atmospheric processes, Ph.D. thesis, Oxford University, Oxford, 1984.

Wale, M. J., and G. D. Peskett, Some aspects of the design and behavior of the Stratospheric and Mesospheric Sounder, *J. Geophys. Res.*, *89*, 5287-5293, 1984.

Wallace, J. M., General circulation of the tropical lower stratosphere, *Rev. Geophys. Spa. Phys.*, *11*, 191-222, 1973.

Wallace, J. M., The climatological mean stationary waves: Observational evidence, in *Large-scale Dynamical Processes in the Atmosphere*, edited by B. J. Hoskins and R. Pearce, pp. 27-53, Academic Press, New York, 1983.

Wallace, J. M., and V. Kousky, Observational evidence of Kelvin waves in the tropical stratosphere, *J. Atmos. Sci.*, *25*, 900-907, 1968.

Wallington, T. J., R. Atkinson, and A. M. Winer, Rate constants for the gas phase reaction of OH radicals with peroxyacetyl nitrate (PAN) at 273 and 297K, *Geophys. Res. Lett.*, *11*, 861-864, 1984.

Wang, P.-H., M. P. McCormick, and W. P. Chu, A study on the planetary wave transport of ozone during the late February 1979 stratospheric warming using the SAGE ozone observation and meteorological information, *J. Atmos. Sci.*, *40*, 2419-2431, 1983.

Wang, W.-C., and P. H. Stone, Effect of ice-albedo on global sensitivity in a one-dimensional radiative-convective climate model, *J. Atmos. Sci.*, *37*, 545-552, 1980

Wang, W.-C., and N. D. Sze, Coupled effects of atmospheric N_2O and O_3 on the Earth's climate, *Nature*, *268*, 589-590, 1980.

Wang, W.-C., J. P. Pinto and Y. L. Yung, Climatic effects due to halogenated compounds in the Earth's atmosphere, *J. Atmos. Sci.*, *37*, 333-338, 1980.

Wang, W.-C., Y. L. Yung, A. A. Lacis, T. Mo and J. E. Hansen, Greenhouse effects due to man-made perturbations of trace gases, *Science*, *194*, 685-690, 1976.

Wang, W.-C., W. B. Rossow, M.-S. Yao and M. Wolfson, Climate sensitivity of a one-dimensional radiative-convective model with cloud feedback, *J. Atmos. Sci.*, *38*, 1167-1178, 1981.

Wang, W.-C., D. J. Wuebbles, W. M. Washington, R. G. Isaacs and G. Molnar, Potential climatic effects of perturbations other than CO_2, Chapter 6, in *State-of-the-art report*, edited by M. C. MacCracken and F. M. Luther, Dept. of Energy, Washington, DC, 1985

Warmbt, W., Results of long term measurements of near surface ozone in the GDR, *Zeit. fuer Met.*, *29*, 24-31, 1979.

Warneck, P., On the role of OH and HO_2 radicals in the troposphere, *Tellus*, *26*, 39-46, 1974.

Washington, W. M., and G. A. Meehl, General circulation model experiments on the climatic effects due to a doubling and quadrupling of carbon dioxide concentration, *J. Geophys. Res.*, *88*, 6600-6610, 1983.

Washington, W. M., and G. A. Meehl, Seasonal cycle experiment on the climate sensitivity due to a doubling of CO_2 with an atmospheric general circulation model coupled to a simple mixed-layer ocean model, *J. Geophys. Res.*, *89*, 9475-9503, 1984.

Watanabe, K., M. Zelikoff, and E. C. Y. Inn, Absorption coefficients of several atmospheric gases, *Geophysical Research Paper No. 21*, Air Force Cambridge Research Lab., Bedford, MA, 1953.

Waters, J. W., J. J. Gustincic, R. K. Kakar, H. K. Roscoe, P. N. Swanson, T. G. Phillips, T. de Graauw, A. R. Kerr, and R. J. Mattauch, Aircraft search for millimeter wavelength emission by stratospheric ClO, *J. Geophys. Res.*, *84*, 7034-7040, 1979.

Waters, J. W., J. C. Hardy, R. F. Jarnot, and H. M. Pickett, Chlorine monoxide radical, ozone, and hydrogen peroxide: Stratospheric measurements by microwave limb sounding, *Science*, *214*, 61-64, 1981.

Waters, J. W., J. C. Hardy, R. F. Jarnot, H. M. Pickett, and P. Zimmermann, A balloon-borne microwave limb sounder for stratospheric measurements, *J. Quant. Spectrosc. Radiat. Transfer*, *32*, 407-433, 1984.

Watson, R. T., Rate constants of reactions of ClO_x of atmospheric interest, *J. Phys. Chem. Ref. Data*, *6*, 871-918, 1977.

Watson, R. T., Balloon intercomparison measurements of minor species, to be published, 1986.

Watson, R. T., J. Rogers, L. Heidt, W. Pollock, K. Mauersberger, D. Kley, A. L. Schmeltekopf, D. L. Albritton, S. Oltmans, J. Mastenbrook, D. Murcray, W. F. J. Evans, C. Midwinter, N. Swann, and E. F. Danielsen, An intercomparison of stratospheric water vapor instruments, to be published, 1986.

Wayne, R. P., *Chemistry of Atmospheres*, 361 pp., Clarendon Press, Oxford, 1985.

WCP, Aerosols and their climatic effects, paper presented at World Climate Research Programme Report, *WCP-55*, Report of the experts meeting, Williamsburg, VA, 28-30 March 1983.

Weaver, C., and R. Pearson, Ozone conservation and transport in cumulus clouds, *Eos Trans. AGU*, *65*, 836, 1984.

Weaver, H., M. J. Mumma, J. L. Faris, T. Kostiuk, and J. J. Hillman, Infrared heterodyne spectroscopy of seven gases in the vicinity of chlorine monoxide lines, *Appl. Opt.*, *22*, 1562-1567, 1983.

REFERENCES

Webster, C. R., and R. T. Menzies, In situ measurements of stratospheric nitric oxide using a balloon-borne tunable diode laser spectrometer, *Appl. Opt.*, *23*, 1140-1142, 1984.

Webster, P. J., and G. L. Stephens, Tropical upper-tropospheric extended clouds: Inferences from Winter MONEX, *J. Atmos. Sci.*, *37*, 1521-1541, 1980.

Weeks, L. H., and L. G. Smith, A rocket measurement of ozone near sunrise, *Planet. Space Sci.*, *16*, 1189-1195, 1968.

Weeks, L. H., R. S. CuiKay, and J. R. Corbin, Ozone measurements in the mesosphere during the solar proton event of 2 November 1969, *J. Atmos. Sci.*, *29*, 1138-1142, 1972.

Wehrbein, W. M., and C. B. Leovy, An accurate radiative heating and cooling algorithm for use in a dynamical model of the middle atmosphere, *J. Atmos. Sci.*, *39*, 1532-1544, 1982.

Weiler, K. H., P. Fabian, G. Flentje, and W. A. Mathews, Stratospheric NO measurements: A new balloon-borne chemiluminescence instrument, *J. Geophys. Res.*, *85*, 7445-7452, 1980.

Weinreb, M. P., W. A. Morgan, I-Lok Chang, L. D. Johnson, P. A. Bridges, and A. C. Neuendorffer, High-altitude balloon test of satellite solar occultation instrument for monitoring stratospheric O_3, H_2O and HNO_3., *J. Atmos. Oc. Tech.*, *1*, 87-100, 1984.

Weinstock, E. M., M. J. Phillips, and J. G. Anderson, In situ observations of ClO in the stratosphere: A review of recent results, *J. Geophys. Res.*, *86*, 7273-7278, 1981.

Weinstock, B., and H. Niki, Carbon monoxide balance in nature, *Science*, *176*, 290-292, 1972.

Weinstock, J., Nonlinear theory of gravity waves: Momentum deposition, generalized Rayleigh friction and diffusion, *J. Atmos. Sci.*, *39*, 1698-1710, 1982.

Weiss, R. F., The temporal and spatial distribution of tropospheric nitrous oxide, *J. Geophys. Res.*, *86*, 7185-7195, 1981.

Weiss, R. F., and H. Craig, Production of atmospheric nitrous oxide by combustion, *Geophys. Res. Lett.*, *3*, 751-753, 1976.

Wesely, M. L., Turbulent transport of ozone to surfaces common in the eastern half of the United States, in *Trace Atmospheric Constituents*, edited by S. E. Schwartz, pp. 345-370, Wiley, New York, 1983.

Wesley, M. L., and B. B. Hicks, Some factors that affect the deposition rates of sulfur dioxide and similar gases on vegetation, *J. Air Poll. Control Assoc.*, *27*, 1110-1116, 1977.

Wesely, M. L., J. A. Eastman, D. R. Cook, and B. B. Hicks, Daytime variations of ozone eddy fluxes to maize, *Boundary-Layer Meteorol.*, *15*, 361-363, 1978.

Wesely, M. L., D. R. Cook, and R. M. Williams, Field measurement of small ozone fluxes to snow, bare wet soil, and lake water, *Boundary-Layer Meteorol.*, *20*, 459-471, 1981.

Wesely, M. L., J. A. Eastman, D. H. Stedman, and E. D. Yalvac, An eddy correlation measurement of NO_2 flux to vegetation and comparison to O_3 flux, *Atmos. Environ.*, *16*, 815-820, 1982.

Wetherald, R. T., and S. Manabe, The effects of changing the solar constant on the climate of a general circulation model, *J. Atmos. Sci.*, *32*, 2044-2059, 1975.

Whitten, G. Z., H. Hogo, and J. P. Killus, The carbon bond mechanism: A condensed kinetic mechanism for photochemical smog, *Environ. Sci. Technol.*, *14*, 690-700, 1980.

Whitten, R. C., W. J. Borucki, H. T. Woodward, L. A. Capone, C. A. Riegel, R. P. Turner, I. G. Poppoff, and K. Santhanam, Implications of smaller concentrations of stratospheric OH: A two-dimensional model study of ozone perturbations, *Atmos. Environ.*, *15*, 1583-1589, 1981.

Wigley, T. M. L., and M. E. Schlesinger, Analytical solution for the effect of increasing CO_2 on global mean temperature, *Nature*, *315*, 649-652, 1985.

Wilkniss, P. E., and R. E. Larson, Atmospheric radon measurements in the Arctic fronts, seasonal observations and transport of continental air to polar regions, *J. Atmos. Sci.*, *41*, 2347-2358, 1984.

Wilkniss, P. E., R. A. Lamontagne, R. E. Larson, J. W. Swinnerton, C. R. Dickson, and T. Thompson, Atmospheric trace gases in the Southern Hemisphere, *Nature*, *245*, 45-47, 1973.

Williams, A. P., Relaxation of the 2.7γ and 4.3γ bands of carbon dioxide, in *Mesospheric Models and Related Experiments*, edited by G. Fiocco, pp. 177-187, D. Reidel, Dordrecht, 1971.

Williams, R. M., Uncertainties in the use of box models for estimating dry deposition velocity, *Atmos. Envir.*, *16*, 2707-2708, 1982.

Williams, W. J., J. J. Kosters, A. Goldman, and D. G. Murcray, Measurements of stratospheric halocarbon distributions using infrared techniques, *Geophys. Res. Lett.*, *3*, 379-382, 1976.

Wine, P. H., and A. R. Ravishankara, Kinetics of OH reactions with tropospheric sulfur compounds, in *2nd Symposium Composition of the Nonurban Troposphere*, pp. 258-260, May 25-28, 1982, Williamsburg, VA, AMS, Boston, MA, 1982.

WMO, *The Stratosphere 1981. Theory and Measurements*, WMO Global Ozone Research and Monitoring Project Report No. *11*, 516 pp., WMO, Geneva, 1982.

WMO, Report of the WMO meeting of experts on potential climatic effects of ozone and other minor trace gases, *WMO Global Ozone Research and Monitoring Project, Report No. 14*, WMO, Geneva, 1983a.

WMO, World Meteorological Organization project on research and monitoring of atmospheric CO_2, *Report No. 10*, edited by R. J. Bojkov, 42 pp., Geneva, 1983b.

WMO, Report of the WMO (CAS) Meeting of Experts on the CO_2 Concentrations from Pre-Industrial Times to I.G.Y. World Climate Programme, *WCP-53*, WMO/ICSU, 34 pp., Geneva, 1983c.

Wofsy, S. C., Interactions of CH_4 and CO in the earth's atmosphere, *Ann. Rev. Earth Planet. Sci.*, *4*, 441-469, 1976.

Wofsy, S. C., J. C. McConnell, and M. B. McElroy, Atmospheric CH_4, CO and CO_2, *J. Geophys. Res.*, *77*, 4477-4493, 1972.

Wofsy, S. C., M. B. McElroy, and Y. L. Yung, The chemistry of atmospheric bromine, *Geophys. Res. Lett.*, *2*, 215-218, 1975.

Wolff, G. T., and P. J. Lioy, Development of an ozone river associated with synoptic scale episodes in the eastern United States, *Environ. Sci. Tech.*, *14*, 1257-1261, 1980.

Woodman, R. F., and A. Giullen, Radar observaqtions of winds and turbulence in the stratosphere and mesosphere, *J. Atmos. Sci.*, *31*, 493-505, 1974.

Wu, M. F., M. A. Geller, J. G. Olson, and M. E. Gelman, Troposphere-Stratosphere (surface-55 km) monthly general circulation statistics for the Northern Hemisphere; 4 year averages, *NASA Techn. Memo. 86182*, NASA Goddard Space Flight Center, Greenbelt, MD, 1984.

Wuebbles, D. J., Chlorocarbon emission scenarios: Potential impact on stratospheric ozone, *J. Geophys. Res.*, *88*, 1433-1443, 1983a.

Wuebbles, D. J., A theoretical analysis of the past variations in global atmospheric composition and temperature structure, *UCRL-53423*, Lawrence Livermore National Laboratory, Livermore, CA, 1983b.

Wuebbles, D. J., and P. S. Connell, Interpreting the 1-D model-calculated nonlinearities from chlorocarbon perturbations, paper presented at International Workshop on Current Issues in our Understanding of the Stratosphere and the Future of the Ozone Layer, BMFT, NASA, FAA, WMO, Feldafing, FRG, June 11-16, 1984.

Wuebbles, D. J., F. M. Luther, and J. E. Penner, Effect of coupled anthropogenic perturbations on stratospheric ozone, *J. Geophys. Res.*, *88*, 1444-1456, 1983.

Wuebbles, D. J., M. C. MacCracken, and F. M. Luther, A proposed reference set of scenarios for radiatively active atmospheric constituents, *Carbon Dioxide Research Division Report DOE/NBB-0066*, U.S. Department of Energy, Lawrence Livermore National Laboratory, Livermore, CA, 1984.

Wyngaard, J. C., Toward convective boundary layer parameterization: A scalar transport module, *J. Atmos. Sci.*, *41*, 1959-1969, 1984.

Yamazaki, K. and C. R. Mechoso, Observations of the final warming in the stratosphere of the Southern Hemisphere during 1979, *J. Atmos. Sci.*, *42*, 1198-1205, 1985.

REFERENCES

Yanai, M., J.-H. Chu, T. E. Stark, and T. Nitta, Response of deep and shallow tropical maritime cumuli to large-scale processes, *J. Atmos. Sci.*, *33*, 976-991, 1976.

Yao, F., I. Wilson, and H. Johnston, Temperature dependent ultraviolet absorption spectrum for dinitrogen pentoxide, *J. Phys. Chem.*, *86*, 3611-3615, 1982.

Yoshida, T., and M. Alexander, Nitrous oxide formations by nitrosomoses europsea and heterotrophic organisms, *Soil Sci. Soc. Am. Proc.*, *34*, 880-882, 1970.

Yoshida, T., and M. Alexander, Hydroxylamine oxidation by nitrosomoses europea, *Soil Sci.*, *3*, 307-312, 1971.

Yoshino, K., D. E. Freeman, J. R. Esmond, and W. H. Parkinson, High resolution absorption cross section measurements and band oscillator strengths of the (1,0) - (12-0) Schumann-Runge bands of O_2, *Planet. Space Sci.*, *31*, 339-353, 1983.

Yung, Y. L., M. B. McElroy, and S. C. Wofsy, Atmospheric halocarbons: A discussion with emphasis on chloroform, *Geophys. Res. Lett.*, *2*, 397-399, 1975.

Yung, Y. L., J. P. Pinto, R. T. Watson, and S. P. Sander, Atmospheric bromine and ozone perturbations in the lower stratosphere, *J. Atmos. Sci.*, *37*, 339-353, 1980.

Zafiriou, O. C., and M. McFarland, Nitric oxide from nitrite photolysis in the central equatorial Pacific, *J. Geophys. Res.*, *86*, 3173-3182, 1981.

Zander, R., Presence de HF dans la stratosphere superieure, *C. R. Acad. Sc. Paris*, *281B*, 213-214, 1975.

Zander, R., Recent observations of HF and HCl in the upper stratosphere, *Geophys. Res. Lett.*, *8*, 413-416, 1981a, Corrections, *Geophys. Res. Lett.*, *8*, 850, 1981.

Zander, R., Evidence for variability in the total column of HCl over the Jungfraujoch Station, to be published, 1986.

Zander, R., Trend in HF above the Jungfraujoch Station, to be published, 1986.

Zander, R., H. Leclerq, and L. D. Kaplan, Concentration of carbon monoxide in the upper stratosphere, *Geophys. Res. Lett.*, *8*, 365-368, 1981.

Zander, R., G. M. Stokes, and J. W. Brault, Simultaneous detection of FC-11, FC-12, and FC-22 through 8 to 13 micrometers IR solar observations from the ground, *Geophys. Res. Lett.*, *10*, 521-524, 1983.

Zander, R., G. M. Stokes, and J. W. Brault, Spectroscopic detection of acetylene and ethane in the earth's atmosphere, through ground-based solar observations, *C. R. Acad. Sc. Paris*, *295*, 583-586, 1982.

Zander, R., N. Louisnard, and M. Bangham, Stratospheric methane concentration profiles measured during the Balloon Intercomparison Campaigns, to be published, 1986.

Zangvil, A. and M. Yanai, Upper tropospheric waves in the tropics. Part I: Dynamical analysis in the wavenumber frequency domain, *J. Atmos. Sci.*, *37*, 283-298, 1980.

Zawodny, J. M., Short-term variability of nitrogen dioxide in the winter stratosphere., *J. Geophys. Res.*, in press, 1985a.

Zawodny, J. M., Short term variability of nitrogen dioxide in the winter stratosphere., Ph.D. thesis, University of Colorado, Boulder, CO, 1985b.

Zipf, E. C., and S. S. Prasad, A mesosphere source of nitrous oxide, *Nature*, *295*, 133-135, 1982.

Zumbrunn, R., A. Neftel, and H. Oeschger, CO_2 measurements on l-cm^3 ice samples with an IR laser spectrometer (IRLS) combined with a new dry extraction device, *Earth and Planetary Space Letters*, *60*, 318-324, 1982.